THE UNIVERSITY
of EDINBURGH

Age estimation on two Mediterranean samples using rib histomorphometry

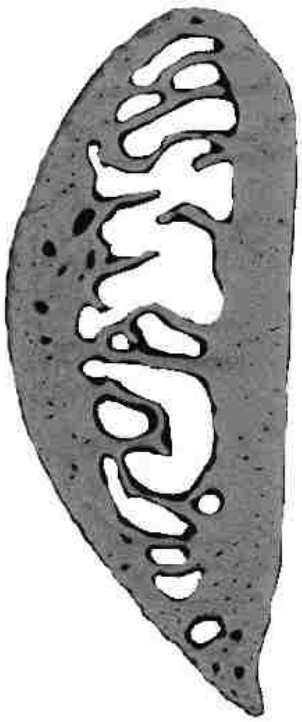

Julia Gómez García-Donas

PhD

The University of Edinburgh

2018

Abstract

Estimation of age is a crucial step for the identification of unknown individuals. Age is commonly assessed through macroscopic analytical methods based on the gross-examination of age degenerative changes in the skeleton. The choice of the methods relies on the taphonomic condition of the human remains and/or the skeletal element that is available. In cases of very fragmented bones, microscopic techniques remain one of the few approaches to estimate age. Thus, many histological age estimation methods have been developed for different bones and on different samples in the last forty years. Numerous intrinsic and extrinsic factors influence bone remodelling rates and have shown to affect the accuracy of histological aging methods. The present study investigates rib thin-sections from two Mediterranean samples, aiming to explore the applicability and reliability of histological methods in estimating age within these samples.

Standard ribs were obtained from males and females (N = 88, Mean age = 60, SD = 17.90) from two samples, Cretans (Greece) and Greek-Cypriots (Republic of Cyprus). The costal elements were processed histologically according to standard protocols and thirteen raw and composite histomorphometric parameters (frequency number of intact and fragmentary osteons, total osteons, osteon population densities – including OPD(I) and OPD(F) – cortical area, total area, endosteal area, relative cortical area, osteon area, osteon perimeter and osteon circularity) were assessed.

Intra- and inter-observer errors were examined. Due to the fragmented nature of the costal elements, sampling error was calculated as a means to explore whether the histological variables vary among six different topographical locations along the rib length. A validation study was carried out by applying four existing histological age prediction equations on the entire dataset and on the sub-datasets (sex and samples separately) in order to verify whether population-specific formulae are required for the Mediterranean samples. The relationship between the histological variables and age, as well as sex and samples, was determined through several statistical tests. Lastly, simple and multiple regression analyses were performed testing all possible combinations of variables. The best models

were finally selected according to prediction power and goodness of fit indicators.

The results from intra- and inter-observer errors indicated that most of the histological parameters achieved high levels of repeatability. The preliminary outcome from the sampling error pilot study suggested low variability among the six thin-sections from each rib. According to the validation study, three of the four age prediction equations resulted in high underestimation of age, indicating that population-specific formulae are needed to provide more accurate age estimates. Most of the histological variables showed a statistically significant correlation with age with some differences observed by sex and by sample. Forty-one models were generated concluding that osteon densities along with rib and osteon measurements formulae produced the most accurate results. The best model generated from the entire dataset included OPD and osteon circularity with a standard error of the estimate of 10.45 years. When sex and samples were separated, the best model selected included OPD and osteon perimeter producing a standard error of the estimate of 8 years for Cypriots.

This research demonstrates that quantitative bone histology is a feasible method to estimate age on the Mediterranean samples obtaining errors rates that are in accordance with macroscopic ageing techniques. Inter-population variation in remodeling rates is suggested; however, the inclusion of other bones presenting different remodelling dynamics (such as femora) is recommended to further explore this hypothesis. This study contributes to the creation of population-specific standards for Cretans and Cypriots.

Declaration of own work

I hereby declare that this thesis has been composed by me; the work presented here is my own and has not been submitted for any other degree or any professional qualification except as specified. Any previous own publication relevant to this work has been referenced in this work when appropriate.

Signed

……..

Acknowledgements

I would like to thank many people that went with me through these years.

First, I would like to thank my supervisor, Elena Kranioti, for all the things she did for me. For her support, encouragement, energy, strength, scientific wisdom….She has been always there when I needed her and always supportive. I am sure this could not have been possible without her, both professionally and personally…since the first time we met, and she said: who said you cannot do this?. I will be always grateful, always. Venceremos, prima!.

I would like to thank Robert Paine because he played an important role in the creation of this work. He was very supportive in the edition, data management, and further discussion of the results. I owe you so many beers, Roberto.

All these people that work with me over the years: Anna Evatt, Philip McMath, Anna Maria Dianna, Laura Girdwood, Mara Karell and Andrea Bonicelli. You were there and this made my years much better. We learnt, cried and laughed together. Thank you guys! Graeme Eskrime….you are also included in this group!

I would like to thank Linda Fibiger for her support, and for giving me all the hours that I needed to survive. Also, thanks for bringing Freya to play (Juji).

Alan Dalton, we made such a nice team. All laboratory, bones and music. This would have not been possible without your help. Always happy to work with you, cocodrilo.

I would like to thank Xavier Rubio-Campillo for his help and support during the statistical analysis. Very much appreciated.

I am thankful to the administrative stuff for helping me and responding my one thousands questions with a smile.

I probably forget people that were there…but it is not a lack of recognition but a product of tiredness. Whoever I forget, sorry and thanks!

Now, I need to talk to my Spanish crew.

Me gustaría agradecer mi familia (tios, tias, primo y prima) por toda la ayuda, el apoyo y la compresión. Especialmente a mis padres, porque siempre han estado

allí cuando lo necesitaba y cuando no. En los últimos meses (que han sido muy duros), vuestro apoyo ha sido el impulso fundamental para que yo esté donde estoy y sólo se podría explicar con amor. Os quiero a todos.

A mis amigos, especialmente a Ana Rodriguez, Tommy Corvate y a Jesus Oliva. Porque al llorar y al reir, siempre me habéis cogido de la mano. Y por darme una bofetada de vez en cuando! Entiendo que no ha sido fácil pero os habéis portado como unos campeones. Sito, muchísimas gracias por la ayuda con la edición, te debo una y te la voy a pagar.

Gracias a Mariam, por la ayuda psicológica, su guía y sus consejos en el último tramo. Me sirvió de mucho tenerte cerca en los peores momentos. Muy profesional.

Gracias a Diego Zamora por la ayuda prestada durante la primera fase.

Por último, quería recordar la memoria de mis abuelos que ya no están, y que siempre han sido un ejemplo para mí. Me gustaría terminar los agradecimientos con una frase que solía decir mi abuelo:

A todos aquellos hombres que al nacer de cada día saben encontrar esas pequeñas cosas que hacen de la vida algo maravillo.

That was me,

Thanks!

Table of Contents

List of Figures

List of Tables

Chapter 1 : INTRODUCTION

Only fools and the dead never change their opinions

James R. Lowell

One of the main tasks of the physical anthropologist is to gather anthropological information from decomposed human remains. Age estimation is an essential step in the creation of the biological profile of an unknown individual in forensic settings. It is also critical for the construction of population demographics from the bioarchaeological context. Whether we are searching for a clearer physiological understanding of skeletal age related changes in bone micro- and macro-anatomy or the specific goal is to create methods for the practitioners to apply, the anthropologist needs a full understanding of the nature, distribution and timing of biological processes related to skeletal age changes.

The interpretation of how age indicators are manifested in the skeleton is crucial due to complex physiological processes during growth, maturation and later in adulthood making the association between age markers and individual´s chronological age imperfectly connected (Garvin et al., 2012). A useful age indicator (trait or process) should present a unidirectional and predictable change with age, demonstrate a strong correlation to chronological age and vary consistently across individuals and among populations (Scientific Working Group for Forensic Anthropology, 2010). As expected, this is not the case for most of the age markers used in age estimation methods (Mays, 2015). Along the years, the scientific community has worked tirelessly on the development of age estimation techniques. This work has also included the testing and improvement of existing age prediction methods (Stout et al., 1996).

Once growth has ceased, the skeleton continues to preserve and maintain its functional and material properties but undergoes a progressive degeneration over time. This process can be assessed both by the naked-eye and/or by the aid of a microscope. The combination of both analytical approaches — macroscopic and microscopic methods — may produce more accurate age estimates (Aiello and Molleson, 1993; Stout et al., 1994). Ultimately, the preference of analytical method is down to the discretion of the investigator, based on equipment available, the skeletal element analysed and its state of preservation, and the nature of the question to be answered and the accuracy of the methods.

Macroscopic methods using gross-examination of degenerative changes on bones have been widely used since they are easy to apply and do not require specific equipment (e.g. Todd, 1920; Lovejoy et al., 1985a; Isçan et al., 1984a, b). However, the macroscopic approach is considered subjective and wide age ranges are generally produced for individuals older than 50 years of age (Christensen et al., 2014). Moreover, the exposure of the age markers to taphonomic processes may invalidate their observation, and thus, precluding them from use (Cappella et al., 2017).

On the other hand, the histological approach was first applied to estimate age on dry bone in the mid- 1960s demonstrating that it could be reliably used for aging unknown individuals (Kerley, 1965). Since then, many histological aging methods have been developed (e.g. Ahlqvist and Damsten, 1969; Stout et al., 1994; Maat et al., 2006; Han et al., 2009). As discussed in *Chapter 2*, the physiological basis of bone remodelling consists of the replacement of older bone and the formation of new bone carried out by the coupled and coordinated activity of bone cells (osteoclasts and osteoblasts) referred to as bone multicellular unit (BMU) or bone remodelling units (Parfitt, 1979). Of the microscopic features formed by remodelling events, secondary osteonal structures densities are strongly correlated to age, increasing with age and removing all evidence of the primary bone commonly seen in young individuals (Stout and Paine, 1992). In summary, age-related bone loss is caused by an imbalance in resorption and formation which accounts for remodelling occurring on the endosteal surface resulting in cortical thinning, and an intra-cortical remodelling imbalance in the Haversian canal surface (constituent feature of the osteonal structure) eliciting higher porosity and a decline in bone mineral density (Russo et al., 2006). Hence, definable age related microstructural changes can be quantified allowing the expert to establish a relationship between the biological processes and chronological age (Streeter, 2012).

An important technical aspect of the application of microscopic method is that specialised training and equipment are necessary for the preparation and assessment of bone thin-sections (Crowder et al., 2012). Several techniques have been proposed and are still being tested and revised in order to improve methodological aspects of the production of bone histological slides (e.g. Beauchesne and Saunders, 2006; De Boer, Aarents and Maat, 2013). Additionally, taphonomic processes can also affect the microscopic analysis of the remains. Post-

mortem changes have an effect on bone microstructures such as bacteria entering the bone via its porous network and expanding differently throughout the cortex (Bell, 2012). Although common in archaeological context, understanding diagenetic processes in forensic cases may also help to identify changes observed in the cross-section and their subsequent interpretation.

As discussed in *Chapter 3* and *4*, other limitations in the application of histological methods must be taken into consideration. For example, sampling area seems to play an important role due to inconsistencies resulting from different topographical locations within the same bone (e.g. higher remodeling rates on muscle attachment areas) or intra- and inter-individual variability in bone microstructure (Mulhern, 2000; Pfeiffer et al., 1995; Pfeiffer et al., 2006).

The first issue relates to the fact that as a result of the normal aging process, the endosteal diaphyseal area is resorbed, and consequently, most of the techniques developed using long bones are limited and focused on the subperiosteal area (Kerley, 1965; Maat et al., 2006). The question of whether the average periosteal remodeling may be an accurate indicator of the individual´s age presents a methodological concern. This issue is prominent when a large cortical area needs to be interpreted, as occurs with the femur, and specific sampling areas within the same cross-section have to be selected (Martin et al., 2015). To overcome these sampling error issues, ribs can be used instead since a full interpretation of the cortex is doable due to their small cortical areas.

The second argument relates to different remodelling rates observed in bones from the same skeleton since weight and non-weight bearing skeletal elements have different mechanical and metabolic responses; consequently, variation in remodelling dynamics might be expected (Mulhern, 2000; Chan et al., 2007). Regardless of the skeletal element used, bone microstructures have shown different degrees of variability and different types of correlation to age (decrease, increase or lack of association) (Barer and Jowsey, 1967; Pfeiffer, 1998; Kim et al., 2007), suggesting that intra- and inter-individual variation exist and must be considered when developing histological age estimation methods. Moreover, inter-population variation must be accounted for intrinsic and extrinsic factors such as physical activity, nutrition and pathology – among others – may alter bone turnover rates (Robling and Stout, 2008). Additionally, remodelling rates do not occur at a predictive rate through time and the mentioned factors may have an impact on

normal bone physiology, further increasing the variability within and among chronological/ geographical populations (Thompson and Gunness-Hey, 1981; Weinstein and Bell, 1988; Cho et al., 2006).

Some studies have focused on applying existing histological aging formulae on target samples not related to the reference population reporting different levels of accuracy and reliability in the estimated ages. An early study performed by Fangwu (1983) applied Kerley´s American age prediction formula (Kerley, 1965) on Modern Chinese femora sample, reporting errors greater than ± 10 years from real age, suggesting so the necessity of population-specific formula.

Based on all these factors, the histomorphological approach has been employed to estimate age exploring different bones and different populations (Ahlqvist and Damsten, 1969; Drusini and Businaro, 1990; Ericksen, 1991; Stout and Paine, 1992; Cho et al., 2002). As mentioned earlier, aging techniques should include age indicators represented and distributed evenly among different geographical samples. As covering the entire age range of variation among humans seems to be a complicated objective (Milner and Boldsen, 2012), the development of population-specific standards is encouraged not only in relation to aging methods, but also towards gaining insights into the relation between remodeling, internal biological mechanisms and age. Over the last two decades, there has been an increment in research focusing on estimating age on advanced age samples due to the increasing life expectancy of recent human population (Ice, 2003).

Moreover, sex related differences might also be manifested on bone microstructure features. Remodelling rates seem to increase after menopause, triggering the differences between women and men of the same age (Oursler et al., 2008; Robling and Stout, 2008). There is still an open debate as to whether sex differences can actually be discerned through the histological approach and to what extent they will bias the overall accuracy of age estimation methods since some studies have reported sex differences while others have not (e.g. Kerley, 1965; Ericksen, 1991).

Lastly, it is important to mention intrinsic methodological issues related to aging old individuals. Some histological variables present limitations to age individuals over 50-60 years old since the correlation between the parameters and age seems to weaken as age advances (e.g. osteon population densities) (Stout

and Crowder, 2012). Although it may vary depending on the remodelling rate of the population and the bone under study, there is a need to explore alternative histological parameters (alone or in combination) and to assess the impact of elderly individuals in microscopic techniques (Trammell and Kroman, 2013; Goliath et al., 2016).

In order to determine whether bones are of forensic significance, the expert needs to examine the remains through the application of appropriate scientific methods and analyse the contextual clues that can lead to a medicolegal investigation (Krogman and Isçan, 1986; Schultz, 2012). In the forensic field where the age estimates may fulfil specific requirements imposed by the legal setting, the choice of the method requires further considerations. Scientific methods must be tested, standardised and error rates known to ensure accurate results that are particularly relevant for court cases (Christensen and Crowder, 2009). Histology has been recommended as one of the aging methods that achieves acceptable error levels although mostly suitable for individuals under 40 (Ritz-Timme et al., 2000). Both in archaeological and forensic contexts the ultimate goal is to produce estimated ages as accurate as possible, and to enable that, development of new methods with proper research design and adequate statistical approaches must be implemented.

Regarding the statistical analysis, regression analysis is commonly used to estimate age although the systematic under and over–estimation of young and old individuals, respectively, remains problematic (Nawrocki, 2010). Furthermore, the inclusion of more parameters in the equation can lead to lower inaccuracy and higher prediction power, but the side effect is that the model increases in complexity in order to fit that specific sample and most likely will not fit the overall population (www.minitab.com). In practicality, a problem arising from adding more variables to the aging formula is the introduction of human error due to greater experience being required for the accurate observation and interpretation of age indicators/variables. Therefore, intra- and inter-observer error must be assessed to ensure the methods´ validity (Christensen et al., 2014). In this case, the complexity of the technique and the experience of the practitioner play a crucial role. All these issues are contemplated in *Chapter 5* and *Chapter 6.*

1.1 Research design and research questions

The present research aims to provide new insights in cortical microstructural changes related to age based on a sample of individuals from Mediterranean origin (N = 88, Mean age = 60, SD = 17.90). The procedures and research questions for this study are (refer to Figure 4.11):

1. Intra and inter-observer error analysis will be evaluated in order to assess the agreement and repeatability of the method considering the variables under examination; an assessment of the possible bias introduced by the same and different observers will be carried out.
2. An assessment of the possible error introduced by different sampling areas along the length of the rib to understand their impact on age estimation techniques.
3. Through the application of existing population-specific formulae, a validation study will be performed to test the accuracy of four microscopic methods to estimate age on the Mediterranean sample/s. The methods performance will clarify if Mediterranean population-specific formulae are ultimately required.
4. The relationship between histological variables and age as well as the relationship between variables and other factors such as sex and samples will be examined though several statistical tests. Once the relationship is established, the results from this assessment will be considered for the generation of regression formulae and to determine the best combination of parameters.
5. The most accurate aging equations based on prediction power based on all previous gathered information will be selected.

The fragmented nature of ribs makes costal element prone to breakage and identification of sampling area becomes an arduous and sometimes impossible task. A pilot study was performed to explore the impact of topographical location along the length of the rib and explore how different sampling locations may or may not have an effect on the histomorphometric variables and on the estimation of age (García-Donas et al., 2016).

As noted above, inter-population variability has been reported and histological methods could decrease in accuracy depending on the sample under study and the method applied (Bouvier and Ubelaker, 1977). The accuracy, reliability and

magnitude of errors of four existing aging methods were evaluated. Reference sample demographics such as age and sex distributions, ethnicity and statistical approaches were considered in the evaluation of the performance of each method.

Before developing the age estimation technique for the sample under study, the relationship between the histological parameters and age needed to be understood. Several statistical approaches were used to determine these correlations. It is recommended to examine other effects that can be attributable to other factors rather than age (e.g. sex and samples origin). This step helps to determine which parameters differ significantly between groups and whether their inclusion in the regression equations is meaningful (Nawrocki, 2010). *A priory*, the comparison of the two samples composing the study sample (Cretans and Cypriots) could yield some interesting remodelling patterns as they share similar culture, dietary habits and climate.

To date, there has not been any study using histology to estimate age on a southern European population. Having taken into account the mean age of the sample, it is imperative to explore age changes in the senile ages and interpret the relationship of age physiological changes and other pathologies associated to the elderly (e.g. osteoporosis associated to postmenopausal women (Parfitt, 1979).

Ultimately, this research aims to generate a method to estimate age for Mediterranean forensic and bio-archaeological burials. At first, a wide range of models were generated with all possible combination of variables. Based on the observed differences between sexes and samples, group specific formulae were developed. For the application of histological methods, certain level of experience in microscopy is required. The method reliability due to data collection and the nature of the parameters has been questioned (Lynnerup et al., 1998; Crowder, 2005), and thus, intra and inter-observer errors are assessed not only to examine agreement between observers, but also as a criterion for model inference considering the method repeatability for future applications. Finally, the more accurate age prediction models were selected according to prediction power, accuracy, feasibility and reliability.

Chapter 2 : BONE ANATOMY, BONE BIOLOGY AND BONE MICROSTRUCTURE

The main topic of this research is based on the understanding of bone histological microstructures related to aging processes and age estimation. In view of interpreting the microstructures observed on the available samples, bone biology and physiology needs to be clearly understood. Bone is a multifunctional tissue that changes and adapts metabolically and mechanically in response to the demands of the organism throughout one´s life (Burr and Akkus, 2013). This chapter presents an extended review in biology, physiology and turnover of bone both as an organ and as a tissue at the macro and micro-structural levels.

2.1 A brief history of bone anatomy and biology

Bone anatomy has represented a magnificent tool for paleo-anatomists, biologists, and physical anthropologists because skeletal features survive harsh environmental conditions (Schoenau et al., 2004; Schaefer and Black, 2005; Travan et al., 2015).

Skeletal anatomic knowledge traditionally comes from gross examination of bone by the naked eye. This includes metric assessment and detailed understanding of outer skeletal features and their range of variability (White and Folkens, 2005). The microscopic observation introduced in the 17th century enabled scientists to study microstructure of bone tissue allowing the understanding of the components of bone matrix and bone cells, as well as the interactions between them. Since then, the knowledge about this field has evolved considerably (Lanyon 1993; Noble and Reeve, 2000; Maggiano, Maggiano, Tiesler et al., 2016).

Martin and Burr (1989) summarised how scientists started perceiving bone microstructure four centuries ago. Clopton Havers (1657-1702) was not the first naturalist to recognise the porous nature of bones, but he was indeed the first one able to describe in detail the microscopic structure and organization of bone as a tissue. Among his findings, he inferred bone as a composite material made of inorganic and organic particles with parallel strings and plates that were arranged longitudinally around the medullary cavity in a tubular fashion. The tubular features found in secondary osteons are known as Haversian systems and are named after Havers. The pores observed in the cortical bone were assumed not to be vascular,

although Havers accurately thought that veins were going through the marrow to provide blood supply. According to him, the lamellae (thin plates of bone matrix) did not run consistently through the length and/or the diameter of bone but instead, different types of hard tissue were described to define the transition from cortical to trabecular bone (Martin and Burr, 1989). His contemporary Van Leeuwenhoeck (1632-1723) defined the different types of pores by their size and their longitudinal arrangement which would be summarised today in features that we recognise as osteocytes, primary and secondary osteons, canaliculi and resorption spaces. More complicated physiological processes were initially understood from the studies driven by Alexander Monro (1697-1767). This pathologist developed a theory based on the microscopic structure of bone matrix being able to explain the changes that bone undergoes during growth and throughout life, giving a first insight of the processes that would be later called modelling and remodelling. He was also the first to adequately defined bone loss both in the medullary cavity and in cortical bone describing formation and resorption processes related to aging. The scientist John Howship (1781-1841) identified large spaces in cortical bone as a result of the resorption process, giving the name to the microstructure known as Howship´s lacunae (Martin and Burr, 1989).

Once the existence of the Haversian canals was established, the discussion shifted to the identification and definition of lamellae in bone. Through staining methods, the organization of bone by the alternation of layers of concentric lamellae with variable degrees of thickness was finally demonstrated (Du Hamel, 1700-1782). Further experiments allowed Lieutaud (1703-1780) to eventually define the laminae of bone and the compact fibers constituted in an irregular arrangement (Martin and Burr, 1989).

In the 19th century, Todd and co-worker were able to define the structure of secondary osteons and lamellae partly due to the advances in bone microscopy and histological preparation of bone (Todd and Bowman, 1857). Tomes and De Morgan (1853) provided new insights on how resorption and formation activity would remove pre-existing older bone and replace it with new tissue as a natural process. The function of secondary osteons, other bone microstructures, and bone formation was then understood through their functional properties related to mechanical stress. Gebhardt (1905) discussed in detail the function of osteonal bone, where osteons were arranged in specific patterns with different angles of lamellae orientation in

order to bear stress trajectories (with fibers in spiral fashion). He also pointed out the differences in arrangement for both trabecular and cortical bone. Further findings about bone modelling and remodelling processes and their impact on bone microstructures would be revealed in the 20th century as it will be presented later in this chapter.

The work carried out by scientists of the 17th-19th centuries and later studies have allowed us to reach a level of comprehensive understanding of bone microanatomy that far exceeds past expectations specific to bone anatomy. Insights towards understanding bone gross anatomy and its characteristics as an organ will be briefly presented. Next, skeletal microanatomy via histological assessment and the theory about bone as a tissue covering its histological level, composition, microstructure and function will be discussed (Table 2.1).

Table 2.1 Hierarchical levels of integration of bone micro-anatomical tissue (adapted **from Francillon-Vieillot et al., 1990).**

Order of structure/ level of integration	Scale (approx.)	Characteristics of the order
First order: ANATOMICAL level	1 m - 1 mm	Bone and tooth morphology and relationships; vascular orientation in compact bone, and trabeculae in spongy bone
Second order: HISTOLOGICAL level	1 mm -100 µm	Orientation, size and number of bone trabeculae; size and number of vascular canals; extracellular matrices structure
Third order: CYTOLOGICAL level	100 µm - 1 µm	Details of cells and extracellular matrices; orientation, quantity, organization and relationship
Fourth order: MOLECULAR level	1 µm - 10 nm	Organic and mineral components: chemical and biophysical organization

2.2. Bone as an organ: gross anatomy, functions and associated tissues within the skeletal system

The human body works as a whole in order to accomplish all the necessary activities for its survival and maintenance. The body systems (integumentary, skeletal-muscular; nervous, endocrine; cardiovascular and lymphatic; respiratory, digestive and urinary; reproductive) perform specific functions necessary for the living organism (Faller and Schuenke, 2004). In anatomy, complementarity of

structure and function is essential as every particularity of the body structures (shape, size, composition) are designed to execute specific activities and help the body function (Thibodeau and Patton, 2007). In such, a hierarchical organization, different subdivisions within the body are found.

Regarding the skeletal system from the anatomical level to the tissue level, we encounter *bones* as the basic element of the skeleton and *bone tissue* as the primary level of organization that forms the bones (Table 2.1). Bones are classified in different types accounting for a variety of shapes, sizes and structures depending on the area of the body that they are located, and therefore, on the function that they perform (Gray et al., 2005).

Movement is one of the main functions of bones within the skeletal system. One can imagine the body without the skeletal structure and the incapacity of movement due to the lack of structural support. Bones are deemed to provide this scaffolding not only for maintaining the posture but also contributing to shape, alignment and positioning of the body parts. Movement is possible due the coordination of bones and skeletal muscles via the tendons and ligaments connecting bone to muscle and bone to bone, respectively. Skeletal muscles are composed of muscular fibers and connective tissue strongly interlinked. Muscle cells are covered by a connective tissue membrane (endomysium) and grouped by skeletal muscle fibers (fascicles) bounded together by another tougher connective tissue called the perimysium. Muscle fibers are surrounded as a whole by a sheath called epimysium (Faller and Schuenke, 2004). All three tissue membranes form a continuum with bone attaching muscle to bone ensuring a hard and firm support for the bones during contraction. The last layer consists of a dense collagen connective tissue sheath (muscle fascia) which encloses the muscle and allows interaction with other related structures. Structurally, bones and skeletal musculature work in combination with another skeletal system element, cartilage, which is an avascular connective fibrous tissue formed by collagen and elastic fibers located in different areas of the human body (Thibodeau and Patton, 2007). Bones and cartilage are organised and grouped to fulfil different functional requirements. Cartilage – like bone – has more extracellular matrix than cells. Other tissues associated with the skeletal system include fibrous and loose connective tissue, nervous tissue, epithelium, blood, lymphatic tissue, myeloid tissue and adipose tissue (Thibodeau and Patton, 2007). As seen later in this chapter, muscles will play an important role

in bone architecture and microstructure being responsible for the highest dynamic strains placed on bone (Frost, 2000).

The skeletal system function is not only limited to the obvious structural support or movement. Bones are indeed multifunctional. Internal organs are protected by the osseous structures and bones also provide storage of needed mineral like calcium, phosphate and others, allowing control of body homeostasis. Bones are a reserve of cytokine and growth factor allowing the balance of body fluids (e.g. fat). Moreover, hematopoietic activity and hormone regulation and production are also performed within the skeletal elements (Francillon-Vieillot et al., 1990; Clarke, 2008).

The majority of bones consist of a porous tissue enclosed in an outer and an inner compact layer. The outer superficial area is surrounded by a dense connective tissue membrane called periosteum. The periosteum varies in thickness depending on the location and it is not found at articular surfaces which are covered by cartilage surrounding the subchondral bone. Sharpey´s fibers (bundles of collagen fibers) fix the periosteum to the bone penetrating at right angles into the outer layer of the membrane. Bone internal superficial area – the endosteum – is lined by a connective tissue with a layer of flattened cells. In gross-morphology, the outer surface is called periosteal surface and the inner surface is known as the endosteal surface (or endocortical). Long bone internal hollow (medullary cavity) houses the bone marrow performing hematopoietic and osteogenic activities. Nutrients are transported via arteries that penetrate the periosteum through the nutrient foramina piercing into the marrow cavity and spreading internally. Marrow cavity sinuses allow the collection and distribution of blood through venous branches in the medullary cavity and the spongy bone, and out again from the marrow cavity via nutrients and metaphyseal veins. Blood supply to the cortical and trabecular bone differs (see below): trabecular blood vessels running within the trabecular space while in the compact bone longitudinal canals are the main means for blood transportation (Burr and Akkus, 2013).

2.3. Bone composition, structure and function

2.3.1. Bone composition

Bone composition consists of around 25% organic material, 65% mineral, and 10% water fractions (Burr and Akkus, 2013). It is a hierarchical material and

composite substance in which all the properties of each fraction interact. Due to its microstructure, material quantity and arrangements change constantly through time and this plays an important role in bone mechanical properties and composition (Currey, 2002; Olszta et al., 2007).

The organic material is secreted in the extracellular matrix and mostly composed of type I collagen (90%) with 10% of non-collagenous proteins (NCPs) which accounts for mineralization, regulation of collagen formation and fibril size, and mechanical functions (Burr and Akkus, 2013). Type II and type V collagen are found in small quantities around the bone cells. The collagen matrix organization consists of amino acid sequences $(Gly\text{-}X\text{-}Y)_n$ [Y usually represent respectively proline and hydroxyproline] (Olszta et al., 2007). Individual collagen molecules (tropocollagen) consist of two α1 chains and one α2 chain arranged in a triple helical structure. Each collagen molecule has a length of 300 nm and a thickness of 1.5 nm; the tropocollagen molecules bond together through covalent interaction between hydroxyl groups of hydroxyproline and water in order to stabilize the structure (Burr and Akkus, 2013). Tropocollagen molecules assemble in quarter-staggered arrays to produce the fibrillary structure organization with spaces between the fibrils that play an important role in the mineralisation phase. The fibrils are around 150 nm in diameter and 10 nm in length; the tropocollagen molecules bond and stack together creating micro fibrils that aggregate in order to form fibrils (Olszta et al., 2007).

Bone mineral crystals are found within the collagen – both surrounding in and embedded within. Bone inorganic constituent is mostly hydroxyapatite, $Ca_{10}(P0_4)_6(OH)_2$, a calcium-deficient apatite constituted by carbonated apatite mineral (Boskey, 2001). The average size and shape of a bone crystal under normal conditions ranges from 30 to 200 nm for width and length although varying noticeably with age (Olszta et al., 2007). Bone apatite crystals are very thin elongated platelets (nanocrystals). Initially, the calcium phosphate is deposited randomly in combination with calcium carbonate. The carbonates are reduced with tissue maturation and small crystals start to be deposited in parallel to each other and longitudinally to individual collagen fibrils. During the mineralisation processes all the spaces are filled with new crystals within the collagen fibrils (via heterogeneous nucleation) increasing the size of the existing crystals (Rey et al., 2009). Due to crystal deposition, bone substance changes its physiological and

mechanical properties. As bone ages, mineral crystals tend to grow and become larger through ion substitution and mineral stoichiometry changing the mechanical behaviour of the material (Burr and Akkus, 2013). Mineralization in secondary bone seems to occur in two phases. Primary mineralization consists of a fast increment in the number of minerals crystals produced by heterogeneous nucleation and the mineral is deposited within the collagen matrix reaching the highest levels of mineralization in 3 weeks from the first deposition; these primary HA_p minerals are more soluble and disorganized. This first phase is followed by a secondary phase of reorganization of the structure based on a slow process of crystal accumulation, growing and maturation until the physiological mineralization level is reached (Burr and Akkus, 2013).

Water can be found within the collagen fibrils and also running along the vascular canals when needed. The water-mineral proportion is 1:1 which influences directly bone tissue mechanical properties as seen in highly mineralised bone with the reduction of water reducing elasticity properties (Burr and Akkus, 2013).

2.3.2. Structure and function of cortical and cancellous bone

There are two types of bone that can be differentiated by gross observation: cortical bone (compact bone) and cancellous bone (more porous bone) (**Figure 2.1**). An alternative terminology for cancellous bone, trabecular bone, is used mostly for the microscopic approach due to its relations to the trabecular spurs but not as a structural element (Burr and Akkus, 2013). Compact and cancellous bone differ in the degree of porosity, function and mechanical properties. The chemical composition of both types of bone is the same but the ratio of the constituents differs. The calcium content, tissue density and ash fraction (both volume fraction and mineral content) is lower in trabecular than in cortical bone tissue (Gong et al., 1964).

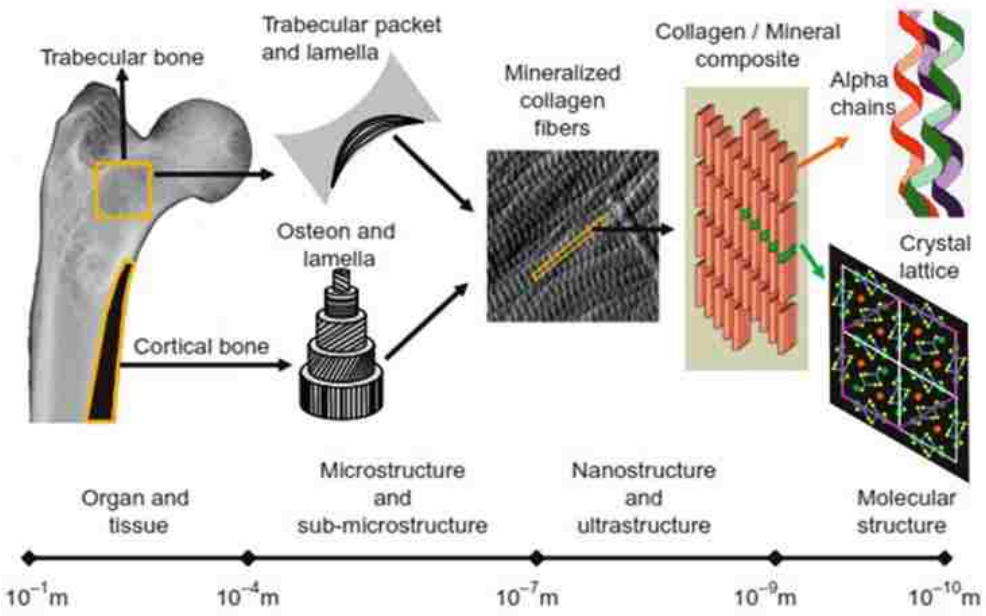

Figure 2.1 Cortical and cancellous bone from the organ and tissue level to the molecular structure (Burr and Akkus, 2013: 4 fig. 1.1).

The solid outer layer of skeletal elements is composed of a dense shell (Guo, 2001). Cortical bone composition compromises mineral (70% mostly hydroxyapatite), type I collagen (22%) and water (8%) (Augat and Schorlemmer, 2006). In the cortical lamellar bone, collagen fibres and ductility through the mineral crystals determine stiffness. The collagen fibrils are arranged cylindrically around an axial canal (see below for a detailed description for osteonal bone tissue). Intracortical porosity (size and distribution of the pores) is strongly related to the material properties of bone. The degree of porosity (intracortical porosity) is around 5% in young individuals and it increases with age with a direct effect on cortical architecture and bone mass (Augat and Schorlemmer, 2006). In such a low porosity (1-5%), size and distribution of the material is also related to the functional and mechanical bone properties. Therefore, the thickness of cortical bone varies depending on the area of the element (i.e. greater bone thickness of the diaphysis compared to the metaphysis). Hence, the balance between resistance to loading and movement is kept through the balance of the structure (Wallace, 2013). When bone turnover is low, bone has a high Young´s modulus (elasticity modulus) with resistance in torsion and bending. Due to its solidity, this type of bone serves functionally as a protective shell for the inner structurally weaker bone (cancellous

bone) (Guo, 2001). Cortical bone receives around 60 % of the blood supply through the endocortical surface and 30% from the intracortical blood flow and periosteal surface (Burr and Akkus, 2013).

Cancellous bone is a porous material composed by both hard and soft tissue found inside flat and irregular bones (i.e. vertebral bodies or pelvis) and in the epiphyses of long bones. Cancellous bone has a honeycomb like network based on an arrangement of plates and thin rods (0.1 mm) that have single or multiple connections between them and are arranged in a directional orientation (Guo, 2001). Each trabecula is oriented accounting parameters such as thickness, spacing, number and connectivity (Wallace, 2013). There are different types of trabecular bone depending on the rod/plates arrangements, size and orientation (Singh, 1978):

- A non-oriented fine rods structure, with either straight or curved rods found inside the long bone marrow cavities.
- A structure built up both by rods and plates (either fine plates found in the pubis body or near the glenoid cavity).
- Bigger irregular plates connected by small ones and rods found in the calcaneus, or a structure with plates parallel to each other connected to adjacent ones via rods found on articulation areas.
- Only trabeculae made of different sizes plates with a great variety in their orientation and density as the one located in the vertebral bodies and most parts of the skeleton.

Depending on the types of trabecular arrangements described, the degree of porosity varies around 75-95%. The architectural structure of the trabecular plates and rods (100-150 um of thickness) accounts for about 30% of the tissue space with the remaining area being filled by bone marrow. This spatial organization provides mechanical support optimising the weight of the bone itself (Martin et al., 2015).

At the tissue level, material properties differ between the cortical and cancellous bone implying differences in their mechanical properties. Both cortical and cancellous bone are not only competent in strength and stiffness but they are also resistant to loading stress and they prevent fatigue (Martin and Burr, 1989). Cancellous bone mechanical properties need to be regarded according to its density and trabecula arrangement. The grains in the lamellar bone are organised fairly

along the length of the sheets with the loading forces being applied at the end of these structures. Thus, the loading forces come in the same direction as the grain providing stiffness and strength to the whole structure; it is dependent of volume fraction and architecture and other factors as age and pathologies (Guo, 2001). The organization of the single trabecula itself gives to cancellous bone its anisotropic property (Currey, 2002). Cortical bone minerals allow the structure to bear compression forces while the competence in tensile forces is provided by the quality of the collagen fibrils and their orientation. Changes in material properties alter the mechanical properties of cortical bone; e.g. from small crystals to large crystal due to the aging processes producing a reduction in elasticity properties of bone tissue (Augat and Schorlemmer, 2006).

The degree of porosity may play an important role in this functional-structural differentiation. Due to its porosity, trabecular bone is weaker than cortical bone (under the same volume of tissue) and in general terms, cortical bone is more resistant in tension and bending while cancellous is stronger in compression (Wallace, 2013). Both cortical and cancellous bone are arranged to build the bone in a way that the whole structure of the skeletal element complies with its specific mechanical and functional requirements. Also, cancellous bone is mechanically more heterogeneous than cortical bone with variation in the degrees of stiffness and strength depending on the area under examination (Rho et al., 1998). Ultimately, material and structural properties of both types of bone are founded as a composite material at the nanostructure level with cortical and trabecular bone differentiation being not so defined. Thus, they account for a similar composition but in different degrees of expression in view of responding to different metabolic demands (e.g. higher remodelling and lower mineralization in trabecular than in cortical bone) (Oftadeh *et al.*, 2015).

2.4. Microstructural level: organization of bone tissue

2.4.1. Histological tissues: woven bone, parallel fibered bone and lamellar bone

Woven, plexiform and lamellar bone are material tissues that differ in material patterns, structural properties and in collagen fibre orientation (Currey, 2002). Woven bone is primarily laid down, and as maturation goes on, it is replaced by lamellar bone (known as Harversian bone) which is the most commonly material

found in bone tissue (Currey, 2003). The distinction between primary and secondary bone – which will be explained in depth in the next section – is fundamentally based on bone deposited *de novo* (primary) and bone being formed on a pre-existing bone surface (secondary) (Martin et al., 2015).

Woven bone is characterised by quick bone deposition (4 μm/day circa) and it is a transient tissue usually found in the foetal skeletal system or in the callus formed during the healing process of bone fracture (Burr and Akkus, 2014; Martin and Burr, 1989). Collagen fibrils are organised in thick bundles (0.1-3 μm in diameter) and randomly oriented in a 3D plane. Consequently, direction of mineralization is hardly predictable and crystals deposition does not follow a regular pattern. This non-homogeneous distribution is related to the formation of numerous centres of mineralisation with some areas not presenting any degree of mineral (Currey, 2002). It contains a large number of isodiametric osteocytes and it is highly vascularised (Currey, 2003). Overall, woven bone shows the same material (chemical) properties of all the other types of bone while structural properties vary considerably in relation with the mentioned collagen fibrils orientation (Currey, 2002). Woven bone is also formed as a repair tissue during fracture healing and in other pathological disorders but also as a response to high excessive mechanical stress (Burr and Akkus, 2013).

Plexiform bone (also known as *parallel fibered bone*) is mostly formed of primary fibrolamellar bone organised in bundles of mineralised collagen fibrils that have been deposited quickly – as woven bone – but presents an unidirectional organization and an improvement in mechanical properties (Burr and Akkus, 2013; Reznikov et al., 2014a). It combines both nonlamellar bone (formed *de novo*) that serves as the core substrate, and primary lamellar bone that lays superficially on the substrate. The result is a structure of buds that start from being deposited perpendicularly on a small space of bone from the envelopes (subperiosteal or subendosteal), to form on most of the surface with the buds being adjacent to each other in a parallel fashion. Theses buds are separated through spaces filled by vascular elements producing a brick wall pattern (**Figure 2.2B**). Normally, it is found in rapidly growing animals but it might be also found in children in relation to maximum growth rate periods (Burr and Akkus, 2014; Martin and Burr, 1989).

Lamellar bone is deposited at a slower rate (less 1 μm per day) on an existing bone surface with collagen fibrils organised in layers (lamellae) and arranged in

bundles of 2-3 μm separated by disorganised material. Specific bone cells (osteocytes) sit in elongated spherical lacunae oriented parallel to the lamella plate. Usually, lamellae organise in arrays of 3-7 μm thickness alternating with thinner lamellae of approximately 1 μm thickness. In these two types of arrays, the crystals assume different structures and orientations (Reznikov et al., 2014b). This configuration influences structural properties resulting in a stronger material tissue. Furthermore, its composition is highly variable according to the area of examination. For example, cancellous lamellar bone presents a particular composition to satisfy mineral homeostatic and haemopoietic functions, while in areas subjected to high mechanical stress the composition is such that it can prevent fracture risks (Weiner et al., 1999; Currey, 2002; Martin and Burr, 1989). Lamellae present different patterns: lamellar bone bordering the endosteal or periosteal surface organised as layers of bone, primary interstitial lamellae (primary lamellar bone deposited *de novo*), or osteonal lamellae (osteonal interstitial lamellae and osteonal concentric lamellae) (Figure 2.2A and 2.2B). There is a highly mineralised lamellar bone type tissue known as interstitial lamellar bone that appear filling the spaces between secondary osteons and represents the traces of primary or secondary lamellae that have been resorbed by latter secondary bone deposition. This layered bone that appears not structurally organised has an older age tissue than the nearby osteonal bone. In adult healthy individuals, approximately half of the bone area is built by osteonal lamellar bone. The remaining area is formed by interstitial bone (Burr and Akkus, 2013). Two morphological types of lamellar bone can be differentiated microscopically: the circumferential lamellar bone at the endosteal and periosteal surfaces, and the osteonal lamellar bone within the intracortical surface (Currey, 2003; Burr and Akkus, 2014; Reznikov et al., 2014a).

2.4.2. Microscopic bone at the tissue level: cortical and trabecular bone

As seen in the previous section, cortical and cancellous bone are different in morphology and functional properties at the tissue level, but at the microscopic tissue level they are both composed of lamellar bone (Table 2.2). In this section, a microscopic detailed description of cortical and trabecular bone will be presented.

Table 2.2 Summary of microstructural and histological characteristics of cortical and trabecular bone (Adapted from Jee, 2001).

Features	Cortical Bone Tissue	Trabecular Bone Tissue
Microstructural	100-300 μm (osteon diameter)	100-640 μm (trabeculae mostly hemiosteons; osteons appear in transitional areas)
Cement line	Surrounding osteonal structures	Cement line surrounding hemiosteons (more numerous)
Lamellar thickness	30-40 μm, 460/mm^2	38-55 μm, 156-577 /mm^2
Bone turnover	3%	26%
Porosity and circulation	5-10% (slow circulation)	50-90% (high diffusion of nutrients and waste)

2.4.2.1 Cortical bone

Cortical bone is organised in the circumferential bands of lamellar bone (3-7 um thickness) separated by approximately 1 um thickness of interlamellar layers; these bands can be found running along the periosteal or endosteal walls, around the vascular channels (primary or secondary osteons) and within the trabeculae (Burr and Akkus, 2013). Their structural and mechanical properties are both determined by the material itself and by its organization accounting for 70-80% of the bone strength as measured by geometrical measurements (Augat and Schorlemmer, 2006). The microscopic structures of not tubular bones are the same (i.e. cranial bone), although histologically a more irregular organization is seen as a result of the different biomechanical forces applied on them (Hillier and Bell, 2007).

Cortical lamellar bone can be further differentiated in circumferential lamellar bone (endosteal and periosteal surfaces) and osteonal lamellar bone (intracortical). In addition, lamellar bone differentiates in two types of bone tissue. They both share the same circumferential lamellae organization and similar osteonal structures but differ in the formation of the tissue: primary lamellar bone and primary osteons, and secondary lamellar bone resulting on secondary osteons (Weiner et al., 1999) . Low mineralization makes primary lamellar bone weaker than secondary bone; however, secondary lamellar is a more brittle material than primary bone due to higher porosity and higher mineralization. As age advances, previous secondary osteons will be overlapped by new depositing bone (newly formed osteonal structures) which will be a phenomenon used for age estimation methods. Hence, different types of

osteonal bone based on unremodelled or remodelled surfaces need to be identified for aging techniques (Kerley, 1965).

Three types of primary bone are found (primary lamellar bone, plexiform – already described – and primary osteons) (Figure 2.2A). Although different in structural and mechanical properties, primary bone is always deposited *de novo* onto a surface that has not been previously remodelled.

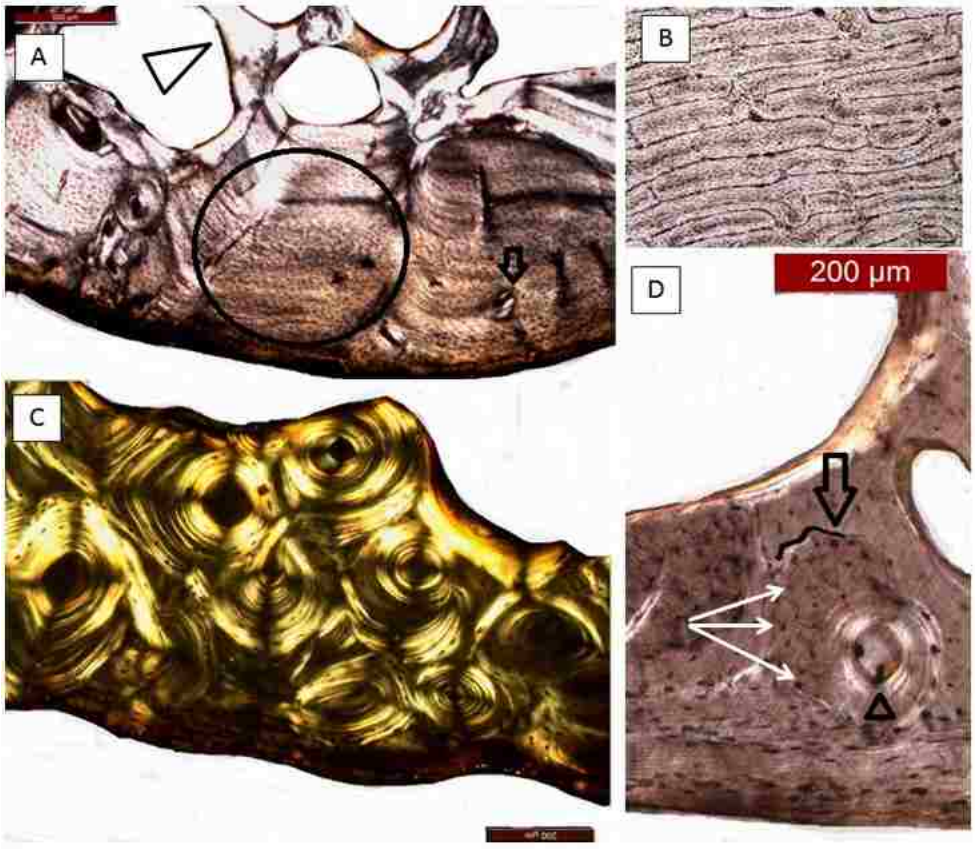

Figure 2.2 Types of primary and secondary bone (A, C and D: human rib cross-section, sample study photomicrographs). A: primary lamellar bone formed by a series of parallel laminar sheet (circle), arrow indicating a primary osteon; trabecular bone (arrowhead) (40x). *B*: plexiform bone: brick-like structure (from Burr and Akkus, 2013: 14 fig. 1.9). ***C*:** dense secondary cortical bone formed by interstitial bone and different types of secondary osteons (100x semi-polarised, study sample). ***D***: single osteon; Haversian canal (arrowhead) (note concentric lamellae surrounding the canal), cement line separating the osteonal structure from the interstitial bone (arrow and black outline), osteocytes (white arrows) (100x, study sample).

Primary lamellar bone is composed of laminal sheets running in a parallel fashion to each other. It is mostly found close to the periosteal surface although it

occurs also on the endosteum and on the trabeculae. Depending on the topographical location, the tissue may change in order to fulfil metabolic demands from dense stable material found on the periosteum to more prone to replacement and turn over as found on the endosteal envelop (Burr and Akkus, 2013).

Primary osteons or primary vascular canals consist of concentric lamellae surrounding a vascular canal with a non-clear delimitation between the osteonal structure and the surrounding bone matrix. It has been suggested that primary osteons have smaller vascular canals and less surrounding lamellae than secondary ones with around 10 lamellae or less and a diameter of approximately 50-100 μm (Martin and Burr, 1989). The concentric layers of bone are added on specific bone areas changing through the length of the vascular canal to accomplish mechanical and physiological requirements. Primary osteons are the result of primary bone laid down from the vascular canal to the outer lamella, as a process of transformation from woven to lamellar bone (Currey, 2002). They are normally found in areas of primary lamellar bone closely located to blood vessels in order to assist in calcium homeostasis, serving as storage of calcium ions (Martin and Burr, 1989). They may appear close to the endosteal surface during endosteal drift or trabecular compaction where the voids will be filled by new bone (Stout and Crowder, 2012).

Secondary lamellar bone implies the apposition of bone tissue by resorption of pre-existing bone and its replacement by newly bone formation (see bone remodelling later in this chapter). This mechanism is known as intra-cortical remodelling activity resulting in the formation of secondary lamellar bone that consists of tubular structures (Figure 2.2C). It consists of the coordination of resorption and formation of bone created by cylindrical arrays of lamellae (Burr and Akkus, 2013). These structures are called Harversian systems or secondary osteons (Currey, 2002). Harversian systems are formed by longitudinal arranged fibres with an average length of 1-10 mm embedded within the interstitial lamellae and delimited from the matrix by a boundary called the cement line (Figure 2.2D). These microstructures are fairly cylindrical in length and they have a diameter of 200-300 μm varying considerably with age and pathological conditions (Currey, 1964; Jowsey, 1966). The concentric lamellae surround a circular canal that varies in shape. The Haversian canal typically has a diameter of around 50-90 μm with the tubular systems running slightly parallel to the axis of the bone (11-17 degrees) (Cohen and Harris, 1958). Haversian canals can branch out and they can vary in

size, shape and orientation along their length (Cohen and Harris, 1958; Stout *et al.*, 1999). Recent research has shown that the branching pattern seems to be either transverse (coming off from the Haversian system) or dichotomous branching (bifurcation of a Harversian system) (Maggiano, Maggiano, Clement et al., 2016). The orientation of the adjacent osteonal lamella varies in a fashion that the layers of lamellae are not either completely parallel or perpendicular to the cylinder axis (Reznikov et al., 2014b). As a general organization, each layer of lamellae has fibrils that are arranged longitudinally in one lamella and circularly in the next, with the bundles of fibrils cutting each other in less than 90 degrees (Weinmann and Sicher, 1955). The orientation of the collagen fibers are organised from helicoidal to orthogonal bundles with an intermediate phase, although it has been also suggested that dense or loose bundled fibers are arranged in pairs of layers (Giraud-Guille, 1988; Marotti, 1993). The different arrangements of the adjacent lamellae in osteonal bone respond to mechanical and physiological demands resulting in a wide variety of types of secondary osteons morphology (Reznikov et al., 2014a).

The Haversian canal contains vessels which diameter is about 15 μm being wider in the endosteal area than in the periosteum. The vessels are surrounded by a basement membrane that regulates the ionic transport though the capillary wall. The vessels communicate to each other transversally perforating the circumferential lamellae to link (branching or merging) adjacent Haversian systems by the so called Volkmann's canals (Reznikov et al., 2014a). They can be seen in a cross-section as a tunnel crossing two Haversian canals. Different types of cells like osteoblasts in different stages (activated or resting), pluripotential mesenchymal cells and lining cells are found between the vessels and the canals´ wall (Martin and Burr, 1989).

Following the orientation of the lamellae, osteocytes are trapped in lacunae (small cavities) (Figure 2.2D). Osteocytes are arranged parallel to the orientation of the collagen fibers (16-20 cylindrical lamellae). The osteocytes are as close as 100-150 μm to the canal from where they receive the necessary blood supply and nutrients. They are connected by canalicular processes (canaliculi). The canaliculi are evenly distributed along the different concentric lamellae levels allowing communication with the surrounded lacunae area and with the extracellular space of the canal wall. The metabolic exchange and regulation of ion passage between bone cells and blood is carried out through the canaliculi network (lacunar-canalicular system) (Martin and Burr, 1989). The canaliculi, which density reduces

with age, may cross the cement line creating an metabolic connection between the blood vessels inside the Haversian systems and the surrounding external bone matrix (Milovanovic et al., 2013).

The Haversian system is delimited by a cement sheath (also known as reversal line). This cement line has a thickness from 1-5 μm that separates the secondary osteon from the rest of the bone matrix (Figure 2.2D). The cement line appears as a local interface when no more bone reabsorption occurs in the tubular structure (*cutting cone*) and the new bone deposition process is about to start; the line represents the traces of reabsorbed surfaces by osteoclast activity (Burr and Akkus, 2013). It is mainly composed of glycosaminoglycans and a low quantity of collagen, although the degree of mineralization in the cement line in comparison to the surrounding bone can vary and different studies have shown controversial findings (Schaffler et al., 1987; Burr et al., 1988; Skedros et al., 2005). Whether high or low mineralization, the mechanical properties still will remain either stopping or preventing crack growth providing resistance to fatigue failure (Burr et al., 1988; Burr and Akkus, 2014). There are other types of histological features known as arrest lines that, although similar to the cement line, they are not indicative of resorption but instead an indication of a temporary interruption of the filling process within the Haversian system which could be diagnostic for specific physiological conditions (Ortner and Turner-Walker, 2003).

The process of formation of the Haversian systems is related to modelling and remodelling mechanisms. Osteoclasts are activated and remove existing bone forming a cutting-cone (about 200um diameter/ 300um thick) (Martin and Burr, 1989). The cylindrical cavity will be filled by deposition of cylindrical layers of bone resulting in the concentric lamellae we observe microscopically (lasting from 2 to 4 months) (**Figures 2.2C** and **2.2D**) (Currey, 2002). Depending on the dispersion of the Haversian system, secondary bone can be divided into irregular (few osteons irregularly placed on the bone matrix), endosteal (located at the endosteal margin and being incomplete and irregular in shape), and dense (bone matrix crowded with numerous Haversian systems) (Enlow and Brown, 1957; Hillier and Bell, 2007).

Cortical bone circumferential lamellae present variations depending on the given bone area and the individual´s age. Periosteal lamellae are more numerous than lamellae found on the endosteal area in young individuals. While with advanced age, the endosteal area experiences reabsorption and the periosteum is

remodelled by secondary osteons. As mentioned earlier, interstitial bone is found within the osteonal structures as part of the entire cortical lamellar picture. Young individuals account for less interstitial bone and more organize osteonal bone than old individuals for which an increase in resorption and deposition processes results in cortical bone to be filled with higher densities of interstitial bone and osteonal structures (Currey, 1964).

2.4.2.2 Trabecular bone

Haversian systems are not formed in trabecular bone. In the trabecular envelope, an equivalent structure known as hemi-osteons is represented by the morphology of half an osteon with an approximate thickness of 35 μm, surrounded by concentric lamellae and missing a central canal (Clarke, 2008). The sheets of lamellae are organised in a mosaic-like microstructure with angular segments in a parallel fashion (called trabecular or lamellar packets) arranged in alignment to the trabeculae. The lamellar packets are organised in arrays in such a fashion that the last deposited lamellar packet is aligned with the most superficial trabecular surface (Guo, 2001). A single trabecula within the lamellar packet is also surrounded –as the secondary osteons- by a boundary (cement line) (Reznikov et al., 2014a; Oftadeh et al., 2015).

2.5. Bone cells

There are three main types of bone cells that are involved in the formation and resorption of bone. Osteoclasts are mainly involved in bone resorption, osteoblasts are responsible for bone deposition, and osteocytes for maintenance and repair of bone. The basic multicellular unit (BMU) responsible for the remodelling process consists of osteoclasts degrading bone and osteoblasts forming bone (Parfitt, 1979).

2.5.1 Osteoclasts

Osteoclasts are multinucleated cells derived from the hematopoietic monocyte – macrophage linage (Jähn and Bonewald, 2012). Osteoclast precursors proliferate in the bone marrow microenvironment in response to growth factors and cytokines. The fusion of mononuclear precursors into multinuclear mature osteoclast takes place at the bone surface level under the influence on RANKL (tumour necrosis factor –TNF- family of ligands) and transmembrane proteins. How osteoclasts move from the bone marrow to the bone surface in order to reabsorb specific bone areas

is still unknown, although it has been suggested that they may receive signals from osteocytes and bone lining cells (Gu et al., 2005; Väänänen and Zhao, 2008). Osteoclast survival, activity and formation are also regulated by steroids hormones (Bellido et al., 2014). The resorption cycle consists of a multistep process in which osteoclasts go cell activation, creation of the sealing zone, polarization, bone removal and cell apoptosis (Väänänen et al., 2000). A single osteoclast can go several resorption cycles before cell apoptosis. Osteoclasts' activation is based on membrane reorganization and formation (Figure 2.3A). In resorption, osteoclast polarization in the different membranes is very high and mostly driven by the activity of integrin receptors (transmembrane proteins) in the sealing zone (Bellido et al., 2014). To prepare for bone removal (cell activation), an apical membrane domain close to the bone surface and a basolateral membrane domain away from the bone surface are created. During osteoclast activation, the sealing zone (acting ring formed as a structure of microfilaments) is created for the adhesion of bone cells to the bone surface. In vitro, the sealing zone appears as a ring of adhered dense structures called podosomes that are essential for bone remodelling activity due to their role in adhesion and degradation of the extracellular matrix (Clarke, 2008). The ruffled zone and the transition zone (separated by the sealing zone) are used for secretion of hydrolytic enzymes and degradation of bone matrix. During osteoclast resorbing cycle, the functional secretory domain (FSD- which is located in the basal membrane) plays an important role for carrying bone degradation products (Nesbitt and Horton, 1997; Salo et al., 1997). After completing the reabsorption, osteoclasts undergo apoptosis (Clarke, 2008).

An active osteoclast is found in specific cavities within the bone surface (resorption lacuna) (Väänänen and Zhao, 2008) . The process of bone mineral dissolution is based on the solubilisation of crystals by lowering the pH in the resorption lacunae by the action of a proton pump (Salo et al., 1997). This allows the cell to survive in a highly mineralised environment. After mineral is removed, the organic matrix is degraded through the activity of two types of proteolytic enzymes both intra and extra-cellular matrices. The degradation products are finally released either by transcytosis from the ruffled border to the basal membrane (FSD) or by continuous removal from the resorption lacunae to the sealing zone (Väänänen and Zhao, 2008).

2.5.2 Osteoblasts

Osteoblasts originate from mesenchymal cell progenitors (Aubin and Triffitt, 2008). Osteoblasts´ function consists of secretion of bone matrix protein and bone mineralization. Their morphology is typical of high protein secretion cells with a polygonal shape, with a large nucleus away from the bone surface and a Golgi apparatus facing the bone surface. The process of bone formation comprises of several phases (Figure 2.3B): proliferation, extracellular development and maturation, mineral deposition and apoptosis. The phenotypic expression of an osteoblast changes depending on the phase (with different cell phenotype in the different stages) (Aubin and Triffitt, 2008). The maturation process of osteoblast concerns the following main stages: preosteoblasts, mature osteoblasts, osteoid osteocytes, early osteocyte and mature osteocyte (trapped in the bone matrix) (Jähn and Bonewald, 2012). Osteoblasts differentiation is controlled by the transcription factor Runx2 which will determine the expression of osteoblast phenotype-specific genes essential for regulation of bone formation and remodelling (Schinke and Karsenty, 2008). There are two signalling path (family of secreted proteins) that activates osteoblasts, contributing to skeletogenesis and homeostasis: BMPs for differentiation of osteoblasts precursors proliferation; and Wnts involved in differentiation, proliferation and cell apoptosis. Osteoblasts secrete large amounts on type I collagen and other matrix proteins, and produce also high levels of alkaline phosphatase (ALP) and osteocalcin (Bellido et al., 2014).

The organic component of bone matrix or osteoid deposited by mature osteoblast is mostly type I collagen which provides tensile strength to bone. Other types of non-collagenous proteins (like osteocalcin) are also secreted in order to form this matrix in the osteoid stem. Subsequently, osteoblasts carry out the mineralisation of osteoid by depositing calcium and phosphate and liberating matrix vesicles (Safadi et al., 2009).

Upon bone deposition, osteoblasts can die by apoptosis or become lining cells. Osteoblasts apoptosis will be the fate of 60-80% of the osteoblasts with cell detachment, composition changes and shrinkage as main characteristics (Jilka et al., 2007). Some of the remaining osteoblast will flatten on the inactive surface of bone (no formation or resorption area) as lining cells. These cells show a flat nuclear profile and they create a connective tissue barrier. Under the right stimulus, lining cells have the ability to become active osteoblasts and produce bone matrix. Lining

cells participate with osteocytes in the exchange of minerals from bone to cells, restrict resorption activity of osteoclast when it is not needed and participate in these cells´ differentiation; they are also part of the remodelling process being a component of the bone multicellular unit (BMU) (Florencio-Silva et al., 2015)

2.5.3 Osteocytes

The other option for the osteoblastic cell is to be entrapped in the bone matrix and remain there for bone maintenance (Figure 2.3C). These types of cells are known as osteocytes. Osteocytes are mesenchymal stem cells that descend from osteoblast differentiation and are responsible of mineral regulation and bone maintenance detecting mechanical stress (see below). Osteocytes transform from the polygonal cell to a star-shaped cell going through changes in gene expression. It seems that specific osteoblast develops cytoplasmic processed resulting in osteocyte differentiation. 5% to 20% of the mature osteoblasts will turn into osteocytes and they are the more numerous bone cells found within the matrix or on the bone surface (90% of the total) (Klein-Nulend and Bonewald, 2008; Bellido et al., 2014).

Osteocyte body is trapped within the matrix (in spaces called lacunae); it has cytoplasmic dendritic projections. For each osteocyte, there are around 50 processes joined via gap junctions which establish intercellular connection in the canaliculi network. These canaliculi allow the transportation of proteins produced and secreted by osteocytes and expands osteocyte activity through the periosteal and endosteal surfaces and on the vicinity of the bone marrow in the trabecular bone (Bellido et al., 2014). Because osteocytes derive from mature osteoblast, they share most of the genes and proteins with those bone cells but in different levels of expression (e.g. osteocytes have higher levels of proteins required for mineralization). Osteocytes are the only bone cells that produce sclerostin which has an effect on osteoblast polarization and activity though controlling BMP and Wnt signalling (Poole et al., 2005). Osteocytes death may be a regulator of osteoclast activity by producing local damage or micro damage of bone and recruiting and activating lining cells and therefore, initiating remodelling activity (Bonewald, 2011).

Osteocytes play an essential role in the detection of mechanical stress, and consequently coordinate the action of osteoblasts and osteoclasts in order to maintain bone integrity trough modelling and remodelling (Lanyon, 1993).

Furthermore, they react to environmental changes and hormonal stimuli balancing bone turnover. Due to their location in the Haversian canal system (Figure 2.2D), osteocyte networks allow the regulation of blood calcium and blood phosphate homeostasis and other protein regulators of mineralization as the aforementioned sclerostin (among others) (Jähn and Bonewald, 2012). Osteocyte life span may be determined by the rate of bone matrix turnover indicating that they may be reabsorbed or "liberated" by active osteoclasts (Klein-Nulend and Bonewald, 2008). These released osteocytes may get trapped again within the matrix during bone formation or undergo definite apoptosis and become phagocytosed (Suzuki et al., 2000). Osteocyte cell death can lead to deficiencies in bone quality and bone mass with the surrounding bone matrix area becoming in fact more brittle and fragile due to the focal hypermineralization of the tissue (Atkins and Findlay, 2012).

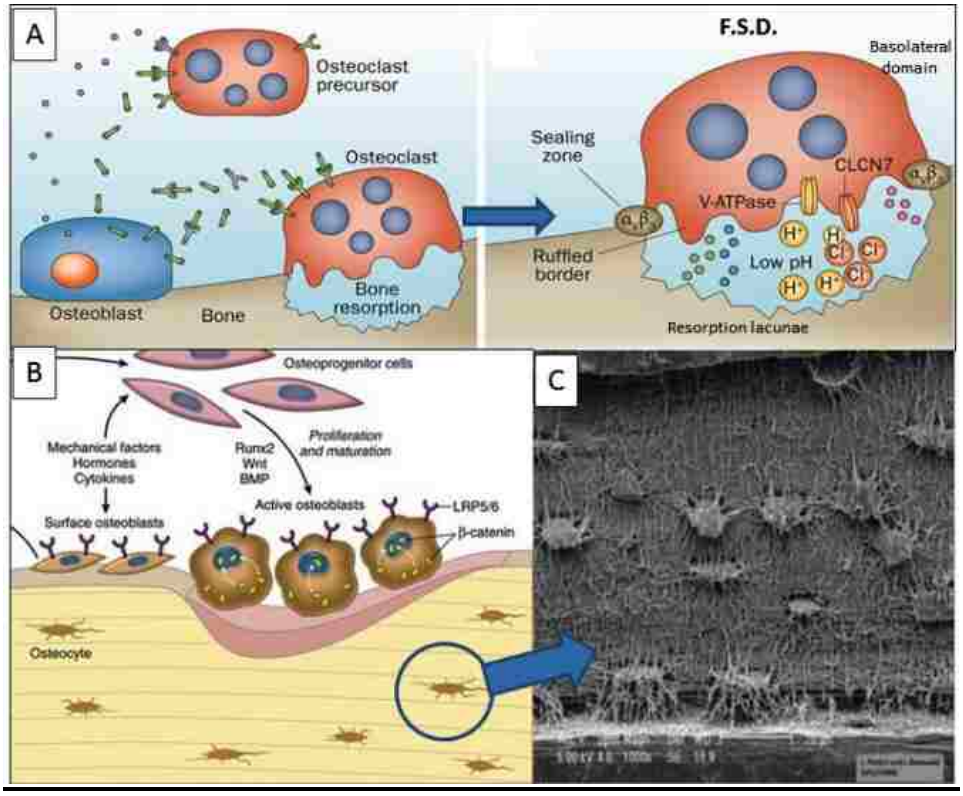

Figure 2.3 Bone cells. A: osteoclast formation and resorption activity on the different membranes (F.S.D = functional secretory domain). B: osteoblast differentiation, formation and activation. C: osteocytes lying within the lacunae spaces and connected by canaliculi network (Images adapted from Adamopoulos and Mellins (2014: 190 fig.1) and Kumar et al. (2015: 63 fig 2.16).

2.6. Bone development and growth

Bone growth is considered a higher level of bone formation that accounts for changes in mass and size. Osteogenesis (bone formation) has two processes: Intramembranous and endochondral ossification. Unless noted, the following discussion is based on the work of Jee (2001), Scheuer and Black (2004) (2004), Maes and Kronenberg (2012) and Weaver and Fuchs (2013).

At the early foetal stages, skeletal development begins with the condensation of mesenchymal cells. The ossification of these structures results in bone membrane and bone cartilage, the first group developing through mesenchymal ossification and the second group through endochondral ossification. Both bone development types follow similar cellular paths. First, there is an increase on the number of cells and fibres followed by cell differentiation. The process finalises with osteoblasts activity laying down the organic matrix and ostecytes proceeding with the mineralisation process. In embryonic bone formation, woven bone is firstly formed and it will be replaced after birth by the bundled lamellar bone. Skeletogenesis is strongly genetically determined with a programmed spatial and temporal patterning of the skeletal element to be formed; however, other factors such as diet, physical activity and vitamin intake – among others – have also an effect on prenatal skeletal development.

Intramembranous ossification is the direct mineralization of a tissue membrane and it forms the bulk that is the precedent of the cortical shell. The process starts with fibrocellular condensation in the embryo, followed by an increase in cells and fibres that produce the formation of the primary centre of ossification. The process continues with apposition of bone. Osteoblasts start forming a diffuse network of bone spicules that will result in the primary spongiosa. The thickness of the spongiosa increases as more osteoids are laid down; compact bone appears when the spaces between the primary trabeculae are occupied by the formation of primary osteonal systems that will be replaced by Haversian systems. Many plate-like bones of the skull, facial bones, parts of the mandible and clavicle, and the sense bones are formed by intramembranous ossification.

Endochondral ossification forms the bulk that will become cancellous bone and it mostly associated with long bones development. The first step is mesenchymal in nature forming hyaline cartilage as a precursor of bone (as there is

no direct replacement of cartilage *per se*). The cartilage usually appears in the embryonic period with chondrocytes (cartilage cells) producing the matrix which will serve as a model of the future bone. The matrix mineralizes and a vascular bud forms an interruption canal that penetrates the periosteal collar allowing osteogenesis to take place. Osteoid appear on the calcified cartilage walls that gradually will be transformed into woven bone. The result is a transformation into primary spongiosa spicules in the form of calcified cores surrounded by woven bone. The periosteal collar is formed and the primary centre of ossification appears. The collar will be replaced by secondary trabecula or by bone marrow. Long bones, vertebrae, tarsals, carpals, sternum and ribs developed via endochondral ossification.

In long bones, growth occurs longitudinally at the growth plate with the cartilage on the metaphyseal side being replaced by calcified tissue. This replacement will push the increase in length of the skeletal element occurring in four zones: reserve (resting), proliferative, hypertrophic and provisional mineralization. The diaphyseal development consists of radially appositional growth with bone formation at the bone surface creating ridges parallel to the blood vessel. The ridges will augment and fuse leaving a longitudinal space in the middle that will become the canal. The canal houses the blood vessel and once the process is completed a typical osteon structure is accomplished (refer to Scheuer and Black (2004) for more detail).

2.7. Bone modelling and remodelling

Bone modelling consists of the coordinated activity of the resorption of bone by osteoclasts and the formation of bone by osteoblasts; this occurs at any bone surface accounting for bone changes related to shape, size and position. Bone remodelling consists of a coupled and coordinated activity of osteoclasts and osteoblasts on a specific bone surface occurring at three sequential steps – activation, resorption and formation- accounting for bone maintenance and repair (Table 2.3) (Stout and Crowder, 2012).

Table 2.3 Summary of bone modelling and remodelling main characteristics. Adapted from Jee (2001) and Allen and Burr (2014).

	Modelling	Remodelling
Goal	Shape bone, increase bone mass	Renew bone
Location	Different surfaces	Spatial
Cell/Mechanism	A-F; A-R	A-R-F
Bone envelopes	Periosteal, endocortical, trabecular	Periosteal, endocortical, trabecular, intracortical
Timing	Continuous	Cyclical
Extent	Large (>90%)	Small (<20%)
Apposition rate	Fast (2-10 /day)	Slow (0.3-1.0 μm /day)
Net effect on bone mass	Net gain (increase)	No change or net loss (maintenance or slight decrease)
Occurrence	Mostly during growth, childhood; special circumstances in adulthood	Throughout life spam
MES threshold	< 200 microstrain	> 1500-2000 microstrain

A=activation, F=formation, R=resorption; MES= *minimum effective strain*

Skeletal growth, development and modelling primarily account for the normal development of the skeleton, although modelling can be distinguished as a sub-process of these two other phenomena. To summarise the differences between bone growth and modelling, bone growth (periosteal and endosteal expansion) accomplishes bone mass peak, whilst bone modelling accounts for diametric shape and curvature and general position in relation to the rest of the skeletal elements through different morphological changes (Frost, 2001; Maggiano, 2012). Hence, different hormonal inputs and biomechanical mechanisms are involved on each process.

Modelling always occurs in a pre-existing bone surface at the periosteal and endosteal membranes (PEM) (Frost, 1973). There is also evidence of bone formation and resorption modelling in random cortical areas domains – termed *foci* according to Frost (1964) – that can be seen as variations in the orientation and depth of the lamellae under polarised light (Maggiano 2012).

In modelling, both osteoclasts and osteoblast work independently and co-ordinately (cell activity at a locus but not necessary at the same time). Resorption is not a pre-requirement for deposition (as it will be in bone remodelling) (Martin et al., 2015). The signal received by the bone cells is based on local tissue strain, and bone formation or bone resorption are respectively initiated depending on the higher

or lower strain stimulation. During modelling, the cellular process compromises first cell activation, followed by either formation or resorption; lining cells are also involved by activation and may become active osteoblasts (Frost, 1973; Allen and Burr, 2013).

The modelling process is more active during development and growth but it is also present during early maturity and occurring at a lower rate during late adulthood (Allen and Burr, 2013). Modelling takes place also in some pathological conditions or with radical changes in the mechanical loading (Ruff et al., 2006; Peck and Stout, 2009). The modelling functions are related to growth, drifts, lamellar compaction (understood as the process of filling empty bone spaces to transform trabecular bone into compact bone when required) and bone adaptation. This is achieved by bone resorption and bone formation on a given bone surface. Modelling formation process consists on the deposition of primary bone that, histologically, may appear as a continuum between woven bone and lamellar bone deposited at a rapid rate, or as lamellar bone with more organised collagen fibrils deposited at a lower rate; in both cases, an increase of bone mass occurs (Maggiano, 2012). Bone shape, seen as morphological adaptation/modification through a geometric determination, is carried out by modelling drifts (Frost, 2001). Modelling drift is driven by bone modelling formation in the diaphysis at both periosteal and endosteal surfaces, and resorption modelling occurring on opposite cortices. The target is to reach the normal adult functional morphology but also to respond to variations in mechanical loading patterns. Two types of modelling cortical drifts have been proposed in long bones. *Linear drift* accounts for the bone changing position in relation to a straight line (e.g. transversally to the bone axis) (Frost, 1973), and *curvilinear drift* which is referred as modular change of the drift direction on one or both envelopes resulting in modifications in shape-size (Maggiano, 2012) (Figure 2.4). Formation and resorption modelling are coordinated at the metaphysis of bones (coupled but independently local activity) resulting in an increase in longitudinal growth which is associated to endochondral ossification. Radial growth is related to the modification of bone shapes: a reduction on the metaphysis in favour of the expansion of the medullary cavity is seen in long bones. This mechanism allows a modification of the cross-sectional geometry to maintain the medullary cavity in balance with the bone axis (Maggiano, Maggiano, Tiesler et al., 2016).

Differences in morphological adaptation also exist depending on the type of bone as flat skeletal elements do not experience diametrical modelling. Sex differences driven by hormonal stimulation – mostly related to puberty and aging – and other factors such as mechanical loading can also alter modelling drifts (Allen and Burr, 2013). In summary, these complex mechanisms will adapt the whole bone not only to the required curvature but also to its relative position in relation to the articulations and to the other elements of the skeleton.

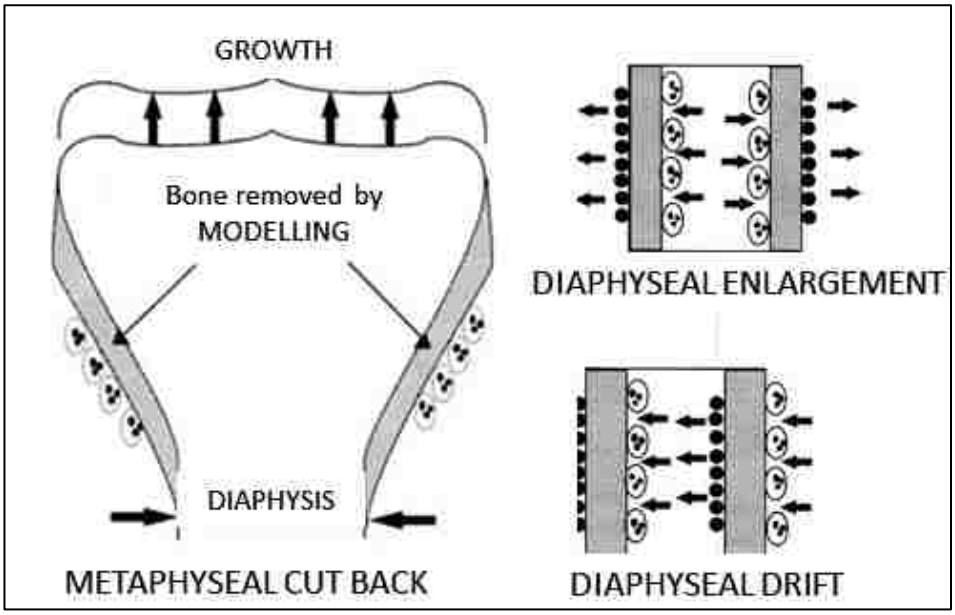

Figure 2.4 Modelling formation and resorption. Left: resorption occurring at the metaphysis and formation on the diaphysis; longitudinal growth at the epiphyseal plate. Right: formation modelling at the periosteal envelope and resorptive modelling at the endosteal envelope (top); modelling diaphyseal drift with displacement towards the left (bottom) (Adapted from Martin et al. 2015: 98 fig. 3.1).

Remodelling is an episodic mechanism that consists on the replacement of older bone by coupled and coordinated activity of osteoclast and osteoblasts. The discrete bone unit (bone structural units, BSU) that is created by osteoclasts and osteoblast activity is the secondary osteons or Haversian systems (Parfitt, 2002; Martin et al., 2015). The main goals of remodelling are mineral homeostasis, bone repair and mechanical adaptation.

Remodelling is a *quantum concept* occurring throughout life in which specific bone sites are replaced with new bone by the activity of groups of osteoclasts and osteoblast -known as basic multicellular units (BMU). BMUs move in a three-dimensional plane creating and refilling a tunnel through the cortical bone or through

trenches on the trabecula (Frost, 1969; Parfitt, 2002). The activity of a BMU is accomplished by a sequence of three main phases: activation, resorption and formation (A-R-F). In the *activation* phase (or origination phase as Parfitt proposed (2002), osteoclasts precursors are recruited to the bone surface where differentiation and fusion of osteoclast occurs. Before mature osteoclasts can start bone resorption, the lining cells retract to expose the bone matrix and to leave space for osteoclasts. Afterwards, bone resorption by the formation of a Howship´s lacuna appears in a longitudinal section seen as a cutting cone that is about 150-300 um diameter to 300 um in length (with variations depending on the remodelling sites) (Parfitt, 1993). The diameter of the cutting cone determines the size of the osteon viewed in cross-section. An approximate resorption rate will follow with 40-50 μm/day in length and 5 μm /day radially (Martin and Burr, 1989). There is a transitional stage between resorption and formation known as the reversal phase in which a group of mononuclear cells smoothen the border of the resorption bay creating the cement or reversal line as a delimitation from the old bone matrix (Martin et al., 2015). Both resorption and reversal phases take around 30 days to be completed. Osteoblasts lay at the edge of the cutting-cone and start depositing the concentric lamellae (formation phase). Over 2-3 weeks, osteoblasts start osteoid mineralization by depositing mineral and phosphate ions within and between the fibres completing about 70% of the total mineralization; finally, the mature mineral will be deposited in a slower rate (up to 1 year). Upon formation completion, the quiescence phase takes place in which secondary osteons maintain their homeostatic and metabolic functions (Martin and Burr, 1989). The remodelling cycle lasts for 2-4 months in healthy individuals (average of 90 days from resorption to completion of the osteon) with time alterations produced by pathological conditions. Figure 2.5 illustrates the formation and timing of the “cutting cone” with a scheme of the A-R-F phases.

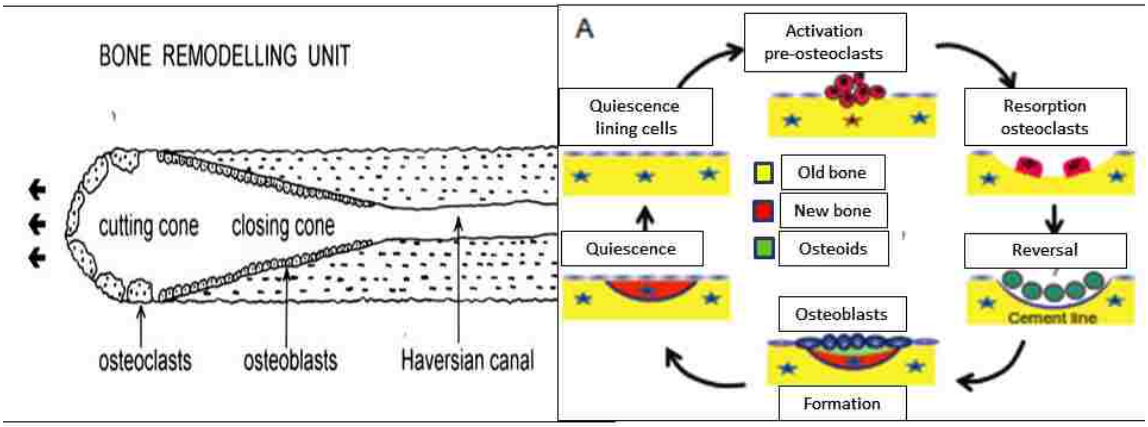

Figure 2.5 Left: cutting cone longitudinal section. Right: Schematic illustration of bone remodelling cycle starting from lining cells on the quiescent bone surface to osteoblast depositing proteins followed by mineralization. Osteocytes (stars) regulate all the resorption and formation processes. Adapted from Chamberlain and Forbes (2005: 44 fig. 1) and Bellido et al. (2014: 28 fig. 2.1).

Two types of bone remodelling can be differentiated. Targeted bone remodelling is a mechanism activated by a specific signal event on a specific focus which can be the response to microdamage and/or osteocyte apoptosis (e.g. microcracks disrupting the osteocyte-canalicular system followed by an activation of osteoclasts resorption) (Burger and Klein-Nulend, 1999). This remodelling accounts for bone repair accelerating bone turnover on a specific damaged site. The second type is known as stochastic remodelling and responds to non-specific signal and location (although probably not completely random) in order to balance calcium homeostasis; only 30% of the remodelling is targeted remodelling (Burr, 2002).

Microdamage seems to activate osteocyte apoptosis in which osteocytes – before they undergo programmed cell death – secrete factors that target the activation of osteoclasts, and therefore, the resorption point stars (Allen and Burr, 2013). The lining cells are also suggested to play the role of initiators of the new BMU formation being activated by stress or microdamage accumulation and producing also intracellular signalling molecules (cyclic AMP) (Eriksen, 2010). Direct and indirect influence of hormones in remodelling – and modelling – like PTH and glucocorticoids (stimulate bone resorption/loss), and Vitamin D and calcitonin (stimulating bone formation/mass) may also activate the formation process (Rodan and Martin, 1981; Eriksen, 2010).

One of the main functions of bone remodelling is bone integrity maintenance. Frost (1964) brought to attention the possibility of bone remodelling as a concept of bone turnover occurring in anatomically discrete foci. Remodelling processes are carried out on the four bone envelopes: periosteum, endosteum, trabeculae and Haversian (intra-cortical). Trabecular bone remodelling presents variations compared to the other envelopes in which a cavity known as the bone remodelling compartment (BRC) appears with the initiation of bone resorption and closes when bone formation finalises. The BRC is identified as a multiple purpose platform where minerals and matrix constituents exchange, and bone cell recruitment and coordination of BMU activities take place (Hauge et al., 2001). Osteonal BMUs in human adult bone is replaced in 3% every year, while remodelling in the endosteum and in the trabecular bone accounts for BMUs in "half-moon" shape erosions (hemi-osteon) with a rate of approximately 25-30% of trabeculae being replaced per year. Also, the trabecular remodelling takes longer than the cortical remodelling, with approximately 200 days to finish the whole process with most of it being bone formation (Kular et al., 2012).

The periosteum has an increase in the remodelling rate with age with the surface becoming scalloped and losing some bone mass, while the endosteal envelope has a similar remodelling rate as the trabecula with some pits that are not eventually filled with new bone resulting in an expansion of the medullary cavity (Martin et al., 2015). Mechanically, it can be said that intra-cortical remodelling (formation of Haversian systems) does not have a clear advantage in comparison with primary bone: the newly formed Haversian systems are even weaker in tension that the primary osteonal structures due to the quick deposition of minerals in the first stage of the formation phase (Currey, 1959). Remodelling rate slows down after the growth period has been completed and it is highly variable during adulthood. Sex, diet, hormones, genetic and environmental factors affect remodelling of the human skeleton (Stout, 1998). Bone cells involved in the remodelling process have a coordinated and coupled but not necessarily balanced activity at the BMU; either a positive or negative imbalance can cause excessive bone deposition or removal (Allen and Burr, 2013). An increase in bone remodelling rates is observed in women with menopause due to the decrease in estrogen, while both sexes experience a lower rate in remodelling after the seventh decade of life (Martin and Burr ,1989; Gosman et al., 2011).

Remodelling events will accumulate in a given bone area throughout age. As noted above, bone remodelling produces quantifiable defined microscopic features appearing as the individual ages, and it is one of the mechanisms assessed for aging histomorphometric analysis (Kerley, 1965). However, it is not only the biological age of the individual what is represented through the remodelled microstructures but also the mean tissue age (MTA) of that specific bone domain (Frost, 1987c; 1987d). This matter will be discussed in the next chapter.

2.8. Theories about bone biology and remodelling

As discussed at the beginning of this chapter, since the 17th-18th centuries, scientists were able to link bone internal structure to its mechanical properties. In the last two centuries, further investigations and the advances in experimental research gave the crucial insights into bone relation not only to mechanics, but also to genetics and chemical components. In order to understand where we are now in our understanding of bone modelling and remodelling, it is important to review the evolution of the theories and how the current concepts of both mechanisms have been built, modified and improved through time.

During the 19th and the 20th centuries, new perceptions about bone physiology and adaptation were defined. The adaptation of bone to stress and the environment was first introduced through the idea of bone physiological homeostasis and the role of bone cells responding to the mechanical environment. It was Julius Wolff (1836-1902) who suggested that mechanical stress applied to bone changes its structure and these changes respond to specific mathematical rules. He understood that bone mass and architecture (internal architecture and external structure) is modified by changes in the form and function (or only function) of bone suggesting hence an adaptation to the mechanical environment surrounding it (Ruff et al., 2006). In a simplistic manner, bone cells would respond to stress and react by adding or removing bone where and when needed (Robling et al., 2013).

Since the 1980s, Harold Frost carried out extensive research on the question of bone adaptive modelling and remodelling (Frost, 1983; 1987d). Frost´s hypothesis, known as the Mechanostat theory, is explained with the following parallelism: a thermostat that would be turned on or off depending on a certain temperature (physiological window in the case of bones) (Frost, 1987a). A relation between bone and bone mass through the mechanostat can be established (Figure

2.6). According to his theory, bone modelling would add new bone onto a bone surface. Higher or lower levels from the minimum effective strain modelling point (MESm, around 1.500-2.500 microstrain for mechanically controlled modelling) would turn modelling drifts on or off, respectively. Strain higher than the MESm activates modelling and provokes an increment in the bone mass, while lower strains do not have any bone mass effects. On the other hand, bone remodelling does not imply always the replacement of all the bone that has been previously removed (A-R-F seen in Haversian system), and thus, an increase in remodelling may decrease bone mass (Frost, 1997; 1998b). In bone remodelling, peak bone strains lower than the MES remodelling threshold (MESr) will increase remodelling by the acceleration in the recruitment of BMU, while higher strains will produce a decline in the BMU recruitment, and thus, bone will be retained. In other words, if the strain is above the set point, it would adjust existing trabecular and cortical-endosteal bone in order to preserved bone mass (even resorption and deposition). This according to Frost is referred to as “conservation-mode” (Frost, 1998b: 115). A decrease in trabecular bone mineral density and an elongation of the medullary cavity will occur if the mechanical usage is below the threshold range reducing bone strength (bone mass decreased due to BMUs resorption higher than deposition, “disuse-mode”) (Frost, 1998b: 115). The disuse mode causes any types of adult osteopenia and it could be the reason of observed 40 % bone mass loss from young to 75 years old adults in which intracortical porosity increases specially in the marrow cavity but there is not decrease in bone external diameter (Frost, 1987a; 1998b; 2000). Modelling and remodelling have opposite responses to mechanical usage with modelling being stimulated with over 2.500 microstrain and remodelling activation reacting to strains falling below 200 microstrain. In summary, when modelling increases, remodelling is inhibited (producing bone deposition on the periosteum and retaining the endosteal expansion); and when remodelling is increased, modelling is inhibited (vice versa effect with an expansion of the marrow cavity) (Martin and Burr, 1989; Robling et al. 2014).

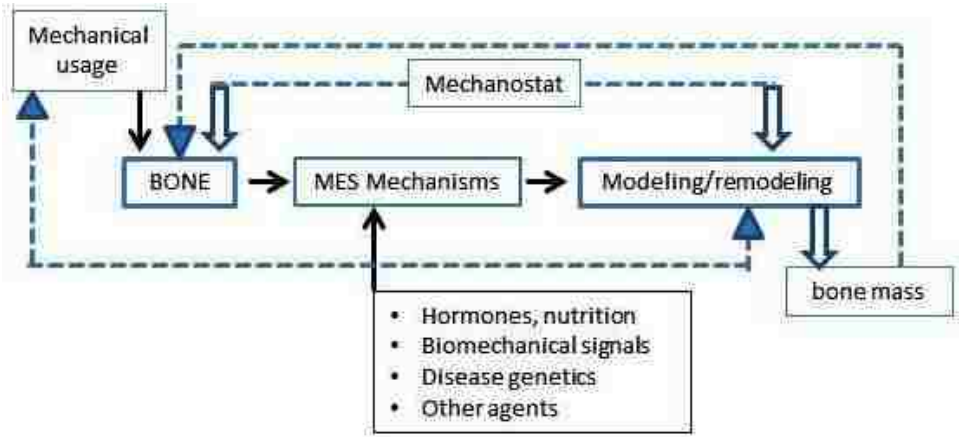

Figure 2.6 The Mechanostat theory: bone responds to mechanical usage (MES) altering its structure and influenced by the mechanical thresholds (modelling/remodelling); bone mass will change accordingly (Adapted from Frost (1987a: 6).

The main proposal from Frost (1987a) was that mechanical usage would induce bone to change its mass according to changes in the strain magnitude. Three mechanisms are involved in the theory of bone adaptation controlled by mechanical usage: growth, modelling and remodelling led by the control and coordination of bone cells responding to the mechanical usage under the normal physical activity of an individual. The sequence of events is based on mechanical loading placed on the bone generating primary signals detected by bone cells that will send secondary signals to activate the different mechanisms (see below). Early in 1960s, Frost already suggested that microcracks produced by repeated strain might initiate bone remodelling (as noted earlier) due to the disruptions that they produce in the canalicular net (Frost, 1960). It is worth mentioning that these biological mechanisms that are guided ultimately by mechanical factors (specially strain) require non-mechanical factors to function, and that muscles strength would also play an important role for bones in relation to development, health and pathologies (Frost, 2004). Regarding baseline factors involved in his theory, biochemical agents or metabolic disorders can evoke changes in the set point increasing or decreasing modelling and remodelling even if the strain threshold has remained stable (Frost 1987; Turner 1999) (Figure 2.6). Specific hormonal imbalances or medication treatments may therefore alter the “normal” points of strain causing alterations and changing consequently the thermostat set-point (Martin et al., 2015).

A further step in the discussion led to the study of cell behaviour in order to understand how and why cells receive specific signals, and how bone deposition and/or resorption (refer here as change in bone mass) react consequently transforming bone structure and improving bone strength (Turner, 1999). Experimental theories could now explain the fact that different sampling sites within the same bone have different MES thresholds. According to Turner (1999), Frost´s Mechanostat model did not acknowledge that bone loss rate due to disuse eventually slows down with time. This new approach known as the "cellular accommodation theory" proposes that bone cells are very reactive to transients in their environment. Hence, they account for a capacity of adaptation to these environmental changes that would make them readjust their sensitivity levels and accommodate to a new steady rate learning from previous loading experiences (cellular memory) (Turner et al., 2002). This adaptation of cells to the local strain environment would change the strain threshold depending on the specific bone site explaining lower set-points of skeletal elements that bear minimal mechanical loads. Frost´s Mechanostat model explained that certain hormones and biochemical agents involved in modelling and remodelling processes could alter the threshold of the Mechanostat (Frost, 1987a). Turner pointed out how certain hormones are responsible of the sensitivity of bone to mechanical strains suggesting that mechanical loading is not the only principal motor of bone formation as Frost claimed (Turner, 1999).

The Utah Paradigm compromises a series of scientific meetings about bone physiology motivated by intensive research carried out by a number of inter and multi-disciplinary researchers (biomechanics, biologists, histologists). 1960 research on growth, architecture, strength and health of the skeleton after birth was believed to be influenced by biomechanical factors controlled by bone cells (Frost, 2000). Although other physiological processes were acknowledged to influence the skeleton, the paradigm considers nonmechanical agents (e.g. growth hormones, genetics, vitamins, minerals…) predominant for bone mass and strength changes (Jee, 2005). With the 1987 Mechanostat as the key concept, skeletal elements not only refer to bones; the importance of muscles, ligaments, tendons and all tissues related to the skeletal system are also considered. In view of the new paradigm, bone is treated as a tissue, organ and at its cellular level further exploring the ideas from Frost about loading forces (Frost, 1999).

In general, these new concepts suggest that non-mechanical factors and biological mechanisms for bone adaptation work jointly in order to maintain the functional demands of the skeletal elements with the latest group controlling changes in bone architecture and strength (Frost, 1999; 2000). At birth, there exists some predetermined baseline conditions that are the effect/result of gene expression patterns. After birth, bone mechanical adaptation rules those biological mechanisms in time and space and the established biological responses to mechanical demands will dominate the spectrum of how, when, how long and where these responses will be activated or not and with what intensity. Non-mechanical factors (as sex, age, minerals, vitamins intake and hormones) are essential as they modulate or influence bone modelling and remodelling but do not replace the postnatal mechanical control (Frost, 2003). Consequently, mechanical usage affects remodelling and modelling in around 40% while only 3-10% will be determined by other non-mechanical factors (Frost, 1998a; 2001). The non-mechanical agents have also a direct effect on bone cells participating in biologic mechanisms. Some evidences support that non-mechanical agents and mechanical factors may interact with the first group altering the mechanical set point or having an effect of the mechanical stimuli (Frost, 1987c; 2000).

As seen at the beginning of this chapter, muscles in coordination with bone play an important role in bone physiology; muscle development is correlated with bone development with strong muscles leading to strong bones and muscles controlling most of the voluntary mechanical loads. Moreover, a genetic correlation between muscle mass and bone mass ensure that both elements´ strength are in accordance (Parfitt, 2004). Also, both hard and soft tissues are affected by any anomalous function in the mechanostat which may cause or trigger disorders like osteoporosis, hernias or ligament ossification, among others (Frost, 2000; 2004).

2.9 Summary

Bones are living elements that are influenced by a wide range of intrinsic and extrinsic factors. These factors determine in different degrees of expression bone composition, structure and architecture from the macroscopic to the microscopic level. Moreover, bones respond to intrinsic and extrinsic stimuli during development and growth, and throughout one´s live. The skeleton changes through time and these changes can be identified and assessed. A detailed discussion about bone remodelling mechanisms was here presented. Remodelling processes interpreted

and recorded applying bone histology, especially for age estimation methods, will be discussed in the next chapter.

Chapter 3 : AGE ESTIMATION AND BONE HISTOLOGY

In disciplines such as bioarchaeology, osteo-archaeology, physical and forensic anthropology, the goal of the expert osteologist is to obtain as much anthropological information as possible about the biological profile of the individual and/or the sample under study. The basic analysis involves sex estimation, age assessment, pathological conditions and ancestry.

The research presented in this document focused on age estimation assessment. By definition, aging is the result of biological natural processes representing a skeletal decline which has hereditary influences and is conditioned to a certain extent by environmental factors (Nakamura, 1991). This chapter discusses age estimation methodologies to assess age at death on dry bones. First, an overview of general macroscopic methods will be presented. Secondly, histological techniques used for age estimation on long bones is debated, followed by a detailed discussion on costal and short skeletal elements histological aging methods. Intrinsic and extrinsic factors having an impact on the aging techniques will close this chapter. Other applications of bone and dental histological analysis are out of the scope of this thesis, but the reader is referred to Crowder and Stout (2012) for a further review.

3.1. Macroscopic methods for age estimation

The estimation of chronological age-at-death for juvenile remains relies on the gross observation of developmental and growth patterns on bone and teeth elements. Analytical methods based on the appearance of centers of ossification, dental age, long bones length and epiphyseal fusion are used for sub-adult age estimation (refer to Scheuer and Black (2004) for a full discussion).

Age estimation in adults is based on the observation and assessment of degenerative changes in the skeleton. Maturity refers to the stage at which the adult function and form have been reached. The most commonly applied methodologies are based on the assessment of the following skeletal features: pubic symphysis, auricular surface, sternal end of the rib, cranial suture closure and dentition. The first three methods rely on degenerative changes on bone joints. Basically, morphological alterations that the specific age indicator gradually undergoes as the individual ages are recorded (Lovejoy et al., 1985a; Todd, 1920; Iscan et al., 1984a,b). Cranial suture has always been controversial due to the high variability of

suture obliteration and large errors in age estimates have been reported; still, the method is commonly used in combination with other techniques (Meindl and Lovejoy, 1985; Byers, 2002). Among the macroscopic techniques, pubic symphysis and rib sternal end age estimation techniques were recommended as anthropological methods fulfilling the accuracy levels for forensic cases although with restrictions related to age cohorts and environmental influences on the expression of the age indicators (Ritz-Timme et al., 2000). A detailed description on gross-examination aging approaches is beyond the scope of this work and further details can be found in Lathan and Finnegan (2010); instead, a brief critic about methodological issues is here provided.

It has been shown that around 60% of the variation observed in age markers is not directly correlated to age but to other parameters like hormones, vitamins, biomechanical markers and inter-population variation which prevents the applicability of the methods as universal standards (Mays, 2015). Hence, the mentioned factors might alter the timing at which the degenerative changes occur, and thus, age standards derived from one population may not be applicable to another one (Lathan and Finnegan, 2010). Even individuals with the same chronological age may show different patterns due to behaviour or plasticity. Different accuracy rates have been achieved while developing aging methods on diverse sample populations, and numerous validation studies have been performed on different ethnic groups reporting variability in age trait expression due to secular trends or geographical location (Buckberry and Chamberlain, 2002; Igarashi et al., 2005; Savall et al., 2015). Not only the inherent variation in aging processes supposes a limitation, but observer´s subjectivity may also introduce certain biases (Garvin et al., 2012). Refinement of the descriptions or changes in the scoring system have improved methodological problems and solved inherent issues related to wide age ranges or errors arising from sexual dimorphic differences (McKern and Steward, 1957; Katz and Suchey, 1986; Nawrocki, 1998; Mulhern and Jones, 2005). Some authors have modified the age estimating techniques by the addition of different mathematical procedures (Samworth and Gowland, 2007) or updating the methodological approaches with the aid of new technologies (Stoyanova et al., 2015).

A recent study tested most aging methods on a Southeast Asian sample. The results demonstrated different levels of accuracy not only for specific methods but

also for different age cohorts (Gocha et al., 2015). The authors improved the accuracy rates by combining multiple indicators obtaining more precise age estimates as confirmed by other studies (Miranker, 2016). Nonetheless, the combination of several age markers may be done cautiously due to problems arising from adding traits from different samples with non-comparable age distributions, and from combining methods developed under different methodological assumptions and/or statistical foundations (Garvin et al., 2012).

3.2. Micro-anatomical features used for age estimation

Bone histomorphometry allows for the quantitative interpretation and assessment of bone microstructures throughout an individual´s life spam. It is an important research tool for the analysis of bone remodelling dynamics, not only in forensic anthropology but also in clinical and pathological studies.

3.2.1. Bone histomorphometry and age: an overview of primary parameters

Age-dependent changes occur in bone microstructures might relate to morphology, size, geometry and frequency number. There is a wide range of studies showing how different types of bone histological features (e.g. types of osteons, area of remodelled bone…) can be applied to estimate age depending on the skeletal elements, sampling location, sample under study and other intrinsic-extrinsic factor affecting the outcome of the research (Stout and Gehlert, 1982; Ericksen, 1991; Pavón, 2007). Due to the amount of data available, this section will focus on the most commonly – but not limited to – age related histomorphometric parameters. Methodological variation between studies must be considered – e.g. different description of the same microstructures – when a specific aging technique is applied.

As part of the normal aging process, a decrease in bone mass is observed after the fourth decade of life. This bone loss implies age related changes in bone macro- and micro-architecture, structure and composition which involved: bone resorption and bone formation uncoupled activities, accumulation of microdamage, changes in cross-sectional geometry due to expansion of the medullary cavity and cortical thinning, accompanied by changes in mineral deposition and protein content (Livshits et al., 1998; Brickley and Ives, 2008). The typical appearance of cortical bone cross-section accounts for lamellar bone at periosteal and endosteal surfaces (outer and inner margins) with the middle area occupied in different proportions by

Haversian systems and interstitial lamellae. Primary vascular canals (primary osteons) reflect the deposition of primary bone with their correlation to age being included in aging techniques for sub-adults (Streeter, 2005; Agnew, 2006). Sub-adult cortical bone consisting of primary lamellae and primary osteons is replaced by secondary bone through modeling and remodeling activity. Resorption spaces are the first sign of secondary osteon creation, and their number seems to increase as age increases; nonetheless, some authors did report none or different age related changes (Sedlin et al., 1963; Ortner, 1975). As already mentioned in the previous chapter, the main distinctive feature to discern between primary and secondary osteons is a histological delimited boundary known as the cement line. The ratio (fractional volume) between primary and secondary osteonal bone increases as primary bone is replaced by secondary bone (Figure 3.1).

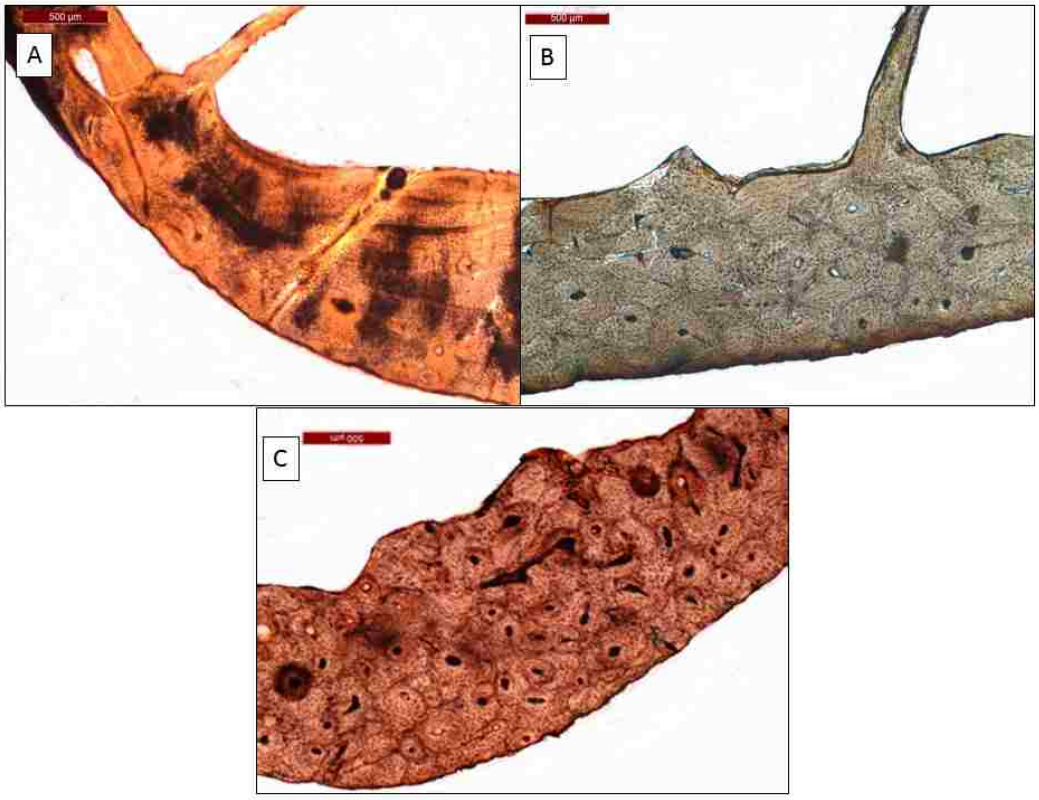

Figure 3.1 Different age stages showing changes on fractional volume of primary and secondary osteonal bone (study sample specimens); A: 6 years old (lamellae and no osteonal structures), B: 35 years old (large osteons and thick cortex,), C: 56 years old (small and numerous osteonal structures) (40x magnification).

Morphology type of secondary osteons was also employed for aging methods. Researchers used the correlation between intact secondary osteons (*type I*) and

age owing that as chronological age advances, secondary osteons increase in frequency number as a result of an increase in bone remodelling rates. Both the reversal line and the Haversian canal must be partially unremodeled to be considered a secondary intact osteon (Robling and Stout, 2008). Osteon accumulation per unit area and the ongoing remodeling result in secondary fragmentary osteons which are commonly defined as osteons that – in different proportions – have been resorbed by the appearance of new osteonal structures. Aging causes the middle and periosteal fractions of bone to be filled by these features due to an increase in numerical osteonal density, while the endosteal lamellae undergoes a decrease in area as a result of endosteal cavity expansion and trabecular remodelling processes (Maat et al., 2006; Keough et al., 2009; Crescimanno and Stout, 2012).

Other types of osteons depending on their morphology were shown to be correlated to age. Drifting osteons (waltzing osteon) exhibit a non-central Haversian canal and a tail formed by lamellae: viewed in cross-section, the tail seems to be the remains of the transverse drift direction advancing through the cortex (Robling and Stout, 1999). Directional and non-directional drifting osteons can be discerned depending on the drift orientation during BSU formation (Crowder, 2005). Drifting osteons occupied more than half of the resorption area in individuals under 10 years old and decrease in number as age increases (Coutelier 1976; Robling and Stout 1999). Drifting osteons may be a response for developing bones in order to maintain mineral homeostasis which is highly needed in growing individuals explaining their high frequency in sub-adults (Coutelier, 1976). Albeit, the relation between metabolic responses and this feature is still unclear (Robling and Stout, 1999). The author has observed drifting osteons in most decades of life in the sample under study but decreasing in number or being absent in over 70 years old individual, which is in agreement with other studies (Robling and Stout, 1999).

Type II osteons (or embedded) are seen in cross-section as a small complete Haversian system sitting on an existing larger osteon and they may be caused by radial remodelling of the previous formed Haversian canal (Richman et al., 1979). The reversal line of the embedded osteon seems to be the result of growth reactivation after a high moment of stress (Stout, 1989). These osteonal structures might be produced by mineral exchange to maintain mineral homeostasis with an increase in their number with increasing age (Ericksen, 1991). However, their

numerical frequency was tested for any association with age with discrepancies arising for this feature (Richman et al., 1979; Yoshino et al., 1994).

Double zonal osteons reveal a hypercalcified ring (arrest line) representing a moment of matrix secretion disruption which forms a boundary separating two zones with identical lamellae orientation (note that no reversal line can be seen in this frontier). Some studies showed either a positive or none correlation to age (Pankovich et al., 1974; Yoshino et al., 1994).

Metric analysis of osteonal microstructures seem to be also related to age with parameters as area, perimeter and diameter of both Haversian systems and Haversian canals being commonly used in aging methods. Haversian systems area decreases as age increases while Haversian canal area shows an inverse correlation with age, fact that would explain intracortical remodeling processes being higher in old individuals with the associated increase in intracortical porosity (Britz et al., 2009). It is worth mentioning that Haversian canal measurements reported some controversial views (Thompson, 1980; Keough et al. 2009).

Cortical and trabecular area aging changes exhibit a general decrease in the former one affected directly by the reabsorption at the endosteal margin produced by remodelling on the trabecular area (Chen et al., 2013). In age histological studies, total cortical area is used as a normalised reference measurement to compute composite parameters such as relative cortical area, among others (Martin and Burr, 1989; Stewart et al., 2015). Age changes observed in the cortical surface area are, to some extent, a biological mechanism observed in the whole skeleton with variation in their magnitude depending on the anatomical location.

3.2.2. Histomorphometric research methods and methodological issues

Bone histomorphometric methods range from the study of dynamic bone cells and function (dynamic histomorphometry) to the assessment of static bone microstructures (static histomorphometry). Static bone histomorphometry – the present study being based on *stereologic analysis of cortical bone* – consists of the study of bone microstructure through the use of optical microscopy to examine histological features in a 2-dimensional plane (Stout and Crowder, 2012). It is worth mentioning other technologies like micro-CT, MRI or spatial analyses software that allow the researcher to observed bone features on a 3-dimensional level (Rose et al., 2012; Maggiano, Maggiano, Clement et al., 2016). Not only a technological

improvement has been achieved; an effort have been made along the years to standardised the nomenclature – proposed by the American Society of Bone and Mineral Research (ASBMR) – and ultimately, to standardise terms cited in histological studies to help researchers to make comparisons between studies feasible (Parfitt, 1988; Dempster et al., 2013).

Important considerations need to be brought to attention about the specific applicability of age estimation through histological analysis. Modeling during growth is responsible of most of the cortical and trabecular bone formation. As mentioned earlier, age-related changes in cortical bone do not have a steady rate throughout the individual´s life span; indeed, osteonal formation rate and bone turnover in the cortex are higher in individuals from 9 to 23 years old than in adults with rapid rates leading to the replacement of primary bone into secondary osteonal bone in the developing skeleton (Robling and Stout, 2008). During adulthood, frequency of BMU activation rates depends on specific mechanical or metabolic demands (Martin and Burr, 1989). Consequently, both intact and fragmentary osteons visible on a cross-section at the time of death are not a representation of all the remodeling accumulated since birth. It is the reflection of the age of the given cortex rather than the chronological age of the individual (Stout and Paine, 1992). This is a combination of aging processes and the mean tissue age (MTA) of a specific bone domain which is determined by both secondary osteons accumulation and other factors such as physical activity, hormonal and metabolic influences and modeling drifts (Frost, 1987b; 1987c). Moreover, the so-called effective age of adult compacta refers to the observable accumulation of secondary osteons (intact and fragments) on a given bone sample (Stout and Jackson, 1990) that reflects the time at which cessation of cortical drifts and growth modeling have occurred, and the tissue has eventually reached maturity for adult compacta (Wu et al., 1970; Stout and Lueck, 1995). Age estimates would therefore depend on this *effective age* and should be theoretically adjusted depending on the given area of bone tissue under analysis.

To some extent, any type of secondary osteons are the evidences of remodeling events but as age advances and osteons start increasing in frequency number, they accumulate in the cortex erasing any traces of previous remodeling events. Osteon overlap (asymptote), in some occasions, implies that the new created osteons will completely refill the Haversian canal of the “old” remodelling event (Martin et al., 2015). Consequently, secondary osteon accumulation entails a

limitation for aging old individuals because remodeling events seen at the moment of death do not reflect the individual´s chronological age (Wu et al., 1970; Robling and Stout, 2008). The point at which osteon population density (OPD) – accounting of intact and fragmentary secondary osteon in relation to cortical area (Stout and Paine, 1992) – reaches asymptote depends on the bone under consideration, remodeling activation rates and other factors. For example, femora present a relatively older age OPD asymptote than ribs due to larger cortical area and a higher remodeling density variation along the cortex (Stout and Crowder, 2012). Above all, pathological conditions and other intrinsic and extrinsic factors will also alter remodeling rates producing variation in OPD asymptotic values (Stout et al., 1996).

Regarding practical concerns, histomorphometric analysis relies on the preparation of thin-sections – both decalcified or undecalcified bone samples, stained or unstained depending on the variables to be assessed – in an histology laboratory (see next chapter for thin-section production). The observation of the organization and structure of bone tissue under the microscope – transmitted and/or polarised light – allows histological interpretation and parameters assessment. Morphometric analysis can be carried out by taking measurements using manual grids and graticules (e.g. Stout and Paine (1992), although new technologies provided the incorporation of computerised methods (Trammell and Kroman, 2013). In spite of the fact that the use of computer software helps to quantify microstructures faster and more accurately, it has been shown that the levels of inter-observer error are still high risking the reliability and repeatability of the techniques, and the use of both microscope and microphotographs have been recommended (Crowder et al., 2012). Due to the high number of features to be counted (e.g. when assessing osteons number frequencies), there is always a certain error introduced due to the imprecision of the observer. Alternatives in the modality of quantification were proposed through changing frequency number by percentages of bone area (Ahlqvist and Damsten, 1969), but some authors suggested that it was not as reliable as osteon counting (Stout and Stanley, 1991). Besides, discrepancies in the parameters descriptions may be a source of error as different authors refer to the same structure using different definitions (Kerley, 1965; Ortner, 1975; Goliath et al., 2016).

As it will be discussed in the next section, methodological issues arising from bone sampling area suggest that original methodology sample sites must be apply

when replicating any histological method due to errors introduced by remodeling rates variability between anatomical locations (Tersigni, 2005). But recent studies reported low variation between different rib numbers and age (Crowder and Rosella 2007). Additionally, even within the same cross-section, the distribution of histological structures on periosteal or endosteal regions would vary as a result of remodeling rates occurring at different paces depending on the bone area (Jowsey, 1966). It is worth mentioning that the feasibility of the method may be affected by the magnitude of the bone read. Rib and femur cross-section areas differ from 10 mm^2 to 300 mm^2, and thus, different methodological approaches can be applied. Furthermore, core samples can be extracted from the skeletal element to avoid endless counting of features and large areas of bone removed (Thompson, 1979). Regarding skeletal sample matters, aging techniques must be ideally developed from a reference sample that represents the demographic structure of the broader population (Aiello and Molleson, 1993). Also, reference sample and target sample should have similar age distribution and be ethnically close enough to prevent inter-population remodeling variation affecting the accuracy of the age estimates (Stout, 1998).

Despite several concerns related to histological methods and age estimation, it is encouraging to explore new possible approaches to further investigate and improve the state of art. In the next section, studies dealing with research issues and other anthropological matters will be discussed.

3.3. Bone histomorphometry for age estimation: methods and bones

3.3.1 Long bones

Long bones have been widely used for developing histological aging methods (Table 3.1). Among the long bones, the femur is an ideal skeletal element for histological analysis since its toughness makes this specific bone likely to be recovered during excavation and the anatomical features over the femur allow the recognition of topographical bone areas for sampling locations.

In the 1960, Jowsey (1960) recorded age changes of histological features on femoral cortical bone. In this study, no difference in remodeling between the four different topographical areas of the cortex within each section was found fact that would be argued in further research. Although this study used a rather small sample

(N = 24), it was the promoter of the quantification of age microstructural changes on this skeletal element. Partly based on the previous study, histomorphometry for aging the skeleton was applied by Kerley (1965) through the analysis of all the three lower limbs bones. Preliminary observation allowed the author to select the most representative areas for histological analysis which seemed to be the anterior, posterior, medial and lateral outer third of the cortex. The advantage of these sampling areas entails that endosteal bone resorption that occurs with age will not affect the observation of the parameters. Kerley carried out the quantification of intact and fragmentary osteons, percentage of lamellar bone and non-Haversian canals on 126 sections of femora, tibiae and fibulae. Using linear and curvilinear regression analysis to examine the data, the author noticed that all variables behaved in the same fashion for the three bones: intact and fragmentary osteons increased in number with advancing age, and the remaining variables decreased from childhood to elderly. The best correlation found was between age and intact and fragmentary osteons for all bones, although the best accuracy produced by a single parameter was reported for fibular fragmentary osteons. A test of the technique was run on a set of 56 specimens using an age profile chart – recommended by the author when multiple bones are available for analysis – which provided estimates falling within ±10 years from chronological age for the entire sample. Kerley pointed out factors such as taphonomic processes of poorly preserved archaeology material or specific pathologies that might affect parameters quantification and the reliability of technique. Neither sex nor ethnicity demonstrated any effect on the histological parameters. In both cases, the scarce number of females and specimens other than Caucasoid in the sample may have had an impact on the outcome. Several problems arose for the applicability of this methodology. In first place, Kerley did not specify the exact bone area that must be read; he just stated that the selected fractions of bone “were representative” which seems to be a subjective criterion (Kerley, 1965: 154). Secondly, the author recommended the microscopic approach over the macroscopic assessment for old age ranges, suggestions that appears to be non-feasible as we will see in the upcoming studies.

Methodological problems observed in this early research drove Ahlqvist and Damsten (1969) to conduct a validation study on 20 modern specimens finding the quantification of the variables unreliable. Instead of counting structures, a method simplification by assessing microstructure percentage – grouped in increasing or

decreasing features in relation to age – was made and using a squared-ruled field the authors were deemed to avoid missing areas on the subperiosteal bone area. Moreover, the field of view was shifted 45 degrees to evade the linea aspera, and thus, avoiding variation observed over the muscle attachments of the crest. Despite the good results on the estimates (standard error of the estimate (SEE) = ± 6.71) and the helpful contribution in constructive critic about Kerley's technique (1965), caution should be taken due to the small sample size. Kerley and Ubelaker (1978) also published a revision of Kerley´s original methodology (1965) providing a correction of the field diameter and a final revision of the regression equation. In 1982, Stout and Gehlert tested the revised method on 20 femora from autopsy samples. They concluded that histological structures are not spaced evenly through the cortex and therefore the specific field of view of the original technique must be applied to ensure that the same microstructures are quantified; by doing so, an improvement in the method reliability is accomplished (Stout and Gehlert, 1982). This sampling error concern has been also discussed by others (Lynnerup et al., 2006).

Stout and Stanley (1991) used radius, tibia and fibula midshafts from 36 cadavers based on Ahlqvist and Damsten´s technique (1969). Topographical variation was tested on the radius based on the assessment of four sampling areas within the same thin-section in comparison to results obtained from the entire surface area, and a significant age correlation was reported only for the latter. Within the same individual the variables under study on the three bones showed statistical differences suggesting that bone turnover variability does exist among different skeletal elements. High correlation with age for osteon counts was reported and osteonal bone percentage was statistically significant only for the upper limb. The authors noted that the research did not fulfil the requirement for the generation of age prediction formula. Instead, it meant an input into the continuous development of histological methods exploring concerns such as the choice of an appropriate sampling location (Ahlqvist and Damsten, 1969).

Another test of the histological variables proposed by Ahlqvist and Damsten (1969) and Kerley (1965) was carried out by Stout and Gehlert in the 80´s demonstrating that Kerley´s formulae performed more accurately for the entire sample (Stout and Gehlert, 1980). Under and over 60 years old age cohorts, however, resulted in one or another technique performing more accurately

depending on the age groups. This outcome might be due to intrinsic methodological issues as sampling area, inter-population specific variation or differences on age distribution between the samples. This research reported no statistical significance between observers suggesting high precision of the methods – as shown somewhere else (Keough et al., 2009). This assertion is in disagreement with Lynnerup et al. (1998) who reported high levels of inter-observer error for specific parameters regardless of the degree of observer experience. This last study suggested intrinsic methodological problems related to the variables under use rather than other sources of error. Osteons fragments quantification seems to be problematic with two major concerns arising: the parameter is a direct representation of aging for middle adults thus it must be present in the analysis, and secondly, the inclusion of intact and fragmentary osteons density do not solve the problem but instead it obscures the assessment.

Further validation of Kerley´s method (Kerley, 1965) was performed by Lynnerup et al. (2006) modifying the original technique by using stereoscopic techniques. The bias introduced by the nature of the original method is reduced by the random selection of small fields of view avoiding error in topographical selection and in variable quantification. Age correlation between secondary intact osteons and age was found after exclusion of one outlier although a larger sample size is required to confirm the results. As it will be discussed, the unsystematic selection of fields presented here may introduce other problematic issues like intra cross-section variation.

This random pattern in the selection of the bone area sampled within the cross-section was tested years before by Singh and Gunberg (1970) using core fragments of mandible, femur and tibia of over 40 years old male specimens (N = 59). The sampling area selected was around 1x1 cm of the cortex of the anterior midshaft femur and tibia, and from posterior border of mandibular ramus. Three parameters were assessed on two microscopic fields from the anterior periosteal third (no exact sampling provided). All variables had certain correlation with age and variability between bones was found when comparing the parameters frequency and distribution. However, comparison is not strictly applicable due to differences in sample size and age distribution between the three skeletal elements within the sample. As the authors noticed, there emerged a confrontation between this study and previous research regarding age effects on the Haversian canal size (e.g. Barer

and Jowsey (1967)) with the present study observing a decrease with age in the Haversian canal diameter. From all the bones, mandible provided the best results with standard error of ± 2.5 years from known age which contradicts later studies that did not show such a high correlation (Drusini and Businaro, 1990).

Thompson (1979) applied the same core extraction procedure on a sample of individuals over 50 years old using both lower and upper extremities and both histological and non-histological parameters. Apart from the advantage of reduction of bone damage, the author included specimens with pathologies known to alter bone turnover – even though separated formulae were generated – under the assumption that is likely that no clinical information is available in forensic cases. Stepwise regression analysis selected osteon area as the variable with the highest accuracy for all the skeletal elements. This variable was also found to accurately age individuals over 55 years old in other long bones (Thompson and Galvin, 1983) and an overall high age correlation somewhere else (Watanabe et al., 1998; Han et al., 2009). Thompson´s method (1979) was validated on a Japanese sample obtaining higher error rates than the reported by the original study. The author included new variables to improve the accuracy but it seems that ethnicity and the skewed age distribution of the Asian sample may have be the cause of this poor results (Narasaki, 1990). Modifications of the core technique were described recently with a less destructive procedure recommended for fossils (Stein and Sander, 2009).

Chan et al. (2007) examined regional remodeling variation – within and between sections – along the midshaft of 5 male femora. The afore mentioned Thompson´s core method (1979) was applied removing sections of bone from anterior, posterior, medial and lateral margins analysing four consecutive fields within these sampling areas. Four parameters were assessed. Inter-section variation produced age estimates that were not statistically significant when applying the original technique with the exception of the posterior shaft area for all five sections. Moreover, the four selected sampling areas were compared to their corresponding topographical areas along the femoral shaft producing age estimates statistically different for most of the midshaft and mid-distal shaft sections likely to be produced by muscle attachment strains (Sobol et al., 2015). A comparison of the estimates obtained through all the sampling locations and the original study midshaft location suggested the use of the anterior portion as the suitable area due to less variability

along the femoral shaft length, although other studies reported different results (Tersigni, 2005). This type of research highlights the importance of validating existing studies, to correctly apply the methods and ensure accurate results.

Several studies have also examined whether spatial variation or the means of variable quantification (e.g. stained or unstained section or counting versus percentage parameters) might have an impact on the reliability and feasibility of histological aging methods on long bones.

Spatial variation was investigated by Iwaniec and colleagues (1998) who sampled several subareas from a total area of 60 mm^2 of the anterior midshaft femur of 35 Inuit and Pueblo agriculturists. The sampling area was divided into columns, and intact and fragmentary secondary osteons were counted to calculate osteons density. The results suggested that small portions of the midshaft representing only 15% of the total area sampled could predict up to 95% of the total OPD, although more or less representation was reported given specific sub-areas. Thus, reducing the observed bone sampled might be feasible and advantageous implying less data collection quantity and time, and lower observer error. Some authors disagreed by considering that a reduction of the area read as an increase of the error (Stout 1989). Whether this pattern is also observed over the entire cross-section topography in large bones such as femora needs further investigation.

A technical approach performed by Martrille et al. (2009) investigated both thin-section staining and aging regression analysis on midshaft femora of 59 specimens. The authors advised that specific staining may facilitate the observation and interpretation of the histological features that are frequently difficult to discern. Computed tomography is applied for reading automatically the variables through microphotographs of 20 different subperiosteal fields. The authors recommended the use of multiple fields, although unfortunately, no detailed topographical description was provided. The highest correlation with age for all ages was reported for fragment secondary osteon density over 20 fields and the most accurate estimates were obtained for age cohort less than 70 years old. Watanabe et al. (1998) examined whether the quality of osteons observation was dependent on thin-section preparation procedures reaching the conclusion that features demarcation was optimised with a specific staining. Osteon perimeter showed the highest correlation with age while stepwise multiple regression provided the best combination of variables (fragment counts, osteon perimeter and Haversian canal

length) with a reported standard error as high as 6 years from known age. As the previous study stated, this research found higher standard error among the oldest age cohorts.

Parameters quantification were explored through body size and percentage of non-remodeled bone on three sampling locations on the most anterior part of 162 Dutch femora (Maat et al., 2006). A new approach in microscope lighting is explained and used to identify the lamellae. Inter-observer error seems to be low although inexperienced observer disagreement was remarked which was reported by previous studies (Lynnerup et al., 1998). Micro-anatomical differences of bone between sexes were not statistically significant; yet, adding cadaver length to the equation improved the SEE to ± 9 years supporting, other studies (Stout et al., 1994).

A sample of 72 Korean cadaver femoral sections from individuals over the age of 35 years was analysed by using the previous staining procedures and a modification of Maat et al.´s method (Han et al., 2009). The histological variables were analysed and averaged on five subperiosteal areas of the most anterior part of the femoral cortex. As in the previous study, statistical analysis did not show any sex differences although there was a low representation of females under 50 years of age; a combined formula for males and females was generated using linear, multiple and stepwise regression equations with the best variables for age estimation including OPD and secondary osteon area. Keough and colleagues (2009) tested 10 histomorphometric variables on femora cores from a 146 South African sample of low socioeconomic background. Only six out of the ten variables used in the research achieved moderate to low correlation with age. Two variables showed statistical significance between sexes and the reported SEE was as high as 15 years suggesting than other factors rather than the expression of age in the histomorphometric variables may have affected the method´s accuracy. Poor health conditions have been proven to impact aging methods in other studies (Paine and Breton, 2006).

A considerably large sample of 328 femora from mixed ethnicity individuals was examined by Ericksen (1991) to create a new histological age estimation method using only the anterior cortex. Apart from the already mentioned variables, resorption spaces and type II osteons were assessed and both remodelled and unremodelled bone percentages were calculated on both photographs and

microscope views. In summary, remodelled and unremodelled bone were found to be respectively positive and negatively correlated to age and the overall accuracy rate was ± 10 years from known age which is slightly higher than previous studies. This research demonstrated higher accuracy provided by sex-specific equations. The author encountered variability in intact and fragmentary osteon frequencies with respect to sex depending on the age cohorts. Haversian canal number and area also showed sexual differences varying with age ranges in a study carried out by Thompson (1980). Moreover, another study found different levels of accuracy rates depending on sex with more reliable estimates produced by male histological features (Samson and Branigan, 1987). Despite Ericksen´s results (1991) are encouraging for further research and it provides the possibility of aging individuals of unknown origin, sex differences between different ethnic groups were not contemplated and bone remodeling rates differences due to inter-population variability are likely to alter the results (Cho et al., 2006). Additionally, if the sample age distribution is skewed towards old age with little representation of individuals under 50 years old, this will have an impact on histomorphometric parameters (Oursler et al., 2008). The study carried out by Mulhern and Van Gerven (1997) explored sex as well as age variation in femoral histological features on an archaeological Nubian population (N = 43). Macroscopic assessment was performed to create the individuals´ biological profile; eight sites along the femur midshaft cross-section (periosteal and endosteal) were sampled and 10 variables proposed by previous age estimation histological studies assessed. Regarding sex differences, some variations were observed in the number of intact osteons (higher in males than in females) and number of fragmentary osteons (reverse to the intacts). Females showed more resorption cavities and bigger osteons which produced a decrease in the number of intact osteons. These findings are in agreement with other studies on the same ethnic population (Martin, 1983). According to the authors, the sexual dimorphism reported on histological features could be explained by cultural factors related to sexual division of labour, and also may imply different biological responses to stress by males and females (Ruff et al., 1984). Caution must be taken when dealing with archaeological human remains with no documented demographic data as the macroscopic assessment might lead to certain bias when conducting individuals' biological profile.

The tibia has been used for developing age estimation formulae with results comparable to those obtained from the femur alone. As well as Kerley did in 1965,

Ortner (1975) explored age changes in the outer cortex of around 101 tibiae ranging from 18 to 88 years old finding the highest correlation with age for complete osteons frequencies; yet, secondary osteon counts were computed as percentages and no change in relation with age was observed. Uytterschaut (1985) used also osteonal bone percentage by applying Ahlqvist and Damsten´s femoral method (1969) on tibiae (and femora) from a Dutch cadaveric sample (N = 20) obtaining accurate results. Furthermore, their formula on the tibia had one of the highest correlations achieved by histological aging techniques (R = 0.95) although this outcome could be due to small sample size. Thompson and Galvin (1983) removed tibial bone cores from an autopsy sample of 53 individuals from European and African American ancestry. The authors applied cortical thickness, bone density, frequency numbers and metrics from secondary osteons and Haversian canals. A slightly higher error in the estimates than the previous study was reported – maximum of 10 years from known to estimated age for all individuals. Differences between specific parameters were found depending on the age cohort (under and over 35 years old) suggesting that two regression formulae should be used if age group can be determined. No sex or inter-population differences were examined although representation of each group was certainly uneven, and thus, this analysis would have been misleading. A pilot study was performed on a small tibia sample in order to explore spatial variation within cross-section over four anatomical sampling sites (Blatch, 2012). The result demonstrated that the higher OPD and remodeled bone values were observed on the anterior area and on the mid-cortical location for the four quadrants. As occurs with the femur, tibia cross-sections present a problem due to the amount of cortical bone needed to be read. Other studies performed on lower limbs agreed on the fact that remodeling variability may have an effect on age prediction equations and caution must be taken when selecting sampling area (Pfeiffer et al. 1995).

Upper limbs have also produced accurate age estimates. Yoshino et al. (1994) sampled cores from proximal diaphysis of the humerus obtaining a SEE of 6 years when eight variables were included in the aging equation. Even if accuracy was high, the assessment of such a high number of variables may introduce error for anthropologist without experience in microscopy. A bigger sample and the inclusion of female individuals are required to corroborate their results. Histology on the humerus was used in addition with other anthropological techniques to create the biological profile of a South African Neanderthal specimen (Pfeiffer and Zehr, 1996)

demonstrating so the further applicability of aging histological methods on paleo-anthropological research.

All long bones were included in a recent study conducted by Nor et al. (2014) on 50 Malaysian males. The authors incorporated both histological and morphological parameters and the lowest deviation from estimates and known age was provided by a formula that included both analytical approaches and it is applicable to both upper and lower limbs. Reliability of the variables was examined on three observers with different anthropological backgrounds and osteon counting was the only parameter that showed slight discrepancies. Although the formula produced error within the range of other histological studies results, the inclusion of females is required for further verification of the results.

In a study performed by Thomas and co-workers (2000), femoral histological analysis on bone porosity plus macroscopic measurements were included with the highest correlation with age produced when these variables were combined with sex, height and weight parameters. The combination of histological and macroscopic parameters has shown to increase the accuracy of aging methods somewhere else (Stout et al., 1994).

Table 3.1 Summary of selected histological aging studies on long bones and mandible.

Author/year	Population / Age Range (mean)/N/ sex distribution (M,F)	Bone/s	Variables/sampling	Nº of fields and field location	R (minimum and maximum)	SEE (years, minimum and maximum)
Kerley (1965)	Caucasoid and Black/ 0-95(41)/126/88,29,9	Femur, tibia and fibula	Intacts and fragments, % lamellar bone and non-Haversian canals on four fractions	Four fields on anterior, posterior, medial and lateral outer cortex	0.92/0.92/0.97	5.27 - 13.85
Ahlqvist and Damsten (1969)	?/? (55)/20/?	femur	% of intact and fragmentary osteons, and % of lamellar bone and non-Haversian canals	adjacent to periosteum (4 fields)	0.96	6.71
Samson and Branigan (1987)	Caucasian/16-91(?)/58/31,27	femur	Haversian canal number and diameter	Not specified (2 fields)	n/a	6(M) - 16(F)
Singh and Gunberg (1970)	?/39-8(62)7/59/59,0	femur, tibia and mandible	Intact osteons, number of lamellae per osteon, Haversian canal diameter	outer third of the cortex (2 fields)	0.89 - 0.96	2.5 -5
Thompson (1979)	Caucasians/30-97(71)/116/64,52	femur, tibia, humeri and ulna	19 variables (see original article)/ various sampling locations	adjacent to periosteum (4 fields)	0.42 - 0.74	6.21 - 9.5
Ericksen (1991)	Mixed ethnicity/14-97(62.7)/ 328/174,154	femur	Osteons intact and fragments, Type II osteons, resorption spaces and non Haversian canals	adjacent to periosteum (5 fields)	0.48 - 0.72	9.96 - 12.21
Han et al. (2009)	Koreans/ 35-94(68)/72/44,28	femur	OPD, Haversian canal, cortical width, osteon area average	anterior midshaft (5 fields)	0.29 - 0.78	6.6 - 13.68
Yoshino et al. (1994)	Japanese/23-80(47)/40/?	humerus	10 variables (see original article)	proximal (5 fields)	0.78 - 0.90	6.1 - 8.8

SEE= standard error of the estimate; M=male, F=female

3.3.2. Ribs and short bones.

Ribs were selected by many researchers as a suitable bone for histological analysis in view of the following assumptions (Table 3.2). Although costal elements undergo constant stress due to breathing; physiological stress on respiration is common to all humans indicating that variation in remodeling rates among individuals might be minimal. Moreover, costal elements are not subjected to high biomechanical loading like it occurs with weight bearing bones as the femur (Crowder and Rosella, 2007). Many clinical studies were carried out during the 50´s and 60´s using ribs because they have an ideal location within the human body that was suitable for bone biopsies in living individuals (Crowder et al., 2012). Consequently, extensive clinical research on rib normal physiology and pathological conditions was done on early and recent studies (Sedlin et al., 1963; Epker and Frost, 1965; Wu et al., 1970; Keshawarz and Recker, 1984). Other advantages of thoracic bones are their easy extraction in autopsy procedures, the non-inclusion of ribs in the standard osteological analysis – e.g. metrics, and the feasibility of assessing the entire cross-section owing the relatively small amount of rib cortical area in comparison to upper and lower extremities (Streeter, 2012). For valuable archaeological specimens for which destructive procedures must be avoided, sampling a rib cross-section is more feasible than sampling a long bone. One more advantage is the possibility of recovery due to the number of ribs found in the human skeleton. One specific limitation of the costal elements is that due to their fragmented nature complications arise from the identification of sampling area and/or rib number, matters that have been tested by some studies as it will be discussed shortly.

Wu et al. (1970) performed a study on Haversian bone formation rates on the 6th rib. Such rates can be calculated based on annual bone formation. This rate is defined as the histologically observed osteon frequency on a given sample and the previous existing osteons not visible at the time of death -computation of missing osteons removed by remodeling activity averaged by the number of years that the osteons took to form. Considering rib cortical transverse drifts during bone compacta formation, the effective birth of rib adult cortex is estimated to be 12.5 years which may differ depending on the given sampling site. A comparison among healthy specimens with those suffering from diabetes, osteoporosis or osteogenesis

imperfecta, as well as with animal bones, demonstrated how pathological conditions produce lower bone formation rates than in healthy individuals.

One of the first aging histomorphometry studies using the 6th rib midshaft was the research performed by Stout (1986) who estimated age-at-death from human remains believed to belong to the Spanish conqueror Francisco Pizarro. The author applied common histomorphometric variables used for aging and additional age related indicators like total osteons creation (estimation of bone remodelling activity – osteons created – through the individual´s life spam), calculation of rib effective age of adult compacta (computed by subtracting 12.5 years from estimated age) and annual creation frequencies (rate of total osteons and Haversian bone creations) (Wu et al., 1970). The histological analysis provided an approximate age of 64 years old (60-69 age range) which is in accordance with the macroscopic observation and records of the deceased. Unfortunately, not much information about demographics, accuracy or even the applied regression formula is provided by the author making comparison with the upcoming studies on the field impossible.

Stout and Paine (1992) assessed histological variables on a sample of 40 ribs and clavicles from a mixed ethnicity American sample with documented sex, age, race and cause of death. The authors generated single and combined bone formulae. Four variables were taken into consideration and the microscopic field examined included the entire bone surface. The results showed standard errors between known and estimated age of -2.7 to +9 years for the rib, and -8.1 to +20.6 for the clavicle, with the combined formula producing errors of -2.5 to + 14.5 years. The entire sample except for one individual fell within 95% of confidence interval. The validation test resulted in highly accurate age estimates. No sex differences were reported although the sample was biased towards male individuals. In 1996, Stout and colleagues (1996) tested the clavicle formula developed by Stout and Paine (1992) on 19th century Swiss individuals to verify whether a different population sample would provide estimates falling within the error rates reported by the original method. The results confirmed a decrease in the accuracy for individuals over 40 years old arguing age distribution differences between reference and target samples as the cause of the high error rates. A new formula combining both samples was provided and recommended for estimating age. Clavicle has been used by other authors to generate population specific standards. OPD, osteon area and relative cortical area parameters were applied on Korean cadavers with the two

first variables being selected as the best indicators to estimate age through stepwise linear regression (Lee et al., 2014). Age estimate errors were similar to those reported by Stout and Paine (1992). Other authors further confirmed clavicles as good skeletal elements for histological age at death (Sobol et al., 2015).

Stout et al. (1994) used multiple criteria by the incorporation of age metamorphosis of rib sternal end and histological assessment of bone microstructures (Isçan et al., 1984a; 1984b). Two estimation formulae were generated using the original Isçan´s sample: one only uses histology and the second applies both analytical methods. The multivariate equation provided more accurate results (SEE = 7.18) than any of the other methods by themselves suggesting than a multiple approach may decrease the error as shown somewhere else (Stout and Gehlert, 1980; Dudar et al., 1993). The combination of micro and macro approaches reflects different age factors, and so, they complement each other for the final estimate. Dudar and colleagues (1993) showed a clear improvement when estimates obtained through gross-examination and histological analysis are averaged avoiding the over and under-estimation produced by the two separate approaches.

Cho et al. (2002) generated population specific formulae from a sample of 154 known African-American and European-American individuals based on three variables (OPD, relative cortical area and mean osteonal area). They concluded that group ancestry accounts for differences on the assessed variables, and consequently, separated equations were generated to improve accuracy levels. The performance of the parameters found in this study supports clinical research concerning differences between white and black populations (e.g. Schnitzler 1993). A study conducted by Cho and colleagues years later deemed to examine whether differences among the mentioned variables and additional histomorphometric parameters exist, and a deeper understanding of remodeling rates variability between sex and ethnic groups was provided (Cho et al., 2006). The results showed interesting variation between both sexes within and between populations, which will be discussed later in this chapter.

Pfeiffer and co-workers (2016) selected 216 mid-thoracic ribs from a South African sample made up by genetically-diverse individuals and different representation of socio-economic backgrounds. The variables assessed by Cho et al. (2002) were assessed and their aging equations validated on the South African

sample. The outcome shows promising results in terms of bias and accuracy with the best performance given by Cho et al.´s unknown-ethnicity formula (2002), with the other two aging equation showing a tendency of under and over-estimation of individuals. Population-specific formula developed from the South African sample did not provide higher accuracy rates, suggesting that for the Kirsten Collection no population specific formula is required.

In contrast with this study, authors developed population specific standards for different populations in order to overcome intrinsic factors influencing bone remodeling rates between populations. Kim et al (2007) used 64 fourth ribs from forensic cases to develop a method to estimate age on Koreans. The authors shifted the sampling area to the sternal end and used as a categorical variable known/unknown sex. Seven variables were tested for generating the most accurate prediction formulae. The results show that histomorphological variables like osteon area and relative cortical area differ significantly between males and females. From all variables, only relative cortical area showed no statistical significance with age for the entire sample, and the strongest correlation was found for OPD and osteon area for both separated and combined sexes formulae. The equations were applied to a validation set of 19 cadavers with 84% of the individual following within ± 5 years for real age, although accuracy rates decreased for over 60 years old individuals (> ± 5 years). This trend was also present for males and females separately (both sex known and sex unknown variable) and reported somewhere else (Martrille et al., 2009). Furthermore, it was confirmed that not only old ages have an impact on accuracy rates but also the inclusion of sex in the equation produce more accurate estimates. Similarly, separate sex equations were developed from a Polish cadaveric sample using osteon density as a single variable reporting similar correlations between sexes and the variable under consideration (Bednarek *et al.*, 2009); unfortunately, the authors did not provide any standard errors of the estimate. These results are not consistent with Kerley (1965) or Stout et al. (1994) – among others – who did not report any sex differences and consequently mixed sexes formulae were generated. Furthermore, the application of other existing equations developed from American populations (Stout and Paine, 1992; Cho et al., 2002) onto the Korean sample resulted in error rates greater than the reported by the original papers bringing into attention the need of Korean population-specific standards. This pattern has been noted in other validation studies in which existing equations were applied on population not closely related to the reference sample

showing a decrease in accuracy levels in the age estimates (Dudar et al., 1993; Pavón et al., 2010).

Not only inter-population variation might increase error estimates, but also rib OPD asymptote suppose a limitation for age estimation in advanced age individuals. This issue was investigated by Goliath et al. (2016) through the assessment of osteon densities, and osteons shape and size on a sample of 27 femora and ribs. None of the variables were correlated to sex except for osteon circularity, while all of them were correlated to age. The increasing rate of osteon circularity with age might be a mechanism to stop the higher frequency of microcracks propagation common in older individuals (Britz et al. 2009). The results are promising with an error from known age of around ± 6 years using just one parameter. The authors confirmed the use osteon circularity for individuals over 50 years old even though a bigger sample is needed to confirm these results.

For the purpose of age estimation, some studies were conducted to explore methodological issues such as sampling area, rib number selection, diagenetic processes or application of the technique on fragile archaeological assemblages.

Cannet and co-workers carried out different methodological approaches on fourth ribs sternal segments from a sample of 80 individuals (Cannet et al., 2011). Ribs were stained and the assessment carried out through ten microphotographs taken from external and internal cortical areas, respectively, to investigate whether parameters distribution variability exist. Most of the variables did not show statistical differences between the two sides of the cortex, and OPD on the internal rib portion was found to be the best age indicator using discriminant function analysis. The internal rib region was also found to be larger and with more homogeneous osteon orientation than the external side most likely due to biomechanical variation resulting from muscle attachment. In summary, the highest classification accuracy was produced by OPD for the youngest age range (30-39 years old) which is in agreement with previous cited studies reporting also more accurate estimates for the young cohorts (Kim et al., 2007). Repeatability of the method was corroborated although osteon number and Haversian canal density were statistical significant between two of the observers. Further inclusion of more females (N = 18) in the sample will validate these results.

Sampling variation was explored by Crowder and Rosella (2007) to test whether OPD variability is remarkably different between cross-sections from the same individual, and between 3th to 8th ribs in relation to the commonly used 6th rib. OPD variation within the same individual was found to be fairly similar although bias and lower values than those obtained from the standard costal element were reported; interestingly, the highest deviation was produced by the 8th rib. Regarding inter-individual variation (OPD for equivalent rib numbers different from the sixth among specimens), no error would be expected in estimating age using costal elements from the 3th to the 7th with the last two ribs being the most accurate. The authors suggest that the main cause of the error produced by 8th ribs might be related to muscle attachment resulting in different biomechanical remodelling. In summary, intra-individual variation produced higher bias from the 6th rib OPD than inter-individual variation indicating that deeper examination of intra-remodeling variability needs to be undertaken.

The taphonomic condition of the remains also affects age estimation techniques. Absolonova et al. (2013) conducted an experimental study to test the feasibility of observation of age related changes in burnt ribs. Bone microstructure changes due to fire induced destruction as well as differences between sexes were tested on 28 variables. Most of the parameters were unobservable after certain level of heat with intact osteons and Haversian canals being the features less affected. Moreover, sex differences related to advancing age were found only on specific parameters on the unburnt sample. Even if the number of females was scarce, these finding support other research outcomes (Ericksen, 1991; Kim et al., 2007). It is concluded that heat alteration on bone microstructures can lead to distorted interpretation of the histological parameters as fire modification replicate age-related changes. A recent taphonomic experimental study demonstrated significant microstructural changes both within the same individual and within the same skeletal element; it is suggested that bone tissue organization and composition, along with material clothes covering the remains, might play an important role in the expression of diagenetic modifications (Kontopoulos et al., 2016).

A Mayan rib archaeological sample was tested by Suzuki et al. (2009) to compare the macroscopic analysis with the histological approach. Two histological existing equations were used for aging the sample (Stout and Paine, 1992; Pavón 2007) with more accurate age estimates being produced by the Mayan method. The

histological approach showed a systematic overestimation of the juveniles and underestimation of the elderly, but when compared to the macroscopic techniques close estimates were obtained suggesting that both analytical approaches might be adequate. A rib modern sample of the same ethnicity was used for the generation of population-specific formulae producing a regression equation with a standard error of ± 6 years from known age (Pavón et al., 2010). Rib bone formation rates on ancient population sample were further examined by Stout and Teitelbaum (1976). Agreement between macroscopic and histological analysis was also corroborated in this study leading to the conclusion that bone physiology dynamics seem to prevail from *Homo Sapiens* to modern human specimens. Although microstructures were fairly observable, previous pathological conditions identified on these samples did not match with the histological analysis mostly because focal nonspecific infectious processes were probably not reflected on the thoracic cage. The potential of histology on paleoanthropological studies is confirmed in this study. However, considerations about the extrapolation of bone physiological mechanisms from extant to modern humans need further attention as bone structure variation related to differences in gracility patterns have been shown between prehistoric modern hominid species (Ryan and Shaw, 2015).

Table 3.2 Summary table of age histomorphometry methods developed using ribs.

Author/year	Population/ Age Range (mean)/N/ sex distribution (M,F)	Variables/sampling	Nº of fields and field location	R^2 (minimum to maximum)	SEE (years minimum to maximum) or accuracy level	Comments
Stout (1986)	?/?/?	see original article	6th rib, Midshaft?	n/a	n/a	Data used from Wu et al. (1970) and Frost (1969)
Stout and Paine (1992)	Mixed American/13-62 (28.6)/40/32,7	OPD	6th rib, midhsaft	0.69-0.77	3.9	Rib and clavicle
Stout et al. (1994)	White/11-88 (39,2)/59/?	OPD	4th rib, sternal end	0.69-0.86	7.2-10.4	Histology and sternal end
Cho et al. (2002)	European and African Americans/17-95 (50)/154/?	OPD, Osteonal Mean area, Relative Cortical Area,	6th rib, midhsaft	0.36-0.59	12.22 (RMSE)	Population specific and non-specific formulae provided
Kim et al. (2007)	Koreans/20-77(?) /64 /36,28	OPD, cortical area, relative cortical Area, average osteon and canal areas	4th rib, sternal end	0.82-0.83	4.8-4.9	Known and unknown sex formulae
Bednarek et al. (2009)	Polish/ 17-88(50)/ 54 /39,35	OPD	left 4th, midshaft	0.57-0.62	n/a	Sex separated equations
Pavón et al. (2010)	Mayan/20-87(43)/36 /34,2	OPD, cortical area, osteon size	4th rib, midshaft	?	6.2-12.8	Population-specific formula required
Absolonova et al. (2013)	Central Europe/19-95/162 (106,56)	see original article	3rd to 10th rib, sternal segment (1 to 4 fields)	0.33-0.70	11.9-15.7	Burnt and unburnt remains
Goliath et al. (2016)	European ancestry/39-82 (62)/27 (11,16)	OPD, osteon area, osteon circularity	standard rib, midshaft	0.65	6.05	Old individuals
Pfeiffer et al. (2016)	South African/17-82(48)/213/138,75	OPD, mean osteonal area, Relative cortical area	Mid thoracic rib, midshaft	0.28-0.35	n/a	No population specific-formula required

SEE= standard error of the estimate, RMSE: root mean squared error, M= male, F= female.

3.4. Factor affecting histological age estimation techniques

Histological age estimation methods rely on bone remodelling rates; the evidence of remodelling activity might be altered by intrinsic and extrinsic factors, and consequently, bias in the age estimates. The most relevant factors will be discussed in this section (Table 3.3).

Table 3.3 Summary table of some factors affecting bone remodelling rates (Adapted from Stout (1998)).

Chronological Age	Genetics	Biomechanics	Drugs	Disease	Others…
Adult compacta birth	Population variation	Spatial variation	Alcohol	Diabetes mellitus	Regional Trauma
Asymptote			Estrogen	Osteomalacia (rickets)	Local infections
Age related pathologies (e.g. senile or postmenopausal osteoporosis)			Corticosteroids	Osteogenesis imperfecta	Nutrition Physical activity
			Anticonvulsant	Paget´s Disease	Hormones

3.4.1. Inter-population Variation

Inter-population variation in remodelling rates is a result of genetics as well as environmental and cultural factors. Two important considerations related to age histological techniques and population specific standards are noted: since remodelling dynamics seem to differ between and within populations, higher errors have emerged from applying existing formula onto an unrelated sample with many researchers accessing to a variety of ethnic origin groups either to test the original method or to develop population-specific formulae.

Ubelaker (1977) used Kerley´s method (1965) on a modern sample from Dominican origin finding higher errors in the estimates than those reported by the original method. Pavón et al. (2010) tested Stout and Paine (1992) and Cho et al. (2002) formulae on ribs from a Mayan population. The first aging method provided reasonable age estimates for the main sample but produced errors around ± 11 years for the control sample, whilst the second methodology overestimated most of the individuals from both main and control samples again producing higher errors for the latter group. The authors suggest that net formation rate may differ between the

three samples due to higher OPD values in comparison to the reference samples. Further investigation is required due to sample size and sex skewness, although the two only females included in the sample fell within the variability produced by their male counterparts. The better performance of Stout and Paine (1992) could be attributed to the European-American origin shared by the two samples. Early studies have shown discrepancies in error rates for different ethnic groups (Thompson and Gunness-Hey, 1981); some recent studies, however, proved same accuracy rates for population-specific and existing formulae (Pfeiffer et al., 2016).

Broadly speaking, bone modelling and remodelling are determined not only genetically but also environmentally. Genetic factors determine bone microstructure in around 33-81% through the regulation of bone cellular machinery, and environmental factors seem to account for 19-61% of population variation; the added influence of specific individual´s life style on bone microarchitecture might also alter population variation and possibly modify heritability patterns within the population sample (Bjørnerem et al., 2015). A study on baboons shown that genetic variation accounts 48-75% of the phenotypic variance in intracortical microstructure variation at normal population-level (Havill et al., 2013). Regarding bone mineral content, depending on the ethnic group, genetic factors are estimated to account for 70–80% of the mineral composition during the early years of life responsible for bone development and posterior bone quality during adulthood (Anderson and Pollitzer, 1994).

In particular, bone turnover seems to be lower in trabecular and cortical bone for African Americans than white Americans having an impact on bone fragility associated with age (Schnitzler, 1993). Moreover, bone density and bone mass are higher in blacks compare to whites, and usually higher in males than in females (Broman et al., 1958). It was noted that cellular mechanisms responsible for bone formation differ between blacks and whites with cells producing a greater amount of growth factors associated with bone formation in blacks during developmental stages, and thus, incrementing general bone mass in this ethnic group (Bell, 1988). Nonetheless, different black-white bone dynamic patterns throughout the life spam could suggest a more complex phenomenon in regard to inter-population variation bone rates. According to the cited literature, African Americans have less risk of suffering from osteopenia in old ages as a result of the mentioned higher bone mass and denser cortical bone due to more subperiosteal deposition and lower endosteal

resorption (Garn, 1981; Anderson and Pollitzer, 1994; Baron et al., 1994), although some studies did not corroborate this. For example, Cho and colleagues (2006) reported that among all the groups, African American females were the only group showing significant expansion of the medullary cavity with age. In this study, most of the variables presented differences between ancestry and sexes. Yet, the relation between these groups and bone dynamics seems to be more complicated than just one group having higher bone remodeling rates than the other. The greatest differences were found between European American males and the remaining groups, especially this ancestry/sex group exhibited the higher bone turnover in young ages in comparison to African American females. Interestingly, European American males total and relative cortical area did not change with age –indicating that they maintain bone mass.

Another research examined osteon and Haversian canal area variability from ribs and femora obtained from 18th to 20th centuries English, Canadian and South African collections (Pfeiffer, 1998). A general trend of larger osteon size in femora than in ribs was found. Histomorphometric parameters differences were observed between the earliest English sample and the modern groups on both skeletal elements. Owing the genetic heterogeneity of the South African sample, it is suggested that environmental factors rather than direct genetic differences might be the cause of the observed variance encountering the non-genetic relatedness of the Canadian and the Cape Town groups (Pfeiffer, 1998). When different femur and rib formulae -mostly developed from American populations- were tested on a large number of individuals on the same English sample, only some histological methods demonstrated fair agreement between known and estimated age (Crowder, 2005); limitations related to biological variability as well as different statistical approaches or methodological issues were attributed as possible factors affecting accuracy rates.

Other ethnic groups, such as Chinese and Japanese population samples, have been revealed to differ demonstrating less cortical bone than American whites; Central American groups showed longer growth development periods than the other populations (Pollitzer and Anderson 1989). Assuming that growth rates are different between ancestries and maturation rates vary between populations, the mean age tissue will be higher or lower depending on the ethnic group and an impact on histological age assessment can be expected.

Cortical rib remodelling in three different archaeological populations and a modern sample demonstrated that although sex differences were not observed, a variation in bone remodelling parameters between the four sub-samples existed – with increasing rates over time (Stout and Lueck, 1995). The authors suggest different subsistence and cultural backgrounds as the cause. However, osteon creations differences in these samples could be a result of variation in skeletal growth cessation, and consequently, differences in effective age of adult compacta would be observed. In summary, although evidences of variability in life cycle spams between the different species of Homo were shown, whether age estimation is directly affected by bone remodelling secular changes need further consideration.

Archaeological samples from Native America displayed different remodelling rates with a higher bone turnover for Eskimos in comparison with Pueblo and Arikara samples indicating different dietary habits as a possible caused for this variability (Richman et al., 1979). Furthermore, when Eskimos from the 19th century were compared to modern White Americans, a higher OPD was reported (Thompson and Gunness-Hey, 1981). Bone mineral content variation between modern Eskimos and White Americans was observed with an earlier and higher age associated mineral loss for the Eskimo population sample becoming highly osteoporotic with advancing age –a fact observed also in Eskimos in the Artic area (Harper et al., 1984).

3.4.2. Sex related variation

Males and females present differences in body size due to sexual dimorphism (e.g. Kranioti and Michalodimitrakis, 2009). Age associated sex differences in endosteal and periosteal measurements are due to a higher periosteal bone apposition in males that balances the bone loss that occurs at the endocortical, trabecular and intracortical level with advancing age. This mechanism is not observed in females provoking an increase in bone stress levels and a decrease in bone strength ,and thus, stressing differences between sexes (Seeman, 2001). Ericksen (1979) reported a higher rate in femoral medullary cavity measurements for females than males throughout all age cohorts, as well as unequal remodelling observed through different femoral sampling sites probably in response to different topographical biomechanical stresses and metabolic demands. Examination of sexual dimorphism among ethnic groups demonstrated that while white males seemed to have larger medullary cavities than their black counterparts, black and

white American females showed different bone loss rates depending on the life decade. An overall higher expansion of the femoral cavity in the African American female group after the fifth decade was observed contrasting findings reported by other authors on the metacarpals (Garn and Shaw, 1977). These discrepancies could be attributed to different remodeling rates between different skeletal elements. For example, sexual and ethnical differences are larger in non-weight bearing bones than in bones subjected to weight strains probably because physical activity on highly active skeletal elements alters in the same fashion the bones, this being the result of the observed sexual differences (Pollitzer and Anderson, 1989). Therefore, caution must be taken when considering remodelling rates in different parts of the skeleton based on site specific effects.

Cho et al. (2006) agreed with Ericksen results (1979). Different values for OPD, osteon area and relative cortical area with age were found among all groups (separated by sex and African-Americans and European-Americans ancestries). Regarding sex differences, European males and African females were the sub-samples that differed the most, with this last group having the lowest OPD and therefore the highest bone density quality. Sexual dimorphism in rib size was confirmed by larger subperiosteal area for younger males from both ancestries. African-American females had larger relative cortical area to endosteal area in younger ages, being the cause of better bone quality in older ages when endosteal area is systematically reduced for all sexes. Conversely, African females at older postmenopausal ages had significantly higher endosteal expansion than any of the other groups. This seems to be balanced by lower intracortical porosity and larger relative cortical areas accounted in early years of life. The authors account ancestral biological differences due to genetic and environmental factors (e.g. lifestyle) as an explanation, although unequal sexes and ancestries distribution among the four sub-samples might have had an impact on the results.

Some factors would affect sex as well as ethnic groups. For example, femoral bone mineral density analysis was determinant of greater bone strength and bone density for black ethnic groups than for white samples. Nelson et al. (1991) studied the differences in bone density and the risk of osteoporosis on each group using principal component analysis. Differences in body size accounts for 50% of the variance in bone density for the two ethnic subsamples, and the results demonstrated that Black women have higher bone density levels than whites do,

and therefore they might have a lower risk of developing osteoporosis. These findings might be explained by biomechanical usage, hormonal activity or cultural and genetic differences between the groups. A higher muscle mass –observed in Black women- increments bone mass, and it is partly responsible of the greater bone mass in this group (Cohn et al., 1977). An interesting research was carried out to investigate the differences in cross-sectional geometry between U.S black and whites, and South African whites and blacks (Nelson et al., 2004). Bone strength in postmenopausal Black females from U.S. and from South Africa was higher than the two white samples for the same age cohorts and cross-sectional geometry comparison resulted in smaller endosteal cavities and higher cortical thickness in the femoral neck for blacks. The same ethnic groups in the two countries present less differences than different ethnic groups within the same country probably due to genetics influences being more determinant than environmental factors. Moreover, both black sub-samples showed greater differences between them than the two white subsamples which could be explained by migration history and admixture of the black population.

Histologically, both Haversian canal distance from the cement line and cement line diameter are measurements that reflect past bone formation activities, and their correlation in healthy human ribs indicates bone quality maintenance (Parfitt, 1979). Osteoporotic samples reflect bone formation rates diminishing in relation to the rate of bone resorption creating imbalance between both cellular activities (formation and resorption of each BSU creates a larger cavity than the BSU that is newly formed). Females over 40 and men over 50 years old are supposed to have a higher risk of osteoporosis due to this imbalance in remodelling rates on endosteal, Haversian surface and periosteal locations. For women in the premenopausal period, bone loss rate is about 0.76% per year compared to the postmenopausal group that have an annual rate of 1.39% due to estrogen deficiency and associated bone turnover imbalance. Recker et al. (2004) indicates that the rate at which bone remodeling occurs in females over 40-50 is not stable with a considerable increase in the first decade after menopause implying an increment in bone fragility.

Having all these facts into account, sex differences have been encountered and studied for anthropological examination of human remains concerning histological age estimation. Although clinical data is ambiguous, there is still an ongoing debate about how sex differences in bone remodeling affects males and

females in histological methods with some studies demonstrating clear differences and some not reporting any. In summary, the question still remains as how age estimation techniques accuracy rates may be decreased in groups of pooled sexes. Factors as menopausal effects (as shown earlier), sex differences in histomorphometric parameters (Tanner, 1978; Thompson, 1979; Burr et al., 1990; Ericksen, 1991; Mulhern and Van Gerven, 1997) and/or sex related variation related to maturation rates between males and females (Tanner, 1978) might be the key answer.

3.4.3. Other factors: pathology, diet and physical activity.

Pathological conditions have been shown to alter modelling and remodelling rates of endosteal, cortical and trabecular bone (Ortner, 2003; Robling and Stout, 2008). Consequently, the microscopic features will induce bias. Paine and Brenton (2006) demonstrated that a South African sample affected by malnutrition produced low OPD levels indicating a slowdown of the bone turn-over. Some researchers have included pathological specimens in their samples, with the assumption that some pathologies are certainly difficult to discern given an unknown individual (Ericksen, 1991); while others discarded pathological cases considering them as outliers for the regression analysis (e.g. Stout et al., 1994). Whether the inclusion of these specimens covers a wider range of remodelling activity on a population basis or actually decreases accuracy rates and reliability when developing an age estimation method is still an open debate.

Metabolic disturbances affect the rates of bone modelling and remodelling. There are specific conditions that are known to alter the histological variables observed in the aging methodologies. Activation frequencies are accelerated under osteogenesis imperfecta or hyperparathyroidism (HP) implying an increase in the number of BMUs created per year, and thus, producing higher OPD values and an overestimation of age at death (Robling and Stout, 2008). Furthermore, the pathognomonic of the HP known as tunnelling resorption could be differentiated and it might be used for diagnosis and observed histologically (McCarthy, 2010). Osteoporosis, that as a calcium deficiency can lead to secondary HP (Raisz, 2005), is commonly associated with age provoking an imbalance in bone formation and resorption and consequent higher bone loss. Moreover, it is attenuated by other factors as menopause, mechanical loading (e.g. disuse or extreme exercise) and population and/or genetic influences, among others (Brickley and Ives, 2008).

Females and males bone loss associated with increasing age accounts for the same rate (around 20-30%), but the factors aforementioned make the subjects (especially women after a certain age) more susceptible to osteoporosis related fractures (Riggs et al., 1998). Histologically, osteoporosis can be seen as an increase in the number frequency and depth of resorption spaces with failure of complete filling of the new created osteons. These patterns can be also observed in other metabolic conditions like vitamin D deficiency -provoking higher resorption rates to give calcium to the blood serum- or in osteopenia (Brickley and Ives, 2008). Moreover, postmenopausal women with osteoporosis are prompted to seasonal vitamin D deficiency triggering the acceleration of bone loss and an increment of poor mineralization (Brickley and Ives, 2008; Stein et al., 2011).

Histological age estimates can be also altered by fractures or local infections resulting in an increase of remodeling rates. According to Frost (1983), the so-called regional acceleratory phenomenon (RAP) would affect only a specific area of the bone surface while other areas will show no effects. If this is the case and just a topographic section altered by the RAP is interpreted, the estimates will not represent the chronological age of the individual (Frost, 1983; Robling and Stout, 2008). Van Der Merwe et al. (2010) described some examples of this alterations and how dry bone histology aids in the diagnosis of these condition. Likewise, increase porosity and Haversian canal size, and smaller osteon area produced by an increase in osteonal remodelling rates may be used as indicators for osteoporosis diagnosis and possible association with higher risk fracture (Squillante and Williams, 1993; Havill et al., 2013). However, caution must be taken since only a limited number of disorders will show pathognomonic features that can be observed on dry bone (De Boer and Van der Merwe, 2016).

Environmental factors such as physical activity may affect also bone modelling and remodelling, and the expression of histological features. The theoretical framework is called mechanotransduction consisting on the conversion of mechanical loading into a reaction of the bone cells that will lead to bone remodelling (Turner and Pavalko, 1998). Differences in bone architecture and cortical density were observed in lower and upper limbs depending on the population subsistence activity or between individuals with various activity levels (Stock and Pfeiffer 2001; Fritz et al. 2016). Burr and colleagues´ data (1990) demonstrated variation in histological features between archaic and industrial

populations ,as well as sexes, as a consequence of different dietary habits and subsistence activities. Histological changes like smaller Haversian canal size or greater OPD values suggest higher remodelling activation rates as a result of higher levels of physical activity. On the other hand, biomechanical effects of no-activity also affect bone external and internal architecture. A pilot study carried out by Inoue et al. (2000) showed how both acceleration in bone resorption and a decline in bone deposition causes bone loss in individuals under bed rest. Bone mineral densities are related not only to physical activity itself but also with type, duration, intensity and occurrence of physical activities with higher or lower benefits for bone quality depending on those factors (Morseth et al., 2011).

As it has been shown, physical activity have an impact on bone histological structures, and although further research is needed, differences between populations likely to be caused by occupational related activities have been reported. The remaining question is how to evaluate and measure the type, intensity and level of activity/strain that may or may not have occurred to actually produce significant differences in intracortical remodeling parameters, and therefore, be able to identify and interpret these variations in age estimation techniques.

3.5 Summary

Since the first studies in 1960, histological aging methods have experienced advances in standardization and in methodological approaches. Most of the bones tested for histological analysis were proven to be suitable for estimating age although intra and inter individual/population variation may be considered and further examined in order to fully understand variability in remodelling rates within and between samples. Upcoming research exploring histomorphometric parameters on different samples will provide deeper insight on how intrinsic and extrinsic factors can alter bone microstructure.

In this thesis, an in-depth histomorphometric investigation using ribs was performed on the two Mediterranean samples in view of exploring the factors and issues discussed during the course of this chapter; and to what extent, these considerations can have an impact on the age-at-death estimation method developed for the sample at hands.

Chapter 4 : MATERIALS AND METHODS

This chapter presents the material and methods used for the research undertaken in this thesis. To begin with, the skeletal material examined will be presented along with relevant demographic data about each sample. Next, a detailed description of the histological methodologies applied for the preparation of the rib cross-sectional slides will be provided. Last, the statistical approach used to assess the data collected will be presented.

4.1. Materials

The skeletal material consists of standard rib samples from modern skeletal remains collected from two Mediterranean samples. The Cretan sample (Crete, Greece) consists of remains acquired from the Cretan Osteological Collection (Crete, Greece) (Kranioti et al., 2008; Kranioti and Michalodimitrakis, 2009) and autopsy samples collected in the Pathology Division Department (University of Crete, Greece). The Cypriot sample consists of human remains collected from an ossuary housed in the Municipal cemetery of Limassol (Republic of Cyprus); this skeletal material comes from the Greek-Cypriot area of the island of Cyprus and it will be referred as Cypriots in this research (Kranioti et al., 2017). Demographic data for the entire sample used for this study is summarised in Table 4.1.

Table 4.1 Demographic data for Cretan and Cypriot study sample together.

		N	Age Range	Mean Age	SD	Skewness
Total sample	Males	40	20-89	60.1	16.52	-0.58
	Females	48	19-100	60.52	19.11	-0.24
	Total	88	19-100	60.33	17.88	-0.21

The costal elements sampled for this study share the same selection criteria. Thus, ribs were collected according to the following characteristics:

- Ribs must be in good preservational condition with no damage on the periosteal surface affecting the cortical bone of the rib. Slight damage of the periosteal surface was allowed if the cortical bone was still intact for observation of microscopic features.
- No trauma or evident pathological condition may be apparent. When the whole skeleton was available for macroscopic examination (occasionally in the Cretan sample and the entire Cypriot sample), all the skeletal elements must be also

examined for possible pathological conditions affecting other areas of the skeleton, and the individual must be discarded if the pathology was considered to have an impact on bone microstructure. Common degenerative changes were often observed on the skeletons and were not considered a criterion of exclusion but a result of aging.

- The third segment of the rib midshaft was the area of interest. If only a segment of the rib was available (see Cretan Collection sample section), the morphology of the rib was assessed with the specimen being discarded if the midshaft was not identified (Figure 4.1).

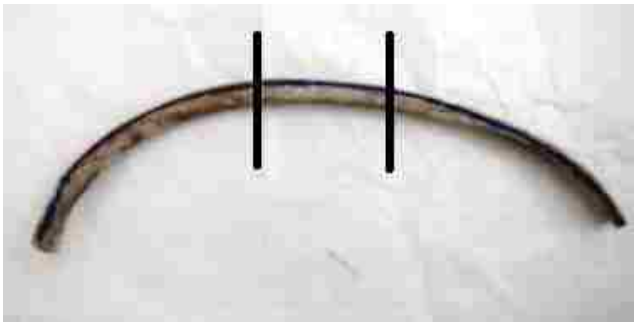

Figure 4.1 Third middle rib segment sampled (area of interest marked by horizontal lines, study sample).

- *A priori* the 6th left rib was selected. This criterion was accomplished by the examination of the entire costal element or shaft portion (if fragmented) through morphological characteristics of the rib. It has been demonstrated that histological age estimation can be reliably applied on ribs from the 3th to the 7th (both right and left) (Crowder and Rosella, 2007). According to this protocol, other standard ribs (4th -7th ribs) apart from the sixth left one were selected from the Cretan and Cypriot samples.

- Age at death and sex of the individuals must be known.

4.1.1. Sampling error pilot study: sub-sample set

An additional 36 rib sections were processed to test whether sampling sites along the length of the rib had an effect on osteon population densities observed through histological examination. Furthermore, the impact of sampling sites on the accuracy of two existing age estimation methods was investigated. Ribs from the Cretan Collection were collected based on the selection criteria, although for this study, the costal elements needed to be also complete along their length from the

sternal to the vertebral end with no apparent damage on the periosteal area. Due to the inclusion criteria, restrictions in sample size and sex selection were experienced and only female specimens were suitable. Six 4th ribs were selected and processed histologically. Age of the individuals ranged from 19 to 58 years old with the oldest individual being under 60 years old to avoid asymptote effects on age estimations (Mean age = 36 years old, SD =14.16) (Table 4.2).

Table 4.2 Sampling error sample demographic data (y.o.= years old).

Rib code	Age	Sex
Rib_1	19 y.o.	Female
Rib_2	27 y.o.	
Rib_3	29 y.o.	
Rib_4	35 y.o.	
Rib_5	46 y.o.	
Rib_6	58 y.o.	
Mean	36 y.o.	

4.1.2. The Cretan sample

Cretan costal elements were obtained from the Cretan Collection, a Modern Osteological Collection housed in the Pathology Division Department which is part of the Ministry of Human Rights and Justice located in Heraklion (Crete, Greece).

The skeletal material corresponds to a modern population (19th and 20th century) from two cemeteries, St. Konstantinos and Pateles, both municipal graveyards in Heraklion city. Heraklion is the largest city of Crete and it is the fourth largest in Greece giving the name to one of the four municipalities of the Crete Island. This prefecture was created after the beginning of the 20th century when the island of Crete joined Greece, and it experienced a population increase of 20% from 1980 to the beginning of 1990 (www.crete.gov.gr). The sample consists of males and females who were born in Crete between 1867 and 1956, and died between 1968 and 1998. In Greece, burial practices dictate that skeletal material must be exhumed after approximately 3 to 5 years unless a rental fee is paid by the family of the deceased in order to keep the remains in the cemetery grave. Otherwise, the Council proceeds to exhume the remains and they are either transferred to be stored in designated areas of the city or cremated (Kranioti et al., 2008; Kranioti and Michalodimitrakis, 2009). Dr Elena Kranioti received the permits from the District Attorney to perform anthropological analysis on them. Consequently, around 200

skeletons were collected, cleaned and stored according to standard protocols (Kranioti Personal communication).

Age at death for each individual is known from census records housed in the City Hall in Heraklion. Unfortunately, this information was not available for all the individuals. Sex was inferred by the examination of the names written on the boxes and was also assessed and corroborated by the macroscopic examination of the pelvis (Krogman and Isçan, 1986). Cause of death was obtained from the archives although this information is only available for a proportion of the individuals (Kranioti et al., 2008). Based on the information available, a number of individuals that migrated from mainland Greece, other Greek islands or other neighbouring countries were excluded. The collection consists of around two-hundred individuals with an age range from 6 to 100 years old (age = 70, SD = 16.11). Due to the high life expectancy in Crete (Males = 77.5 years old, Females = 82.6) (www.healthgain.eu/casestudy/crete-greece)(www.healthgain.eu/casestudy/crete-greece) the individuals from the Cretan Collection are inevitably skewed towards older ages.

A total of 60 rib samples from the Cretan Collection (approximately 5 centimetres of the entire rib) were received at the Archaeology Department in the School of History, Classics and Archaeology (SHCA, University of Edinburgh) by the author for performing histological analysis (see permits in Appendix A.1). Of the 60 rib samples available for assessment only 40 of them met the selection criteria. Most of them are discarded due to sampling area not corresponding to the specific sampling site chosen for this research and for pathological conditions seen through gross-morphology. Hence, a total of 40 ribs from the Cretan Collection were eventually selected for histological analysis and processed accordingly in the laboratory (see Methods section). Moreover, the author had the opportunity of performing macroscopic examination of some of the skeletons in order to confirm that pathological disorders were not present on the remaining skeletal elements. In some instances, while no specific pathologies were found through gross examination of the costal elements, the individual had to be excluded due to obvious pathological conditions that were observed through histological observation (see Appendix A.1). An under 13 years old male individual was also excluded due to cortical drifts during development and growth affecting the histological assessment of age. According to Wu et al. (1970), the effective age of birth of the adult compacta

occurs at this stage, therefore individuals under this age had to be removed from the total sample.

The final sample set comprises 34 individuals with a mean age of 60.55 (SD = 20.23) (18 males and 16 females). The mean age for males is 55.54 years (SD = 20.50) and females with a mean age of 60.23 years (SD = 20.50) (Table 4.3).

The second set of Cretan specimens consists of the middle third of the 6th rib collected during routine autopsies. The costal elements were obtained from forensic cases received at the Pathology Department, University of Crete (Greece) following next of kin consent for the study according to the protocol that was approved by the Ethics Committee of the University Hospital of Heraklion in Crete. A total of 14 individuals were first processed histologically. After the examination of the autopsy reports, seven of them were excluded due to pathological conditions and to avoid their possible impact upon the accuracy of age estimation (Paine and Brenton, 2006a). One specimen was identified as a non-Greek individual and therefore excluded from the final set (see Appendix A.1). The final autopsy sample consists of seven specimens with an age range from 20-69 years old (Mean Age = 42.57, SD = 20.61) with a total of five males and two females with a mean age of 37.8 (SD = 20.80) and 54.5 (SD = 20.50), respectively.

The total Cretan sample includes a total of 41 individuals (Males = 23 and Females = 18) with an age range from 19 to 98 years old (Mean age = 57.48, SD = 21.17) (Table 4.3). The sample age distribution corresponds to 24.4% of individuals from the 19-39 age range, 26.8% within the 40-59 age bracket and over 48% of the individuals over 60 years old. Figure 4.2 represents age distribution for males and females divided into age cohorts for the entire Cretan sample.

Table 4.3 Demographic data for the total Cretan sample.

		N	Age Range	Mean Age	SD	Skewness
Total Cretan sample	Males	23	19-89	55.54	20.50	-0.31
	Females	18	27-98	60.23	22.42	0.07
	Total	*41*	*19-98*	*57.48*	*21.17*	*0.25*

SD=standard deviation

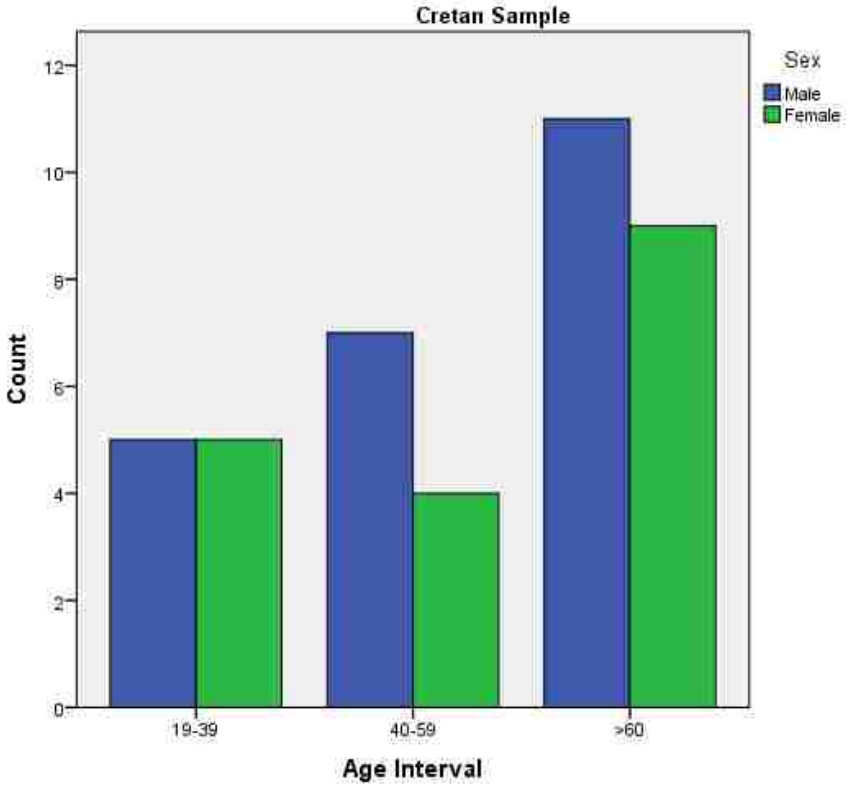

Figure 4.2 Age distribution for the entire Cretan sample by sex.

4.1.3. The Cypriot sample

The Cypriot Osteological Collection comprises approximately 200 individuals whose remains are housed in the Municipal Ossuary inside St. Nicholas Cemetery, in Limassol (Republic of Cyprus) (Kranioti et al., 2017). The individuals are part of the ossuary and according to the Cypriot burial custom, the remains are buried for five years, and after this period, exhumed and moved to the cemetery ossuary. Permit for access to the human remains had to be obtained from the Priest in charge of the Municipal Cemetery and all the documentation required was presented and access granted. This is a relative new osteological collection for

which research studies are being published (Almeida Prado et al. 2016; Cawley and Paine 2015; Kranioti et al. 2017; García-Donas, Ekizogu, Bozdag et al., 2017).

The skeletal material ranges from 1 day to 100 years old consisting of individuals who died between 1976 and 2003 and were buried in Limassol Municipal cemetery. Limassol is the second largest city of Cyprus. It experienced a considerable population increment after the division of Cyprus in 1974 when Greek-Cypriot refugees moved to Limassol (around forty-three thousand people). The development of urban areas provoked a population displacement from the countryside. In the 1980´s and 1990´s, further population increase resulted from other external factor such as the Lebanon war and the accession of Cyprus in the European Union (Edoc.coe.int/en, 2013).

The author personally collected the costal elements as part of a project funded by the University of Edinburgh (Challenge Investment Fund, SCHA). A total of seventy individuals were originally collected as being suitable for this research based on the rib selection criteria aforementioned. Each individual is kept in a metallic or wooden box with the deceased´s name written on it. As occurs with the Cretan collection, Greek names are either female or male so no confusion with the individual´s sex is possible. Based on the available demographic information and the deceased's surnames, individuals that were not born in Cyprus were excluded. Age at death was obtained from the archives. For some of the individuals, age was not available *in situ* but they were collected anyway in view of gathering this information through other sources (e.g. City Hall records). No clinical data are available for this collection but gross examination of all the individuals was carried out by the author in order to exclude those specimens with obvious pathological conditions.

All the costal elements were sent to the Archaeology Department (University of Edinburgh) and the samples were cleaned and prepared for histological examination. From the 70 ribs originally collected, age at death information was not available for 19 individuals, and thus, they were excluded from the final sample. Histologically, no obvious pathological conditions were observed but three rib samples were discarded due to taphonomic alterations that deemed microscopic observation impossible (see Appendix A.2). The only sub-adult individual in the sample was also excluded (6 years old). Thus, the total study sample finally consists of 47 individuals (M = 17 and Females = 30, Figure 4.3) ranging from 20 to 100 years old with a mean age of 62.81 (SD = 14.20) (Table 4.4).

Table 4.4 Age and sex distribution for the Cypriot sample.

		N	Age Range	Mean Age	SD	Skewness
Cypriot sample	Males	17	42-84	64.11	10.9	-0.08
	Females	30	45-100	62.06	15.90	0.16
	Total	47	20-100	62.81	14.20	-0.59

SD=standard deviation

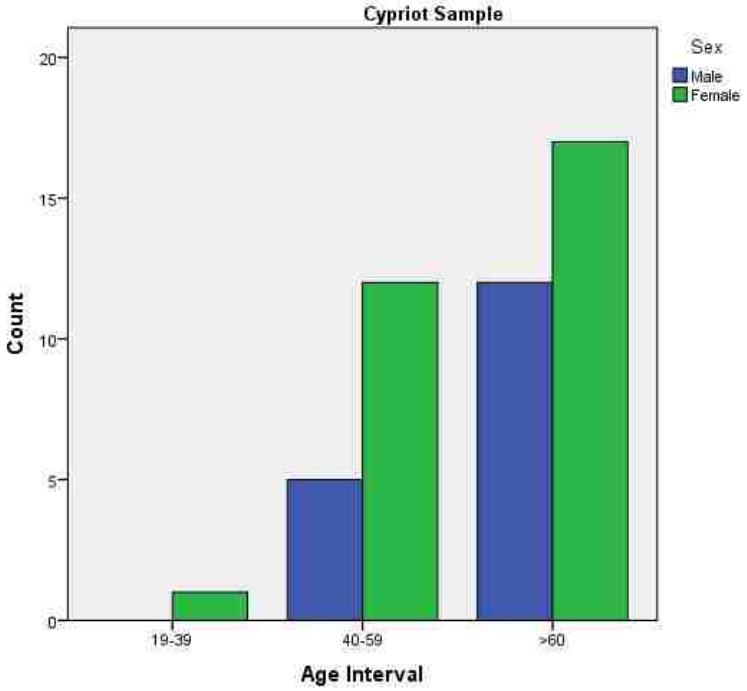

Figure 4.3 Age distribution of the Cypriot sample by sex.

4.1.4. The Mediterranean sample: Cretan and Cypriot samples

The original sample consisted of 105 individuals that were processed histologically for developing the age estimation method. The final sample (both Cretans and Cypriots together) consisted of 88 individuals, 40 males and 48 females (see Table 4.1); the mean age for the total sample is 60.33 with a standard deviation of 17.88. See Appendix A.3 for a detailed numerical description of individuals per decade.

The composition and size of the sample is inevitably determined by availability and criteria selection, and even though total sample sex distribution is fairly

balanced, age distribution for both population samples is skewed toward old ages (Figure 4.4 and Figure 4.5).

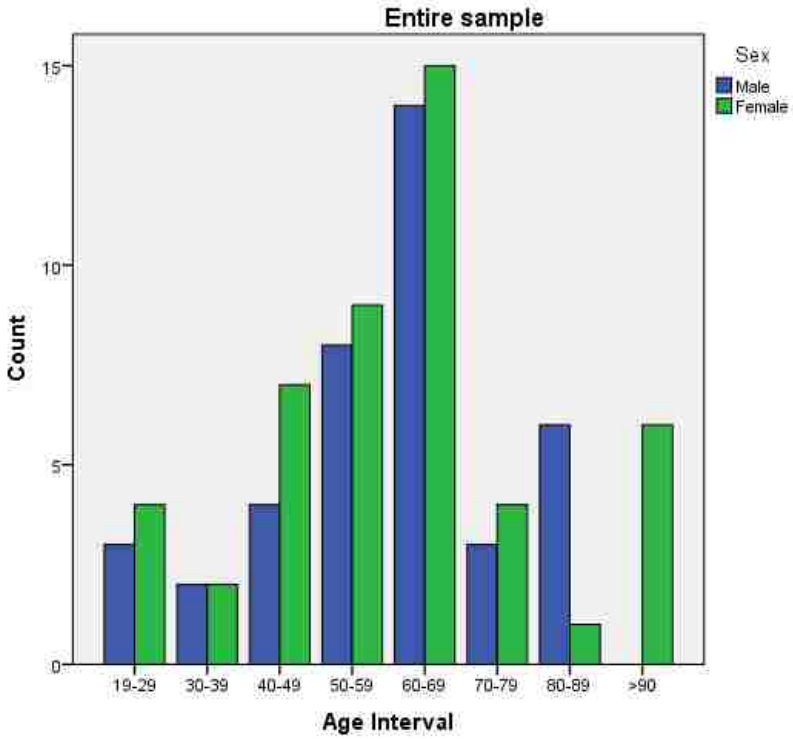

Figure 4.4 Age distribution of Cretan and Cypriot sample together.

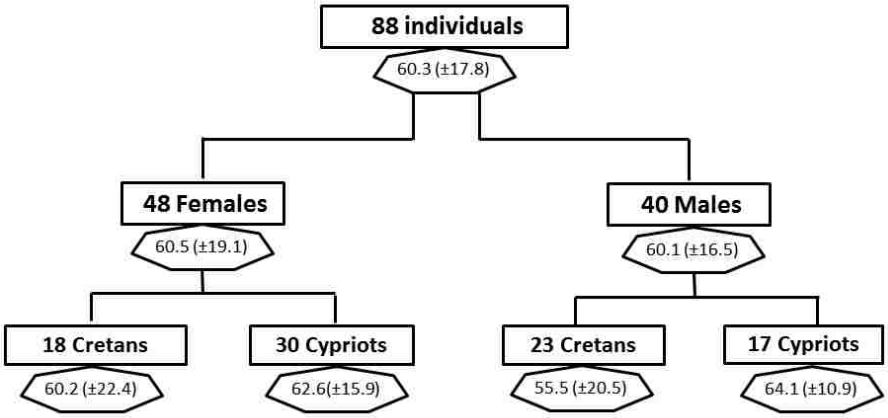

Figure 4.5 Entire sample composition based on sex and population samples with mean age and standard deviation for each (sub)-group.

4.2. Methods

4.2.1. Sample histological preparation

The preparation of the rib thin-sections was carried out in the Bone Histology Laboratory housed at the School of Anatomy (University of Edinburgh). The required Health and Safety documents and guidelines have been followed according to the University of Edinburgh *Health and Safety Department* (Safety Notes for Students working in teaching laboratories (BMTO); Archaeology Laboratories–Safe Working Practices (December 2012)) (www.ed.ac.uk/schools-departments/health-safety). The researcher has attended the *Health and Safety Seminars* provided by the University of Edinburgh for all laboratory users (February, 2013, 2014, 2015). Moreover, the required Control of Substances Hazardous to Health (COSHH) application forms based on the University of Edinburgh Regulations (2005) were submitted for the chemicals used during the process of thin-section preparation. All the required approvals were awarded.

Two histological techniques were used for the preparation of the thin-sections. The first sample set (most of the Cretan Collection sample and a small proportion of the Cypriot sample) was processed according to the technique described in Cho (2012) and Paine (2007) (named in this thesis *Methodology A*). A few modifications have been made in light of the available laboratory equipment and the option of using computer software for histomorphometric analysis. The second set of specimens (a small proportion of the Cretan Collections sample, the Cretan autopsy sample and most of the Cypriot sample) was prepared following a revision of petrographic methods for thin-section preparation (*Methodology B*) (García-Donas, Dalton, Chaplin et al., 2017). It is extremely important that all the steps described in this chapter will be carefully followed; the quality of the slides is crucial for the acquisition of the data. It is recommended for safety issues to have all the necessary tools and equipment ready before starting each step. Only one single section per specimen was assessed following standard protocols (e.g. Cho et al., 2002; Pfeiffer et al., 2016; Goliath et al., 2016); there is no improvement in age estimates when results from serial thin-sections are averaged, although it can be used to examine intra-individual variability (Crowder, 2005). Unless stated otherwise, Buehler equipment and consumables were used for the histological preparation (Buehler, Esslingen am Neckar, Germany).

4.2.1.1. Specimens preparation: *Methodology A*

a. *Rib preparation*

Ribs from each individual were received in properly labelled plastic bags. New codes and labels were attributed to each specimen as a necessary procedure for creating the dataset: information recorded included rib codes, collection point or origin, rib number, side, age, sex, rib description and additional information or comments.

The ribs were complete or fragmented, and in both cases it was imperative to select the specific area on which the cross-section has to be cut off. Once the desired area was identified, a rib segment was removed taking into consideration that the piece of bone had to fit in the space between the bone chuck and the width of the tank (IsoMet 1000 Precision Saw) which generally was not more than 7 cm. This first segment had an approximate length of 4 cm and was extracted manually using a Dremel 3000 variable speed multi-tool fitted with a diamond-cutting wheel.

Three sides of each rib –superior, anterior and posterior- were marked with different coloured permanent markers with the purpose of being able to identify the location area of each bone once they were processed. The colour code was as follows: blue represents superior edge, red corresponds to ventral area and green corresponds to cutaneous area (Figure 4.6).

Figure 4.6 Colour coding of ribs (superior, ventral and cutaneous surfaces, study sample).

If the skeletal material is fresh, it should not be necessary to embed the specimens in hard epoxy resin. However, as the sample included fragile specimens, like individuals of advanced age with bone with thin cortical areas, the embedding process was carried out on all the specimens ensuring the integrity of the skeletal material during the cutting procedure. Apart from protecting the bone from flaking off, the epoxy resin provides a better precision in sectioning and handling of the specimen. EpoThin Resin 1® and 2® are suitable embedding agents able to fill the voids, pores and cracks present in dry bone tissues. The embedding solution is a mixture of Buehler EpoThin resin and Buehler EpoThin hardener in ratios as specified by the manufacturer. The quantities of both chemicals had to be modified according to the size of the rib to be embedded. Attention must be paid when mixing both chemicals in order to prevent overheating of the substance and air-bubbles. The solution was left to settle for at least five minutes before embedding the skeletal sample.

The next step consists of encapsulation. Different sizes of hard and silicone moulds were used as containers for the embedding process. The selection of the container/mould depends on the size and shape of the ribs, and frequently modifications of the rib length might be advisable to make them fit into the molds. The sample was immersed in the mixture following these steps.

- First, a piece of paper with the code of the individual written on it was placed at the bottom of the mould to keep track of the rib code.
- Second, a thin layer of the mixture is placed over the paper covering the whole of the base of the mould.
- Third, the bone was deposited over this first layer.
- Last, the remaining solution was poured until the rib was completely covered by the EpoThin mixture.

After a maximum of 72 hours at room temperature (for EphoThin 1; EpoThin 2 curing time was improved to 9 hours at most), the solution was solidified. If the trabecular bone area had not been fully filled, a second deposition of resin must be done placing the rib vertically and making sure that the trabecular voids were now filled by the solution.

c. *Cutting and thin-sectioning preparation*

The embedded rib samples are now ready for the thin-section cutting process. The embedding resin can be grounded down to remove the unnecessary plastic from the sample and/or to modify the specimen shape if it does not fit the bone chuck (diamond grit paper can be used for faster grinding).

An IsoMet 1000 Precision Saw fitted with a 15LC diamond wafer blade (blade thickness 0.5 mm) is used for the generation of thin-sections. The tank of the cutting machine must be filled with approximately 60 centimetres of water, and optionally, some ordinary washing soap to ensure a smooth wet cutting and prevent damage from overheating. The specimen must be tightly held in the single saddle chuck suitable for rib bone size. The distance between the lever and the blade need to be adjusted to approximately 1 mm thick through the automatic distance control panel (it could be reduced up to 0.6 mm to minimise the grinding process).

c. *Grinding and mounting slides*

Before mounting the thin-section onto the grinding slide for continuing with the polishing process, the thin-section needs to be slightly polished on the corners to eliminate peaks or pointed edges that would not prevent the sample making contact with the grinding slide. Afterwards, the grinding slide is frosted using the MetaServ 250 equipped with a Vector 250 power head. Placing the slide into a petro slide holder, the frosting process is carried out by hand with the aid of coarse grinding paper (CarbiMet Abrasive Disc 80, P-600 mm), which is an abrasive disc used for polishing processes. Regulating the speed of the MetaServ (at approximately 150 RPM) and lubricating the sand paper with some water, the slide surface is ready to be adhered onto the slide.

The frosted slide is correctly labelled providing each specimen a case code. Permount Mounting Media glue (Fisher Scientific®) is placed on the slide and the thin section placed over the glue and pressed gently with a wooden stick. Then, it is covered with paper towel and the sample secured using two paper clips making sure that pressure is applied on the thin-section. Three to four days at room temperature are necessary for the adherent agent to dry.

d. *Grinding and mounting thin sections*

After removing the paper clips and most of the towel paper, the grinding slide is placed again onto the petro slide holder and carefully polished using the MetaServ 250 at a speed 150 with 400 grinding sand paper to a thickness of 70-50 µm. During this procedure, it is extremely important to evenly press the whole surface of the specimen obtaining an equally polished thin-section. It is recommended to check the transparency of the section under a transmitted and polarised light microscope until the desirable features are visible.

Once the thin section was readable, the grinding slide is placed inside a glass jar with Xylene (or other special glue solvent such as Neo-Clear®). An Ultra Sonic Cleaner (Buehler Ltd UK) water bath is used to help the dissolution of the glue through the agitation of the grinding slides. The jar is deposited inside the cleaner and left there for 5-10 minutes until the bone thin-section is released from the slide. It is then removed from the jar and left on towel to dry. The remaining xylene can be reused always following the Health and Safety requirements for hazardous chemicals.

The reading slides are correctly coded (case number). Permount glue is gently spread on the slide and the thin-section is placed on the glue. A small quantity of glue is again deposited over the thin section and a wooden stick is used to lightly press the section to the reading slide. A glass cover slip is deposited over the bone section to protect it from future damages. A maximum of two days are necessary for the glue to dry.

4.2.1.2. Specimen preparation: *Methodology B*

The revised method was incorporated after a training session (funded by SCHA) carried out by Ian Chaplin, an expert on thin-section production, at the University of Durham (England). The method was recently published (García-Donas, Dalton, Chaplin et al., 2017). It is a modification of published methodologies (Chinsamy and Raath, 1992; Beauchesne and Saunders, 2006; Tiesler et al., 2006; Paine, 2007; Crowder et al., 2012; De Boer, Aarents and Maat, 2013), adapted to the sample under study (dry-bone) and to the equipment and consumables available at the Bone Histology Laboratory (Edinburgh).

As *methodology A* and *B* shared common steps, they will not be repeated but just mentioned. Rib preparation and embedding are the same in both methodologies. Before the cutting process, one of the ends of the resin block was grounded using an UltraPrep 20 µm diamond abrasive disc fitted to a MetaServ 250. The end of the resin block needs to be as even as possible and clean from imperfections because this surface will be directly bound on the glass slide and observed under the microscope. For polishing this area, a silicon carbide abrasive disc fitted in the grinder-polisher is used. The grinding discs used ranged from abrasive (CarbiMet P1200 [FEPA]) to fine (MicroCut P2500 [FEPA]): initial polishing is achieved using an abrasive grade the polishing process is finished using a fine grinding disc (MicroCut P4000)

As in *Methodology A*, the glass slide needs to be frosted before the resin block is mounted. This procedure is performed by taking the plane slide and frosting the surface using a glass plate. Logitech 15 µm calcined aluminium oxide powder is spread over the glass plate and the plain grinding slide is frosted applying moderate pressure and some water. Once the surface is evenly frosted, it is ready to be mounted on the resin block. The frosted slide is cleaned with soap and water.

In this method, resin is also used as a mounting agent. A small quantity of resin is placed on the ground surface of the resin block and gently spread. This surface is then pressed against the frosted surface of the glass slide applying slight pressure in circular movements. It is recommended to use weighted bonding jigs to ensure that it does not lift while the resin is curing.

A glass slide chuck is used to cut the thin-section – in this case, a 27 × 46 mm slides chuck holder. A 1 mm thin-section was then cut using the IsoMet 1000. As a result, a section already mounted onto the grinding slice is now ready for polishing. For this final step, the same procedure as in *Methodology A* is applied for polishing the thin-section to a thickness of 70-50 µm. The final polishing is carried out using a MicroCut P4000 disc resulting in a clean and polished thin-section. A cover slip may be placed on the sample by again using resin as a bonding agent by following the same procedure explained in *Methodology A*.

4.2.1.3. Maceration protocol (Cretan Autopsy sample)

The autopsy sample is partially cleaned by an autopsy technician in Crete when the rib midshafts were extracted from the chest plate of the deceased. When

received in the Bone Histology Laboratory at the University of Edinburgh there were remaining flesh and bone marrow, and thus, cleaning and maceration procedures were carried out. The maceration procedure was performed in the Public Morgue (Edinburgh) following standard procedures. Previous removal of the adhering tissue before boiling is recommended. The samples are covered with clothing material and labelled and coded accordingly. Biological powder was used to boil the specimens with boiling time varying depending on the size of the sample and the amount of adhering flesh (a minimum of 40 minutes is required). After boiling, the tissue started to soften and could be easily removed manually using a scalpel. Special care must be taken not to damage the periosteal surface. The protocol was updated from other standards maceration procedures (Fenton et al. 2003). The biological material was disposed following the standard procedures from the University of Edinburgh (COSHH form).

4.2.1.4. Validation pilot study: sample preparation

For the validation study, thin-section preparation followed all the steps included in *Methodology A*. A modification of the first step was necessary in view of extracting the six thin-sections from the length of the rib. The entire length was divided into three equal sections (labelled as proximal (vertebral), medial (midshaft) and distal (sternal)) and two thin-sections were taken from each segment. In order to cover all possible sampling sites within each segment, the three equal sections were divided into two equal length fragments and the two thin-sections were extracted from the middle of the two portions (Figure 4.7). *A* total of 36 sections were produced for this pilot study (6 thin-sections per rib). The sections were labelled as follows:

- Proximal 1 (V1) and proximal 2 (V2) = most vertebral section (V1) and most sternal section (V2).
- Distal 1 (S1) and distal 2 (S2) = most sternal section (S1), more proximal section (S2).
- Midshaft 1 (M1) and midshaft 2 (M2) = most sternal section (M1) and most vertebral section (M2).

Figure 4.7 Preparation process for the pilot study sample: segment cutting for the extraction of six sections per rib (study sample).

4.2.2. Data collection

4.2.2.1. Rib parameters selection

Histological estimation of age in human cortical bone is based on the observation of age-related changes in bone microstructure patterns. The repeatability and accuracy of the parameters depends on the population under consideration, the criteria of the researcher and the research question. Ultimately, the target of this study is not only to find the best equation for age prediction on the Mediterranean samples, but also to find the most suitable equation based on method repeatability.

4.2.2.2. Histomorphometry

Unless stated otherwise, the abbreviations used for microscopic analysis were adopted from Parfitt et al. (1987); modifications have been applied in order to follow the recommendations and recent update from the American Society for Bone and Mineral Research Committee (Dempster et al., 2013). The following histomorphometric variables were collected (Table 4.5):

A. *Measurements related to osteon number frequencies and densities* (Figure 4.8):

A. *Variables related to osteonal structures*:

1. ***Intact osteon number*** (*N.On*): frequency number of intact osteons showing equal or more than 90% of the perimeter of the Haversian canal with no evidence of resorption (Stout and Paine, 1992). The following additional criteria were applied (Crowder, 2005; Heinrich, 2015):

-Two or more structures that shared a Haversian canal and there was no evidence (cement line) of two different events of bone remodelling but instead a single reversal line is observed. These structures were counted as one intact osteon.

-Structures that were connected by a clear Volkmann´s canal were counted as two separate osteons.

-Hemi-osteons appearing on the trabecular envelope as part of trabeculae plates were not counted as structures.

- Primary vascular canals (primary osteons) were not counted as single intact osteons.

2. ***Fragmentary osteons number*** *(N.On.Fg):* frequency number of intact secondary osteons that are a result of resorption due to subsequent deposition of osteonal structures having at least 10% of the Haversian canal perimeter remodeled (if present) (Stout and Paine, 1992). The following additional criteria were considered:

- Fragmentary osteons with the canal not present due to remodelling can be differentiated from the interstitial bone by the identification of the concentric lamellae, the concentric direction of the osteocytes and the reversal line with a clear and irregular margin. Observation of the surrounding osteonal structures and lamellar bone is recommended in order to discern this type of fragmentary osteons.

- Differentiation between interstitial lamellar bone and fragmentary osteons was achieved only if the previous criterion was observed; therefore, interstitial bone may include fragments of osteonal bone that cannot be identified due to posterior remodelling events removing the above-mentioned evidence.

**Drifting osteons* for both the identification of intact and fragmentary secondary osteons require special attention. This type of osteon is considered as stated by Robling and Stout (1999) as Haversian systems in which continuous resorption occurs on one side and continuous deposition occurs on the other producing an osteons that is surrounded by 4-8 concentric lamellae with one side showing an elongated “hemicyclically deposited tail” (Robling and Stout, 1999:193) . The length and shape of the tail is the result of transverse drift. When observing this type of structures, it is important to use both transmitted and polarised light while observing the tail of the drifting osteon; the continuous waves of concentric lamellae may appear as fragmentary osteons while in reality they are just continuous bone

formation of the same intact drifting osteon. There are cases in which the tail expands until it finds another previous structure and both osteonal systems overlap; in these cases, a clear cement line is observed delimiting the end of the drifting osteon tail and the beginning of the associated fragmentary osteon.

3. ***Total Osteons*** (N.On.Tt): the sum of secondary intact and fragmentary osteon numbers. As follows:

$$N.On.Tt = N.On + N.On.Fg$$

Note that the symbols used to refer to osteon population densities –both intact and fragmentary densities- differ depending on the authors (Kerley, 1965; Stout and Paine, 1992; Goliath et al., 2016). For this study, the abbreviation proposed by Robling (1998) about intact and fragmentary osteon densities (N.On and N.On.Fg, respectively) was not followed due to possible confusion with intact and fragmentary osteons frequency number; instead, it is used for denoting number of structures as recommend elsewhere (e.g. Parfitt et al. 1987). In order to make a clear distinction between number of osteons and osteon population densities, the abbreviated nomenclature from Heinrich et al. (2012) for intact and fragmentary osteon density will be used. OPD abbreviation was used for osteon population density as in Stout and Paine (1992) and Goliath et al. (2016).

4. ***Intact osteon density*** (OPD(I)) in number of osteons/mm^2: the number of secondary intact osteons per mm^2 (Stout and Paine, 1992). To calculate OPD(I), intact osteon number is divided by cortical area:

$$OPD(I) = N.On / Ct.Ar$$

5. ***Fragmentary Osteon Density*** (OPD(F)) in number of osteons/mm^2: the number of secondary osteons per mm^2. The number of fragmentary osteons is divided by cortical area:

$$OPD(F) = N.On.Fg / Ct. Ar$$

6. ***Total visible osteon density*** (OPD) number of osteons/mm^2: the sum of the number of intact osteons and the number of fragmentary osteons visible on the surface area sampled, corresponding to total number of osteons divided by cortical area as follows:

$$OPD = N.On.Tt / Ct. Ar$$

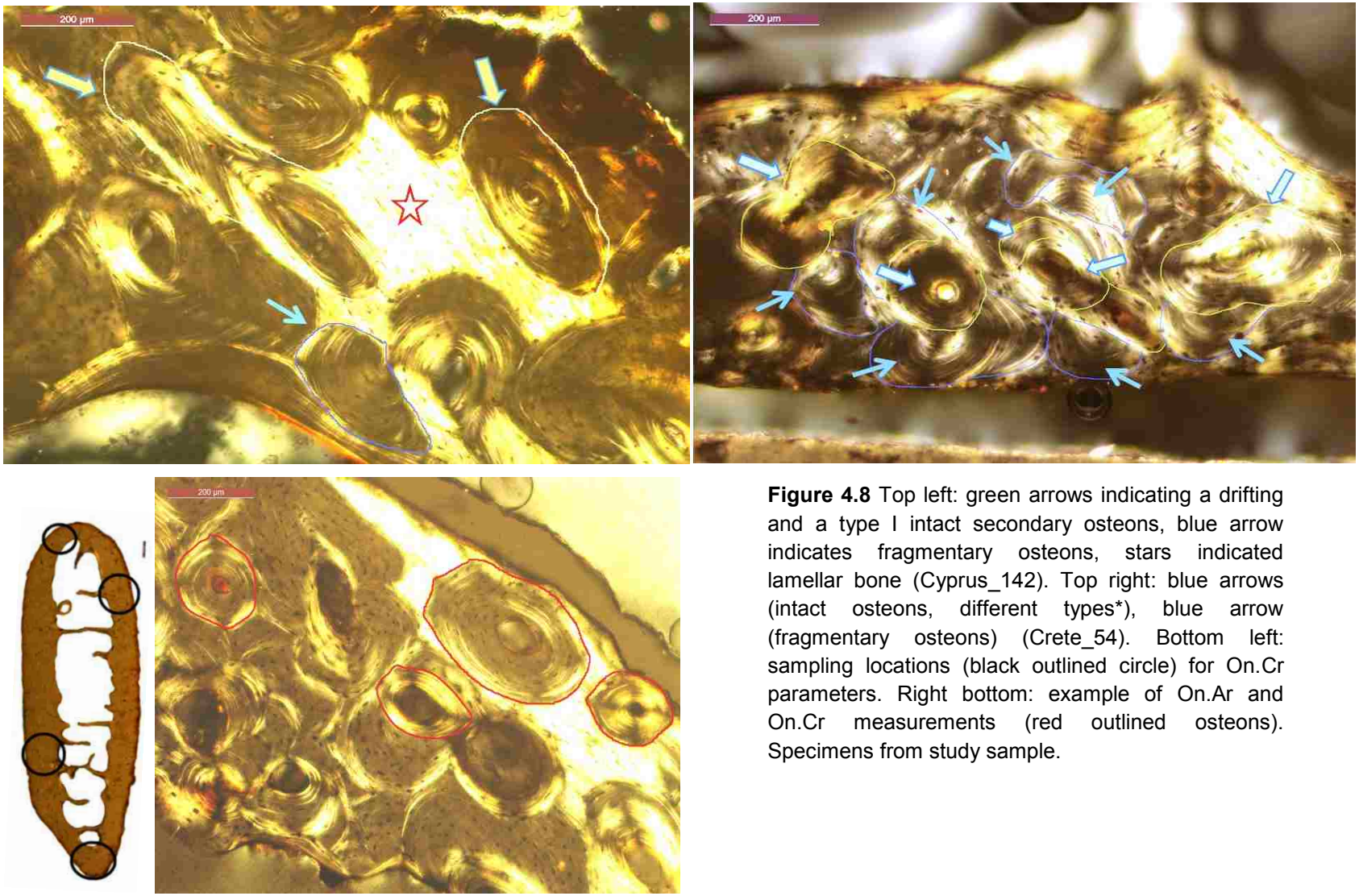

Figure 4.8 Top left: green arrows indicating a drifting and a type I intact secondary osteons, blue arrow indicates fragmentary osteons, stars indicated lamellar bone (Cyprus_142). Top right: blue arrows (intact osteons, different types*), blue arrow (fragmentary osteons) (Crete_54). Bottom left: sampling locations (black outlined circle) for On.Cr parameters. Right bottom: example of On.Ar and On.Cr measurements (red outlined osteons). Specimens from study sample.

B. *Measurements on bone surface related to cortical and trabecular bone areas* (Figure 4.9):

7. ***Cortical Area*** (Ct.Ar): amount of total cortical area sampled per section excluding the marrow cavity (cortical area per section, in mm^2) (Parfitt et al., 1987; Pfeiffer et al., 2016); it corresponds to the extraction of the endosteal area to the total area as follows:

$$Ct.Ar = Tt.Ar - Es.Ar$$

Where,

8. ***Total subperiosteal Area*** (Tt.Ar): the total bone surface that is surrounded by the outer periosteal perimeter, including cortical area, trabecular area and marrow cavity (Cho et al., 2006) (Figure 4.9).
9. ***Endosteal Area*** (Es.Ar): the medullary cavity space which corresponds to the area under the marrow cavity (Cho et al., 2006; Ruff, 2008). The endosteal area is defined as the limit between the cortical area and the trabecular area. This delineation is somewhat subjective, (e.g. Crowder et al., 2012). In this study, endosteal area is measured as shown in the microphotographs in Figure 4.9; the limitation is defined by intracortical remodelling being not obvious anymore and trabecular area morphology appearing at the endosteal limits.
10. ***Relative Cortical Area*** (Ct.Ar/Tt.Ar): the relative amount of cortical bone in the cross-sectional area. It is calculated as the ratio of cortical area to total area (Cho et al., 2006). It measures the amount of cortical area that is independent of absolute bone size (Stewart et al., 2015).

Figure 4.9 Rib Area measurements: blue outline (Total Area), green outline (Endosteal Area).

C. *Osteons measurements* (Figure 4.8):

11. ***Mean Osteonal cross-sectional Area*** (On.Ar) in mm^2*:* the average area of bone contained within the cement line of an intact osteon that has an intact cement line (including both circumferential lamellae and Haversian canal). Osteons showing Haversian canals deviating considerably from even circular profiles are excluded. For this parameter, the most circular osteon shapes were sought. In the case of drifting osteons, for example, no measurements were taken if the drifting osteon deviated considerably from circular shape (i.e. elongated tails) (Cho et al., 2002; Goliath et al., 2016). On.Ar is calculated as the average of a minimum of 25 to a maximum of 30 osteons with these characteristics within the entire surface area.
12. ***Osteon perimeter*** (On.Pm): the perimeter of the osteon area that corresponds to the area of bone contained by the cement line of an intact osteon (both circumferential lamellae and Haversian canal) (Thompson and Galvin, 1983). Osteons that deviated strongly from a circular shape are excluded. Mean osteonal perimeter is calculated as the average of the osteonal perimeter of a minimum of 25-30 osteons with these characteristics within the entire surface area.
13. ***Osteon circularity*** *(On.Cr):* the parameter is defined by the circularity index that reflects the similarity of a measured object to the shape of a true circle. The index ranges from 1 to 0, with 1 indicating a true circle and 0 referring to elongated shapes. As recommended by Goliath et al.

(2016), only osteons that had intact cement lines and round Haversian canals are measured. Due to strain differences in osteon shape depending on the cortical bone area (van Oers et al., 2008), different locations within the same surface area need to be sampled. A minimum of 25-30 osteons are assessed. The index is calculated as follows:

$$On.Cr = (4\pi\ (area/perimeter^2))$$

Note: For On.Ar and On.Pm, it is recommended to sample different areas of the surface of the rib in order to cover all different sizes along the morphology of the cross-section. For the On.Cr parameter, four topographical areas over the rib surface must be sampled: superior, inferior and cutaneous and pleural areas (see Figure 4.8). Approximately six to eight osteons were measured on each sampling area. Due to the advanced age of most of the individuals included in this sample and thinning in the cortical area due to osteoporosis, the osteons could not be found within these four topographical areas in some cases, and therefore other areas were sampled. Moreover, as the age of the individuals increased, the possibility of finding "structurally complete intact osteons" (Goliath et al., 2016:282.e2) became more difficult as remodeling event started overlapping with each other over the entire cross-sections. These concerns must be considered for future application of these parameters in old age skeletal samples.

Table 4.5 Summary of variables under consideration.

Variable	Abbreviation	Brief Definition	Author	Calculation	Data acquisition
1. Intact osteon number	N.On	secondary osteon number with at least 90% of the of the Haversian canal perimeter visible	Stout and Paine (1992)	n/a	Microscopy and photomicrographs: histomorphology qualitative observation)
2. Fragmentary osteon number	N.On.Fg	secondary osteon number with at least 10% of the Haversian canal perimeter visible or not present		n/a	
3. Total osteons	N.On.Tt	Sum of intact osteons and fragmentary osteons		N.On + N.On.Fg.	
4. Intact osteon density	OPD(I)	Intact osteon number divided by cortical area (#/mm^2)		N.On/ Ct. Ar.	
5. Fragmentary osteon density	OPD(F)	Fragmentary osteon number divided by cortical area (#/mm^2)		N.On.Fg / Ct.Ar	
6. Total visible osteon density	OPD	Sum of Intact osteons and Fragmentary osteons divided by cortical area (#/mm^2)		N.On + N.On.Fg/ Ct.Ar	
7. Cortical area	Ct.Ar	Cortical area sampled (mm^2)	Cho et al. (2006)	Tt.Ar-Es.Ar	ImageJ software (polygon selection tool)
8. Total area	Tt.Ar	Surface area including cortical and trabecular areas (mm^2)		n/a	
9. Endosteal area	Es.Ar	area occupied by trabecular bone (mm^2)		n/a	
10. Relative cortical area	Ct.Ar/Tt.Ar	Ratio of cortical area to total area (mm^2)		Ct.Ar./Tt.Ar.	
11. Osteon area	On.Ar	Area within the cement line of an intact secondary osteon (mm^2)	Cho et al. (2002)	On.Ar	ImageJ software (freehand selection tool)
12. Osteon perimeter	On.Pm	Perimeter of the area within the cement line of an intact secondary osteon (mm)	Thompson and Galvin (1983)	On.Pm	
13. Osteon circularity	On.Cr	Measure of the proximity of an osteon to a true circle (index)	Goliath et al. (2016)	(4π (area/perimeter2)	

4.2.3. Data acquisition: microscopy and photomicrographs

Data acquisition took place at the microscope laboratory in the Archaeology Department (SHCA, University of Edinburgh) and it was carried out by the author of this thesis. A standard research microscope (Leica DM750P with transmitted light) equipped with 4x, 10x and 20x objective lens and a 10x ocular lens was used to collect the histomorphometric data for each rib. These lenses are necessary for the interpretation of the parameters with the medium magnification being used for osteon counting switching from x10 to x20 objectives to have a better understanding of the osteonal microstructures (Crowder et al., 2012). The microscope has a polarising filter, and so, both transmitted and polarised light were used in order to discern more clearly the histomorphometric variables and recognise specific features such as intact and fragmentary secondary osteons cement lines. The light and the filter were manipulated by the researcher depending on the thin-section under assessment to adjust transmitted-polarised views. Several trials were performed for the researcher to become comfortable with both the parameters and the equipment; results were compared in order to adjust the microscope settings before carrying out the final assessment on each rib.

The Stout and Paine (1992) method consists of calibrating the microscope image with 10x oculars fitted with a standard counting reticule for area measurement and microscopic field delineation. This approach provided good results and is commonly used. For the present study a research microscope with a fitted camera was used for performing the histomorphometric analysis. It allows the researcher to capture photomicrographs of all the rib areas sampled and use image analysis software in combination with microscopic observation.

A Leica DM750P research microscope equipped with 4x, 10x, 20x and 50x objective lenses and 10x ocular lenses fitted with a Leica MC170 HD camera was used to obtain the microphotographs. A minimum of 30 and a maximum of 80 single high-resolution microphotographs (depending on the amount of cortical area) from the entire cortex of each rib were taken at both 40x and 100x magnification. The Leica software provides the user with the option of incorporating a digital scale on the images. The scale function was adapted accordingly depending on the magnification used. The 40x magnification microphotographs were used to create a complete cross-section montage by using the 'stitching' option provided by the software; the compound image incorporates a calibrated scale allowing

measurement collection. The 100x magnification microphotographs were used for the collection of single osteon measurements. The images were saved in TIFF format for post-hoc analysis.

For frequency number assessment (N.On and N.On.Fg) direct microscopic observation (as explained above) and microphotographs were used for collecting the data and ensuring the appropriate interpretation of the variables and accurate counting of structures. ImageJ software provides an option (multipoint selection) to create a permanent record on the image (numbered) as the structures are counted. This ensures that microstructures are not missed or counted twice by the observer.

In order to measure rib area parameters (Tt.Ar, Es.Ar, Ct.Ar) and osteon size and shape (On.Ar, On.Pm and On.Cr) a free software platform (ImageJ 1.48) is used to perform the measurements (Schneider et al., 2012). To calibrate the images, the researcher needs to convert from millimetres or microns to pixel counts the length of the scale incorporated in the image by using the 'Set scale' command in the software. Once the images were calibrated, measurements can be taken. Rib area measurements are performed using the 'Polygon selection tool'. A variation in the methodology was carried out for the calculation of cortical area parameter in the sampling error pilot study sub-set. A digital handheld microscope – a Dino Lite® – was used to take a picture of the entire cross-section and then ImageJ 1.48 was used to measure the area (Figure 4.10).

Figure 4.10 Dino Lite® photograph; outlined in black (A) trabecular area selection (study sample).

Osteon size and shape measurements were taken by using the 'freehand selection tool' and selecting the area and shape descriptors commands (see Figure 4.8 left bottom image for an example); each individual osteon is outlined (for area

and perimeter together, and separately for circularity) and the osteonal variables were then averaged.

Image capturing allows for the assessment of the histomorphometric variables and it is deemed to be a suitable viewing format for histomorphometric analysis as shown by Britz et al. (2009), Goliath et al. (2016) and Crowder et al. (2012).

4.2.4. Statistical analysis

The following statistical methods are used to answer the research questions presented in this thesis (Figure 4.11):

1. TEM analysis and Bland and Altman test are used to examine the repeatability and agreement between observers for the assessment of the histological variables.
2. Descriptive statistics and errors are calculated to explore the impact of sampling location on the age estimates.
3. Inaccuracy and bias along with other statistical approaches are used to verify whether four existing histological methods are suitable for the sample under study.
4. Different statistical tests are chosen depending on the nature of the parameters to assess the relationship between the histological variables and age. The outcome is taken under consideration for the next statistical analysis.
5. Those variables with the highest correlation with age are used for the generation of linear and multiple regression formulae (total study sample, and sex and population samples separately). The best formulae are selected based on accuracy and parsimony indicators (R^2, SEE, AIC and BIC)
6. Two different techniques for the preparation of bone thin-sections are tested and the results compared qualitatively.

The terms used during the course of this study are defined as follows. Repeatability refers to the capability of the same observer or different observers to reproduce the same value by measuring the same parameter under the same conditions. Accuracy is defined as the amount of error produced by an estimation, assessed as the difference between the estimate and the true value (in this study,

age at death). The prediction power accounts for the strength of the estimated age in comparison to the true age.

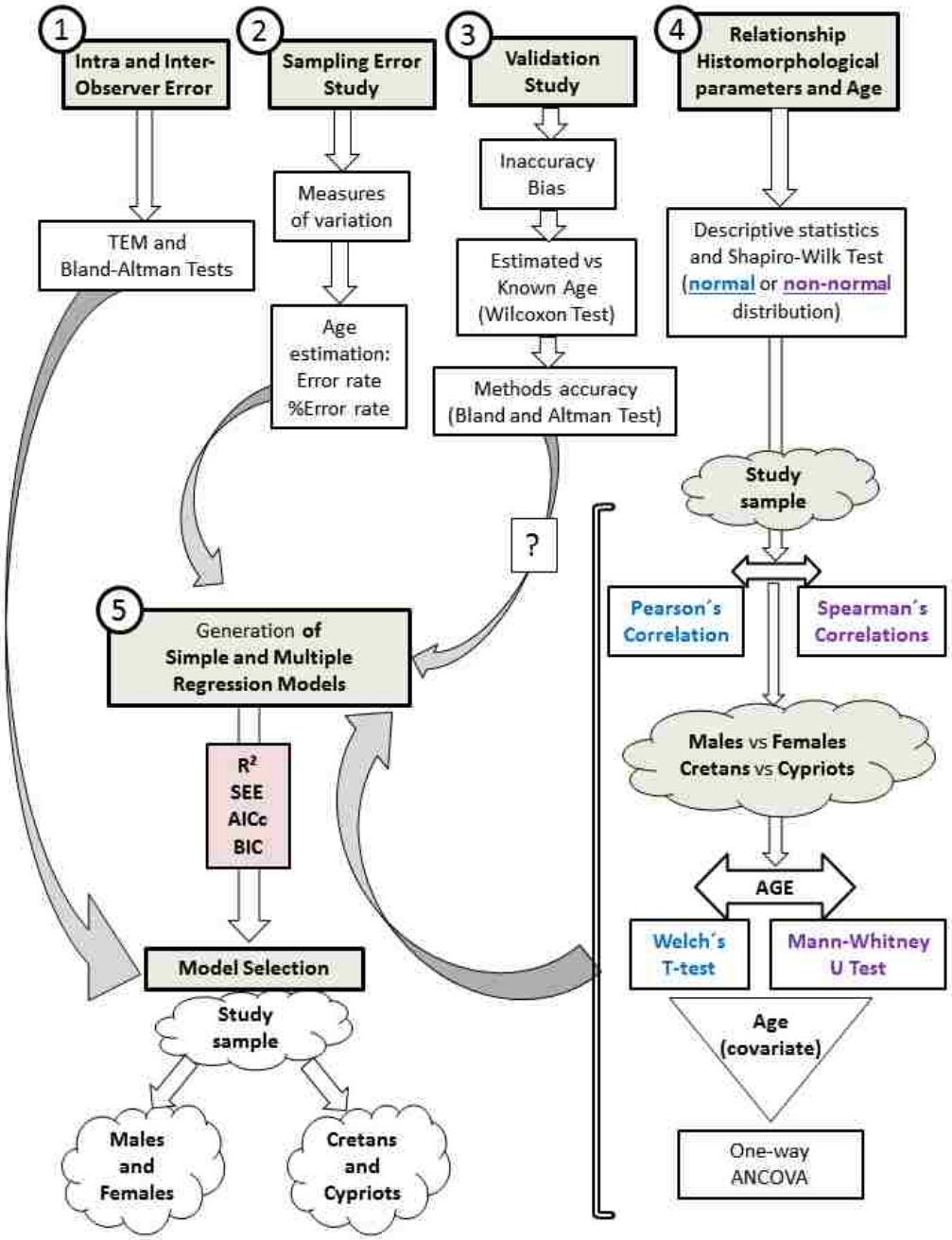

Figure 4.11 Diagram for the research questions and statistical analysis applied (SEE=standard error of the estimate).

4.2.4.1. Inter and intra-observer error evaluation

Intra-observer error was examined by assessing OPD raw and composite parameters and Ct.Ar/Tt.Ar on 36 thin-sections. Osteon measurements variables (On.Ar, On.Pm and On.Cr) were assessed on 20 slides for which microphotographs were available. The observations were carried out with three months between first and second observation. Inter-observer error was tested using two different individuals. An observer with at least 30 years of experience assessed OPD raw and composite parameters on 16 thin-sections. These parameters are commonly considered to be biased by the observers´ experience. A second observer with three years of experience in histology (similar to the author´s experience) was used to assess the same parameters as well as osteon measurements on 20 slides. The target of this analysis was to test whether the observer´s experience has an impact on the repeatability. Each observer was given the necessary instructions and descriptions for successfully accomplished data collection. Ultimately, the observers´ scores were introduced in several age prediction formulae to understand to what extent observer error has an impact on the age estimates. All thin-sections for this analysis were selected at random from the total sample set.

Repeatability between observations/observers was assessed calculating the *Technical error of measurement* (TEM), *relative technical error of measurement* (rTEM) and associated *R* coefficient (R). These values give an indication of the imprecision of the two observations (Ulijaszek and Kerr 1999). TEM **(1)** is defined as the square root of measurement error variance and calculated as follows,

$$\text{TEM}=\sqrt{\frac{(\Sigma D^2)}{2N}} \qquad \textbf{(1)}$$

Where D corresponds to the difference between the two observers or observations 1 and 2, and *N* is the number of cases observed. It is commonly used to assess repeatability providing a measurement of the imprecision of variance when the same sample of subjects is assessed, and it is expressed with the same units as the variables that are measured (Dahlberg, 1940; Harris and Smith, 2009).

TEM can be transformed into the *relative TEM (rTEM)* **(2)** calculated as the standard deviation divided by the average of all the observations. It corresponds to a percentage based on the error related to the size of the variable (Harris and Smith, 2009). It is formulated in the following way:

$$\text{rTEM} = \left(\frac{TEM}{mean}\right) \times 100 \quad \textbf{(2)}$$

Although left to the discretion of the researcher, a common threshold for agreement between observations is set up to 5% cut off value (Crowder, 2013).

The *coefficient of Reliability* (*R*) **(3)** is used to assess repeatability in anthropometric measurement (De Onis, 2006); it has the advantage of allowing comparison between variables calculated as follows:

$$R = 1 - \left(\frac{(TotalTEM)^2}{SD^2}\right) \quad \textbf{(3)}$$

The formula in parenthesis corresponds to the squared of TEM (calculated as expressed in **(1)**), and the squared root of the standard deviation (inter-subject variance). It ranges from 0 to 1 (or expressed as percentage) indicating the proportion of error that is not related to measurement error. Acceptable levels of R are established to be > 95%, although it is dependent on the sample or population under study (Ulijaszek and Kerr, 1999). For example, other anthropometric studies considered 60 to 80% as substantial agreement (De Onis, 2006). If the differences between the observations are not normally distributed (assessed by Shapiro-Wilk Test (*S-W*)), natural log transformation of the parameters will be required (Giavarina, 2015).

The Bland-Altman analysis (B&A) (Bland and Altman 1986; 1995) was used to compare the assessment between observers and the possible proportional bias. The mean difference between observations must not be statistically significant different from zero. Mean difference between observations and its standard deviation were used to calculate the limits of agreement estimated as two standard deviation (1.96*SD) plus/minus the mean difference. The values are displayed on a scatter plot with the *x*-axis representing mean difference of the observations (due to the true value being unknown for the variables) and the *y*-axis representing differences between observations. The line of equality – in which all values should fall if there would be perfect agreement – is placed in the plot in order to evaluate bias. Through this analysis, the magnitude of variability in the measurements that is not represented by the TEM test is explored. To assess repeatability of the methods, the *coefficient of repeatability* (*CR*) **(4)** is calculated as follows:

$$CR =: 1.96 * \sqrt{\frac{\Sigma(d2-d1)^2}{n}} \quad \textbf{(4)}$$

Where *d*2 and *d1* is difference between measurements and *n* is the number of observations. 95% of the differences must fall within two standard deviations of the limits of agreement and the coefficient of variability to achieve repeatability (Barnhart and Barboriak, 2009; Vaz et al., 2013; Giavarina, 2015).

4.2.4.2. Pilot study: sampling error.

A pilot study was conducted to test whether rib sampling area has an effect on the age estimates. The null hypothesis (H_0) states the following: minimum differences in the parameters values within the six thin-sections exist, and thus, accuracy levels are not biased by rib sampling area. If rejected, some differences would be observed for OPD along the length of the rib (H_1). For this study, one single variable was assessed (OPD). To test the effect that sampling sites can have in the estimation of age-at-death, two existing histological formulae were applied and the estimates for the sample under study calculated (Stout and Paine, 1992; Stout et al., 1994) (see **Table 4.6** in next sub-section for respective methods information).

The degree of variability within the six sections of the same rib was explored by calculating basic descriptive statistics as well as range, variance, interquartile range and the coefficient of variability (*CV*: ratio of SD) for the histological variables and estimated ages for each individual. These values give an approximation of the dispersion of the scores obtained by each thin-section within the same rib. The range simply indicates the difference between the highest value and the lowest value. Variance represents the squared average of the difference in relation to the mean with larger variance indicating more variability. The interquartile range is again an indication of the variability although without taking into consideration extreme values, calculated by extracting the 75th percentile and the 25th percentile (Cramer and Howitt, 2004). The thin-sections with the largest and lowest values for each variable *per* individual were identified to examine whether there was a recognisable pattern.

The age estimates obtained by each method (Stout and Paine, 1992; Stout et al., 1994) were used to explore the intra-costal *mean error rates* (mean difference between the errors in the age estimates produced by the six sections within the same rib **(5)**) and *mean percentage error rates* **(6)** (average of percentage error

calculated by comparison between the age estimates and known age), calculated as follows:

$$(Mean)\ Error\ Rate = Estimated\ Age - Known\ Age \quad \textbf{(5)}$$

$$(Mean)\ Percentage\ Error\ Rate = (100 * Mean\ Error\ Rate) \div Know\ Age \quad \textbf{(6)}$$

4.2.4.3. Validation pilot study

To explore whether population specific standards were required for the study sample, four existing age prediction methods (Stout and Paine, 1992; Stout et al., 1994; Cho et al., 2002; Goliath et al., 2016) (Table 4.6) were applied to the entire sample.

Table 4.6 Existing age prediction formulae and standards applied on the Mediterranean samples.

Author/year	Methodology	Formulae	SEE
Stout and Paine (1992)	6th rib, middle third	Ln_Age= 2.343 + 0.050877(OPD)	3.9*
Stout et al. (1994)	4th rib, sternal sampling area	Age = 18.389 - 0.731 * (OPD) + 0.110 * (OPD)²	10.43
Cho et al. (2002)	6th rib / middle third	European-American: Age=38.029+1.603(OPD)-882.210(On.Ar*1)-51.228(Ct.Ar/Tt. Ar)+57.441(Ct.Ar/Tt. Ar*1)	12.22
		Unknown Ethnicity: Age =29.524 + 1.560 (OPD) + 4.786 (Ct.Ar/Tt.Ar) - 592.899(On.Ar)	
		African-American: Age=38.029+1.603(OPD)-51.228(Ct.Ar/Tt. Ar)	
Goliath et al. (2016)	standard rib, middle third	Age= -472.331 + 591.369 (On.Cr)	6.06

*Absolute difference from known and estimated age

Four histomorphometric parameters were assessed (OPD, Ct.Ar/Tt.Ar, On.Ar and On.Cr) according to the description provided by the original methodologies (Stout and Paine, 1992; Stout et al., 1994; Cho et al., 2002; Goliath et al., 2016). The values obtained from the histomorphometric parameters were entered in the original formulae and age estimates calculated. Descriptive statistics, test of normality and Pearson´s Correlations for the entire dataset and the data separated in groups (sex and samples, separately) were used to examine the data.

According to Lovejoy and co-workers (1985b) to test *inaccuracy* **(7)** and *bias* **(8)** of the methodologies, these values must be calculated on the entire sample, the entire sample divided in age cohorts, and on sub-sample sets (both sex and samples subgroups). The following formulae are applied:

$$\text{Inaccuracy (years)} = \Sigma|estimated\ age - actual\ age|/N \quad \textbf{(7)}$$

$$\text{Bias} = \Sigma\ (estimated\ age - actual\ age)/N \quad \textbf{(8)}$$

Where inaccuracy **(7)** corresponds to the sum of all the absolute errors obtained from each case divided by the number of individuals; and bias **(8)** represents the sum of the errors obtained from each case divided by the number of cases. The absolute average error represented by the calculation of inaccuracy while the term bias would reflect whether a systemic over- or under-estimation of age was produced by the existing formulae.

To test whether the age estimates were significantly different from the known ages, Wilcoxon signed rank test was performed on the entire sample and sub-sample sets. This statistical test takes the difference between the scores and ranks the data in positive and negative values assuming as null hypothesis that the median difference between pairs equals to zero, and therefore, no statistical significant difference exists (McDonald, 2014).

The level of agreement between the age estimates and known age was represented graphically by B&A plots (Bland and Altman, 1986; 1995). Difference between estimates and known age were calculated and the mean difference was tested statistically. If not significant, the difference between estimated age and known age was plotted against known ages; the previous calculated bias was set on the plot and the upper and lower limits of agreement calculated (as expressed previously). The best line of fit was also represented to examine the over- or under-estimation of the methods.

4.2.4.4. Age and histological variables analysis

The data were analysed based on the following null hypothesis (Ho): there is no relation between age and the variables observed in the microstructure of rib cortical bone in the means of the sample under study. If the data demonstrate the opposite as stated before (H1), then the null hypothesis is rejected indicating that there is a correlation between histological variables and age.

Several statistical tests were performed to examine the relationship between the variables and age for the entire sample, and for sub-sample sets (males and females and Cretans and Cypriots, separately). General summary descriptive statistics were used as a first approach to the data. Normal distribution indicators (skewness and kurtosis) along with Shapiro-Wilk Test (*S-W*) were used to examine the distribution of each variable**.** Skewness and kurtosis values, and *Z-score* for skewness and kurtosis (respective value divided by its standard error) should fall between the threshold of ± 2; this threshold indicates a 95% confidence interval representing the two standard deviations limits expected for data normally distributed (Cramer, 1997; Tabachnick and Fidell, 2007). The Shapiro-Wilk Test (*S-W)* indicated whether the sample distribution was statistically significantly different from a normal distribution (Shapiro and Wilk, 1965). The *S-W* Test is commonly applied to small and medium sample sizes, although for samples bigger than 40 cases the normality assumption should not cause major statistical violations (Ghasemi and Zahediasl, 2012). Pearson´s correlation coefficients were used to determine the direction and strength of the linear relationship between age and all the variables included in this study providing a range of values from -1 to +1 (0 being no correlation between the continuous variables). For those parameters that are not normally distributed, the non-parametric alternative to Pearson´s correlation coefficients - Spearman´s Rank Order Correlation Coefficient - was calculated (Cramer and Howitt, 2004).

In testing sex and sample histological parameters variation, the null hypothesis (H_0) states that no difference between the parameters (both raw and composite variables) exists between the sexes and between the samples. If rejected, the alternative hypothesis will confirm differences between the parameters and the sub-groups (H_1).

The age distribution between sexes and samples was compared using a Welch's t-test (Kohr and Games, 1974). Depending on whether the assumption of normalcy was confirmed or not, parametric (Welch´s t-test) or non-parametric test (Mann-Whitney *U*) were performed to compare the two groups (Figure 4.11). Welch´s t-test responds to unequal variances and unequal sample sizes to compare two independent samples (Welch, 1951). Mann-Whitney *U* compares one group to the other by ranking the number of times scores considering that the two samples´ scores have been treated as a single group. If each sample counts with more than

20 cases, as in this study, the *U* values are transformed into *z*-values that have to be equal or more than 1.96 to be statistically significant at 0.05 two-tailed level (Cramer and Howitt, 2004).

Next, One-way ANCOVA was performed to further explore the relationship between age, samples and the parameters. The dependent variable was each histological parameter, group was set as the factor (either sex or sample), and age as the covariate. This analysis will allow to determine whether group membership has a significant effect on the dependent variables and whether age is a significant covariate (Kim et al. 2007; Huitema, 2011; Crowder, 2013). If the variables were not normally distributed, the natural log transformation was performed. The statistical assumptions tested for ANCOVA analysis were the following: linearity, homogeneity of regression slopes, normal distribution of standardised residuals, homoscedasticity of residuals, homogeneity of variances and identification of outliers (Tabachnick and Fidell, 2014). Variable transformation and bootstrapping procedures were carried out to confirm the results on those variables violating any of the assumptions (Huitema, 2011; Johnson, 2016; Laerd Statistics, 2017).

Finally, general linear models (GLM) with Chow test were performed in an exploratory basis in order to verify whether the regression slopes for each variable in relation to each group differ. The slopes and intercepts were tested for equality by taking the dependent variable (age), the group (sex or sample) as a fixed factor and the predictor (histological variables) as covariates. In the GLM analysis menu, the design subcommand was modified as follows: /Design = x Group*x. The *Group* term was included to determine if the intercept differed between the groups and the *Group*x* to determine if the slopes were different (Crowder, 2005).

4.2.4.5. Generalised Linear Models.

The relationship between the histological parameters and age, as well as sex and samples, was previously assessed. The information gathered was then used for the generation of age-predicting formulae through regression analysis. Even though most of the statistical analysis consisted of linear regression, different types of modelling (e.g. curvilinear models) were tested to assess the best fit of the data (Aykroyd and Lucy, 1997).

The main purpose of the regression analysis is to find the best fit of the data based on the least squared criterion. The so-called “best fit model” is meant to

minimise the sum of squared errors that are called residuals which represents the difference between the model prediction and the true data (see below). Following the general procedure for this type of statistics, the general form for a simple linear regression model is expressed by the following mathematical formula **(9)**:

$$Y = \alpha + \beta x + \varepsilon \qquad \textbf{(9)}$$

where *Y* is the dependent variable or criterion variable (age); α is the constant (intercept of *Y*, point of intersection of the *Y*-axis); *β* is the regression coefficient that corresponds to the slope of the regression line indicating how many units the dependent variable will change given a one-unit change in the independent variable), and *X* corresponds to the observed variable named independent or predictor variable (e.g. OPD). *Ɛ* represents the error of prediction or residuals which accounts for the portion of *Y* that was not predicted by *X*.

The regression line for the sample (prediction model) (**10)** describes the data as follows:

$$\hat{y} = b_0 + b_1 x \qquad \textbf{(10)}$$

Where $\hat{y}$ corresponds to a specific predicted or estimated *y* and x to the actual observed value for that specific case. Therefore, the regression model includes the prediction error while the prediction models has it implicit in $\hat{y}$ by the presence of the error between estimates and *true* values (Lomax and Hahs-Vaughn, 2012). The values b_0 and b_1 are again the slope (**11a)** and the intercept (**11b**), respectively, and they are estimated from the dataset values as follows:

$$\beta_{YX} = \rho_{YX} \frac{\sigma_Y}{\sigma_X} \qquad\qquad \alpha_{YX} = \mu_Y - \beta_{YX}\mu_X \qquad \textbf{(11a, 11b)}$$

Where *σ* for *x* and *y* is the population standard deviations, respectively; ρ_{YX} is the population correlation between *x* and *y*, and *μ* are the population means for both *x* and *y*, respectively (Lomax and Hahs-Vaughn, 2012).

The *regression coefficient value* is not proportional to the relative strength of the relationship between the variables. Instead, it reports the percentage of variance of the dependent variable explained by the regression model. Thus, the *coefficient of determination* or R^2 value provides information about how well the model fits the data. This value is obtained through the square of the *correlation coefficient* (R^2).

$$R^2 = \frac{SSR}{SST} \qquad \textbf{(12)}$$

Where SS_R is the regression total sum of squares and SS_T refers to the total sum of squares. The subjective power of the effect size of the R^2 coefficient differs according to different authors´ opinions (e.g. Smithson, 2001).

The goodness of fit statistics are also examined by observing results from several significance tests and the confidence interval (see below). The significance test involves evaluating whether the dependent variable is actually a significant predictor of the independent variable (using *F statistics* at the 0.05 significance level and evaluating the standard errors, two-sided p-values for the *t* statistics for the regression coefficients). As expected, the relation between dependent and independent variables is inexact, and therefore, the estimated values obtained through the prediction equation present certain proportion of errors. The *residual values* are known also as *error of estimate*, which is calculated by subtracting expected values (Y'_i) from actual values (Y_i) for each individual **(13)**, with the purpose of estimating the error term predicted by the statistical model:

$$e_i = Y_i - Y'_i \qquad \textbf{(13)}$$

Residuals were tested through visual assessment of diagnostic plots for each relevant model. The corresponding statistical tests, as the *S-W* Test, and skewness and kurtosis values were also reported. Note that graphical methods such as a Q-Q plots in sample size larger than 50 are highly recommended due to Shapiro-Wilk test flagging minor deviations from normality as statistically significant (Laerd Statistics, 2017). The assumptions of *linearity, normality, independence and homogeneity of variance* of the residuals were assessed through the examination of residuals *versus* predicted values, Q-Q plots, scale-location plots and standardised residuals versus Leverage values (Kutner et al., 2005; Kim, 2015). Test for independence of residuals (Durbin-Watson) was also reported for the generated models with an acceptable level for values ranging from 1 to 3 (Field, 2009). Independence of errors was further assessed by standardised residuals versus standardised predicted scatter plot for which all values should fall within ± 3 with a non-specific pattern (Lucy, 2005). Extreme values were examined by studentised residuals, Leverage values and Cook's distance values in order to identify influential cases (Cook and Weisberg, 1982; Fox, 1991). When a case was considered to be a regression influential outlier, the regression analysis was repeated without this case and hypothesis testing, beta coefficients and standard errors and prediction accuracy rates compared between the models. Diagnostic plots examination will verify

whether the model is appropriate and the assumptions of the regression analysis have been violated. However, minor violations of these assumptions are generally accepted in least square regression analysis as it is a robust statistical analysis (Lucy 2005).

After calculating all error values for each case, the total prediction error (*TPE*) is obtained. It will be replaced by the sum of the squares of errors (*SSE*) **(14)** representing the line that actually minimises the error rates. It is calculated as follows:

$$SSE = \sum (Y_i - \hat{Y}_i)^2 \quad \textbf{(14)}$$

The variation for all the prediction errors around the regression line can be estimated as:

$$S_e = \sqrt{\frac{(Yi - \hat{Y}i)2}{n-2}} \quad \textbf{(15)}$$

This last formula is the so called *standard error of estimates* (also known as *Root Mean Squared Error*) **(15)** that corresponds to the estimated standard deviation of the actual *Y* from the predicted $\hat{Y}$. As suggested in other studies, the confidence interval for *Y* at a given value of *X* can be calculated using the standard error of the estimate (generally falling in 95% of confidence for an estimated age for this type of studies) (see Giles and Klepinger (1988) for a detailed description). A prediction interval can be also calculated as the estimation of the value of the independent variable to a particular value of the response variable (Utts and Heckard, 2014).

In the case of incorporating multiple independent variables to the equation, Multiple Linear Regression was applied**.** Multiple regression is a statistical tool that investigates the simultaneous relationship between several independent or response variables and a single dependent or criterion variable (age). Considering the overall model fit of the independent variables included in the equation as aggregate, the null and alternative hypotheses for multiple linear regression states that the regression coefficients would be equal or different from zero (respectively):

$$H_0: \beta_1 = \beta_2 = \ldots = \beta_k = 0$$

$$H_1 : \text{not all the } \beta_k = 0$$

Most of the principles described previously for the linear regression are also valid for multiple regression with some minor modifications. Therefore, only theoretical definitions (for those that change from one model to the other) will be presented here. One remarkable difference in that in this case, the relation between dependent variables and the independent one is represented in a three dimensional plane (Lomax and Hahs-Vaughn, 2012). The multiple regression formula for the sample prediction model **(16)** is expressed as follows:

$$Y'_i = \alpha + \beta_1 X_{1i} + \beta_2 X_{2i} + \ldots + \beta_k X_{ki} \qquad \textbf{(16)}$$

Where α is the intercept of the regression line for Y'_i predicted by a group of values of X_k´*s* (predictors where k=1,…,m) and β_k is the partial slope for the regression line for that particular X_k value. The errors are calculated as previously and the least squared criterion is also applied to minimise the residuals or squared prediction errors. The *multiple coefficient of determination* (R^2) is expressed as $R^2_{y.1,\ldots,m}$ where the subscript Y is the dependent variable and $X_{1,\ldots,m}$ are the various independent variables. The *adjusted* R^2 is used for interpreting the amount of variation in Y explained by the set of X variables by adjusting for sample size and number of predictors. Testing the goodness of fit for the model requires the same concepts as described earlier for the simple regression analysis (Lucy, 2005).

Partial correlations and multicollinearity between the independent variables must be examined to verify whether there is certain degree of dependency between the predictors, and therefore overlapping of their variances. Tolerance indicates the unique proportion of variance of an independent variable, and the variance inflation factors statistics (*VIF,* inverse to tolerance) corresponds to the variance of the estimate coefficient from an independent variable inflated when compared to a non-collinearity case. Generally, values of more than 10 for *VIF* are associated to multicollinearity issues (O'Brien, 2007; York, 2012). Multicollinearity can be also examined by performing regression of the independent variable on the remaining variables, with R^2 less than 0.90 suggesting non-collinearity (Lomax and Hahs-Vaughn, 2012).

The inclusion of dummy variables (group variables) such as sex and/or population to test the impact of the inclusion of the categorical predictors was examined. The groups were coded in a process called "dummy coding". The

variables were then inserted in the regression functions and the models fitted and examined.

The General Linear Models (*GLM*) models are performed using Gaussian link function and maximum likelihood fitting assessing model selection according to significance levels, ANOVA x^2 test and Akaike information criterion (AIC). Special attention in the criteria used for model selection based on goodness of fit and number of parameters. The already mentioned R^2 and *SEE* were considered to compare the results of this analysis with previous published works. Statistical model selection estimators generally not used in previous histological studies – but commonly used in ecology – were applied on the basis of parsimony through assessing best fit and complexity of the model (Aho et al., 2014). The parsimony relates to the concepts of under-fitting and over-fitting of a given model taking into account the number of parameters, the model structure and the variables under consideration; the goal is to choose a model that is as simple as possible (Burnham and Anderson, 2002).

AIC criterion is a measure based on the relative likelihood of the model given the data; it considers all the generated models with penalization of the model complexity (Akaike, 1973). In a model given *p* parameters the AIC calculation **(17)** is as follows:

$$AIC = -2 \ln L(\hat{\theta}) + 2p \quad \textbf{(17)}$$

Where $L(\hat{\theta})$ is the maximum likelihood of the estimated model that in regression includes the likehood of the model parameters in $N(0,\hat{\sigma}^2)$ representing the model residuals, while $\hat{\sigma}^2$ represents the "maximum likelihood estimate for the variance of the error term distribution" and *p* corresponds to the total number of parameters estimated to be in the model (Aho et al. 2014:632). A modification of AIC, known as AIC_c **(18)**, accounts for a correction factor for sample size calculated as:

$$AIC_c = AIC+(2K(K+1))/(n-K-1) \quad \textbf{(18)}$$

Where *K* expresses the total estimable number of the parameters included in the model and *n* corresponds to the sample size.

According to *Kullback-Leibler (K-L) information*, the strength of each hypothesis (each model) can be measured and compared to other hypotheses (models) (i.e. from H_i to H_R) based on the estimators obtained (AIC in this specific case). Thus, comparison across models is the only viable way to approximate to the "best model" (Burnham et al., 2011). The computation of the difference between AIC values (Δ) provides results that can be interpreted and used to rank the models and support the selection of one model over the other, as follows **(19)**:

$$\Delta_i = AICc_i - AICc_{min}; \quad \text{for i ¼ 1; 2; . . . ,} R. \qquad \textbf{(19)}$$

Where the $AICc_{min}$ is the minimum AIC value obtained for *R* models and it commonly used for model inference and define a rank of the generated models (Burnham and Anderson, 2002).

The other estimator used is the *Bayesian information criterion* (BIC) **(20)** (Schwarz, 1978) which is defined as follows:

$$BIC = -2 \ln L(\hat{\theta}) + p \ln n \qquad \textbf{(20)}$$

Where *n* refers to the sample size (see description for **(17)**). BIC penalizes model selection strongly than AIC and it is independent of sample size (Aho et al., 2014).

For both AIC and BIC indices, the smaller the value the better the model.

All data analysis was conducted using IBM SPSS version 22.0 (SPSS, Inc., Chicago, IL) and RStudio version 3.4.1 (RStudio Team, 2015).

4.2.4.6. Thin-section preparation

The last section corresponds to the comparison of the two methodologies (*A* and *B*) used for the preparation of the thin-sections. A qualitative analysis of the quality of slides obtained by each method was presented.

4.2.5 Summary

Most of the Cretan and Cypriot rib samples were obtained from two cemetery populations from Heraklion (Crete) and Limassol (Cyprus). Seven Cretan individuals from forensic cases were included in the data set. From the original dataset (N = 105), a number of cases were discarded due to following reasons: pathological

conditions (N = 11), under-aged individuals (N = 2), non-Greek origin (N = 1) and diagenesis (N = 3). The final study sample consists of 88 individuals with an age range from 19-100 years and a mean age of 60 years (SD = 17.88) (Figure 4.5). The entire sample comprised an even number of males and females (Males = 40, Females = 48). An additional 36 thin-sections (six sections extracted from six ribs) were processed and assessed for the sampling error pilot study.

As presented in section 4.2.4, the statistical approach comprises five main tests (Figure 4.11). Two methods for the preparation of bone histological slides were applied. The technical aspects of each method were explained in detail and they will be discussed in the next chapter.

Chapter 5 : RESULTS

This chapter is organized in six sections. Section 5.1 presents the results for intra- and inter-observer error. Section 5.2 covers the outcome of the pilot study exploring sampling error of six different rib sections along the length of six different ribs. Section 5.3 presents the results of the validation of four different existing age prediction methods. Sections 5.4 and 5.5 focus on the main statistical analysis for the generation of the age prediction models. The last section (5.6) offers a qualitative comparison of the thin-section prepared using the two different histological techniques.

5.1. Intra- and inter-observer error

5.1.1. Intra-observer error

Intra-observer error was analysed through TEM and Bland-Altman (B&A) plot analysis on a sub-sample of 36 thin-sections. All of the parameters related to the composite variable OPD and its raw parameters (N.On, N.On.Fg, N.On.Tt, OPD(I), OPD(F), Tt.Ar, Es.Ar, Ct.Ar and Ct.Ar/Tt.Ar) were examined for the sub-sample. Variables related to secondary osteon measurements (On.Ar, On.Pm and On.Cr) were assessed on 20 slides from the total sub-sample set.

Intra-observer TEM results are shown in Table 5.1. All variables except On.Cr showed error rates with $R > 0.97$ which indicates that about 3% of the variance can be attributed to intra-observer measurement error. This falls within the 5% accepted threshold (Ulijaszek and Kerr, 1999).

Table 5.1 TEM results for intra-observer error.

	TEM	Relative TEM	R
N.On	1.89	1.37	0.99
N.On.Fg	1.94	2.94	0.99
N.On.Tt	2.57	1.26	0.99
OPD (I)	0.13	1.86	0.99
OPD(F)	0.12	2.91	0.98
OPD	0.19	1.69	0.99
Tt.Ar	0.46	0.87	0.97
Es.Ar	0.44	1.35	0.99
Ct.Ar	0.36	1.77	0.98
Ct.Ar/Tt.Ar	0.006	1.33	0.99
On.Ar	0.002	2.90	0.99
On.Pm	0.02	2.86	0.97
On.Cr	0.01	1.16	0.90

All the values obtained from Bland-Altman (B&A) analysis for all of the mentioned variables are reported here. The Shapiro-Wilk test (*S-W*) was performed on the difference between observation with all the variables being normally distributed (*S-W* p-value < 0.05) except for OPD, Es.Ar, Ct.Ar/Tt.Ar and On.Pm for which a natural log transformation of the parameters was recommended. The mean difference between observations was not statistically significant from zero as indicated by one sample T-test except for OPD(F) and Tt.Ar ($p = 0.037$ and $p = 0.030$, respectively). No further analysis was carried out on these two variables as repeatability was not achieved through this test. The B&A coefficient of repeatability for N.On was ± 5.24 with a mean difference of -0.05 in osteon number ($p = 0.90$). N.On.Fg produced a mean difference between observations of -0.44 ($p = 0.33$) with a coefficient of repeatability of ± 5.36. N.On.Tt mean difference accounted for -0.38 ($p = 0.53$) with a coefficient of ± 7.12. OPD(I) presented a mean difference of -0.01 ($p = 0.65$) with coefficient of repeatability of ± 0.36. The B&A repeatability coefficient for LnOPD was ± 0.058 with a mean difference of -0.01 ($p = 0.07$). The mean difference calculated for LnEs.Ar was 0.003 with a coefficient of repeatability being ± 0.037. Ct.Ar coefficient of repeatability was estimated as ± 1.01 with a mean difference between observations of 0.16 ($p = 0.07$). LnCt.Ar/Tt.Ar mean difference was 0.0014 with a coefficient of repeatability of ± 0.037. On.Ar mean difference was calculated as 0.001 not being statistically significant ($p = 0.29$) and presenting a coefficient of repeatability of ± 0.003. LnOn.Pm obtained a mean difference of -

0.013 (p = 0.09) with a repeatability coefficient of ± 0.06. Lastly, On.Cr presented a coefficient of repeatability of ± 0.029 with a mean difference of 0.17 (p = 0.17).

All of the values obtained from the B&A analyses are represented in a scatter plot (see Figure 5.1). The limits of agreement and coefficients of repeatability for each parameter were calculated as described in the previous chapter (section 4.2.4.1) and were included in the scatter plot along with the reported mean differences. In this section, the B&A plot for LnOPD is used as an example (Figure 5.1). The LnOPD Bland-Altman plot shows a random distribution of points indicating no proportional bias with 95% of the values falling within the limits of agreement (solid line); the coefficient of repeatability limits are represented by the dashed line where 95% of the variability is expected to fall The limits of agreement can be calculated on the original scale by taking the anti-log of these values (upper and lower limits of agreement of 1.05 and 0.94, respectively) (Grilo and Grilo, 2012). The remaining B&A plots for intra-observer error are presented in Appendix B.1.

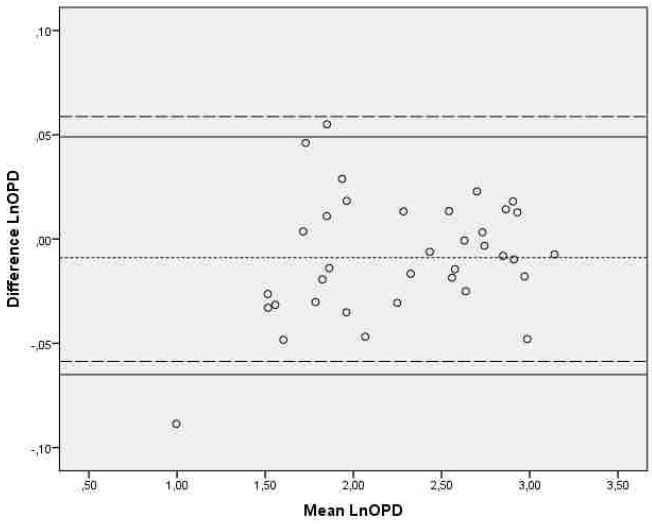

Figure 5.1 Intra-observer error B&A plot (LnOPD): limits of agreement represented by the solid line, coefficient of repeatability by the dashed line, and mean difference by the dotted line.

5.1.2 Inter-observer error

Inter-observer error was assessed by conducting TEM and B&A analyses from two different observers with different levels of histological experience –one highly experienced observer (observer A) and one individual with similar level of experience (observer B). All the raw variables included in the calculation of OPD

were examined as well as the composite variables that are commonly used in aging methods (e.g. Cho et al. 2002).

The TEM, relative TEM (*rTEM*) and associated R values indicated that high reliability was achieved for most of the parameters except for N.On.Fg and OPD(F) for both observers (Table 5.2). Results for N.On and N.On.Tt suggested that no more that 3% of the variance was attributed to measurement error with *rTEM* not exceeding the 5% threshold. N.On.Fg results indicated that between 19% and 12% of the variance was due to measurement error for observer A and observer B, respectively, with an *rTEM* above the limit of acceptance. OPD(I) *rTEM* results for the observer A was just above the 5% threshold (5.30) with 5% of the variance attributed to measurement error while the observer B achieved higher repeatability with only 2% of the variance attributable to measurement error. As a variable collected by multiple observers, OPD(F) demonstrated low reliability. This was indicated by the *rTEM* assessment value, which was higher than the accepted threshold for both observers. R values indicated that around 20% of the variance was attributed to measurement error for observer A while 14% of the variance was related to error for observer B. OPD scores produced an *rTEM* below the 5% threshold with 3% of the variance related to measurement error for the experienced observer; the same parameter produced an *rTEM* slightly above the threshold (7.20) with 6% of the variance attributable to error for observer B. The remaining variables (Tt.Ar, Es.Ar, Ct.Ar and Ct.Ar/Tt.Ar) were all under the 5% threshold for *rTEM* with only Es.Ar slightly exceeding the 5% threshold for observer A. However, all these parameters demonstrate high repeatability with no more than 4% of the variance due to measurement error.

Table 5.2 TEM results for inter-observer (experienced histologist – observer A – and similar level of experience observer – observer B).

	Experienced histologist A (N=16)			*Same experience observer B (N=20)*		
	TEM	**Relative TEM**	**R**	**TEM**	**Relative TEM**	**R**
N.On	0.37	4.84	0.97	5.38	3.79	0.99
N.On.Fg	5.28	20.67	0.81	13.84	15.54	0.88
N.On.Tt	3.49	2.22	0.98	16.22	7.02	0.96
OPD (I)	0.26	5.30	0.95	0.14	1.60	0.98
OPD(F)	0.20	19.73	0.79	0.96	16.43	0.86
OPD	0.22	3.71	0.97	1.04	7.20	0.94
Tt.Ar	2.12	3.75	0.96	0.26	0.51	0.99
Es.Ar	1.81	5.96	0.97	0.22	0.61	0.99
Ct.Ar	0.90	3.43	0.97	0.25	1.58	0.99
Ct.Ar/Tt.Ar	0.01	3.77	0.97	0.004	1.22	0.99

Inter-observer error for On.Ar and On.Pm obtained TEM values of 0.001 and 0.010, and *rTEM* values of 3.06 and 1.58, respectively (observer B). The amount of variance that was related to measurement error was 2% and 1% (R being 0.98 and 0.99 for On.Ar and On.Pm, respectively). All values fell within the acceptable levels indicating that high repeatability was achieved. TEM and *rTEM* values for On.Cr were 0.014 and 1.56; a low *R* value was obtained (0.62) indicating that only substantial agreement was accomplished.

B&A analysis was determined for observer A with the following results. According to one sample T-test results, statistical significance was found for N.On.Fg, OPD(F), Tt.Ar, Es.Ar and Ct.Ar/Tt.Ar ($p < 0.05$). Based on these results, no further analysis was performed on these parameters. The remaining variables were tested for normality indicating that they approximated a normal distribution (*S-W* > 0.05). N.On repeatability coefficient was ± 17.67 with a mean difference of -3.31 ($p = 0.15$). N.On.Tt repeatability coefficient was estimated to be ± 9.68 with a mean difference between observations of -0.62 ($p = 0.96$). For OPD(I), the mean difference between values was -0.03 ($p = 0.77$) and the repeatability coefficient ± 0.74. OPD coefficient of repeatability was ± 0.61 with a mean difference between values of 0.16 ($p = 0.23$). Ct.Ar mean difference was -0.33 ($p = 0.31$) and the coefficient of repeatability estimated as ± 2.49. According to the B&A plots for OPD, 94% of the cases fall within the limits of agreement and the coefficient of

repeatability (Figure 5.2). No proportional bias is observed as assessed by the random distribution of values above and below the mean difference line.

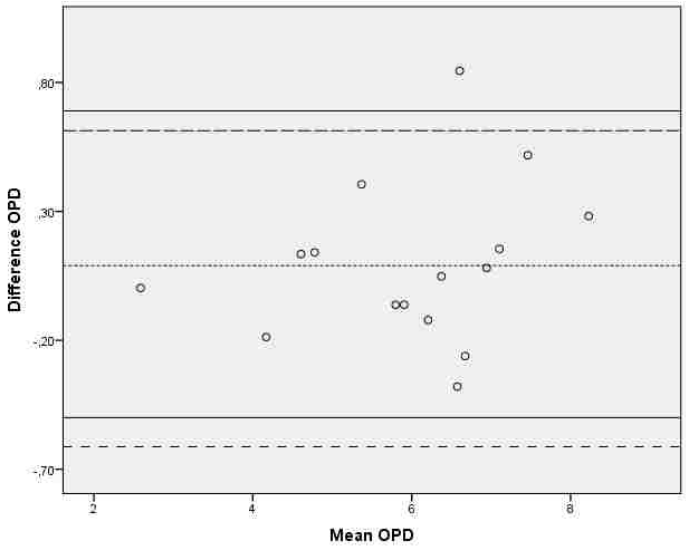

Figure 5.2 B&A plot (OPD), experienced histologist (observer A): limits of agreement represented by the solid line, coefficient of repeatability by the dashed line, and mean difference by the dotted line.

B&A plots were also generated for the same level of experience observer (observer B). One sample T-test results indicated that N.On.Fg and OPD(F) mean differences were statistically significant ($p < 0.010$), and thus, these variables were excluded from further analysis. Test of normality indicated that all variables were normally distributed except for On.Ar (*S-W* $p < 0.05$). For N.On, the repeatability coefficient was ± 14.92 with a mean difference of -2.7 ($p = 0.15$). N.On.Tt produced a coefficient of repeatability corresponding to ± 44.98 and a mean difference of 8.7 ($p = 0.09$). OPD(I) mean difference was reported to be -0.07 ($p = 0.11$) and the repeatability coefficient was ± 0.38. OPD had a mean difference of 0.61 ($p = 0.07$) and a coefficient of repeatability of ± 2.88. The variables related to rib area measurements produced the following mean differences and coefficients of repeatability: Ct.Ar: 0.14 ($p = 0.08$), ± 0.72; Tt.Ar: 0.11 ($p = 0.18$), ± 0.73; Es.Ar: -0.032 ($p = 0.65$), ± 0.62; and Ct.Ar/Tt.Ar: 0.002 ($p = 0.21$), ± 0.01, respectively. LnOn.Ar obtained a mean difference of -0.002 ($p = 0.92$) with a coefficient of repeatability of ± 0.18, and On.Pm presented a mean difference of -0.003 ($p = 0.42$) with ± 0.029 coefficient of repeatability. LnOn.Cr produced a mean difference of 0.007 with a coefficient of repeatability of ± 0.05 ($p = 0.16$).

Figure 5.3 presents the B&A plot for OPD differences between observations against OPD mean differences. All values fall within the upper and lower limits of agreement and coefficient of repeatability. Examination of the plots suggests no proportional bias as all the cases are randomly distributed above and below the mean difference line. The remaining B&A plots for intra-observer error can be found in Appendix B.1.

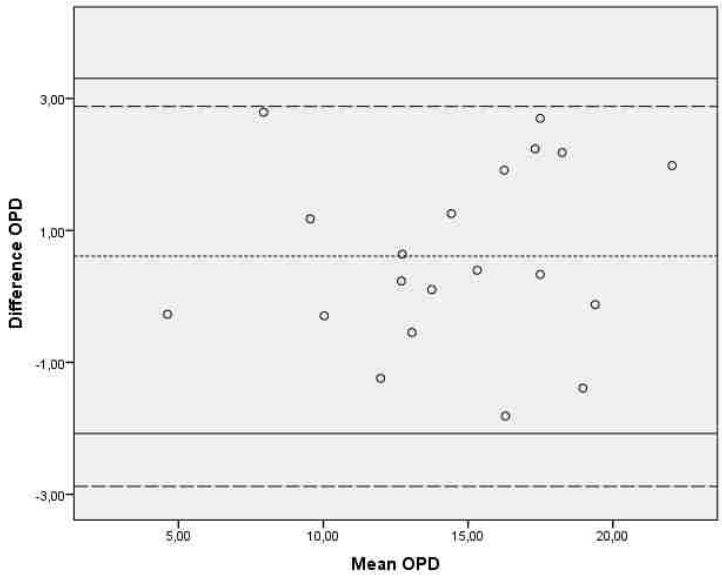

Figure 5.3 B&A plot (OPD) same level of experience observer: limits of agreement represented by the solid line, coefficient of repeatability by the dashed line, and mean difference by the dotted line.

In order to examine whether intra and inter-observer error has an impact on age estimation methods, the values obtained from each observation were inserted into Stout and Paine´s aging formula (1992) (see Table 4.6 in previous chapter). Age estimates for each OPD score were calculated and the mean differences between age estimates tested for significance using paired T-test or Wilcoxon Test. None of the estimated ages were statistically significant ($p < 0.05$) indicating that the reported differences between observations did not have an impact on the age estimates. A final test was performed to clarify if other parameters apart from OPD would imply potential differences in the estimated ages. The values obtained for OPD, On.Ar and Ct.Ar/Tt.Ar were inserted into the Cho et al. (2002) unknown ethnicity formula and into Goliath et al.´s (2016) formula (refer to Table 4.6). Neither intra- nor inter-observer errors seemed to affect the age estimates, which were not statistically significantly different ($p < 0.05$).

5.2. Pilot study: sampling error

A single composite parameter, OPD, was assessed on six cross-sections from six Cretan rib samples (6 sections per rib, N = 36). Two age estimation formulae (Stout and Paine (1992) *Ln_Age= 2.343 + 0.05087(OPD)*; Stout et al. (1994) *Age = 18.389 - 0.731(OPD) + 0.110(OPD)²*) were applied. The main purpose of this test does not relate to the inaccuracy or bias of the methods, that matter will be examined in the next section. Instead, it aims to explore the performance of the six different histological sections within a rib to test the effect of sampling sites on the OPD values and on the individuals´ estimated ages. The demographics for this sub-sample included an age range of 19-58 years and all female individuals (refer to Table 4.2).

5.2.1. Intra and inter-costal histological variables differences

N.On.Tt descriptive statistics for the intra-costal data are presented in Table 5.3. In comparing the number of secondary osteons counted by segment within the same rib, the 27-year-old individual exhibited the maximum difference of 171 secondary osteons among the intra-shaft sections. A minimum difference of 37 secondary osteons among intra-shaft rib sections was observed in a 46-year-old.

Taking into account the variability of the measured values –standard deviation from the mean (SD), range and variance – the highest variability was produced for the youngest individual while the lowest variability values were observed for the 46-year-old individual. A fairly similar interquartile range was observed for all the ribs with the exception of the youngest individual and the 46-year-old individual that presented the highest and the lowest interquartile range, respectively. There seemed to be a trend on N.On.Tt reported by each segment. For half of the sample the lowest N.On.Tt was produced for the sternal segment while the highest N.On.Tt was usually seen in the vertebral segment. The highest variation according to the CV was produced for the two youngest individuals.

Descriptive statistics for Ct.Ar are presented in Table 5.4. A decrease in Ct.Ar with increasing age was observed. The maximum difference for Ct.Ar between the six sections within the same rib was evident in the youngest individual (with the highest SD) and the minimum difference was observed in the oldest individual (producing the lowest SD): note that variability for the remaining individuals was fairly similar. The highest interquartile range was evident in the 29-year-old

individual and the lowest interquartile range in the oldest individual. A pattern was observed for the Ct.Ar by segments with the smallest area given by the sternal segments while the largest areas were mostly produced by the vertebral segments. The highest and lowest CV were seen in the youngest and the oldest individuals, respectively, with the other samples showing similar values.

Descriptive statistics for OPD values are presented in Table 5.5. There was an observed trend with increasing OPD as age increased. The difference between OPD maximum and minimum values for all the six segments within the same rib ranged from a minimum of 2.11 to a maximum of 6.22 corresponding to the 29-year- old individual and the 58-year-old individual, respectively. The highest SD, range and variance were observed for the oldest individual while the lowest variability was seen in the 29-year-old individual. Interquartile ranges varied from a minimum of 1.15 for the 29-year-old individual to a maximum of 2.96 for the 46-year-old individual. OPD lowest and highest values within the same rib did not seem to have a pattern related to sampling area, at least for the small sample tested here. When the average of the two sections extracted from the same segment was computed, the two youngest individuals produced the highest OPD values from the vertebral segment, the two middle age individuals from the middle segment and the individuals that were 46 and 58 years of age from the sternal and middle segments, respectively. Half of the sample produced the lowest OPD from the sternal segment while the remaining values appeared to be random. CV values suggested than the two youngest individuals obtained the highest variability within their OPD values with the remaining individuals reporting similar values.

Table 5.3 Descriptive statistics and variability values for N.On.Tt on the six ribs.

Known Age	Min	Max	Mean	SE	SD	Range	Variance	Interquartile range	Lowest Segment	Highest Segment	CV
19	100	269	160.17	27.52	67.43	169	4546.10	122	M1	V1	0.42
27	51	222	152.67	23.93	58.62	171	3436.66	82	S1	V2	0.38
29	125	235	181.67	18.71	45.84	110	2101.46	91	S1	V2	0.25
35	87	168	136.67	14.84	36.37	81	1322.66	72	S2	V1	0.27
46	159	196	179	7.18	17.61	37	310	36	M1	S1	0.10
58	128	245	184.67	17.82	43.65	117	1905.46	82	V1	M2	0.24

Min=minimum, Max=maximum, SE=standard error of the mean, SD=standard deviation, S=sternal, M=middle, V=vertebral, 1=1st section and 2=2nd section (extracted from vertebral to sternal), CV= coefficient of variation

Table 5.4 Descriptive statistics and variability values for Ct.Ar on the six ribs.

Known Age	Min	Max	Mean	SE	SD	Range	Variance	Interquartile range	Lowest Segment	Highest Segment	CV
19	11.45	34.84	23.57	3.13	7.68	23.39	59.01	10.51	S2	V1	0.33
27	19.69	31.79	26.36	2.18	5.35	12.10	28.69	11.13	S1	V2	0.20
29	21.28	34.88	30.22	2.41	5.91	13.60	35.03	11.21	S1	M1	0.20
35	14.63	25.68	18.96	1.66	4.07	11.05	16.62	6.95	S1	V1	0.22
46	15.70	24.99	20.29	1.67	4.09	9.29	16.78	8.63	S1	V2	0.20
58	11.97	17.21	15.21	0.78	1.92	5.24	3.71	3.28	S2	V1	0.13

Min=minimum, Max=maximum, SE=standard error of the mean, SD=standard deviation, S=sternal, M=middle, V=vertebral, 1=1st section and 2=2nd section (extracted from vertebral to sternal); CV= coefficient of variation

Table 5.5 Descriptive statistics and variability values for OPD on the six ribs.

Known Age	Min	Max	Mean	SE	SD	Range	Variance	Interquartile range	Lowest Segment	Highest Segment	CV
19	4.07	8.99	6.89	0.71	1.73	4.92	3.01	2.70	M1	S2	0.25
27	2.58	7.33	5.68	0.73	1.77	4.43	3.14	2.92	S1	S2	0.31
29	4.85	6.95	5.99	0.29	0.73	2.11	0.53	1.15	V1	V2	0.12
35	5.75	8.74	7.17	0.45	1.10	2.96	1.21	1.85	S2	M1	0.15
46	7.18	11.01	9.06	0.66	1.61	3.83	2.58	2.96	M1	S1	0.18
58	8.38	14.6	12.17	0.84	2.07	6.22	4.29	2.53	V2	M1	0.17

Min=minimum, Max=maximum, SE=standard error of the mean, SD=standard deviation, S=sternal, M=middle, V=vertebral, 1=1st section and 2=2nd section (extracted from vertebral to sternal); CV= coefficient of variation

5.2.2. Age estimates differences between sampling areas

Two different formulae – Stout and Paine (1992) and Stout et al. (1994) – were used to explore differences in the level of accuracy related to intra-costal variation (comparison of estimated ages produced by the six thin-sections along the length of the rib). OPD values from each section were inserted into each formula and estimated ages were calculated (García-Donas et al., 2016).

A summary of the accuracy levels based on mean error and mean percentage error rates are presented in Table 5.6. When Stout and Paine (1992) formula was applied for aging the specimens, the youngest individual (19 years old) produced the lowest mean error ranging from -2.54 to -6.19 with a percentage mean error ranging from -13.38 to -32.57. For the oldest individual included in the study sample (58 years old), the error ranged from -36.10 to -42.06 producing error percentages from -65.10 to -72.52. Both mean errors and mean percentage errors increased gradually as individuals´ age increased.

Overall, the mean error and mean percentage errors obtained by the application of Stout et al. formula (1994) were slightly lower than the ones obtained from Stout and Paine formula (1992) (Table 5.6). The youngest individual estimated ages produced errors ranging from -1.17 to 1.72 with percentage errors varying from -1.66 to 9.06. The oldest individual in the sample obtained estimates ranging from -26.81 to -30.20 errors and percentage errors from -46.23 to -65.56.

As seen in Table 5.6, the differences between the lowest and the highest errors produced by the six sampling areas for each individual did not show a major difference when compare to the differences between estimated age and known age. The error range for the entire sample was from 4 to 38 years when using the Stout and Paine (1992) equation while the error ranged from a minimum of 0.15 to a maximum of 32 while using Stout et al. (1994) equation.

In summary, the absolute maximum difference between the errors obtained by the six thin-sections within the same rib did not exceed 6 years for Stout and Paine (1992), and a maximum error difference of 11 years when using Stout et al. (1994) (both for the oldest individual in the sample) (Table 5.6). Some variation was observed in relation to which rib sampling area performed better according to the closest estimated age to known age. For both methods, the second sternal sections were more accurate for the two youngest individuals, while for the middle age

individuals (29 and 35 years old) second vertebral and first middle shaft sections produced the closest age estimations, respectively. The two oldest specimens produced the closest estimated ages through first sternal and first middle sections.

Table 5.6 Mean error, mean percentage error and maximum difference between errors and percentage errors for the six sections within the same rib.

	Stout and Paine (1992)			Stout et al. (1994)		
	Mean Error (years)	Mean error %	ABS Max. error diff. (years)	Mean Error (years)	Mean error %	ABS Max. error diff.(years)
19 y.o.	-4.17	-21.95	3.65	-0.15	-0.8	1.46
27 y.o.	-13.05	-48.33	3.24	-8.92	-33.05	1.71
29 y.o.	-14.87	-51.28	1.09	-11	-37.92	1.22
35 y.o.	-19.99	-57.1	1.81	-16.09	-45.97	2.56
46 y.o.	-29.45	-64.01	3.23	-24.97	-54.29	4.87
58 y.o.	-38.64	-66.63	5.96	-31.96	-55.11	11.2

*Mean Error= Real Age-Estimated Age; % Error rate=100*Mean Error/Known Age; Abs. Max. diff.: absolute maximum difference; y.o= years old.

Table 5.7 provides a summary of the measurements of variability obtained by the estimated ages by applying the two formulae. For Stout and Paine (1992) the highest range, SD and interquartile range were found for the oldest individual. The same specimen produced the highest variability values for Stout et al. (1994) showing a noticeable difference in comparison with the rest of the specimens considering all values as an aggregate. This difference may be due to the estimated ages produced by this individual as the lowest age is 20 years old (second vertebral thin-section) while the highest estimate was 31 years old (first middle thin section). The CV obtained for estimated ages on each specimen performed similarly indicating that estimated ages produced by the six thin-sections along the length of the rib did not vary dramatically.

Table 5.7 Descriptive statistics and variability values for estimated ages using Stout and Paine (1992) and Stout et al. (1994) age estimation equations.

	Known Age	Min	Max	Mean	SE	SD	Range	Variance	Interquartile range	CV
Stout and Paine (1992)	19	12.81	16.46	14.83	0.52	1.28	3.65	1.64	2.01	0.09
	27	11.88	15.12	13.95	0.49	1.2	3.24	1.46	2.04	0.09
	29	13.33	14.83	14.13	0.21	0.52	1.5	0.27	0.82	0.04
	35	13.98	16.25	15.02	0.34	0.84	2.27	0.72	1.42	0.06
	46	15	18.24	16.55	0.55	1.35	3.24	1.84	2.49	0.08
	58	15.94	21.9	19.35	0.8	1.96	5.96	3.84	2.46	0.10
Stout et al. (1994)	19	17.24	20.72	18.95	0.5	1.23	3.48	1.51	1.98	0.07
	27	17.23	18.94	18.1	0.27	0.67	1.71	0.46	1.38	0.04
	29	17.43	18.63	18.01	0.17	0.42	1.2	0.17	0.66	0.02
	35	17.84	20.41	18.91	0.39	0.96	2.57	0.95	1.59	0.05
	46	18.81	23.68	21.03	0.83	2.03	4.87	4.14	3.72	0.10
	58	19.89	31.19	26.3	1.49	3.66	11.21	13.41	4.76	0.14

Min=minimum, Max=maximum, SE=standard error of the mean, SD=standard deviation, CV = coefficient of variation

5.3 Validation study: rib histological methods

In the previous section, under- or over-estimation of the individuals´ age by the two aging equations has been ignored. In this section, the entire sample (N = 88) was tested against four existing methodologies (Stout and Paine, 1992; Stout et al., 1994; Cho et al., 2002; Goliath et al., 2016) to determine the performance of the aging techniques on the Mediterranean sample (Table 4.6). Cho et al. (2002) method includes three different formulae developed for specific ancestry groups (European, Unknown ethnicity and African-American).

Firstly, the entire dataset was used to explore the overall accuracy rates of the four methods. A test of normality (Shapiro-Wilk (*SW*)) was run on the entire sample in order to explore the distribution of the data. *S-W* assessment indicated that the age distribution fitted the theoretical normal distribution (SW = 0.98, df = 88, p = 0.25). Pearson´s Correlations showed a significant positive correlation for all the age estimates and known age, at p-value < 0.01 (Stout and Paine (1992), r = 0.66; Stout et al. (1994), r = 0.67; Cho et al. (2002): European-American r = 0.75, Unknown Ethnicity r = 0.76, African-American r = 0.70; Goliath et al. (2016), r = 0.67). Descriptive statistics are shown in Table 5.8.

Table 5.8 Descriptive statistics for the entire sample and age estimates obtained using the four methods. Note that the age estimates for Stout et al. (1994) are significantly skewed.

N=88		Min	Max	Mean	SE	SD	Skewness	Z_Skewness	Kurtosis	Z_Kurtosis
Known Age		19	100	60.33	1.91	17.89	-0.21	-0.82	0.04	0.08
Stout and Paine (1992)		13.03	33.68	22.47	0.46	4.30	0.35	1.30	0.07	0.14
Stout et al. (1994)		17.32	71.87	35.39	1.27	11.95	0.96	3.70	0.81	1.60
Cho et al. (2002)	European-American	7.60	66.20	36.63	1.43	13.37	-0.07	-0.28	-0.76	-1.51
	Unknown Ethnicity	11.51	61.01	36.23	1.15	10.81	-0.05	-0.18	-0.64	-1.25
	African-American	15.29	54.62	37.92	0.97	9.08	-0.43	-1.60	-0.46	-0.91
Goliath 2016		35.05	86.42	65.94	1.36	12.76	-0.51	-1.99	-0.43	-0.85

Min: minimum age, Max=maximum age, SE=standard error, SD=standard deviation.

As recommended by Lovejoy et al. (1985b), inaccuracy and bias were calculated to test the performance of each method. The sample was divided by age cohorts taking into account the number of individuals for each age group. Moreover, the entire sample was divided into under and over 60 years of age. This was done to consider the idea that OPD asymptote occurs at this age (Robling and Stout, 2008). As observed in Table 5.9**,** there was a general underestimation trend for all methods except for Goliath et al. (2016). When the sample was divided into four age categories, the formulae developed by Stout and Paine (1992), Stout et al. (1994) and Cho et al. (2002) showed a noticeable increase in inaccuracy for individuals over the age of 40. The highest values of inaccuracy were seen for the individuals over the age of 80. The Stout and Paine (1992) age estimation equation produced the highest error values. The opposite trend was observed in the application of Goliath et al. (2016) formula for which the highest inaccuracy and bias values were observed in the youngest group (20-39 years old) while the lowest were evident in the 60-79 years age cohort. The only underestimation observed by using this method corresponds to the over 80 years of age group.

As seen in Table 5.9, there is an increase in inaccuracy and bias values when the sample is divided into under and over 60 years old for which the values almost double between the young and the old age cohorts. This pattern was observed in the application of Stout and Paine (1992), Stout et al. (1994) and all three formulae developed by Cho et al. (2002) suggesting a trend of increasing inaccuracy and bias

in older age categories. Goliath et al. (2016) followed the opposite pattern with decreasing inaccuracy and bias values with increasing age. For the entire sample, Stout and Paine (1992) formula produced values that surpassed Stout et al. (1994) and Cho et al. (2002) methods in more than 10 years of difference being the least accurate method. From the three formulae applied from Cho et al. (2002), the African-American ancestry one showed the lowest inaccuracy and bias values although a similar performance was observed by the three age predicting equations. Overall, Stout et al. (1994) and Cho et al. (2002) performed similarly. Comparing all four methods applied, Goliath et al. (2016) was the method that most accurately predicted age in the sample under study.

Table 5.9 Inaccuracy and bias values for the entire sample by age cohorts.

						Cho et al. (2002)							
		Stout and Paine (1992)		Stout et al. (1994)		European formula		Unknown formula		African-American formula		Goliath et al. (2016)	
n	Age range	Inaccuracy	Bias	Inaccuracy	Bias	Inaccuracy	Bias	Inaccuracy	Bias	Inaccuracy	Bias	Inaccuracy	Bias
11	19-39	10.38	-10.38	6.19	-3.73	10.70	-5.90	8.72	-3.94	10.34	-0.36	22.52	22.52
28	40-59	31.22	-31.22	22.72	-22.72	22.87	-22.87	21.68	-21.68	18.72	-18.72	11.37	9.14
36	60-79	42.73	-42.73	27.17	-27.17	24.41	-24.41	25.85	-25.85	24.86	-24.86	6.87	4.05
13	80	61.94	-61.94	41.48	-41.48	38.58	-38.58	41.49	-41.49	42.24	-42.24	12.62	-12.01
39	under 60	25.34	-25.34	18.06	-17.36	19.44	-23.23	18.02	-16.68	16.35	-13.54	14.52	12.91
49	over 60	47.83	-47.83	30.97	-30.97	28.17	-28.17	30.00	-30.00	29.47	-29.47	8.40	-0.21
88	ALL	37.86	-37.86	25.24	-24.94	24.30	-23.70	24.69	-24.10	23.66	-22.41	11.11	5.61

The entire sample was separated by sex to examine whether there were differences between the estimated ages obtained for males and females. The results for the normality test showed that both sexes age distributions appeared to be normally distributed (Males, *SW* = 0.96, df = 40, p = 0.22; Females *SW* = 0.97, df = 48, p = 0.42). The estimated ages also corresponded to a normal distribution (*S-W* p-value > 0.05). Descriptive statistics for estimated ages by sex are presented in Table 5.10. The closest mean estimated age to mean known age for both males and females was produced using Goliath et al. (2016); for the remaining methods, the lowest mean estimated age was provided by Stout and Paine (1992) while Stout et al. (1994) and Cho et al. (2002) produced very similar inaccuracy and bias results. Table 5.11 shows Pearson´s correlation coefficients between estimated age and known age for males and females for all the formulae. Correlations were slightly stronger for males than for females for Stout and Paine (1992) and Stout et al. (1994) while the inverse was observed for the remaining formulae (especially for Cho et al. (2002) African-American formula).

Table 5.10 Descriptive statistics for estimated age using the four methods for males and females.

			Min	Max	Mean	SE	SD	Skew-ness	Z_ Skewness	Kurtosis	Z_ Kurtosis
MALES n=40	Known Age		20	89	60.1	2.63	16.53	-0.58	-1.55	0.19	0.27
	Stout and Paine (1992)		15.36	32.80	22.46	0.66	4.18	0.97	2.60	0.37	0.50
	Stout et al. (1994)		19.23	68.52	35.20	1.95	12.38	1.33	3.56	1.13	1.53
	Cho et al. (2002)	European-American	12.29	57.31	36.17	1.99	12.6	-0.1	-0.27	-0.76	-1.03
		Unknown Ethnicity	16.27	54.67	35.93	1.60	10.14	0.07	0.18	-0.68	-0.92
		African-American	16.82	54.13	38.85	1.31	8.33	-0.35	-0.94	0.01	0,01
	Goliath et al. (2016)		35.05	86.42	67.63	2.05	12.97	-0.70	-1.88	-0.02	-0.03
FEMALES n=48	Known Age		19	100	60.52	2.75	19.11	-0.02	-0.05	-0.03	-0.04
	Stout and Paine (1992)		13.03	33.68	22.46	0.64	4.43	-0.08	-0.20	-0.01	-0.02
	Stout et al. (1994)		17.32	71.87	35.54	1.68	11.70	0.64	1.72	0.78	1.06
	Cho et al. (2002)	European-American	7.60	66.20	37.01	2.03	14.09	-0.67	-1.79	-0.78	-1.06
		Unknown Ethnicity	11.51	61.01	36.48	1.64	11.42	-0.13	-0.35	-0.61	-0.83
		African-American	15.29	54.62	37.14	1.39	9.67	-0.41	-1.10	-0.77	-1.05
	Goliath et al. (2016)		35.64	84.56	64.51	1.80	12.52	-0.40	-1.07	-0.57	-0.78

Min: minimum, Max=maximum, SE=standard error, SD=standard deviation.

Table 5.11 Pearson´s correlations between age and estimated age for males and females.

			Cho et al. (2002)			
	Stout and Paine (1992)	**Stout et al. (1994)**	European-American	Unknown Ethnicity	African-American	**Goliath et al. (2016)**
MALE	0.71**	0.68**	0.72**	0.74**	0.58**	0.67**
FEMALE	0.69**	0.67**	0.77**	0.77**	0.79**	0.68**

** p-value significant at 0.01 level

Table 5.12 shows the results for both sexes with the sample divided in four age cohorts, under and over 60 years old, and the entire sex sub-samples separately. The pattern seen for the entire sample was also observed for the two sexes, with increasing inaccuracy and bias values towards increasing age for all methods except for Goliath et al. (2016). Stout and Paine formula (1992) produced the highest inaccuracy and bias values and Stout et al. (1994) and Cho et al. (2002) performed similarly for the two sub-samples. When divided into age cohorts, females over 80 years of age produced higher inaccuracy and bias values than their male counterparts for all methods. This trend was marked for Goliath et al. (2016).

Table 5.12 Inaccuracy and bias values for the entire sample and age cohorts divided by sexes.

							Cho et al. (2002)							
			Stout and Paine (1992)		Stout et al. (1994)		European Formula		Unknown Formula		African-American Formula		Goliath et al. (2016)	
	N	Age range	Inaccuracy	Bias	Inaccuracy	Bias	Inaccuracy	Bias	Inaccuracy	Bias	Inaccuracy	Bias	Inaccuracy	Bias
MALES (n=40)	5	20-39	10.39	-10.39	6.97	-4.43	13.17	-6.86	10.57	-4.46	12.59	2.14	22.24	22.24
	12	40-59	32.43	-32.43	24.79	-24.79	23.40	-23.40	22.48	-22.48	17.13	-17.13	12.92	9.98
	17	60-79	42.62	-42.62	27.39	-27.39	25.42	-25.42	26.55	-26.55	24.93	-24.93	7.46	6.58
	6	80	56.61	-56.61	35.08	-35.08	34.99	-34.99	37.24	-37.24	38.53	-38.53	8.24	-6.91
	17	< 60	25.95	-25.95	19.55	-18.80	20.39	-18.54	18.97	-17.18	15.80	-11.47	15.66	13.59
	23	> 60	46.27	-46.27	29.40	-29.40	27.92	-27.92	29.34	-29.34	28.48	-28.48	7.66	3.06
	40	ALL	37.63	-37.63	25.21	-24.89	24.72	-23.93	24.93	-24.17	23.09	-21.25	11.06	7.54
FEMALES (n=48)	6	19-39	10.37	-10.37	5.54	-3.14	8.65	-5.11	7.17	-3.51	8.47	-2.45	22.76	22.76
	16	40-59	30.31	-30.31	21.16	-21.16	22.47	-22.47	21.08	-21.08	19.90	-19.90	10.21	8.50
	19	60-79	42.84	-42.84	26.98	-26.98	23.51	-23.51	25.23	-25.23	24.80	-24.80	6.35	1.79
	7	80	66.51	-66.51	46.96	-46.96	41.65	-41.65	45.13	-45.13	45.41	-45.41	16.38	-16.38
	22	< 60	24.87	-24.87	16.90	-16.25	18.70	-17.74	17.28	-16.29	16.78	-15.14	13.63	12.39
	26	> 60	49.21	-49.21	32.36	-32.36	28.40	-28.40	30.59	-30.59	30.35	-30.35	9.05	-3.10
	48	ALL	38.05	-38.05	25.27	-24.97	23.95	-23.51	24.49	-24.04	24.13	-23.38	11.15	4.00

The entire data set was divided into the two samples, Cretans and Cypriots, to explore whether there were differences in estimated ages between the two groups. The test of normality indicated that the age distributions for each group were close to the theoretical normal distribution (Cretans, *SW* = 0.97, df = 41, p = 0.48; Cypriots *SW* = 0.96, df = 47, p = 0.11). All estimated ages produced for Cretans and Cypriots by each formulae approximated a normal distribution except for Stout et al. (1994) (Cretans, *SW* = 0.97, df = 41, p = 0.005; Cypriots *SW* = 0.94, df = 47, p = 0.019). Descriptive statistics are presented in Table 5.13. Comparing the mean known age and the mean estimated age produced by each method on each sample it can be seen that Cypriots obtained slightly higher estimated mean age than the Cretans for all the formulae. Overall, the two samples performed similarly with the closest mean estimated age to mean known age produced by Goliath et al. (2016). Correlations between estimated ages and known age indicated a stronger correlation for Cypriots than Cretans for all methods except for Goliath et al. (2016) that performed similarly (Table 5.14).

Table 5.15 presents inaccuracy and bias values for the Cretan and Cypriot samples. Similar values for the four age categories between the two groups were observed for Stout and Paine (1992), Stout et al. (1994), Cho et al. (2002) and Goliath et al. (2016) with slightly higher inaccuracy and bias values for the Cypriot sample. It must be noted that even if sample sizes were uneven, similar results as the ones obtained for the entire data set and separated sexes were produced. Again, Stout and Paine (1992) method showed the highest bias and inaccuracy values. When all individuals included in each sample were compared, Cypriots showed slightly higher inaccuracy and bias values than the Cretans. Among the three formulae of Cho et al. (2002), the African-American formula performed slightly better than the others did although the difference was very small.

Table 5.13 Descriptive statistics for estimated age using the four methods for Cretans and Cypriots.

			Min.	Max.	Mean	SE	SD	Skew-ness	Z_ Skewness	Kurto-sis	Z_ Kurtosis
CRETE n=40	Known Age		19	98	57.49	3.3	21.17	-0.07	-0.20	-0.82	-1.13
	Stout and Paine (1992)		13.03	32.8	21.57	0.67	4.32	0.39	1.05	0.39	0.53
	Stout et al. (1994)		17.32	68.52	33.10	1.79	11.46	1.16	3.15	1.50	2.07
	Cho et al. (2002)	European-American	7.60	59.12	36.49	2.21	14.16	-0.28	-0.75	-0.86	-1.19
		Unknown Ethnicity	11.51	54.67	35.68	1.78	11.42	-0.24	-0.65	-0.69	-0.95
		African-American	15.29	51.81	37.20	1.48	9.53	-0.70	-1.88	-0.37	-0.50
	Goliath et al. (2016)		35.05	84.99	63.51	2.11	13.54	-0.39	-1.06	-0.84	-1.15
CYPRUS n=48	Known Age		20	100	62.81	2.07	14.2	0.06	0.18	1.57	2.30
	Stout and Paine (1992)		15.66	33.68	23.25	0.61	4.16	0.41	1.19	-0.08	-0.11
	Stout et al. (1994)		19.61	71.87	37.39	1.76	12.11	0.88	2.54	0.70	1.03
	Cho et al. (2002)	European-American	15.9	66.2	36.75	1.86	12.79	0.17	0.49	-0.66	-0.97
		Unknown Ethnicity	19.8	61.01	36.71	1.5	10.33	0.21	0.60	-0.66	-0.97
		African-American	19.46	54.62	38.55	1.27	8.71	-0.10	-0.29	-0.79	-1.16
	Goliath et al. (2016)		35.64	86.42	68.05	1.72	11.76	-0.56	-1.62	0.04	0.06

Min: minimum, Max=maximum, SE=standard error, SD=standard deviation

Table 5.14 Pearson´s correlations between known age and estimated age for Cretans and Cypriots.

			Cho et al. (2002)			
	Stout and Paine (1992)	**Stout et al. (1994)**	European-American	Unknown Ethnicity	African-American	**Goliath et al. (2016)**
CRETE	0.67**	0.67**	0.74**	0.74**	0.64**	0.68**
CYPRUS	0.74**	0.74**	0.80**	0.80**	0.79**	0.64**

** p-value significant at .01 level; Stout et al. (1994) refers to Spearman´s correlations.

Table 5.15 Inaccuracy and bias values for the entire sample and age cohorts divided by samples.

							Cho et al. (2002)							
			Stout and Paine (1992)		Stout et al. (1994)		European Formula		Unknown Formula		African-American Formula		Goliath et al. (2016)	
	N	Age range	Inaccuracy	Bias	Inaccuracy	Bias	Inaccuracy	Bias	Inaccuracy	Bias	Inaccuracy	Bias	Inaccuracy	Bias
CRETE (n=41)	10	19-39	11.19	-11.19	6.51	-4.39	11.75	-6.52	9.29	-4.63	10.71	-1.06	21.51	21.51
	11	40-59	30.94	-30.94	22.08	-22.08	19.65	-19.65	19.41	-19.41	15.93	-15.93	10.65	8.78
	12	60-79	43.42	-43.42	29.14	-29.14	21.07	-21.07	23.96	-23.96	24.48	-24.48	4.77	2.36
	8	80	62.44	-62.44	45.45	-45.45	40.83	-40.83	43.32	-43.32	44.03	-44.03	12.64	-11.65
	21	under 60	21.54	-21.54	14.67	-13.66	15.89	-13.40	14.59	-12.38	13.45	-8.85	15.82	14.84
	20	over 60	51.02	-51.02	35.66	-35.66	28.97	-28.97	31.70	-31.70	32.30	-32.30	7.92	-3.24
	41	ALL	35.92	-35.92	24.91	-24.39	22.27	-21.00	22.94	-21.80	22.64	-20.29	11.97	6.02
CYPRUS (n=47)	1	20-39	2.26	-2.26	2.94	2.94	0.25	0.25	2.94	2.94	6.64	6.64	32.67	32.67
	17	40-59	31.40	-31.40	23.13	-23.13	24.95	-24.95	23.14	-23.14	20.52	-20.52	11.84	9.36
	24	60-79	42.39	-42.39	26.19	-26.19	26.09	-26.09	26.80	-26.80	25.05	-25.05	7.92	4.90
	5	80	61.16	-61.16	35.12	-35.12	34.97	-34.97	38.56	-38.56	39.37	-39.37	12.59	-12.59
	18	under 60	29.78	-29.78	22.01	-21.68	23.58	-23.55	22.02	-21.69	19.75	-19.01	12.99	10.66
	29	over 60	45.63	-45.63	27.73	-27.73	27.62	-27.62	28.83	-28.83	27.52	-27.52	8.72	1.88
	47	ALL	39.56	-39.56	25.54	-25.41	26.07	-26.06	26.22	-26.10	24.54	-24.26	10.36	5.25

In summary, Stout and Paine (1992), Stout et al. (1994) and Cho et al. (2002) aging formulae produced high inaccuracy and bias values, with a significant underestimation for the sample under study, especially for the over 50-60 years of age individuals. Goliath et al. (2016) formula seemed to estimate age more accurately for old individuals than for young ones. Further steps on the validation study were carried out only on the entire data set based on the similar inaccuracy and bias trend reported for entire sample and for the sub-samples. Next, Wilcoxon signed rank test was performed to verify whether the values for known age differed significantly from the estimated age for the entire sample and the sample divided into age cohorts (Table 5.16).

Due to the high inaccuracy and bias values, Stout and Paine (1992) underestimated age in all age cohorts with p-values less than the 0.05 threshold (Table 5.16). Only individuals under 40 years of age showed non-statistically significant differences between estimated age and known age for Stout et al. (1994) and for all the three formulae from Cho et al. (2002). When the sample was divided into 20 year age cohorts, Goliath et al. (2016) method produced estimated ages that were statistically significantly different from zero for all the sub-groups. However, this method produced estimated ages not statistically significantly different from known age for over 60 years of age individuals suggesting that it can accurately estimate age in old specimens.

Table 5.16 Wilcoxon paired test between known age and estimated age.

						Cho et al. (2002)							
		Stout and Paine (1992)		**Stout et al. (1994)**		European formula		Unknown formula		African-American formula		**Goliath et al. (2016)**	
N	**Age range**	**Z**	**p-value**	**Z**	**p-value**	**Z**	**p-value**	**Z**	**p-value**	**Z**	**p-value**	**Z**	**p-value**
11	20-39	-2.93	0.003	-1.33	**0.18**	-1.51	**0.13**	-1.24	**0.21**	-0.09	**0.93**	-2.93	< 0.001
28	40-59	-2.93	<0.001	-2.93	< 0.001	-2.93	< 0.001	-2.93	< 0.001	-2.93	< 0.001	-3.69	< 0.001
36	60-79	-5.23	<0.001	-5.23	< 0.001	-5.23	< 0.001	-5.23	< 0.001	-5.23	< 0.001	-5.23	< 0.001
13	80	-3.18	<0.001	-3.18	< 0.001	-3.18	< 0.001	-3.18	< 0.001	-3.18	< 0.001	-3.18	< 0.001
39	under 60	-5.44	<0.001	-5.2	< 0.001	-5.17	< 0.001	-5.17	< 0.001	-4.7	< 0.001	-4.77	< 0.001
49	over 60	-6.09	<0.001	-6.09	< 0.001	-6.09	< 0.001	-6.09	< 0.001	-6.09	< 0.001	-0.41	**0.68**
88	ALL	-8.14	<0.001	-8.07	< 0.001	-8.06	< 0.001	-8.07	< 0.001	-7.92	< 0.001	-3.88	< 0.001

In bold non-statistically significant

In the final stage of the analysis, B&A analysis was used to assess the agreement interval produced by the estimated ages; only those age categories that presented non-statistically significant differences between estimated and known age were tested (Bland and Altman 1986; 1995). Mean differences, and upper and lower limits of agreement were calculated as described in section 4.2.4.3.

For Stout et al. (1994) and Cho et al. (2002) methods, plots are not presented due to the low number of cases (n = 11). A one sample T-test confirmed that the difference between estimated and know age was non-statistically significant from zero (p-value > 0.05). The upper and lower limits of agreement for the formula developed by Stout et al. (1994) ranged between 10.94 and -18.38 with a bias of -3.72. Cho et al. (2002) European formula had agreement levels of 17.7 and -27.7 with a bias of -5.9. Cho et al. (2002) unknown formula limits of agreement ranged from 15.3 and -23.3 with a bias of -3.9; and the African-American formula presented 23.61 and -24.3 upper and lower limits of agreement with a bias of -0.36. All the cases fell within the limits of agreement calculated for each formula. Among these methods, Stout et al. (1994) produced the narrowest limits of agreement.

Due to larger sample size, the over 60 years old age cohort was tested with the B&A plot to graphically examine the agreement between estimated and known age for Goliath et al. (2016) (n = 49). One sample t-test confirmed that the difference between scores was not statistically significant (p-value > 0.05). The upper and lower limits of agreement correspond to 21.52 and -21.93 (solid lines). Figure 5.4 shows that only two cases fall outside the limits of agreement (4% of the total sample) with a bias of -0.21 (dotted line). The best-fit line (coloured line) indicates a general underestimation of individuals older than 75 years of age.

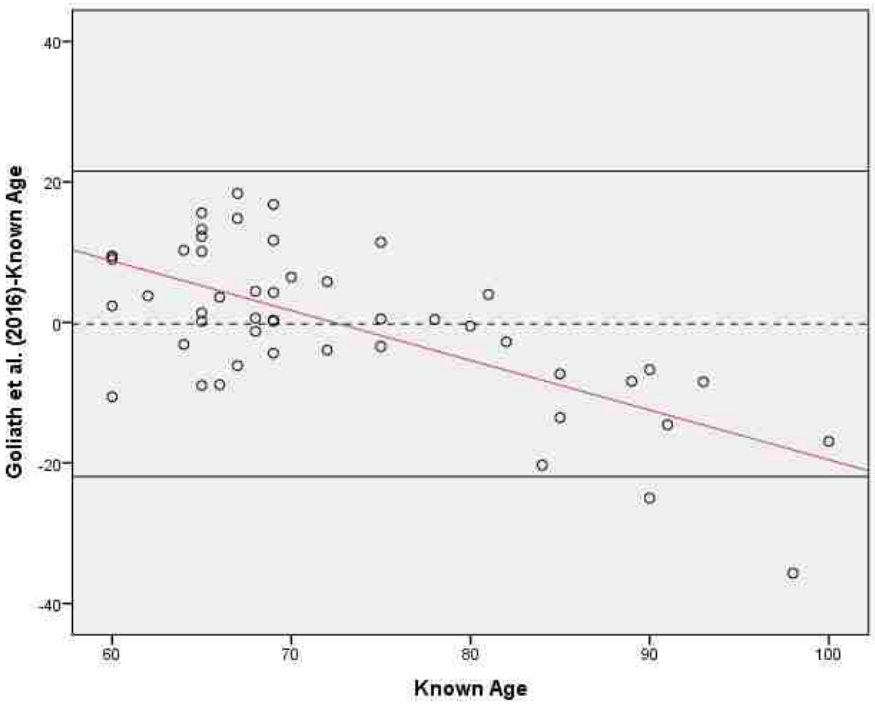

Figure 5.4 Difference in Goliath et al. (2016) estimated ages and known age against known age for the over 60 years old sub-sample set.

5.4. Histological variables and age

Statistical analysis was performed to examine the relation between age and histological variables for the entire dataset, and for sexes and samples separately.

5.4.1. Age and histological variables on the entire sample

Descriptive statistics for all variables on the entire sample are presented in Table 5.17**.** Those variables for which there was an indication of non-normal distribution are highlighted and the results accounted for further analyses.

The age distribution for the entire sample is represented in Figure 5.5 (Mean age = 60.33, SD = 17.89)**.** A normal shape distribution is observed in the histogram and confirmed by skewness and by the *S-W* test (skewness: -0.21, SE = 0.26; *S-W* = 0.98, df = 88, p = 0.25).

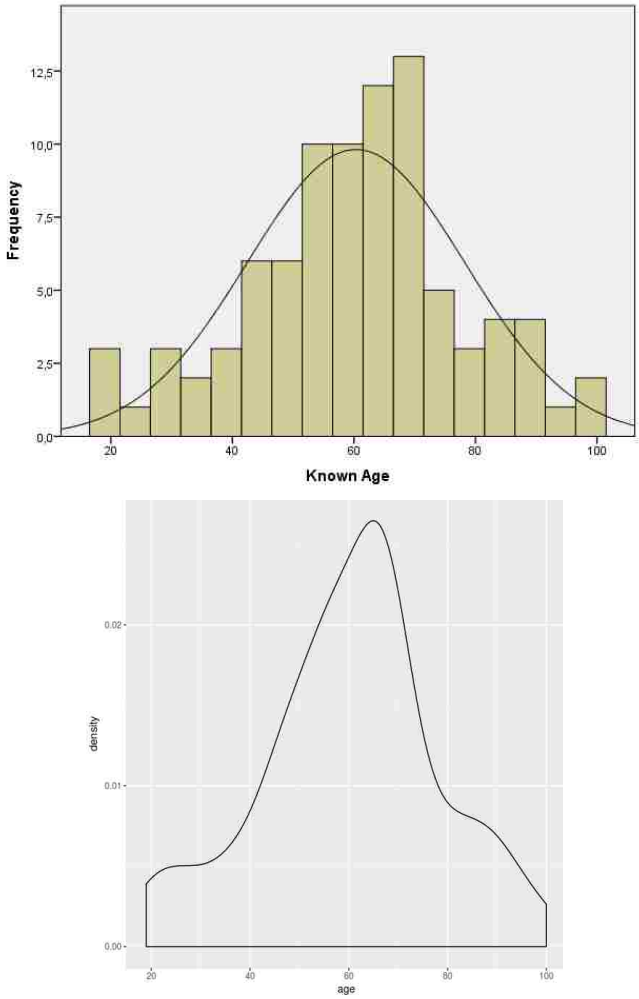

Figure 5.5 Age distribution histogram (top) and density plot (bottom) for the entire population.

Histograms were generated to graphically examine the distribution of the raw and composite parameters used in this research. Note that only the histogram for OPD is shown in this section. The remaining histograms can be consulted in Appendix B.2. The distribution of all variables related to osteon frequency number did not pass the normality assumption with positively skewed distribution for N.On and N.On.Fg (Table 5.17). Secondary osteon frequency numbers were inconsistent with the bell-shaped curve as assessed by S-W test ($p < 0.05$). OPD(I) and OPD(F) values were consistent with normal distribution according to skewness and *S-W* statistics. *S-W* test and skewness value for OPD indicate normalcy which was corroborated through the examination of the histograms (Figure 5.6)**.** Rib area parameters all provide statistically significant p-values ($p < 0.05$). Moreover, Ct.Ar, Tt.Ar and Es.Ar distribution showed positive skewness with excessive kurtosis for Es.Ar (3.53, SE = 0.51) (Table 5.17).

For secondary osteon measurements, only On.Cr presented *S-W* statistics lower than 0.05 suggesting non-normal distribution of the data (Table 5.17).

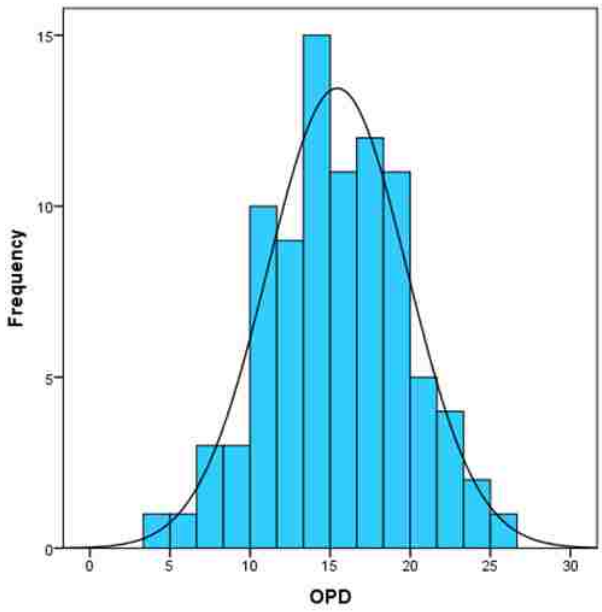

Figure 5.6 Histogram with normal curve fitted for OPD.

Table 5.17 Descriptive statistics for all the raw and composite parameters for the entire sample.

	N=88	Min	Max	Mean	SE	SD	Skewness	$Z_{Skeweness}$	Kurtosis	$Z_{Kurtosis}$	Shapiro-Wilk	p-value
VARIABLES	Known Age	19	100	60.33	1.91	17.89	-0.21	-0.82	0.04	0.08	0.98	0.22
	N.On	46	399	173	7.83	73.49	.063	2.45	0.30	0.59	0.97	0.02
	N.On.Fg	23	224	110	4.89	45.90	0.545	2.12	-0.49	-0.97	0.96	0.01
	N.On.Tt	96	583	282	11.49	107.81	0.47	1.83	-0.25	-0.50	0.97	0.03
	OPD(I)	3.56	13.72	9.16	0.24	2.23	-0.28	-1.10	-0.34	-0.66	0.98	0.21
	OPD(F)	0.93	12.85	6.28	0.29	2.69	0.38	1.48	-0.31	-0.61	0.98	0.12
	OPD	4.49	25.62	15.44	0.46	4.35	-0.01	-0.02	-0.01	-0.02	0.99	0.96
	Ct.Ar	6.38	44.77	19.21	0.85	7.98	1.09	4.27	1.29	2.54	0.92	< 0.001
	Tt.Ar	26.82	155.25	63.38	2.52	23.61	0.94	3.66	1.29	2.54	0.94	< 0.001
	Es.Ar	13.64	141.09	44.17	2.28	21.37	1.33	5.19	3.54	6.96	0.91	< 0.001
	Ct.Ar/Tt.Ar	0.091	0.596	0.322	0.01	0.12	0.43	1.69	-0.78	-1.53	0.96	0.005
	On.Ar	0.015	0.052	0.032	0.001	0.01	0.14	0.56	-0.86	-1.69	0.97	0.07
	On.Pm	0.433	0.831	0.632	0.01	0.10	-0.07	-0.28	-0.95	-1.87	0.97	0.06
	On.Cr	0.858	0.945	0.910	0.001	0.02	-0.51	-1.98	-0.41	-0.81	0.96	0.02

Grey values indicate skewness and kurtosis over the limit and not normal distribution of the data; Min=minimum, Max=maximum, SEE=standard error, SD=standard deviation

A summary of the OPD composite variables, Ct.Ar and Ct.Ar/Tt.Ar and secondary osteon measurements parameters for the entire sample divided into twenty decades age cohorts is presented in Table 5.18. Refer to Appendix B.3 for numerical descriptive statistics for the remaining raw variables included in this study. As expected, OPD values increase with increasing age (both mean and range values) and only OPD(F) shows *S-W* p-value inconsistent with a normal distribution in the 60-79 years old age group. Ct.Ar and Ct.Ar/Tt.Ar measurements decrease gradually with increasing age with the two older age cohorts showing a non-normal distribution of the data for both variables (*S-W* p-values < 0.05). Moreover, Ct.Ar has a positively skewed distribution for the second older age cohort (skewness = 0.93, SE = 0.44). Ct.Ar/Tt.Ar also exhibits a positively skewed distribution for the 60-79 and > 80 years age groups (1.19, SE = 0.39; 1.996, SE = 0.62, respectively). On.Ar and On.Pm decrease with increasing age whilst On.Cr increases with increasing age. For the oldest age categories, all these parameters showed *S-W* values lower than 0.05 indicating inconsistencies with a normal distribution; a positively skewed and excessive kurtosis were observed for On.Ar and On.Pm (over accepted limits for both values).

To further explore the relationship between age and all the variables included in this study, a Pearson´s Correlation test was computed on the entire sample. As seen in Table 5.19A**,** results indicated significant correlation between age and most of the variables with different degrees of strength in their association (Cohen, 1988). For secondary osteon frequency number, an inverse weak relation was observed between age and N.On ($r(86) = -0.23$, $p < 0.01$) while a stronger but still weak positive correlation was observed for age and N.On.Fg ($r(86) = 0.03$, $p < 0.01$): no significant correlation was reported for N.On.Tt probably due to this parameter being the sum of both intact and fragmentary secondary osteons. All OPD parameters exhibit a positive correlation with age indicating that osteon densities increase as age increases. A moderate association was seen between age and OPD(I) ($r(86) = 0.43$, $p < 0.01$), and a strong correlation was reported for age and OPD(F) ($r(86) = 0.78$, $p < 0.01$). OPD presented a slightly lower, but still strong, relationship with age ($r(86) = 0.71$, $p < 0.01$) than OPD(F). As observed in Table 5.19A, the strongest correlation between age and rib area measurements was observed for Ct.Ar indicating that this parameter decreases with increasing age ($r(86) = -0.58$, $p < 0.01$). An inverse correlation is observed for On.Ar and On.Pm whilst a positive

strong correlation is observed for On.Cr ($r(86) = -0.67$, $p < 0.01$): note that all osteon measurements parameters show a similar strength.

S-W results for normality suggest that eight parameters did not meet the assumption of normal distribution (see Table 5.17). Spearman's Rank correlations were computed to corroborate the correlation between age and these variables (refer to statistics diagram Figure 4.11). All associations were in accordance with the ones obtained through Pearson's Correlation analysis (Table 5.19B) (Evans, 1996).

Figure 5.7 presents the scatter plot for the association of known age and OPD with the best line of fit. The remaining variables are graphically illustrated in Appendix B.4.

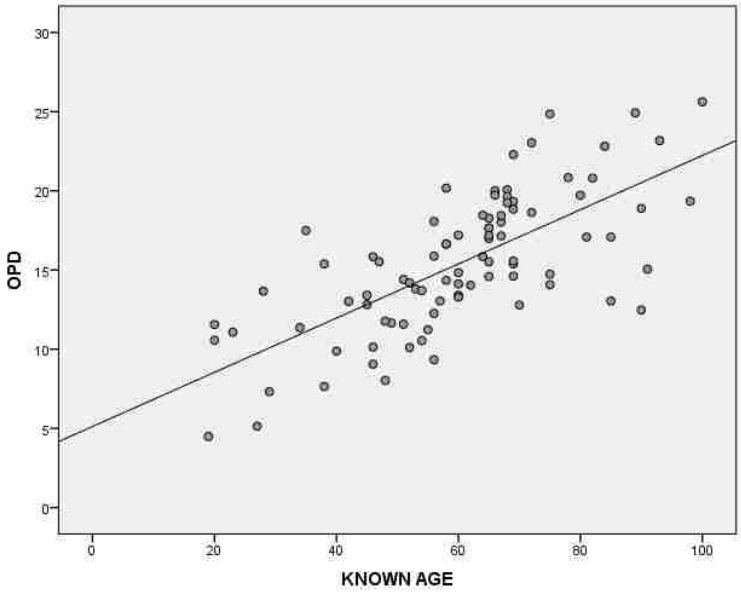

Figure 5.7 Scatter plot representing the association between known age and OPD on the entire sample.

Table 5.18 Summary table of descriptive statistics for compute variables in the entire sample divided in 20 years age cohorts.

	Variable	Min	Max	Mean	SE	SD	Skewness	$Z_{Skewness}$	Kurtosis	$Z_{Kurtosis}$	Shapiro-Wilk	p-value
19-39 years old (N=11)	Known Age	19	38	28.27	2.17	7.21	0.08	0.12	-1.55	-1.21	0.91	0.22
	OPD(I)	3.56	11.50	7.51	0.81	2.70	-0.08	-0.12	-1.02	-0.79	0.91	0.27
	OPD(F)	.93	6.27	3.01	0.47	1.58	0.85	1.29	0.56	0.44	0.94	0.48
	OPD	4.49	17.49	10.52	1.23	4.10	0.10	0.15	-0.69	-0.54	0.96	0.82
	Ct.Ar	15.78	42.11	26.42	2.67	8.87	0.67	1.01	-0.59	-0.46	0.92	0.36
	Ct.Ar/Tt.Ar	0.199	0.596	0.415	0.04	0.13	-0.37	-0.56	-0.82	-0.64	0.94	0.49
	On.Ar	0.025	0.049	0.040	0.001	0.01	-0.92	-1.39	-0.09	-0.08	0.89	0.14
	On.Pm	0.575	0.809	0.722	0.02	0.07	-1.13	-1.71	0.43	0.34	0.87	0.09
	On.Cr	0.858	0.916	0.885	0.01	0.02	0.45	0.68	-1.47	-1.15	0.89	0.15
40-59 years old (N=28)	Known Age	40	58	51.32	1.00	5.29	-0.41	-0.92	-0.92	-1.07	0.93	0.07
	OPD(I)	4.48	11.84	8.37	0.35	1.85	0.01	0.01	-0.36	-0.41	0.98	0.86
	OPD(F)	2.30	8.33	4.74	0.29	1.51	0.48	1.09	-0.43	-0.50	0.96	0.46
	OPD	8.03	20.17	13.11	0.55	2.90	0.41	0.93	-0.09	-0.11	0.98	0.88
	Ct.Ar	9.26	44.77	22.60	1.59	8.42	0.93	2.11	0.88	1.02	0.94	0.11
	Ct.Ar/Tt.Ar	0.091	0.556	0.377	0.02	0.11	-0.61	-1.39	0.26	0.30	0.97	0.52
	On.Ar	0.016	0.052	0.037	0.002	0.01	-0.27	-0.61	0.30	0.35	0.97	0.59
	On.Pm	0.446	0.831	0.691	0.02	0.09	-0.67	-1.53	0.95	1.11	0.96	0.32
	On.Cr	0.859	0.933	0.901	0.001	0.02	0.02	0.04	-0.056	-0.65	0.97	0.66

Grey values indicate not normal distribution of the data; Min=minimum, Max=maximum, SE=standard error, SD=standard deviation

Table 5.18. (***Continued***) Summary table of descriptive statistics for compute variables in the entire sample divided in 20 years age.

	Variable	Min	Max	Mean	SE	SD	Skewness	$Z_{Skeweness}$	Kurtosis	$Z_{Kurtosis}$	Shapiro-Wilk	p-value
60-79 years old (N=36)	Known Age	60	78	67.03	0.75	4.53	0.38	0.98	0.05	0.06	0.95	0.09
	OPD(I)	5.38	12.44	9.89	0.28	1.67	-0.54	-1.37	0.07	0.09	0.96	0.22
	OPD(F)	3.78	12.85	7.50	0.36	2.14	0.74	1.88	-0.14	-0.18	0.93	0.03
	OPD	12.79	24.85	17.40	0.48	2.88	0.49	1.24	-0.05	-0.06	0.96	0.29
	Ct.Ar	8.91	28.58	16.49	0.85	5.09	0.73	1.86	0.19	0.26	0.93	0.03
	Ct.Ar/Tt.Ar	0.152	0.550	0.279	0.02	0.09	1.19	3.04	1.18	1.54	0.90	0.01
	On.Ar	0.015	0.046	0.028	0.001	0.01	0.24	0.61	-0.41	-0.54	0.98	0.62
	On.Pm	0.433	0.768	0.595	0.01	0.08	-0.05	-0.12	-0.71	-0.92	0.98	0.75
	On.Cr	0.882	0.945	0.919	0.002	0.01	-0.22	-0.57	0.09	0.12	0.98	0.83
>80 years old (N=13)	Known Age	80	100	88.31	1.73	6.25	0.51	0.83	-0.51	-0.43	0.94	0.51
	OPD(I)	6.06	13.72	10.26	0.75	2.72	-0.30	-0.49	-1.49	-1.25	0.91	0.15
	OPD(F)	5.92	12.64	8.97	0.58	2.09	0.17	0.28	-0.77	-0.64	0.97	0.85
	OPD	12.48	25.62	19.23	1.17	4.23	-0.11	-0.17	-0.91	-0.77	0.96	0.78
	Ct.Ar	6.38	24.44	13.37	1.44	5.19	0.75	1.22	0.03	0.03	0.94	0.49
	Ct.Ar/Tt.Ar	0.130	0.548	0.241	0.03	0.11	1.99	3.24	4.64	3.89	0.79	0.01
	On.Ar	0.016	0.041	0.023	0.002	0.01	1.66	2.69	3.11	2.62	0.84	0.02
	On.Pm	0.457	0.723	0.536	0.02	0.07	1.52	2.46	2.79	2.34	0.87	0.04
	On.Cr	0.904	0.942	0.928	0.004	0.01	-0.80	-1.29	-0.83	-0.69	0.86	0.04

Grey values indicate not normal distribution of the data; Min=minimum, Max=maximum, SE=standard error, SD=standard deviation

Table 5.19 Pearson´s correlation (A) and Spearman´s correlation (B) coefficients for age and all the variables for the entire sample

5.19A	1	2	3	4	5	6	7	8	9	10	11	12	13	14
1. Known Age	1													
2. N.On	-0.23*	1												
3. N.On.Fg	0.35**	0.61**	1											
4. N.On.Tt	-0.01	0.94**	0.84**	1										
5. OPD(I)	0.43**	0.41**	0.52**	0.50**	1									
6. OPD(F)	0.78**	-0.14	0.61**	0.16	0.55**	1								
7. OPD	0.71**	0.12	0.64**	0.36**	0.86**	0.91**	1							
8. Ct.Ar	-0.56**	0.79**	0.28**	0.66**	-0.18	-0.52**	-0.41**	1						
9. Tt.Ar	-0.13	0.43**	0.33**	0.43**	-0.02	-0.09	-0.06	0.44**	1					
10. Es.Ar	0.07	0.17	0.26*	0.23*	0.06	0.09	0.09	0.11	0.94**	1				
11. Ct.Ar/Tt.Ar	-0.49**	0.39**	-0.07	0.24*	-0.14	-0.51**	-0.38**	0.56**	-0.41**	-0.66**	1			
12. On.Ar	-0.64**	0.35**	-0.11	0.19	-0.35**	-0.61**	-0.56**	0.61**	0.04	-0.17	0.61**	1		
13. On.Pm	-0.67**	0.36**	-0.12	0.19	-0.34**	-0.63**	-0.56**	0.62**	0.05	-0.17	0.62**	0.99**	1	
14. On.Cr	0.67**	-0.06	0.38**	0.12	0.35**	0.60**	0.55**	-0.31**	0.04	0.17	-0.41**	-0.54**	-0.58**	1

5.19B	1	2	3	4	8	9	10	11	14
1. Known Age	1								
2. N.On	-0.23*	1							
3. N.On.Fg	0.31**	0.64**	1						
4. N.On.Tt	-0.02	0.93**	0.86**	1					
8. Ct.Ar	-0.58**	0.78**	0.34**	0.67**	1				
9. Tt.Ar	-0.09	0.43**	0.39**	0.49**	0.45**	1			
10. Es.Ar	0.16	0.21*	0.36**	0.32**	0.13	0.93**	1		
11. Ct.Ar/Tt.Ar	-0.55**	0.43**	0.01	0.26*	0.61**	-0.39**	-0.68**	1	
14. On.Cr	0.67**	-0.07	0.35**	0.11	-0.32**	0.05	0.22*	-0.39**	1

Correlation significant at 0.05, ** Correlation significant at 0.01

5.4.2 Age and histological variables by sexes and samples

The entire sample was divided into sub-sample sets in order to explore the relationship between the histological variables and sex and sample (Cretans and Cypriots), respectively.

All numerical descriptive statistics for males and females are shown in Table 5.20. Mean age for both males (n = 40) and females (n = 48) is very close. Moreover, normal distribution for both sexes was reported (Male, *SW* = 0.96, df = 40, p = 0.22; Females, *SW* = 0.97, df = 48, p = 0.42). Figure 5.8 shows age distribution and density plots for both sexes separately: it can be observed in the histograms that males have a higher frequency of cases ranging from 50 to 70 years of age while females exhibit a more even age range distribution; however, both sexes present similar density plots. Some differences in the number of osteons were observed with males having generally more N.On, N.On.Fg and N.On.Tt than females. Osteon population densities showed similar values between sexes with slightly larger OPD(I) for males and slightly larger OPD(F) for females. Sexually dimorphic differences were observed in the rib area parameters (Ct.Ar, Tt.Ar and Es.Ar) with males exhibiting larger values than females; however, Ct.Ar/Tt.Ar appeared to be larger in females than in males. On.Ar, On.Pm and On.Cr did not exhibit apparent differences between sexes. Four parameters for males and five parameters for females showed *S-W* p-values inconsistent with a normal distribution (Table 5.20). Figure 5.9 presents scatterplots showing the association between known age and OPD for males and females, separetely. The remaining scatter plots can be found in Appendix B.5.

Table 5.20 Descriptive statistics for the entire sample divided by sex.

VARIABLES	**MALE** N=40 / **FEMALE** N=48	Statistics										
		Min	Max	Mean	SE	SD	Skewness	$Z_{Skewness}$	Kurtosis	$Z_{Kurtosis}$	Shapiro-Wilk	p-value
	Known Age	20	89	60.10	2.61	16.53	-0.58	-1.56	0.20	0.27	0.96	0.22
		19	100	60.52	2.76	19.11	-0.02	-0.07	-0.03	-0.05	0.97	0.42
	N.On	66	399	194.80	11.78	74.52	0.47	1.27	0.31	0.42	0.98	0.57
		46	355	154.54	9.83	68.09	0.81	**2.36**	0.77	1.14	0.95	0.04
	N.On.Fg	47	212	118.00	7.18	45.44	0.46	1.23	-0.81	-1.10	0.95	0.08
		23	224	102.65	6.58	45.58	0.68	1.98	-0.07	-0.10	0.95	0.06
	N.On.Tt	142	583	312.80	17.05	107.8	0.50	1.34	-0.07	-0.09	0.97	0.26
		96	507	257.19	14.74	102.1	0.47	1.36	-0.55	-0.81	0.96	**0.07**
	OPD(I)	5.38	13.04	9.38	0.32	2.02	0.09	0.25	-0.66	-0.90	0.95	0.06
		3.56	13.72	8.98	0.35	2.40	-0.41	-1.18	-0.41	-0.61	0.97	0.34
	OPD(F)	2.18	12.85	6.10	0.42	2.66	0.82	**2.19**	0.04	0.06	0.93	**0.02**
		0.93	12.64	6.43	0.40	2.74	0.05	0.16	-0.31	-0.47	0.98	0.56
	OPD	7.65	24.93	15.48	0.65	4.08	0.74	1.99	0.03	0.04	0.93	**0.02**
		4.49	25.62	15.42	0.66	4.61	-0.42	-1.23	-0.02	-0.03	0.97	0.34
	Ct.Ar	9.26	44.77	21.16	1.37	8.64	**1.13**	**3.03**	0.92	1.26	0.89	**0.01**
		6.38	39.95	17.59	1.02	7.07	0.92	**2.67**	1.15	1.70	0.94	**0.02**

In bold values over the limit of skewness and kurtosis; p-values < 0.05; Male (grey coloured), Female (non-coloured); Min=minimum, Max=maximum, SE=standard error, SD=standard deviation

Table 5.20. (***Continued***) Descriptive statistics for the entire sample divided by sex.

	MALE N= 40	Statistics										
	FEMALE N= 48	Min	Max	Mean	SE	SD	Skewness	$Z_{Skewness}$	Kurtosis	$Z_{Kurtosis}$	Shapiro-Wilk	p-value
VARIABLES	Tt.Ar	26.82	155.25	74.66	4.24	26.79	0.40	1.06	0.65	0.89	0.97	0.33
		32.65	90.60	53.98	2.23	15.42	0.72	**2.11**	-0.08	-0.12	0.94	**0.01**
	Es.Ar	14.52	141.09	53.50	3.97	25.12	0.95	**2.54**	2.20	**3.00**	0.93	**0.02**
		13.64	72.87	36.39	1.97	13.64	0.48	1.41	0.01	0.01	0.97	0.30
	Ct.Ar/Tt.Ar	0.091	0.572	0.304	0.02	0.12	0.49	1.30	-0.35	-0.48	0.97	0.36
		0.152	0.596	0.336	0.02	0.13	0.37	1.09	-1.06	-1.57	0.94	**0.01**
	On.Ar	0.016	0.052	0.032	0.001	0.01	0.43	1.16	-0.60	-0.82	0.96	0.12
		0.015	0.051	0.031	0.001	0.01	-0.03	-0.09	-1.07	-1.58	0.96	0.08
	On.Pm	0.446	0.831	0.636	0.02	0.10	0.18	0.48	-0.62	-0.84	0.97	0.47
		0.433	0.818	0.629	0.02	0.11	-0.19	-0.55	-1.19	-1.76	0.95	**0.03**
	On.Cr	0.858	0.945	0.913	0.003	0.02	-0.69	-1.85	0.02	0.02	0.95	0.08
		0.859	0.942	0.908	0.002	0.02	-0.40	-1.17	-0.57	-0.85	0.97	0.18

In bold values over the limit of skewness and kurtosis; p-values < 0.05; Male (grey coloured), Female (non-coloured) Min=minimum, Max=maximum, SE=standard error, SD=standard deviation

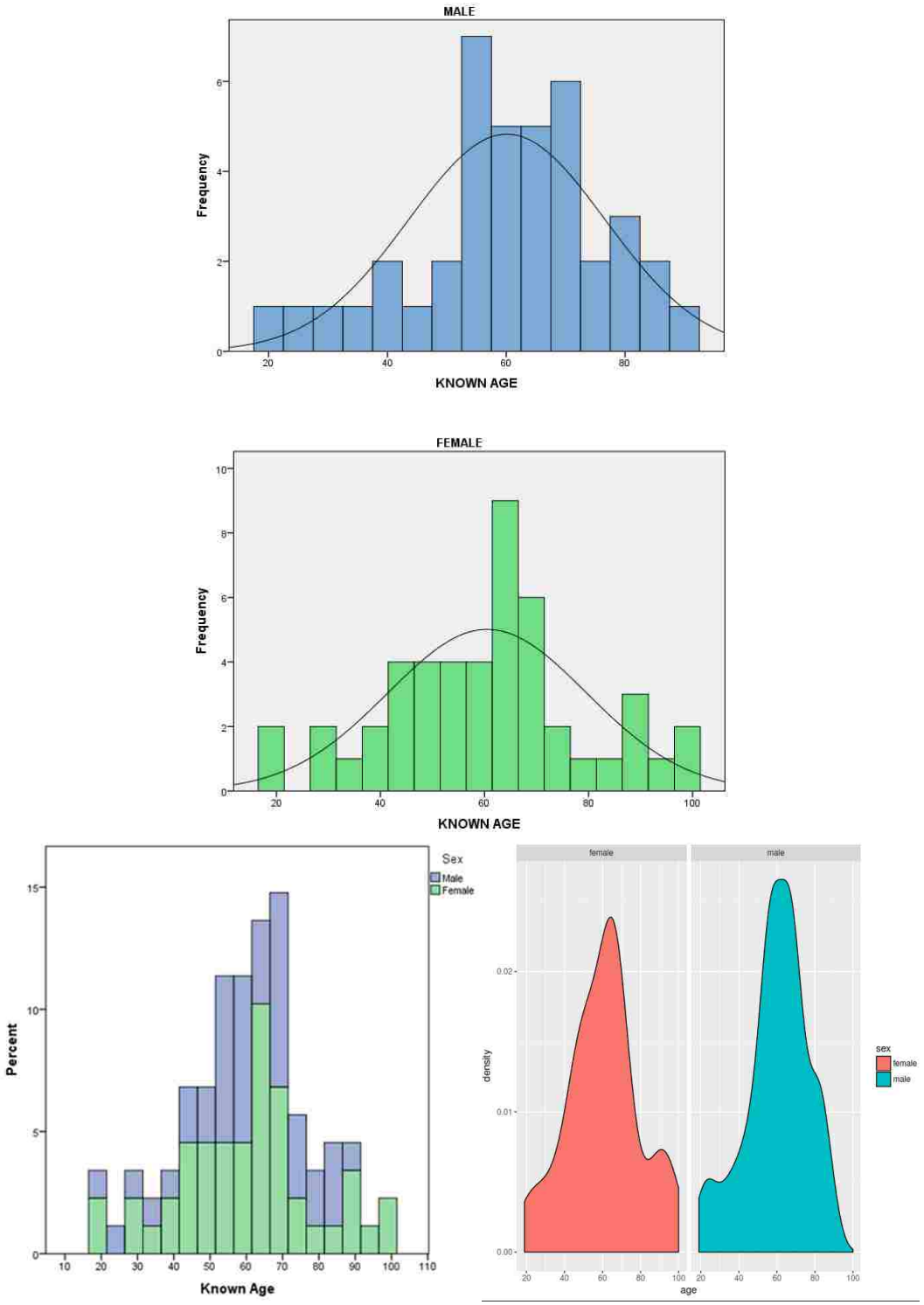

Figure 5.8 Sex histograms; both sexes percentages (males-blue, females-green) (bottom left); density plots by sexes (males –blue, females-pink) (bottom right).

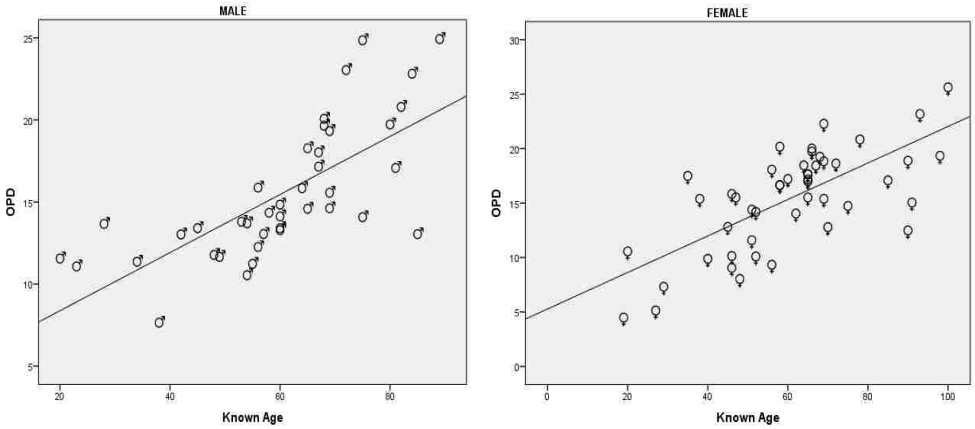

Figure 5.9 Scatter plot for association between known age and OPD: males (left), females (right).

Descriptive statistics for Cretans and Cypriots samples separately are presented in Table 5.21. Age distributions for both population samples are shown in Figure 5.10. Both samples presented approximately normal age distributions (Crete, *SW* = 0.97, df = 41, p = 0.48; Cypriots, *SW* = 0.96, df = 47, p = 0.11). It can be observed through the histograms that the Cretan sample was more evenly distributed with individuals representing all age ranges. The Cypriot sample, however, had a higher number of individual older than 60 years old and fewer cases under 40-50 years of age. As a general trend, values for the Cypriot sample were higher than values for the Cretan sample (Table 5.21). All osteons frequency numbers (N.On, N.On.Fg and N.On.Tt) were higher for Greek-Cypriots than for Cretans. The same pattern was observed for osteon densities values with the more noticeable difference between the two samples being accounted by OPD. Rib area and secondary osteons measurements presented the same trend for which all values were higher for the Cypriots. Seven parameters for the Cretan sample and three parameters for the Cypriot sample showed non-normal distribution according to the *S-W* test ($p < 0.05$). Associations between age and OPD for each sub-sample are shown in Figure 5.11. The remaining scatter plots can be consulted in Appendix B.6.

Table 5.21 Descriptive statistics for the sample divided by samples.

	CRETE N=41	Statistics										
	CYPRUS N=47	Min	Max	Mean	SE	SD	Skewness	$Z_{Skewness}$	Kurtosis	$Z_{Kurtosis}$	Shapiro-Wilk	p-value
VARIABLES	Known Age	19	98	57.49	3.31	21.17	-0.07	-0.20	-0.82	-1.13	0.97	0.49
		20	100	62.81	2.07	14.20	0.06	0.18	1.57	**2.30**	0.96	0.11
	N.On	60	299	150.10	9.18	58.81	0.42	1.13	-0.59	-0.81	0.96	0.14
		46	399	192.68	11.62	79.64	0.46	1.32	0.07	0.11	0.97	0.50
	N.On.Fg	23	183	86.83	5.24	33.58	0.98	**2.65**	1.28	1.77	0.92	**0.01**
		50	224	129.51	6.74	46.23	0.09	0.27	-0.78	-1.15	0.97	0.39
	N.On.Tt	111	482	236.93	12.82	82.11	0.69	1.88	0.33	0.46	0.95	0.07
		96	583	322.19	16.41	112.51	0.06	0.18	-0.33	-0.49	0.98	0.71
	OPD(I)	3.56	13.04	8.85	0.36	2.33	-0.31	-0.83	-0.35	-0.49	0.97	0.38
		4.48	13.72	9.44	0.31	2.14	-0.21	-0.60	-0.38	-0.56	0.98	0.81
	OPD(F)	0.93	11.88	5.66	0.42	2.71	0.52	1.40	-0.06	-0.08	0.96	0.17
		2.25	12.85	6.83	0.38	2.59	0.38	1.09	-0.35	-0.51	0.97	0.39
	OPD	4.49	24.93	14.50	0.70	4.50	-0.01	-0.04	0.23	0.31	0.98	0.91
		8.03	25.62	16.26	0.60	4.09	0.14	0.42	-0.36	-0.52	0.98	0.89
	Ct.Ar	8.17	42.11	17.74	1.19	7.63	1.05	**2.85**	1.19	1.65	0.92	**0.01**
		6.38	44.77	20.49	1.19	8.13	1.19	3.43	1.48	**2.18**	0.91	**0.001**

In bold values over the limit of skewness and kurtosis; p-values < 0.05; Male (grey coloured), Female (non-coloured) Min=minimum, Max=maximum, SE=standard error, SD=standard deviation

Table 5.21. ***(Continued)*** Descriptive statistics for the dataset divided by samples.

	CRETE N=41	Statistics										
	CYPRUS N=47	Min	Max	Mean	SE	SD	Skewness	$Z_{Skewness}$	Kurtosis	$Z_{Kurtosis}$	Shapiro-Wilk	p-value
VARIABLES	Tt.Ar	26.82	155.25	60.29	3.74	23.96	1.64	**4.44**	4.77	**6.58**	0.88	**< 0.001**
		33.50	115.65	66.08	3.39	23.23	0.37	1.08	-0.98	-1.44	0.94	**0.02**
	Es.Ar	13.64	141.09	42.55	3.61	23.12	2.09	**5.66**	7.10	9.80	0.83	**< 0.001**
		15.07	87.79	45.58	2.90	19.87	0.44	1.26	-0.68	-1.00	0.95	0.06
	Ct.Ar/Tt.Ar	0.091	0.596	0.316	0.02	0.13	0.49	1.33	-0.67	-0.93	0.95	0.07
		0.156	0.556	0.326	0.02	0.11	0.42	1.20	-0.96	-1.41	0.94	**0.03**
	On.Ar	0.016	0.050	0.030	0.001	0.01	0.32	0.85	-1.08	-1.50	0.96	**0.04**
		0.015	0.052	0.033	0.001	0.01	0.08	0.24	-0.45	-0.66	0.98	0.87
	On.Pm	0.446	0.809	0.622	0.02	0.11	0.16	0.43	-1.25	-1.72	0.95	**0.03**
		0.433	0.831	0.646	0.01	0.09	-0.23	-0.67	-0.39	-0.57	0.98	0.82
	On.Cr	0.858	0.942	0.905	0.003	0.02	-0.39	-1.06	-0.79	-1.10	0.92	0.15
		0.859	0.945	0.913	0.002	0.02	-0.56	-1.62	0.04	0.06	0.97	0.24

In bold values over the limit of skewness and kurtosis; p-values < 0.05; Male (grey coloured), Female (non-coloured) Min=minimum, Max=maximum, SE=standard error, SD=standard deviation

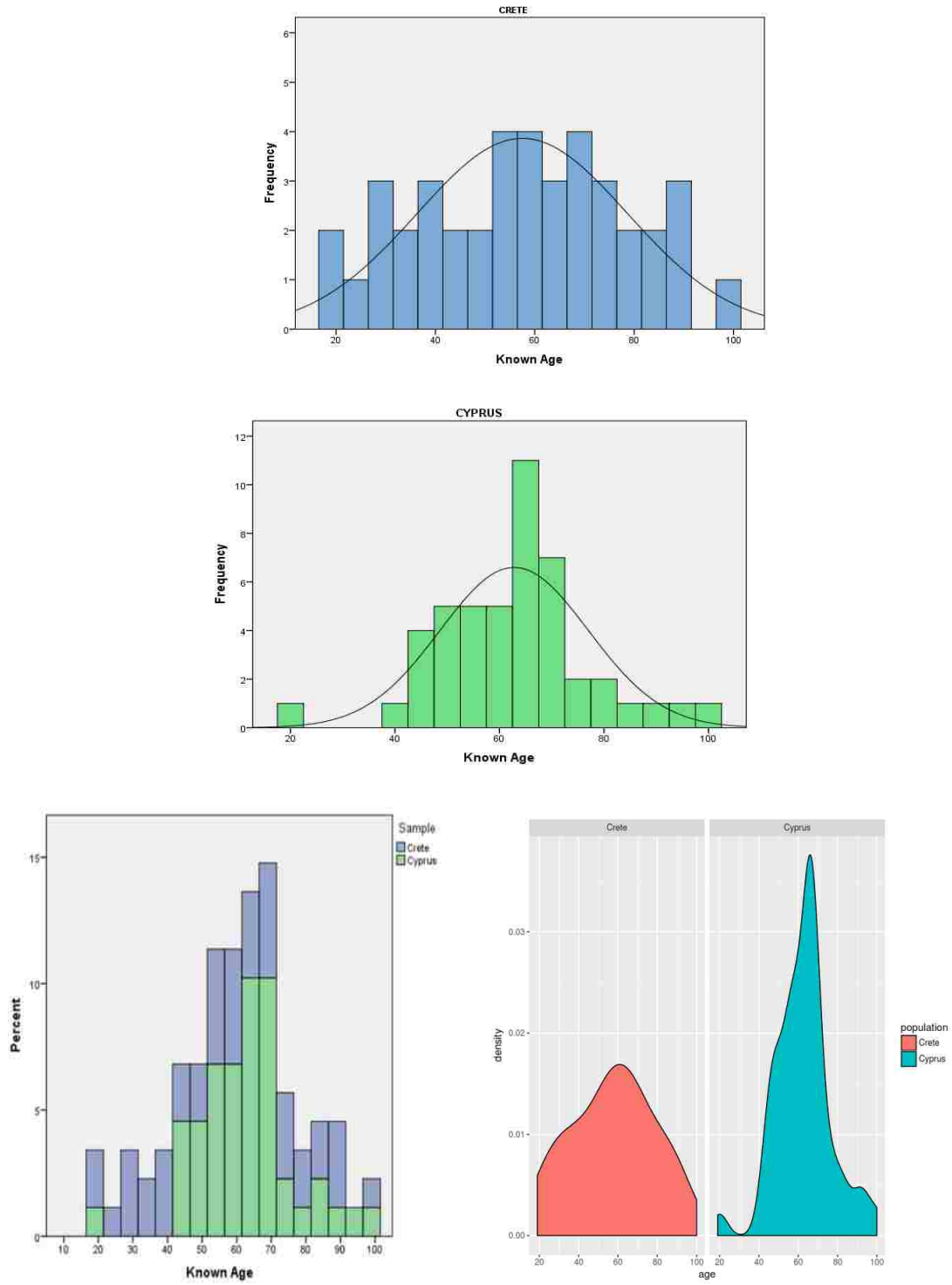

Figure 5.10 Sample histograms; both samples percentages (Crete-blue, Cyprus-green) (bottom left), and density plots by sample (Crete-pink, Cyprus-blue) (bottom right).

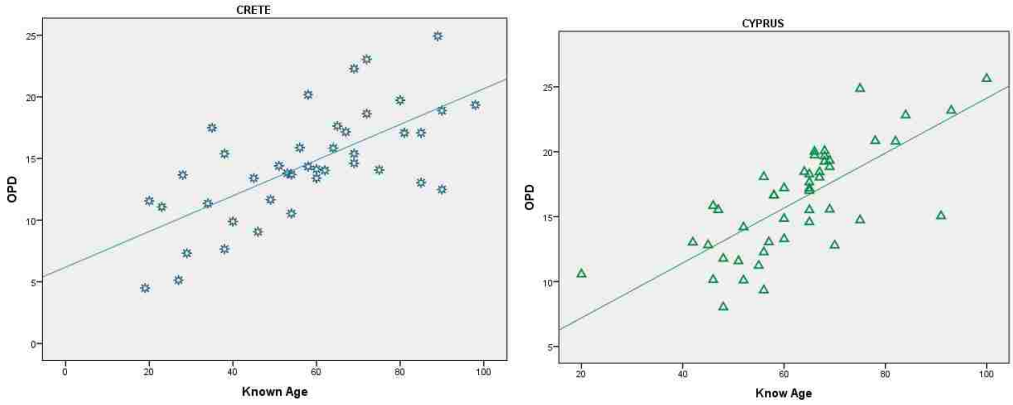

Figure 5.11 Association between age and histological variables for Cretans (left) and Cypriots (right).

Pearson´s correlation coefficients were computed for each sub-group (sex and sample) to assess the strength and direction of the relationship between known age and each variable (Table 5.22). A similar pattern in the direction of the association (positive or negative) as seen for the entire sample was observed on most of the variables for the four sub-groups.

Table 5.22 Pearson´s correlation coefficients between all the variables and age by groups: sex and sample.

	SEX		SAMPLE	
	MALE	FEMALE	CRETE	CYPRUS
1. N.On	-0.11	-0.34* (*-0.36***)	-0.27	-0.34*
2. N.On.Fg	0.44**	0. 29*	0.37* (*0.31**)	0.31*
3. N.On.Tt	0.11	-0.11	-0.05	-0.11
4. OPD(I)	0.51**	0.39**	0.42**	0.43**
5. OPD(F)	0.71** (*0.79***)	0.82**	0.77**	0.81**
6. OPD	0.72**(*0.79***)	0.69**	0.68**	0.73**
7. Ct.Ar	-0.40* (*-0.42***)	-0.73** (*-0.732***)	-0.63** (*-0.68***)	-0.59** (*-0.58***)
8. Tt.Ar	-0.11	-0.18(*-0.07*)	-0.26 (*-0.30*)	-0.01 (0.08)
9. Es.Ar	0.01 (*0.08*)	0.17	-0.06 (*0.10*)	0.23
10. Ct.Ar/Tt.Ar	-0.27	-0.66**(*-0.70***)	-0.43**	-0.65** (*-0.72***)
11. On.Ar	-0.54**	-0.69**	-0.64** (*-0.66***)	-0.73**
12. On.Pm	-0.58**	-0.73**(*-0.77***)	-0.68** (*-0.69***)	-0.76**
13. On.Cr	0.67**	0.68**	0.68**	0.64**

* Correlation significant at 0.05, ** Correlation significant at 0.01; italics indicates Spearman´s Rank Correlation for non-normally distributed variable

As exceptions, N.On.Tt, Tt.Ar and Es.Ar results suggested direct or inverse associations depending on the sub-groups (Table 5.22). For males N.On.Tt exhibited a positive association indicating that, although not statistically significant,

this variable tends to increase with age for males. Based on the high skewness value reported for this variable, Spearman´s correlation was recommended (Mukaka, 2012).In the Cretan sample, there was an outlier for both Tt.Ar and Es.Ar (155 and 141 mm^2, respectively); after examination of the values, not obvious pathological or metabolic explanation was identified, and thus, this individual was kept for further analysis. This might have caused the direction discrepancies between Pearson´s and Spearman´s correlation coefficients for Es.Ar results. The Cypriot sample results indicated a difference in the direction of the correlation on Tt.Ar and Es.Ar (note that the values were all close to zero). The reported differences may be also the result of intrinsic size differences between males and females within the two samples.

In order to compare the sub-samples age distributions, a Welch's t-test was applied for comparison on each pair of groups – males and females, Cretans and Cypriots (Kohr and, Games 1974). Next, a parametric – Welch´s t-test – or non-parametric –Mann-Whitney U test (Mann and Whitney, 1947), were applied based on the results of testing the normality of distribution of the variables (see Table 5.20 and Table 5.21 for S-W for sexes and samples means).

Welch t-test results by sex did not indicate any statistically significant difference between age distributions among males and females ($t(85.86) = 0.01$, $p = 0.91$). This suggested that the samples can be compared for differences in the histomorphometric variables. Two variables indicated statistically significant differences between the sexes. The N.On.Tt mean for males is 313 while females report a mean of 257 with a different distribution between the sexes as seen in Table 5.23. The remaining variables did not show any statistically significant difference. The Mann-Whitney U test was run for the non-normally distributed variables. Three variables were found to be statistically significantly different between the two groups. N.On, Tt.Ar and Es.Ar present significantly higher values for males than for females (see mean ranks in Table 5.24). The remaining histomorphometric variables did not show any statistically significant difference between the sexes.

Table 5.23 Welch´s t-test by sex.

Welch´s Test	Statistics	df2	p-value
N.On.Fg	2.48	83.26	0.12
N.On.Tt	6.09	81.38	0.02
OPD(I)	0.70	85.99	0.41
On.Ar	0.16	84.73	0.69
On.Cr	1.18	82.28	0.28

Table 5.24 Mann-Whitney U Test by sex.

Mann-Whitney U		Mean Rank	U	Z	p-value
N.On	Male	52.29	149	-2.61	0.009
	Female	38.01			
OPD(F)	Male	41.38	836	-1.04	0.29
	Female	47.10			
OPD	Male	42.93	897	-0.53	0.59
	Female	45.81			
Ct.Ar	Male	49.91	744	-3.86	0.07
	Female	39.99			
Tt.Ar	Male	56.03	499	-3.86	0.001
	Female	34.90			
Es.Ar	Male	54.85	546	-3.47	0.001
	Female	35.88			
Ct.Ar/Tt.Ar	Male	41.53	841	-1.00	0.32
	Female	46.97			
On.Pm	Male	45.03	939	-0.18	0.86
	Female	44.06			

Regarding samples differences, the results from the Welch t-test for Cretans and Cypriots also exhibited non-statistically significant difference between the two samples´ age distributions (t (68.41) = 1.85, p = 0.18). Note that through visual inspection of the histograms differences in the age distributions of the two samples were noticed (Figure 5.10). Thus, the bootstrapping method was used to confirm the preliminary results and the same outcome was obtained.

Welch´s Test results for the normally distributed variables indicated that four variables were different between the samples (Table 5.25). The N.On was statistically significant higher in Cypriots than in Cretans (the means are 192.7 and 150.1, respectively). The N.On.Tt mean for Cretans was 237 while Cypriots presented a significantly higher mean of 322. OPD(F) was statistically significantly higher for Cypriots (mean = 6.83) than for Cretans (mean = 5.66). The remaining variables did not show any differences. Mann-Whitney U Test results indicated that

just one variable differed between the samples with Cretans showing a lower number of N.On.Fg (mean rank = 31.72) than Cypriots (mean rank = 55.65) (Table 5.26).

Table 5.25 Welch´s t-test by samples.

Welch´s Test	Statistics	df2	p-value
N.On	8.27	83.82	0.005
N.On.Tt	16.76	83.52	< 0.001
OPD(I)	1.51	81.94	0.22
OPD(F)	4.25	83.26	0.042
OPD	3.64	81.64	0.06
On.Cr	3.02	80.27	0.08

Table 5.26 Mann-Whitney U Test by samples.

Mann-Whitney U		Mean Rank	U	Z	p-value
N.On.Fg	Crete	31.72	440	-4.38	< 0.001
	Cyprus	55.65			
Ct.Ar	Crete	39.12	743	-1.84	0.06
	Cyprus	49.19			
Tt.Ar	Crete	40.78	811	-1.28	0.20
	Cyprus	47.74			
Es.Ar	Crete	41.29	832	-1.10	0.27
	Cyprus	47.30			
Ct.Ar/Tt.Ar	Crete	42.85	896	-0.56	0.57
	Cyprus	45.94			
On.Ar	Crete	40.24	789	-1.46	0.14
	Cyprus	48.21			
On.Pm	Crete	40.83	813	-1.26	0.21
	Cyprus	47.70			

5.4.2.1 One-Way ANCOVA: sex and sample effect

Further investigation of the differences among histological parameters between sexes and samples was carried out using an analysis of covariance (One-way ANCOVA). Note that for this test only the histological variables that showed a significant relation with age for entire sample and subgroups will be examined.

Results from ANCOVA testing assumptions indicated the following: the examination of scatterplots for both males and females, and Cretans and Cypriots, suggests a fairly linear relation between all parameters and each sub-group (see

Appendix B.5 and B.6). Hence, linearity assumption was assumed for all the variables. The interaction term was non-statistically significant indicating that homogeneity of regression slopes assumption was met. Standardised residuals for each sex/sample and for the overall model were tested for normality using *S-W* test. Non-normality was suggested by a p-value less than the cut-off ($p < 0.05$). If this assumption was violated, it will be reported in the text. Homoscedasticity was tested by the examination of standardised residuals versus predicted values; with all the scatter plots indicating a random distribution of the values. Moreover, values were equally spread along the axes. Homogeneity of variances assumption was checked through Levene´s test. The identification of outliers in the data was done by inspection of the residuals minimum and maximum values confirming that all cases fell within ± 3 standard deviations. Thus, this assumption was also met for all the parameters.

One-way ANCOVA was run to determine the sex effect on the following variables: N.On.Fg, OPD(I), OPD(F), OPD, Ct.Ar, Ct.Ar/Tt.Ar, and secondary osteon measurements (On.Ar, On.Pm and On.Cr), with age as a covariate. For all the dependent variables, known age was reported to be a statistically significant covariate. Table 5.27 presents the means and adjusted means for all the dependent variables by sex as well as p-values for homogeneity of regression slopes and Levene´s Test results.

Table 5.27 ANCOVA results for: means and adjusted means for males and females as groups and age as a covariate; homogeneity of regression slopes and Levene´s Test p-values.

		Unadjusted		Adjusted		Homogeneity of regression slopes		Levene´s test	Sex effect
		Mean	SD	Mean	SE	F* (1,84)	p-value	p-value	
N.On.Fg	M	118	7.18	118.21	6.76	0.958	0.33	0.44	NO
	F	102.65	6.58	102.50	6.17				
OPD(I)	M	9.38	2.02	9.38	0.321	0.264	0.61	0.04	NO
	F	8.98	2.4	8.98	0.293				
OPD(F)	M	6.10	2.66	6.12	0.270	0.025	0.87	0.15	NO
	F	6.43	2.74	6.41	0.247				
OPD	M	15.48	4.08	15.51	0.494	0.061	0.81	0.14	NO
	F	15.42	4.06	15.38	0.451				
Ct.Ar	M	21.16	8.64	21.10	1.02	0.610	0.44	0.01	YES
	F	17.59	7.06	17.63	0.93				
Ct.Ar/Tt.Ar	M	0.304	0.12	0.303	0.02	3.55	0.06	0.46	NO
	F	0.336	0.13	0.337	0.01				
On.Ar	M	0.0323	0.01	0.032	0.001	0.366	0.55	0.61	NO
	F	0.0315	0.01	0.032	0.001				
On.Pm	M	0.637	0.09	0.636	0.01	0.764	0.38	0.95	NO
	F	0.629	0.11	0.630	0.011				
On.Cr	M	0.913	0.02	0.913	0.003	0.409	0.52	0.71	NO
	F	0.908	0.02	0.908	0.002				

M= male, F= female, SD= standard error, SE= standard error; Sex*Age interaction

ANCOVA results for N.On.Fg indicates that standardised residuals for females and the overall model were not normally distributed (p = 0.03 and p = 0.02, respectively). When age was adjusted, the sex effect was shown to be not statistically significant $F(1, 85) = 2.94$, $p = 0.090$, partial $\eta^2 = 0.034$. Based on the violation of normality, LnN.On.Fg was used as the dependent variable and the analysis performed again. Normality of residuals was confirmed for both sexes and the overall model, and the remaining assumptions were also met. The sex effect was also reported as non-statistically significant ($F(1, 85) = 3.77$, $p = 0.060$, partial $\eta^2 = .043$) with the bootstrapping procedure confirming these results.

For OPD(F) and OPD, normality of standardised residuals was not statistically significant for each sex and for the overall model (p > 0.05). However, OPD(I)

showed a deviation from normal distribution for the male group (*S-W* p = 0.047). Homogeneity of variances was assessed by Levene´s test indicating no violation for OPD(F) and OPD, although a p-value less than 0.05 was reported for OPD(I) (Table 27). The final results indicated that there was no statistically significant difference between sexes for OPD(F) and OPD as assessed by the sex effect being reported as $F(1, 85) = 0.607$, $p = 0.438$, partial $\eta^2 = 0.007$, and ($F(1, 85) = 0.038$, $p = 0.846$, partial $\eta^2 = 0.005$, respectively.

Based on the violations observed for OPD(I), ANCOVA analysis was performed on LnOPD(I) as the dependent variable. All the previous assumptions were met except for normality of standardised residual both for each sex and for the overall model ($p < 0.05$), and for homogeneity of variances (Levene´s Test $p < 0.05$). If the results were interpreted ignoring these violations, the same pattern was observed for the non-transformed and the Ln-transformed parameter with non-statistically significant sex effect (OPD(I)= $F(1, 85) = 0.918$, $p = 0.341$, partial $\eta^2 = 0.011$ and LnOPD(I)= $F(1, 85) = 1.45$, $p = 0.232$, partial $\eta^2 = 0.017$). No further transformation of this variable was performed as ANCOVA is considered a robust test for normality violation. Moreover, further transformation of the data will complicate the interpretation of the results. Lastly, bootstrapping confirmed the non-statistically significant sex effect for OPD(I).

As seen in Table 5.27, homogeneity of variance assumption was violated for Ct.Ar. Moreover, non-normality of standardised residuals for the overall model was reported (S-W test < 0.05). With adjustment of age as a covariate, a statistically significant sex effect was found for Ct.Ar (($F(1, 85) = 6.26$, $p < 0.010$, partial $\eta^2 = 0.069$). Based on the violations reported, LnCt.Ar was used as the dependent variable. In this case, normality of standardised residuals was confirmed for both sexes separately and the overall model ($p > 0.05$). The homogeneity of variance was still an issue (Levene´s test significance p-value < 0.05). After the adjustment of age, the sex effect was still statistically significant ($F(1, 85) = 7.36$, $p < 0.010$, partial $\eta^2 = 0.080$). Post hoc analysis with Bonferroni adjustment for non-transformed Ct.Ar showed that this parameter was higher in males than in females with a mean difference of 3.46 (95% CI, 0.713-6.219, $p < 0.010$). Again, the bootstrapping process confirmed the reported results.

All assumptions for Ct.Ar/Tt.Ar were met, and the effect of sex after the adjustment of age was not statically significant as assessed by the ANCOVA results ($F(1, 85) = 2.204$, $p = 0.141$, partial $\eta^2 = 0.025$).

The remaining variables are related to secondary osteons measurements. On.Ar, On.Pm and On Cr ANCOVA results showed that with age as a covariate, the effect of sex on these variables was not statistically significant $F(1, 85) = 0.176$, $p = 0.676$, partial $\eta^2 = 0.002$; ($F(1,85) = 0.130$, $p = 0.719$, partial $\eta^2 = 0.002$; ($F(1,85) = 2.436$, $p = 0.122$, partial $\eta^2 = 0.028$, respectively).

The same histological parameters were used to determine whether age was a significant covariate and sample effect (Crete and Cyprus) was statistically significant. In this analysis, the covariate of age was also found to be statistically significant for all the models. Table 5.28 reports means and adjusted means for all the dependent variables by sample**,** homogeneity of regression slopes and Levene´s Test p-values.

Table 5.28 ANCOVA results for means and adjusted means for Cretans and Cypriots as groups and age as a covariate; Homogeneity of regression slopes and Levene´s Test p-values.

		Unadjusted		**Adjusted**		**Homogeneity of regression slopes**		**Levene´s test**	**Sample effect**
		Mean	SD	Mean	SE	F (1,84)*	p-value	p-value	
OPD(I)	CR	8.84	2.32	8.99	0.32	0.472	0.49	0.42	NO
	CY	9.43	2.13	9.31	0.29				
OPD	CR	14.5	4.49	14.98	0.49	2.91	0.09	0.49	NO
	CY	16.26	4.09	15.85	0.45				
Ct.Ar	CR	17.74	7.63	16.98	0.99	1.98	0.16	0.34	YES
	CY	20.49	8.13	21.15	0.93				
Ct.Ar/Tt.Ar	CR	0.316	0.13	0.306	0.02	3.59	0.06	0.20	NO
	CY	0.326	0.11	0.335	0.02				
On.Ar	CR	0.303	0.01	0.029	0.001	2.98	0.09	0.24	YES
	CY	0.033	0.01	0.034	0.001				
On.Pm	CR	0.617	0.11	0.606	0.01	2.30	0.13	0.12	YES
	CY	0.645	0.09	0.656	0.01				
On.Cr	CR	0.905	0.02	0.908	0.003	0.624	0.43	0.49	NO
	CY	0.913	0.02	0.912	0.002				

CR=Crete, CY=Cyprus, SD=standard error, SE=standard error; Sample*Age interaction

The homogeneity of regression slopes assumption for N.On.Fg and for OPD(F) was violated as indicated by the interaction term being statistically significant ($F(1,84) = 21.83$, $p < 0.001$; $F(1,84) = 5.386$, $p < 0.05$, respectively). Thus, no further analysis was performed.

Standardised residuals obtained by OPD(I) for each sample and for the overall model were examined for normality assumption which was violated for Cypriots and for the overall model (*S-W* $p < 0.05$). When age was adjusted as a covariate, the sample effect was not statistically significant for OPD(I) ($F(1,85) = 0.489$, $p = 0.486$ partial $\eta^2 = 0.006$). Based on the violation of normality, the analysis was repeated using LnOPD(I). All the assumptions met in the previous test were met apart from normality of standardised residuals for both samples and the overall model (Cretans $p < 0.05$, Cypriots and overall model $p < 0.001$). The results for the transformed variable indicated that the sample effect on OPD(I) after adjustment of age was still not statistically significant ($F(1,85) = 0.612$, $p = 0.436$ partial $\eta^2 = 0.007$) with bootstrapping confirming this outcome.

OPD standardised residuals were not normally distributed for Cypriots ($p < 0.05$), although the overall model approximated normality. The sample effect was found to be non-statistically significant after the age adjustment ($F(1,85) = 1.674$, $p = 0.199$, partial $\eta^2 = 0.019$). The transformation of OPD was performed with LnOPD ANCOVA results and bootstrapping indicating non-statistical significance ($F(1,85) = 2.118$, $p = 0.143$, partial $\eta^2 = 0.025$); however, the normality assumption was still violated for the Cypriot sample ($p < 0.01$).

Ct.Ar standardised residuals for each sample and for the overall model were not normally distributed ($p < 0.001$). After adjustment of age, sample effect was found statistically significant for Ct.Ar ($F(1,85) = 9.162$, $p < 0.010$, partial $\eta^2 = 0.097$). Post-hoc analysis was carried out with Bonferroni adjustment showing that the mean difference was statistically significant with Cypriots Ct.Ar being 4.16 larger than the Cretans Ct.Ar (95% CI: 1.429 to 6.901, $p < 0.001$). Based on the violation of residuals normality, LnCt.Ar was used as the dependent variable. The standardised residuals seemed to be normally distributed for both samples and overall the model after the variable transformation ($p > 0.05$). These results indicated that sample effect was still different between Cretans and Cypriots ($F(1,85) = 12.15$, $p < 0.010$, partial $\eta^2 = 0.125$) and it is further confirmed by the bootstrapping procedure.

Normality of standardised residuals for Ct.Ar/Tt.Ar was violated for the Cypriot sample ($p < 0.01$). No sample effect was found for the dependent variable as assessed by $F(1,85) = 1.573$, $p = 0.213$, partial $\eta^2 = 0.018$). LnCt.Ar/Tt.Ar was then used as the dependent variable and normality of the standardised residuals was achieved for both samples and the overall model ($p > 0.05$). The effect of sample on LnCt.Ar/Tt.Ar was still non-statistically significant as demonstrated by the ANCOVA results ($F(1,85) = 2.596$, $p = .111$, partial $\eta^2 = .030$).

When age was adjust as a covariate, the sample effect was statistically significant for On.Ar and On.Pm ($F(1,85) = 9.996$, $p < 0.010$, partial $\eta^2 = 0.105$, and $F(1,85) = 9.992$, $p < 0.010$, partial $\eta^2 = 0.106$, respectively). Post hoc test with Bonferroni adjustment indicated that the Cypriot sample has a greater On.Ar than the Cretan sample with a significant mean difference of 0.005 (95% CI: 0.002 to 0.008, $p < 0.01$) and a higher value for On.Pm than the Cretan sample with a mean difference of 0.05 (95% CI: 0.019 to 0.082, $p < 0.01$).

Finally, after adjustment of age, there was no statistically significant difference between Cretan and Cypriots found for On.Cr ($F(1,85) = 1,178$, $p = 0.281$, partial $\eta^2 = 0.014$).

Group differences were further explored using the General Linear Model (*GLM*) in combination with Chow test to determine if the slopes and intercepts between sex and samples for each independent variables (parameters) were equal or differ (Crowder, 2013). The analysis was performed as described in (section 4.2.4.4). Those parameters not normally distributed were ln-transformed (Table 5.17)**.**The results are shown in Table 5.29. Regarding slope differences between sexes, none of the variables were found to be statistically significant. Results by samples indicated that the regression slopes were significantly different between Cretans and Cypriots for LnCt.Ar, LnCt.Ar/Tt.Ar, On.Ar and On.Pm.

Table 5.29 Chow test results with age as the dependent variable by sex and by sample.

SEX			SAMPLE	
Interaction	p-value		Interaction	p-value
Sex*LnN.On.Fg	0.45		Sample*LnN.On.Fg	0.74
Sex*OPD(I)	0.72		Sample*OPD(I)	0.44
Sex*OPD(F)	0.94		Sample*OPD(F)	0.34
Sex*OPD	0.84		Sample*OPD	0.85
Sex*LnCt.Ar	0.06		Sample*LnCt.Ar	0.001
Sex*LnCt.Ar/Tt.Ar	0.12		Sample*LnCt.Ar/Tt.Ar	0.03
Sex*On.Ar	0.60		Sample*On.Ar	0.002
Sex*On.Pm	0.76		Sample*On.Pm	0.002
Sex*LnOn.Cr	0.37		Sample*LnOn.Cr	0.53

5.5. Simple and Multiple GLM

Generalised linear models were built to determine the relationship between the dependent variable (age) and the independent variables (histological parameters). Values related to the goodness of fit are reported in order to finally select the best model. Regression analysis of those variables that did not demonstrate any statistically significant relationship with age in the previous section showed a poor fit with the data, and they were excluded from further analysis. Diagnostic plots for the first model will be presented here as an example and the remaining diagnostic plots from the main models can be consulted in Appendix B.7 and B.10). In the case of any assumptions being violated, a correction of the model and/or further examination of the specific statistical requirement was considered and will be discussed here.

5.5.1. Simple regression models

The relationship between the histomorphometric variables and known age was examined through simple linear models as described in section 4.2.4.5. The entire dataset was used at this stage of the analysis (N = 88).Ten simple linear models were generated. Table 5.30 presents a summary of all univariate models for secondary osteon frequency numbers and densities, rib area and secondary osteons measurements. Diagnostic plots can be consulted in Appendix B.7.

The null hypothesis was rejected for *Model 1* (N.On) (F (1,86) = 4.91, p = 0.029). R^2 indicated that a very small proportion of the variance was expressed by the model (SEE = 17.49). AIC_c and BIC values were the highest of all the generated simple regression models (Table 5.30).The regression slope coefficient for the predictor was statistically significant (t = -2.22, p = 0.029). The model seemed to violate the assumption of independence of errors (Durbin-Watson, *DW* = 0.51). Further examination of standardised residuals against standardised predicted (error independence scatter plot) demonstrated a roughly rectangular pattern with all values falling within ± 3, and thus, suggesting that independence of errors assumption was met (Lomax and Hahs-Vaughn, 2012). A review of normality test (*S-W* = 0.98, df = 88, p = 0.27) and skewness and kurtosis (-0.305 and 0.149, respectively) of the unstandardized residuals suggested reasonable normality. Further assessment of the diagnostic plots indicates evidences for linearity and normal distribution of the residuals (Figure 5.12.1 and 5.12.2); Figure 5.12.3 suggests homogeneity of variance and no case is identified as an influential outlier as assessed by Figure 5.12.4. Cook's distance values were examined with all cases within the acceptable level (less than 1).

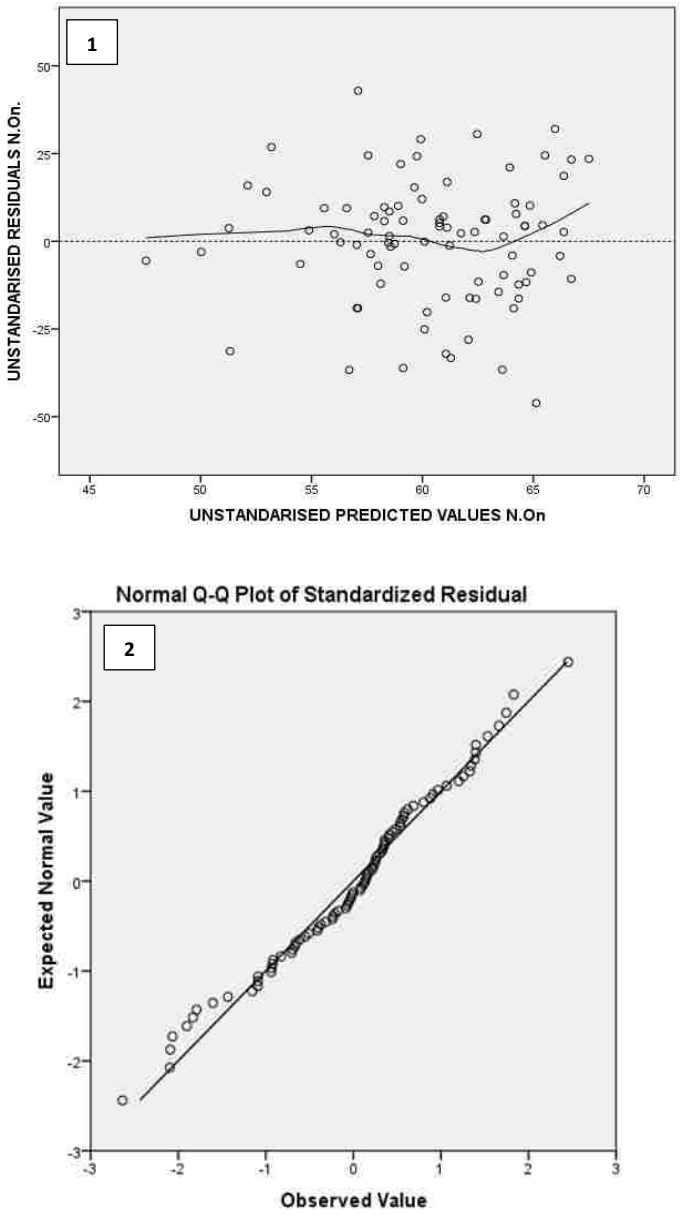

Figure 5.12 Diagnostic plots Model 1. Residuals vs fitted (1): roughly horizontal line with a random distribution of values indicating linearity. Q-Q plot (2): normal distribution of residuals represented by values not deviating drastically from the straight line.

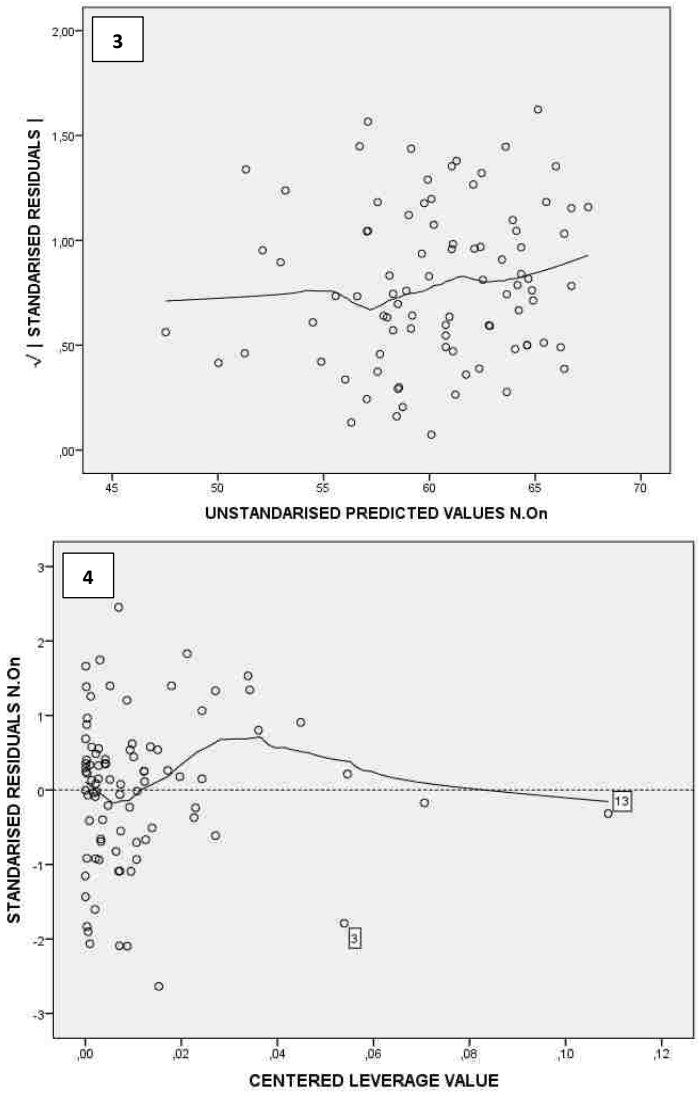

Figure 5.12. (***Continued***) Scale-location plot **(3)**: residuals spread equally along the predicted value axis with a roughly horizontal line indicating homogeneity of variance (homoscedasticity). Residuals vs Leverage´s values **(4)**: no cases outlying on the top and bottom right corner along with Leverage values suggesting no influential regression outliers.

Model 2 (N.On.Fg) regression model was statistically significant (F(1,86) = 11.09, p = 0.001) with standardised and unstandardized slope coefficients for N.On.Fg being statistically significant (t = 3.45, p = 0.001) (Table 5.30). The proportion of the variation of age explained by the model was low (R^2 = 0.12, *SEE* = 16.9) in comparison with the remaining generated models. Residuals analysis indicated violation of the assumption of independence (*DW* = 0.51). Linearity and slightly normal distribution of the residuals was observed through the diagnostic

plots. Equal variances assumption was met and no outliers were identified. A slightly better fit of the data than the previous model was observed for N.On.Fg based on AIC_c and BIC values.

Based on the hypothesis that OPD values reach an asymptote after 60 years of age, both linear and curvilinear models were tested in order to evaluate which regression model better fits the data.

The null hypothesis was rejected for the model including OPD(I) as a predictor $F(1,86) = 19.77$, $p < 0.001$) (*Model 3*) (Table 5.30). Beta unstandarised and standardised coefficients were statistically significant ($t = 4.44$, $p < 0.001$). AIC_c and BIC values decrease in comparison with osteon counting models although the prediction power of the model is low ($R^2 = 0.19$, *SEE* = 16.22). Durbin-Watson (D-W) value (0.68) suggests that the assumption of independent errors was not meet but the standardised residuals versus standardised predicted scatter plot indicated reasonable independence. Non-normality of the distribution of the residuals was reported (*S-W* = 0.97, df = 88, p = 0.034) although skewness and kurtosis values were within the acceptable range (0.073 and 0.640, respectively). Further assessment of the diagnostic plots suggested evidences of linearity and slightly normal distribution of the residuals with some deviation observed on the tails. When quadratic regression was applied for explaining the relation between OPD(I) and age, the model predictive power decreased slightly (multiple adjusted $R^2 = 0.17$, *SEE* = 16.30) and parsimony values increased ($AIC_c = 746.29$, BIC = 755.72). The standardised and unstandarised partial slopes for the predictor became non-statistically significant ($t = 0.162$, df = 86 , $p = 0.82$ and $t = 0.601$, df = 86 , $p = 0.60$, respectively for OPD(I) and $OPD(I)^2$) suggesting than the curvilinear model did not improve the fit of the data to the model.

With OPD(F) as the independent variable (*Model 4*), a noticeably higher proportion of the variation was explained by the independent variable ($R^2 = 0.60$, SEE = 11.30) along with a decrease in AICc and BIC values. The regression model and the standardised and unstandardized coefficients for the slope were statistical significant ($F(1,86) = 131.16$, $p < 0.001$). As seen in Table 5.30, independence of errors seemed reasonably met (*DW* = 1.24). Unstandarised residuals normality tests indicated normality (S-W = 0.99, df = 88, p = 0.93; skewness and kurtosis values of 0.3 and 0.10, respectively) and it was further confirmed by the QQ-plot.

Table 5.30 Summary of simple models in the entire sample set.

	N=88	ANOVA						Parameters Estimates						Model Summary					Goodness of fit	
Model	Variable		Sum of Squares	df	Mean Square	F value	Pr > F		Unstandarised Coefficients		Standarised Coefficients	T-Value	Pr>|t|	R	R^2	Adj. R^2	SEE	D-W	AICc	BIC
									B	SE	Beta									
M1	**N.On**	Regression	1504.41	1	1504.41	4.91	0.029	(Constant)	70.11	4.79		14.638	< 0.001	0.23	0.05	0.04	17.49	0.51	757	764.8
		Residuals	26325.02	86	306.1			N.On.	-0.057	0.03	-0.233	-2.217	0.029							
		Total	27829.44	87																
M2	**N.On.Fg**	Regression	3383.66	1	3383.66	11.90	0.001	(Constant)	45.436	4.68		9.717	< 0.001	0.35	0.12	0.11	16.86	0.69	751.2	758.3
		Residuals	24445.77	86	284.25			N.On.Fg	0.136	0.04	0.349	3.45	0,001							
		Total	27829.44	87																
M3	**OPD(I)**	Regression	5201.26	1	5201.26	19.7	< 0.001	(Constant)	28.631	7.34		3.903	< 0.001	0.43	0.19	0.18	16.22	0.68	744.4	751.5
		Residuals	22628.17	86	263.11			OPD(I)	3.46	0.78	0.432	4.446	< 0.001							
		Total	27829.44	87																
M4	**OPD(F)**	Regression	16808.28	1	16808.28	131.8	< 0.001	(Constant)	27.935	3.07		9.083	< 0.001	0.78	**0.60**	0.59	11.32	1.24	688.2	691.2
		Residuals	11021.15	86	128.15			OPD(F)	5.158	0.45	0.777	11.452	< 0.001							
		Total	27829.44	87																
M5	**OPD**	Regression	13774.9	1	13774.93	84.28	< 0.001	(Constant)	15.66	5.05		3.099	0.003	0.70	**0.49**	0.49	12.78	1.12	702.5	709.6
		Residuals	14054.54	86	163.42			OPD	2.893	0.31	0.704	9.181	< 0.001							
		Total	27829.44	87																

*M= model, SE=standard error, SEE= standard error of the estimate, D-W=Durbin-Watson; **In bold SEE < 15 years

Table 5.30. (***Continued***) Summary of simple models in the entire sample set.

	N=88	ANOVA						Parameters Estimates						Model Summary					Goodness of fit	
Model	Variable		Sum of Squares	df	Mean Square	F value	Pr > F		Unstandarised Coefficients		Standarised Coefficients	T-Value	Pr>|t|	R	R^2	Adj. R^2	SEE	D-W	AICc	BIC
									B	SE	Beta									
M6	**Ct.Ar**	Regression	8646.56	1	8646.56	38.76	< 0.001	(Constant)	84.337	4.17		20.217	< 0.001	0.56	**0.31**	0.30	14.93	0.66	729.6	729.8
		Residuals	19182.87	86	223.05			Ct.Ar	-1.249	0.20	-0.557	-6.226	< 0.001							
		Total	27829.44	87																
M7	**Ct.Ar/Tt.Ar**	Regression	6900.58	1	6900.58	28.35	< 0.001	(Constant)	83.823	4.71		17.778	< 0.001	0.49	0.25	0.24	15.6	0.47	737.5	744.66
		Residuals	20928.85	86	243.35			Ct.Ar/Tt.Ar	-73.003	13.71	-0.498	-5.325	< 0.001							
		Total	27829.44	87																
M8	**On.Ar**	Regression	11250.83	1	11250.83	58.36	< 0.001	(Constant)	97.473	5.08		19.179	< 0.001	0.64	**0.40**	0.39	13.88	0.83	717	724.1
		Residuals	16578.6	86	192.77			On.Ar	-1163.81	152.3	-0.636	-7.64	< 0.001							
		Total	27829.44	87																
M9	**On.Pm**	Regression	12463.76	1	12463.76	69.75	< 0.001	(Constant)	133.224	8.84		15.065	< 0.001	0.67	**0.45**	0.44	13.36	0.94	710.3	717.5
		Residuals	15365.67	86	178.67			On.Pm	-115.24	13.79	-0.669	-8.352	< 0.001							
		Total	27829.44	87																
M10	**On.Cr**	Regression	12398.55	1	12398.55	69.1	< 0.001	(Constant)	-445.296	60.84		-7.319	< 0.001	0.67	**0.45**	0.44	13.39	0.76	710.7	717.8
		Residuals	15430.89	86	179.42			On.Cr	555.582	66.83	0.667	8.313	< 0.001							
		Total	27829.44	87																

*M= model, SE=standard error, SEE= standard error of the estimate, D-W=Durbin-Watson, **In bold SEE< 15 years

There was a certain curvilinear tendency observed in the residuals versus the fitted diagnostic scatterplot for *Model 4*. Homoscedasticity was assumed although after 70 years of age there is a slope in the trend line. No influential cases were identified according to Cook´s Distance values.

Curvilinear regression analysis for *Model 4* suggested that OPD(F) was slightly better explained through a quadratic model. The model fit values were improved (multiple adjusted R^2 = 0.63, *SEE* = 10.80; AIC_c and BIC values of 673.9 and 683.4, respectively). The regression model was statistically significant (F(1,86) = 76.81, p < 0.001) and it met the assumption of normality of residuals (*SW* = 0.988, df = 88, p = 0.62; kurtosis = 0.43, skewness = 0.207) and independence of errors (*DW* = 1.34). Standardised and unstandarised partial slope coefficients were statistically significant (Table 5.31). The examination of diagnostic residual plots suggested an improvement in the curvilinear pattern previously observed in the linear model.

Table 5.31 Summary of quadratic *Model 4*.

Variable	B	SEB	β	t	Pr >| t |
Intercept	12.371	5.84		2.118	0.037
OPD(F)	10.631	1.827	1.602	5.819	< 0.001
OPD(F)2	-0.404	0.131	-0.849	-3.082	< 0.001

Model 5 includes OPD as an independent variable; the null hypothesis is rejected (F(1,86) = 84.29, p < 0.001) (Table 5.30). Standardised and unstandarised slope for OPD were significantly different from zero (t = 0.704, p < 0.001). Around 50% of the variance in age can be explained by OPD (*SEE* = 12.7). A slight decrease in model fit of the data was observed through an increase in the AIC_c and BIC values compared to *Model 4*. Independence of errors and normality of the residuals are reasonable (DW = 1.12, skewness (0.23) and kurtosis (1.16)). Further examination of studentised residuals against predicted values plot indicated a random display of points suggesting independence. There is evidence for normality of residuals (*S-W* = 0.97, df = 88, p = 0.30). Visual examination of diagnostic plots suggested a random and a normal distribution of the residuals; assumption of equal variance was met and no influential cases are noted. Only one case seemed to be an outlier although Cook's Distance and Leverage values indicate no influence on the regression. Curvilinear regression analysis did not improve the linear model

based on the values obtained by prediction accuracy rates and model fit values (multiple adjusted R^2 = 0.486, *SEE* = 12.8, AIC_c = 704.2, BIC = 713.6). Standardised and unstandardized slope coefficients for OPD squared (-0.036 and -0.277, respectively, t = -0.687, p = 0.494) suggested that the inclusion of this variable into the model did not improve the fit of the data.

Model 6 and *Model 7* included predictors related to Ct.Ar and Ct.Ar/Tt.Ar. Summarising, all coefficients for both models were statistically significant at the p-value < 0.001 (Table 5.30). Ct.Ar accounted for a higher R^2 than Ct.Ar/Tt.Ar explaining around 31% of the variance of the response variable and providing a *SEE* of around 15 years; while 24% of the variance of age was explained in *Model 7* with slightly lower prediction accuracy (15.6 years). Based on the lower prediction power of these two models, no further discussion will be held.

The remaining models (*Model 8, 9* and *10*) include secondary osteon measurements as independent variables (Table 5.30). Among all the models, On.Ar produced the lower explanatory power (R^2 = 0.40) and the highest AIC_c and BIC values (717 and 724, respectively). The model was statistically significant with F(1,86)= 58.36, p < 0.001. Standardised and unstandarised slopes for the independent variable were statistically significant (t = 19.17 and t = -7.64 at p < 0.001, respectively). Independence of errors was not confirmed by statistics (*DW* = 0.83) but it was suggested by visual examination of error independence scatter plot. Skewness and kurtosis fell within the acceptable range (-0.47 and 0.45) and normal distribution of the residual was confirmed through the analysis of unstandarised residuals (*S-W* = 0.97, df = 88, p = 0.15).

Model 9 included On.Pm accounting for 45% of the variance in age (SEE = 13.36); AIC_c and BIC values were the lowest among the three models that include secondary osteon measurement parameters. It presented a slope of the regression line statistically significantly different from zero (F(1,86) = 69.75, p < 0.001) with both standardised and unstandarised slopes falling at the p < 0.001 level (t = 15.06 and t = -8.35, respectively) (Table 5.30). As seen in the previous model, the independence of errors was just under the expected level (*DW* = 0.94) with skewness (-0.49), and kurtosis (0.34) within the range. Unstandarised residuals were normally distributed (*S-W* = 0.979, df = 88, p = 0.17).

Model 10 (On.Cr as predictor) explained similar variance as On.Pm model (45%) and the regression slope was statistically different from zero (F (1,86) = 69.10, p < 0.001). Standardised and unstandarised slopes were statistically significant (t = -7.32 and t = 8.31, respectively, p < 0.001). Independence of errors was violated according to D-W statistics (0.77), although studentised residual against predicted values plot did provide evidence of independence. Normality tests suggest normal distribution of residuals (*S-W* = 0.51, skewness = -0.03, kurtosis = 0.91).

The diagnostic plots for all models (Appendix B.7) suggest that the assumptions of residuals were met with 95% of the standardised residuals falling within ± 2. The cases identified as possible outliers were examined for standardised residuals, leverage and Cook's distance values concluding that none of them were influential cases for the regression models.

5.5.2. Multiple regression models

The results for the multiple regression models are organised first with the models including OPD variables and secondary osteon measurements, and the remaining models only including secondary osteons measurements and rib area parameters. Sixteen models are presented in Table 5.32 and Table 5.34. Due to the large amount of data, only those models that showed a clear improvement in prediction accuracy rates and goodness of fit values compared to the univariate models will be presented in this section. Diagnostic plots for multiple linear models can be found in Appendix B.8.

Five models were generated using OPD and secondary osteons measurements (*Model 11* to *Model 15*). The first three models in Table 5.32 (*Model 11* to *13*) include two independent variables. The prediction accuracy rates were fairly similar although a slightly higher SEE, lower multiple R^2 and AIC_c and BIC values was obtained by the combination of OPD and On.Ar (*Model 11*). The null hypothesis was rejected with all the models being statistically significant from zero, and all partial slope coefficients were shown to be statistically significant at < 0.001 level. D-W statistics were within ±2 for the three models and independence of errors was further confirmed by standardised residuals and standardised predicted values scatter plots. While *S-W* test indicated non-normal distribution of unstandarised residuals (*S-W* = 0.966, df = 88, p = 0.022; S-W = 0.96, df = 88, p = 0.034; and *S-W*

= 0.97, df = 88, p = 0.040, *Model 11, 12* and *13* respectively), skewness and kurtosis values were acceptable (-0.272 and 1.12; -0.33 and 1.05; 0.345 and 1.57, respectively). Multicollinearity between the independent variables was reviewed through the tolerance and variance inflation factor (*VIF*) values that fell within the limits of acceptance for the three models. However, the eigenvalues for all of them were close to zero (*Model 11*: OPD = 0.123, On.Ar = 0.02; *Model 12*: OPD = 0.10 and On.Pm = 0.006; *Model 13*: OPD = 0.05, On.Cr = 0.002). Further analysis of the regression of OPD on the osteon measurement parameters resulted in R^2 not higher than 0.35 suggesting that in aggregate multicollinearity was not a problem.

Visual examination of residuals plots suggests the following assumptions. Linearity of residuals was assumed based on the random distribution of points in the residuals versus predicted values plot. Q-Q plots indicated relative normality with minor deviations at the tails (more pronounced for *Model 11).* Homogeneity of variance was confirmed, and a review of the case wise diagnosis based on Cook's distance and Leverage values was indicative of no cases exerting influence on the models (refer to Appendix B.8).

Table 5.32 Summary of selected multiple models including OPD variables for the entire sample (best model fit and accuracy rates).

	N=88	ANOVA						Parameters Estimates							Model Summary					Goodness of fit	
Model	Variables		Sum of Squares	df	Mean Square	F value	Pr > F		Unstandarised Coefficients		Standarised Coefficients	T-Value	Pr>|t|	Collinearity Diagnosis		R	R^2	Adj. R^2	SEE	D-W	AICc	BIC
									B	SE	Beta			Tolerance	VIF							
M11	OPD+On.Ar	Regression	16144.02	2	8072.01	58.71	< 0.001	(Constant)	48.77	9.22		5.287	< 0.001			0.76	0.58	0.57	11.72	1.14	688.4	697.8
		Residuals	11685.41	85	137.47			OPD	2.081	0.35	0.506	5.964	< 0.001	0.686	1.458							
		Total	27829.44	87				On.Ar	-644.567	155.26	-0.352	-4.151	< 0.001									
M12	OPD+On.Pm	Regression	16815.23	2	8407.61	64.88	< 0.001	(Constant)	73.515	12.76		5.76	< 0.001			0.78	0.60	0.59	11.38	1.21	683.2	692.6
		Residuals	11014.21	85	129.57			OPD	1.967	0.34	0.478	5.794	< 0.001	0.683	1.464							
		Total	27829.44	87				On.Pm	-68.866	14.21	-0.400	-4.844	< 0.001									
M13	OPD+On.Cr	Regression	16900.43	2	8450.21	65.72	< 0.001	(Constant)	-274.568	59.03		-4.651	< 0.001			0.78	0.61	0.59	11.34	1.21	682.5	691.9
		Residuals	10929	85	128.57			OPD	1.982	0.33	0.482	5.917	< 0.001	0.696	1.437							
		Total	27829.44	87				On.Cr	334.353	67.81	0.402	4.93	< 0.001									
M14	OPD+On.Ar+ On.Cr	Regression	17925.26	3	5975.08	50.67	< 0.001	(Constant)	-193.379	62.88		-3.075	0.003			0.80	0.64	0.63	10.85	1.25	676.1	687.8
		Residuals	9904.17	84	117.90			OPD	1.599	0.34	0.389	4.62	< 0.001	0.598	1.673							
		Total	27829.44	87				On.Ar	-449.111	152.33	-0.245	-2.948	< 0.001	0.611	1.636							
								On.Cr	267.398	68.79	0.321	3.887	< 0.001	0.62	1.612							
M15	OPD+On.Pm+ On.Cr	Regression	18194.45	3	6064.81	52.87	< 0.001	(Constant)	-153.132	66.45		-2.304	0.024			0.81	0.65	0.64	10.71	1.28	673.7	685.3
		Residuals	9634.98	84	114.70			OPD	1.577	0.34	0.383	4.656	< 0.001	0.608	1.646							
		Total	27829.44	87				On.Pm	-48.909	14.56	-0.284	-3.359	0.001	0.576	1.735							
								On.Cr	241.791	69.72	0.29	3.468	0.001	0.587	1.703							
M16	OPD(F)+On.Ar	Regression	17955.64	2	8977.82	77.28	< 0.001	(Constant)	49.465	7.45		6.639	< 0.001			0.80	0.64	0.64	10.7	1.22	673.6	683
		Residuals	9873.8	85	116.16			OPD(F)	4.116	0.542	0.62	7.596	< 0.001	0.626	1.597							
		Total	27829.44	87				On.Ar	-469.546	149.40	-0.257	-3.143	0.002	0.626	1.597							
M17	OPD(F)+On.Pm	Regression	18333.81	2	9166.90	82.05	< 0.001	(Constant)	68.487	11.34		6.038	< 0.001			0.81	0.66	0.65	10.56	1.25	670.2	679.6
		Residuals	9495.63	85	111.71			OPD(F)	3.909	0.539	0.589	7.248	< 0.001	0.608	1.645							
		Total	27829.44	87				On.Pm	-51.715	13.99	-0.300	-3.695	< 0.001	0.608	1.645							
M18	OPD(F)+On.Cr	Regression	18545.24	2	9272.62	84.89	< 0.001	(Constant)	-201.271	57.54		-3.498	0.001			0.82	0.67	0.66	10.45	1.34	668.2	677.6
		Residuals	9284.19	85	109.22			OPD(F)	3.907	0.521	0.589	7.502	< 0.001	0.637	1.569							
		Total	27829.44	87				On.Cr	260.484	65.32	0.313	3.988	< 0.001	0.637	1.569							
M19	OPD(F)+On.Ar+ On.Cr	Regression	19101.96	3	6367.32	61.28	< 0.001	(Constant)	-149.78	60.38		-2.48	0.015			0.83	0.69	0.67	10.2	1.31	664.9	676.6
		Residuals	8727.48	84	103.89			OPD(F)	3.35	0.562	0.505	5.962	0.001	0.521	1.921							
		Total	27829.44	87				On.Ar	-339.413	146.62	-0.186	-2.315	0.023	0.581	1.72							
								On.Cr	219.594	66.11	0.264	3.322	0.001	0.592	1.69							
M20	OPD(F)+On.Pm + On.Cr	Regression	19262.82	3	6420.94	62.96	< 0.001	(Constant)	-120.205	63.45		-1.894	0.062			0.83	0.69	0.68	10.10	1.33	663.3	675.1
		Residuals	8566.62	84	101.98			OPD(F)	3.281	0.56	0.494	5.904	< 0.001	0.523	1.914							
		Total	27829.44	87				On.Pm	-37.581	14.16	-0.218	-2.653	0.01	0.541	1.847							
								On.Cr	201.846	66.87	0.242	3.018	0.003	0.568	1.762							

*M= model, SE=standard error, SEE= standard error of the estimate, D-W=Durbin-Watson

A third variable (On.Cr) was added to previous *Models 11* and *12* in order to examine whether a better fit of the data was obtained. The results provided by *Model 14* and *Model 15* demonstrated a very similar outcome. The combination of OPD, On.Pm and On.Cr (*Model 15*) produced a slightly higher multiple R^2 and prediction accuracy (multiple R^2 = 0.64, *SEE* = 10.71) than *Model 14*. Hierarchical regression indicated that the addition of On.Cr improved prediction with R^2-change of 0.05 (*F* change = 12.02, p = 0.001). The smallest AIC_c and BIC values were produced for *Model 15*. As seen in Table 5.32, *F-values*, unstandarised and standardised partial slopes for the three variables regression models are similar and statistically significant. *Model 14* and *Model 15* statistical tests suggest normality of the residuals (*SW* = 0.98, df = 88, p = 0.243, skewness = -0.169, kurtosis = 1.18; and *SW* = 0.98, df = 88,p = 0.317, skewness = -0.229, kurtosis = 1.04, respectively). Tolerance and *VIF* values indicated that multicollinearity was not an issue. However, eigenvalues for On.Cr as the third parameter were close to zero for both cases with a condition index of more than 30; the redundant inclusion of both area and perimeter in the calculation of On.Cr may be the reason. A review of regression of all the possible combinations for *Model 14* and for *Model 15* indicated that none of the R^2 obtained were higher than 0.45. Comparing diagnostic plots for each model, assumptions of normality, linearity, normality, equal variances and non-influential cases were reasonably met.

First, four different multiple linear models were generated combining OPD(F) and secondary osteon measurements. Simple regression results previously demonstrated that OPD(F) models were better fitted by curvilinear regression. In summary, a general decrease in AIC_c and BIC values in comparison to the models that included OPD was observed.

Model 16, 17 and *18* include two predictors each. All the models rejected the null hypothesis and reported standardised and unstandarised partial coefficients that were statistically significant (Table 5.32). Overall, independence of errors was reasonably met as assessed by D-W statistics and visual examination of scatter plots. Normal distribution of the residuals was confirmed by skewness and kurtosis (-0.269 and 0.513; 0.306 and 0.534; and -0.012 and 0.558, *Model 16, 17* and *18,* respectively). This assumption was further confirmed by *S-W* test normality test (*S-W*, p = 0.68, p = 0.57, p = 0.96, respectively). Statistics reported for tolerance and *VIF* values indicated that multicollinearity was not an issue and although

eigenvalues for the second predictor were close to zero (as with the previous models), the condition indices and the regression of all possible combination of independent parameters suggested non-collinearity.

As seen in Table 5.32, *Model 19* and *Model 20* performed very similarly with slightly higher explanatory power and better goodness of fit given by *Model 2*0 with the combination of OPD(F), On.Pm and On.Cr. Unstandarised and standardised partial slopes for the three variables were reported to be significant for both models (note the intercept for *Model 20* is not statistically significant (t = -1.89, p = 0.062). *Model 19* and *Model 20* independence of errors was confirmed by D-W statistics and statistical tests suggesting normality of the residuals (*SW* = 0.99, df = 88, p = 0.809, skewness = -0.169, kurtosis = 1.18; *SW* = 0.991, df = 88, p = 0.785, skewness = -0.317, kurtosis = 0.472, respectively). Looking at multicollinearity diagnosis for *Model 19* and *20*, tolerance and *VIF* values suggested that multicollinearity was not an issue; however, further assessment of a third variable (On.Cr) included in either of the two models suggest that a third predictor may cause some collinearity problems. Regression of all the possible combinations for *Model 19* and for *Model 20* resulted in multiple R^2 lower than 0.90. Comparing diagnostic plots for each model, assumption of normality, linearity, equal variances and non-influential cases were reasonable met.

In all the five models (*Models 16* to *20*), a certain curvilinear pattern was observed in the trend lines. It suggests that the linear model might not be the best fit to the data with non-linear relationships between dependent and independent variables not being totally explained by the linear model (see Univariate Models section for OPD(F) and Appendix B.8).

Curvilinear regression was conducted using hierarchical multiple regression analysis to test whether an increase in explanatory power is observed. Results for curvilinear regression models are summarised in Table 5.33. All the curvilinear models produced multiple R^2 and *F-statistics* changes that were statistically significant ($p < 0.05$) indicating that the curvilinear effect improves prediction to different degrees. Multicollinearity seemed to be an issue with tolerance around 0.05 and *VIF* values higher than the threshold of 10, which for these models was expected due to the correlation between the OPD(F) variable included twice in the equation. The examination of the diagnostic plots suggested that the assumptions for regression analysis were met. Furthermore, the curvilinear trend lines observed

in the multiple linear models show a fairly horizontal pattern with residual equally spread along the range of values.

Table 5.33 Summary table of curvilinear models for OPD(F) and osteons measurements as independent variables.

Quadratic Models	F	R	R^2	SEE	AIC_C	BIC	D-W	Quadratic regression equation
Model 16	57.62	0.82	0.67	10.41	668.7	680.3	1.23	Age=33.132+8.911(OPD(F)-401.271(On.Ar)-0.342(OPD(F)^2)
Model 17	60.71	0.83	0.68	10.23	665.5	677.2	1.27	Age=50.724+8.525(OPD(F)-45.233(On.Pm)-0.329(OPD(F)^2)
Model 18	63.12	0.83	0.69	10.09	663.2	674.8	1.29	Age=-190.406+8.545(OPD(F)+233.568(On.Cr)-0.332(OPD(F)^2)
Model 19	50.10	0.84	0.71	9.91	661.3	675.1	1.31	Age=-147.369+7.586(OPD(F)-201.328(On.Ar)+201.328(On.Cr)-0.298(OPD(F)^2)
Model 20	51.35	0.84	0.71	9.82	668.7	673.6	1.33	Age=-120.593+7.44(OPD(F)-32.967(On.Pm)+185.352(On.Cr)-0.293(OPD(F)^2)

SEE= standard error of the estimate, D-W= Durbin-Watson

The last set of multiple models for the entire sample includes histomorphometric variables that are related to rib area and secondary osteons measurements and shape. Six models were generated. As seen in Table 5.34, the combination of osteon measurements with Ct.Ar/Tt.Ar was redundant as demonstrated by the p-value produced by the inclusion of the last variable into the equation. Only the model that demonstrated an improvement in goodness of fit (R^2, SEE, AIC_c and BIC) in comparison to the simple linear models will be discussed here. Diagnostic plots for the best two models (*Model 25* and *26*) can be consulted in Appendix B.8.

Model 25 (On.Cr and Ct.Ar) explained a significant amount of the variance in age (58%) with a *SEE* of 11.72 years (F (2.85) = 58.73, $p < 0.001$). AIC_c and BIC values were the smallest among these models. Standardised and unstandarised partial coefficients for On.Cr and Ct.Ar were statistically significant at the $p < 0.001$ level (t = 7.387and t = -5.22, respectively). D-W statistics (1.28) indicated independence of errors and test statistics suggested normal distribution of the residuals (*S-W* = 0.98 df = 88, p = 0.308; skewness = -0.328; kurtosis = 0.917). Although the eigenvalues for the second variable were close to zero and exceeding

the condition index threshold, further review of On.Cr regressed on Ct.Ar produced multiple R^2 of 0.087 providing no further evidence of multicollinearity issues. No regression influential cases were identified and the assumptions were reasonably met.

Table 5.34 Multiple Regression Models for rib area and osteons measurements variables for the entire sample.

	N=88	ANOVA						Parameters Estimates							Model Summary					Goodness of fit	
Model	Variables		Sum of Squares	df	Mean Square	F value	Pr > F		Unstandarised Coefficients		Standarised Coefficients	T-Value	Pr>| t |	Collinearity Diagnosis		R	R^2	Adj. R^2	SEE	D-W	AICc	BIC
									B	SE	Beta			Tolerance	VIF							
M21	On.Ar+Ct.Ar	Regression	12501.41	2	6250.70	34.66	< 0.001	(Constant)	99.409	4.97		20.01	< 0.001			0.67	0.45	0.44	13.42	1.12	716.9	724.1
		Residuals	15328.02	85	180.33			On.Ar	-862.451	186.53	-0.471	-4.62	< 0.001	0.623	1.604							
		Total	27829.44	87				Ct.Ar	-.601	0.23	-0.268	-2.63	0.010	0.623	1.604							
M22	On.Ar+ Ct.Ar/Tt.Ar	Regression	11766.92	2	5883.46	31.13	< 0.001	(Constant)	99.413	5.16		19.239	< 0.001			0.65	0.42	0.41	13.74	1.14	716.4	725.8
		Residuals	16062.51	85	188.97			On.Ar	-969.984	191.13	-0.53	-5.075	< 0.001	0.622	1.607							
		Total	27829.44	87				Ct.Ar/Tt.Ar	-25.231	15.32	-0.17	-1.647	**0.103**	0.622	1.607							
M23	On.Pm+Ct.Ar	Regression	13390.22	2	6695.11	39.41	< 0.001	(Constant)	127.576	8.95		14.245	< 0.001			0.69	0.48	0.47	13.03	1.13	707.1	716.5
		Residuals	14439.21	85	169.87			O.Pm	-90.503	17.13	-0.53	-5.284	< 0.001	0.617	1.621							
		Total	27829.44	87				Ct.Ar	-.52	0.22	-0.23	-2.334	0.022	0.617	1.621							
M24	On.Pm+ Ct.Ar/Tt.Ar	Regression	12758.03	2	6379.01	35.97	< 0.001	(Constant)	130.491	9.06		14.4	< 0.001			0.68	0.46	0.45	13.32	1.12	710.8	720.2
		Residuals	15071.41	85	177.31			O.Pm	-101.117	17.59	-0.59	-5.748	< 0.001	0.61	1.638							
		Total	27829.44	87				Ct.Ar/Tt.Ar	-19.269	14.97	-0.131	-1.287	**0.202**	0.61	1.638							
M25	On.Cr+Ct.Ar	Regression	16146.31	2	8073.15	58.73	< 0.001	(Constant)	-337.07	57.14		-5.899	< 0.001			0.76	0.58	0.57	11.72	1.38	688.4	697.8
		Residuals	11683.12	85	137.44			On.Cr	454.948	61.59	0.55	7.387	< 0.001	0.902	1.109							
		Total	27829.44	87				Ct.Ar	-.866	0.16	-0.386	-5.222	< 0.001	0.902	1.109							
M26	On.Cr+ Ct.Ar/Tt.Ar	Regression	14082.16	2	7041.08	43.53	< 0.001	(Constant)	-348.847	65.04		-5.363	< 0.001			0.71	0.51	0.49	12.72	1.15	702.7	712.1
		Residuals	13747.27	85	161.73			On.Cr	463.584	69.56	0.56	6.664	< 0.001	0.832	1.202							
		Total	27829.44	87				Ct.Ar/Tt.Ar	-39.534	12.25	-0.27	-3.226	0.002	0.832	1.202							

*M= model, SE=standard error, SEE= standard error of the estimate, D-W=Durbin-Watson, in bold p > 0.05

5.5.3. GLM separated by groups

5.5.3.1. GLM for sex

The grouping variable, sex, was transformed into a dummy variable (Male = 0, Female = 1) to determine whether the inclusion of sex in the regression models improved the prediction accuracy.

First, all the histological variables were combined with the sex grouping variable. The regression analysis indicated that the single histological variables for the entire dataset performed more accurately than the combination of the histological variable and sex, as assessed by the non-statistical significance of sex for any of the models (p-value > 0.05). Hierarchical linear regression indicated than the only slight improvement from the univariate model was obtained for Ct.Ar and sexes (see Appendix B.9 and Table 5.30 for *Model 6* values). Due to the little improvement observed, no further analysis of residuals was performed on this model.

Multiple hierarchical regression was performed to examine whether the inclusion of sex as a categorical variable improved the previous multiple models built for the entire sample (refer to Table 5.32 and Table 5.34). No increment in multiple R^2 was observed for any of the new generated models. Additionally no statistical significance was reported for the incorporation of the categorical variable.

Further exploration of possible regression formulae for sex specific datasets including only histological variables was performed. Only the equations that provided a clear improvement in prediction accuracy based on indicators as R^2, SEE, AIC_c and BIC values are reported and discussed. Multiple linear regression and stepwise multiple linear regression were used to obtained the most accurate combination of variables for each sex. The results are presented in Table 5.35. Diagnostic plots can be consulted in Appendix B.10.

As seen in Table 5.35, the null hypothesis was rejected at the $p < 0.001$ level for the best three models generated for males (*Model 27*, *28* and *29*). Between 43% and 63% of the variance in age can be explained by these models with SEE ranging from 10 to 12 years. All the standardised and unstandarised (partial) slopes were significantly different from zero. The lowest AIC_c and BIC values were reported for *Model 29*. Independence of errors seemed to be an issue for *model 28* (D-W= 0.89);

however, inspection of standardised residuals versus standardised predicted values provided a random display of point falling within ± 3. *Model 27* presented non-normality of residuals through the pattern observed in the Q-Q plot and confirmed by *S-W* test (*S-W* = 0.943, df = 40, p = 0.045). However, other indicators suggested reasonable normality (skewness (-0.297) and kurtosis (1.734)). Assumption of equality of variance appeared constant although a deviation around 50 year was observed. Unstandarised residuals normality was confirmed for the remaining *Model 27* and *29* (*S-W* p-value > 0.05; skewness and kurtosis: -0.393 and 0.642, 0.714 and 1.4, respectively).

Curvilinear regression analysis was performed on OPD equation (*Model 27*). The quadratic model for OPD statistically significantly predicts age in the male sample ($F(1,38) = 21.50$, $p < 0.001$; multiple $R^2 = 0.51$, SEE = 11.54; AIC = 315.19, BIC = 320.81). Standardised and unstandarised partial slope coefficients for OPD squared ($t = -1.366$, $p = 0.180$) suggests that the inclusion of this variable into the model is redundant. The assumption of normality of residuals was corrected by the curvilinear model (S-W = 0.925, df = 40, p = 0.086) and the remaining assumption were also reasonably met. The quadratic equation is as follows:

$$Age = -19.957 + 7.340\,(OPD) - 0.131(OPD^2)$$

Weighted least squares regression explores the correction of heteroscedasticity observed in *Model 27*. The new model produced an R^2 of 0.58 ($F(1,38) = 54.43$, $p < 0.001$). Unstandarised and standardised coefficients are statistically significant ($t = 3.10$, $p = 0.004$, $t = 7.38$, $p < 0.001$) providing the following formulae:

$$Age = 19.94 + 2.06(OPD)$$

Table 5.35 Summary of selected simple and multiple regression models for males and females.

Males	Females	ANOVA						Parameters Estimates						Model Summary							Goodness of fit	
Model	Variables		Sum of Squares	df	Mean Square	F value	Pr > F		Unstandarised Coefficients		Standarised Coefficients	T-Value	Pr>|t|	Collinearity Diagnosis		R	R²	Adj. R²	SEE	D-W	AICc	BIC
									B	SE	Beta			Tolerance	VIF							
M27	OPD	Regression	5478.40	1	5478.40	40.226	< 0.001	(Constant)	15.15	7.323		2.070	0.045			0.72	0.51	0.51	11.70	1.22	314.7	319.1
		Residuals	5175.19	38	136.18			OPD	2.904	0.458	0.717	6.342	< 0.001									
		Total	10653.60	39																		
M28	On.Cr	Regression	4762.47	1	4762.47	30.72	< 0.001	(Constant)	-402.715	83.52		-4821	< 0.001			0.67	0.45	0.43	12.45	0.89	319.8	324.3
		Residuals	5891.12	38	155.02			On.Cr	507.025	91.47	0.669	5543	< 0.001									
		Total	10653.60	39																		
M29	OPD + On.Cr	Regression	6692.97	2	3346.48	31.26	< 0.001	(Constant)	-247.98	78.388		-3.3164	0.003			0.79	0.63	0.61	10.35	1.30	306.5	312.1
		Residuals	3960.62	37	1070.44			OPD	2.04	0.48	0.504	4.247	< 0.001									
		Total	10653.6	39				On.Cr	302.931	89.932	0.399	3.368	0.002	0.71	1.40							
M30	OPD(F)	Regression	11686.65	1	11686.65	98	< 0.001	(Constant)	23.511	4.05		5.795	< 0.001			0.82	0.68	0.67	10.90	1.32	370.2	375.3
		Residuals	5485.32	46	11.924			OPD(F)	5.753	0.58	0.825	9.900	< 0.001									
		Total	17171.97	47																		
M31	Ct.Ar	Regression	9248.99	1	9248.99	53.69	< 0.001	(Constant)	95.428	5.13		18.615	< 0.001			0.73	0.54	0.53	13.12	1.19	387.9	392.9
		Residuals	7922.98	46	172.23			Ct.Ar	-1.984	0.27	-0.734	-7.328	< 0.001									
		Total	17171.97	47																		
M32	On.Pm+Ct.Ar	Regression	11055.76	2	5527.88	40.67	< 0.001	(Constant)	128.742	10.21		12.61	< 0.001			0.80	0.64	0.63	11.65	1.25	377.8	384.4
		Residuals	6116.21	45	135.91			On.Pm	-74.338	20.39	-0.43	-3.646	0.001									
		Total	17171.97	47				Ct.Ar	-1.220	0.32	-.0451	-3.823	< 0.001	0.56	1.76							
M33	On.Cr+Ct.Ar	Regression	11960.07	2	5980.038	51.63	< 0.001	(Constant)	-276.939	77.08		-3.593	0.001			0.83	0.69	0.68	10.76	1.47	370.1	376.7
		Residuals	5211.90	45	115.82			On.Cr	399.886	82.65	0.443	4.838	< 0.001									
		Total	17171.97	47				Ct.Ar	-1.453	0.25	-0.537	-5.866	< 0.001	0.84	1.24							
M34	OPD(F)+Ct.Ar	Regression	13585.87	2	6792.93	85.24	< 0.001	(Constant)	52.44	6.79		7722	< 0.001			0.89	0.79	0.78	8.93	1.42	352.2	358.7
		Residuals	3586.1	45	79.69			OPD(F)	4.21	0.57	0.604	7377	< 0.001									
		Total	17171.97	47				Ct.Ar	-1.080	0.22	-0.399	-4,882	< 0.001	0.69	1.44							

*M= model, SE=standard error, SEE= standard error of the estimate, D-W=Durbin-Watson

The female sub-dataset was used for the generation of sex specific formulae (Table 5.35). Two simple linear models and three multiple linear models were generated. For the models including just one single predictor, OPD(F) produces the highest R^2 and lowest AIC_c and BIC values. Independence of errors and normality of standardised residuals assumption were met for both *Model 30* and *31* (*S-W* p-value > 0.05; skewness and kurtosis 0.469 and 0.761, -0.154 and 1.09, respectively). Visual examination of diagnostic plots suggested a slight curvilinear trend for *Model 30*. The quadratic regression model statistically significantly predicted age in the female sample ($F(1,46) = 52.05$, $p < 0.001$; multiple $R^2 = 0.685$, SEE = 10.73; AIC = 369.87, BIC = 376.43). Beta standardised and unstandarised partial slope coefficients for OPD and OPD squared suggest that $OPD(F)^2$ was not statistically significant ($t=4.231$, $p < 0.001$ and $t = -1.621$, $p = 0.112$, respectively). The diagnostic plots indicate that regression assumptions were met and a correction of the curvilinear pattern was observed indicating more approximate equality of variances. The quadratic equation is as follows:

$$Age = 14.09 + 9.275(OPD(F)) - 0.271(OPD(F)^2)$$

Three multivariate models produced the highest prediction accuracy for the female sample. Among them, stepwise regression analysis selected as the best combination of variables for females OPD(F) and Ct.Ar (*Model 34*) (Table 5.35). This model explains 79% of the variance in age with a standard error of the estimate of 9 year from real age. Multicollinearity was not an issue based on tolerance and VIF values (0.693 and 1.443 respectively). Independence of residuals assumption was met (*DW* = 1.42) and statistics test indicated that residuals were normally distributed (S-W = 0.96, df = 48, p = 0.117). A curvilinear pattern in the trend line was observed in the scale-location plot suggesting issues in the equality of variances. The possibility of correcting the curvilinear pattern by performing quadratic regression was not recommended due to the sample size and the impact of adding a third variable into the model.

For the remaining models (*Model 31,32* and 33), the null hypothesis was rejected at the $p < 0.001$ level and they all met the regression assumptions (Appendix B.10).

5.5.3.2. GLM for samples

The grouping variable sample was transformed into a dummy variable (Crete = 0, Cyprus = 1) in order to include it as a categorical variable in the regression equations. Multiple linear regression models were built with single histological variables and sample, as well as for the combination of several histological variables and sample as predictors.

For all the models, a decrease in the prediction was observed when combining the continuous and the categorical predictors, except for Ct.Ar, Cr.Ar/Tt.Ar, On.Ar and On.Pm (refer to Appendix B.9). Although the categorical variable as well as F-statistics change were statistically significant for all the new generated models, the combination of sample, secondary osteon measurements and Ct.Ar/Tt.Ar makes this last predictor to become non-statistically significant. Based on the little improvement provided by the inclusion of sample as a categorical predictor, no further analysis of residuals will be performed on the models.

The entire dataset was divided into two sub-datasets (Cretans and Cypriots) to examine whether regression models performed better if only histological predictors are considered for each sample. Only simple and multiple regression models that produced an improvement in goodness of fit values (R^2 and SEE, AICc and BIC) in comparison to the models generated using the entire database are reported.

Simple linear models were built for the Cretan sample testing each histological variable and age. None of the models improved the results from the previous regression analysis. Multiple regression analysis was run for all possible combinations of histological parameters and age. The multiple regression models did not show higher prediction accuracy rates indicating that a general formula can be better used for Cretans.

The Cypriot sub-dataset was used to generate simple and multiple regression equations. Most of the simple and multiple regression models resulted in an improvement of prediction accuracy in comparison to the regression models generated from the entire database. Only the two best models are discussed here although all models summary statistics can be seen in Table 5.36. Diagnostic plots are presented in Appendix B.11.

All the simple linear regression models generated rejected the null hypothesis (Table 5.36). The highest R^2, and the lowest SEE, AICc and BIC values are obtained by *model 35* (OPD(F)). The second best model according to the goodness of fit values was *Model 38*, which includes On.Pm as a single predictor. Independence of errors indicated acceptable values and was further confirmed by standardised residuals against standardised predicted values scatter plots. Normality test suggested non-violation of normality for unstandarised residuals for all models (S-W p-value > 0.05) and reasonable values for skewness and kurtosis (*Model 35*: 0.192 and 1.18, and *Model 38*: =-0.145 and 1.03, respectively).

As seen for *Model 35,* the diagnostic plots indicated a random distribution of the residuals although a slope was observed in the trend line. A curvilinear pattern in the distribution of the residuals along the predictor ranges was again observed suggesting certain violation of homoscedasticity (Appendix B.11). Curvilinear regression was performed with the inclusion of $OPD(F)^2$ in the equation being not statistically significant (F change p = 0.079) although the null hypothesis was rejected (F (2,44)= 45.38, p value < 0.001) with multiple R^2 was slightly higher that with the single model (0.67). The curvilinear pattern previously seen was slightly corrected; however, the curvilinear trend line was still observed indicating that certain heteroscedasticity was present in the model. The transformation of the dependent variable (LnAge) was tested to examine whether a correction of the trend line pattern was possible but no improvement was achieved. Weighted least squared regression was performed to correct heteroscedasticity of the residuals obtaining a statistically significant model (F (1,45)=89.57, p < 0.001, R^2 = 0.66); the following regression equation for OPD(F):

$$Age = 29.689 + 4.870\ (OPD(F))$$

Three multiple regression models are reported based on the multiple R^2 and goodness of fit values produced (Table 5.36). Stepwise regression selected as the most suitable combination of variables OPD(F) and On.Pm which predicted age with a *SEE* of 7.7 years and a multiple R^2 of 0.72. Among all the multiple models developed from the Cypriots dataset, *Model 39* provided the smallest AIC_c and BIC values followed by the model including OPD and On.Pm (*Model 40*) (Table 5.36). No violation of independence of errors and normality of unstandarised residuals was suggested by statistical tests for the three models (S-W p > 0.05; skewness and kurtosis being *Model 39*: 0.62 and .91, Model 40 = 0.28 and 1.35, Model 41: 0.28

and 0.12). Multicollinearity was examined through tolerance and *VIF* values for all models, and regression was carried out on all possible combinations of variables obtaining multiple R^2 less than 0.50; hence, collinearity might not be an issue. Diagnostic plots indicated no potential violation of regression assumptions. This statement applies for all the models generated for Cypriots.

As a general trend, for most of the formulae developed from the Cypriot database, case 1 (20-year-old) was identified as a possible outlier. For all the selected models, this case was examined closely through the standardised residual, studentised residuals, Cook´s distance and Leverage values. After considering these values as an aggregate, this case was not considered a regression outlier that could influence the coefficients values and/or the prediction accuracy of the formulae. Moreover, simple and multiple regression was performed on the database excluding case 1, and predicted response, slope coefficients and hypothesis test results were not affected by this case suggesting its inclusion to generate the regression formulae.

Table 5.36 Selected simple and multiple regression models for Cypriots.

	Cyprus	ANOVA						Parameters Estimates						Model Summary					Goodness of fit			
Model	Variables		Sum of Squares	df	Mean Square	F value	Pr > F		Unstandarised Coefficients		Standarised Coefficients	T-Value	Pr>| t |	Collinearity Diagnosis		R	R^2	Adj. R^2	SEE	D-W	AICc	BIC
									B	SE	Beta			Tolerance	VIF							
M35	OPD(F)	Regression	6027.69	1	6027.69	83.36	< 0.001	(Constant)	32.66	3.52		9.26	< 0.001			0.81	0.65	0.64	8.50	1.10	339.1	344.1
		Residuals	3253.58	45	72.302			OPD(F)	4.417	0.484	0.806	9.131	< 0.001									
		Total	9281.27	46																		
M36	OPD	Regression	5004.88	1	5004.69	52.66	< 0.001	(Constant)	21.36	5.88		3.629	< 0.001			0.73	0.54	0.53	9.75	1.10	351.9	356.9
		Residuals	4276.38	45	95.03			OPD	2.549	0.35	0.734	7.257	< 0.001									
		Total	9281.38	46																		
M37	Ct.Ar/Tt.Ar	Regression	3890.26	1	3890.26	32.47	< 0.001	(Constant)	89.238	4.90		18.19	< 0.001			0.65	0.42	0.41	10.95	.99	362.8	367.8
		Residuals	5391.01	45	119.8			Ct.Ar/Tt.Ar	-80.95	14.21	-0.647	-5.69	< 0.001									
		Total	9281.27	46																		
M38	On.Pm	Regression	531.215	1	5312.15	60.22	< 0.001	(Constant)	136.234	9.56		14.25	< 0.001			0.76	0.57	0.56	9.40	1.22	348.4	353.4
		Residuals	3969.11	45	88.20			On.Pm	-113.681	14.64	-0.757	-7.761	< 0.001									
		Total	9281.27	46																		
M39	OPD(F)+ On.Pm	Regression	6677.58	2	33.387	56.42	< 0.001	(Constant)	78.819	14.28		5.51	< 0.001			0.85	0.72	0.71	7.69	1.21	331	337.5
		Residuals	260.369	44	59.17			OPD(F)	2.97	0.618	0.542	4.80	< 0.001									
		Total	9281.27	46				On.Pm	-56.171	16.95	-0.374	-3.314	< 0.001	0.51	1.99							
M40	OPD+On.Pm	Regression	6410.16	2	3205.08	49.12	< 0.001	(Constant)	85.982	14.75		5.828	< 0.001			0.83	0.69	0.68	8.10	1.20	335.6	342
		Residuals	2871.09	44	65.25			OPD	1.507	0.367	0.434	4.102	< 0.001									
		Total	9281.27	46				On.Pm	-73.831	15.91	-0.491	-4.641	< 0.001	0.63	1.59							
M41	On.Pm+ Ct.Ar/Tt.Ar	Regression	5977.45	2	2988.73	39.80	< 0.001	(Constant)	131.744	8.94		14.722	< 0.001			0.80	0.64	0.63	8.66	1.22	341.2	348.6
		Residuals	3303.82	44	75.08			On.Pm	-86.248	16.35	-0.574	-5.272	< 0.001									
		Total	9281.28	46				Ct.Ar/Tt.Ar	-40.518	13.61	-0.324	-2.977	0.005	0.68	1.46							

*M= model, SE=standard error, SEE= standard error of the estimate, D-W=Durbin-Watson

5.5.4. Summary of best regression formulae: model selection

As described in the previous chapter (section 4.2.4.5), several indicators of goodness of fit were used as a means of model selection. R^2 corresponds to an expression of the best fit of the line to the data representing the proportion of the variance in the dependent variable that is expressed by the regression model (Zar, 2010). Standard error of the estimates (*SEE*) is a measure of how accurate the predictions made through a specific model are. Two parsimony indicators are also computed. AIC_c is preferred in this study as it comprises a correction of AIC in relation to sample size and it is assessed to evaluate which is the best model based on prediction power (Hurvich and Tsai, 1989). BIC values for each model are also reported to examine which model adjusts the best to the data (Aho et al., 2014).

Table 5.37 presents a summary of the selection of the best models generated in this study based on the aforementioned values. The nature of the parameters was considered (i.e. formulae including densities versus formulae including metric parameters) and both simple and multiple models were included. Moreover, the reliability of the variables was also taken into account (i.e. OPD(F) demonstrated high inter-observer error). Issues concerning the repeatability and practical application of the models will be fully discussed in the next chapter.

Table 5.37 Summary of the best models generated based on entire dataset and sub-data sets.

	Model / variable		Formula	R^2	SEE	AICc	BIC
Entire sample	Model 5	OPD	Age = 15.66 + 2.893(OPD)	0.49	12.78	702.50	709.62
	Model 9	On.Pm	Age = 133.224 – 115.24(On.Pm)	0.45	13.36	710.30	717.47
	Model 13	OPD, On.Cr	Age = -274.568 + 1.982(OPD) + 334.535(On.Cr)	0.61	10.45	668.18	677.61
	Model 15	OPD, On.Pm, On.Cr	Age = -153.132 + 1.577(OPD) – 48.909(On.Pm) + 241.791(On.Cr)	0.65	10.71	673.69	685.35
	Model 25	On.Cr, Ct.Ar	Age = -337.948 + 454.948(On.Cr) – 0.866(Ct.Ar)	0.58	11.72	688.40	697.83
Males	Model 29	OPD, On.Cr	Age = -247.98 + 2.04(OPD) + 302.931(On.Cr)	0.63	10.35	306.47	312.10
Females	Model 32	On.Pm, Ct.Ar	Age = 128.742 – 74.338(On.Pm) – 1.220(Ct.Ar)	0.64	11.65	377.14	384.38
	Model 33	On.Cr, Ct.Ar	Age = -276.939 – 399.886(On.Cr) – 1.453(Ct.Ar)	0.69	10.76	370.14	376.70
Cyprus	Model 36	OPD	Age = 21.36 + 2.549(OPD)	0.54	9.75	351.94	356.93
	Model 38	On.Pm	Age = 136.234 – 113.681(On.Pm)	0.57	9.40	348.61	353.43
	Model 40	OPD, On.Pm	Age = 85.982 + 1.507(OPD) – 73.831(On.Pm)	0.69	8.10	335.61	342.05
	Model 41	On.Pm, Ct.Ar/Tt.Ar	Age = 131.744 – 86.248(On.Pm) – 40.518(Ct.Ar/Tt.Ar)	0.64	8.66	341.20	348.65

SEE= standard error of the estimate

The prediction equations are used as follows: if an individual from Mediterranean origin is found and the histological variables OPD (20.50) and On.Cr (0.913) are assessed, these values would be inserted in *Model 13* (as an example) and age would be estimated in the following manner:

$$\text{Age} = -274.568 + 1.982(20.50) + 334.535(0.913)$$

$$\text{Age} = 71.49$$

The estimated age is 71.49 years with a range of 61 to 81 years since the SEE for the generated model is roughly 10 years.

5.6. Thin-section preparation methodologies comparison

A qualitative assessment of the thin-sections produced by *methodology A* and *methodology B* was done to test whether both histological techniques produced thin-section of similar quality. As seen in Figure 5.13, the histological features are equally observable under 4×, 10× and 40× magnification on microphotographs obtained by each method (both transmitted and polarised light microscopy). The only minor drawback that was noticed when using the revised method consisted of blurred areas appearing on the thin-section due to water penetrating the space between the thin-section and the glass slides. The application of a larger quantity of resin in the mounting procedure seemed to solve this technical issue.

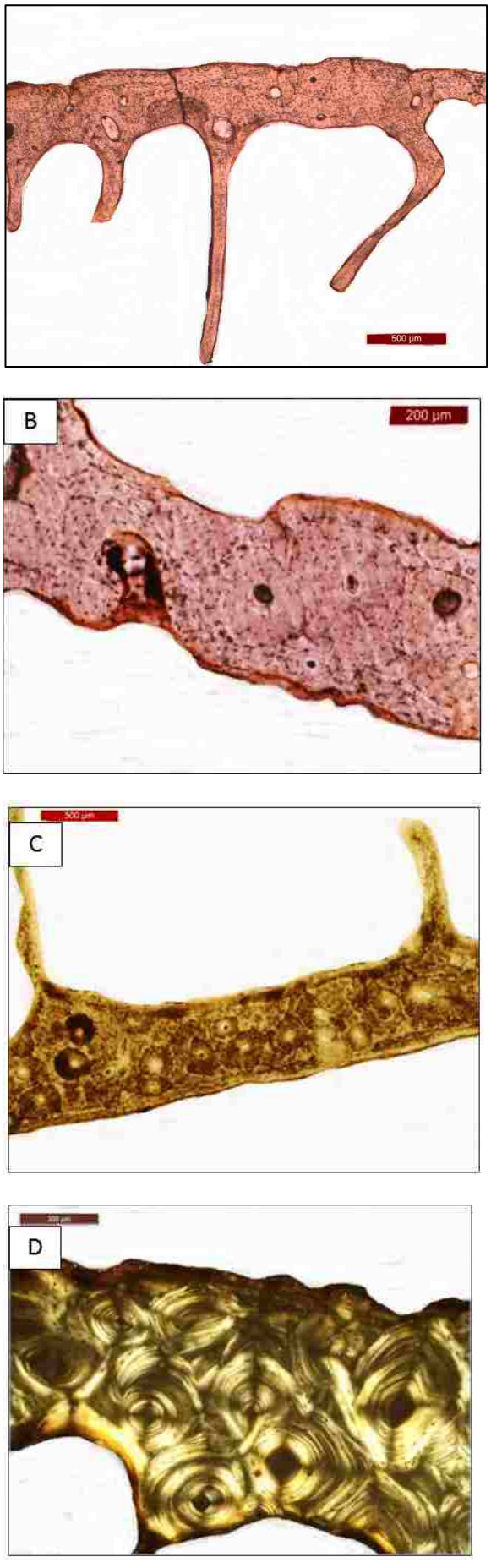

Figure 5.13 Study sample examples of four microphotographs taken with a research microscope (Leica DM750P equipped with a Leica MC170 HD camera). A (40×) and B (100×): rib sections processed using methodology A. C (40×) and D (100×): ribs sections processed applying the revised method (under semi-polarised light).

Chapter 6 : RESEARCH LIMITATIONS

Although the present research was carefully designed and it reached its aims, some limitations should be taken under consideration when interpreting the results. The current shortcomings presented here will lead to future research directions to improve the method and provide more insight in age-related changes in cortical bone on Mediterranean samples.

First, one of the main limitations of this research relates to the nature of the sample which was limited in representation of individuals for specific age ranges. *A prio*ri, a larger sample size was sought but a proportion of the specimens was finally discarded from the final dataset due to the following reasons: lack of basic information of the rib samples originally collected, pathological conditions observed microscopically or obtained through archives or autopsy reports, and diagenetic processes observed microscopically. The final sample study – total and separated by sexes and by samples – was, however, suitable for histological analysis since histological aging formulae have been developed with less or similar number of individuals (Stout et al., 1994; Kim et al., 2007; Pavón et al., 2010; Goliath et al., 2016). Nonetheless, larger samples are always desirable in order to have a full representation of the population under study. In this research, an improvement in number of individuals is required to balance the age categories in the youngest and the oldest age cohorts (under 40 and over 80 years, refer to Appendix A.3). On one hand, the low number of individuals under 40 years old may cause a potential impact in the future application of the method: if a young individual´s age is estimated applying the generated models, inaccurate results could be expected due to their under-representation in the sample. On the other hand, it was noted while collecting the rib samples that old individuals were naturally over-represented in both osteological collections, which is indicative of the increasing trend of advanced ages in recent human populations (Ice, 2003). From this point of view, the developed method would respond to current methodological needs.

This links to the second potential limitation. Based on the mean age of the sample, cortical bone microstructures observed may have been influenced by pathologies, such as osteoporosis related to advanced age (Curtis et al., 2016). The inclusion of younger individuals would help to better understand bone remodelling dynamics along the life span. When pathological information was available or anomalous histological microstructures were observed, these individuals were excluded from the final study sample. However, for most of the individuals no pathological data was available. There are only a limited number of diseases that

are pathognomonic and are reflected by histological alterations (De Boer, Van de Merwe and Maat, 2013). Therefore, those disorders that cannot be discerned through the histological approach could not be acknowledged. From the physiological perspective, whether the inclusion of pathological individuals would lead to a more accurate representation of the population is an open debate, with some authors excluding pathological cases while others included them in their samples (Stout et al., 1994; Ericksen, 1991; Goliath et al., 2016). From the statistical point of view, pathological individuals may produce values that are outwith the range of the overall sample trend (Stout et al., 1994). In this study, when a case was seen as a potential regression outlier during the regression analysis, this case was excluded and the analysis performed again. From the practical aspect, the author would like to remark that in the circumstance of including some pathological individuals, such as cases CC22 or CC203 (see Appendix A.2), data collection would have been complicated due to the impossibility of accurate identification of microstructural features (e.g., Haversian systems presented elongated canals and irregular surrounding lamellae with some cortical bone areas lacking any sign of osteonal structures).

Moreover, most of the individuals come from two cemetery populations associated with the largest cities, Heraklion and Limassol. Osteological collections may be biased towards individuals falling in a specific category (health, social status, cultural habits) (DiGangi and Moore, 2013). Whether a different pattern in bone turnover would be observed if the individuals were from other areas of the islands needs to be further investigated. Additionally, an improvement in the number of forensic cases in the samples would probably represent the current health status of the population; dietary habits seemed to have changed in the last decades and thus, an impact on bone cortical microstructure and bone turnover due to nutrition could be further explored (Vardavas et al., 2010; Angastinioti and Hutchins-Wiese, 2016).

Third, several statistical tests were performed to examine the influence of sex (males and females) as well as samples (Cretans and Cypriots) on the histomorphometric variables (Figure 4.11). Due to the limited and uneven number of individuals for each group separately – Cretan males, Cretan females, Cypriot males, and Cypriot females (Figure 4.5) – the differences between each group could not be assessed since the low representation of individuals in each age cohort would have resulted in misleading conclusions. Thus, the conclusions derived from this analysis are strictly limited to the fact that the subgroups could not be divided.

As mentioned above, the inclusion of more individuals would verify whether differences ultimately exist.

Fourth, bone turnover might be altered by intrinsic and extrinsic factors, such as physical activity, nutrition, and pathological disorders, among others (see Table 3.3). The lack of information (neither medical history nor life style) about the majority of the individuals included in the study sample prevents the author from drawing further conclusions about the obtained results.

Fifth, only rib samples were used due to time constrains and the invasive nature of the histological technique. The advantages of using costal elements for histological analysis have been discussed previously (Stout and Paine, 1992), but other skeletal elements could provide more insights in bone remodelling rates and bone turnover. Bones, such as the femur, with slower remodelling rates and larger cortical areas than ribs present a later OPD asymptote, and thus, may be more suitable for histological age estimation. However, other factors like remodelling spatial variation within the cross-section or complex biomechanical factors should then be considered (Gocha and Agnew, 2016).

Sixth, sampling area error testing was performed on six ribs from female individuals from the Cretan collection. Most of the ribs found were taphonomically affected and the entire length of the costal element was not available. Due to the small sample size, this study should be considered as an exploratory analysis and caution is warranted when drawing any conclusion.

Lastly, inter-observer error was performed using two individuals with different levels of histological experience. As previously stated, histological analysis requires specific training and experience has been shown to play an important role in the application of the method (Lynnerup et al., 1998; Stewart et al., 2013). The possibility of an inexperienced forensic anthropologist applying the method and obtaining higher inter-observer error rates should be borne in mind. This suggests that in real settings, the method needs to be applied by someone with histological experience to avoid inaccurate results. Thus, further examination on the magnitude of error for practitioners without any histological experience may be included in future research. The high number of old individuals and the consequent difficulties observed for variable identification in the sample under study (e.g. differentiation between interstitial bone and fragmentary secondary osteons) entails a limitation in the application of the method in practise.

Chapter 7 : DISCUSSION

The anthropologist can save himself/herself a lot of time by not trying to make more precise estimates of age than are warranted by the nature of the material.

S. L. Washburn (1958)

The successful use of bone histology for biological and anthropological research has been corroborated along the years (Kerley, 1965; Pfeiffer, 1998; Cuijpers, 2006). The application of hard tissue quantitative histology has covered a wide spectrum of research like comparative anatomy (Cvetkovic et al., 2013), taphonomic studies (Bell, 2012; Fernández Castillo et al., 2013; Hollund et al., 2015; Kontopoulos et al., 2016), ontogeny (Goldman et al., 2009; Jasinoski and Chinsamy, 2012) and pathological assessment (De Boer et al., 2015; De Boer and Maat, 2016), among others. Animal and human bones have been assessed through bone microscopy demonstrating the application of bone histomorphometry in the identification of different patterns in bone microstructural organization (Hillier and Bell, 2007). As discussed in *Chapter 3*, there has been an extensive age estimation research carried out on different past and modern populations and on a variety of skeletal elements (Yoshino et al., 1994; Stout and Jackson 1990; Dudar et al., 1993; Maat et al., 2006). There are intrinsic and extrinsic factors such as within and between population remodeling rates variation, pathological conditions and/or methodological discrepancies that may have an impact on age histological assessment (Robling and Stout, 2008).

Age estimation is a crucial step for the creation of the biological profile of an individual. Macroscopic methods are frequently the first approach used by osteoarchaeologist and forensic anthropologist to estimate age. However, when human skeletal remains are very fragmented and/or post-mortem thaphonomic effects have eroded bone surfaces, bone histomorphometry is one of the few available analytical methods that can be used (Stout, 1988). As noted above, several factors are known to affect bone microstructure and intra-individual and inter-population variation may be taken into consideration when developing new population-specific standards and when testing existing aging histological methods (Chan et al., 2007; Kim et al., 2007; Peck and Stout, 2007). This research aimed to explore intra-individual variability in rib bone microstructures, validate existing histological methods, examine the relationship between histological parameters and age, and develop population-specific standards for the sample under study. The accuracy of the developed aging formulae was analysed in the previous chapter and will be discussed along the course of the following sections. Overall, the results

indicated that the application of quantitative histological methods for estimating age on the Mediterranean sample is feasible producing error rates comparable to those reported by macroscopic methods and by other histological studies (Dudar et al., 1993; Stout et al., 1994; Cho et al., 2002).

7.1 Intra and inter-observer error

The methods commonly used to gather anthropological information from skeletal remains are scrutinized to evaluate measurement error, and to identify – when possible- the degree of error related to practitioners experience and/or to technical methodological aspects (Krishan and Kanchan, 2016).

In this study, the histological variables were tested for agreement and repeatability within and between observers. The results showed acceptable levels of intra-observer error as reported elsewhere (Keough et al., 2009; Goliath et al., 2016). Yet, higher variability in the levels of agreement between observers was noticed. As a result of this finding, special attention must be drawn to the variables included in the best models selected for the Mediterranean samples.

OPD is one of the most commonly used variables in histological studies (Stout and Stanley, 1991; Stout and Paine, 1992; Pfeiffer et al., 2016). As it is a composite variable, its constituent parameters were analysed individually. Through the course of data collection, the author noticed that N.On.Fg was difficult to assess due to both the definition and the nature of the parameter. The description of N.On.Fg adopted for this research states that at least 10% of the Haversian canal perimeter must exhibit evidence of resorption (Stout and Paine, 1992). This implies that the observer must estimate the missing percentage and could mislead differentiation between intact and fragmentary osteons. It is recommended that the observer calibrates his/her scores before final data collection. This can be done by comparing results in fragmentary secondary osteon count with the count results from an experienced bone histologist.

In samples of advance age, the entire cortex becomes less structured and more crowded with bone features. Fragmentary secondary osteons are very numerous in older individuals and their identification becomes problematic due to the increase of surrounding microstructures like intact osteons and interstitial bone. Inter-observer error results showed that both N.On.Fg and OPD(F) demonstrate low repeatability regardless individuals experience, which is in agreement with other studies (Lynnerup et al., 1998; Crowder, 2005). On the other hand, neither N.On nor OPD(I) showed poor agreement between observers. Lastly, OPD demonstrates

acceptable levels of inter-observer error suggesting that despite the observed discrepancies regarding OPD(F), the combination of OPD(I) and OPD(F) compensates measurement inconsistencies as it has been acknowledged elsewhere (Crowder, 2005; Cannet et al., 2011).

For the remaining histological variables, intra and inter-observer error values as an aggregate achieved repeatability standards. Rib area measurements are easily performed although Es.Ar has been shown to be the more subjective parameter due to difficulties in the identification of the transition from endosteal bone to intracortical remodelling (Agnew and Stout, 2012; Crowder et al., 2012). The technical aspects of the acquisition of rib area parameters through Dino Lite images could be further tested in future research as this specific data collection protocol has not been applied previously (Stewart et al., 2013).

On.Cr produced a high proportion of within-subjects variance as indicated by TEM R values for both for intra- and inter-observer. Nonetheless, *rTEM* and repeatability assessed through Bland and Altman analysis were within the acceptable thresholds. Other studies did not find intra-observer differences for this parameter but their statistical approach did not include TEM analysis (Crescimanno and Stout, 2012; Goliath et al., 2016). Photomicrographs are used for the assessment of On.Cr and ImageJ software calculates automatically the circularity index including area and perimeter (Rasband, 2000). The possible combination of both parameters may have induced more variability in the measurement as it was noted by other authors testing On.Cr data acquisition protocols (Mears et al., 2014). Finally, the author noticed a possible drawback in On.Cr data collection: as osteons overlap with age, measuring circularity becomes an arduous task due to the difficulty of finding “intact osteons with complete reversal lines and round Haversian canals” on the selected rib areas (Goliath et al. 2016: 282.e2). This methodological issue has been also noticed by other researchers (Goliath, 2010).

Histomorphometric methods are considered experience-based techniques (Garvin and Passalacqua, 2012). Two individuals with different levels of experience were used in this research to test whether histological training has an impact on the inter-observer error levels. Interestingly, the same parameters demonstrated inconsistencies for both observers suggesting that factors other than practitioner expertise may play an important role in the method’s reliability. As mentioned previously, one of the issues might be the definition of microstructures which may lead to subjective evaluation. Regarding possible technical issues, a standard counting reticule was not used in this study but instead the assessment was carried

out through microscopy and photomicrographs as suggested in other studies (Crowder and Rosella, 2007; Cannet et al., 2011; Absolonova et al., 2013; Goliath et al., 2016). It is unlikely that the counting of features as fragmentary osteons would be drastically altered due to the data collection protocol. Inherent methodological limitations might have counted as sources of error (Lynnerup et al., 1998).

Despite the reported inter-observer error for some of the histomorphometric parameters, age estimates produced by the scores obtained by each observer were very similar (Figure 7.1). Other studies have shown the same pattern suggesting that inter-observer error does not affect the final calculation of predicted ages (Stout and Gehlert, 1980; Cannet et al., 2011).

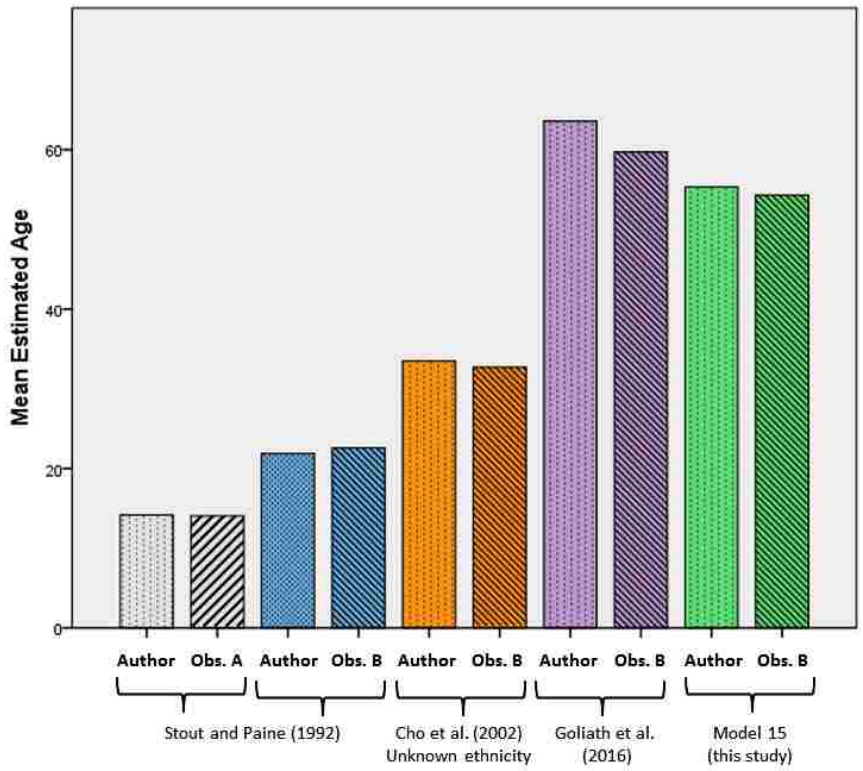

Figure 7.1 Histogram presenting mean estimated ages obtained by each observer (y axis) applying three formulae (Stout and Paine (1992); Cho et al. (2002), Goliath et al. (2016), Model 15 (x axis).

A possible research direction that would contribute to standardization, improvement of data collection and reliability of bone histological methods could focus on the analysis and assessment of intra- and inter-observer error in future studies. While intra-observer error is sometimes reported in published histological studies (Goliath et al., 2016), the inter-observer error does not seem to be so commonly undertaken (Pfeiffer et al., 2016; Goliath et al., 2016). In other instances, none of them are even evaluated (Stout et al., 1994; Watanabe et al., 1998; Cho et

al., 2002; Han et al., 2009; Lee et al., 2014). This trend may decrease scientific reliability and limit the use of microscopic methods for expert witness testimony in the court room, even if the method accurately estimate age of unknown individuals (Christensen et al., 2014).

7.2. Sampling error pilot study

Sampling area seems to be a significant factor in the application of histological aging methods. Both intra- and inter-section variation due to topographical differences in cortical bone remodelling have been previously reported (Tersigni, 2005; Chan et al., 2007). For example, femoral intra-section heterogeneity –i.e. from periosteal to endosteal area – may produce discrepancies in the age estimates depending on the sampling location (Pfeiffer et al., 1995). A common belief for long bones is that muscle attachment areas should be avoided in histological sampling due to high remodelling variability as a result of muscle attachment strains (Ahlqvist and Damsten, 1969; Sobol et al., 2015). Gocha and Agnew (2016) found high variation in remodelling densities across the midshaft femoral cortex with the antero-lateral periosteal area exhibiting the highest OPD values in individuals over 35 years old. Effective age of adult compacta of this specific location might be affected by modelling and remodelling drifts during development, and the diaphyseal biomechanical tensile loading on this area might be the cause of higher OPD values (Skedros, 2012; Gocha and Agnew, 2016). Other studies have shown remodelling variability for serial sections along the length of long bones resulting in biased estimated age (Tersigni, 2005). This fact indicates that a complex and heterogeneous mapping of remodelling rates in loading bones might be considered when choosing sampling areas for aging techniques.

Costal elements contrary to long bones are fragile and their fragmented nature makes the identification of sampling area difficult. Ribs are not exposed to weight bearing forces, and so, less involved in complex biomechanical interactions (Andriacchi et al., 1974; Tommerup et al., 1993). However, costal elements are subjected to constant respiratory mechanical activity and also contribute to other body movements. The main vertebro-costal muscle attachments are the intercostal and the inferior muscles and superior serratus posterior muscle which are involved in respiration (Ombregt, 2013). The sternal segment would be biomechanically affected by the transversus thoracic and the pectoralis minor muscles, while the main attachment on middle antero-lateral area corresponds to the serratus anterior muscle mostly related to scapular movements (Andriacchi et al., 1974; Ombregt, 2013). The rib area close to the costovertebral joint is the scaffolding for the

musculature of the vertebral column playing an important role in stabilization, movement and respiration (Saker et al., 2016). Although it seems that ribs might undergo complex biomechanical interactions based on muscles attachments and related movements, costal elements account for a medium influence of soft tissue (muscle, ligaments and tendons) (Skedros, 2012). Based on the constant respiratory mechanics, remodelling rates would be assumed to be also constant through the length of the rib. Yet, there is a lack of studies testing that hypothesis.

Intra-section variation was explored between the internal and external cortex in a study by Cannet and colleagues (2011) and it was found to be significant for only specific histological parameters. Taking into account the lack of studies on inter-section variation and the possible effect that it could have on age estimation methods, a pilot study was conducted on six thin-sections extracted from the length of six 4th rib samples to test whether intra-costal sampling area had an impact on the values obtained for raw parameters (N.On.Tt and Ct.Ar) and for the composite variable (OPD) (Tables 5.3-5).

The preliminary results of the analysis performed in this research indicated that the highest variability for N.On.Tt was produced by the two youngest individuals. Inter-section comparison showed that the highest number of osteonal structures was mostly produced by vertebral sections of the rib. Distal sections extracted from clavicles showed higher osteonal frequency numbers than middle-shaft sections which could be attributed to pulling forces applied by muscles attachments on the distal areas (Sobol et al., 2015).

An examination of Ct.Ar values suggested that the highest variation was observed also for the youngest individuals. For all the specimens, the lowest area was produced by the sternal segment while the highest was produced by the vertebral segments. The anatomical morphology of the rib supports this finding as the area closest to the vertebral end is larger in order to articulate with the 4th thoracic vertebrae (Figure 7.2). The transition from the midshaft to the rib neck and head requires a more consistent osseous structure than the sternal segment (Roberts and Chen, 1972).

Figure 7.2 29- year-old individual showing the difference in Ct.Ar: sternal end (left), vertebral end (right). Image captured with Dino Lite®.

Crowder and Rosella (2007) assessed the relation between N.On.Tt and Ct.Ar/Tt.Ar on intra-individual sections concluding that higher number of osteonal structures does not always imply higher Ct.Ar/Tt.Ar. Further analysis of Ct.Ar/Tt.Ar on the Cretan sample supported this suggestion. However, vertebral segments matched high values for N.On.Tt and Ct.Ar for most of the individuals under 35 years old which might indicate that certain correlation exists between these two parameters. While Ct.Ar/Tt.Ar is a measurement independent of body size, Ct.Ar is directly related to bone size and robustness (Stewart et al., 2015). Rib-cross section area reaches a maximum around 30 years old and then declines as a result of endosteal resorption (Takahashi and Frost, 1966). To the author´s knowledge, no other studies have been performed on the entire length of the rib, and thus, comparative data are not available.

OPD values increased with age and inter-section variation ranged from a minimum of two points for the 29-year-old individual to a maximum of six for the 58-year-old individual. The two youngest individuals presented the highest intra-section variation as assessed by all variability values as an aggregate. Remodelling rates expressed as OPD values might indicate a more heterogeneous remodelling pattern along the length of the rib for these two specimens. The shape and size of the rib cage is transformed during growth and development through modelling drifts and cortical drifts in order to achieve the adult proportions; when maturity is reached, a decrease occurs (Frost, 1987a). Growth spurt ends around 17-25 years of age for females with the appearance of the articular area of the tubercle and the final fusion of the rib head (Scheuer and Black, 2004). Although smaller ontogenetic changes are present at this stage – and some still unknown – an increase in vertical thoracic height is still observed in late adolescence possibly related to an increase in height and changes in sub-thoracic organs (Bastir et al., 2013). Streeter (2005) developed an aging method based on histomorphological patterns in sub-adults midshaft ribs

identifying intense remodelling in both cutaneous and pleural cortex for 18- and 21-year-old individuals.

Regarding inter-section OPD results, three specimens produced the highest OPD values by sternal segment while there seems to be a random pattern in the distribution of the lowest OPD values (Figure 7.3). A previous study published by the author and colleagues focused on the impact of sampling area on age estimation techniques on the six Cretan individuals (García-Donas et al., 2016). OPD values were inserted into two existing histological formulae (Stout and Paine, 1992; Stout *et al.*, 1994) to verify the magnitude of error that could be attributed to sampling area. A systematic underestimation of all the individuals was noticed: only the two youngest specimens fell within the error rates reported by both methods and error rates increased as the age of the individuals increases (refer to Table 5.6) (García-Donas et al., 2016). As the authors noticed, rib number or rib segment may have introduced some error based on the standards reported by each method. Crowder and Rosella´s findings (2007) indicate that standard ribs can be reliably used without introducing a major bias in OPD values. On the other hand, it seemed that no specific segment performed systematically more accurately than the other suggesting that rib sampling area might not alter significantly the age estimates. The overall error resulting from the under-estimation of the individuals is higher than the possible error introduced by each segment along the rib length (García-Donas et al., 2016).

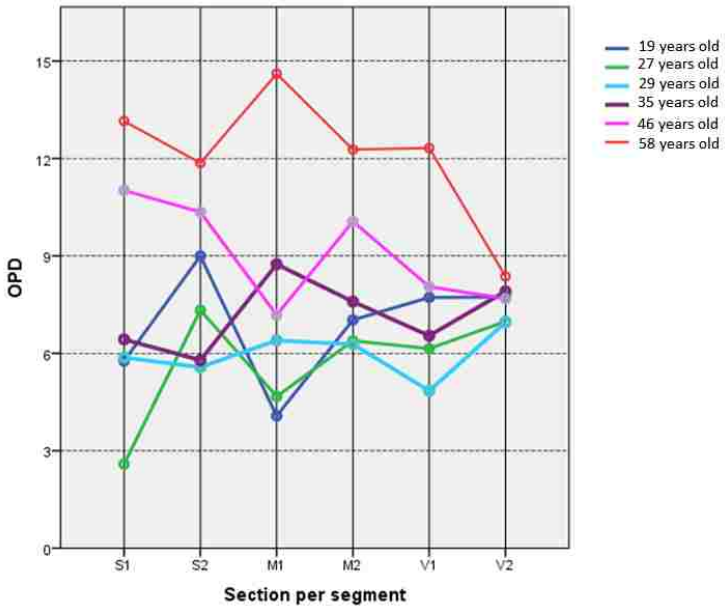

Figure 7.3 OPD values for each thin-section extracted from each individual. X axis represents sections codes from sternal to vertebral end: S1=first sternal, S2=second sternal, M1=first middle, M2= second middle, V1= first vertebral, V2= second vertebral.

In summary, a generally low variation in relation to the OPD produced by each thin-section from the same individual was observed. Moreover, intra-section variation indicated that no specific sampling site performs better when applying two existing formula; hence, any segment might be possibly used if the topographical area along the rib cannot be identified. Due to the small sample size, this is an exploratory analysis and a larger and more heterogeneous sample is required to verify the preliminary results. Further research could examine intra-costal bone remodelling rates variation along the rib length within the same individual as clinical and anthropological studies have already noticed (Frost, 1969; Frost, 1987b; Crowder and Rosella, 2007). Moreover, a larger sample size will verify if other factors as sex differences, inter-population variation or pathological conditions may be causing the discrepancies between known and estimated age (Burr et al., 1990; Paine and Brenton, 2006a; Kim et al., 2007; Oursler et al., 2008).

7.3. Validation study

A forensic anthropologist is often tasked with the examination of skeletal human remains and reconstruction of the biological profile through the application of peer-reviewed methods (Byers, 2011). Age estimation is one of the first steps in the identification process and the choice of the method is crucial to ensure accurate results (Merritt, 2013). Occasionally, the fragmented nature of human remains makes histological methods one of the few tools available for estimating age. Bone remodeling have shown inter-population variation and methods developed from populations not closely related to the target sample demonstrated a decrease in the accuracy rates (Stout et al., 1996; Kim et al., 2007; Pavón et al., 2010). Therefore, validation studies testing histological aging methods are required to guarantee reliable results in forensic cases or in osteo-archaeological samples (Stout and Gehlert, 1980; Crowder and Pfeiffer, 2010). In order to assess the accuracy of aging techniques and verify whether population-specific formulae were required for the Mediterranean sample, four existing aging equations are applied and the results scrutinised (Stout and Paine, 1992; Stout et al., 1994; Cho et al., 2002; Goliath et al., 2016).

Inaccuracy and bias are commonly used for evaluation of methods reliability (Lovejoy et al., 1985b; Crowder, 2005). The outcome from this research showed a general pattern of underestimation for all the applied methods except for Goliath et al. (2016) formula. The main factors affecting the methods´ performances are: differences in demographic characteristics and biological affinity between reference and target samples (age and sex distribution, inter-population variability…), inherent

limitations related to histological age estimation techniques (i.e. OPD asymptote), and methodological issues related to the statistical approach (Figure 7.4).

Regarding the entire Mediterranean sample, the results indicated that Stout and Paine method (1992) produced grossly inaccurate age estimates which is in accordance with other studies (Dudar et al., 1993; Pratte and Pfeiffer, 1999; Crowder and Pfeiffer, 2010). Stout et al. (1994) and Cho et al. (2002) formulae performed similarly with a slightly lower accuracy and bias values seen for Cho et al.´s African-American equation. Goliath et al. formulae (2016) provided the best performance overall, although it showed a tendency of overestimation of young individuals and underestimation of the oldest age cohort. The same tendency was observed for sexes and samples (Cretans and Cypriots) for all predicting equations displaying only discrepancies for specific age categories. Overall, Stout and Paine (1994), Stout et al. (1994) and Cho et al. (2002) methods showed a gradual increase of inaccuracy and bias values with increasing individuals´ chronological age. When the sample and sub-samples were truncated at 60 years of age, a substantial decrease in accuracy and bias was seen for the formulae including OPD as a predictor. This observation has been reported by other studies (Crowder and Pfeiffer, 2010), and it might be explained by OPD rib asymptote occurring at this age and provoking a dissociation between chronological and estimated age (Stout and Crowder, 2012). Furthermore, the under 60 years old age cohort in the Mediterranean sample presented a closer mean age to the mean age of the reference samples explaining to some extent its higher accuracy (Figure 7.4). In reverse, Goliath et al. (2016) formula only includes On.Cr as a single predictor. It has been suggested that osteon circularity may be a mechanism for providing support to the loading forces and for preventing micro-damage, and thus, being positively correlated to age (Schaffler et al., 1995). Hence, the better performance of this method is presumed since it is not affected by osteon densities plateau. The low number of young individuals included in Goliath et al. (2016) original reference sample (7% of the total) could explain the higher inaccuracy and bias of this formula for the young Mediterranean individuals.

Rib samples from both males and females produced very similar results when compared as a whole group. However, females exhibited slightly higher inaccuracy and bias values than males when the sample was divided in age categories. The differences between sexes are especially noticeable for the over 80 years old age group. For the three methods including OPD as predictor (Stout and Paine, 1992; Stout *et al.*, 1994; Cho *et al.*, 2002), this might suggest more variability in remodelling rates within the female group, along with a higher mean age for females

(Females = 92 years old, Male = 83 years old). Moreover, the increment in bone remodelling rates related to post-menopause is not steady throughout time and it is also triggered by other diseases that are potentially appearing with advanced age (Recker et al., 2004). Other studies observed a similar trend for females in their samples (Crowder, 2005).

Goliath et al. formulae (2016) produced the same outcome with higher inaccuracy for the oldest female category when compared to their male counterparts. Britz et al. (2009) did not find any correlation between femoral On.Cr and sex, although On.Ar and sex were correlated. The relationship between age and a decrease in On.Ar may result in more circular osteons with weight, strains and loading complexity possibly affecting osteon size (Currey, 1964; Van Oers *et al.*, 2008; Britz *et al.*, 2009). However, other factors such as genetics and physiological mechanisms might play an important role in On.Ar (Dominguez and Agnew, 2016). Some studies reported sexual differences in osteon size (Burr et al. 1990; Kim et al. 2007) and others contradicted this outcome (Pfeiffer, 1998). Even if circularity increases with age, the possibility of potential age pathological conditions related to the female group (as postmenopausal osteoporosis (Frost, 2003)) might affect osteonal structures morphology and the appearance of the rib cortex. Thus, a possible reason for the observed sex discrepancies could be the On.Cr data collection issue mentioned previously. Whether the higher variability observed in Goliath et al. formula (2016) for the oldest female group was due to intrinsic factors or to age related changes needs to be further examined with a larger sample size for this particular age cohort.

Cretans and Cypriots showed the same underestimation tendency for all histological methods except for Goliath et al. formulae (2016) that still produced the optimal results. Overall, both samples showed similar accuracy and bias values with slight differences observed by age cohorts. It is worth noticing the under-representation of Cypriot individuals younger than 40 years which produces an unbalance of the age distribution. However, the Cretan sample did not perform better; hence, it seems that there might be a secondary reason. Probably, the overall skewed age distribution of the Mediterranean samples affected the general performance of the methods (Figure 7.4).

Based on the low accuracy of three of the four formulae applied (Stout and Paine, 1992; Stout *et al.*, 1994; Cho *et al.*, 2002), inter-population differences in bone remodelling between the reference samples and the Mediterranean samples might be considered as their biological affinity is not ensured (Hughey et al., 2013;

Hellenthal et al., 2014; Heraclides et al., 2017). This matter has been previously reported for other histological studies (Kim et al., 2007). Population specific variability in bone mass and bone structure have been shown (Weinstein and Bell, 1988; Ericksen, 1991; Schnitzler, 1993), and discrepancies between known and estimated age were noticed (Crowder 2005; Pavón et al. 2010; García-Donas, School, Paine et al., 2017). While this could be a true statement for formulae accounting for remodelling rates variables (such as OPD), it appears that when an alternative parameter is used (On.Cr for Goliath et al. formula (2016)), the possible inter-population differences seem to be minimised. A recent research found low accurate age estimates when methods based on degenerative articular changes were applied on the Cretan Collection (Michopoulou et al., 2017). One of the authors' explanations is that the expression of the age indicators may not be strongly correlated to age as they were for the reference sample resulting in unreliable age estimates.

The general inaccuracy and bias values produced by this validation study did not show major differences when sub-groups were compared (sexes and samples, separately). Attention must be drawn to the fact that inherent sexual and genetic differences could not been discern within sexes and within samples due to sample size and uneven number of individuals for each sub-group (see previous chapter). Further research will elucidate whether the spotted differences are meaningful but conclusion are now limited to the given sample.

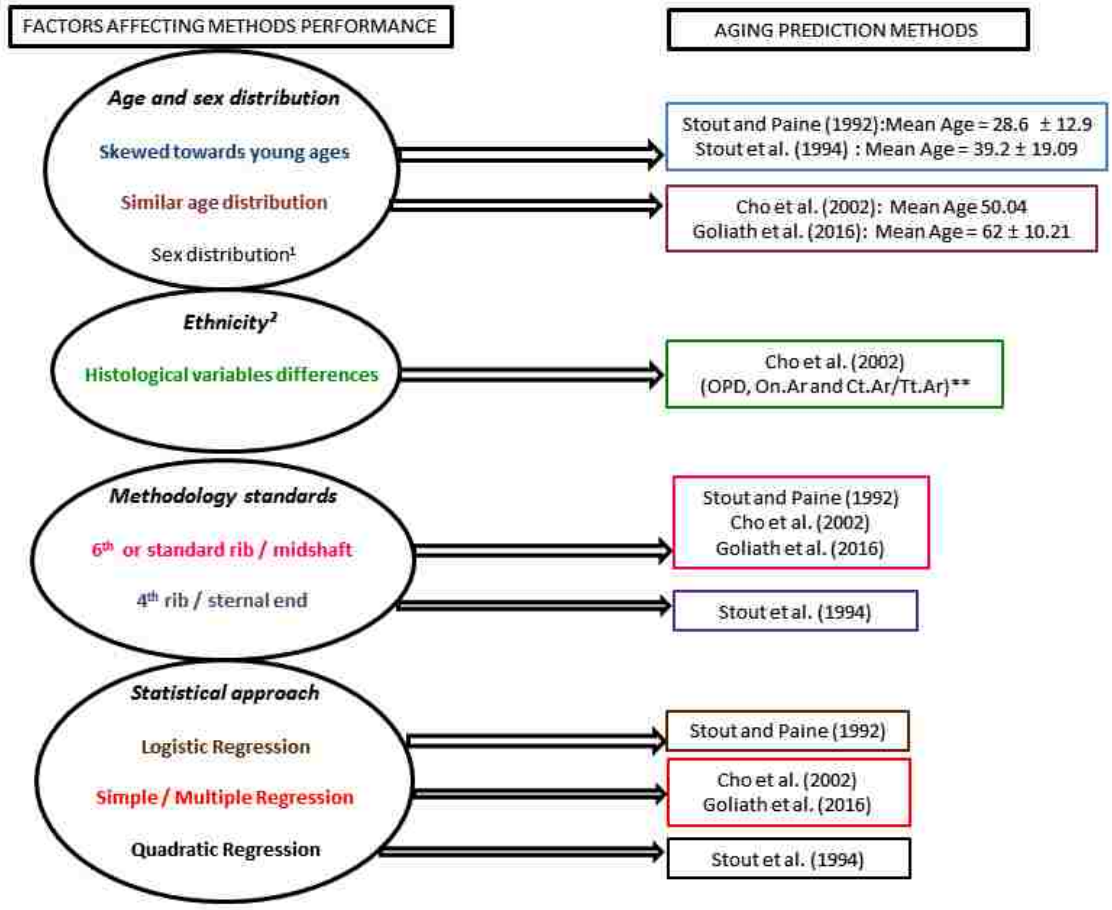

Figure 7.4 Factors biasing the performance of Stout and Paine (1992), Stout et al. (1994) Cho et al. (2002) and Goliath et al. (2017) methods on the study sample. [1]Sex distribution only similar for Goliath et al. (2016); Colours indicate the basis of each method, [2]All samples are Americans with European ancestry or African-Americans (see **Table 7.3**).

Age and sex distribution differences between reference and target samples may have an impact on the methods reliability (Bouvier and Ubelaker, 1977; Aiello and Molleson, 1993). As seen in Figure 7.4, Stout and Paine (1992), Stout et al. (1994) and Cho et al. (2002) samples differ from a minimum of 10 to a maximum of 30 years from the Mediterranean sample mean age (60 years), with Stout and Paine (1992) accounting for the highest mean age difference between reference and target samples. According to Bland and Altman results, Stout et al. (1994) is recommended to age young individuals as assessed by the limits of agreement and bias. All formulae generated by Cho et al. (2002) produced similar accuracy and prediction power; however, the ethnicity unknown equation performed the best as noticed by other studies (Pfeiffer et al., 2016). Goliath et al. (2016) sample age distribution matches the mean age of the sample under study supporting its overall good performance. This method estimated age within the limits of agreement for 96% of individuals older than 60 years of age. Regarding sex distribution, Stout and

Paine (1992) is skewed towards males while Goliath et al. (2016) accounts for a more even sex distribution which might also influence the validation study results.

Sampling area and/or rib number could be the cause of the poor performance for Stout et al. (1994) (Figure 7.4). The sampling error pilot study conducted by the author and colleagues (García-Donas et al., 2016) suggested that other inherent factor as inter-population variability rather than rib topographical location could be the major causes of the reported errors. As far as sampling area is concerned, this matter has been discussed in the previous section so no further debate will be hold here. Regarding rib number, ribs from the Mediterranean samples consists mostly of 4th ribs and it could be thought that certain bias is introduced by the fact that Stout and Paine (1992) standards comprises the 6th costal element. As noted above, standard ribs did not introduce major bias on the methods reliability (Crowder and Rosella, 2007). Indeed, recent histological aging studies do not specify or report rib number in their standards (Goliath et al., 2016; Pfeiffer et al., 2016).

Differences between histological variables values among the samples were examined for their potential impact on the methods performance. The Mediterranean mean OPD value was of the same general magnitude as those reported by Stout and Paine (1992) and Stout et al. (1994) (Paine personal communication) (see Table 7.3 in next section). However, the Mediterranean sample presented a higher mean age. A larger difference was noted for mean OPD, On.Ar and Ct.Ar/Tt.Ar values between European and African-American ethnicity groups and the study sample. Moreover, the larger variation was accounted among Cretans and African-Americans (note Ct.Ar/Tt.Ar between Cretans and African-Americans being 32% and 35%, respectively). On.Cr mean value for Goliath et al. reference sample (2016) was comparable to that obtained by the study sample supporting its better performance (0.905 versus 0.910). Excluding possible inter-observer errors differences – that are not analysed by any of the methods under consideration, and therefore, impossible to assess – possible differences in bone remodelling rates between populations might be drawn to attention. This issue will be further discussed in the next section of this chapter.

The last argument concerns the statistical approach undertaken by the four aging prediction methods used for this validation study. Stout and Paine (1992) method applies logarithmic transformed data and its systematic underestimation on independent samples has been reported by several studies (Dudar et al., 1993; Pratte and Pfeiffer, 1999; Crowder, 2005). Transformation from logarithmic data into arithmetic units induce an underestimation bias due to the geometric mean used for

making the predictions being always less that the transformed arithmetic mean (Smith, 1993). While the common statistical procedure to estimate age is the least square linear regression, some authors have demonstrated systemic under- and over-estimation issues and the use of classical calibration (dependent variable being the age indicator) was presented as an alternative (Rogers and Stout, 1998). If that approach would be applied, confidence intervals and source of errors would be more difficult to be established (Aykroyd and Lucy, 1997). The application of Bayes´ theorem should be explored as a possible alternative to avoid systemic under and over-estimation (Samworth and Gowland, 2007).

7.4. Histological variables and age

Many researchers as the means to estimate age have used bone histomorphometry. As presented in the first two chapters, microscopic age changes are the result of concurrent physiological mechanisms that bone undergoes throughout one´s life. The foundation for histomorphometric age estimation relies on bone modelling and remodelling processes with the latter being the focus of adult age assessment (Trammell and Kroman, 2013). Remodelling discrete cellular packets (BMU) can be assessed qualitatively and quantitatively (e.g. frequency number, morphology, size, geometrical properties) along with age-dependent alterations in cortical and trabecular micro and macrostructure. Hereby, the direct or inverse relationship of the microscopic indicator with age can be effectively applied for age prediction. Unfortunately, the relationship between histomorphological features and age is not fully consistent as it happens with other biological age markers (Mays, 2015). Thus, intra- and inter-variability due to sex, pathology, nutrition, physical activity and genetics – among others factors – may consequently affect not only the application of the methods but also the expression of the microstructural features (Robling and Stout, 2008). Histomorphological features have demonstrated different degrees of variability and different types of age correlation (Jowsey, 1966; Pfeiffer, 1998; Kim et al., 2007). The main parameters assessed in this research, and particularly the ones included in the best models, will be discussed according to the results obtained in the previous chapter.

As a general concept, frequency number of secondary osteons (N.On, N.On.Fg and N.On.Tt) has a direct age effect with an increasing number of osteonal structures associated with an increasing age (Kerley, 1965). The underlying biological mechanism relates to the fact that remodelling occurs throughout life as a response to maintain bone material and functional properties and capacities; the replacement of specific bone sites is carried out by the coupled and coordinated

activity of osteoblasts and osteoclasts seen in a 2D plane as new BMU appearing in the cortex (Frost, 1969; Parfitt, 2002). Considering all the individuals included in this study, N.On presented an average of 190 for the 20-30 age range with the highest peak reached in individuals between 40 and 50 years old. This trend reflects the increase in intact osteons with age as lamellar bone is replaced by secondary bone. However, a general decrease was observed for individuals over 60 years of age with an average of 170 intact osteons (Table 7.1). This indicates a statically significant although weak decrease in N.On which was reported somewhere else (Mulhern and Van Gerven, 1997), but contradicts other research results (Yoshino et al., 1994; Pfeiffer et al., 2016). In Kerley´s study (1965), a plateau for intact secondary osteons for individuals older than 50 years of age can be seen in all the skeletal elements used. Moreover, the number of complete and mature osteons with a high density mineral inner lamellae decreases with age as a result of more variability in the time required to accomplished full mineralization (Ortner, 1975). New forming osteons create a new canal (cutting cone) but also they may obliterate previous osteons canals removing any evidence of intact osteons (Martin and Burr, 1989). Thus, the frequency number of intact osteons observed might be related to the osteonal mineralization or due to osteon overlapping with the underlying effect of the advance age of the individuals under study.

N.On.Fg demonstrates a statistically significant increase with age as shown somewhere else (Kerley, 1965; Keough et al., 2009; Pfeiffer et al., 2016). As noted previously, this parameter reflects the relative appearance of new osteonal structures removing partially or completely existing intact osteons. A common pattern observed in the Mediterranean sample was enlarged resorption spaces or Haversian canals that failed to refill with may be an indication of osteoporosis and related bone loss (Raisz, 2005). As a result, an increment in consequent creation of fragmentary osteons occurs (Figure 7.5).

Table 7.1 N.On, N.On.Fg and N.On.Tt for the Mediterranean sample by decades.

	Decades						
	20 (N=7)	30 (N=4)	40 (N=11)	50 (N=17)	60 (N=29)	70 (N=7)	> 80 (N=13)
N.On	183 ± 81	195 ± 43	198 ± 102	186 ± 74	173 ± 62	129 ± 43	144 ± 79
N.On.Fg	65 ± 27	81 ± 18	88 ± 45	113 ± 35	123 ± 44	116 ± 56	120 ± 53
N.On.Tt	248 ± 103	276 ± 54	286 ± 146	299 ± 102	296 ± 96	246 ± 98	264 ± 129

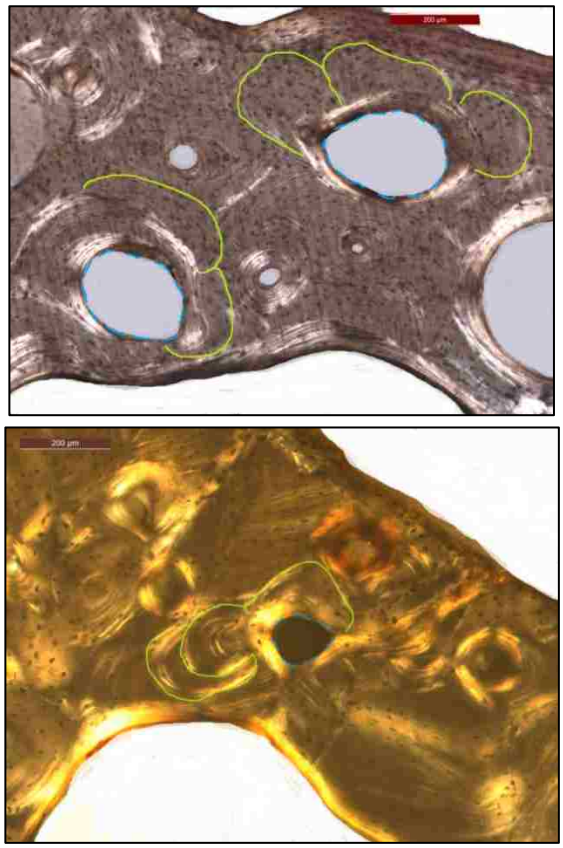

Figure 7.5 Example of enlarged canal (dotted blue line) that removed previous Haversian systems resulting in N.On.Fg (green outline) (10x semi-polarised microphotographs; top: female Cretan, 56 years old; bottom: female Cyprus, 67 years old. Note also low number of N.On.

A non-statistically significant association with age was observed for N.On.Tt, what it is expected due to the negative and positive relationship of the two constituent parameters (N.On and N.On.Fg). Yet, an increase in N.On.Tt was seen until the 50-60 decades of life, and afterwards it seems that senile degenerative changes may have affected the results with a lower rate of osteons creations as stated elsewhere (Table 7.1) (Wu et al., 1970). The frequency number of osteons – both observed osteonal structures and estimated missing osteons – created per year per unit area represents the mean activation frequency (Wu et al., 1970). This parameter along with mean annual bone formation rate show a decrease pattern in their relation to age (Stout and Lueck, 1995). As shown by Frost (1964), mean activation frequency can be shown as a function of osteonal remodelling ranging from a higher peak in childhood to a decline at 35 years of age, to again increase afterwards around 60 years old and reaching a minimum value in the latter decades of life. The physiological mechanism reflects the pattern of rapid bone turnover and new osteons creations driven by modeling cortical drifts during growth; this implies the replacement of primary bone into osteonal bone. In adulthood, the activation rate is maintained to a minimum and only increased when needed for metabolic or

mechanical demands; it demonstrates a senile remodeling deficit for the last three decades of life (Martin and Burr, 1989).

These age-related associations observed for the raw frequency number parameters are strongly coupled with a decrease in the amount of cortical area with increasing age, and thus, accounting for one of the best indicators in histological aging methods, OPD (Stout and Paine, 1992; Kim et al., 2007; Lee et al., 2014; Pfeiffer et al., 2016). Indeed, most of the rib histological studies performed in the later years do not report frequency numbers for any of the osteonal structures, but instead focus on the number of structure per unit area (Cho *et al.*, 2002; Pavón et al., 2010; Goliath et al., 2016).

Ct.Ar decrease with age is related to an expansion of the medullary cavity and trabecularization of the cortex expressed as the difference between Tt.Ar and Es.Ar. In this study, Tt.Ar seems to be fairly stable through age although a slightly larger total periosteal area is seen in the individuals under 60 years old in comparison to the older age cohort (Martin et al., 1980). Es.Ar has been recalled a problematic measurement due to the trabecularization of the endosteal envelope (more extensive and irregular in ribs than in long bones). Some studies suggest the inclusion of the transitional zone to further improve bone loss and endosteal resorption measurements although methodological drawbacks and difficulties in its identification are being still questioned (Dominguez and Agnew, 2014; Zebaze and Seeman, 2015). In general terms, the thinning of the cortex along with an additional increment of intracortical porosity and remodelling rates will result in bone loss with advanced age in all skeletal elements. The amount of rib Ct.Ar increases until 25-30 years of age and decreases sharply afterwards (about 25-30% of bone mass loss) (Takahashi and Frost, 1966). Nonetheless, it is important to consider the factors affecting Ct.Ar aging changes such as sex and population differences, body size, muscle mass decrease, bone site and type, mechanical adaptation, hormonal alterations, nutrition and other still unknown biomolecular mechanisms (Gosman et al., 2011; Jepsen and Andarawis-Puri, 2012). Ct.Ar/Tt.Ar is commonly incorporated in histological studies as it shows a negative correlation with age (Cho et al., 2002; Pfeiffer et al., 2016), though some studies did not report any age association (Kim et al., 2007). This parameter represents a measure of cortical area unrelated to body size (Stewart et al., 2015).

OPD has been shown to be one of the best age predictors in this study confirmed by its inclusion in most of the generated models. OPD composite variables (OPD(I) and OPD(F)) shown also a positive correlation with age with the

latter reporting a stronger age association. This trend has been shown by other studies concluding that the predicting power of OPD can be mostly attributed to OPD(F) (Crowder, 2013). Other studies showed no age associated correlation for OPD(I) on femora (Crowder and Dominguez, 2012). Caution must be taken here. The loading experienced by weight bearing bones (such as femora) is not comparable to the stress applied to non-weight bearing bones (such as ribs) with studies showing differences between intra-individual skeletal elements depending on their loading environment (Tommerup et al., 1993; Cho and Stout, 2011). Most of the published histological studies on ribs did not report the composite variables for OPD, and thus, no robust comparable data is available. Nonetheless, published data demonstrate the OPD prediction power for age estimation on costal elements (Stout and Paine, 1992; Stout et al., 1994; Cho et al., 2002; Kim et al., 2007; Pavón et al., 2010; Pfeiffer et al., 2016).

Osteon size indicated an inverse relation with age for On.Ar and On.Pm and a positive age association for On.Cr. The results of this research are in consensus with other studies (Cho et al., 2002; Kim et al., 2007; Goliath et al., 2016), although non-significant correlation between osteon size and age was also reported (Burr et al., 1990; Pfeiffer, 1998). Osteons dimensions tend to decrease as age advances according to several theories (Abbott, Trinkaus and Burr, 1996) (Abbott et al., 1996). Osteon measurements performed in this study included the Haversian canal. Early research stated that the activity of both osteoclasts and osteoblast seems to be reduced with increasing age the first removing less bone and the second refilling with less efficacy resulting in smaller osteons but with larger Haversian canal area, and thus, producing an increment in intracortical porosity (Martin et al., 1980). A significant relationship between On.Ar and Haversian canal size have been noted although with differences between remodelling sites possibly attributed to different circulation at the periosteal or endosteal envelopes (Qiu et al., 2010). Experimental studies showed an inverse relationship between osteon diameter and large strains (Van Oers *et al.*, 2008). If this is the case, then osteon dimensions may explain physical activity although the evidences suggest that other factors than strains may play a role in osteons size (Pfeiffer et al., 2006). However, a study conducted in osteon dimension to discern between animals and humans found that differentiation between species was accurately achieved by On.Ar indicating that locomotion loading experiences have a clear effect on osteonal dimensions (Dominguez and Crowder, 2012). Moreover, ribs could benefit from the constant respiratory movement as normal strain levels related to physical activity have a positive effect on bone (Qiu et al., 2003). Dominguez and Agnew´s research noted that age and

Ct.Ar/Tt.Ar influence On.Ar in ribs being larger in the pleural cortex than in the cutaneous cortex possibly due to a compensatory response to higher cortical loss in the latter (Dominguez and Agnew, 2016). Further research on the sample under study comparing intra-section variability might verify this outcome. A more methodological issue than a physiological response was also suggested. Age changes in osteon size may be an artefact of a higher remodelling activity and the consequent overlapping and removal of larger osteons in older individuals, thus, leaving only smaller osteonal structures to be measured (Takahashi and Frost, 1966).

Osteon cross-sectional shape (On.Cr) has been recently used as means for age estimation although the appreciation of more circular osteons appearing with age was acknowledged in early research (Currey, 1964). The inverse relationship between On.Ar and On.Cr is confirmed by this research. It has been also suggested that the increase in On.Cr may be a product of increase in OPD as it implies the appearance of new osteons would remove larger and irregular previous osteonal structures (Britz et al., 2009). In relation to weight loading bones, more circular osteons may be a mechanism for providing support to the loading forces and preventing micro-damage, which will explain its positive correlation to age (Schaffler et al., 1995). This biomechanical property would be also correlated to small osteons dimensions. The reciprocity between more and smaller osteonal structures would help to stop fatigue microcracks propagation since numerous and closer cement lines would serve as a boundary (Schaffler et al., 1995; van Oers et al., 2008). This acts as a balance to compensate senile effects in bone material properties and to increase bone energy absorbing capacities (Burr et al., 1990).

Moreover, osteon size might determine osteon packing arrangement on a given area of the cortex with the possibility of smaller osteons allowing higher osteon accumulation per squared millimetre (Figure 7.6). It implies the observations of more intact and fragmentary osteonal structures on that given area (Robling and Stout, 2008). Also, this packing density is related to the aforementioned energy absorption mechanism limiting micro-crack propagation (Martin et al., 1998).

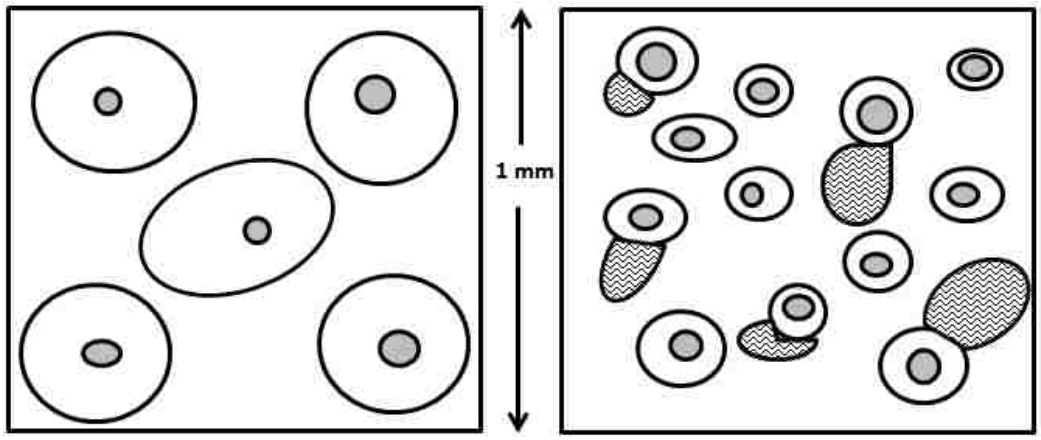

Figure 7.6 Packing effect: relation between osteon area and number of osteons that can accumulate on a given cortical area. Grey shapes represent fragmentary osteons (Adapted from Wu et al. 1970).

These mentioned dynamics between histomorphometric variables play an important role in bone osteonal remodelling. Nevertheless, other intrinsic and extrinsic factors take part in the expression of histological parameters.

7.4.1. Sex variation

As expressed in the previous chapter, the highlighted sexual and sample differences might be affected by sexual dimorphic patterns when the two samples were compared or by Cretan and Cypriots inter-variability when the two sexes were tested against each other. Therefore, conclusions are currently drawn based on the given sample and its implicit limitations.

There is still an open debate regarding sex differences in histomorphometric variables with some studies reporting sexual differences (Samson and Branigan, 1987; Ericksen, 1991; Burr et al., 1990; Cho et al., 2006) whilst other did not report any (Kerley, 1965; Thompson and Galvin, 1983; Han et al., 2009). The maturation rate of the cortex varies between sexes (Tanner, 1978). Whether the earlier completion of the cortex in females would have an impact on the histological variables and on the age estimates due to differences in the mean tissue age needs further investigation (Robling and Stout, 2008). In the early years of adulthood, males present around 40% larger bone areas than females which is also associated with their larger body size; a decrease in cortical area produced by periosteal and endosteal remodelling is observed for both sexes in the middle age (Riggs et al., 2004). With aging, both sexes experienced a general decline in bone formation at the periosteal surface, and a reduction in bone formation and continued resorption at the BMU level which produces a negative remodelling imbalance (Seeman, 2008). This imbalance gets triggered by the increase cortical remodelling which

accelerates cortical and trabecular thinning with interstitial bone becoming highly mineralised in postmenopausal women (Seeman, 2008). According to the literature, menopause causes an increase in bone loss, partly associated with estrogen deficiency, while men undergo the same process but in a slower rate (Frost, 2003; Khurana and Fitzpatrick, 2009). This would be a potential cause for the differences observed in histomorphometric parameters. Considering that 73% of the females in this sample are over 50 years old, some differences may be found due to postmenopausal associated osteoporosis and related bone loss.

Several parameters accounted for sex differences in this research (see Tables 5.23, 5.24 and 5.27), in consensus with other studies (Ericksen, 1991; Mulhern and Van Gerven, 1997), although caution with microstructures definition and skeletal element used by the other authors must be bore in mind.

Ct.Ar showed significant differences between sexes in this research which is in agreement with other studies (Takahashi and Frost, 1966). More specifically, females showed a lower number of secondary osteons compared to their male counterparts (see Table 5.24). This observation is in accordance with Ericksen (1991) who found that the number of secondary intact osteons reached a plateau at the age of 60 years in females while the number increases steadily with age in males.

Differences were also observed for both Tt.Ar and Es.Ar between sexes. This can be simply a reflection of sexual dimorphism in rib size in agreement with other studies carried out on Cretans and Cypriots that demonstrated substantial sexual dimorphism in other bones (Kranioti et al., 2008; Kranioti and Michalodimitrakis, 2009; Osipov et al., 2013; Nathena et al., 2015; Kranioti et al., 2017). Furthermore, periosteal apposition is seen in postmenopausal women as an adaptive response to the decrease of cortical bone strength and increase in bone fragility (Ahlborg et al., 2003). Szulc et al. (2006) proposed that after menopause an imbalance occurs with periosteal apposition decreasing while endosteal expansion increases at its maximum producing progressive fragility in the later years. A study using vertebrae demonstrated that bone loss for males is mostly associated to more periosteal apposition than to endosteal resorption (Seeman, 2001). Thus these differences may be due to a combination of factors including sexual dimorphism in rib size and hormonal influences. Supporting the size differences between sexes, Ct.Ar/Tt.Ar was not statistically different between sexes as it is an expression of Ct.Ar unrelated to body size (Stewart et al., 2015).

The remaining variables did not show any difference between sexes supporting the findings of other studies (Thompson and Galvin, 1983; Pfeiffer, 1998). OPD is the most commonly used variable in age estimation equations, thus the existence of sexual dimorphism would greatly affect the applicability of histological age estimation methods. This study reported non-statistically significant differences between the two sexes but the contradicting results of other studies create the need for further research using larger samples to confirm or reject these observations (Cho et al., 2006; Kim et al., 2007).

7.4.2 Sample variation

Regarding Cretans and Cypriots, both samples share dietary and cultural habits and similar climate (Kranioti et al., 2017), so at first glance minor differences could be expected. However, several histomorphometric variables were found to vary within the two groups. Frequency number of osteons and Ct.Ar showed significant differences with higher values for Cypriots in comparison to Cretans. A possible sex effect could be influencing the samples differences as the same parameters were statistically significant between males and females. Among osteon population densities, only OPD(F) demonstrated differences between the two samples. It is worth noting that even if OPD did not show any statistical significant difference, the p-value showed a trend towards significance when age was not controlled as a covariate ($p = 0.60$). As noted above, OPD(F) seems to be the most powerful indicator of age and the highlighted differences might be because Cypriots presents a higher mean age than Cretans rather than inter-population variations. Nonetheless, On.Ar and On.Pm were also statistically significantly higher for Cypriots. This would mean that the aforementioned packing factor relating osteons number, osteon size and cortex dimensions – see Figure 7.6 – may be reflected in the patterns observed for OPDs between the samples (mean OPDs: Cretans = 14.50, Cypriots = 16.30).

Inter-sample differences in bone microstructure parameters may be attributed to several factors. As discussed in previous chapters, differences in bone mass and mineral densities between populations have been reported (Broman et al., 1958; Pollitzer and Anderson, 1989; Schnitzler, 1993; Anderson and Pollitzer, 1994). The crucial question remains as how and to what extent growth and development, genetic and environmental factors contribute to the perceived differences in histomorphometric structures.

Cortical bone phenotypic traits – as cross-sectional area and density - are determined in the early years of life; however, during growth and development these

traits are also modulated by environmental factors as disease and life-style which will influence the amount of bone mass reached later in life (Cooper et al., 1995). For example, physical activity expressed as mechanical loading has an active role on cortical bone during pre-pubertal and early years of adulthood (Gosman et al., 2011). Growth and maturation account for an increase in bone strength and stiffness with changes in chemical and collagen composition and structure having a determinant effect on posterior aging processes (Wang et al., 2002). Through one´s life and particularly in later adulthood, bone responds to age through a constant reconstruction of its microstructure in order to maintain material and functional properties. Remodelling imbalance processes occurring with advanced age will increase bone loss and skeletal mass degradation (Gosman et al., 2011). Polygenetic interactions and aging effects on the molecular and cellular processes, decrease of muscle mass and life style – among others factors – are responsible of inter-individual and inter-population variability (Gosman et al., 2011).

Bjørnerem et al. (2015) concluded that genetics influence both cortical and trabecular bone microstructure and remodelling markers up to 62%, although variations may exist depending on age, life style and on the skeletal part under examination (Pocock et al., 1987; Bjørnerem et al., 2015). Yet, the same type of genetic factors operates on weight bearing and non-weight bearing bones. In fact, bone mineral density is highly influenced by heritability which explains around 60% of the total variation in bone mass (Livshits et al., 1998).

Some studies have reported some differences between Cretans and Cypriots. For example, Kranioti et al. (2017) found differences in tibial metrics for Cretans and Cypriots individuals in only two variables (maximum length and transverse diameter of the nutrient foramen) for both males and females. Along with possible sample effects, the authors suggested that the variation could be attributed to possible genetic differences between the two samples. In addition, a study on crania of Cretans, Greek-Cypriots and Turkish from Izmir showed slight differences between Cretan and Greek-Cypriots to the extent that they were merged as one group to develop ancestry estimation formulae (Kranioti personal communication).

Early and recent research suggest little admixture between other populations and modern Cretans (Coon, 1954; Hughey et al., 2013). Actually, Cretans from Heraklion and Lasithi prefecture were found to be more closely related to Minoans than to Greeks from Chios, Euboea or Laconia (Hughey et al., 2013). Nathena et al. (2015) tested mainland Greek metric standards to estimate sex on the Cretan population obtaining high errors of misclassification which could be attributed to

biological differences or sample effects. Regarding Cypriots, genetic studies have revealed that 23% of their DNA is correlated to Greek markers and 14% to Iranian markers. Yet, they seem to cluster closer to Greeks from Laconia, Chios, Euobea and Byzantine populations than from Cretans (Hellenthal et al., 2014). Heraclides et al. (2017), on the other hand, suggests that Greek-Cypriots and Turkish-Cypriots share a common pre-Ottoman paternal linage. The closest affinity between Greek-Cypriots and seventeen different populations (Europe, North Africa and Middle-East) was found for Turkish-Cypriots (27% common haplotypes), followed by Greeks, Albanians, Lebanese and Italians (ranging from 5-3%). In contradiction with Hellenthal et al. (2014), Heraclides and colleagues (2017) suggests that the closest genetic proximity between Cypriots and sub-groups of Greeks is with Cretans-Greeks which might be explained by similar migratory history between the two islands. However, this research did not explore the differences within the Cretan population (e.g. different areas from the island) and a larger sample of Cretans and Aegean islands individuals is required to verify the highlighted genetic influences between Greek-Cypriot and the Cretan populations (Heraclides et al., 2017). In addition the latter study is focusing on Y-haplotypes while the first on SNPs which may be the reason for what appear to be slightly contradicting results. Anyhow, the extent of genetic similarity of the two samples does not guarantee aetiology for the differences in the histomorphometric variables as it is not possible to explore if they are controlled by any potentially common genetic markers between the samples. This topic definitely deserves further investigation.

It seems adequate to compare environmental factors such as diet and lifestyle between the two samples as these aspects may help to explain remodelling dynamics (Richman et al., 1979; Ruff et al., 1984; Mulhern and Van Gerven, 1997; Pratte and Pfeiffer, 1999; Paine and Brenton, 2006). The Cretan diet consists of a high consumption of vegetables, whole grains, nuts, fruits, olive oil and moderate consumption of fish (Porrini, 2013). Although being reduce in the past years, the importance of agriculture in the island´s economy has implied a regular physical activity that in combination with the Mediterranean diet may have induced to low coronary disease propensity and low rates of obesity (Willett et al., 1995). The Cypriot dietary habits are also based on the traditional products of the Mediterranean diet, and thus, closely related to general Cretan eating patterns. The Mediterranean diet is one of the heathiest in the world with low rates of morbidity and mortality (Caretto and Lagattolla, 2015). In the last 50 years the inclusion of western food, however, may have resulted in a decrease in the health status in Crete (Vardavas et al., 2010). In Cyprus, dietary habits started to shift at the

beginning of the 20th century with an increment of the importation of foodstuffs (Kazamias and Panayiotou, 2015). Nutritional disorders as vitamin deficiencies or malnutrition episodes can affect remodelling resulting in lower rates than the expected (Paine and Brenton, 2006a). Besides, alcohol intake has been demonstrated to produce a considerable impact reducing bone formation rate and turnover and a high risk factor for osteoporosis (Ortner, 1970; Pratte and Pfeiffer, 1999; Iwaniec et al., 2008). For example, chronic alcoholism is not an issue in Greece but daily alcohol intake seems to be very common (Liakos et al., 1980; World Health Organization, 2014). Further research including individuals´ life story and habits would provide new insights about their impact on the observed results.

One of the means to understand the levels of physical activity among the two samples is to explore their economy. One of the most important economic activities in the island of Crete is agriculture (Chartzoulakis and Psarras, 2005). Nonetheless, at the end of the 20th century there was a noticeable decrease of production from the primary sector (agriculture) in favour of industry and energy (in second place), and the highest increase and development being observed in the contribution of Trade and Tourism activities. These changes in economy imply also a drift in occupational activities with an employment reduction from 76% to 48% in the primary sector in favour of an employment increase in industry, tourism and finances (www.crete.gov.gr). Changes in lifestyle and an increase in tourism industry have produced a reduction in physical activity and this may have had an impact on the population health. To illustrate this, Cretan farmers over 40 years old seem to have increased their body mass index (BMI) by seven points from the 1960 to 2005 (Hoffman and Gerber, 2012).

In Cyprus, the general economy of the country grew after the II World War. Agriculture has been the main economic activity with 60% of the exportation being agricultural products in early 1960 (Panagides, 1967). After the Turkish invasion and the consequent division of the Republic of Cyprus into Turkish northern area and the southern Cypriot area, the economy experienced several drawbacks resulting in a rise in unemployment (30%) and increase in poverty levels. It was in the last two decades, when the economy focused on tourism and all related sectors favouring, for example, women active participation (50% at the present to under 29% before the conflict) (Edoc.coe.int/en, 2013). Manufacturing seemed to improve during 1980 becoming the second source of employment, although poor working conditions and poor products quality would become an obstacle for future industrial development. The third economic sector (construction) also experienced a real input when tourism started being one of the main economical motors (Solsten, 1991).

Burr et al. (1990) conducted a femoral histological study between an archaeological native American population and modern samples suggesting that higher OPD values might be an indicative of higher physical activity. Whether non-weight bearing bones such as ribs could also reflect this pattern is unclear. Other factors rather than the differences in biomechanical response such as intrinsic remodelling rates and metabolic activity between different skeletal sites may influence the expression of the histomorphometric parameters (Pfeiffer, 1998; Pfeiffer et al., 2006).

Pathological conditions may cause alterations in the normal physiological appearance of bone tissue. De Boer and Van der Merwe (2016) conducted an extensive review in histological diagnosis of pathology on dry bone. The authors state that dry bone histology can be a valuable approach in combination with other diagnostic tools as the pathognomonic signs may disappear as the bone tissue dries. The histological slides used in this research were examined for sings of abnormal histomorphology that can be discerned through the methodological approach applied (De Boer, Van Der Merwe and Maat, 2013). If alterations in bone microstructures were found, the specimens were removed from the sample (see Appendix A2). However, thin cortical areas were common among the sample. In the lack of medical history, it was assumed to be part of the normal aging process rather than a pathological disorder. On the other hand, various pathologies may have not been diagnosed by the time of death of the individual. Other factors such as drug consumption, disease periods, genetic disorders or specific mechanical usage or disuse are well-known to affect remodelling rates (Frost, 1987b). Unfortunately, this could not be deduced from the material under study.

7.5. Rib histological population-specific formulae for the Mediterranean sample

The ultimate research goal of this study was the generation of rib histological age estimation method. As seen in the validation study, most of the histological aging equations tested did not perform accurately on the Mediterranean samples. Therefore, it was expected that population-specific formulae could provide better results. For this purpose, the histomorphometric parameters were regressed onto age using different datasets in order to select the models that better fit the data as assessed by prediction accuracy and goodness of fit indicators.

A total of forty-one regression models were generated using the entire dataset and sub-datasets (sexes and Cretans and Cypriots, separately) (Table 5.30-37). The rationale of such a wide range of models was to explore which parameters

could predict age more accurately on the sample/s under study. However, one needs to consider possible drawbacks in the assessment of some of the variables included (see for example OPD(F) versus osteon measurements inter-observer errors). Practical aspects of the application of the models were considered and the equations that included OPD(F) as a variable were discarded at the final stage of the analysis.

Among all the generated models, twelve were selected as the best according to measures of dispersion and goodness of fit values (Table 5.37). Several indicators as the coefficient of determination (R^2) and standard error of the estimates were assessed. These values are normally reported by histological age prediction studies in order to give the reader an indication on how well the model fits the data and what prediction interval error should be expected when estimating age through the proposed equations (Maat et al., 2006; Han et al., 2009; Goliath et al., 2016). Based on the sample size and the possibility of using other indicators equivalent to cross-validation, another methodological approach was used in this study by the incorporation of AIC_c and BIC values. These parsimony indicators helped in multi-model inference by comparison of their values (the smallest, the best). The difference between AIC_c values can be compared (smallest AIC_c minus AIC_c from remaining models) in order to rank the models generated (Burnham and Anderson, 2004). In practise, they are both important because they estimate both fit of the data and complexity of the model (Aho et al., 2014). AIC approach is based on minimizing prediction error and model overfitting or underfitting (noise or bias that will be introduced in the model if used for future predictions), while BIC indicates the correct model consistently – as it is not influenced by sample size – based on all the possible given models (Aho et al., 2014). Due to all these reasons, the mentioned parsimony indicators were chosen to test all the selection models created in the present study. However, the cross-validation approach could be further examined on the sample under study. This technique is commonly used in regression analysis, although validation set sample size and number of estimators needs to be considered to produce consistent results (Zhang and Yang, 2015). The main purpose of cross-validation techniques is to avoid overfitting of the model, and although it was assessed by the AIC indicator and it is a valid approach to assess overfitting (www.petrkeil.com), cross-validation would give specific percentages of prediction accuracy. Therefore, this statistical approach could further clarify the error expected when the formula is applied to estimate age of an unknown individual.

In real life, some practitioners might prefer a complex model that provides more anthropological information but is less accurate to a simplistic model reflecting

less biological information but performing more precisely in aging an individual. The optimal choice depends on the question that needs to be answered. An overview of the methodological approach adopted in this study can be seen in Figure 4.11.

Figure 7.7 presents a summary graph for the best twelve models selected with the values for goodness of fit indicators and inaccuracy rates as previously calculated (Lovejoy et al., 1985b). For the entire sample, *Model 13*, *15* and *25* provided very similar values with a difference in AIC_c of 5 points leading to a plausible hypothesis that all models are adequate for the given dataset (Burnham et al., 2011). Considering all the estimated values, the models that best explain the data are *Model 13* and *Model 15* which included OPD and osteon size and shape providing the lowest inaccuracy (Figure 7.7A). In the case of a less experience observer having difficulties in assessing OPD, *Model 25* is recommended as it yielded also acceptable accuracy and goodness of fit values. If the sex of the individuals is known, the use of sex specific prediction equations (*Model 29* and *Model 33*) is recommended since they provide slightly more accurate results than the general equations. The best single model for males included OPD and On.Cr, while for females *Model 33* (On.Cr and Ct.Ar) would be selected according to R^2, AIC_c and BIC values (Figure 7.7B).

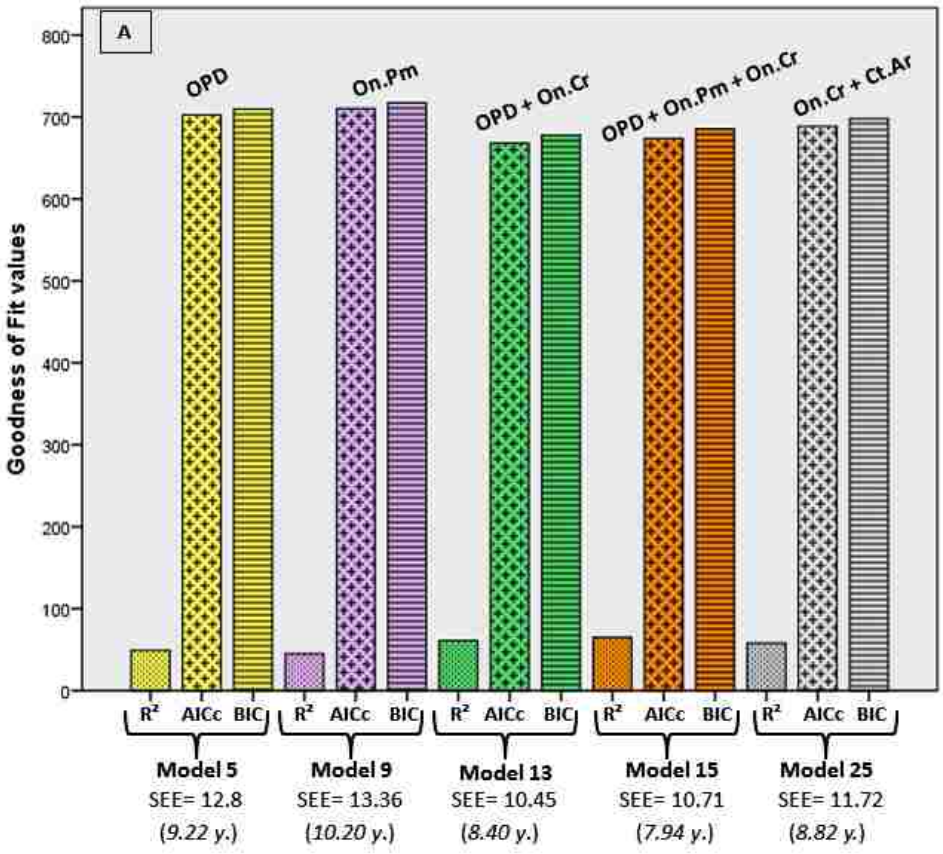

Figure 7.7 Graphs showing differences in Goodness of Fit indicators (R2, AICc, BIC) for the best selected models for the entire sample (A). SEE= standard error of the

estimated. Models inaccuracy (parenthesis; y.=years). R^2 is presented here as a percentage.

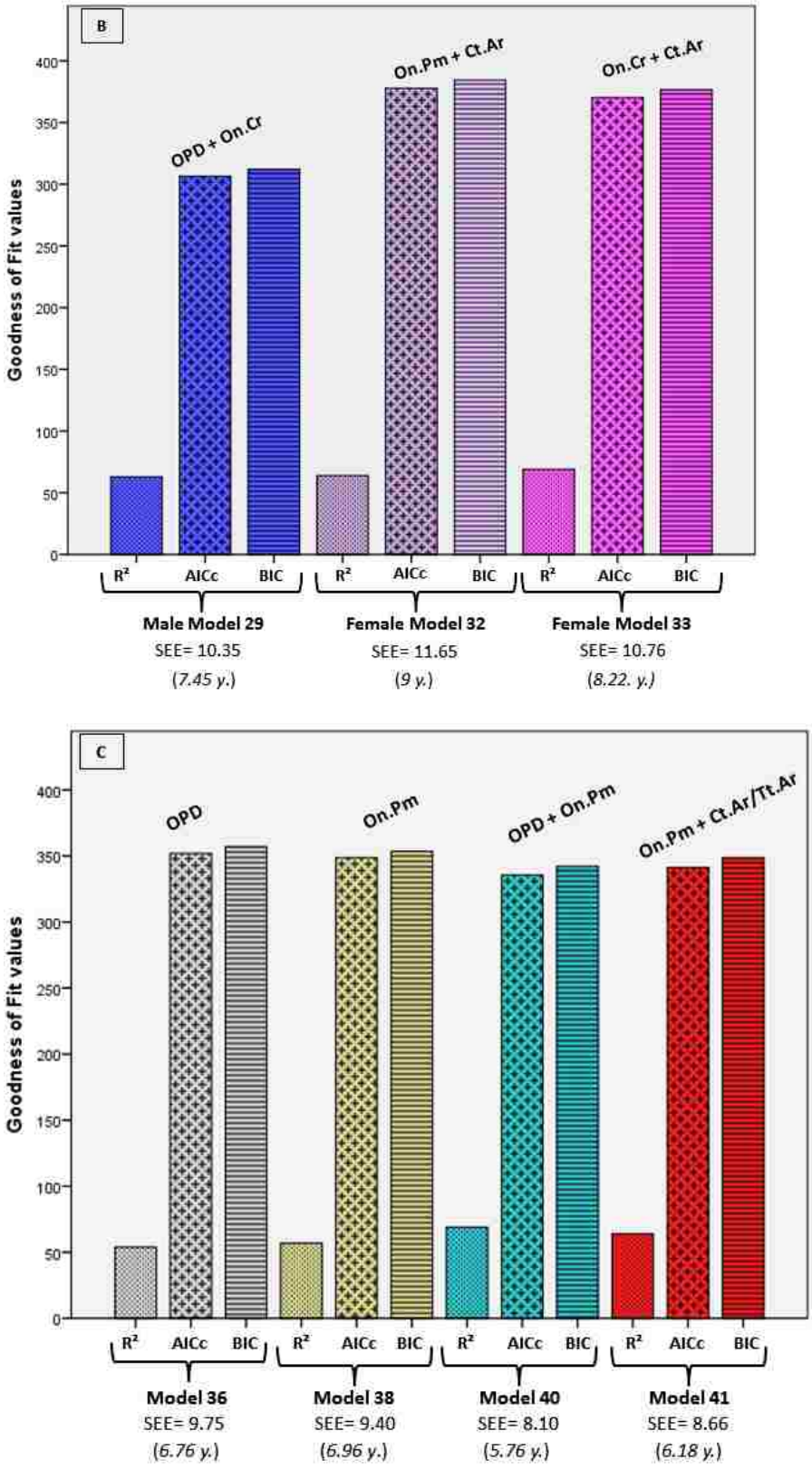

Figure 7.7. (Continued) Graph showing differences in Goodness of Fit indicators (R^2, AIC_c, BIC) for the best selected models for Males **(B)** and for Cypriots **(*C*)**.

As seen in the *Results chapter*, Cretans did not show any improvement when the Cretan sub-dataset was used for the generation of sample-specific models. On the other hand, Cypriots did produce better results. The Cypriot sample is more homogeneous that the Cretan sample due to both males and females presenting a similar mean age and thus producing lower standard errors. As seen in Figure 7.7C, OPD and On.Pm (*Model 40*) would be the most optimal choice for estimation of age in a Cypriot individual obtaining the lowest inaccuracy from all the tested models. The same principle applies here for the use of *Model 41* to avoid the assessment of osteons densities by an inexperienced anthropologist. The twelve best models reported very similar prediction and accuracy values indicating that all of them are suitable to estimate age on the sample under study. As discussed, a closer examination of inaccuracy rates along with goodness of fit values suggested that *Models 13*, *15*, *25*, *29 33*, *40* and *41* can be more appropriate (Table 7.2).

It seems relevant to remark that most of the selected models included osteon population densities and/or osteon measurements as predictors. This indicates that even if OPD is still one of the best predictors, the addition of osteon size, perimeter and shape improves considerably the prediction power of the method. These parameters are known to have negative and positive relation to age (respectively) and they are not affected by any asymptotic effect as OPD is. Hence, their inclusion in histological techniques to estimate age in old individuals is recommended (Goliath et al., 2016). On.Pm was also selected as a powerful age predictor in other studies (Watanabe et al., 1998). It is worth mentioning that the combination of osteon size and/or osteon shape and cortical area produced the best results for the female sub-sample. As discussed earlier, Ct.Ar decreases with age and sexual differences are noted with females experiencing a higher thinning in the cortex than males –more marked after menopause (Russo et al., 2006). Considering the mean age for women in the Mediterranean sample, the use of this parameter for estimating age in females seems reasonable.

Inaccuracy values have been highly improved in comparison with the results obtained from the validation pilot study. Estimated ages and know ages were tested for statistical significance and none of the p-values were over the 0.05 threshold. Estimated ages across the age span were also examined and a general pattern of overestimation for young individuals (under 40 years of age) and underestimation of oldest individuals (over 80 years of age) was observed which is a standard result of least-squares regression (Martrille et al., 2007; Nawrocki, 2010). However, when the samples were divided in under and over 60 years old age groups, an even distribution of inaccuracy and bias was seen with slightly higher values for the

younger age cohort (Table 7.2). Besides, a negative bias is observed for the oldest age cohort reflecting the underestimation of individuals over 80 years old. The lowest inaccuracy and bias was obtained for individuals from 40 to 79 years since the overall mean age of the sample falls within that age range. It is likely that future predictions will produce higher error in individuals under 40 years old due to the low number of cases included in the Mediterranean sample. A larger sample size of young individuals is required for further developed this aging method and achieve a more accurate reflection of the population.

Table 7.2 Inaccuracy and bias values for best final Models: entire sample, sexes and Cypriots sub-samples.

	Entire sample						Males		Females		Cypriots			
	Model 13		Model 15		Model 25		Model 29		Model 33		Model 40		Model 41	
	Inac	Bias	Inac	Bias	Inac	Bias	Inac	Bias	Inac	Bias	Inac	Bias	Inac	Bias
< 60	9.11	4.83	8.53	4.06	9.62	5.38	8.62	8.62	7.41	4.32	5.65	3.09	6.73	4.05
> 60	7.82	-3.85	7.47	-3.23	8.19	-4.29	6.59	-2.98	8.92	-3.65	6.03	-1.92	6.06	-2.51

Inac.= Inaccuracy

In summary, the results produced by the twelve best models are comparable to other studies using rib histomorphometry for age estimation (refer to Table 3.2). The histological parameters are used as predictors of chronological age, here understood as the length of time that the individual has lived. The biological age of the individuals (referred here as physiological age) is not perfectly associated with chronological age and this association gets less precise in elderly individuals. This phenomenon, known as the "trajectory effect" (Nawrocki 2010: 88), implies that biomechanical and physiological changes in the aging indicators undergo more alterations as the later years in the life span are approaching. These complex interactions make us expect more errors associated to samples of advance age. Even if this is the case, older individuals are now found in most of the populations and increasing in number. Hence, anthropological methods for this specific age cohorts are currently required (Ice, 2003).

7.5.1. Anthropological standards and research on the Cretan and Cypriot Collections

Extensive anthropological research on the Cretan Collection has been carried out in the last two decades. A wide range of studies have focused on the development of sex estimation population specific-standards (Kranioti et al., 2008; Kranioti and Michalodimitrakis, 2009; Osipov et al., 2013; Kranioti et al., 2014; Nathena et al., 2015; Kranioti, 2017). Others have examined the application of novel

computerised method to sort commingled remains (Tsiminikaki et al., 2017) or validated existing age estimation macroscopic methods on the Cretan Collection (Michopoulou *et al.*, 2017). In addition, age estimation methods based on rib biomechanical properties were developed from autopsy samples in Crete (Bonicelli et al., 2017).

The recent access to the Cypriot Collection has promoted research on different topics like discrete non-metric cranial trait analysis (Almeida Prado et al., 2016) or differential diagnosis of reactive arthritis on a Cypriot individual (Cawley and Paine, 2015). Sexual dimorphism on the tibia was investigated and sex population-specific standards developed for this population (Kranioti et al., 2017). Furthermore, a validation study tested reliability of existing sex estimation formulae developed from South European standards obtaining acceptable levels of accuracy for the Cypriots (García-Donas, Ekizogu, Bozdag et al., 2017).

Thereby, active research has been and is being performed in order to develop new anthropological methods, validate the existing ones and explore methodological applications. This thesis aims to be a new contribution to the mentioned investigations. The research presented here is the first exhaustive study conducted on the Cretan and Cypriot samples for age estimation through histological analysis and offered age estimation standards to assist in the creation of biological profiling and identification in future forensic cases. This contribution is especially important for the Cypriot sample since there are still around 1500 Greek-Cypriot missing individuals to be identified (www.cmp-cyprus.org).

7.6 The Mediterranean samples and other populations: histomorphometric parameters comparison

Histological studies have demonstrated different remodelling rates between and within populations, and lower reliability have been reported when a population-specific equation was applied to an independent sample (Burr et al. 1990; Stout and Lueck 1995; Crowder 2005; Cho et al. 2006; Kim et al. 2007; Pavón et al. 2010; García-Donas, School, Paine et al., 2017).

Table 7.3 summarises rib histological values from published studies and for the Mediterranean samples. Note that the qualitative comparisons are limited to the data provided by the original methods and the variables assessed in the present research. Possible intrinsic and extrinsic factors affecting bone remodelling rates have been discussed along the course of this thesis. Thus, only the relevant

information gathered from the similarities and/or differences between published data and this research will be presented here.

First, none of the communities from which the rib histological standards for age estimation were created can be considered closely related to the Mediterranean samples. Generally speaking, one could assume that American samples coming from European ancestries might reflect less genetic differentiation with the Cretan and Cypriot samples than the other populations. This would be the case for the studies conducted by Cho et al. (2002) European-Americans sample and Goliath et al. 's sample (2016) (Table 7.3). Cho et al. (2002) OPD value is relatively higher than the ones obtained by the samples under study. On the other hand, their sample accounts for a slightly higher On.Ar and a comparatively larger Ct.Ar. The Mediterranean sample is just slightly younger than Goliath et al. (2016) making the comparisons more feasible. The values suggest that OPD is considerably higher than the obtained for the Mediterranean sample but also On.Ar is noticeable smaller. Ct.Ar is not reported by this study but considering the aforementioned packing effect, a higher OPD for the European-Americans would be expected with such as small osteon size.

Observing the reported values for the histomorphometric variables regardless population affinity, the least difference in magnitude among the Mediterranean samples and the other populations was observed for the data provided by Stout et al. (1994), Stout and Lueck (1995), Pratte and Pfeiffer (1999), Muhlern (2000) and Paine and Brenton (2006). Paine and Brenton (2006) reported the lowest OPD for the Black South Africans, among all the studies under consideration (OPD= 13.50) (Table 7.3). All these populations mean age is around 40 years old except for Pratte and Pfeiffer (1999) and Paine and Brenton (2006) that are closer to the Mediterranean samples which might make comparisons between the samples more convenient.

Pratte and Pfeiffer (1999) applied two existing formulae to their South African sample – one of them Stout and Paine (1992) – obtaining a systemic underestimation of age. In addition, OPD values obtained by the target sample were lower than the ones reported for the reference samples. Along with genetic and intrinsic methodological factors, the authors attribute this outcome to the fact that part of the sample is supposed to suffer from alcoholism and/or malnutrition. This may have caused a decrease in remodelling rates, and thus, resulted in the low OPD (Pratte and Pfeiffer, 1999). Moreover, OPD and age were not statistically significantly correlated (only for males older than 50 years of age), possibly due to

the general health condition of the sample. Paine and Brenton (2006) also tested Stout and Paine (1992) method on a South African Black sample, reporting again an underestimation of the individuals´ age. Health status and dietary disorders are pointed out as the causes of a slowdown in bone turnover rates producing low osteon densities and inaccurate age estimates. However, as already mentioned, other studies demonstrated a systematic underestimation when using this particular equation with no reported or apparent health issues in their samples (Crowder, 2005; Kim et al., 2007).

Taking this under consideration, the question now remains whether pathological disorders are partly responsible for the osteonal density reported for the sample under study. Due to the lack of complete medical history, consistent reporting of medical conditions and cause of death in the medical certificates, and the absence of census data along with the fact that pathology could have gone undiagnosed at the time of death; such hypothesis cannot be tested properly. In addition, the risk of pathology bias should be similar for both samples taking into account the age range and social and cultural status. Modern collections may be biased towards specific demographics depending on cultural and social reasons (e.g. who donates the human remains and why) (DiGangi and Moore, 2013). Except for the seven autopsy samples, both samples come from cemetery populations which may represent individuals with a low-socioeconomic background resulting in poorer health and deficient diets. It is worthy to remark that individuals from both samples died between 1960 and 2003; the consequences of political conflicts such as the German invasion of Crete in the mid 40´s or the Turkish invasion of Cyprus in the mid 70´s had economic and social repercussion for the inhabitants of both islands (Edson, 1967; Papadakis et al., 2006).

Table 7.3 Histological parameters values (mean and standard deviation) for rib histological studies and the Mediterranean sample.

Author/year	Histomorphometric reported values	Demographics	
		Age	Ethnicity / other information
Stout and Paine (1992)	On.Ar = 0.039 Ct.Ar = 22.36	28.6 (SD ± 12.9)	Mostly American whites
Stout et al. (1994)	OPD = 16.01 (SEM ± 0.73)	38.51	Iscan et al. (1984a; 1984b) sample
Stout and Lueck (1995)	OPD = 18.8 (SEM ± 1.07)	34.9 (± 3.09)	Modern sample from Stout and Paine (1992) sample
Pratte and Pfeiffer (1999)	OPD = 15 ± 3.26 Ct.Ar= 18.10 ± 5.03	62 (range 24-95)	South Africans-Cape Town (black, white and coloured), possible pathology
Mulhern (2000)*	OPD = 14.24 (SEM ± 0.07)	15-50	Nubian
Cho et al. (2002)	OPD = 18.70 (SEM ± 0.71) On.Ar = 0.039 (SEM ± 0.001) Ct.Ar = 21.43 (SEM ± 0.73) Ct.Ar/Tt.Ar = 0.343 (SEM ± 0.023)	38.18 (SEM ± 2.97)	European-Americans; includes Stout and Paine (1992) sample
	OPD = 20.10 (SEM ± 0.97) On.Ar = 0.036 (SEM ± 0.001) Ct.Ar = 20.92 (SEM ± 0.75) Ct.Ar/Tt.Ar = 0.350 (SEM ± 0.015)	50.69 (SEM ± 2.27)	African-American
Paine and Brenton (2006)	OPD = 13.54	50.20	Dart Collection, South Africa; 38% died from pellagra
Kim et al. (2007)	OPD = 21.60 ± 6.58 On.Ar = 0.021 ± 0.005 Ct.Ar/Tt.Ar = 0.333 ± 0.088	Males: 44.8 (± 11.7) Females: 38.6 ± 11.1)	Koreans
Pavón et al. (2010)	OPD = 28.76 ± 6.48 On.Ar = 0.03 ± 0.007 Ct.Ar = 18.07 ± 4.83 Ct.Ar/Tt.Ar = 0.35 ± 0.10	43.8 (range 20-87)	Mayan population; mostly males
Goliath et al. (2016)	OPD = 23.52 ± 5.93 On.Ar = 0.024 ± 0.009 On.Cr = 0.905 ± 0.014	62.96 ± 10.21	European-Americans; 52% died from cancer
Pfeiffer et al. (2016)	OPD = 19.90 ± 5.30 On.Ar = 0.034 ± 0.008 Ct.Ar/Tt.Ar = 0.38 ± 0.011	47.96 ± 15.70	South Africans (Cape Town: black, white and coloured)
Sample under study	OPD = 15.44 ± 4.35 On.Ar = 0.032 ± 0.009 On.Cr= 0.910 ± 0.021 Ct.Ar = 19.21 ± 7.97 Ct.Ar/Tt.Ar = 0.319 ± 0.121	All: 60.33 ± 17.89	Mediterranean samples (Cretans and Cypriots)
	OPD = 14.50 ± 4.49 On.Ar = 0.030 ± 0.010 On.Cr = 0.906 ± 0.023 Ct.Ar = 17.74 ± 7.63 Ct.Ar/Tt.Ar = 0.316 ± 0.132	Cretans: 57.50 ± 21.17	
	OPD = 16.26 ± 4.09 On.Ar = 0.033 ± 0.009 On.Cr = 0.913 ± 0.019 Ct.Ar = 20.49 ± 8.13 Ct.Ar/Tt.Ar = 0.326 ± 0.113	Cypriots: 62.81 ± 14.20	

N/A=not available, SEM= standard error of the mean, * Archaeological sample.

Assuming that, to some extent, dietary disorders might have be the cause of the low OPD, it could be presumed that both Cretans and Cypriots would suffer from this nutritional deficiency as they share the same dietary habits.

Heinrich (2015) examined nutritional and physiological stress differences in rib cortical bone microstructure on a sample of heterogeneous origins (Canada, Unites States and South Africans). Comparing low and high stress males groups, a lower OPD(I) and OPD was observed for the group suffering from chronic nutritional and physiological stress. Moreover, a negative shift is reported for OPD(I). Nonetheless, male OPD(I) and OPD did show a similar rate of change throughout age. This suggests that even if values were lower between the male sub-groups, nutritional and physiological stress does not alter dramatically bone modelling and remodelling rates during adulthood. The author proposed that the mentioned histological differences might be a reflection of nutritional and physiological stress delaying growth spurt and peak bone mass during adolescence producing a relatively younger mean age tissue that the healthy individuals. Consequently, no stress effect on the remodelling rates and age is seen in the later years of life. Additionally, no differences for any of the OPDs were found for low and high stress females groups indicating that female may respond differently to chronic nutritional and physiological stress due to an earlier timing of puberty and lower growth rate during adolescence (Heinrich, 2015).

Table 7.4 Comparison of Heinrich (2015) high nutritional and physiological stress samples with the Mediterranean sample.

	Age		OPD(I)		OPD(F)		OPD		On.Ar		Ct.Ar	
	Mean	SD	Mean	SD	Mean	SD	Mean	SD	Mean	SD	Mean	SD
M*	45.86	16.79	9.95	1.99	6.43	2.71	16.37	4.17	0.041	0.010	26.09	7.32
M	60.10	16.52	9.40	2.02	6.10	2.66	15.74	4.08	0.032	0.009	21.16	8.63
F*	45.38	15.67	11.03	1.97	6.91	2.85	17.94	4.36	0.040	0.001	25.36	5.91
F	60.52	19.11	8.98	2.40	6.43	2.74	15.42	4.60	0.031	0.010	17.59	7.06

M=Male, F=Female, Grey coloured= Heinrich (2015) values; SD= standard deviation

Table 7.4 summarises the values between sexes for the high nutritional and physiological stress sample and for the Mediterranean sample. The values obtained for OPD(I), OPD(F) and OPD are very similar between Mediterranean males and Heinrich males (2015), but slightly different values are observed for females particularly for OPD(I), and OPD. This outcome might reflect post-menopausal age-related alterations on bone turnover and thinning of cortical area (notice mean age and Ct.Ar differences for the samples) (Feng and McDonald, 2011). Mediterranean females over the post-menopausal window (N = 35, Mean age = 69) produced an

OPD(I) of 9.5 and a OPD(F) of 7.65 (OPD = 17.10). When compared to healthy individuals, postmenopausal females with symptomatic osteoporosis showed rather small osteon size, a reduced average number of intact osteons and an increase average of fragmentary osteons; moreover, bone formation rates fell below expected (Wu et al., 1970). A different pattern in the observation of osteon frequency number was seen for both sexes and samples which could be indicative of age related resorption-formation imbalance resulting in osteoporosis for both sexes and increased in women due to postmenopause (refer to Figure 7.5). According to Thompson (1980), intracortical porosity in men is attributed to higher number of osteons whilst in females is due to larger Haversian canals. Influences of the samples when comparing the sexes and vice versa could hide the within sub-samples variability. A more quantitative approach such as Haversian canal measurements should be performed to test this hypothesis (De Boer and Van der Merwe, 2016).

While considering other pathological conditions in the Mediterranean sample, a pilot study conducted by the author and colleagues on Cretans and Cypriots individuals demonstrated that healthy individuals and individuals affected by chronic metabolic diseases produced different results for osteons densities (Lill et al., 2017). OPD obtained by the metabolically affected sub-group did not show any correlation to age while the healthy sub-group did produce a positive statistical significant association. This is consistent with the Pratte and Pfeiffer (1999) results. For the Mediterranean sample under study, osteon population densities demonstrated a positive moderate to strong correlation to age in accordance with the healthy individuals trend (Lill et al., 2017).

At this stage, it seems reasonable to find another potential factors contributing to the OPD value reported by this research. Stout and Lueck (1995) stated that different effective age of adult compacta may provoke differences in OPD values. This would imply that skeletal maturity has been reached at an earlier or later age; thus, the mean tissue age would present higher or lower osteons population densities, respectively, since it had more or less time to accumulate in the cortex (Frost, 1987a; 1987b). The effective birth of age of rib adult compacta is estimated to occur around 12.5 years old (Wu et al., 1970). Mechanical usage during growth, genetics, sex, nutrition, activity levels and skeletal site – among others –are possible factors impacting the age at which the adult cortex would be complete (Wu et al., 1970; Burr et al., 1990; Robling and Stout, 2008; Cho and Stout, 2011).

Growth and maturation rates differ between sexes and between populations (Crowder and Austin, 2005; O'Connor et al., 2008). Multiple factors that incorporate genetic and environmental influences play a significant role on skeletal maturation. For example, a delay of almost 2 years was observed in children from low socio-economic status and poor nutrition (Frisancho et al., 1970). Genetic inputs, however, seems to be crucial: an earlier maturation in Bosnian than in American adolescents was seen despite the adverse living circumstances of the former due to political conflicts (Schaefer and Black, 2005). Whether skeletal growth is different in the Mediterranean samples, and therefore, a more prolonged duration and slower rate of cortical drifts resulted in an older effective age of adult compacta and lower osteon densities needs to be further explored.

Supporting inter-population variation, several facts can be drawn to attention from the data gathered in Table 7.3. The OPD asymptotic value is reached when osteonal bone occupies the entire cortex and previous evidence of osteonal structures are removed (Frost, 1987b). The highest OPD value for the entire Mediterranean sample is reported to be 25.63 (On.Ar = 0.025) for the 100-year-old female individual. The highest OPD value for Pavón et al. (2010) is 43.05 (On.Ar = 0.033) for the second oldest individual in their sample (84 years old). None of the OPD values from the sample used by Goliath et al. (2016) exceeds the average value of 30 with the exception of an outlier reporting an OPD of 42.30. Overall, the asymptotic value for OPD was different between the populations. Again this may be a subject of sample variation or could be attributed to the removal of outliers which is a common strategy in many studies (Stout et al., 1994; Lynneru et al., 2006; Crowder, 2013).

Further population differences can be discerned from Kim et al. (2007) and Pavón et al. (2010) studies which have same age and sex distribution but differ in ethnic origin. The mean OPD for Korean males is 23.82 (± 6.56) with a mean On.Ar of 0.019 mm^2, while the Mayan males present an OPD of 28.76 (± 6.48) with a mean On.Ar of 0.03 mm^2. Comparisons between Mayans and African-Americans result in larger differences yet, demographics are also slightly different (Cho et al., 2002).

At this stage the author would like to make the last remarks. Firstly, some individuals in the sample showed lamellar bone at ages in which this type of bone tissue should have been replaced by secondary osteonal bone (Figure 7.8). Whether this is a physiological trend in the samples under study or the expression of some kind of disorder needs further examination. Secondly, only 25% of the

individuals are under 50 years old in the Mediterranean sample. Remodelling seems to experience a decrease around the seventh decade (Allen and Burr, 2013). Considering that the asymptotic effect will remove past-remodelling events in ribs around 50-60 years of age, a lower OPD, at least to some extent, should be expected as a result of the asymptotic bias. Nevertheless, cortical area does not change in a perfect linear proportion to the increment of age introducing additional variability to the parameter.

Based on the data obtained from the published studies and the present research, interesting patterns were seen for osteonal remodelling between the samples. Genetics partly determine bone mass, density and bone turnover (Schnitzler, 1993; Cho et al., 2006). An interaction between genetic influences and environmental factors during growth and development is also crucial for bone material and functional properties later in adulthood. Other factors such as age, sex, hormones, metabolic and genetic disorders, mechanical usage or disuse, nutrition and regional trauma are known to play a direct or indirect role in osteonal remodelling (Frost, 1987b). Exhaustive measurements of bone formation rates and activation frequencies from different and heterogeneous populations are required to provide more insight from the findings obtained from this research and the other histological studies.

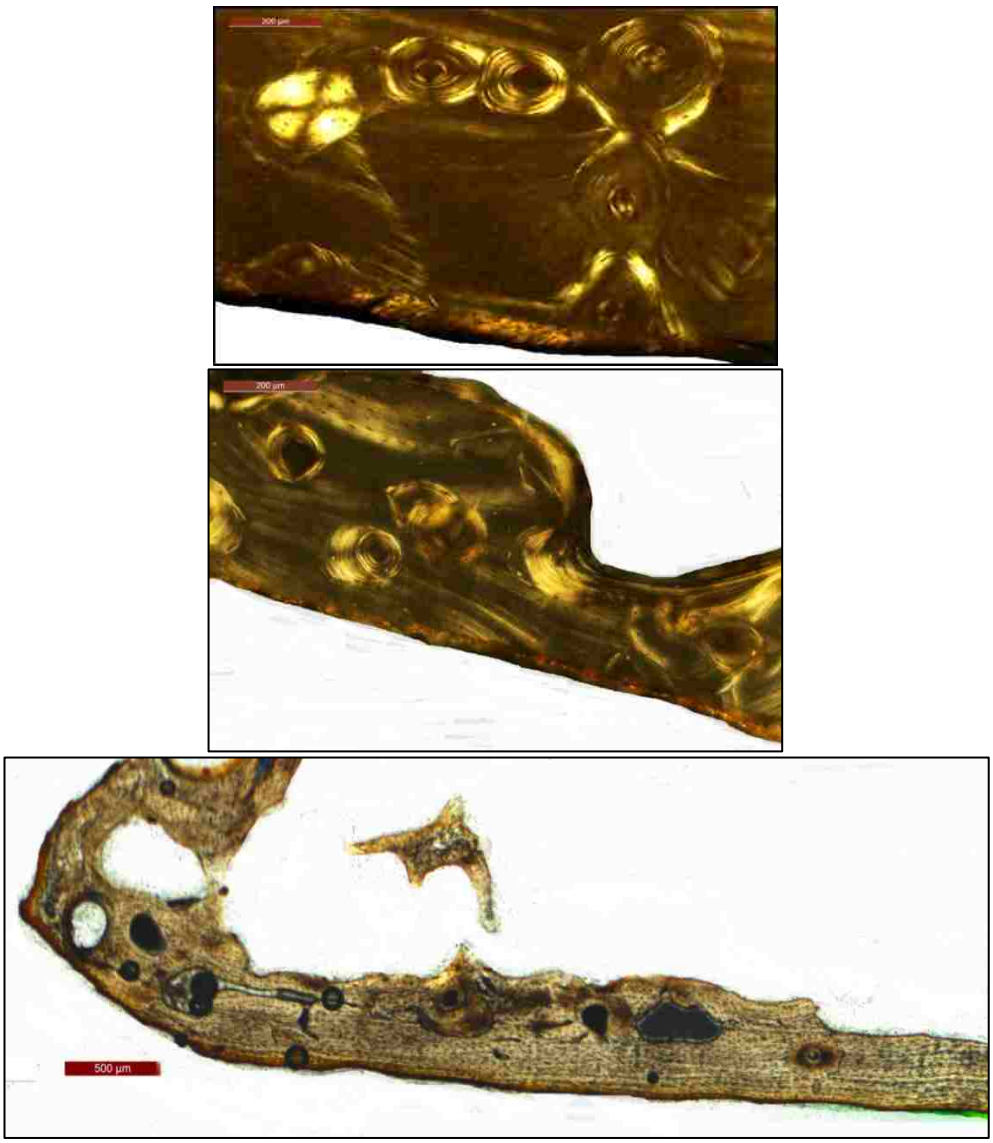

Figure 7.8 Examples of ribs from the sample showing lamellar bone: Cypriot female 48 years old (top left) and Cretan female 98 years old (top right) (semipolarised 10x); Cypriot female 56 years old (bottom) (40x).

7.7. Revised technique for the preparation of dry bone thin-sections

In microscopic studies, appropriate data collection relies on the quality of the thin-sections. Over the years, methods addressing the production of histological slides have been developed that attempt to improve the state of art (Chinsamy and Raath, 1992; Beauchesne and Saunders, 2006; Paine, 2007; De Boer, Aarents, Maat et al., 2013). The technique proposed here is a combination of existing methods (Caropreso et al., 2000; Tiesler et al., 2006; Paine, 2007), and it was developed based on the type of bone used, the equipment and consumables available at the histology laboratory and the research question. This revised methods is equivalent to other published studies since it produced the same high-quality thin-sections (Paine, 2007; Crowder et al., 2012). However, the number of

steps required and the amount of consumables needed has been reduced improving time efficiency and decreasing costs. There is still need to test the technique on other types of bone such as femora where a higher porosity and a large cross-sectional area of cortical bone may cause technical issues when using the glass slide or the resin applied for ribs (García-Donas, Dalton, Chaplin et al., 2017).

7.8. Conclusions

Estimation of age is a critical step in the identification process of unknown human remains. Several anthropological age estimation techniques are available for the expert and the choice of the methods depends on the skeletal element, the preservation of the bone and the equipment available. When laboratory facilities and equipment are available, microscopic methods can be successfully conducted for age estimation since they have shown similar levels of accuracy as the traditional macroscopic approach (Garvin et al., 2012). Some occasions laboratory based methods have been considered more reliable (Bonicelli et al., 2017). Yet, several limitations regarding their application may be an obstacle in the routine use of histological analysis.

Firstly, the method itself requires specific equipment and training for the preparation of the thin-sections and for the interpretation of the variables. This implies an impediment when compare to the relatively easy and inexpensive gross-examination of morphological age indicators. Regarding histological variable selection, caution is warranted in interpreting specific parameters due to high levels of inter-observer error being reported (Lynnerup et al., 1998). Henceforth, other types of approaches introducing technological innovations for data collection should be investigated (Cooper et al., 2007; Rose et al., 2012) and the incorporation of variables expressing more precise relation to age should be tested (Bonicelli et al., 2017). Secondly, some bias might be introduced due to intrinsic and extrinsic factors affecting in different degrees the skeletal elements and the topographical locations within the same bone (Pfeiffer et al., 1995). Thirdly, histological age estimation relies on the fact that remodelling events accumulate in the cortex throughout one´s life and can be assessed through quantitative analysis. However, sex and inter-population differences could be expected since bone remodelling rates variability have been shown (Cho et al., 2006; Abdullah et al., 2016). As a consequence, aging methods should be scrutinised and continuously updated by validating existing equations on target samples to ensure accurate age estimates (Stout and Gehlert, 1980; Crowder, 2005). Ultimately, as different patterns in bone turnover between and within samples may have an impact on the age estimation methods, the

development of population-specific standards is recommended to reliably estimate age (Cho et al., 2002; Kim et al., 2007; Pavón et al., 2010).

Forensic anthropology is an interdisciplinary field. Generally, the methods developed from physical anthropology are shared by both osteo-archaeological and forensic experts. It is obvious that in both fields high accuracy in age estimation is sought. However, the final target in a medicolegal investigation does concern the positive identification of a particular individual and standardised peer-reviewed methodologies with known error rates are demanded in court to assure consistency and reliability (Christensen and Crowder, 2009). In general, histological methods are suitable for age estimation in adults from modern human remains and historic and archaeological assemblages accounting for standard error of the estimate within 5-12 years and fulfilling the above mentioned court requirements (Ritz-Timme et al., 2000; Rösing et al., 2007).

The aging method developed in this research may help forensic experts dealing with the identification of unknown skeletal remains. The proposed aging equations can be applied depending on the available information about the unknown individual (sex and/or ethnic affiliation) in future forensic cases in Crete and in Cyprus. After the invasion of Cyprus in 1974, positive identification of exhumed skeletons became crucial since there are more than a thousand individuals that have yet to be identified, according to the Committee of Missing Persons (www.cmp-cyprus.org). As with the recent immigration events in Italy, Greece and other Mediterranean countries, the large number of deaths related to this transnational tragedy requires methods for identifying individuals from these communities. Understanding the identification parameters (age determination and sex identification) specific for the local Mediterranean populations is a starting point for this assessment.

Summarising, the following conclusions have been reached amending the research questions presented along the course of this thesis:

• Inter-observer errors present different levels of repeatability and agreement. It should be considered when assessing specific histomorphometric parameters regardless the experience of the observer. Moderate to high agreement between observers is reported for most of the parameters used in this research suggesting that repeatability standards were achieved. Most of the studies published (e.g. Cho et al., 2002) did not explore intra and inter-observer errors, and thus, this thesis presents an exhaustive examination not only of the variables themselves but also of the practical application of the method.

• Sampling location showed no major variability for OPD for the six sampling sites along the length of the rib. This suggests that sampling site has no major effect in age estimation methods. A larger and more heterogeneous sample is required to verify this preliminary observation. The inclusion of other parameters as osteon measurements will help to better understand intra-rib variability. The contribution of rib sampling location in relation to age estimation was explored in this study contributing to future applications of the histological methods considering the fragmented nature of costal elements.

• The existing methods applied to estimate age at death on the Mediterranean samples demonstrated that Stout and Paine (1992), Stout et al. (1994) and Cho et al. (2002) aging equation did not perform accurately on the Mediterranean sample producing a systemic underestimation of the individuals. For these three aging techniques, a substantial increase in inaccuracy and bias rates was noticed for individuals over 60 years. This fact might be related to the rib cortex reaching OPD asymptote at this age. Different age and sex distribution between the reference and the target sample, inter-population remodelling rates variability and methodological issues were also considered as factors affecting the poor accuracy. Goliath et al. (2016) produced the best performance although overestimation of young individuals was detected. These results demonstrated the necessity of population-specific formulae showing the error that can be introduced if one method developed from a reference sample is used to estimate age on a not related target sample.

• When examining the relationship between the histological parameters and age, differences in the histomorphometric variables showed interesting patterns when sexes and samples were compared. Conclusions are limited to the fact that sub-groups could not be separated due to the small sample size. Further investigation of this matter is required to verify whether remodelling rates actually differ between and within the sub-groups.

• Population-specific formulae were developed for the entire dataset, sub-datasets separated by sexes (males and females) and sub-datasets separated by samples (Cretans and Cypriots). Through model inference a final set of twelve models was selected based on prediction power, model fit and overall accuracy. The standard error of the estimate ranged from 8 to 13 years and R^2 varied from 0.45 to 0.69 which is in accordance with other histological studies. The formulae generated in this thesis had made a contribution to the development of population-specific standards for Mediterranean samples offering the possibility of their application in future forensic cases.

• Differences in the mean OPD values and other histomorphometric variables were reported between the Mediterranean sample and other populations. The differences could be a function of genetic, environmental, socioeconomic, nutritional and pathological factors (or any combination of them) and sample variation and the obtained results provided new information about remodelling processes in the samples under study. Yet, the current dataset was limiting in exploring these factors further.

Future research to be conducted:

• The method has still difficult application due to both the ambiguity of description of some variables and the means of data collection. Further improvement of the technique through computerised methods should be investigated.

• A larger sample is required to verify the differences between sexes and samples, and to further examine the accuracy and reliability of the generated models. Ideally, the inclusion of young individuals will help to better cover the full spectrum of the population and validate the obtained results.

• The use of other skeletal elements that were proven to be suitable for histological age estimation such as the femur is recommended to obtain a full picture of remodelling rates between bones and within individuals.

• Multifactorial approach could improve the accuracy rates obtained in the present research. The assessment of age changes on the sternal end may increase the prediction power of the method (Stout et al., 1994).

• As George Box said: Essentially, all models are wrong but some are useful. Other statistical approaches such as Bayesian statistics should be explored to prevent the under and overestimation produced by regression analysis.

Bibliography

Abbott, S., Trinkaus, E. and Burr, D. B. (1996) 'Dynamic bone remodeling in Later Pleistocene fossil hominids', *American Journal of Physical Anthropology*, 99(4), pp. 585–601. doi: 10.1002/(SICI)1096-8644(199604)99:4<585::AID-AJPA5>3.0.CO;2-T.

Abdullah, H., Nor, M. and Abdul Jamil, M. (2016) 'Human Bone Histomorphological Pattern Differences Between Genders: A Review', in Ibrahim, F., Usman, J., Mohktar, M., and Ahmad, M. (eds) *International Conference for Innovation in Biomedical Engineering and Life Sciences*. Springer, pp. 183–187. doi: 10.1007/978-981-10-0266-3.

Absolonova, K., Veleminsky, P., Dobisikova, M., Beran, M. and Zocova, J. (2013) 'Histological Estimation of Age at Death from the Compact Bone of Burned and Unburned Human Ribs', *Journal of Forensic Sciences*, 58(SUPPL.1), pp. 135–145. doi: 10.1111/j.1556-4029.2012.02303.x.

Adamopoulos, I. E. and Mellins, E. D. (2014) 'Alternative pathways of osteoclastogenesis in inflammatory arthritis', *Nature Reviews Rheumatology*, 11(3), pp. 189–194. doi: 10.1038/nrrheum.2014.198.

Agnew, A. M. (2006) *Histomorphological aging of subadults: A test of Streeter's method on a medieval archaeological population*. The Ohio State University.

Agnew, A. M. and Stout, S. D. (2012) 'Brief communication: Reevaluating osteoporosis in human ribs: The role of intracortical porosity', *American Journal of Physical Anthropology*, 148(3), pp. 462–466. doi: 10.1002/ajpa.22048.

Ahlborg, H., Johnell, O., Turner, C., Rannevik, G. and Karlsson, M. (2003) 'Bone loss and bone size after menopause', *The New England Journal of Medicine*, 349(4), pp. 327–334.

Ahlqvist, J. and Damsten, O. (1969) 'A modification of Kerley´s Method for the microscopic determination of age in human bone', *Journal of Forensic Sciences*, 14(2), pp. 205–212.

Aho, K., DerryBerry, D. and Peterson, T. (2014) 'Model selection for ecologists: the worldviews of AIC and BIC', *Ecology*, (95), pp. 631–636.

Aiello, L. C. and Molleson, T. (1993) 'Are microscopic ageing techniques more accurate than macroscopic ageing techniques?', *Journal of Archaeological Science*, pp. 689–704. doi: 10.1006/jasc.1993.1043.

Akaike, H. (1973) 'Information theory and an extension of the maximum likelihood principle', in Petrov, B. and Caski, S. (eds) *Proceedings of the Second International Symposium on Information Theory*. Budapest, Hungary: Akademiai Kaido, pp. 267–281.

Allen, M. R. and Burr, D. B. (2013) 'Bone modeling and remodeling', in Burr, D. B. and Allen, M. R. (eds) *Basic and applied bone biology*. London: Academic Press, pp. 75–90. doi: 10.1016/B978-0-12-416015-6.00004-6.

Almeida Prado, P. S., Garcia-Donas, J. G., Langstaff, H., Cunha, E., Kyriakou, P. and Kranioti, E. F. (2016) 'Os parietale partitum: Exploring the prevalence of this trait in four contemporary populations', *Journal of Comparative Human Biology*, 67(4), pp. 261–272. doi: 10.1016/j.jchb.2016.04.001.

Anderson, J. and Pollitzer, W. (1994) 'Ethnic and genetic differences in susceptibility osteoporotic fractures', in Draper, H. H. (ed.) *Nutrition and Osteoporosis. Advances in Nutritional Research*. Boston: Springer, pp. 129–149.

Andriacchi, T., Schultz, A., Belytschko, T. and Galante, J. (1974) 'A model for studies of mechanical interactions between the human spine and rib cage.', *Journal of Biomechanics*, 7(6), pp. 497–507. doi: 10.1016/0021-9290(74)90084-0.

Angastinioti, E. and Hutchins-Wiese, H. (2016) 'Perception of and Adherence to a Mediterranean Diet In Cyprus and the United States', *Journal of the Academy of Nutrition and Dietetics*, 116(9), p. A88. doi: 10.1016/j.jand.2016.06.318.

Atkins, G. J. and Findlay, D. M. (2012) 'Osteocyte regulation of bone mineral: A little give and take', *Osteoporosis International*, 23(8), pp. 2067–2079. doi: 10.1007/s00198-012-1915-z.

Aubin, J. and Triffitt, J. (2008) 'Mesenchymal stem cells and osteoblast differentiation', in Bilezikian, J., Lawrence, G., and Martin, T. (eds) *Principles of bone biology*. 3rd edn. U.S.A.: Academic Press, pp. 85–107. doi: http://dx.doi.org/10.1016/B978-0-12-373884-4.00026-4.

Augat, P. and Schorlemmer, S. (2006) 'The role of cortical bone and its microstructure in bone strength', *Age and Ageing*, 35(SUPPL.2), pp. 27–31. doi: 10.1093/ageing/afl081.

Aykroyd, R. G. and Lucy, D. (1997) 'Technical note: regression analysis in adult age estimation', *American Journal of Physical Anthropology*, 104, pp. 259–265.

Barer, M. and Jowsey, J. (1967) 'Bone formation and resorption in normal human rib: A study of persons from 11 to 88 years of age', *Clinical Orthopaedics and Related Research*, 52, pp. 241–247.

Barnhart, H. X. and Barboriak, D. P. (2009) 'Applications of the repeatability of quantitative imaging biomarkers : A review of statistical analysis of repeat data sets', *Translational Oncology*, 2(4), pp. 231–235. doi: 10.1593/tlo.09268.

Baron, J., Barrett, J., Malenka, D., Fisher, E., Kniffin, W., Bubolz, T. and Tosteson, T. (1994) 'Racial differences in fracture risk', *Osteoporosis International*, (5), pp. 42–47.

Bastir, M., García Martínez, D., Recheis, W., Barash, A., Coquerelle, M., Rios, L., Peña-Melián, A., García Río, F. and O'Higgins, P. (2013) 'Differential growth and development of the upper and lower human thorax', *PLoS ONE*, 8(9), pp. 1–13. doi: 10.1371/journal.pone.0075128.

Beauchesne, P. and Saunders, S. (2006) 'A test of the revised Frost's "rapid manual method" for the preparation of bone thin sections', *International Journal of Osteoarchaeology*, 16(1), pp. 82–87. doi: 10.1002/oa.804.

Bednarek, J., Awska, E. B., Engelgardt, P. and Wolska, E. (2009) 'Validity of histomorphometric rib assessment for age at death prediction', *Problems of Forensic Sciences*, LXXX, pp. 403–410.

Bell, K. (1988) 'Cellular mechanisms', *American Journal of Medicine*, (84), pp. 275–282.

Bell, L. (2012) 'Histotaphonomy', in Crowder, C. and Stout, S. (eds) *Bone Histology: An anthropological perspective*. U.S.A.: CRC Press, pp. 241–252.

Bellido, T., Plotkin, L. I. and Bruzzaniti, A. (2013) 'Bone cells', in Burr, D. B. and Allen, M. R. (eds) *Basic and applied bone biology*. London: Academic Press, pp. 27–45. doi: 10.1016/B978-0-12-416015-6.00002-2.

Bjørnerem, A., Bui, M., Wang, X., Ghasem-Zadeh, A., Hopper, J., Zebaze, R. and Seeman, E. (2015) 'Genetic and environmental variances of bone microarchitecture and bone

remodeling markers: a twin study', *Journal of Bone and Mineral Research*, 30(3), pp. 519–527. doi: 10.1002/jbmr.2365.

Bland, J. M. and Altman, D. (1995) 'Comparing methods of measurement: why plotting difference against standard method is misleading', *Lancet*, (346), pp. 1085–1087.

Bland, J. M. and Altman, D. G. (1986) 'Statistical methods for assessing agreement between two methods of clinical measurement', *Lancet*, (8476), pp. 307–310.

Blatch, S. N. (2012) *Histomorphometric Differences in Tibial Cortical Bone Based on Sampling Location*. Stony Brook University.

Bonewald, L. F. (2011) 'The amazing osteocyte', *Journal of Bone and Mineral Research*, 26(2), pp. 229–238. doi: 10.1002/jbmr.320.

Bonicelli, A., Xhemali, B., Kranioti, E. F. and Zioupos, P. (2017) 'Rib biomechanical properties exhibit diagnostic potential for accurate ageing in forensic investigations', *PLoS ONE*, 12(5). doi: 10.1371/journal.pone.0176785.

Boskey, A. (2001) 'Bone Mineralization', in Cowin, S. (ed.) *Bone Mechanics: Handbook*. 2nd edn. Boca Ratón: CRC Press, p. 5.1-5.13.

Bouvier, M. and Ubelaker, D. H. (1977) 'A comparison of two methods for the microscopic determination of age at death.', *American Journal of Physical Anthropology*, 46, pp. 391–4. doi: 10.1002/ajpa.1330460303.

Brenton, B. P. and Paine, R. R. (2007) 'Reevaluating the health and nutritional status of maize-dependent populations: evidence for the impact of pellagra on human skeletons from South Africa'', *Ecology of Food and Nutrition*, 46(5–6), pp. 345–360. doi: 10.1080/03670240701486545.

Brickley, M. and Ives, R. (2008) *The Bioarchaeology of Metabolic Bone Disease*. 1st edn. Hungary: Academic Press.

Britz, H. M., Thomas, C. D. L., Clement, J. G. and Cooper, D. M. L. (2009) 'The relation of femoral osteon geometry to age, sex, height and weight', *Bone*, 45(1), pp. 77–83. doi: 10.1016/j.bone.2009.03.654.

Broman, G. E., Trotter, M. and Peterson, R. R. (1958) 'The density of selected bones of the human skeleton', *American Journal of Physical Anthropology*, 16(2), pp. 197–211. doi: 10.1002/ajpa.1330160205.

Buckberry, J. L. and Chamberlain, A. T. (2002) 'Age estimation from the auricular surface of the ilium: A revised method', *American Journal of Physical Anthropology*, 119(3), pp. 231–239. doi: 10.1002/ajpa.10130.

Burger, E. H. and Klein-Nulend, J. (1999) 'Mechanotransduction in bone - role of the lacuno-canalicular network', *The FASEB Journal*, 13(9001), pp. S101–S112.

Burnham, K. P. and Anderson, D. (2002) *Model Selection and Multimodel Inference. A practical Information-Theoretical approach*. 2nd edn. Springer US.

Burnham, K. P. and Anderson, D. R. (2004) 'Multimodel inference', *Sociological Methods & Research*, 33(2), pp. 261–304. doi: 10.1177/0049124104268644.

Burnham, K. P., Anderson, D. R. and Huyvaert, K. P. (2011) 'AIC model selection and multimodel inference in behavioral ecology : some background , observations , and

comparisons', *Behavioral Ecology and Sociobiology*, (65), pp. 23–35. doi: 10.1007/s00265-010-1029-6.

Burr, D. B. (2002) 'Targeted and nontargeted remodeling', *Bone*, 30(1), pp. 2–4. doi: 10.1016/S8756-3282(01)00619-6.

Burr, D. B. and Akkus, O. (2013) *Bone morphology and organization*, *Basic and applied bone biology*. Edited by D. B. Burr and M. R. Allen. Academic Press. doi: 10.1016/B978-0-12-416015-6.00001-0.

Burr, D. B., Ruff, C. B. and Thompson, D. D. (1990) 'Patterns of skeletal histologic change through time: Comparison of an archaic native american population with modern populations', *The Anatomical Record*, 226(3), pp. 307–313. doi: 10.1002/ar.1092260306.

Burr, D. B., Schaffler, M. B. and Frederickson, R. G. (1988) 'Composition of the cement line and its possible mechanical role as a local interface in human compact bone', *Journal of Biomechanics*, 21(11), pp. 939–945.

Byers, S. (2011) *Introduction to Forensic Anthropology: A textbook*. 4th edn. New York: Routledge.

Cannet, C., Baraybar, J. P., Kolopp, M., Meyer, P. and Ludes, B. (2011) 'Histomorphometric estimation of age in paraffin-embedded ribs: A feasibility study', *International Journal of Legal Medicine*, 125(4), pp. 493–502. doi: 10.1007/s00414-010-0444-6.

Cappella, A., Cummaudo, M., Arrigoni, E., Collini, F. and Cattaneo, C. (2017) 'The issue of age estimation in a modern skeletal population: are even the more modern current aging methods satisfactory for the elderly', *Journal of Forensic Sciences*, 62(1), pp. 12–17. doi: 10.1111/1556-4029.13220.

Caretto, A. and Lagattolla, V. (2015) 'Non-communicable diseases and adherence to Mediterranean diet', *Endocrine, Metabolic and Inmune disorder drug tagets*, 15(1), pp. 10–17.

Caropreso, S., Bondioli, L., Capannolo, D., Cerroni, L., Macchiarelli, R. and Condò, S. G. (2000) 'Thin sections for hard tissue histology: A new procedure', *Journal of Microscopy*, 199(3), pp. 244–247. doi: 10.1046/j.1365-2818.2000.00731.x.

Cawley, W. and Paine, R. (2015) 'Skeletal indicators of reactive arthritis : A case study comparison to other skeletal conditions , such as rheumatoid arthritis , ankylosing spondylitis , ankylosing sero-negative SpA , and DISH', *International Journal of Paleopathology*, 11, pp. 70–74. doi: 10.1016/j.ijpp.2015.10.001.

Chamberlain, A. T. and Forbes, S. (2005) 'A preliminary study of microscopic evidence for lactation in cattle', in Mulville, J. and Outram, A. (eds) *The Zooarchaeology of Fats, Oils, Milk and Dairying*. Oxbow Books, pp. 44–49.

Chan, A. H., Crowder, C. M. and Rogers, T. L. (2007) 'Variation in cortical bone histology within the human femur and its impact on estimating age at death', *American Journal of Physical Anthropology*, 132, pp. 80–88.

Chartzoulakis, K. and Psarras, G. (2005) 'Global change effects on crop photosynthesis and production in Mediterranean : the case of Crete , Greece', *Agriculture, Ecosystems and Environment*, 106, pp. 147–157. doi: 10.1016/j.agee.2004.10.004.

Chen, H., Zhou, X., Fujita, H., Onozuka, M. and Kubo, K. Y. (2013) 'Age-related changes in trabecular and cortical bone microstructure', *International Journal of Endocrinology*, 2013,

p. 213234. doi: 10.1155/2013/213234.

Chinsamy, A. and Raath, M. a. (1992) 'Preparation of fossil bone for histological examination', *Palaeontologia Africana*, 29(I), pp. 39–44.

Cho, H. (2012) 'The histological laboratory and principles of of microscope instrumentation', in Crowder, C. and Stout, S. (eds) *Bone Histology: An anthropological perspective*. U.S.A.: CRC Press, pp. 341–359.

Cho, H. and Stout, S. D. (2011) 'Age-associated bone loss and intraskeletal variability in the Imperial Romans', *Journal of Anthropological Sciences*, 89, pp. 109–125. doi: 10.4436/jass.89007.

Cho, H., Stout, S. D. and Bishop, T. A. (2006) 'Cortical bone remodeling rates in a sample of African American and European American descent groups from the American midwest: Comparisons of age and sex in ribs', *American Journal of Physical Anthropology*, 130(2), pp. 214–226. doi: 10.1002/ajpa.20312.

Cho, H., Stout, S. D., Madsen, R. W. and Streeter, M. a (2002) 'Population-specific histological age-estimating method: a model for known African-American and European-American skeletal remains', *Journal of Forensic Sciences*, 47(1), pp. 12–18.

Christensen, A. M. and Crowder, C. M. (2009) 'Evidentiary standards for forensic anthropology', *Journal of Forensic Sciences*, 54(6), pp. 1211–1216. doi: 10.1111/j.1556-4029.2009.01176.x.

Christensen, A. M., Crowder, C. M., Ousley, S. D. and Houck, M. M. (2014) 'Error and its meaning in forensic science', *Journal of Forensic Sciences*, 59(1), pp. 123–126. doi: 10.1111/1556-4029.12275.

Christensen, A. M., Passalacqua, N. V. and Bartelink, E. J. (2014) *Age Estimation*, *Forensic anthropology: current methods and practice*. U.S.A.: Academic Press. doi: 10.1016/B978-0-12-418671-2.00010-0.

Clarke, B. (2008) 'Normal bone anatomy and physiology', *Clinical Journal of the American Society of Nephrology*, 3(Suppl 3), pp. 131–139. doi: 10.2215/CJN.04151206.

Cohen, J. (1988) *Statistical power analysis for the behavioral sciences*. USA: Routledge.

Cohen, J. and Harris, W. (1958) 'The three-dimensional anatomy of Haversian systems', *Journal of Bone Joint Surgery*, (40A), pp. 419–434.

Cohn, S. H., Abesamis, C., Yasumura, S., Aloia, J. F., Zanzi, I. and Ellis, K. J. (1977) 'Comparative skeletal mass and radial bone mineral content in black and white women', *Metabolism*, 26(2), pp. 171–178. doi: 10.1016/0026-0495(77)90052-X.

Cook, R. and Weisberg, S. (1982) *Residuals and influence in regression*. New York, NY: Chapman & Hall.

Coon, C. (1954) *The Races of Europe*. New York: MacMillan Company.

Cooper, C., Cawley, M., Bhalla, A., Egger, P., Ring, F., Morton, L. and Barker, D. (1995) 'Childhood growth, physical activity, and peak bone mass in women', *Journal of Bone and Mineral Research*, 10(6), pp. 940–947.

Cooper, D. M. L., Thomas, C. D. L., Clement, J. G., Turinsky, A. L., Sensen, C. W. and Hallgrímsson, B. (2007) 'Age-dependent change in the 3D structure of cortical porosity at

the human femoral midshaft', *Bone*, 40(4), pp. 957–965. doi: 10.1016/j.bone.2006.11.011.

Coutelier, L. (1976) 'Le remaniement interne de l'os compact chez l'enfant', *Bulletin de l Association des Anatomistes*, (60), pp. 95–110.

Cramer, D. (1997) *Basic statistics for social research*. New-York: Routledge.

Cramer, D. and Howitt, D. (2004) *The SAGE dictionary of statistics*. London: SAGE Publications.

Crescimanno, A. and Stout, S. D. (2012) 'Differentiating fragmented human and nonhuman long Bone using osteon circularity', *Journal of Forensic Sciences*, 57(2), pp. 287–294. doi: 10.1111/j.1556-4029.2011.01973.x.

Crowder, C. M. (2005) *Evaluating the use of quantitative bone histology to estimate adult age at death*. University of Toronto.

Crowder, C. M. (2013) *Estimation of age at death using cortical bone histomorphometry*. New York, NY

Crowder, C. M. and Austin, D. (2005) 'Age ranges of epiphyseal fusion in the distal tibia and fibula of contemporary males and females', *Journal of Forensic Sciences*, 50(5), pp. 1001–1007. doi: 10.1520/JFS2004542.

Crowder, C. M. and Rosella, L. (2007) 'Assessment of intra- and intercostal variation in rib histomorphometry: Its impact on evidentiary examination', *Journal of Forensic Sciences*, 52(2), pp. 271–276. doi: 10.1111/j.1556-4029.2007.00388.x.

Crowder, C. M. and Pfeiffer, S. (2010) 'The application of cortical bone histomorphometry to estimate age at death', in Latham, K. and Finnegan, M. (eds) *Age Estimation of the Human Skeleton*. Charles C Thomas, pp. 193–215.

Crowder, C. M. and Dominguez, V. M. (2012) 'A new method for histological age estimation of the femur', in *American Academy of Forensic Sciences Annual Meeting*. Atlanta, pp. 374–375.

Crowder, C. M. and Stout, S. D. (2012) *Bone Histology. An anthropological perspective*. USA: CRC Press.

Crowder, C. M., Heinrich, J. and Stout, S. (2012) 'Rib Histomorphometry for Adult Age Estimation', in Bell, L. (ed.) *Forensic Microscopy for skeletal tissues. Methods and protocols*. London: Humana Press, pp. 109–128.

Cuijpers, A. G. F. M. (2006) 'Histological identification of bone fragments in archaeology: Telling humans apart from horses and cattle', *International Journal of Osteoarchaeology*, 16(6), pp. 465–480. doi: 10.1002/oa.848.

Currey, J. D. (1959) 'Differences in the tensile strength of bone of different histological types', *Journal of Anatomy*, 93(1), pp. 87–95.

Currey, J. D. (1964) 'Some effects of ageing in human haversian systems', *Journal of Anatomy*, 98(1), pp. 69–75.

Currey, J. D. (2002) *Bones: structure and mechanism*. Pricenton: Princeton University Press.

Currey, J. D. (2003) 'The many adaptations of bone', *Journal of Biomechanics*, 36(10), pp. 1487–1495. doi: 10.1016/S0021-9290(03)00124-6.

Curtis, E. M., Moon, R. J., Dennison, E. M., Harvey, N. C. and Cooper, C. (2016) 'Recent advances in the pathogenesis and treatment of osteoporosis', *Clinical Medicine*, 16(4), pp. 360–4. doi: 10.7861/clinmedicine.15-6-s92.Recent.

Cvetkovic, V. J., Najman, S. J., Rajkovic, J. S., Zabar, A. L. J., Vasiljevic, P. J., Djordjevic, L. J. B. and Trajanovic, M. D. (2013) 'A comparison of the microarchitecture of lower limb long bones between some animal models and humans: A review', *Veterinarni Medicina*, 58(7), pp. 339–351.

Dahlberg, G. (1940) *Statistical methods for medical and biological students.* London: George Allen & Unwin, Ltd.

De Boer, H. H., Aarents, M. J. and Maat, G. J. R. (2013) 'Manual for the preparation and staining of embedded natural Dry bone tissue sections for microscopy', *International Journal of Osteoarchaeology*, 23(1), pp. 83–93. doi: 10.1002/oa.1242.

De Boer, H. H., Van der Merwe, A. and Maat, G. J. . (2013) 'The diagnostic value of microscopy in dry bone palaeopathology: a review.', *International Journal of Paleopathology*, 3(2), pp. 113–121.

De Boer, H. H., Van der Merwe, A. E., Hammer, S., Steyn, M. and Maat, G. J. R. (2015) 'Assessing post-traumatic time interval in human dry bone', International Journal of Osteoarchaeology, 25(1), pp. 98–109. doi: 10.1002/oa.2267.

De Boer, H. H. and Maat, G. J. R. (2016) 'Dry bone histology of bone tumours', *International Journal of Paleopathology*. Elsevier Inc. doi: 10.1016/j.ijpp.2016.11.005.

De Boer, H. H. and Van der Merwe, A. E. (2016) 'Diagnostic dry bone histology in human paleopathology', *Clinical Anatomy*, 29(7), pp. 831–843. doi: 10.1002/ca.22753.

Dempster, D. W., Compston, J. E., Drezner, M. K., Glorieux, F. H., Kanis, J. A., Malluche, H., Meunier, P. J., Ott, S. M., Recker, R. R. and Parfitt, A. M. (2013) 'Standardized nomenclature, symbols, and units for bone histomorphometry: A 2012 update of the report of the ASBMR Histomorphometry Nomenclature Committee', *Journal of Bone and Mineral Research*, 28(1), pp. 2–17. doi: 10.1002/jbmr.1805.

DiGangi, E. A. and Moore, M. K. (2013) 'Application of the Scientific Method to Skeletal Biology', in DiGangi, E. and Moore, M. (eds) *Research methods in human skeletal biology*. Oxford: Elsevier, pp. 29–59. doi: 10.1016/B978-0-12-385189-5.00001-7.

Dominguez, V. M. and Agnew, A. M. (2016) 'Examination of factors potentially influencing osteon size in the human rib'', *The Anatomical Records*, 299, pp. 313–324. doi: 10.1002/ar.23305.

Dominguez, V. M. and Agnew, A. (2014) 'Patterns in resorptive spaces in elderly rib cortices.', in *83rd Annual Meeting of the American Association of Physical Anthropologists*. Calgary, Alberta, Canada., p. 107. doi: 10.1002/ajpa/22488.

Dominguez, V. M. and Crowder, C. M. (2012) 'The utility of osteon shape and circularity for differentiating human and non-human Haversian bone', *American Journal of Physical Anthropology*, 149(1), pp. 84–91. doi: 10.1002/ajpa.22097.

Drusini, A. and Businaro, F. (1990) 'Skeletal age determination by mandibular histomorphometry', *International Journal of Anthropology*, (5), pp. 235–243.

Dudar, J. C., Pfeiffer, S. and Saunders, S. R. (1993a) 'Evaluation of morphological and histological adult skeletal age-at-death estimation techniques using ribs', *Journal of forensic*

sciences, 38(3), pp. 677–85.

Edoc.coe.int/en (2013) *Intercultural Cities- Building the future of Diversity. City of Limassol*.

Edson, C. (1967) 'Greece in the second world war', *Balkan Studies*, 8(2), pp. 225–238.

Enlow, D. and Brown, S. (1957) 'A comparative histological study of fossil and recent bone tissues. Part II', *Texas Journal of Science*, (2), pp. 186–203.

Epker, B. N. and Frost, H. M. (1965) 'A histological study of remodeling at the periosteal, haversian canal, cortical endosteal, and trabecular endosteal surfaces in human rib', *The Anatomical Record*, 152(2), pp. 129–135. doi: 10.1002/ar.1091520203.

Ericksen, M. F. (1979) 'Aging changes in the medullary cavity of the proximal femur in American Blacks and Whites', *American Journal of Physical Anthropology*, 51(4), pp. 563–569. doi: 10.1002/ajpa.1330510408.

Ericksen, M. F. (1991) 'Histologic estimation of age at death using the anterior cortex of the femur', *American Journal of Physical Anthropology*, 84(2), pp. 171–179.

Eriksen, E. F. (2010) 'Cellular mechanisms of bone remodeling', *Reviews in Endocrine and Metabolic Disorders*, 11(4), pp. 219–227. doi: 10.1007/s11154-010-9153-1.

Evans, J. (1996) *Straightforward statistics for the behavioural sciences*. Pacific Grove, CA: Brooks/Cole.

Faller, A. and Schuenke, M. (2004) *The human body - an introduction to structure and function*. New York: Thieme. doi: 10.1017/CBO9781107415324.004.

Fanguw, Z. (1983) 'Preliminary study on determination of bone age by microscopic method', *Acta Anthropology Sinica*, II, pp. 142–151.

Feng, X. and McDonald, J. (2011) 'Disorders of bone remodeling', *Annual Review Pathology: Mechanism of Disease*, (6), pp. 121–145. doi: 10.1146/annurev-pathol-011110-130203.Disorders.

Fenton, T. W., Birkby, W. H. and Cornelison, J. (2003) 'A fast and safe non-bleaching method for forensic skeletal preparation', *Journal of Forensic Sciences*, 48(2), pp. 274–276.

Fernández Castillo, R., Ubelaker, D. H., Acosta, J. A. L., de la Rosa, R. J. E. and Garcia, I. G. (2013) 'Effect of temperature on bone tissue: histological changes', *Journal of Forensic Sciences*, 58(3), pp. 578–582. doi: 10.1111/1556-4029.12093.

Field, A. (2009) *Discovering statistics using SPSS: and sex and drugs and rock 'n' roll*. 3rd ed. London: Sage.

Florencio-Silva, R., Rodrigues, G., Sasso-cerri, E., Simões, M. J., Cerri, P. S. and Cells, B. (2015) 'Biology of bone tissue : Structure , function , and factors that influence bone cells', *BioMed Research International*, p. doi.org/10.1155/2015/421746. doi: 10.1155/2015/421746.

Fox, J. (1991) *Regression diagnostics*. Newbury Park, CA: Sage.

Francillon-Vieillot, H., Buffrénil, V. de, Castanet, J., Géraudie, J., Meunier, F. J., Sire, J. Y., Zylberberg, L. and Ricqlès, A. de (1990) 'Microstructure and mineralization of vertebrate skeletal tissues', in Carter, J. (ed.) *Skeletal biomineralization: patterns, processes and evolutionary trends*. New York: Van Nostrand Reinhold.

Frisancho, A., Garn, S. and Ascoli, W. (1970) 'Unequal influence of low dietary intakes on skeletal maturation during childhood and adolescence', *American Journal of Clinical Nutrition*, 23(9), pp. 1220–1227.

Fritz, J., Duckham, R. L., Rantalainen, T., Rosengren, B. E., Karlsson, M. K. and Daly, R. M. (2016) 'Influence of a school-based physical activity intervention on cortical bone mass distribution: a 7-year intervention study', *Calcified Tissue International*, 99(5), pp. 443–453. doi: 10.1007/s00223-016-0174-y.

Frost, H. M. (1960) 'Presence of microscopic cracks in vivo in bone', *Henry Ford Hospital Medical Bulletin*, (8), pp. 25–35.

Frost, H. M. (1964) *The laws of bone structure*. Springfield: Charles C Thomas.

Frost, H. M. (1969) 'Tetracycline-based histological analysis of bone remodeling', *Calcified Tissue Research*, 3(1), pp. 211–237. doi: 10.1007/BF02058664.

Frost, H. M. (1973) *Bone modeling and skeletal modeling errors. Orthopaedic Lectures Volume IV*. Springfield, IL: Charles C. Thomas.

Frost, H. M. (1983) 'The regional acceleratory phenomenon: a review', *Henry Ford Hospital Medical Bulletin*, 31, pp. 3–9.

Frost, H. M. (1987a) 'Bone "mass" and the "mechanostat": a proposal', *The Anatomical record*, a(1), pp. 1–9. doi: 10.1002/ar.1092190104.

Frost, H. M. (1987b) 'Secondary osteon population densities: An algorithm for estimating the missing osteons', *American Journal of Physical Anthropology*, (30), pp. 239–254. doi: 10.1002/ajpa.1330300513.

Frost, H. M. (1987c) 'Secondary osteon populations: An algorithm for determining mean bone tissue age', *American Journal of Physical Anthropology*, (30), pp. 221–238. doi: 10.1002/ajpa.1330300512.

Frost, H. M. (1987d) 'Secondary osteon populations: An algorithm for effects of biomechanics, modeling patterns, chronological age and tissue age', *Yearbook of Physical Anthropology*, (30), pp. 239–254.

Frost, H. M. (1997) 'Why do marathon runners have less bone than weight lifters? A vital-biomechanical view and explanation', *Bone*, 20(3), pp. 183–189. doi: 10.1016/S8756-3282(96)00311-0.

Frost, H. M. (1998a) 'Changing concepts in skeletal physiology : Wolff ' s Law , the Mechanostat , and the "' Utah Paradigm '"', *American Journal of Human Biology*, 10(July 1997), pp. 599–605. doi: 10.1002/(SICI)1520-6300(1998)10:5<599::AID-AJHB6>3.0.CO;2-9.

Frost, H. M. (1998b) 'On rho, a marrow mediator, and estrogen: Their roles in bone strength and "mass" in human females, osteopenias, and osteoporoses insights from a new paradigm', *Journal of Bone and Mineral Metabolism*, 16(2), pp. 113–123. doi: 10.1007/s007740050035.

Frost, H. M. (1999) 'An approach to estimating bone and joint loads and muscle strength in living subjects and skeletal remains', *American journal of human biology*, 11(February 1998), pp. 437–455. doi: 10.1002/(SICI)1520-6300(1999)11:4<437::AID-AJHB4>3.0.CO;2-K.

Frost, H. M. (2000) 'The Utah paradigm of skeletal physiology: an overview of its insights for bone, cartilage and collagenous tissue organs', *Journal of Bone and Mineral Metabolism*,

18(6), pp. 305–316. doi: 10.1007/s007740070001.

Frost, H. M. (2001) 'From Wolff's law to the Utah paradigm: Insights about bone physiology and its clinical applications', *Anatomical Record*, 262(4), pp. 398–419. doi: 10.1002/ar.1049.

Frost, H. M. (2003) 'Bone's mechanostat: A 2003 update', *the Anatomical Record Part a*, 275A(August), pp. 1081–1101. doi: 10.1002/ar.a.10119.

Frost, H. M. (2004) 'A 2003 update of bone physiology and Wolff s law for clinicians', *Angle Orthodontist*, 74(1), pp. 3–15. doi: 10.1043/0003-3219(2004)074<0003:AUOBPA>2.0.CO;2.

García-Donas, J. G., Dyke, J., Paine, R., Nathena, D. and Kranioti, E. (2016) 'Accuracy and sampling error of two age estimation techniques using rib histomorphometry on a modern sample', *Journal of Forensic and Legal Medicine*, 38, pp. 28–35. doi: 10.1016/j.jflm.2015.11.012.

García-Donas, J. G., Ekizoglu, O., Er, A., Bozdag, M., Akcaoglu, M., Can, I. and Kranioti, E. (2017) 'Accuracy and reliability of Southern European standards for the tibia : a test of two Mediterranean populations', *Journal of Forensic Science and Criminology*, 2(1), pp. 1–5. doi: 10.15761/FSC.1000107.

García-Donas, J., Scholl, A., A, D., Paine, R. and Kranioti, E. (2017) 'Histological Age Estimation on two Mediterranean Populations: A Validation study of four Existing Methodologies', in *The 86th Annual Meeting of the American Association of Physical Anthropologists*. New Orleans, p. 190.

García-Donas, J. G., Dalton, A., Chaplin, I. and Kranioti, E. F. (2017) 'A revised method for the preparation of dry bone samples used in histological examination: Five simple steps', *Journal of Comparative Human Biology*, 68(4), pp. 283–288. doi: 10.1016/j.jchb.2017.07.001.

Garn, S. (1981) 'The phenomenon of bone formation and bone loss', in DeLuca, H., Frost, H., Jee, W., Johnston, C., and Parfitt, A. (eds) *Osteoporosis: recent advances in pathogenesis and treatment*. Baltimore: University Park Press, pp. 3–18.

Garn, S. and Shaw, H. (1977) 'Extending the Trotter model of bone gain and bone loss', in Buettner-Janusch, J. (ed.) *Yearbook of Physical Anthropology*. Washington DC, pp. 45–56.

Garvin, H. M., Nicholas, V. and Uhl, N. M. (2012) 'Developments in forensic anthropology: Age- at-Death estimation', in Dirkmaat, D. (ed.) *A companion to forensic anthropology*. West Sussex: Wiley-Blackwell, pp. 202–223. doi: 10.1002/9781118255377.ch10.

Garvin, H. M. and Passalacqua, N. V. (2012) 'Current practices by forensic anthropologists in adult skeletal age estimation', *Journal of Forensic Sciences*, 57(2), pp. 427–433. doi: 10.1111/j.1556-4029.2011.01979.x.

Gebhardt, W. (1905) *Ueber Funktionell Wichtige Anordungsweisen Des Grberen Und Feineren Bauelemente Des Wirbelthierknochens II*. Edited by Spezieler Teil.1. Der Bau der Haversaschen Lamellensyteme und seine funktionelle Bedeutung. Roux´s Archives.

Ghasemi, A. and Zahediasl, S. (2012) 'Normality tests for statistical analysis: A guide for non-statisticians', *International Journal of Endocrinology and Metabolism*, 10(2), pp. 486–489. doi: 10.5812/ijem.3505.

Giavarina, D. (2015) 'Understanding Bland Altman analysis', *Biochemia Medica*, 25(2), pp. 141–151. doi: 10.11613/BM.2015.015.

Giles, E. and Klepinger, L. L. (1988) 'Confidence intervals for estimates based on linear regression in forensic anthropology', *Journal of forensic sciences*, 33(5), pp. 1218–22. Available at: http://www.ncbi.nlm.nih.gov/pubmed/3193077.

Giraud-Guille, M. M. (1988) 'Twisted plywood architecture of collagen fibrils in human compact bone osteons', *Calcified Tissue International*, 42(3), pp. 167–180. doi: 10.1007/BF02556330.

Gocha, T. P. and Agnew, A. M. (2016) 'Spatial variation in osteon population density at the human femoral midshaft: Histomorphometric adaptations to habitual load environment', *Journal of Anatomy*, 228(5), pp. 733–745. doi: 10.1111/joa.12433.

Gocha, T. P., Ingvoldstad, M. E., Kolatorowicz, A., Cosgriff-Hernandez, M. T. J. and Sciulli, P. W. (2015) 'Testing the applicability of six macroscopic skeletal aging techniques on a modern Southeast Asian sample', *Forensic Science International*. Elsevier Ireland Ltd, 249, pp. 318–318. doi: 10.1016/j.forsciint.2014.12.015.

Goldman, H. M., McFarlin, S. C., Cooper, D. M. L., Thomas, C. D. L. and Clement, J. G. (2009) 'Ontogenetic patterning of cortical bone microstructure and geometry at the human mid-shaft femur', *Anatomical Record*, 292(1), pp. 48–64. doi: 10.1002/ar.20778.

Goliath, J. R. (2010) *Variation in osteon circularity and its impact on estimating age at death*, *MA Thesis*. The Ohio State University.

Goliath, J. R., Stewart, M. C. and Stout, S. D. (2016) 'Variation in osteon histomorphometrics and their impact on age-at-death estimation in older individuals', *Forensic Science International*. Elsevier Ireland Ltd, 262, p. 282.e1-282.e6. doi: 10.1016/j.forsciint.2016.02.053.

Gong, J. K., Arnold, J. S. and Cohn, S. H. (1964) 'Composition of trabecular and cortical bone', *The Anatomical Record*, 149(3), pp. 325–331. doi: 10.1002/ar.1091490303.

Gosman, J. H., Stout, S. D. and Larsen, C. S. (2011) 'Skeletal biology over the life span: A view from the surfaces', *American Journal of Physical Anthropology*, 146(SUPPL. 53), pp. 86–98. doi: 10.1002/ajpa.21612.

Gray, H., Standring, S., Ellis, H. and Berkovitz, B. (2005) 'Musculoskeletal system', in Standing, S. (ed.) *Gray´s Anatomy*. 39th ed. New York: Elsevier Churchill Livingstone, pp. 83–135.

Grilo, L. M. and Grilo, H. L. (2012) 'Comparison of clinical data based on limits of agreement', *Biometrical Letters*, 49(1), pp. 45–56. doi: 10.2478/bile-2013-0003.

Gu, G., Mulari, M., Peng, Z., Hentunen, T. A. and Väänänen, H. K. (2005) 'Death of osteocytes turns off the inhibition of osteoclasts and triggers local bone resorption', *Biochemical and Biophysical Research Communications*, 335(4), pp. 1095–1101. doi: 10.1016/j.bbrc.2005.06.211.

Guo, X. (2001) 'Mechanical properties of cortical bone and cancellous bone tissue', in Cowin, S. (ed.) *Bone Mechanics Handbook*. 2nd edn. Boca Ratón: CRC Press, p. 10.1-10.19.

Han, S. H., Kim, S. H., Ahn, Y. W., Huh, G. Y., Kwak, D. S., Park, D. K., Lee, U. Y. and Kim, Y. S. (2009) 'Microscopic age estimation from the anterior cortex of the femur in Korean adults', *Journal of Forensic Sciences*, 54(3), pp. 519–522. doi: 10.1111/j.1556-4029.2009.01003.x.

Harper, A., Laughlins, W. and Mazess, R. (1984) 'Bone mineral content in St. Lawrence Island Eskimos', *Human Biology*, (56), pp. 63–78.

Harris, E. F. and Smith, R. N. (2009) 'Accounting for measurement error: A critical but often overlooked process', *Archives of Oral Biology*, 54(SUPPL. 1), pp. 107–117. doi: 10.1016/j.archoralbio.2008.04.010.

Hauge, E. M., Qvesel, D., Eriksen, E. F., Mosekilde, L. and Melsen, F. (2001) 'Cancellous bone remodeling occurs in specialized compartments lined by cells expressing osteoblastic markers', *Journal of Bone and Mineral Research*, 16(9), pp. 1575–1582. doi: 10.1359/jbmr.2001.16.9.1575.

Havill, L. M., Allen, M. R., Harris, J. A. K., Levine, S. M., Coan, H. B., Mahaney, M. C. and Nicolella, D. P. (2013) 'Intracortical bone remodeling variation shows strong genetic effects', *Calcified Tissue International*, 93(5), pp. 472–480. doi: 10.1007/s00223-013-9775-x.

Heinrich, J. T. (2015) *Spatial characterization of rib cortical bone microstructure and the effect of nutritional and physiological stresses*. University of Toronto.

Heinrich, J. T., Crowder, C. M. and Pinto, D. (2012) 'Proposal and validation of definitions for intact and fragmented osteons', in *81st annual meeting of the American Association of Physical Anthropologists,*. Portland, Oregon.

Hellenthal, G., Busby, G. B. J., Band, G., Wilson, J. F., Capelli, C., Falush, D. and Myers, S. (2014) 'A genetic atlas of human admixture history', *Science*, 343(6172), pp. 747–751. doi: 10.1126/science.1243518.

Heraclides, A., Bashiardes, E., Fernández-Domínguez, E., Bertoncini, S., Chimonas, M., Christofi, V., King, J., Budowle, B., Manoli, P. and Cariolou, M. A. (2017) 'Y-chromosomal analysis of Greek Cypriots reveals a primarily common pre-Ottoman paternal ancestry with Turkish Cypriots', *PLoS ONE*, 12(6), pp. 1–26. doi: 10.1371/journal.pone.0179474.

Hillier, M. L. and Bell, L. S. (2007) 'Differentiating human bone from animal bone: A review of histological methods', *Journal of Forensic Sciences*, 52(2), pp. 249–263. doi: 10.1111/j.1556-4029.2006.00368.x.

Hoffman, R. and Gerber, M. (2012) *The Mediterranean Diet: health and science*. Chichester, West Sussex, UK: Wiley-Blackwell.

Hollund, H. I., Arts, N., Jans, M. M. E. and Kars, H. (2015) 'Are teeth better? histological characterization of diagenesis in archaeological bone-tooth pairs and a discussion of the consequences for archaeometric sample selection and analyses', *International Journal of Osteoarchaeology*, 25(6), pp. 901–911. doi: 10.1002/oa.2376.

Hughey, J. R., Paschou, P., Drineas, P., Mastropaolo, D., Lotakis, D. M., Navas, P. A., Michalodimitrakis, M., Stamatoyannopoulos, J. A. and Stamatoyannopoulos, G. (2013) 'A European population in minoan Bronze age crete', *Archives of Hellenic Medicine*. Nature Publishing Group, 30(4), pp. 456–466. doi: 10.1038/ncomms2871.

Huitema, B. (2011) *The analysis of covariance and alternatives: statistical methods for experiments, quasi-experiments, and single-case studies*. 2nd ed. Hoboken, NJ: Wiley, Inc.

Hurvich, C. and Tsai, C. (1989) 'Regression and time series model selection in small samples', *Biometrika*, 76(2), pp. 297–307. doi: 10.1093/biomet/76.2.297.

Ice, G. (2003) 'Biological anthropology of aging - past, present and future', *Collegium Antropologicum*, 27(1), pp. 1–6.

Igarashi, Y., Uesu, K., Wakebe, T. and Kanazawa, E. (2005) 'New method for estimation of adult skeletal age at death from the morphology of the auricular surface of the ilium',

American Journal of Physical Anthropology, (128), pp. 324–339.

Inoue, M., Tanaka, H., Moriwake, T., Oka, M., Sekiguchi, C. and Seino, Y. (2000) 'Altered biochemical markers of bone turnover in humans during 120 days of bed rest', *Bone*, 26(3), pp. 281–286. doi: 10.1016/S8756-3282(99)00282-3.

Isçan, M., Loth, S. and Wright, R. (1984a) 'Age Estimation from the Rib by Phase Analysis: White Females', *Journal of Forensic Sciences*, 30(853–863). doi: 10.1520/JFS11018J.

Isçan, M., Loth, S. and Wright, R. (1984b) 'Age Estimation from the Rib by Phase Analysis: White Males', *Journal of Forensic Science*, 29, pp. 1094–1104. doi: 10.1520/JFS11018J.

Iwaniec, U. T., Crenshaw, T. D., Schoieninger, M. J., Stout, S. D. and Erickensen, M. F. (1998) 'Methods for improving the efficiency of estimating total osteon density in the human anterior mid-diaphyseal femur', *American Journal of Physical Anthropology*, 107(March), pp. 13–24.

Iwaniec, U. T., Wronski, T. and Turner, R. (2008) 'Histological Analysis of Bone', *Alcohol. Methods in Molecular Biology*. Edited by L. E. Nagy. Humana Press, pp. 325–341.

Jähn, K. and Bonewald, L. F. (2012) 'Bone Cell Biology: Osteoclasts, Osteoblasts, Osteocytes', in Glorieux, F., Pettifor, J., and Juppner, H. (eds) *Pediatric Bone*. 2nd edn. U.S.A.: Academic Press, pp. 1–8. doi: 10.1016/B978-0-12-382040-2.10001-2.

Jasinoski, S. C. and Chinsamy, A. (2012) 'Mandibular histology and growth of the nonmammaliaform cynodont Tritylodon', *Journal of Anatomy*, 220(6), pp. 564–579. doi: 10.1111/j.1469-7580.2012.01494.x.

Jee, W. S. S. (2001) 'Integrated bone tissue physiology: anatomy and physiology', in Cowin, S. (ed.) *Bone Mechanics: Handbook*. 2nd edn. Boca Ratón: CRC Press, p. 1.1-1.34.

Jee, W. S. S. (2005) 'The past, present, and future of bone morphometry: Its contribution to an improved understanding of bone biology', *Journal of Bone and Mineral Metabolism*, 23(SUPPL. 1), pp. 1–10. doi: 10.1007/BF03026316.

Jepsen, K. J. and Andarawis-Puri, N. (2012) 'The amount of periosteal apposition required to maintain bone strength during aging depends on adult bone morphology and tissue-modulus degradation rate', *Journal of Bone and Mineral Research*, 27(9), pp. 1916–1926. doi: 10.1002/jbmr.1643.

Jilka, R. L., Weinstein, R. S., Parfitt, A. M. and Manolagas, S. C. (2007) 'Quantifying osteoblast and osteocyte apoptosis: Challenges and rewards', *Journal of Bone and Mineral Research*, 22(10), pp. 1492–1501. doi: 10.1359/jbmr.070518.

Johnson, T. R. (2016) 'Violation of the homogeneity of regression slopes assumption in ANCOVA for two-group pre-post designs: Tutorial on a modified Johnson-Neyman procedure', *The Quantitative Methods for Psychology*, 12(3), pp. 253–263. doi: 10.20982/tqmp.12.3.p253.

Jowsey, J. (1960) 'Age Changes in Human Bone', *Clinical Orthopaedics*, 17, pp. 210–218.

Jowsey, J. (1966) 'Studies of Haversian systems in man and some animals', *Journal of Anatomy*, 100(Pt 4), pp. 857–64. doi: 10.1002/ajpa.

Katz, D. and Suchey, J. M. (1986) 'Age determination of the male Os pubis', *American Journal of Physical Anthropology*, 69(4), pp. 427–435. doi: 10.1002/ajpa.1330690402.

Kazamias, G. and Panayiotou, M. (2015) 'Foodstuffs imports and diet change in Cyprus, 1881–1946/7 *', *Modern Greek Studies Association of New Zealand*, pp. 239–250.

Keough, N., L'Abbé, E. N. and Steyn, M. (2009) 'The evaluation of age-related histomorphometric variables in a cadaver sample of lower socioeconomic status: implications for estimating age at death', *Forensic Science International*, 191(1–3), pp. 12–15. doi: 10.1016/j.forsciint.2009.07.012.

Kerley, E. R. (1965) 'The microscopic determination of age in human bone', *American Journal of Physical Anthropology*, 23(2), pp. 149–164.

Kerley, E. R. and Ubelaker, D. H. (1978) 'Revisions in the microscopic method of estimating age at death in human cortical bone', *American Journal of Physical Anthropology*, 49(4), pp. 545–546. doi: 10.1002/ajpa.1330490414.

Keshawarz, N. M. and Recker, R. R. (1984) 'Expansion of the medullary cavity at the expense of cortex in postmenopausal osteoporosis', *Metabolic Bone Disease and Related Research*, 5(5), pp. 223–228. doi: 10.1016/0221-8747(84)90063-8.

Khurana, J. and Fitzpatrick, L. (2009) 'Osteoporosis and Metabolic Bone Disease', in Khurana, J. (ed.) *Bone Pathology*. 2nd ed. Humana Press, pp. 217–238.

Kim, B. (2015) *Understanding diagnostic plots for linear regression analysis*, *University of Virginia Library*. Available at: http://data.library.virginia.edu/diagnostic-plots/ (Accessed: 15 May 2017).

Kim, Y. S., Kim, D. I., Park, D. K., Lee, J. H., Chung, N. E., Lee, W. T. and Han, S. H. (2007) 'Assessment of histomorphological features of the sternal end of the fourth rib for age estimation in Koreans', *Journal of Forensic Sciences*, 52(6), pp. 1237–1242. doi: 10.1111/j.1556-4029.2007.00566.x.

Klein-Nulend, J. and Bonewald, L. F. (2008) 'The Osteocyte', in Bilezikian, J., Lawrence, G., and Martin, T. (eds) *Principles of bone biology*. 3rd edn. U.S.A.: Academic Press, pp. 153–174. doi: http://dx.doi.org/10.1016/B978-0-12-373884-4.00028-8.

Kohr, R. L. and Games, P. A. (1974) 'Robustness of the analysis of variance, the welch procedure and a box procedure to heterogeneous variances', *Journal of Experimental Education*, 43(1), pp. 61–69. doi: 10.1080/00220973.1974.10806305.

Kontopoulos, I., Nystrom, P. and White, L. (2016) 'Experimental taphonomy: post-mortem microstructural modifications in Sus scrofa domesticus bone', *Forensic Science International*, 266, pp. 320–328. doi: 10.1016/j.forsciint.2016.06.024.

Kranioti, E. F. (2017) 'Radiometry versus osteometry in sex assessment: a study of the Cretan radius', *Australian Journal of Forensic Sciences*, 618(December), pp. 1–14. doi: 10.1080/00450618.2017.1329849.

Kranioti, E. F., Işcan, M. Y. and Michalodimitrakis, M. (2008) 'Craniometric analysis of the modern Cretan population', *Forensic Science International*, 180(2–3), pp. 1–5. doi: 10.1016/j.forsciint.2008.06.018.

Kranioti, E. F. and Michalodimitrakis, M. (2009) 'Sexual Dimorphism of the Humerus in Contemporary Cretans — A Population-Specific Study and a Review of the Literature *', *Journal of Forensic Sciences*, 54(5), pp. 3–5. doi: 10.1111/j.1556-4029.2009.01103.x.

Kranioti, E. F., García-Donas, J. G. and Langstaff, H. (2014) 'Sex estimation of the Greek mandible with the aid of discriminant function analysis and posterior probabilities',

Romanian Journal of Legal Medicine, 22(2). doi: 10.4323/rjlm.2014.101.

Kranioti, E. F., García-Donas, J. G., Almeida Prado, P. S., Kyriakou, X. P. and Langstaff, H. C. (2017) 'Sexual dimorphism of the tibia in contemporary Greek-Cypriots and Cretans: Forensic applications', *Forensic Science International*. Elsevier Ireland Ltd, 271, p. 129.e1-129.e7. doi: 10.1016/j.forsciint.2016.11.018.

Krishan, T. and Kanchan, T. (2016) 'Measurement Error in Anthropometric Studies and its Significance in Forensic Casework', *Annals of Medical and Health Science Research*, 1(6), pp. 62–63. doi: 10.4103/2141-9248.180277.

Krogman, W. and Isçan, M. (1986) *The human skeleton in forensic medicine*. 2nd edn. Springfield, Ill: Charles C. Thomas.

Kular, J., Tickner, J., Chim, S. M. and Xu, J. (2012) 'An overview of the regulation of bone remodelling at the cellular level', *Clinical Biochemistry*. The Canadian Society of Clinical Chemists, 45(12), pp. 863–873. doi: 10.1016/j.clinbiochem.2012.03.021.

Kumar, V., Abbas, A., Aster, J. and Cotran, R. (2015) *Robbins and Cotran Pathologic basis of bone Disease*. 9th edn. Philadelphia: Elsevier.

Kutner, M., Nachtsheim, C., Neter, J. and Li, W. (2005) *Applied linear statistical models*. 5th ed. New York, NY: McGraw-Hill.

Laerd Statistics (2017) *One-way ANCOVA using SPSS Statistics. Statistical tutorials and software guides*. Available at: https://statistics.laerd.com/ (Accessed: 10 May 2017).

Lanyon, L. E. (1993) 'Osteocytes, strain detection, bone modeling and remodeling', *Calcified Tissue International*, 53(S1), pp. S102–S107. doi: 10.1007/BF01673415.

Lathan, K. and Finnegan, M. (2010) *Age estimation of the human skeleton*. Springfield, IL: Springfield : Charles C Thomas.

Lee, U. Y., Jung, G. U., Choi, S. G. and Kim, Y. S. (2014) 'Anthropological age estimation with bone histomorphometry from the human clavicle', *Anthropologist*, 17(3), pp. 929–936.

Liakos, A., Madianos, M. and Stefanis, C. (1980) 'Alcohol consumption and rates of alcoholism in Greece', *Drug and Alcohol Dependence*, 6(6), pp. 425–430. doi: 10.1016/0022-5088(68)90136-7.

Lill, C., García-Donas, J. G., Xhemali, B. and Kranioti, E. (2017) 'The effect of pathology on bone microstructure: implications for histological age estimation'', in *The 86th Annual Meeting of the American Association of Physical Anthropologists*. New Orleans, p. 263.

Livshits, G., Karasik, D., Otremski, I. and Kobyliansky, E. (1998) 'Genes play an important role in bone aging', *American Journal of Human Biology*, 10(December 1996), pp. 421–438.

Lomax, R. and Hahs-Vaughn, D. (2012) *An introduction to statistical concepts*. Third edn. New York: Routledge, pp. 610–656.

Lovejoy, C., Meindl, R., Pryzbeck, T. R. and Mensforth, R. P. (1985a) 'Chronological metamorphosis of the auricular aurface of the ilium: a new method for the determination of adult skeletal age at death', *American Journal of Physical Anthropology*, 68(1), pp. 15–28.

Lovejoy, C., Meindl, S., Mensforth, R. and Barton, T. (1985b) 'Multifactoral Determination of Skeletal Age at Death: A Method and Blind Test of its Accuracy', *American Journal of Physical Anthropology*, 68(1), pp. 1–14. doi: 10.1002/ajpa.1330680102.

Lucy, D. (2005) 'Regression and Calibration', in *Introduction to Statistics for Forensic Scientists*. England: John Wiley & Sons, pp. 75–92.

Lynnerup, N., Thomsen, J. L. and Frohlich, B. (1998) 'Intra- and inter-observer variation in histological criteria used in age at death determination based on femoral cortical bone', *Forensic Science International*, 91(3), pp. 219–230. doi: 10.1016/S0379-0738(97)00197-7.

Lynnerup, N., Frohlich, B. and Thomsen, J. L. (2006) 'Assessment of age at death by microscopy: Unbiased quantification of secondary osteons in femoral cross sections', *Forensic Science International*, 159(1), pp. 100–103. doi: 10.1016/j.forsciint.2006.02.023.

Maat, G. J. R., Maes, A., Aarents, M. J. and Nagelkerke, N. J. D. (2006) 'Histological age prediction from the femur in a contemporary Dutch sample: The decrease of nonremodeled bone in the anterior cortex', *Journal of Forensic Sciences*, 51(2), pp. 230–237. doi: 10.1111/j.1556-4029.2006.00062.x.

Maes, C. and Kronenberg, H. M. (2012) 'Postnatal bone growth: growth plate biology, bone formation, and remodeling', in Glorieux, F., Pettifor, J., and Juppner, H. (eds) *Pediatric Bone*. 2nd edn. U.S.A.: Elsevier Inc., pp. 55–82. doi: 10.1016/B978-0-12-382040-2.10004-8.

Maggiano, C. (2012) 'Making the Mold: a microstructural persepctive of bone modeling during growth and mechanical adaptation', in Corwder, S. and Stout, S. D. (eds) *Bone Histology: An anthropological perspective*. CRC Press, pp. 45–82.

Maggiano, C., Maggiano, I., Tiesler, V., Chi-Keb, J. and Stout, S. (2016) 'Methods and theory in bone modeling drift: Comparing spatial analyses of primary bone distributions in the human humerus', *Journal of Anatomy*, 228(1), pp. 190–202. doi: 10.1111/joa.12383.

Maggiano, I. S., Maggiano, C. M., Clement, J. G., Thomas, C. D. L., Carter, Y. and Cooper, D. M. L. (2016) 'Three-dimensional reconstruction of Haversian systems in human cortical bone using synchrotron radiation-based micro-CT: Morphology and quantification of branching and transverse connections across age', *Journal of Anatomy*, 228(5), pp. 719–732. doi: 10.1111/joa.12430.

Mann, H. and Whitney, D. (1947) 'On a Test of Whether one of Two Random Variables is Stochastically Larger than the Other', *Annals of the Institute of Statistical Mathematics*, 18(1), pp. 50–60. doi: 10.1214/aoms/1177728422.

Marotti, G. (1993) 'A new theory of bone lamellation', *Calcified Tissue International*, 53(1 Supplement). doi: 10.1007/BF01673402.

Martin, R. B. (1983) *Paleophysiological aspects of bone remodeling in the Meroitic, X-Group and Christian populations from Sudanese Nubia*. University of Massachusetts.

Martin, R. B. and Burr, D. B. (1989b) *Structure, function and adaptation of bone*. New York: Raven Press.

Martin, R. B., Burr, D. B. and Sharkey, N. A. (1998) 'Growth, modeling and remodeling of bone', in *Skeletal Tissue Mechanics*. New York: Springer, pp. 95–168.

Martin, R. B., Pickett, J. C. and Zinaich, S. (1980) 'Studies of skeletal remodeling in aging men.', *Clinical Orthopaedics and related Research*, pp. 268–282.

Martin, R., Burr, D., Sharkey, N. and Fyhrie, D. (2015) 'Growth, Modeling and Remodeling of Bone', in *Skeletal Tissue Mechanics*. 2nd. ed. Springer, pp. 95–174.

Martrille, L., Ubelaker, D. H., Cattaneo, C., Seguret, F., Tremblay, M. and Baccino, E. (2007)

'Comparison of four skeletal methods for the estimation of age at death on white and black adults', *Journal of Forensic Sciences*, 52(2), pp. 302–307. doi: 10.1111/j.1556-4029.2006.00367.x.

Martrille, L., Irinopoulou, T., Bruneval, P., Baccino, E. and Fornes, P. (2009) 'Age at death estimation in adults by computer-assisted histomorphometry of decalcified femur cortex', *Journal of Forensic Sciences*, 54(6), pp. 1231–1237. doi: 10.1111/j.1556-4029.2009.01178.x.

Mays, S. (2015) 'The effect of factors other than age upon skeletal age indicators in the adult', *Annals of Human Biology*, 42(4), pp. 332–341. doi: 10.3109/03014460.2015.1044470.

McCarthy, E. F. (2010) 'Metabolic Bone Disorders', in Khurana, J., McCarthy, E., and Zhang, P. (eds) *Essentials in Bone and Soft-Tissue Pathology*. Springer, pp. 1829–1841. doi: 10.1007/978-0-387-89845-2.

McDonald, J. H. (2014) *Handbook of biological statistics*. 3rd edn. Maryland, Baltimore: Sparky House Publishing.

McKern, T. and Steward, T. (1957) *Skeletal age changes in young American males, analysed from the standpoint of age identification*. Technical. Natick, Mass. : Headquarters, Quartermaster Research & Development Command.

Mears, C. S., Litton, S. M., Phippen, C. M., Langston, T. D., Keenan, K. E. and Skedros, J. G. (2014) 'Improving accuracy , precision , and efficiency in analysis of osteon cross-sectional shape'', *American Journal of Physical Anthropology*, 154, p. 223.

Meindl, R. and Lovejoy, C. O. (1985) 'Ectocranial accuracy , precision , and efficiency in analysis of osteon cross-sectional shape'', *American Journal of Physical Anthropology*, 68(1), pp. 57–66.

Merritt, C. (2013) 'Testing the accuracy of adult skeletal age estimation methods: original methods versus revised and newer methods', *Vis-à-vis: Explorations in Anthropology*, 12(1), pp. 102–119. doi: http://vav.library.utoronto.ca/index.php/vav/article/view/19146.

Van Der Merwe, A. E., Maata, G. J. R. and Steyn, M. (2010) 'Ossified haematomas and infectious bone changes on the anterior tibia: Histomorphological features as an aid for accurate diagnosis', *International Journal of Osteoarchaeology*, 20(2), pp. 227–239. doi: 10.1002/oa.1026.

Michopoulou, E., Negre, P., Nikita, E. and Kranioti, E. F. (2017) 'The auricular surface as age indicator in a modern Greek sample: A test of two qualitative methods', *Forensic Science International*, 280, p. 246.e1-246.e7. doi: 10.1016/j.forsciint.2017.08.004.

Milner, G. and Boldsen, J. (2012) 'Skeletal Age Estimation: Where We Are and Where We Should Go', in Dirkmaat (ed.) *A companion to forensic anthropology*. West Sussex: Wiley-Blackwell, pp. 224–238.

Milovanovic, P., Zimmermann, E. A., Hahn, M., Djonic, D., Püschel, K., Djuric, M., Amling, M. and Busse, B. (2013) 'Osteocytic canalicular networks: Morphological implications for altered mechanosensitivity', *American Chemical Society Nano*, 7(9), pp. 7542–7551. doi: 10.1021/nn401360u.

Miranker, M. (2016) 'A comparison of different age estimation methods of the adult pelvis', *Journal of Forensic Sciences*, 61(5). doi: 10.1111/1556-4029.13130.

Morseth, B., Emaus, N. and Jørgensen, L. (2011) 'Physical activity and bone: The importance

of the various mechanical stimuli for bone mineral density. A review', *Norsk Epidemiologi*, 20(2), pp. 173–178.

Mukaka, M. M. (2012) 'Statistics corner: A guide to appropriate use of correlation coefficient in medical research', *Malawi Medical Journal*, 24(3), pp. 69–71. doi: 10.1016/j.cmpb.2016.01.020.

Mulhern, D. M. (2000) 'Rib remodeling dynamics in a skeletal population from Kulubnarti, Nubia', *American Journal of Physical Anthropology*, 111(4), pp. 519–530. doi: 10.1002/(SICI)1096-8644(200004)111:4<519::AID-AJPA7>3.0.CO;2-7.

Mulhern, D. M. and Jones, E. B. (2005) 'Test of revised method of age estimation from the auricular surface of the ilium', *American Journal of Physical Anthropology*, 126(1), pp. 61–65. doi: 10.1002/ajpa.10410.

Nakamura, E. (1991) 'A study on the basic nature of human biological aging processes based upon a hierarchical factor solution of the age-related physiological variables', *Mechanisms of Ageing and Development*, 60(2), pp. 153–170. doi: 10.1016/0047-6374(91)90128-M.

Narasaki, S. (1990) 'Estimation of age at death by femoral osteon remodeling: application of Thompson's core technique to modern Japanese', *Journal of the Anthropological Society of Nippon*, (98), pp. 29–38.

Nathena, D., Gambaro, L., Tzanakis, N., Michalodimitrakis, M. and Kranioti, E. F. (2015) 'Sexual dimorphism of the metacarpals in contemporary Cretans : Are there differences with mainland Greeks ?', *Forensic Science International*, 257, pp. 1–8.

Nawrocki, S. (1998) 'Regression formulae for the estimation of age from cranial suture closure', in Reichs, K. (ed.) *Forensic Osteology: Advances in the Identification of Human Remains*. 2nd edn. Springfield: Charles C. Thomas, pp. 276–292.

Nawrocki, S. (2010) 'The nature and sources of error in the estimation of age at death from the skeleton', in Krista, E. and Finnegan, M. (eds) *Age estimation of the human skeleton*. Springfield: Charles C Thomas.

Nelson, D. A., Feingold, M., Bolin, F. and Parfitt, A. M. (1991) 'Principal components analysis of regional bone density in black and white women: Relationship to body size and composition', *American Journal of Physical Anthropology*, 86, pp. 507–514.

Nelson, D. a, Pettifor, J. M., Barondess, D. a, Cody, D. D., Uusi-Rasi, K. and Beck, T. J. (2004) 'Comparison of cross-sectional geometry of the proximal femur in white and black women from Detroit and Johannesburg', *Journal of bone and mineral research*, 19(4), pp. 560–5. doi: 10.1359/JBMR.040104.

Nesbitt, S. and Horton, M. (1997) 'Trafficking of matrix collagens through bone-resorbing osteoclasts', *Science*, 276(5310), pp. 266–269.

Noble, B. S. and Reeve, J. (2000) 'Osteocyte function, osteocyte death and bone fracture resistance', *Molecular and Cellular Endocrinology*, 159(1–2), pp. 7–13. doi: 10.1016/S0303-7207(99)00174-4.

Nor, F. M., Pastor, R. F. and Schutkowski, H. (2014) 'Age at death estimation from bone histology in Malaysian males', *Medicine, Science, and the Law*, 54(4), pp. 203–8. doi: 10.1177/0025802413506573.

O'Brien, R. M. (2007) 'A caution regarding rules of thumb for variance inflation factors',

Quality and Quantity, 41(5), pp. 673–690. doi: 10.1007/s11135-006-9018-6.

O'Connor, J. E., Bogue, C., Spence, L. D. and Last, J. (2008) 'A method to establish the relationship between chronological age and stage of union from radiographic assessment of epiphyseal fusion at the knee: An Irish population study', *Journal of Anatomy*, 212(2), pp. 198–209. doi: 10.1111/j.1469-7580.2007.00847.x.

Van Oers, R. F. M., Ruimerman, R., van Rietbergen, B., Hilbers, P. A. J. and Huiskes, R. (2008) 'Relating osteon diameter to strain', *Bone*, 43(3), pp. 476–482. doi: 10.1016/j.bone.2008.05.015.

Oftadeh, R., Perez-Viloria, M., Villa-Camacho, J., Vaziri, A. and Nazarian, A. (2015) 'Biomechanics and mechanobiology of trabecular bone: a review', *Journal of Biomechanical Engineering*, 137(1), pp. 108021–1080215.

Olszta, M. J., Cheng, X., Jee, S. S., Kumar, R., Kim, Y. Y., Kaufman, M. J., Douglas, E. P. and Gower, L. B. (2007) 'Bone structure and formation: A new perspective', *Materials Science and Engineering: R: Reports*, 58(3–5), pp. 77–116. doi: 10.1016/j.mser.2007.05.001.

Ombregt, L. (2013) 'Applied anatomy of the thorax and abdomen', in *A System of Orthopaedic Medicine*. 3rd ed. Churchill Livingstone Elsevier, pp. e157–e168. doi: 10.1016/B978-0-7020-3145-8.00075-2.

De Onis, M. (2006) 'Reliability of anthropometric measurements in the WHO Multicentre Growth Reference Study', *Acta Paediatrica, International Journal of Paediatrics*, 95(SUPPL. 450), pp. 38–46. doi: 10.1080/08035320500494464.

Ortner, D. (2003) *Identification of pathological conditions in human skeletal remains.* 2nd edn. U.S.A.: Academic Press.

Ortner, D. J. (1970) *The effects of aging and disease on the micromorphology of human compact bone*. University of Kansas, Lawrence.

Ortner, D. J. (1975) 'Aging effects on osteon remodeling', *Calcified Tissue Researchssue research*, 18, pp. 27–36. doi: 10.1007/BF02546224.

Ortner, D. and Turner-Walker, G. (2003) 'The Biology of Skeletal Tissues', in *Identification of pathological conditions in human skeletal remains*. 2nd edn. U.S.A.: Acedmic Press, pp. 11–36.

Osipov, B., Harvati, K., Nathena, D., Spanakis, K., Karantanas, A. and Kranioti, E. F. (2013) 'Sexual dimorphism of the bony labyrinth: A new age-independent method', *American Journal of Physical Anthropology*, 151(2), pp. 290–301. doi: 10.1002/ajpa.22279.

Oursler, M., Kassem, M., Turner, R., Riggs, B. and Spelsberg, T. (2008) 'Regulation of bone cell function by gonadal steroids', in Marcus, R., Feldman, D., Nelson, D., and Rosen, C. (eds) *Osteoporosis*. 3rd edn. New York: Academic Press, pp. 237–260.

Paine, R. R. (2007) 'How to equip a basic histological lab for the anthropological assessment of human bone and teeth', *Journal of Anthropological Sciences*, 85, pp. 213–219.

Paine, R. R. and Brenton, B. P. (2006a) 'Dietary health does affect histological age assessment: An evaluation of the Stout and Paine (1992) age estimation equation using secondary osteons from the rib', *Journal of Forensic Sciences*, 51(3), pp. 489–492. doi: 10.1111/j.1556-4029.2006.00118.x.

Paine, R. R. and Brenton, B. P. (2006b) 'The paleopathology of pellagra: investigating the

impact of prehistoric and historical dietary transitions to maize', *Journal of Anthropological Sciences*, 84, pp. 125–135. Available at: http://www.isita-org.com/jass/Contents/2006 vol84/Jass2006Final/08-PAINE_BRENTON.pdf.

Panagides, S. S. (1967) *An econometric study of the Cyprus economy*. Iowa State University.

Pankovich, A., Simmons, D. and Kulkarni, V. (1974) 'Zonal Osteons in Cortical Bone', *Clinical orthopaedics and related research*, (100), pp. 356–363.

Papadakis, Y., Peristianis, N. and Welz, G. (2006) *Divided Cyprus : modernity, history, and an island in conflict*. Bloomington : Indiana University Pres.

Parfitt, A. M. (1979) 'Quantum concept of bone remodeling and turnover: implications for the pathogenesis of osteoporosis', *Calcified tissue international*, 28(1), pp. 1–5. doi: 10.1007/BF02441211.

Parfitt, A. M. (1988) 'Bone histomorphometry: Standardization of nomenclature, symbols and units (summary of proposed system)', *Bone*, 9(1), pp. 67–69. doi: 10.1016/8756-3282(88)90029-4.

Parfitt, A. M. (1993) 'Morphometry of bone resorption: Introduction and overview', *Bone*, 14(3), pp. 435–441. doi: 10.1016/8756-3282(93)90176-B.

Parfitt, A. M. (2002) 'Targeted and non-targeted bone remodeling: Relationship to basic multicellular unit origination and progression', *Bone*, 30(1), pp. 5–7. doi: 10.1016/S8756-3282(01)00642-1.

Parfitt, A. M. (2004) 'The attainment of peak bone mass: What is the relationship between muscle growth and bone growth?', *Bone*, 34(5), pp. 767–770. doi: 10.1016/j.bone.2004.01.023.

Parfitt, A. M., Drezner, M., Glorieux, F., Kanis, J., Malluche, H., Meunier, P., Ott, S. and Recker, R. (1987) 'Bone Histomorphometry: Standarization of nomenclature, symbols and units', *Journal of Bone and Mineral Research*, (6), pp. 595–610.

Pavón, M. V. (2007) *Indicadores estándares de edad basados en análisis histomorfométricos de la cuarta costilla desarrollados en muestras forenses del Estado de Yucatán, México.* Universidad Autonoma de Yucatán.

Pavón, M. V., Cucina, A. and Tiesler, V. (2010) 'New formulas to estimate age at death in Maya populations using histomorphological changes in the fourth human rib', *Journal of Forensic Sciences*, 55(2), pp. 473–477. doi: 10.1111/j.1556-4029.2009.01265.x.

Peck, J. J. and Stout, S. D. (2009) 'The effects of total hip arthroplasty on the structural and biomechanical properties of adult bone', *American Journal of Physical Anthropology*, 138(2), pp. 221–230. doi: 10.1002/ajpa.20921.

Peck, J. and Stout, S. (2007) 'Intraskeletal Variability in Bone Mass', *American Journal of Physical Anthropology*, (89–97). doi: 10.1002/ajpa.

Pfeiffer, S. (1998) 'Variability in osteon size in recent human populations', *American Journal of Physical Anthropology*, 106(2), pp. 219–227. doi: 10.1002/(SICI)1096-8644(199806)106:2<219::AID-AJPA8>3.0.CO;2-K.

Pfeiffer, S., Crowder, C. M., Harrington, L. and Brown, M. (2006) 'Secondary osteon and Haversian canal dimensions as behavioural indicators', *American Journal of physical anthropo*, 131(4), pp. 460–468. doi: 10.1002/ajpa.

Pfeiffer, S., Lazenby, R. and Chiang, J. (1995) 'Brief communication: Cortical remodeling data are affected by sampling location', *American Journal of Physical Anthropology*, 96(1), pp. 89–92. doi: 10.1002/ajpa.1330960110.

Pfeiffer, S. and Zehr, M. (1996) 'A morphological and histological study of the human humerus from Border Cave', *Journal of Human Evolution*, (31), pp. 49–59.

Pfeiffer, S., Heinrich, J., Beresheim, A. and Alblas, M. (2016) 'Cortical bone histomorphology of known-age skeletons from the Kirsten collection, Stellenbosch university, South Africa', *American Journal of Physical Anthropology*, 147(February), pp. 137–147. doi: 10.1002/ajpa.22951.

Pocock, N. A., Eisman, J. A., Hopper, J. L., Yeates, M. G., Sambrook, P. N. and Eberl, S. (1987) 'Genetic determinants of bone mass in adults: A twin study', *Journal of Clinical Investigation*, 80(3), pp. 706–710. doi: 10.1172/jci113125.

Pollitzer, S. and Anderson, J. (1989) 'Special Ethnic and genetic differences in bone mass : hereditary vs environmental Articles a review with a', *American Journal of Clinical Nutrition*, 50, pp. 1244–1259.

Poole, K., Bezooijen, R., Loveridge, N., Hamersma, H., Papapoulos, S., Löwik, C. and Reeve, J. (2005) 'Sclerostin is a delayed secreted product of osteocytes that inhibits bone formation', *FASEB*, (19), pp. 1842–1844.

Porrini, M. (2013) 'Is the Mediterranean diet the best ne in Europe?', in *Annals of Nutrition and Metabolism*. Granada, Spain, p. 115.

Pratte, D. G. and Pfeiffer, S. (1999) 'Histological age estimation of a cadaveral sample of diverse origins', *Journal of the Canadian Society of Forensic Science*, 32(4), pp. 155–167. doi: 10.1080/00085030.1999.10757496.

Qiu, S., Fyhrie, D. P., Palnitkar, S. and Rao, D. S. (2003) 'Histomorphometric assessment of Haversian canal and osteocyte lacunae in different-sized osteons in human rib.', *The Anatomical Record. Part A, Discoveries in molecular, cellular, and evolutionary biology*, 272(2), pp. 520–525. doi: 10.1002/ar.a.10058.

Qiu, S., Rao, D. S., Palnitkar, S. and Parfitt, A. M. (2010) 'Dependence of bone yield (volume of bone formed per unit of cement surface area) on resorption cavity size during osteonal remodeling in human rib: implications for osteoblast function and the pathogenesis of age-related bone loss', *Journal of Bone and Mineral Research*, 25(2), pp. 423–430. doi: 10.1359/jbmr.091003.

Raisz, L. G. (2005) 'Pathogenesis of osteoporosis : concepts , conflicts , and prospects', *Science in Medicine*, 115(12). doi: 10.1172/JCI27071.3318.

Rasband, W. (2000) *https://imagej.nih.gov/ij/plugins/circularity.html*.

Recker, R., Lappe, J., Davies, K. M. and Heaney, R. (2004) 'Bone Remodeling Increases Substantially in the Years After Menopause and Remains Increased in Older Osteoporosis Patients', *Journal of Bone and Mineral Research*, 19(10), pp. 1628–1633. doi: 10.1359/JBMR.040710.

Rey, C., Combes, C., Drouet, C. and Glimcher, M. J. (2009) 'Bone mineral: Update on chemical composition and structure', *Osteoporosis International*, 20(6), pp. 1013–1021. doi: 10.1007/s00198-009-0860-y.

Reznikov, N., Shahar, R. and Weiner, S. (2014a) 'Bone hierarchical structure in three

dimensions', *Acta Biomaterialia*, 10(9), pp. 3815–3826. doi: 10.1016/j.actbio.2014.05.024.

Reznikov, N., Shahar, R. and Weiner, S. (2014b) 'Three-dimensional structure of human lamellar bone: The presence of two different materials and new insights into the hierarchical organization', *Bone*, 59, pp. 93–104. doi: 10.1016/j.bone.2013.10.023.

Rho, J. Y., Kuhn-Spearing, L. and Zioupos, P. (1998) 'Mechanical properties and the hierarchical structure of bone', *Medical Engineering and Physics*, 20(2), pp. 92–102. doi: 10.1016/S1350-4533(98)00007-1.

Richman, E. A., Ortner, D. J. and Schulter-Ellis, F. P. (1979) 'Differences in intracortical bone remodeling in three aboriginal American populations: Possible dietary factors', *Calcified Tissue International*, 28(1), pp. 209–214. doi: 10.1007/BF02441238.

Riggs, B. L., Khosla, S. and Melton, L. J. (1998) 'A unitary model for involutional osteoporosis: estrogen deficiency causes both type I and type II osteoporosis in postmenopausal women and contributes to bone loss in aging men', *Journal of bone and mineral*, 13(5), pp. 763–73. doi: 10.1359/jbmr.1998.13.5.763.

Riggs, B. L., Melton, L. J., Robb, R. A., Camp, J. J., Atkinson, E. J., Peterson, J. M., Rouleau, P. A., McCollough, C. H., Bouxsein, M. L. and Khosla, S. (2004) 'Population-Based study of age and sex differences in bone volumetric density, size, geometry, and structure at different skeletal sites', *Journal of Bone and Mineral Research*, 19(12), pp. 1945–1954. doi: 10.1359/jbmr.040916.

Ritz-Timme, S., Cattaneo, C., Collins, M., Waite, E., Shütz, H., Kaatsch, H. and Borrman, H. (2000) 'Age estimation : The state of the art in relation to the specific demands of forensic practise', *International Journal of Legal Medicine*, 113(3), pp. 129–136.

Roberts, S. B. and Chen, P. H. (1972) 'Global geometric characteristics of typical human ribs', *Journal of Biomechanics*, 5(2), pp. 191–201. doi: 10.1016/0021-9290(72)90055-3.

Robling, A. (1998) *Histomorphometric assessment of mechanical loading history from human skeletal remains: The relation between micromorphology and macromorphology at the femoral midshaft.* University of Missouri, Columbia.

Robling, A. G. and Stout, S. D. (1999) 'Morphology of the drifting osteon', *Cells Tissues Organs*, 164(4), pp. 192–204. doi: 10.1159/000016659.

Robling, A. G. and Stout, S. D. (2008) 'Histomorphometry of human cortical bone: applications to age estimation', in Katzenberg, M. and S. S. (ed.) *Biological Anthropology of the Human Skeleton*. 2nd edn. New Yersey: Wiley-Liss, pp. 149–182.

Robling, A. G., Fuchs, R. K. and Burr, D. B. (2013) 'Mechanical adaptation', in Burr, D. B. and Allen, M. R. (eds) *Basic and applied bone biology*. London: Academic Press, pp. 175–204.

Rodan, G. A. and Martin, T. J. (1981) 'Role of osteoblasts in hormonal control of bone resorption-A hypothesis', *Calcified Tissue International*, 33(1), pp. 349–351. doi: 10.1007/BF02409454.

Rogers, N. and Stout, S. (1998) 'Selecting a calibration method to reduce bias in histological aging methods', *American Journal of Physical Anthropology*, 105(s26), p. 191.

Rose, D. C., Agnew, A. M., Gocha, T. P., Stout, S. D. and Field, J. S. (2012) 'Technical note: The use of geographical information systems software for the spatial analysis of bone

microstructure', *American Journal of Physical Anthropology*, 148(4), pp. 648–654. doi: 10.1002/ajpa.22099.

Rösing, F. W., Graw, M., Marré, B., Ritz-Timme, S., Rothschild, M. A., Rötzscher, K., Schmeling, A., Schröder, I. and Geserick, G. (2007) 'Recommendations for the forensic diagnosis of sex and age from skeletons', *Journal of Comparative Human Biology*, 58(1), pp. 75–89. doi: 10.1016/j.jchb.2005.07.002.

RStudio Team (2015) 'RStudio: Integrated Development for R. RStudio'. Inc., Boston, MA. Available at: http://www.rstudio.com.

Ruff, C. B. (2008) 'Biomechanical analysis of archaeological human skeletons', in Katzenberg, M. and Saunders, S. (eds) *Biological Anthropology of the Human Skeleton*. 2nd edn. USA: Willey-Liss, pp. 183–206.

Ruff, C. B., Larsen, C. S. and Hayes, W. C. (1984) 'Structural changes in the femur with the transition to agriculture on the Georgia coast', *American Journal of Physical Anthropology*, 64(2), pp. 125–136. doi: 10.1002/ajpa.1330640205.

Ruff, C., Holt, B. and Trinkaus, E. (2006) 'Who's Afraid of the Big Bad Wolff?: "'Wolff's Law"' and Bone Functional Adaptation', *American Journal of Physical Anthropology*, 129, pp. 484–498. doi: 10.1002/ajpa.

Russo, C. R., Lauretani, F., Seeman, E., Bartali, B., Bandinelli, S., Di Iorio, A., Guralnik, J. and Ferrucci, L. (2006) 'Structural adaptations to bone loss in aging men and women', *Bone*, 38(1), pp. 112–118. doi: 10.1016/j.bone.2005.07.025.

Ryan, T. M. and Shaw, C. N. (2015) 'Gracility of the modern *Homo sapiens* skeleton is the result of decreased biomechanical loading', *Proceedings of the National Academy of Sciences*, 112(2), pp. 372–377. doi: 10.1073/pnas.1418646112.

Safadi, F., Barbe, M., Abdelmagid, S., Rico, M., Aswad, R., Litvin, J. and Popoff, S. (2009) 'Bone structure, development and bone biology', in Khurana, J. S. (ed.) *Bone Pathology*. 2nd edn. Humana Press, pp. 1–50. doi: 10.1007/978-1-59745-347-9.

Saker, E., Graham, R. A., Nicholas, R., D'Antoni, A. V, Loukas, M., Oskouian, R. J. and Tubbs, R. S. (2016) 'Ligaments of the costovertebral joints including biomechanics, innervations, and clinical applications', *Cureus*, 8(11), p. e874. doi: 10.7759/cureus.874.

Salo, J., Lehenkari, P., Mulari, M., Metsikkö, K. and Väänänen, H. (1997) 'Removal of osteoclast bone resorption products by transcytosis', *Science*, 276(5310), pp. 270–273.

Samson, D. and Branigan, K. (1987) 'A new method of estimating age at death from fragmentary and weathered bone', in Bodington, A., Garland, A., and JAnaway, R. (eds) *Death, decay, and reconstruction: approaches to archaeology and forensic science*. Great Britain: Manchester University Press, pp. 101–108.

Samworth, R. and Gowland, R. (2007) 'Estimation of adult skeletal age-at-death: Statistical assumptions and applications', *International Journal of Osteoarchaeology*, 17(2), pp. 174–188. doi: 10.1002/oa.867.

Savall, F., Rérolle, C., Hérin, F., Dédouit, F., Rougé, D., Telmon, N. and Saint-Martin, P. (2015) 'Reliability of the Suchey-Brooks method for a French contemporary population', *Forensic Science International*, 266, pp. 1–5. doi: 10.1016/j.forsciint.2016.04.030.

Schaefer, M. C. and Black, S. M. (2005) 'Comparison of ages of epiphyseal union in North American and Bosnian skeletal material', *Journal of forensic sciences*, 50(4), pp. 777–784.

doi: 10.1520/JFS2004497.

Schaffler, M. B., Burr, D. B. and Frederickson, R. G. (1987) 'Morphology of the osteonal cement line in human bone', *The Anatomical Record*, 217(3), pp. 223–228. doi: 10.1002/ar.1092170302.

Schaffler, M. B., Choi, K. and Milgrom, C. (1995) 'Aging and matrix microdamage accumulation in human compact bone', *Bone*, 17(6), pp. 521–525. doi: 10.1016/8756-3282(95)00370-3.

Scheuer, L. and Black, S. (2004) *The juvenile skeleton*. London: Elsevier Academic Press.

Schinke, T. and Karsenty, G. (2008) 'Transcriptional Control of Osteoblast Differentiation', in Bilezikian, J., Lawrence, G., and Martin, T. (eds) *Principles of Bone Biology*. 3rd edn. U.S.A.: Academic Press, pp. 205–217. doi: 10.1210/endo.142.7.8306.

Schneider, C., Rasband, W. and Eliceiri, K. (2012) 'NIH Image to ImageJ: 25 years of image analysis', *Nature Methods*, 9, pp. 671–675.

Schnitzler, C. M. (1993) 'Bone quality: A determinant for certain risk factors for bone fragility', *Calcified Tissue International*, 53(SUPPL.1). doi: 10.1007/BF01673398.

Schoenau, E., Saggese, G., Peter, F., Baroncelli, G. I., Shaw, N. J., Crabtree, N. J., Zadik, Z., Neu, C. M., Noordam, C., Radetti, G. and Hochberg, Z. (2004) 'From bone biology to bone analysis', *Hormone Research*, 61(6), pp. 257–269. doi: 10.1159/000076635.

Schultz, J. J. (2012) 'Determining the forensic significance of skeletal remains', in Dirkmaat, D. (ed.) *A companion to forensic anthropology*. West Sussex: Wiley-Blackwell, pp. 66–84.

Schwarz, G. (1978) 'Estimating the dimension of a model', *Annals of Statistics*, (6), pp. 461–464.

Scientific Working Group for Forensic Anthropology (2010) *Age Estimation Revision*.

Sedlin, E. D., Frost, H. M. and Villanueva, A. R. (1963) 'Age changes in resorption in human rib cortex', *Journal of Gerontology*, 18(4), pp. 345–349. doi: 10.1093/geronj/18.4.345.

Seeman, E. (2001) 'During aging, men lose less bone than women because they gain more periosteal bone, not because they resorb less endosteal bone', *Calcified Tissue International*, 69(4), pp. 205–208. doi: 10.1007/s00223-001-1040-z.

Seeman, E. (2008) 'Structural basis of growth-related gain and age-related loss of bone strength', *Rheumatology*, 47(SUPPL. 4), pp. 2–8. doi: 10.1093/rheumatology/ken177.

Shapiro, A. S. S. and Wilk, M. B. (1965) 'An analysis of variance test for normality (complete samples', *Biometrika*, 52(3), pp. 591–611.

Singh, I. (1978) 'The architecture of cancellous bone', *Journal of Anatomy*, 127(2), pp. 305–310.

Singh, I. J. and Gunberg, D. L. (1970) 'Estimation of age at death in human males from quantitative histology of bone fragments', *American Journal of Physical Anthropology*, 33(3), pp. 373–381. doi: 10.1002/ajpa.1330330311.

Skedros, J. (2012) 'Interpreting load history in limb-bone diaphyses: important considerations and their biomechanical foundations', in Crowder, C. and Stout, S. (eds) *Bone Histology: An anthropological perspective*. Boca Raton: CRC Press Taylor and Francis Group, pp. 153–220.

Skedros, J. G., Holmes, J. L., Vajda, E. G. and Bloebaum, R. D. (2005) 'Cement lines of secondary osteons in human bone are not mineral-deficient: New data in a historical perspective', *Anatomical Record*, 286(1), pp. 781–803. doi: 10.1002/ar.a.20214.

Smith, R. J. (1993) 'Logarithmic transformation bias in allometry', *American Journal of Physical Anthropology*, 90(2), pp. 215–228. doi: 10.1002/ajpa.1330900208.

Smithson, M. (2001) 'Correct confidence intervals for various regression effect sizes and parameters: The importance of non-central distribution in computing intervals', *Educational and Psychological Measurement*, 61(4), pp. 605–632.

Sobol, J., Ptaszyñska-Sarosiek, I., Charuta, A., Oklota-Horba, M., Zaba, C. Z. and Niemcunowicz-Janica, A. (2015) 'Estimation of age at death: Examination of variation in cortical bone histology within the human clavicle', *Folia Morphologica (Poland)*, 74(3), pp. 378–388. doi: 10.5603/FM.2015.0021.

Solsten, E. (1991) *Cyprus: A country study*. Edited by F. Bunge. Washington DC: Federal Research Division, Library of Congress.

Squillante, R. G. and Williams, J. L. (1993) 'Videodensitometry of osteons in females with femoral neck fractures', *Calcified Tissue International*, 52(4), pp. 273–277. doi: 10.1007/BF00296651.

Steadman, D., Diantonio, L., Wilson, J., Sheridan, K. and Tammariello, S. (2006) 'The Effects of Chemical and Heat Maceration Techniques on the Recovery of Nuclear and Mitochondrial DNA from Bone Ã', *Journal of Forensic Sciences*, 51(1), pp. 11–17. doi: 10.1111/j.1556-4029.2005.00001.x.

Stein, K. W. H. and Sander, M. (2009) 'Histological core drilling: a less destructive method for studying bone histology', *In fossil preparation: proceedings of the first annual fossil preparation and collections symposium*, (October), pp. 69–80.

Stein, E. M., Dempster, D. W., Udesky, J., Zhou, H., Bilezikian, J. P., Shane, E. and Silverberg, S. J. (2011) 'Vitamin D deficiency influences histomorphometric features of bone in primary hyperparathyroidism', *Bone*, 48(3), pp. 557–561. doi: 10.1016/j.bone.2010.10.004.

Stewart, M. C., Goliath, J. R. and Stout, S. A. M. D. (2015) 'Intraskeletal Variability of Relative Cortical Area in Humans', *The anatomical Record*, 1643(298), pp. 1635–1643. doi: 10.1002/ar.23181.

Stewart, M. C., McCormick, L. E., Goliath, J. R., Sciulli, P. W. and Stout, S. D. (2013) 'A Comparison of Histomorphometric Data Collection Methods', *Journal of Forensic Sciences*, 58(1), pp. 109–113. doi: 10.1111/j.1556-4029.2012.02195.x.

Stock, J., Pfeiffer, S. (2001) 'Linking structural variability in long bone daiphyses to habitual behaviors: Forager from the Sother African Later Stone Age and the Andaman Islands', *American Journal of Physical Anthropology*, 115(4), pp. 337–348. doi: 10.1002/ajpa.1090.

Stout, S. D. (1986) 'The use of bone histomorphometry in skeletal identification: the case of Francisco Pizarro', *J Forensic Sci*, 31(1), pp. 296–300.

Stout, S. D. (1988) 'The use of histomorphology to estimate age', *J Forensic Sci*, 33(1), pp. 121–125.

Stout, S. D. (1989) 'Histomorphometric analysis of human skeletal remains', in Kenedy, K. A. R. (ed.) *Reconstruction of life from the skeleton*. New York: Alan R. Liss, pp. 41–52.

Stout, S. D. (1998) 'The Application of Histological techniques for Age at death Determination', in Reichs, J. (ed.) *Forensic Osteology: Advances in the Identification of Human Remains*. Springfield, Illinois: Charles C. Thomas, pp. 237–252.

Stout, S. D. and Teitelbaum, S. L. (1976) 'Histological analysis of undecalcified thin sections of archaeological bone', *American Journal of Physical Anthropology*, 44, pp. 263–270.

Stout, S. D. and Gehlert, S. J. (1980) 'The relative accuracy and reliability of histological aging methods', *Forensic Science International*, 15, pp. 181–190.

Stout, S. D. and Gehlert, S. J. (1982) 'Effects of field size when using Kerley's histological method for determination of age at death', *American Journal of Physical Anthropology*, 58(2), pp. 123–125. doi: 10.1002/ajpa.1330580203.

Stout, S. D. and Jackson (1990) 'Comparative cortical bone histomorphometry in ancient populations', in *Para conocer al hombre, Homenaje a Santiago Genovés*. Mexico: Dirección General de Publicaciones, Universidad de Mexico, pp. 273–280.

Stout, S. D. and Stanley, S. C. (1991) 'Percent osteonal bone versus osteon counts: The variable of choice for estimating age at death', *American Journal of Physical Anthropology*, 86(4), pp. 515–519. doi: 10.1002/ajpa.1330860407.

Stout, S. D. and Paine, R. (1992) 'Brief communication: Histological age estimation using rib and clavicle', *American Journal of Physical Anthropology*, 87(1), pp. 111–115.

Stout, S. D., Dietze, W. H., Iscan, M. Y. and Loth, S. R. (1994) 'Estimation of age at death using cortical histomorphometry of the sternal end of the fourth rib', *Journal of Forensic Sciences*, 39(3), pp. 778–784.

Stout, S. D. and Lueck, R. (1995) 'Bone remodeling rates and skeletal maturation in three archaeological skeletal populations', *American Journal of Physical Anthropology*, 98(2), pp. 161–171. doi: 10.1002/ajpa.1330980206.

Stout, S. D., Porro, M. A. and Perotti, B. (1996) 'Brief Communication: A test and correction of the clavicle method for histological age determination of skeletal remains', *American Journal of Physical Anthropology*, 100(1), pp. 139–142.

Stout, S. D., Brunsden, B. S., Hildebolt, C. F., Commean, P. K., Smith, K. E. and Tappen, N. C. (1999) 'Computer-assisted 3D reconstruction of serial sections of cortical bone to determine the 3D structure of osteons', *Calcified Tissue International*, 65(4), pp. 280–284. doi: 10.1007/s002239900699.

Stout, S. D. and Crowder, C. (2012) 'Bone remodeling, histomorphology and histomormetry', in Crowder, C. and Stout, S. D. (eds) *Bone Biology. An anthropological perspective*. U.S.A.: CRC Press, pp. 1–22.

Stoyanova, D., Algee-Hewitt, B. F. B. and Slice, D. E. (2015) 'An enhanced computational method for age-at-death estimation based on the pubic symphysis using 3D laser scans and thin plate splines', *American Journal of Physical Anthropology*, 158(3), pp. 431–440. doi: 10.1002/ajpa.22797.

Streeter, M. (2005) *Histomorphometric characteristics of the subadult rib cortex:normal patterns of dynamic bone modeling and remodeling during growth and development*. University of Missouri, Columbia.

Streeter, M. (2012) 'Histological Age-at-death estimation', in Crowder, C. M. and Stout, S. D. (eds) *Book Histology. An anthropological perspective*. U.S.A.: CRC Press, pp. 135–152.

Suzuki, R., Domon, T. and Wakita, M. (2000) 'Some osteocytes released from their lacunae are embedded again in the bone and not engulfed by osteoclasts during bone remodeling', *Anatomy and Embryology*, pp. 119–128.

Suzuki, S., Cucina, A., Tiesler, V. and Sosa, T. S. (2009) 'Morir en xcambo: evaluación de la mortalidad en un sitio costero maya del clásico a partir del análisis histomorfológico', in *XXII Simposio de Investigaciones Arqueológicas en Guatemala*, pp. 853–864.

Szulc, P., Seeman, E., Duboeuf, F., Sornay-Rendu, E. and Delmas, P. D. (2006) 'Bone fragility: failure of periosteal apposition to compensate for increased endocortical resorption in postmenopausal women.', *Journal of Bone and Mineral Research*, 21(12), pp. 1856–63. doi: 10.1359/jbmr.060904.

Tabachnick, B. and Fidell, L. (2007) *Using mulivariate statistics*. 5th ed. London: Boston, Mass. ; London : Allyn & Bacon.

Tabachnick, B. and Fidell, L. (2014) 'Analysis of covariate', in *Using Multivairate Statistics*. 6th ed. Harlow, Essex, England : Pearson: Pearson, pp. 235–284.

Takahashi, H. and Frost, H. M. (1966) 'Age and sex related changes in the amount of cortex of normal human ribs', *Acta Orthopaedica Scandinavica*, 37(March), pp. 122–130. doi: 10.3109/17453676608993272.

Tanner, J. (1978) *Fetus into man: physical growth from conception to maturity*. Cambridge, MA: Harvard University Press.

Tersigni, M. A. (2005) *Serial long bone histology: inter- and intra-bone age estimation*. University of Tennessee, Knoxville.

Thibodeau, G. and Patton, K. (2007) 'Organization of the body', in *Anatomy & physiology*. 6th edn. St. Louis: Mosby Elsevier, pp. 5–27. Available at: http://trove.nla.gov.au/work/6529284?q&sort=holdings+desc&_=1502203568384&versionId=210616029+227534189.

Thomas, C. D., Stein, M. S., Feik, S. a, Wark, J. D. and Clement, J. G. (2000) 'Determination of age at death using combined morphology and histology of the femur.', *Journal of anatomy*, 196 (Pt 3, pp. 463–471. doi: 10.1046/j.1469-7580.2000.19630463.x.

Thompson, D. D. (1979) 'The Core Technique in the Determination of Age at Death in Skeletons', *Journal of forensic sciencess*, 24(4), pp. 902–915.

Thompson, D. D. (1980) 'Age changes in bone mineralization, cortical thickness, and haversian canal area', *Calcified Tissue International*, 31, pp. 5–11.

Thompson, D. D. and Gunness-Hey, M. (1981) 'Bone mineral-osteon analysis of Yupi k-Inupiaq skeletons', *American Journal of Physical Anthropology*, 55(1), pp. 1–7.

Thompson, D. D. and Galvin, C. A. (1983) 'Estimation of Age At Death By Tibial Osteon Remodeling in an Autopsy Series', *Forensic Science International*, 22(2–3), pp. 203–211. doi: 10.1016/0379-0738(83)90015-4.

Tiesler, V., Cucina, A. and Streeter, M. (2006) *Manual de Histomorfologia en hueso no decalcificado*. Mérida, México: Universidad Autónoma de Yucatán.

Todd, T. W. (1920) 'Age changes in the pubic bone. I. The male white pubis', *American Journal of Physical Anthropology*, 3(3), pp. 285–334. doi: 10.1002/ajpa.1330030301.

Todd, RB, Bowman, W. (1857) *The physiological anatomy and the physiology of man*. Philadelphia: Blanchard and Lea.

Tomes, J. and De Morgan, C. (1853) 'Observations on the structure and development of bone', *Philosophical Transactions of the Royal Society of London*, (143), pp. 109–139.

Tommerup, J., Raab, D., Crensha, T. and Smith, E. (1993) 'Does weight-bearing exercise affect non-weight-bearing bone?', *Journal of Bone and Mineral Research*, 8(9), pp. 1053–1058.

Trammell, L. H. and Kroman, A. M. (2013) 'Bone and dental histology', in DiGangi, A. and Moore, M. (eds) *Research methods in human skeletal biology*. Oxford: Elsevier, pp. 361–395. doi: 10.1016/B978-0-12-385189-5.00013-3.

Travan, L., Saccheri, P., Gregoraci, G., Mardegan, C. and Crivellato, E. (2015) 'Normal anatomy and anatomic variants of vascular foramens in the cervical vertebrae: a paleo-osteological study and review of the literature', *Anatomical Science International*. Springer Japan, 90(4), pp. 308–323. doi: 10.1007/s12565-014-0270-x.

Tsiminikaki, K., Karell, M., Halazonetis, D. and Kranioti, E. (2017) 'Pair-matching phalanges using an automated digital Mesh-to-Mesh Value Comparison method', *La Revue de Médecine Légale*, 8(4), pp. 191–192.

Turner, C. H. (1999) 'Toward a mathematical description of bone biology: The principle of cellular accommodation', *Calcified Tissue International*, 65(6), pp. 466–471. doi: 10.1007/s002239900734.

Turner, C. H. and Pavalko, F. M. (1998) 'Mechanotransduction and functional response of the skeleton to physical stress: The mechanisms and mechanics of bone adaptation', *Journal of Orthopaedic Science*, 3(6), pp. 346–355. doi: 10.1007/s007760050064.

Turner, C. H., Robling, A. G., Duncan, R. L. and Burr, D. B. (2002) 'Do bone cells behave like a neuronal network?', *Calcified Tissue International*, 70(6), pp. 435–442. doi: 10.1007/s00223-001-1024-z.

Ubelaker, D. (1977) 'Problems with the microscopic determination of age at death', in *29th Meeting of the American Academy of Forensic Sciences*. San Diego, California.

Ulijaszek, S. J. and Kerr, D. A. (1999) 'Anthropometric measurement error and the assessment of nutritional status', *British Journal of Nutrition*, 44(1999), pp. 165–177.

Utts, J. and Heckard, R. (2014) *Mind on Statistics*. 5th edn. Cengage Learning.

Uytterschaut, H. . T. . (1985) 'Determination of skeletal age by histological methods', *Zeitschrift für Morphologie und Anthropologie*, (75), pp. 331–340.

Väänänen, H. K. and Zhao, H. (2008) 'Osteoclast Function. Biology and Mechanisms.', in Bilezikian, J., Raisz, L., and Martin, T. (eds) *Principles of Bone Biology*. 3rd ed. U.S.A.: Academic Press, pp. 193–209. doi: 10.1016/B978-0-12-373884-4.00030-6.

Väänänen, H. K., Zhao, H., Mulari, M. and Halleen, J. M. (2000) 'The cell biology of osteoclast function', *Journal of Cell Science*, 113(3), pp. 377–381. Available at: http://www.ncbi.nlm.nih.gov/pubmed/10639325.

Vardavas, C. I., Linardakis, M. K., Hatzis, C. M., Saris, W. H. M. and Kafatos, A. G. (2010) 'Cardiovascular disease risk factors and dietary habits of farmers from Crete 45 years after the first description of the Mediterranean diet', *European Journal of Preventive Cardiology*,

17(4), pp. 440–446. doi: 10.1097/HJR.0b013e32833692ea.

Vaz, S., Falkmer, T., Passmore, A. E., Parsons, R., Vaz, S., Falkmer, T., Passmore, A. E., Parsons, R. (2013) 'The case for using the repeatability coefficient when calculating test – retest reliability'', *PLoS ONE*, (8). doi: 10.1371/journal.pone.0073990.

Wallace, J. M. (2013) 'Skeletal hard tissue biomechanics', in Burr, D. B. and Allen, M. R. (eds) *Basic and applied bone biology*. London: Academic Press, pp. 115–130. doi: 10.1016/B978-0-12-416015-6.00006-X.

Wang, X., Shen, X., Li, X. and Mauli Agrawal, C. (2002) 'Age-related changes in the collagen network and toughness of bone', *Bone*, 31(1), pp. 1–7. doi: 10.1016/S8756-3282(01)00697-4.

Watanabe, Y., Konishi, M., Shimada, M., Ohara, H. and Iwamoto, S. (1998) 'Estimation of age from the femur of Japanese cadavers', *Forensic Science International*, 98(1–2), pp. 55–65. doi: 10.1016/S0379-0738(98)00136-4.

Weaver, C. M. and Fuchs, R. K. (2013) 'Skeletal growth and development', in Burr, D. B. and Allen, M. R. (eds) *Basic and applied bone biology*. London: Academic Press, pp. 245–260. doi: 10.1016/B978-0-12-416015-6.00012-5.

Weiner, S. (2006) 'Transient precursor strategy in mineral formation of bone', *Bone*, 39(3), pp. 431–433. doi: 10.1016/j.bone.2006.02.058.

Weiner, S., Traub, W. and Wagner, H. D. (1999) 'Lamellar bone: structure– function relations.', *Journal of Structural Biology*, 126, pp. 241–255.

Weinmann, J. and Sicher, H. (1955) *Bone and bones: Fundamentals of bone biology*. 2nd edn. London: Henry Kimpton.

Weinstein, R. and Bell, N. (1988) 'Diminished rates of bone formation in normal black adults', *The New England Journal of Medicine*, 319, pp. 1698–1701.

Welch, B. (1951) 'On the Comparison of Several Mean Values: An Alternative Approach', *Biometrika*, (38), pp. 330–336.

White, T. and Folkens, P. (2005) *The human bone manual*. 1st edn. U.S.A: Elsevier Academic Press.

Willett, W., Sacks, F., Trichopoulou, A., Drescher, G., Ferro-Luzzi, A., Helsing, E. and Trichopoulos, D. (1995) 'Mediterranean diet pyramid: a cultural model for healthy eating', *American Journal of Clinical Nutrition*, 61(6), p. 1402S–1406S.

World Health Organization (2014) *Alcohol consumptions: Levels and Patterns, Greece*.

Wu, K., Schubeck, K. E., Frost, H. M. and Villanueva, A. (1970) 'Haversian bone formation rates determined by a new method in a mastodon, and in human diabetes mellitus and osteoporosis', *Calcified Tissue Research*, 6(1), pp. 204–219. doi: 10.1007/BF02196201.

www.cmp-cyprus.org *www.cmp-cyprus.org/ (*Accessed 30 October 2017)

www.crete.gov.gr/index. (Accessed 25 May 2016)

www.healthgain.eu/casestudy/crete-greece (no date) *www.healthgain.eu/casestudy/crete-greece*.(Accessed 30 June 2017)

www.minitab.com (no date). Available at: http://blog.minitab.com/blog/adventures-in-

statistics-2/the-danger-of-overfitting-regression-models (Accessed: 25 June 2017).

http://www.petrkeil.com/?p=836 (Accessed on 20 June 2018)

York, R. (2012) 'Residualization is not the answer : Rethinking how to address multicollinearity', *Social Science Research*, 41(6), pp. 1379–1386. doi: 10.1016/j.ssresearch.2012.05.014.

Yoshino, M., Imaizumi, K., Miyasaka, S. and Seta, S. (1994) 'Histological estimation of age at death using microradiographs of humeral compact bone', *Forensic Science International*, 64(2–3), pp. 191–198. doi: 10.1016/0379-0738(94)90231-3.

Zar, J. (2010) *Biostatistical Analysis*. 5th ed. London: Upper Saddle River, N.J.Pearson Education International Publication Date C.

Zebaze, R. and Seeman, E. (2015) 'Cortical Bone: A Challenging Geography', *Journal of Bone and Mineral Research*, 30(1), pp. 24–29. doi: 10.1002/jbmr.2292.

Zhang, Y. and Yang, Y. (2015) 'Cross-validation for selecting a model selection procedure', *Journal of Econometrics*, 187(1), pp. 95–112. doi: 10.1016/j.jeconom.2015.02.006.

APPENDIX A

Appendix A.1 Ethical Approval

SCHOOL OF HISTORY, CLASSICS and ARCHAEOLOGY
ETHICS STATEMENT

In my view, ethical issues regarding this research project:

have been satisfactorily addressed,

OR
have arisen and the steps taken to address them are listed below:
**delete as appropriate*

Name: Julieta Gómez García-Donas
Matriculation/Personnel Number: s1061835
Research Proposal Title: ….Age estimation on two Mediterranean samples using rib histomorphometry

Body (if applicable):

Issues (if none, please state none):

The material used in this project will be provided by the department of Forensic Sciences of the University of Crete, Greece. The material will consist of small segments of ribs extracted from individuals of Greek origin that are submitted to autopsy. The sampling of the rib will be stated in the autopsy protocol and ethical permission to use this material for research will be granted by the Ethics Committee of the Medical School of the University of Crete. Since similar permits have been granted previously for projects requiring tissue sampling it is expected that there will be no problem in the approval of the project. Additionally the Procurator Fiscal of Scotland has been contacted with an enquiry for the use of modern skeletal material from Greece for research. According to his response he has no authority on material outwith Scotland thus there seems to be no issue for the use of the autopsy samples for the current project. The rib samples constitute biological material thus all the appropriate health and safety regulations must be met for the sample preparation, shipping, delivery, storage and handling of the material. We will follow the standard protocol of the department of Forensic Sciences of the University of Crete, Greece for the shipping of the material, in accordance with the UK standards and the material will be stored in deep fridge until the initiation of the thin sectioning. The remaining biological material after the handling of the specimens will be disposed according to standard protocols for biological material.

Signature: Julieta Gómez García-Donas

Date: 29 January 2013

Appendix A.2 Pathological samples and exclusion criteria

Pathology*

Collection	Rib Code	Age	Sex	Pathology	Comments
Cretan	Baby	4	Male		Sub-adult
Cretan*	CC13	60	Male	Gastric Cancer	abnormal bone formation, irregular bone
Cretan*	CC22	55	Male	Brain cancer	Enlarged Haversian canal
Cretan*	CC45	64	Female	Lung cancer	Normal appearance; few osteons
Cretan*	CC63	83	Male	Periostitis	abnormal bone formation, irregular bone
Cretan*	CC203	85	Male	Lung infection	Cutaneous side irregular abnormal bone
Cretan*	FC2	68	Male	hypertension, coronary artery disease/Progressive supranuclear palsy	Forensic Case
Cretan*	FC9	57	Male	Atherosclerosis, Coronary stenosis	Heavy smoker, Alcohol abuse, Forensic Case
Cretan	FC10	47	Male		Forensic Case / no-Greek
Cretan*	FC13	52	Male	Atherosclerosis, myocardial infarction, coronary obstruction	Forensic Case
Cretan*	FC12	48	Male	fatty liver,myocardial infarction, CAD.	Forensic Case
Cretan*	FC15	59	Male	myocardial infarction, CAD	Forensic Case
Cretan*	FC21	49	Male	Coronary disease, diabetes, COPD	Forensic Case
Cyprus	13	6	Female		sub-adult
Cyprus	32	86	Male		taphonomy
Cyprus	117	55	Male		taphonomy
Cyprus	118	50	Male		taphonomy

*Pathological rib samples

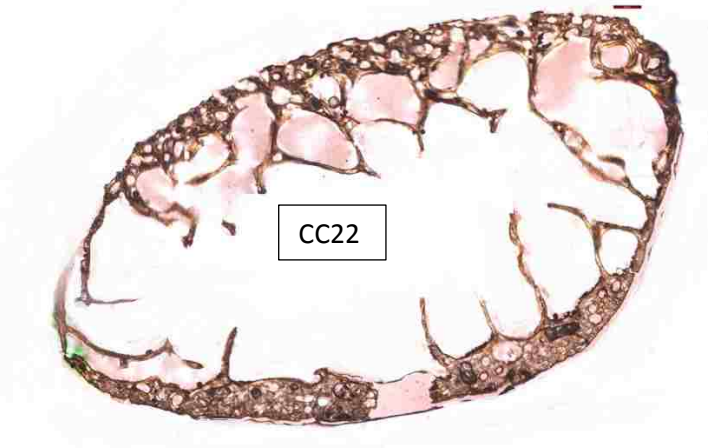

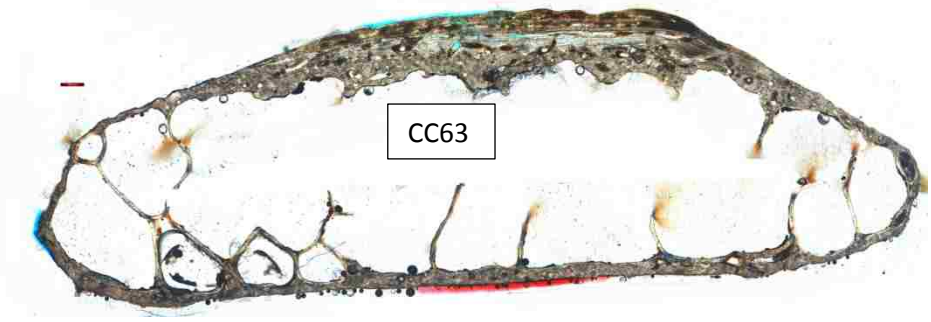

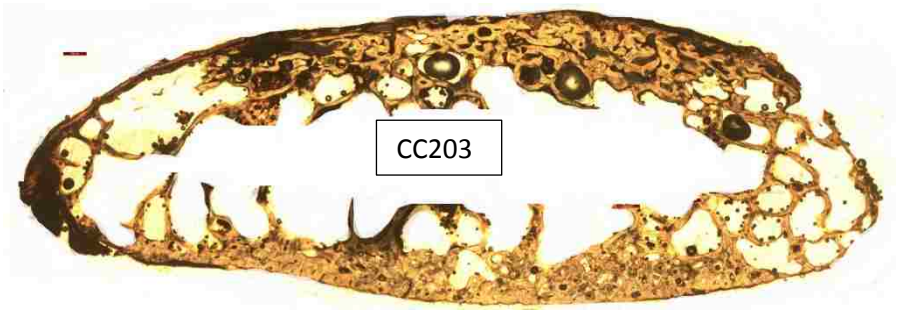

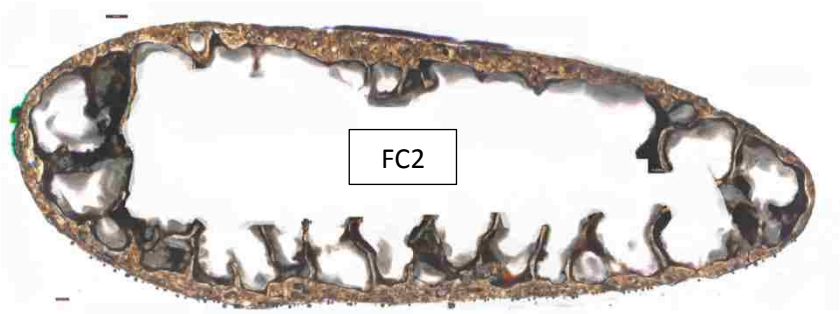

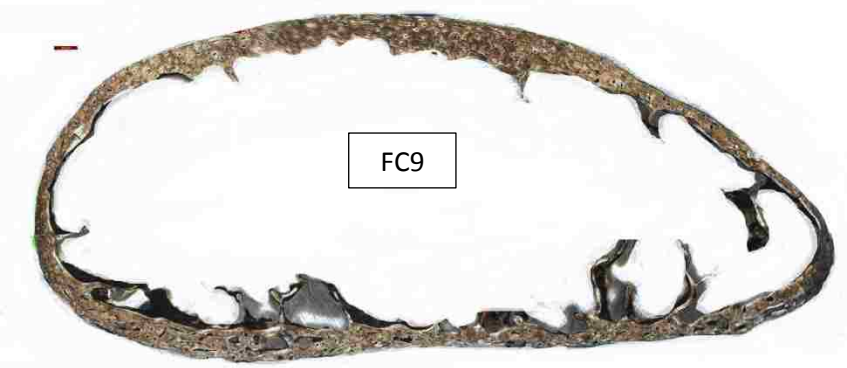

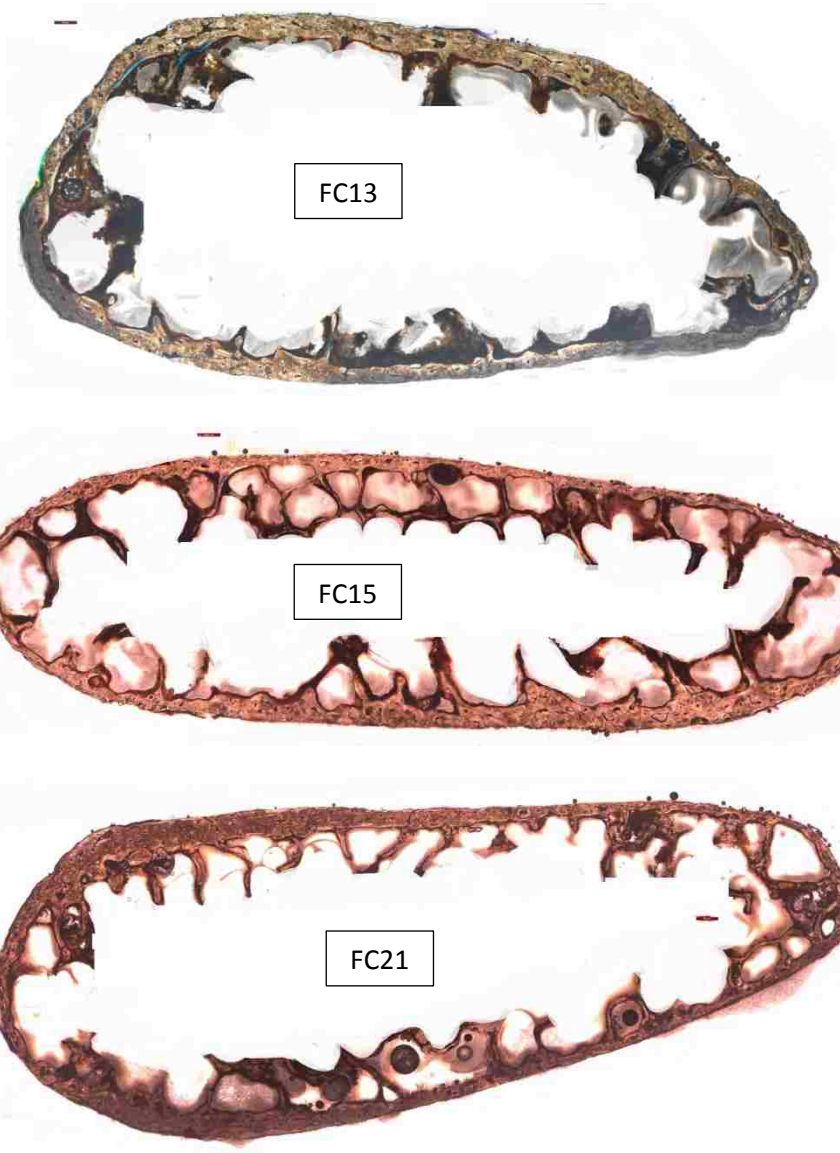

All rib samples presented same taphonomic alteration (example)

Appendix A.3 Total study sample individuals per age group

Age Group	Crete (total sample)		Greek-Cypriots		Study sample	
	n (Males)	n (Females)	n (Males)	n (Females)	n (Males)	n (Females)
4-20 y.o.	1	1	0	1	1	2
21-30 y.o.	2	2	0	0	2	2
31-40 y.o.	2	3	0	0	2	3
41-50 y.o.	2	1	2	5	4	6
51-60 y.o.	7	2	5	8	12	10
61-70 y.o.	3	4	7	10	10	14
71-80 y.o.	3	1	1	3	4	4
81-90 y.o.	3	1	2	0	5	1
< 91 y.o.	0	3	0	3	0	6
Total	23	18	17	30	40	48

APPENDIX B

Appendix B.1 Intra- and inter-observer error

Intra-observer error: Bland-Altman plots

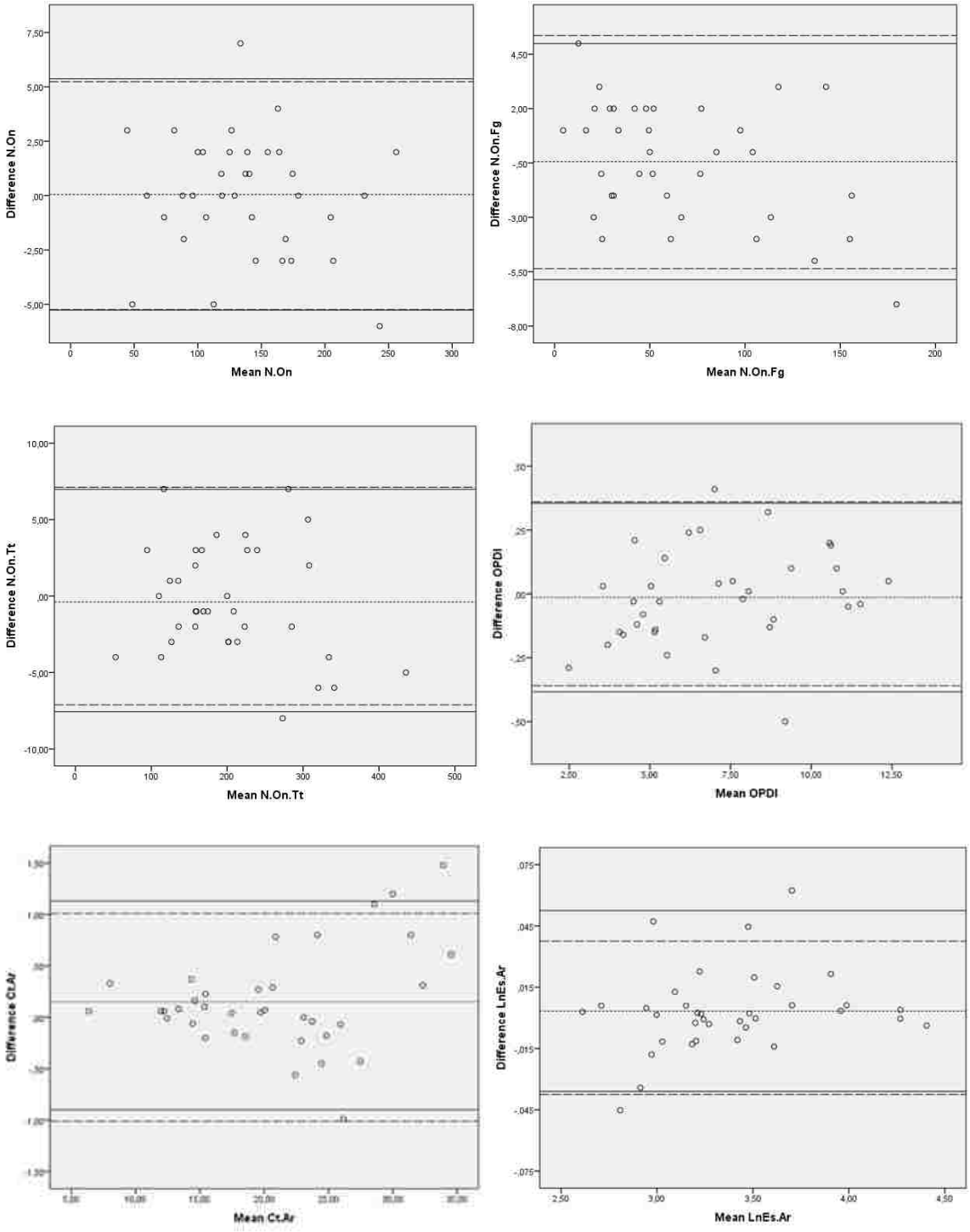

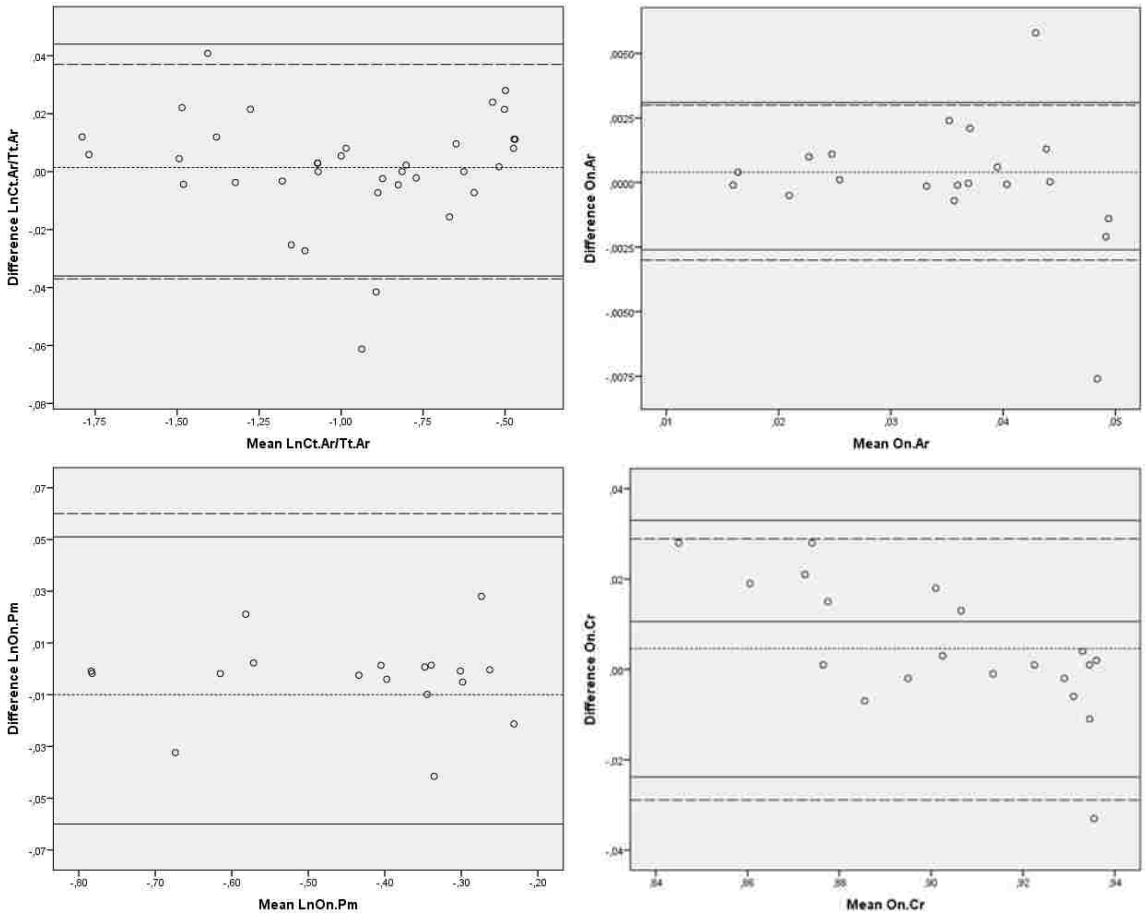

Inter-observer error (experienced histologist): Bland-Altman plots

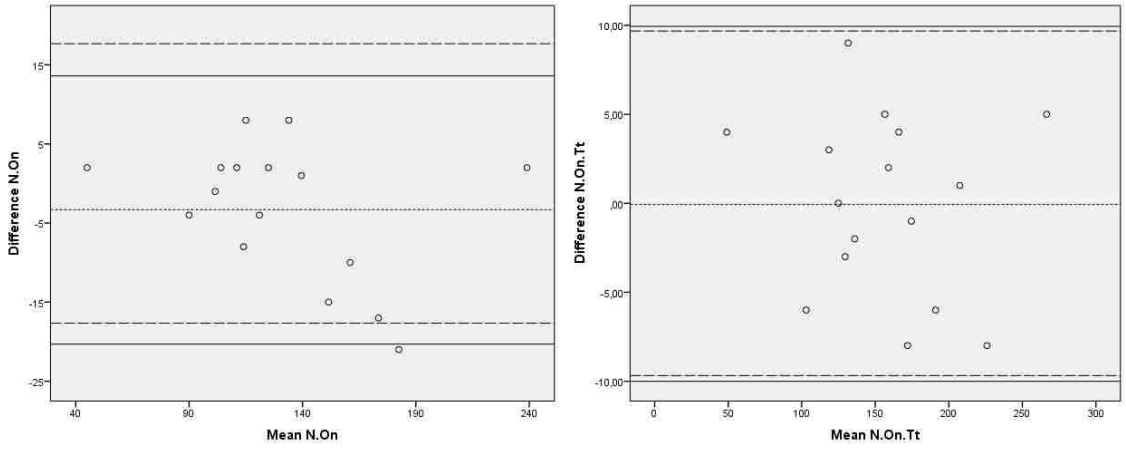

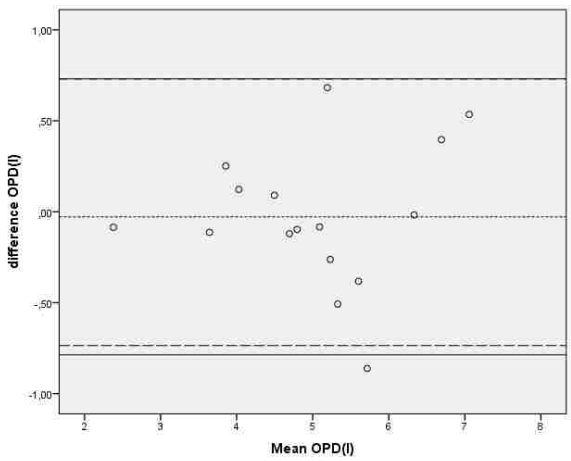

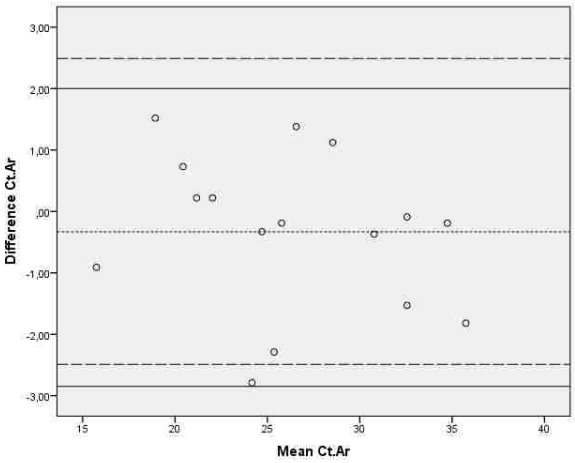

Inter-observer error (same level of experience observer): Bland-Altman plots

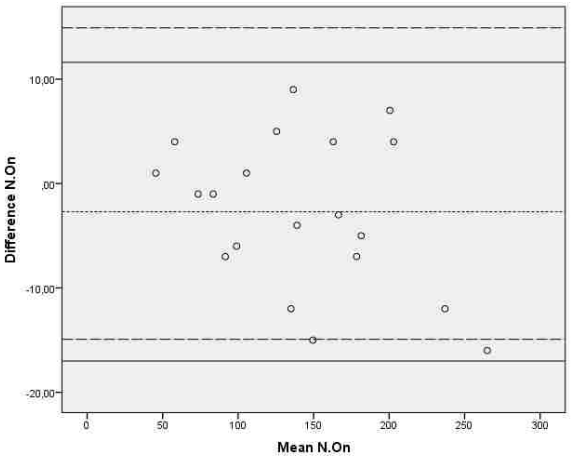

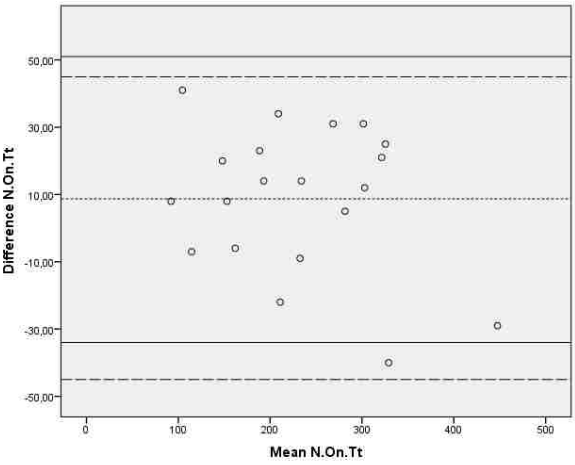

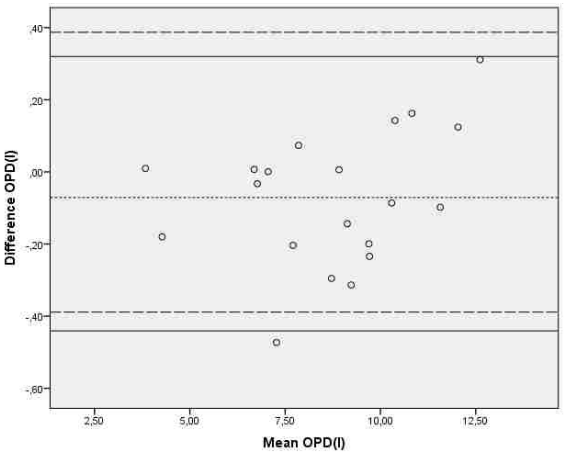

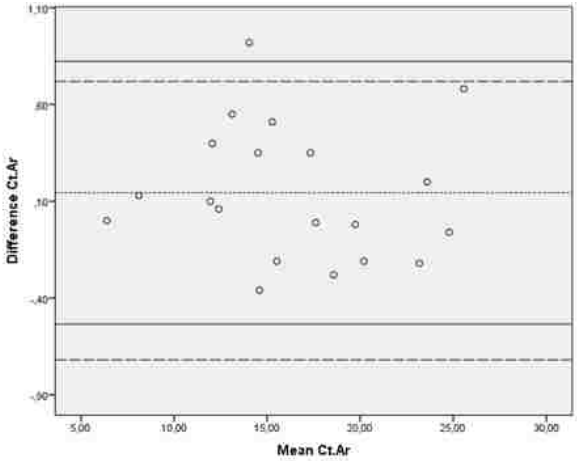

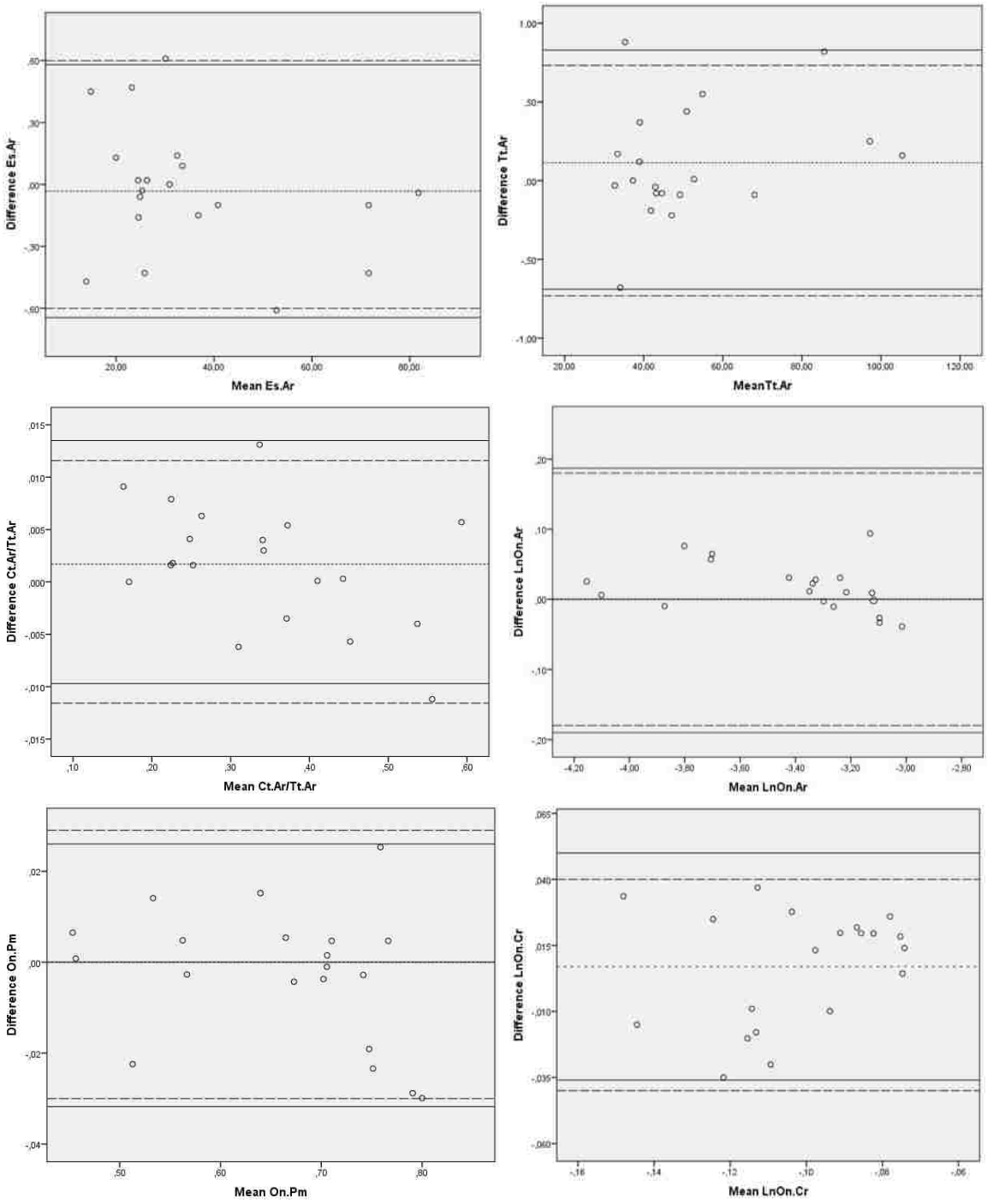

Appendix B.2 Histograms (with normal curve fitted) of the variables assessed on the sample

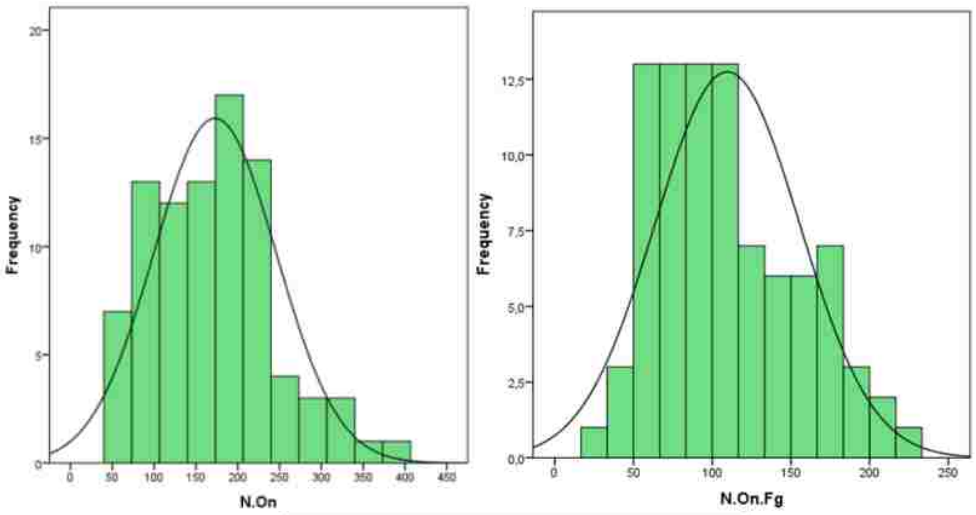

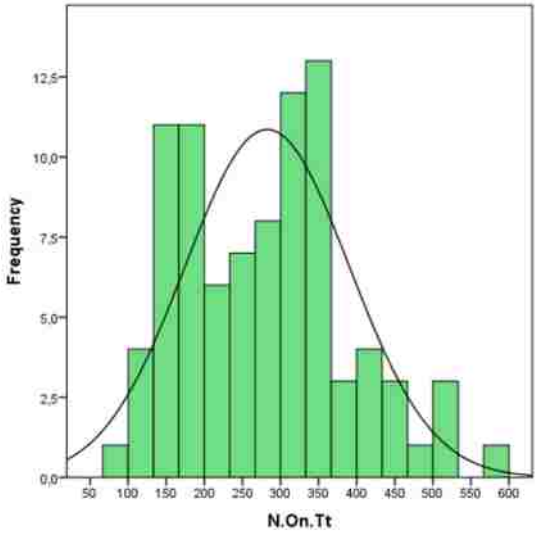

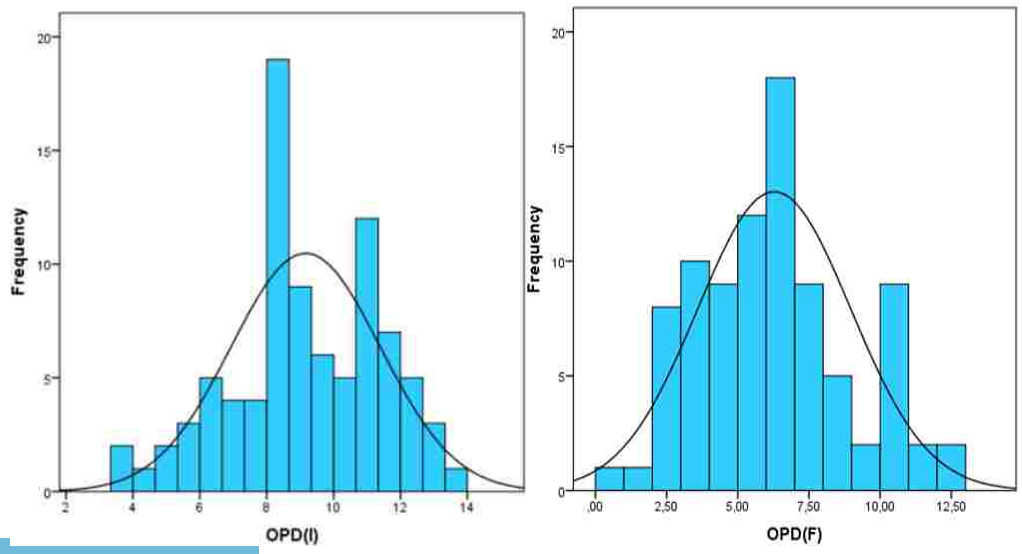

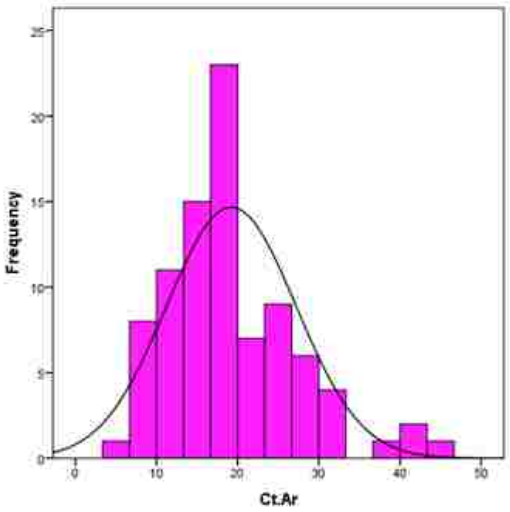

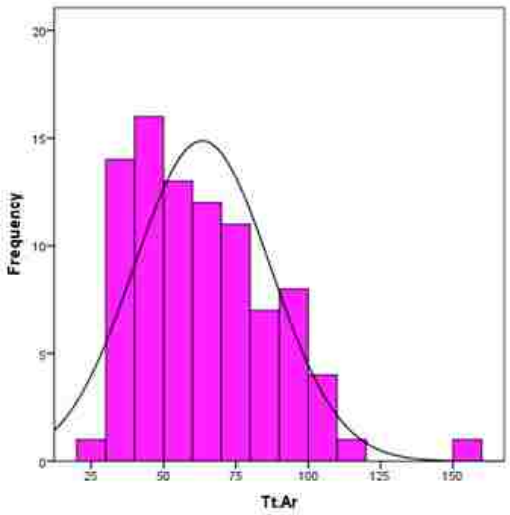

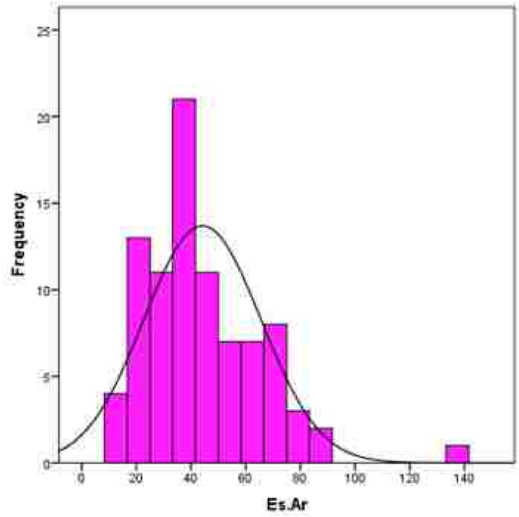

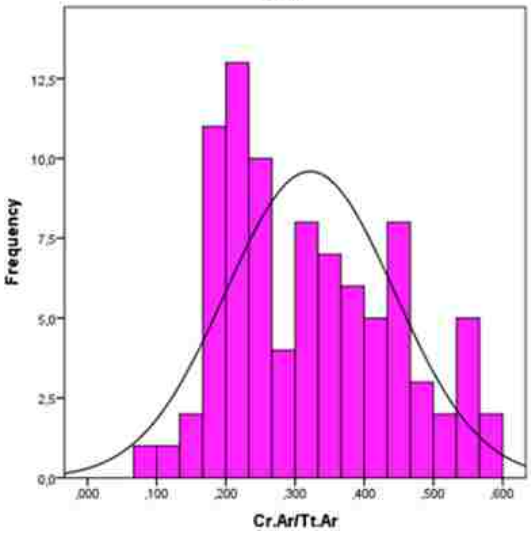

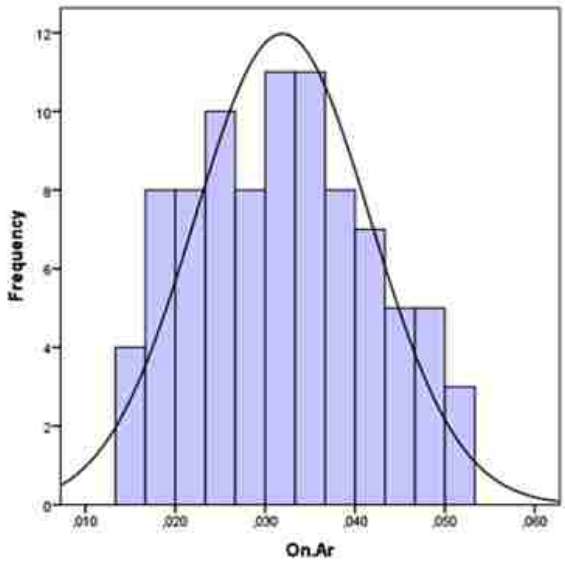

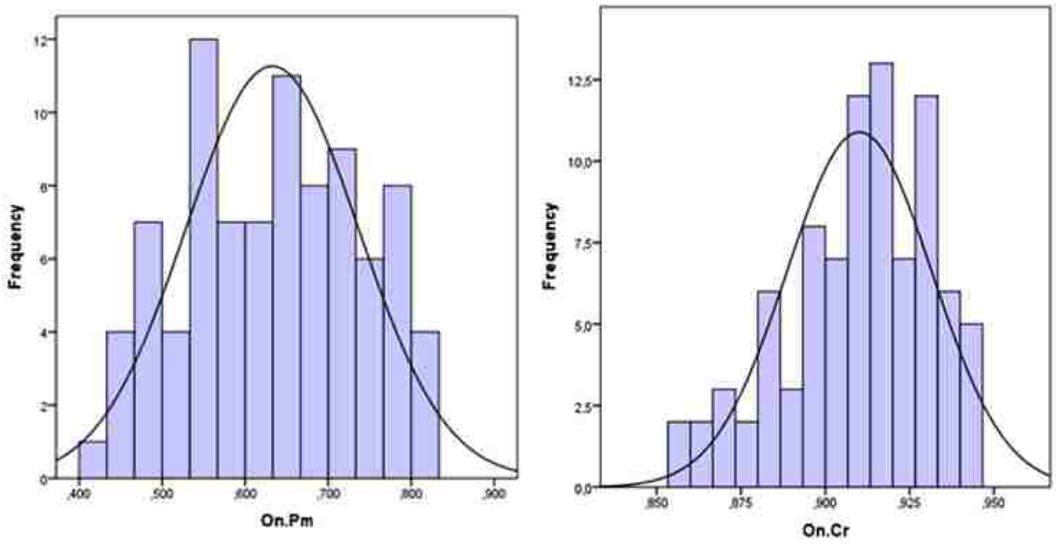

Appendix B.3 Remaining histological parameters (*N.On, N.On.Fg, N.On.Tt, Tt.Ar* and *Es.Ar*) separated by 20 age cohorts

.

N=11											
19-39 years old	Min	Max	Mean	SE	SD	Skewness	Z_Skeweness	Kurtosis	Z_Kurtosis	Shapiro-Wilk	p-value
Known Age	19	38	28.27	2.17	7.21	0.08	0.13	-1.55	-1.21	0.91	0.22
N.On	88	332	187.45	20.48	67.94	0.69	1.06	0.83	0.65	0.96	0.73
N.On.Fg	23	99	71.54	7.47	24.79	-1.01	-1.52	0.02	0.02	0.88	0.12
N.On.Tt	111	422	259.00	26.09	86.52	0.02	0.04	0.34	0.27	0.98	0.94
Tt.Ar	33.72	91.21	67.03	5.94	19.69	-0.22	-0.34	-0.97	-0.76	0.93	0.45
Es.Ar	13.64	72.89	40.61	5.58	18.51	0.43	0.66	-0.79	-0.62	0.96	0.73

Grey values indicate not normal distribution of the data; Min=minimum, Max=maximum, SE=standard error, SD=standard deviation

295

Remaining histological parameters (*N.On, N.On.Fg, N.On.Tt, Tt.Ar* and *Es.Ar*) separated by 20 age cohorts.

N=28											
40-59 years old	Min	Max	Mean	SE	SD	Skewness	Z_Skeweness	Kurtosis	Z_Kurtosis	Shapiro-Wilk	p-value
Known Age	40	58	51.32	1.00	5.29	-0.41	-0.92	-0.92	-1.07	0.93	0.07
N.On	60	399	190.79	16.02	84.77	0.69	1.56	0.09	0.11	0.95	0.17
N.On.Fg	47	184	103.64	7.72	40.84	0.31	0.71	-0.88	-1.02	0.94	0.13
N.On.Tt	125	583	294.43	22.55	119.35	0.54	1.23	-0.27	-0.32	0.94	0.11
Tt.Ar	26.82	155.25	65.19	5.55	29.39	1.17	2.66	1.72	2.00	0.89	0.01
Es.Ar	16.06	141.09	42.59	5.12	27.10	2.02	4.58	5.42	6.31	0.81	0.001

Grey values indicate not normal distribution of the data; Min=minimum, Max=maximum, SE=standard error, SD=standard deviation

296

N=36											
60-79 years old	Min	Max	Mean	SE	SD	Skewness	Z_Skeweness	Kurtosis	Z_Kurtosis	Shapiro-Wilk	p-value
Known Age	60	78	67.03	0.75	4.53	0.39	0.984	0.05	0.06	0.95	0.09
N.On	66	318	164.61	10.13	60.81	0.53	1.349	0.19	0.24	0.96	0.30
N.On.Fg	60	212	122.14	7.63	45.81	0.42	1.069	-0.99	-1.29	0.94	0.04
N.On.Tt	129	523	286.75	16.31	97.88	0.53	1.344	0.04	0.05	0.95	0.15
Tt.Ar	33.50	105.44	62.31	3.47	20.80	0.64	1.627	-0.59	-0.76	0.93	0.02
Es.Ar	15.07	81.74	45.82	3.00	18.02	0.37	0.945	-0.70	-0.91	0.96	0.18

Grey values indicate not normal distribution of the data; Min=minimum, Max=maximum, SE=standard error, SD=standard deviation

Remaining histological parameters (*N.On, N.On.Fg, N.On.Tt, Tt.Ar* and *Es.Ar*) separated by 20 age cohorts.

N=13											
>80 years old	Min	Max	Mean	SE	SD	Skewness	Z_Skeweness	Kurtosis	Z_Kurtosis	Shapiro-Wilk	p-value
Known Age	80	100	88.31	1.73	6.25	0.51	0.83	-0.51	-0.43	0.94	0.51
N.On	46	299	144.62	22.08	79.62	0.44	0.72	-0.85	-0.72	0.93	0.32
N.On.Fg	50	224	120.08	14.91	53.77	0.59	0.97	-0.71	-0.59	0.93	0.33
N.On.Tt	96	482	264.69	35.95	129.62	0.39	0.66	-1.18	-0.99	0.94	0.41
Tt.Ar	32.09	107.17	59.36	6.04	21.77	0.76	1.23	0.44	0.37	0.95	0.54
Es.Ar	14.52	87.79	45.99	5.53	19.95	0.67	1.08	0.41	0.34	0.96	0.70

Grey values indicate not normal distribution of the data; Min=minimum, Max=maximum, SE=standard error, SD=standard deviation

297

Appendix B.4 Scatter plots representing the association between known age and variables for the entire dataset

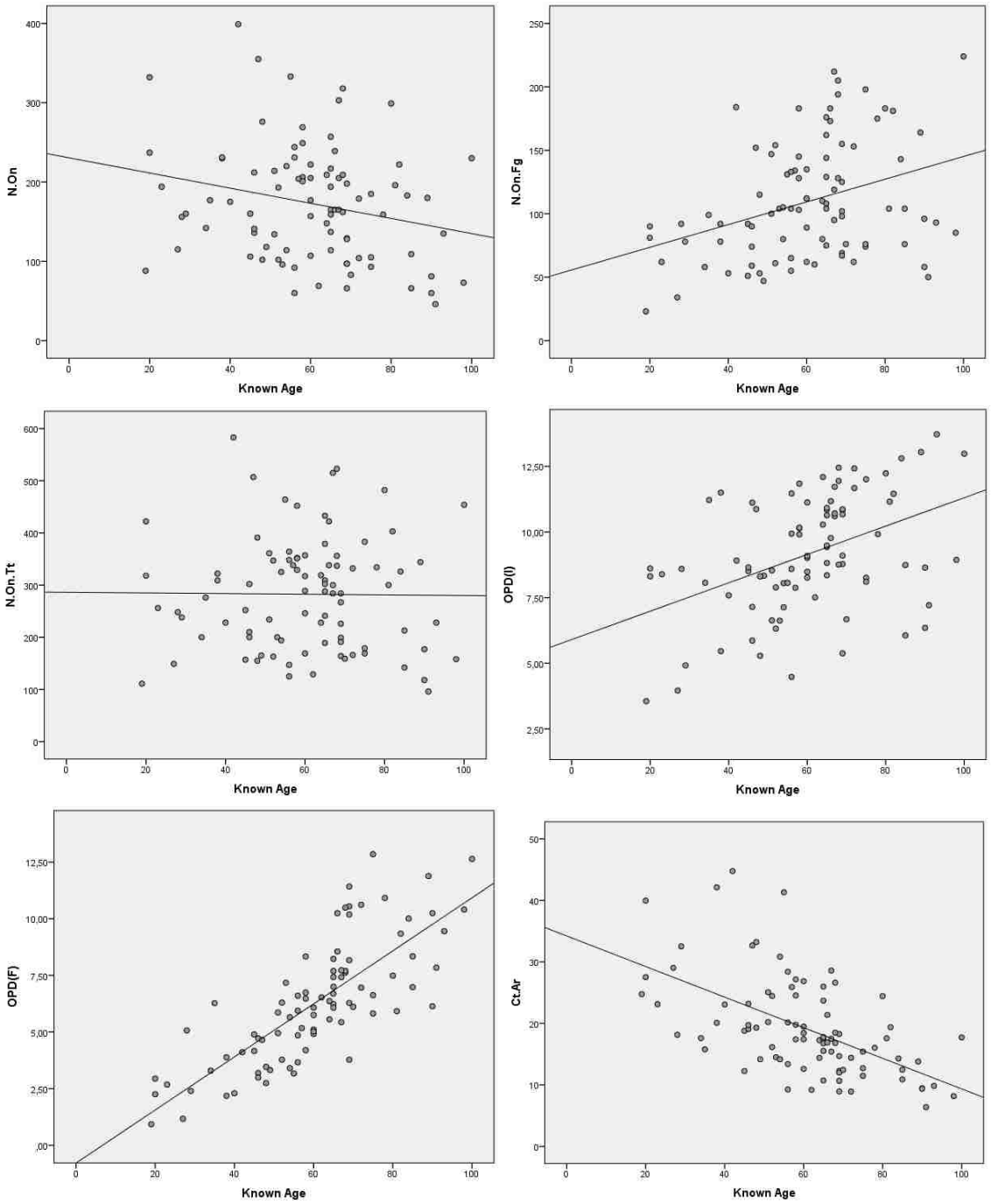

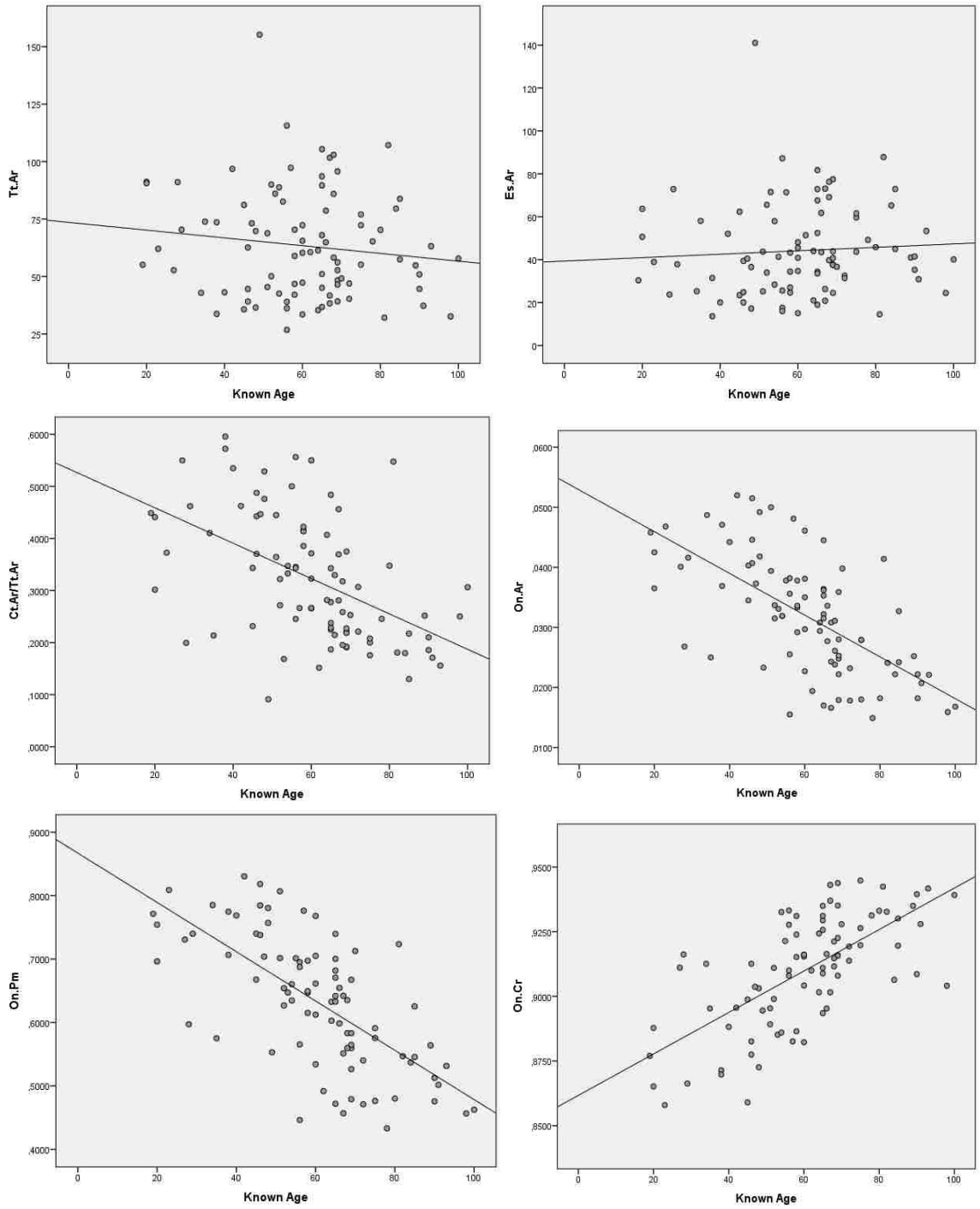

Appendix B.5 Scatter plots representing the association between known age and variables for males and females

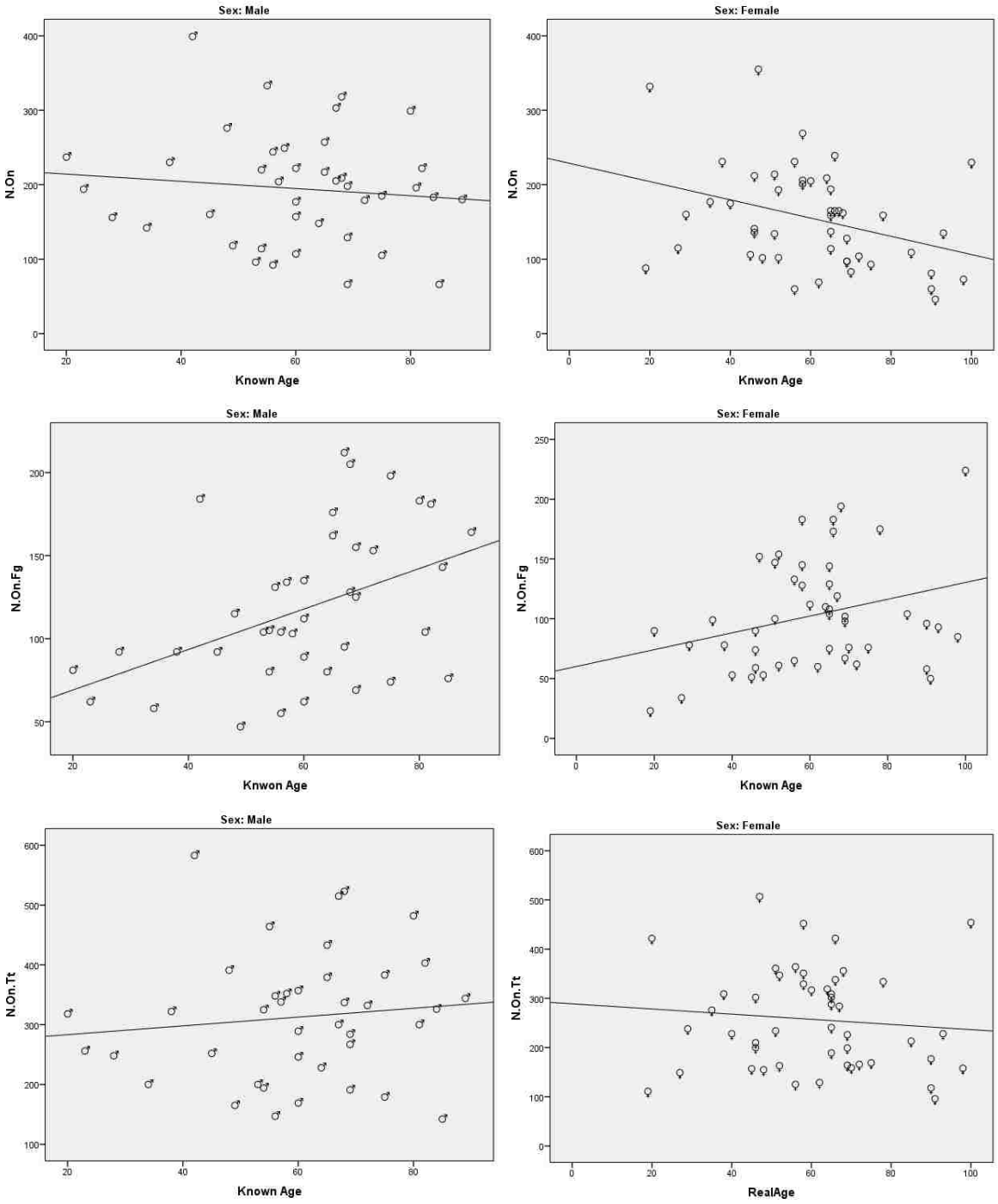

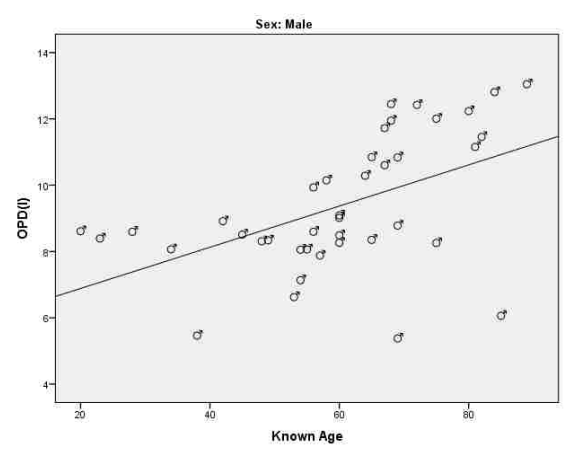

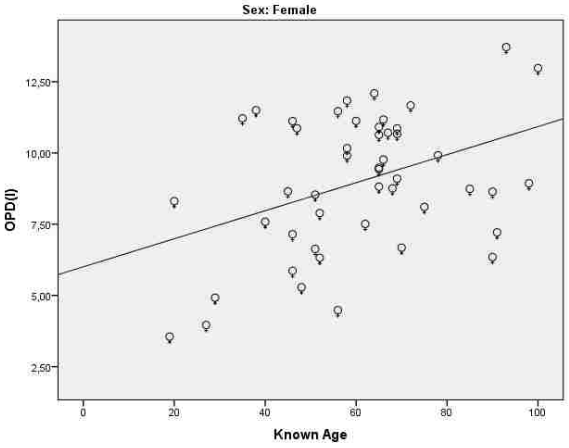

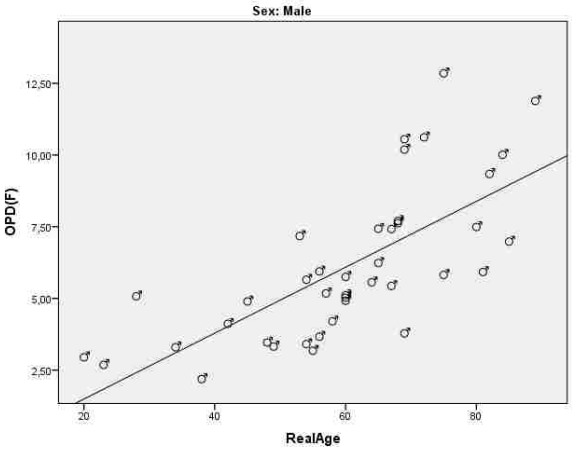

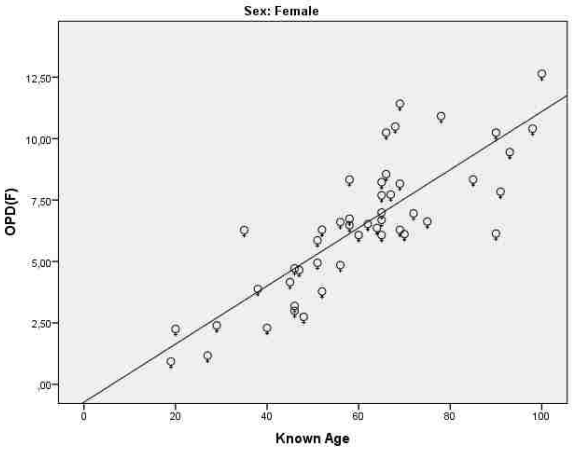

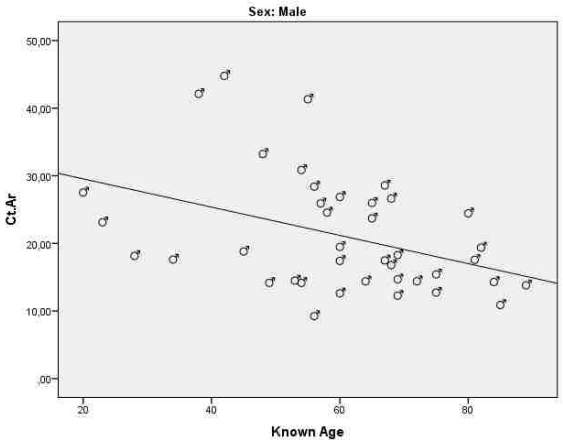

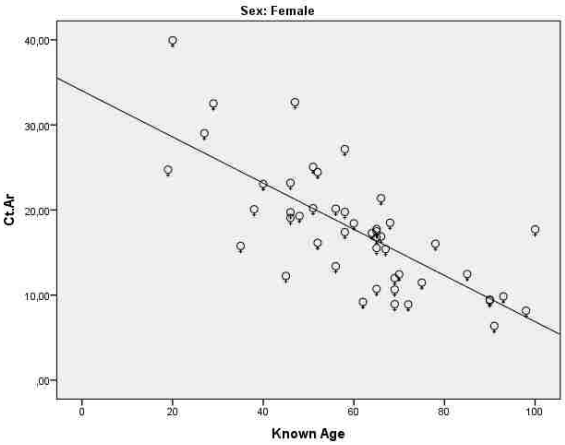

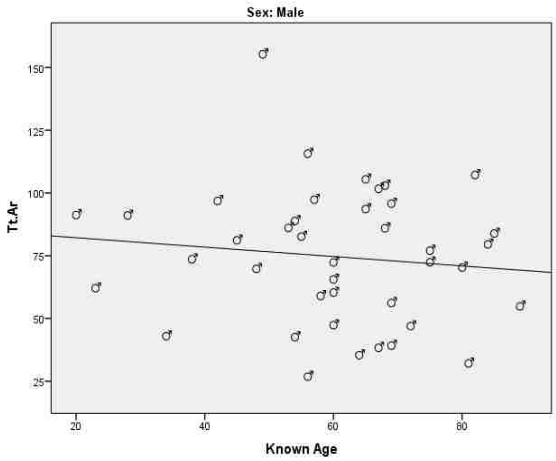

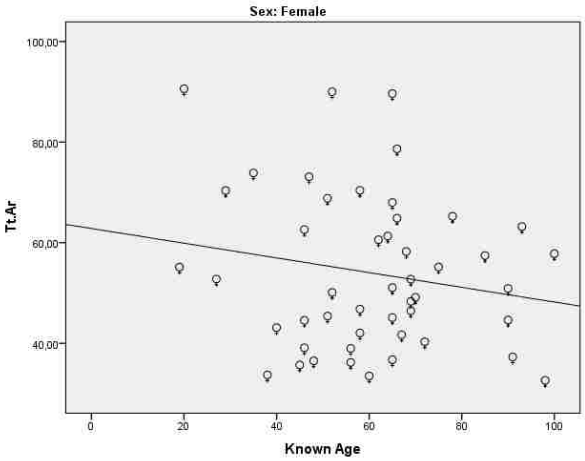

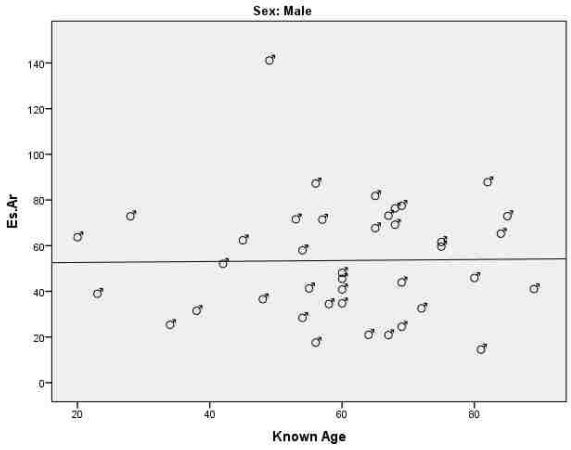

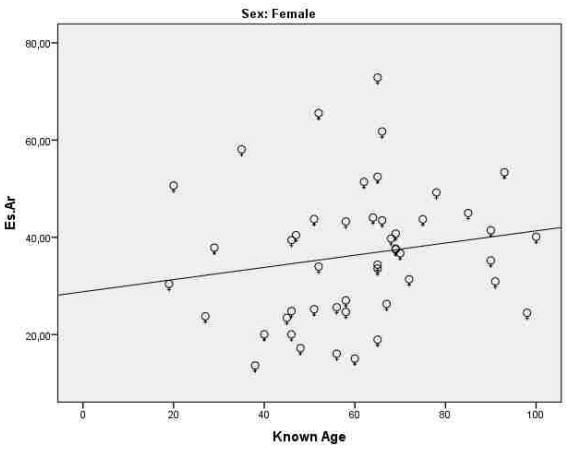

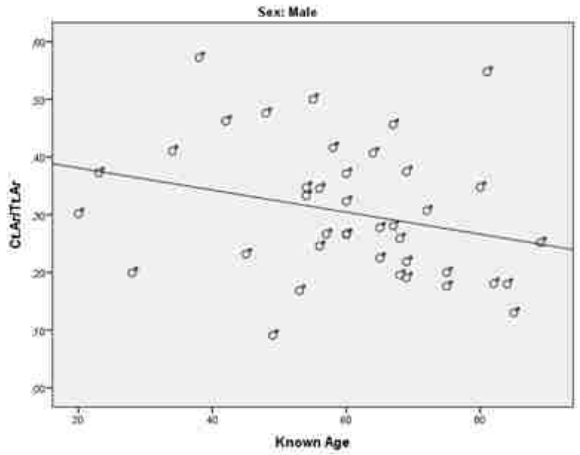

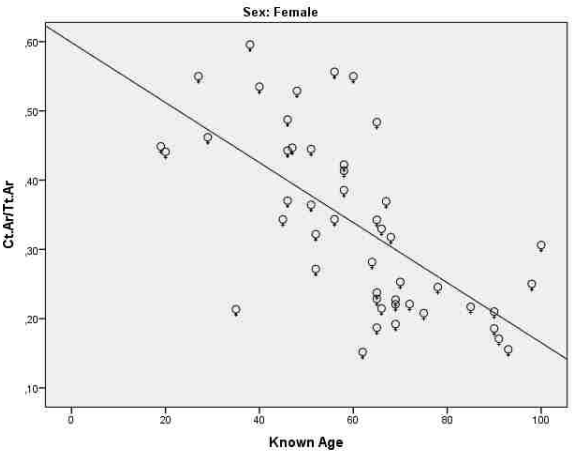

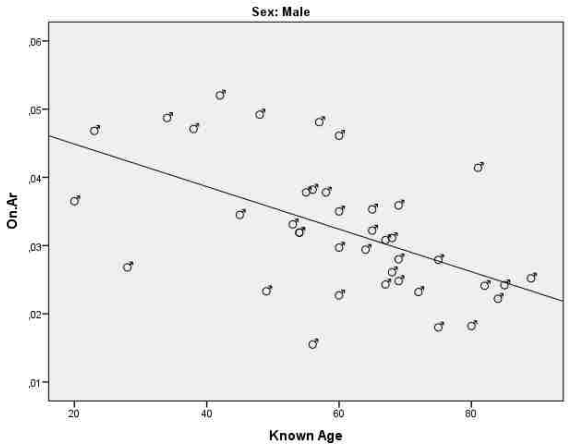

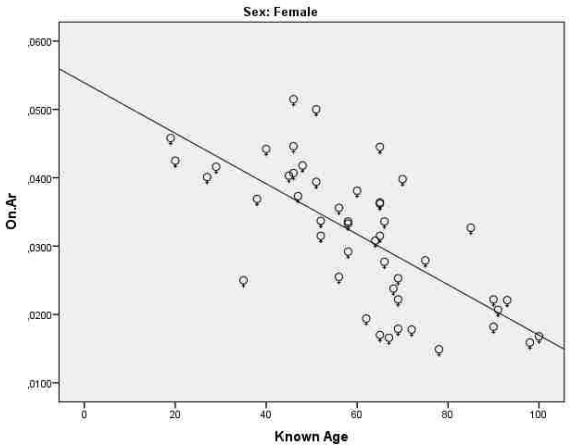

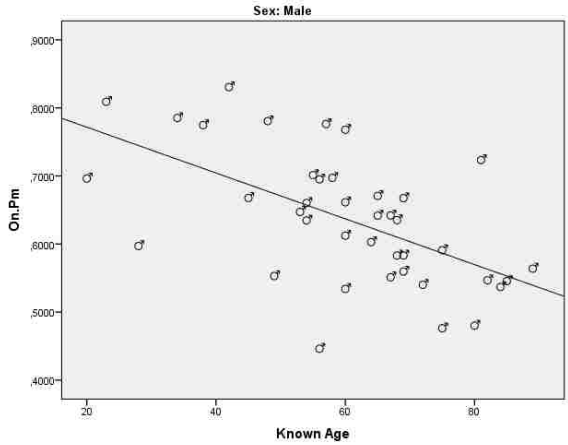

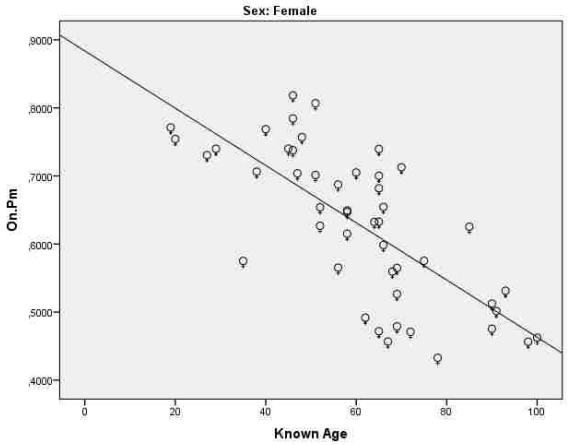

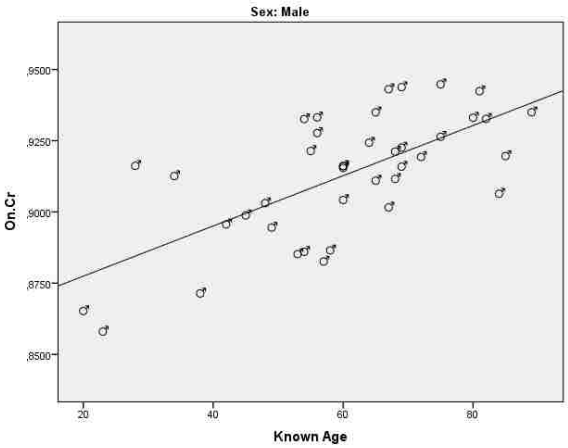

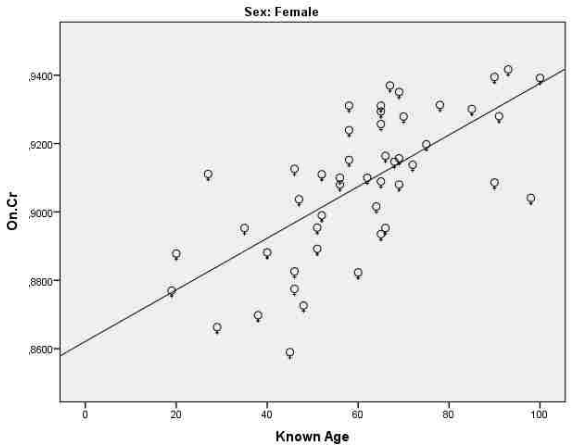

Appendix B.6 Scatter plots representing the association between known age and variables for *Cretans and $^{\Delta}$Cypriots

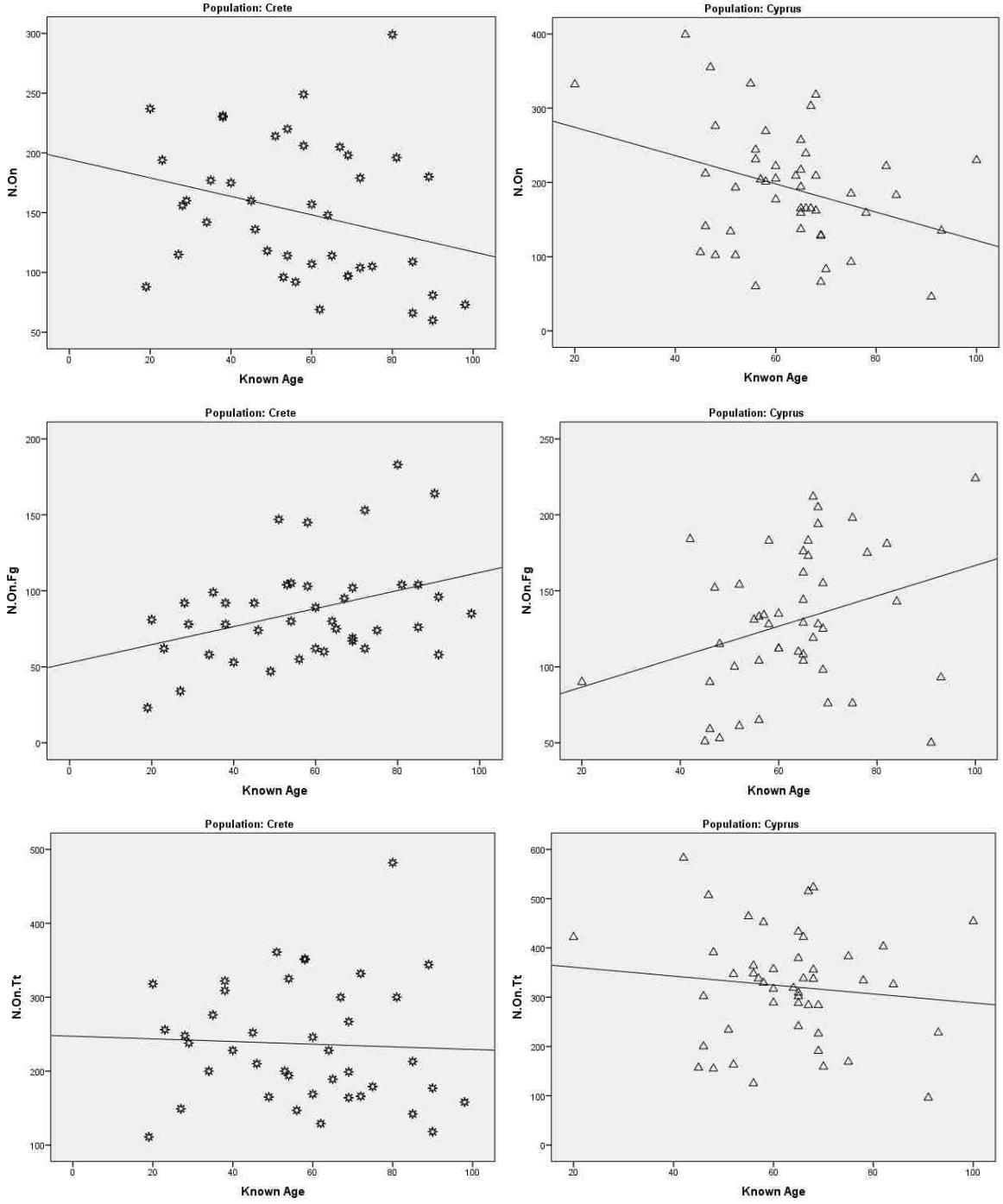

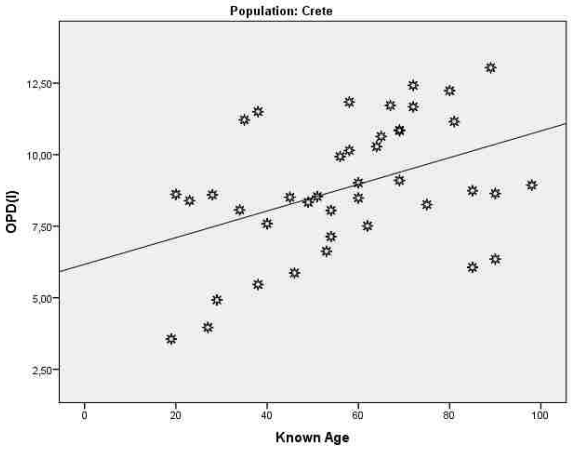

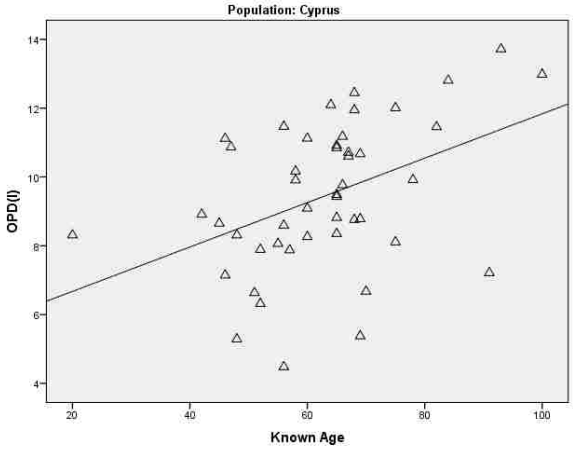

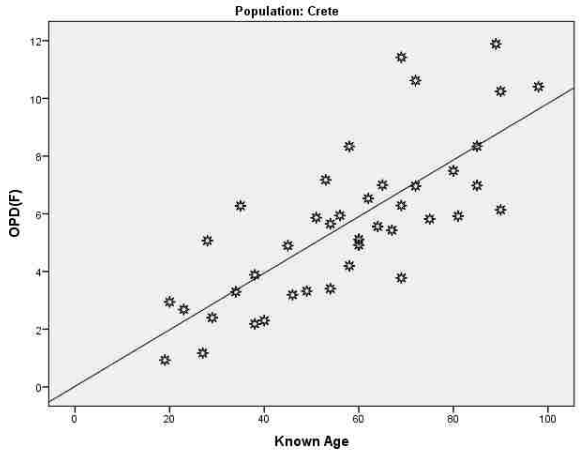

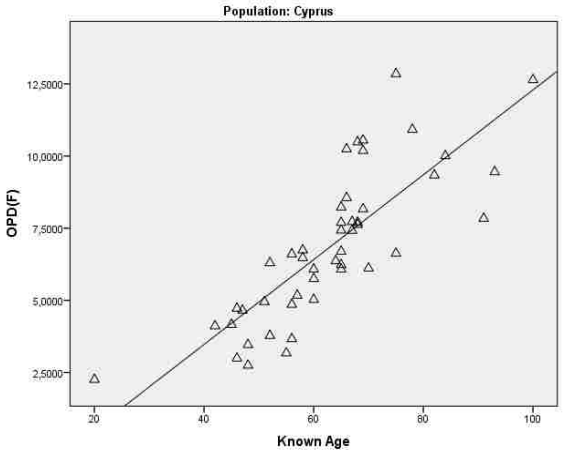

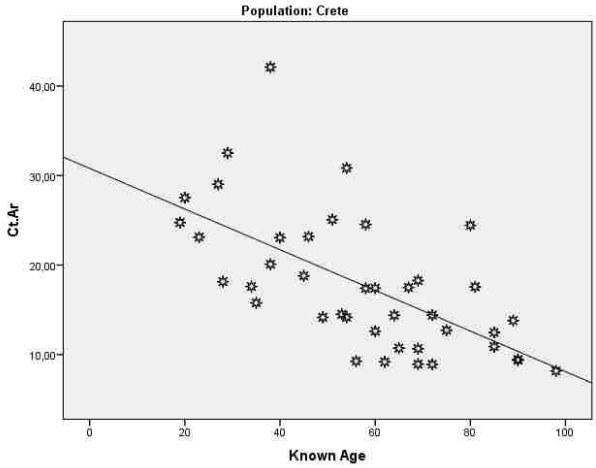

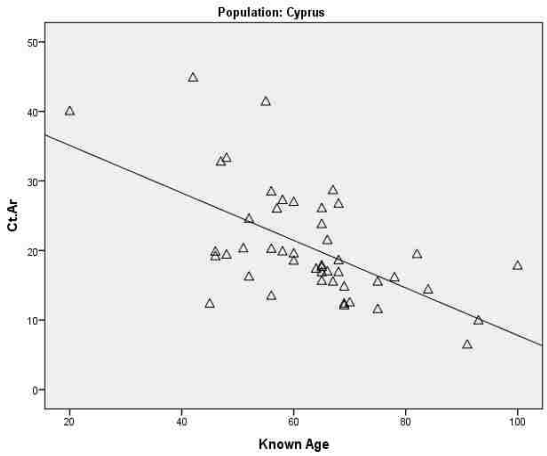

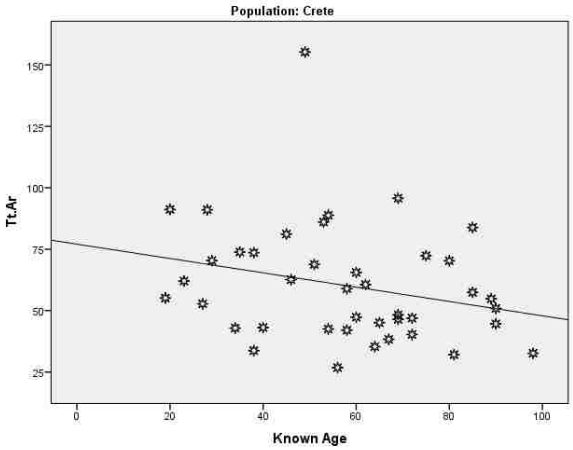

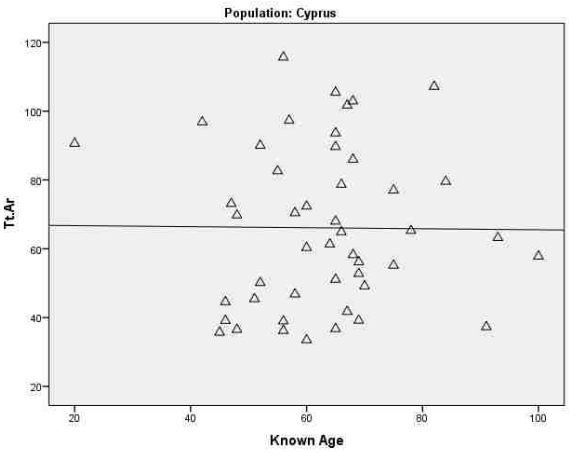

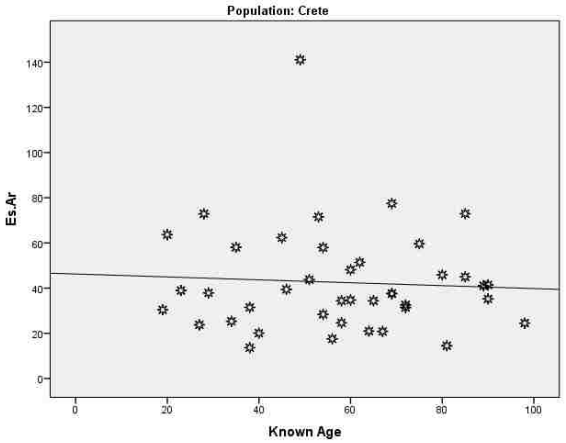

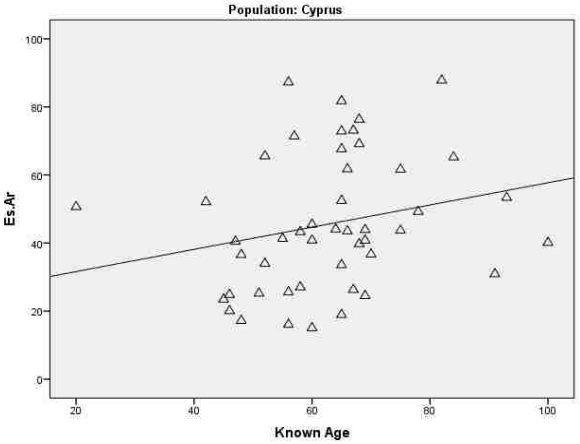

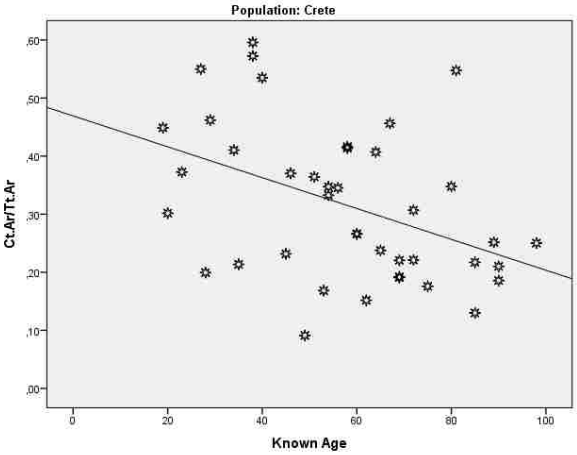

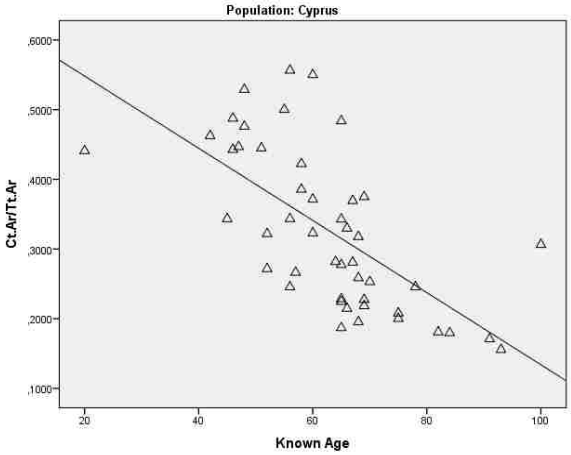

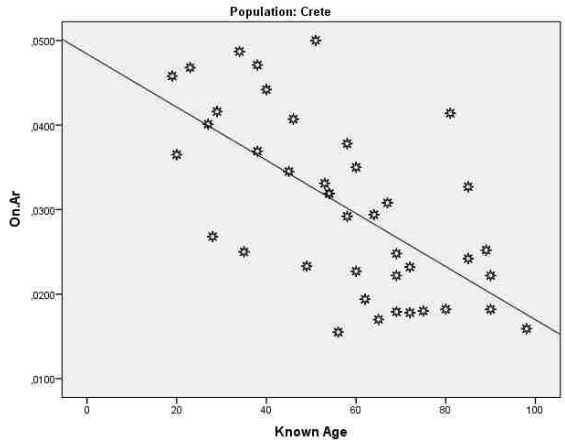

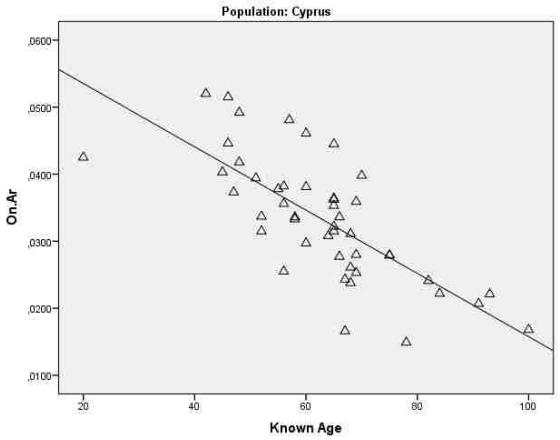

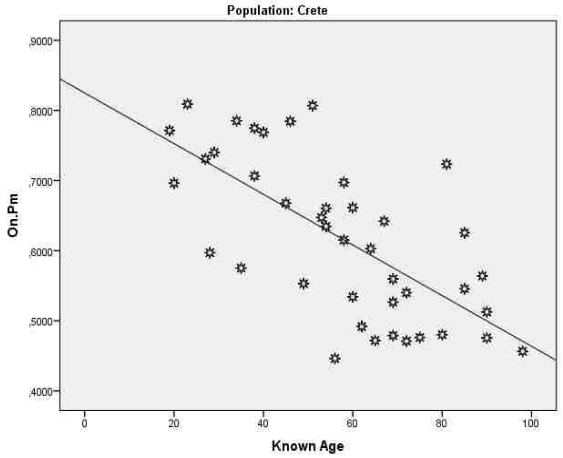

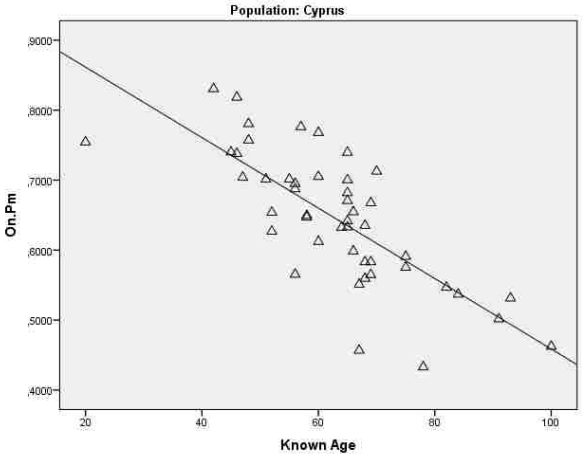

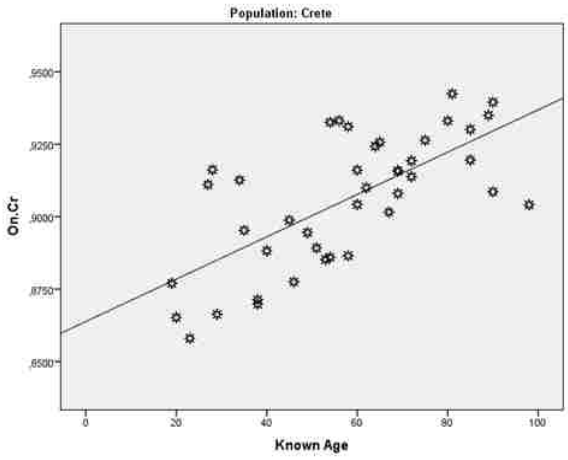

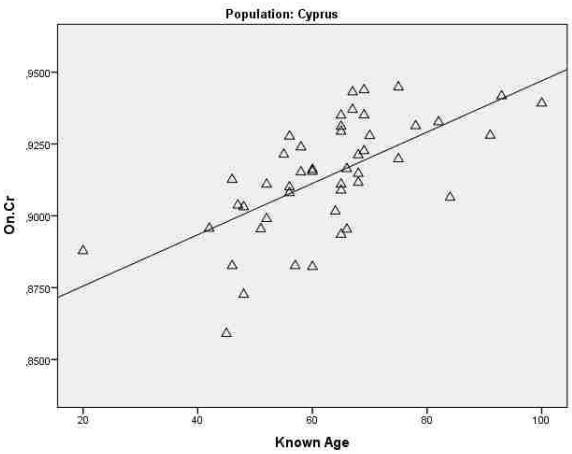

Appendix B.7 Diagnostic plots for regression models: <u>Simple Linear Models</u>

Residuals vs fitted plot, Q-Q plot,
Scale-location plot, Residuals vs Leverage´s values

MODEL 2: 45.44 + 0.136(N.On.Fg)

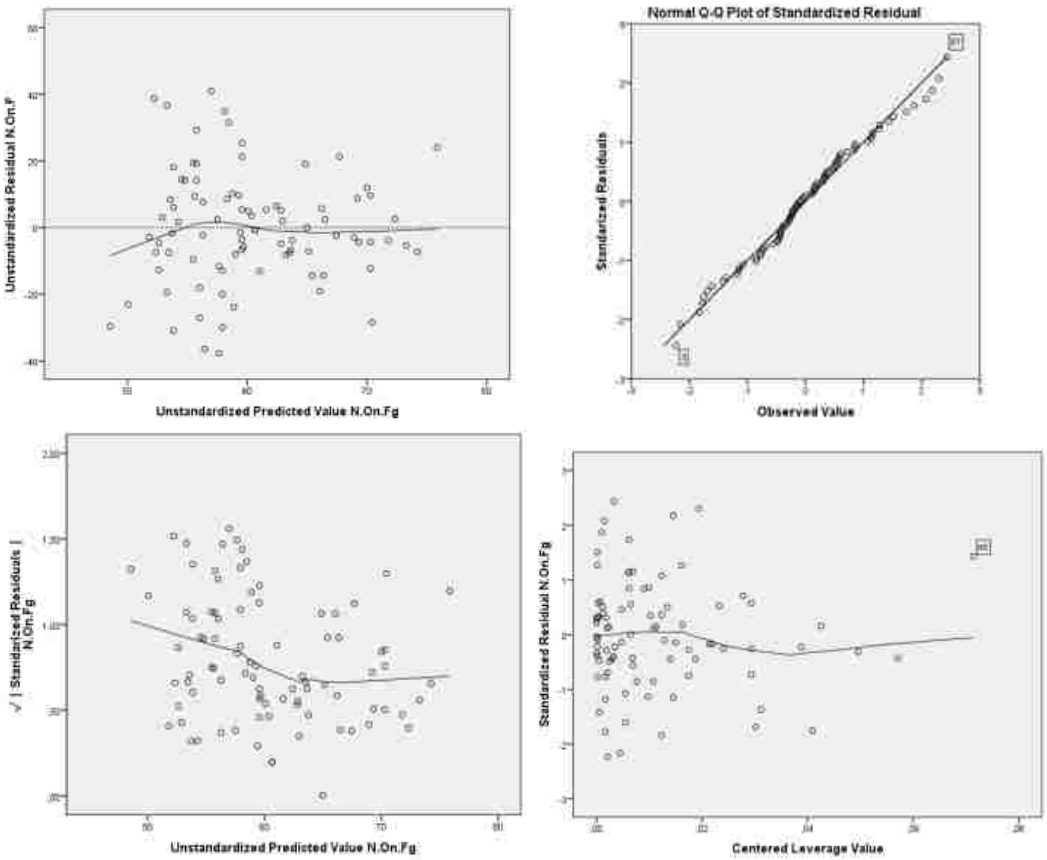

MODEL 3: 28.631 + 3.46(OPD(I))

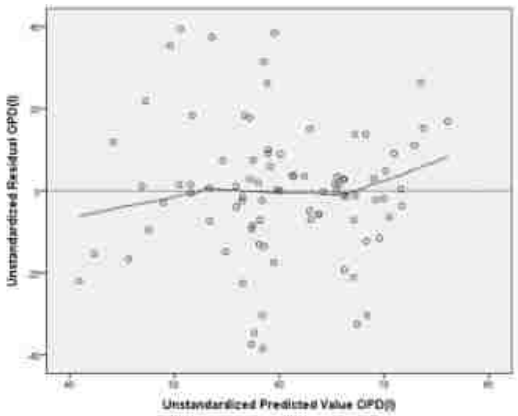

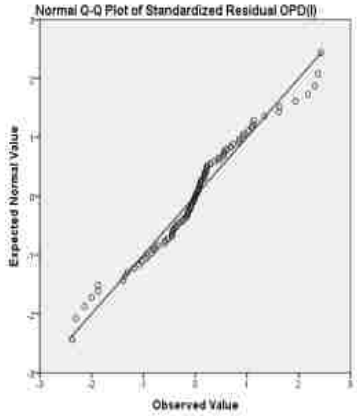

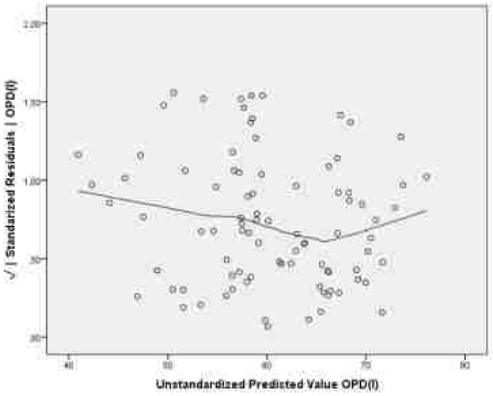

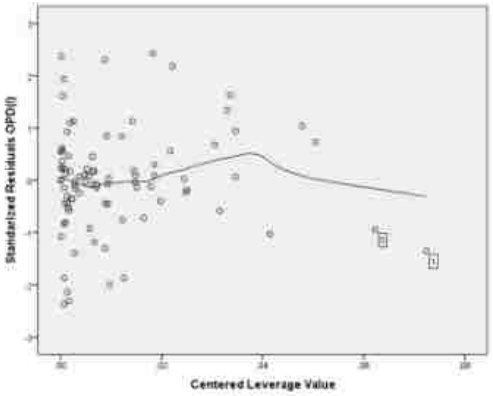

MODEL 4: 27.935 + 5.158(OPD(F))

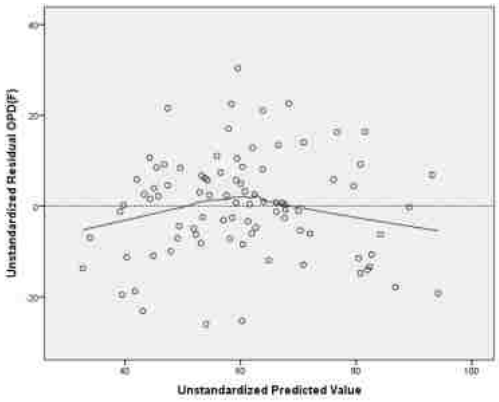

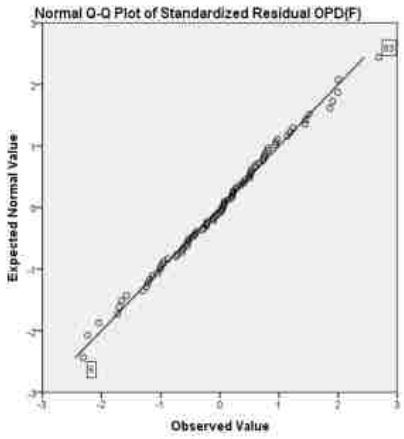

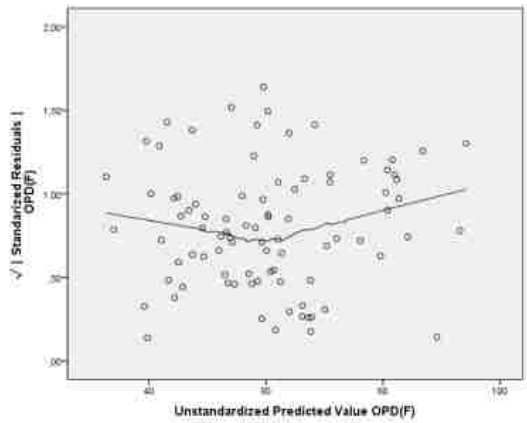

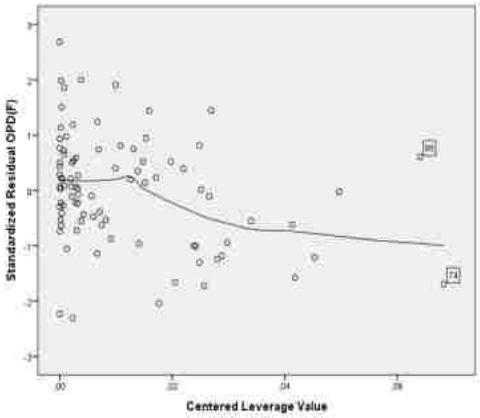

MODEL 5: 15.66 + 2.893(OPD)

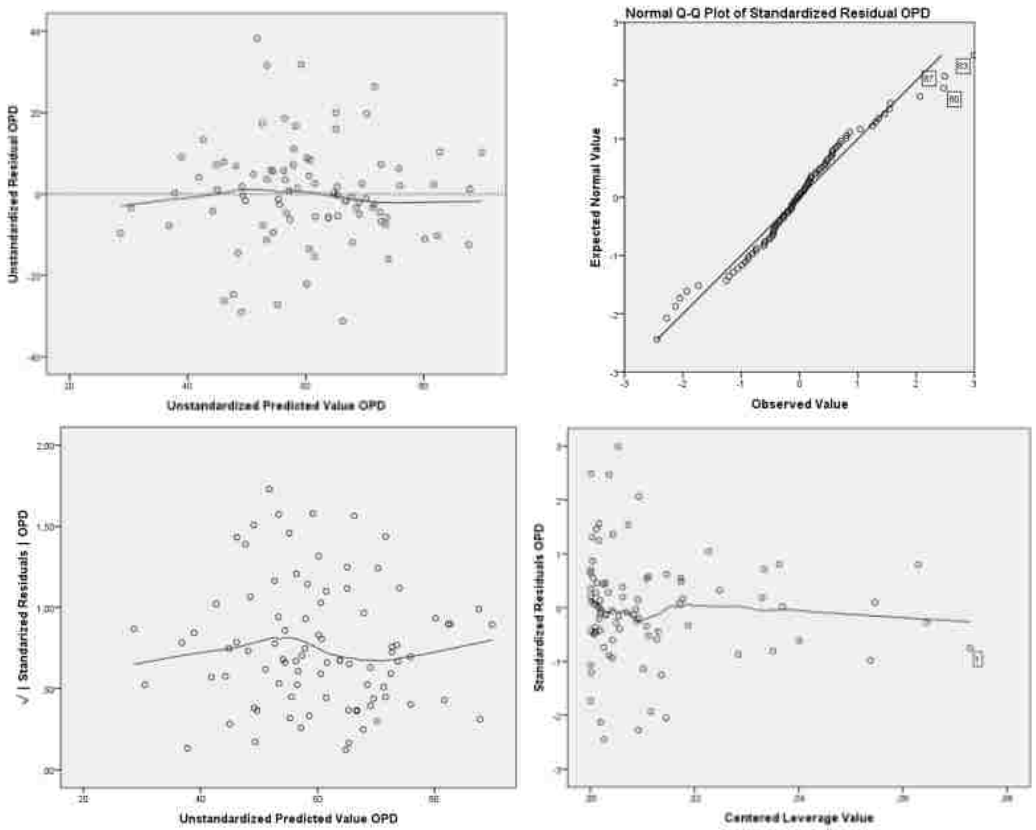

MODEL 6: 84.337 – 1.249 (Ct.Ar)

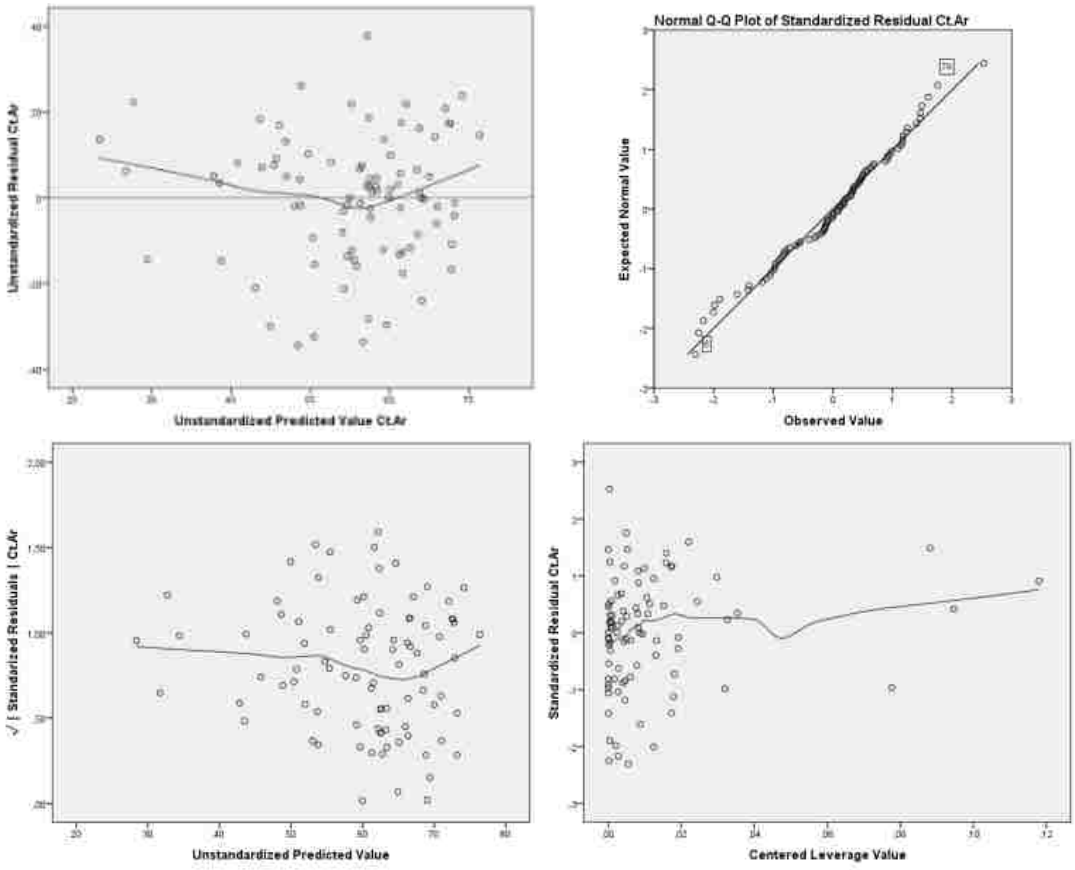

MODEL 7: 83.823 – 73.003 (Ct.Ar/Tt.Ar)

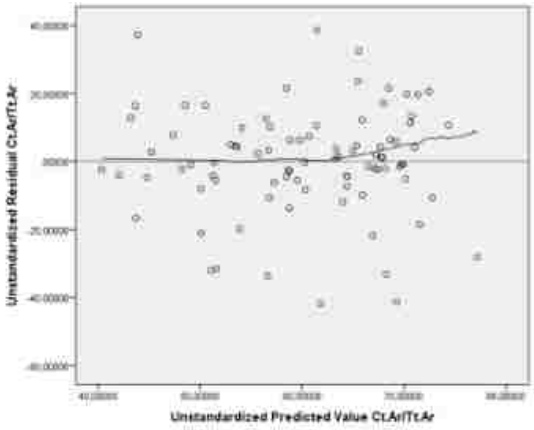

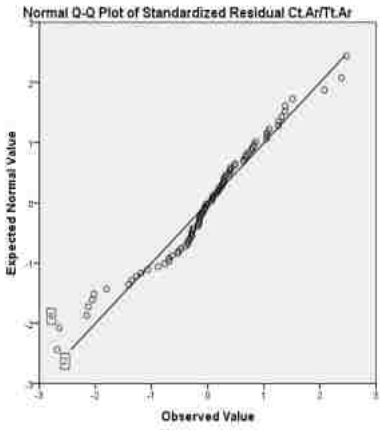

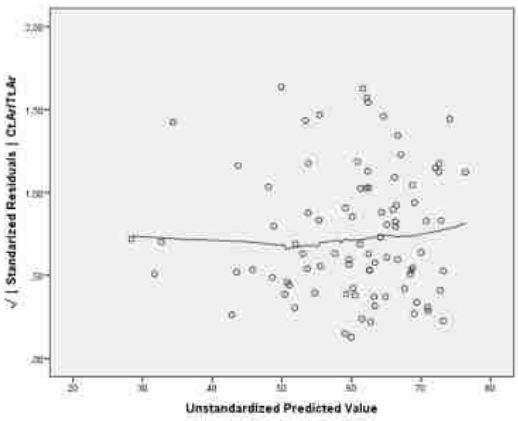

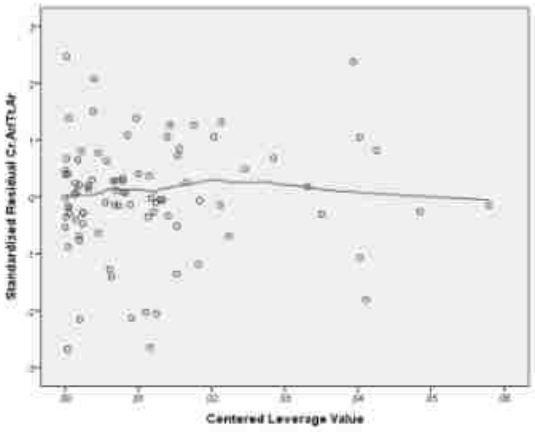

MODEL 8: 97.473 – 1163.81(On.Ar)

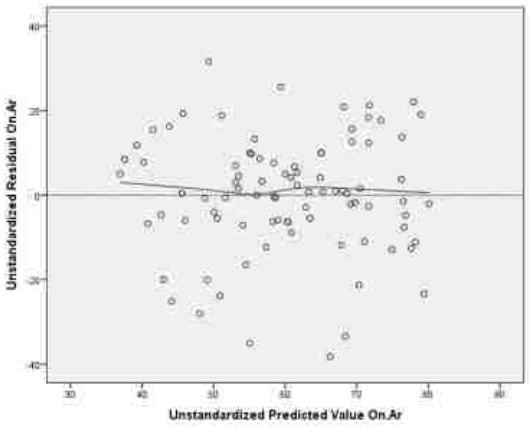

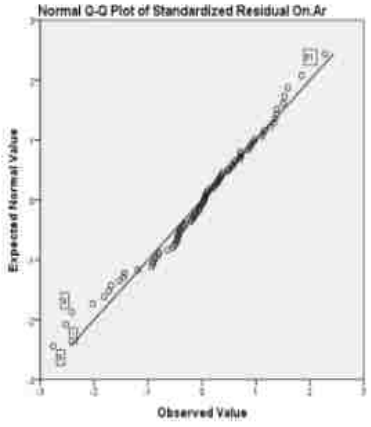

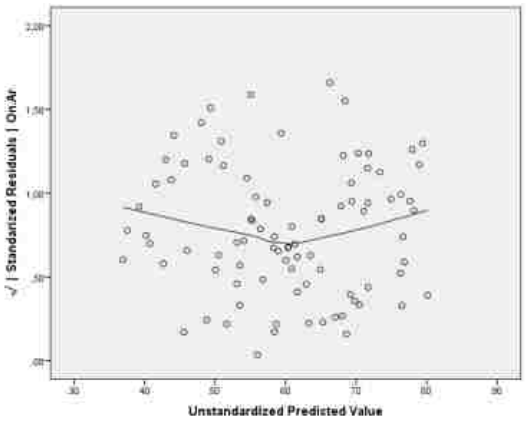

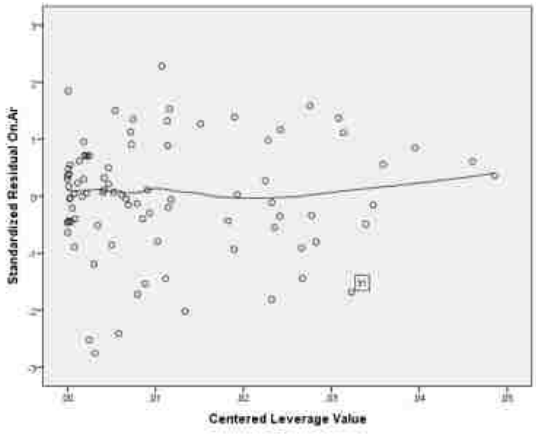

MODEL 9: 133.224 – 115.24(On.Pm)

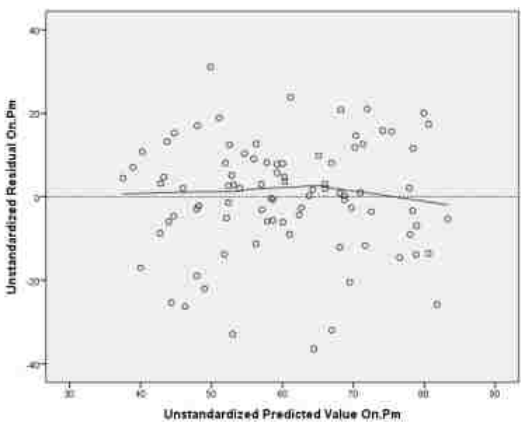

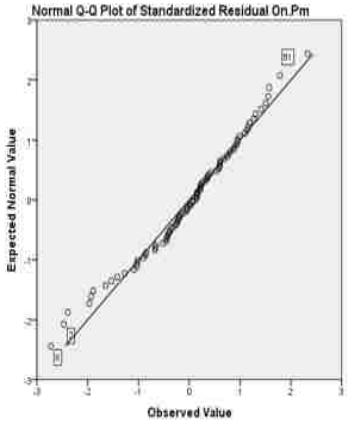

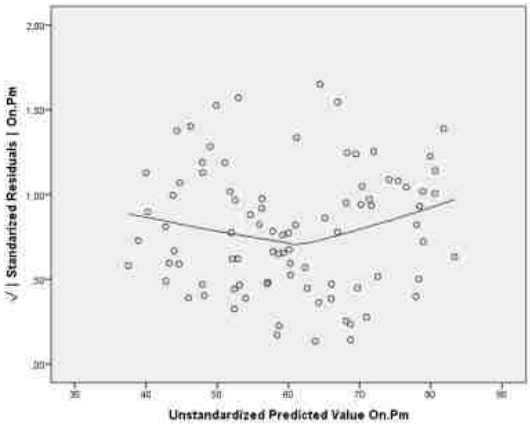

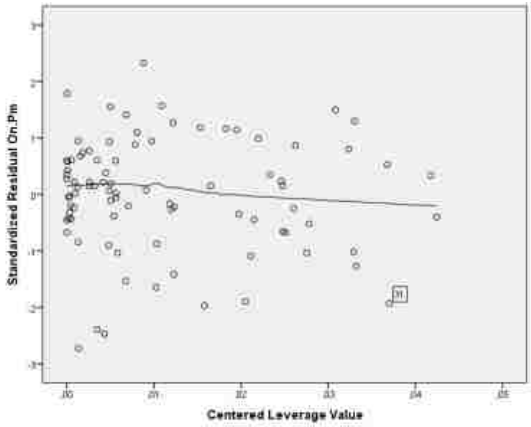

MODEL 10:-445.296 + 555.582(On.Cr)

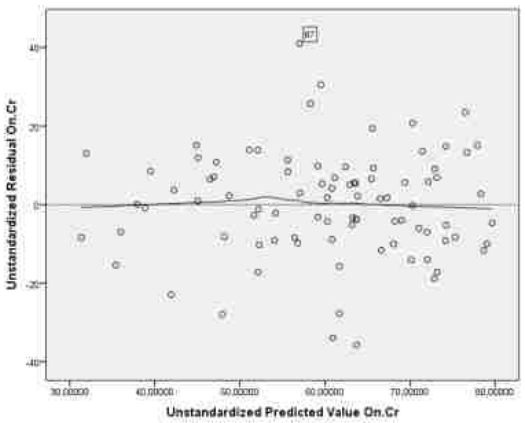

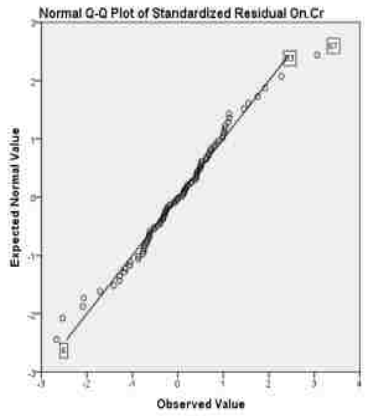

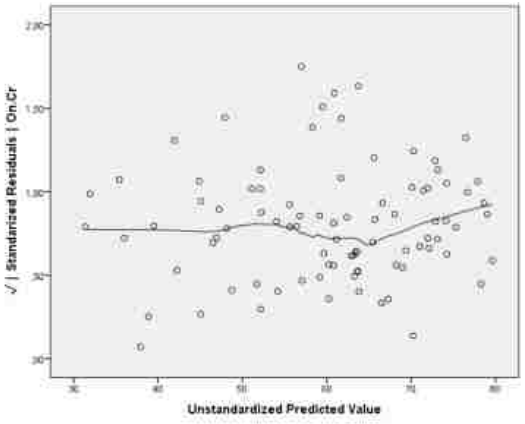

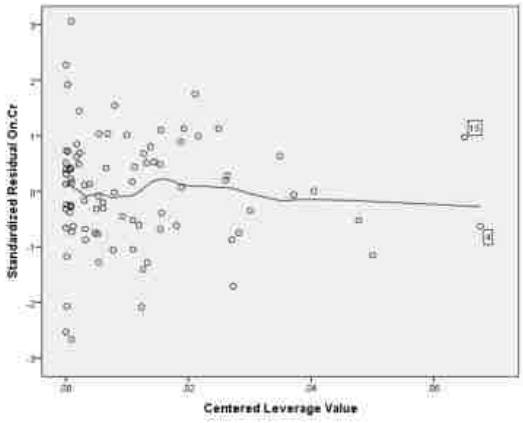

Appendix B.8 Diagnostic plots for regression models: <u>Multiple Linear Models</u>

Residuals vs fitted plot, Q-Q plot,
Scale-location plot, Residuals vs Leverage´s values

MODEL 11: 48.77 + 2.0818(OPD) – 644.567(On.Ar)

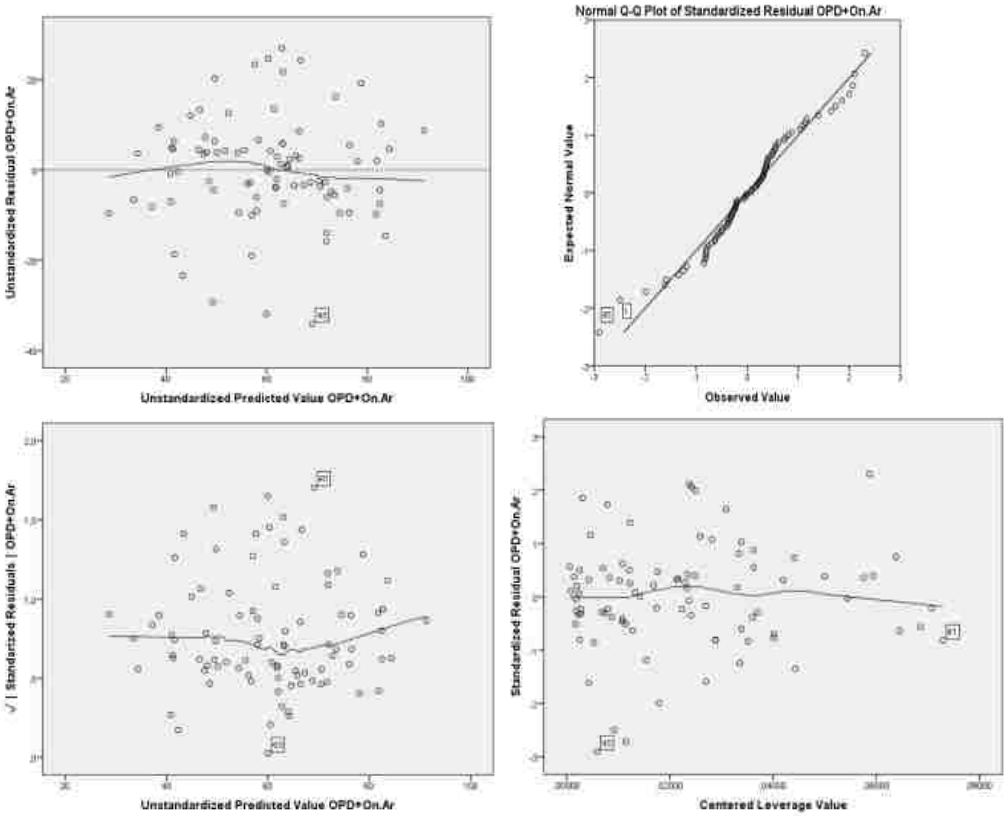

MODEL 12: 73.515 + 1.967(OPD) – 274.568(On.Pm)

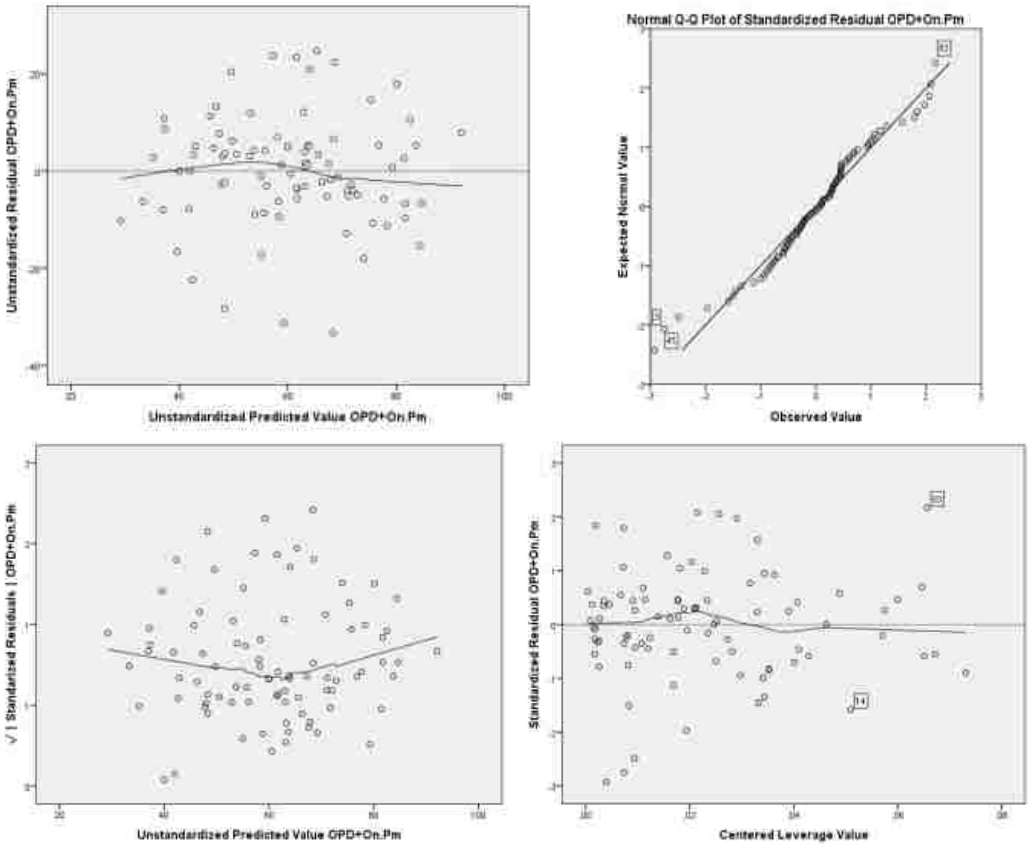

MODEL 13: -274.568 + 1.982(OPD) + 334.535(On.Cr)

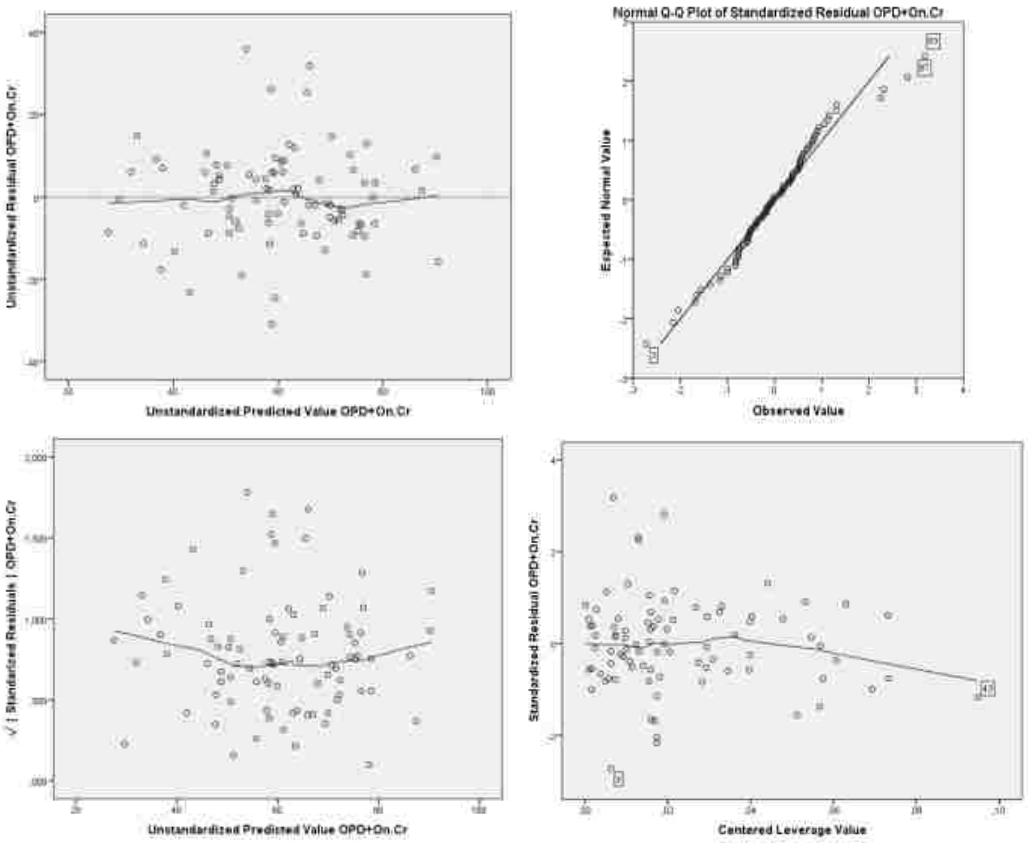

MODEL 14: -193.379 + 1.599(OPD) – 449.111(On.Ar) + 267.398(On.Cr)

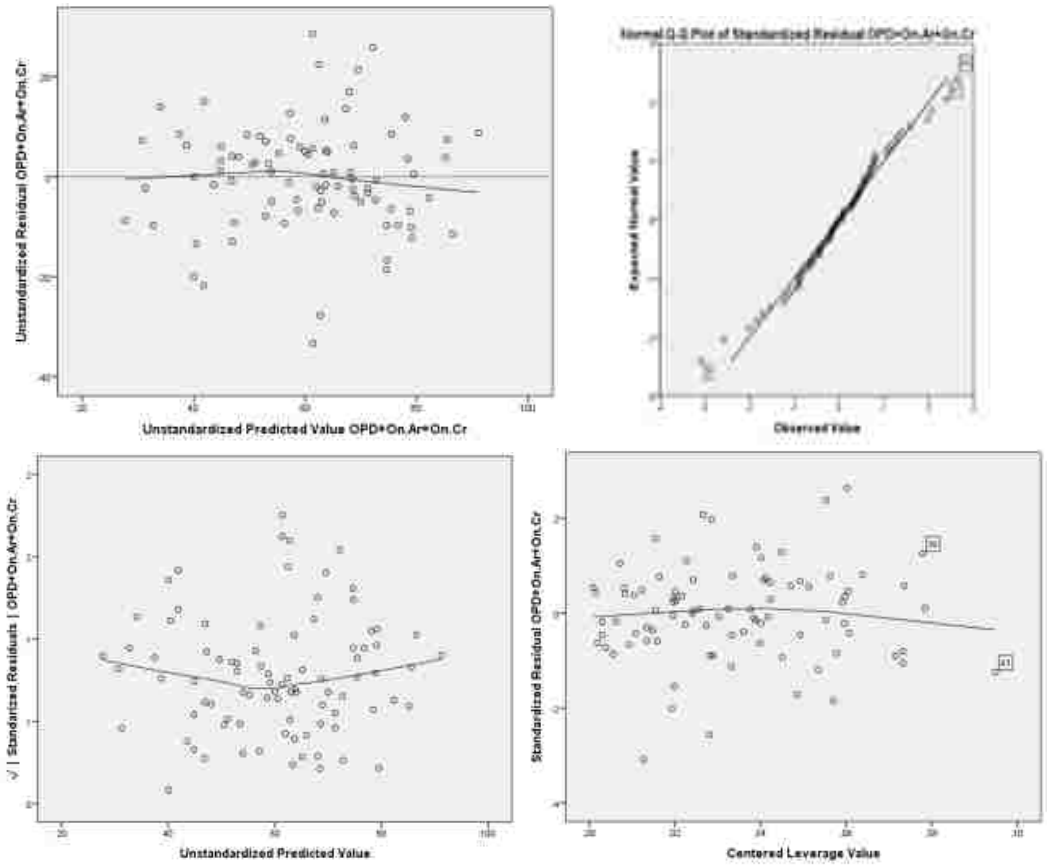

MODEL 15: -153.132 + 1.577(OPD) – 48.909(On.Pm) + 241.791(On.Cr)

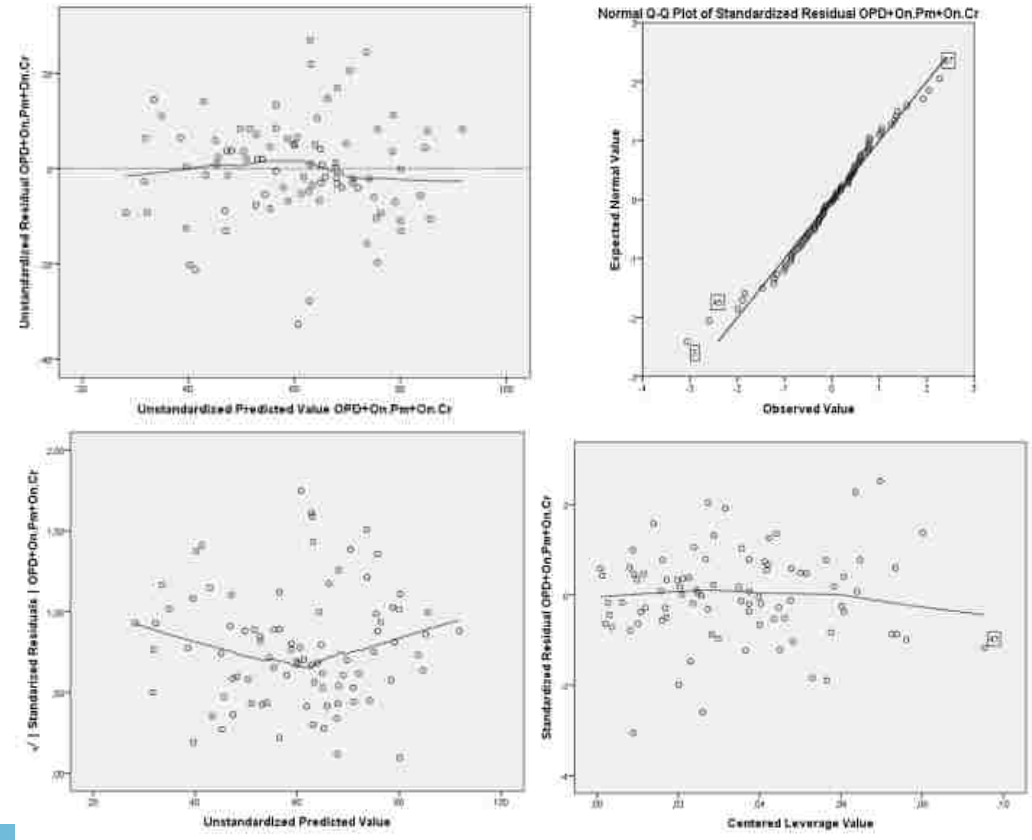

MODEL 16: 49.465 + 4.116(OPD(F)) – 469.456(On.Ar)

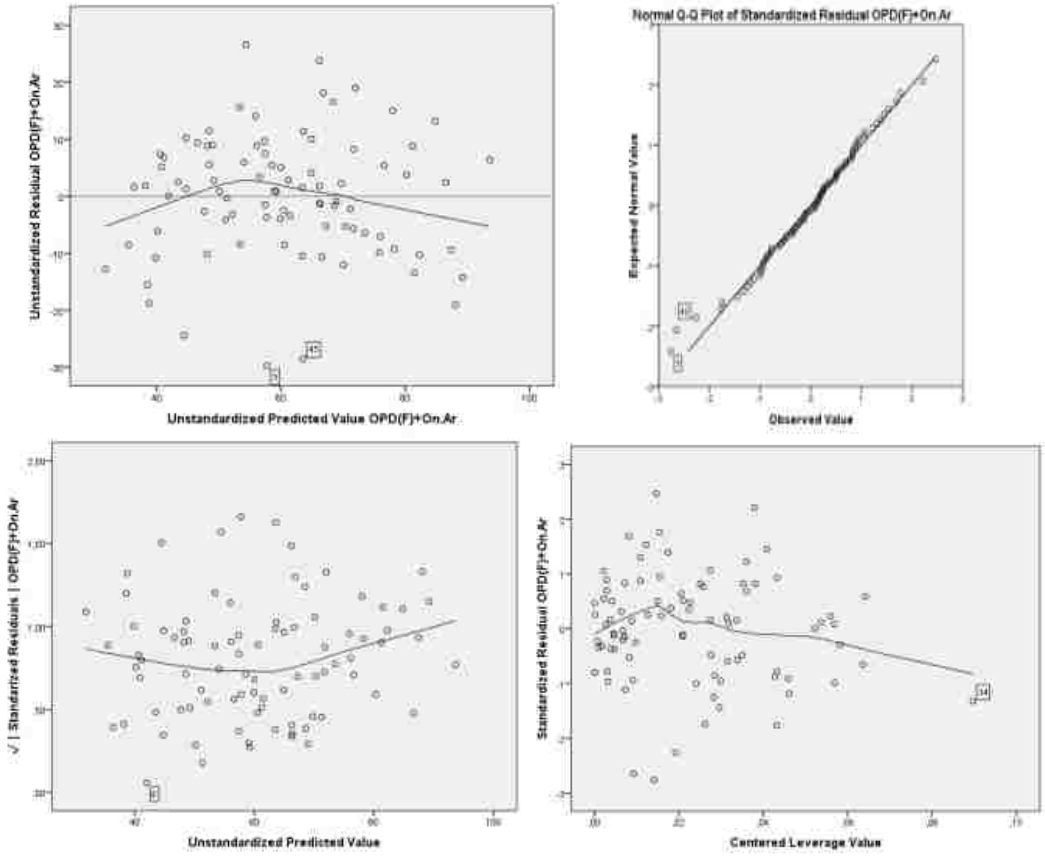

MODEL 17: 68.487 + 3.909(OPD(F)) – 51.715(On.Pm)

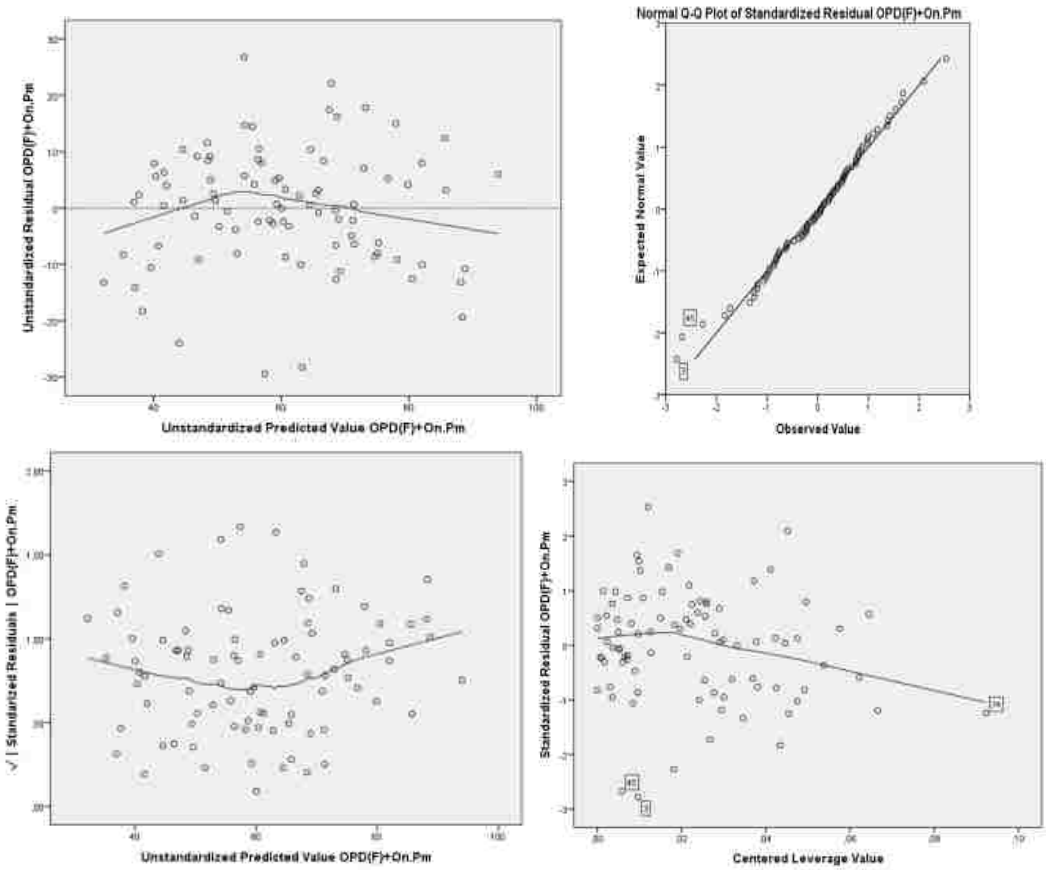

MODEL 18: -201.271 + 3.907(OPD(F)) + 260.484(On.Cr)

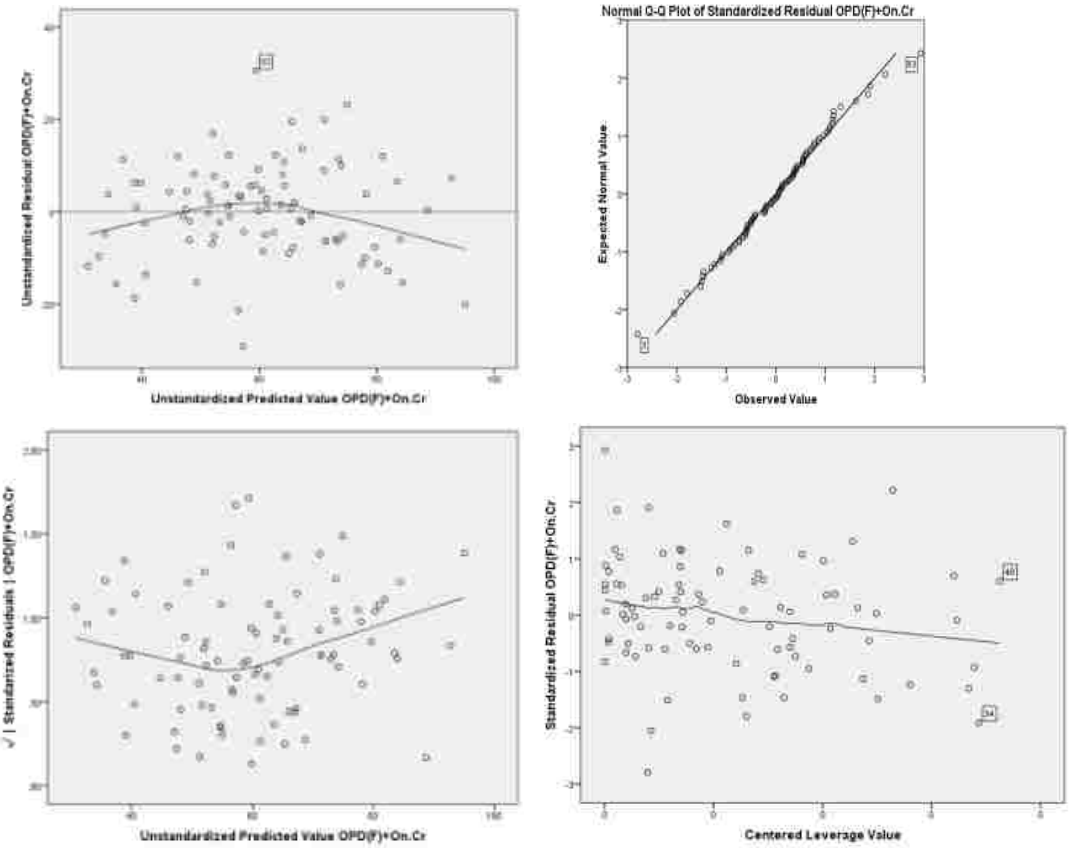

MODEL 19: -149.78 + 3.35(OPD(F)) – 339.413(On.Ar) + 219.594(On.Cr)

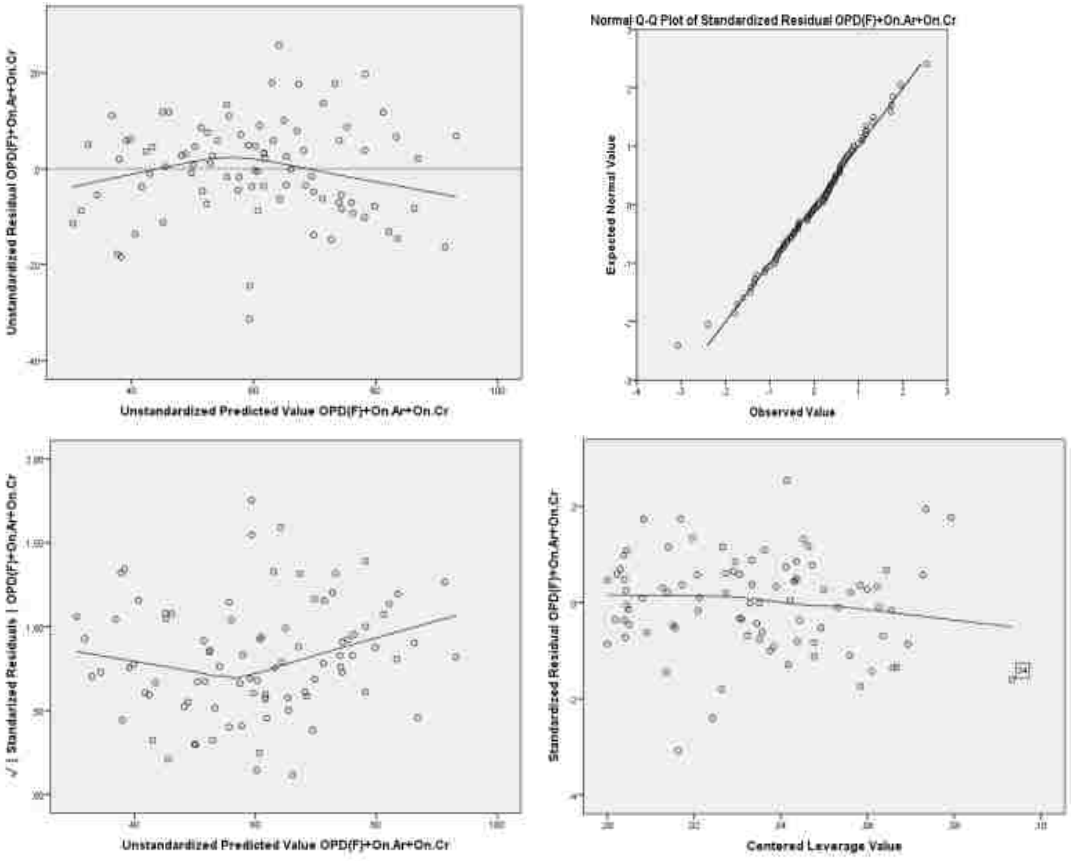

MODEL 20: -120.205 + 3.281(OPD(F)) – 37.581(On.Pm) + 201.846(On.Cr)

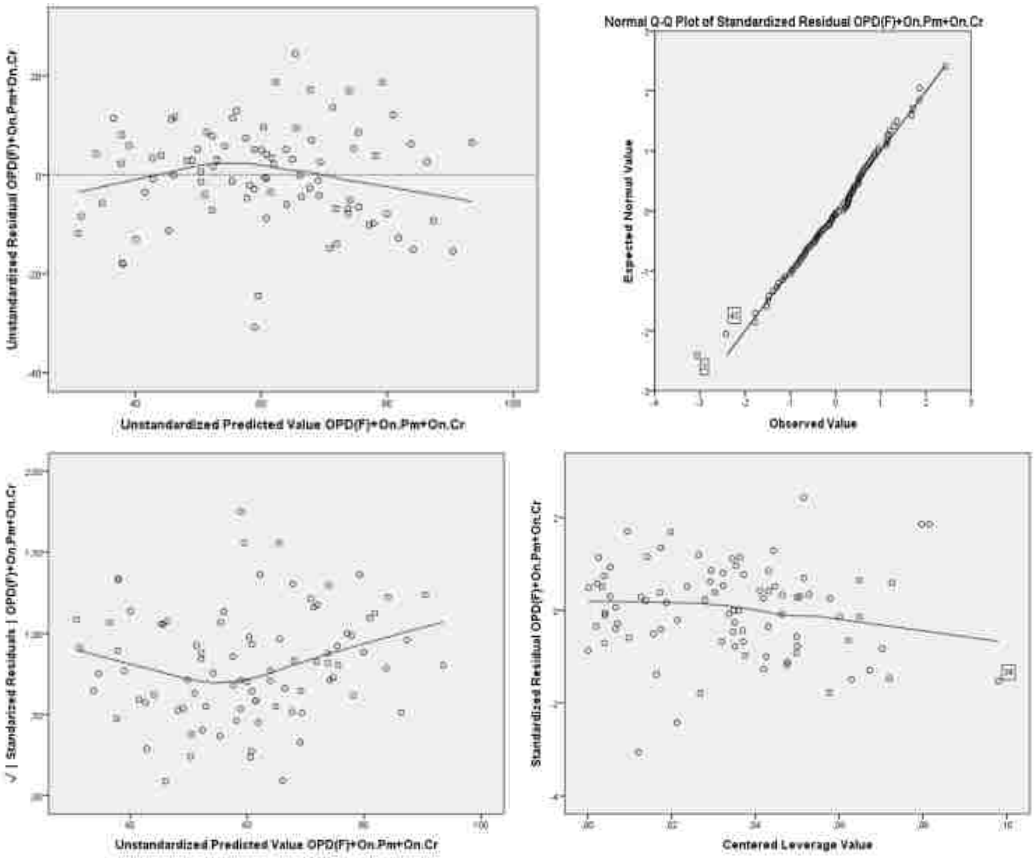

MODEL 25: -337.948 + 454.948(On.Cr) – 0.866(Ct.Ar)

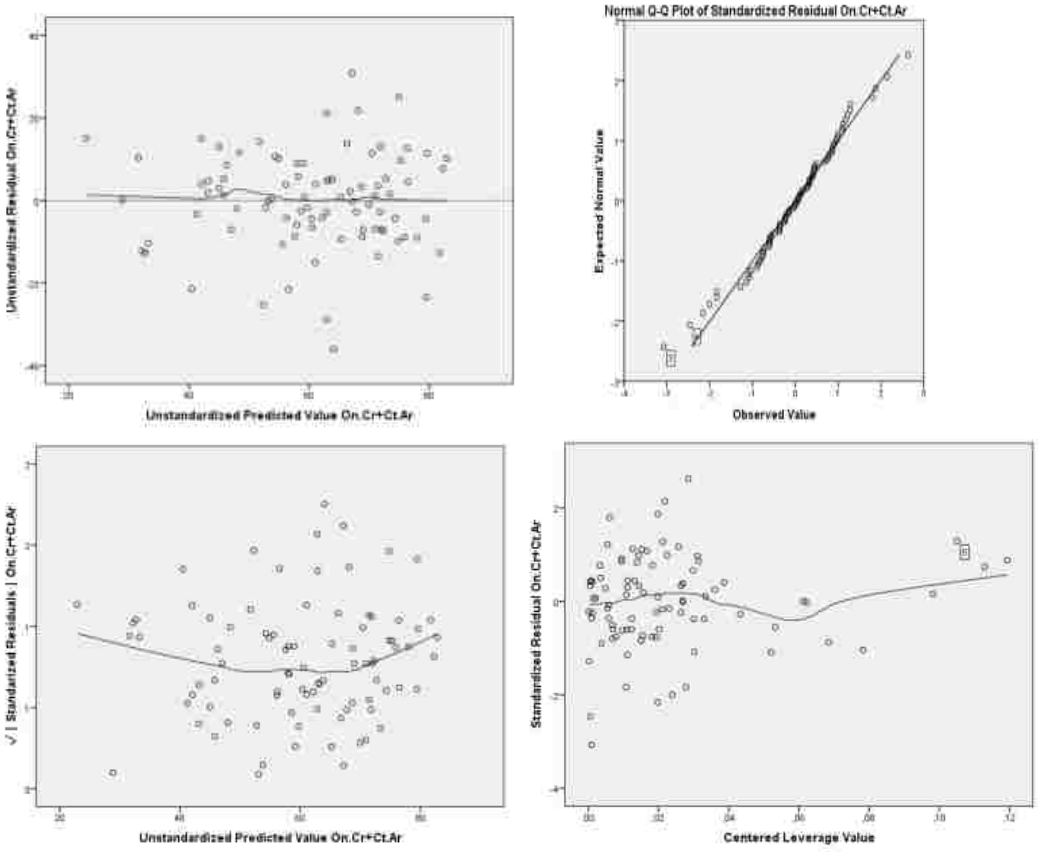

MODEL 26: -348.847 + 463.584(On.Cr) – 39.534(Ct.Ar/Tt.Ar)

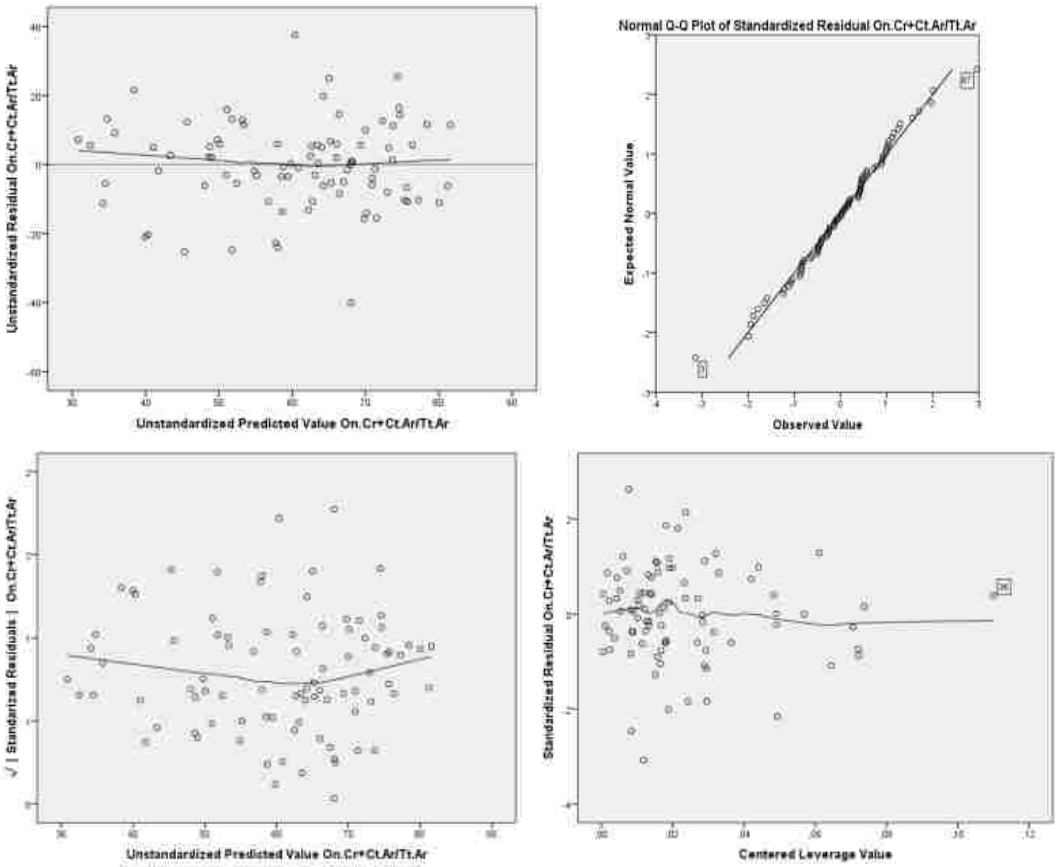

Appendix B.9 Regression Models with sex and sample as categorical variables

Summary of hierarchical regression for predicting age from Ct.Ar and sex as categorical variable.

	Model 6 + Sex	
Variable	B	β
Constant	87.807**	
Ct.Ar	-1.309**	-0.584
Sex	-4.245	-0.119
R2	0.324	
F	20.386	
Δ R2	0.013	
Δ F	1.695	
SEE	14.87	

**p-value <.001, N=88, Male is 0

Hierarchical regression results for simple models improved accuracy of single histological variables and sample as categorical predictor.

	Model 6 + sample			Model 7 + sample			Model 8 + sample			Model 9 + sample	
Variable	B	β	Variable	B	β	Variable	B	β	Variable	B	β
Constant	84.401**		Constant	80.915**		Constant	94.92**		Constant	132.247**	
Ct.Ar	-1.348**	-0.60	Ct.Ar/Tt.Ar	-74.032**	-0.505	On.Ar	-1234.279**	-0.67	On.Pm	-121.118**	-0.703
Sample	9.02*	0.253	Sample	6.064	0.170	Sample	8.991**	0.252	Sample	8.791*	0.247
R2	0.373		R2	0.248		R2	0.466		R2	0.508	
F	25.270		F	16.270		F	37.148		F	43.796	
Δ R2	0.062		Δ R2	0.029		Δ R2	0.062		Δ R2	0.060	
Δ F	8.429*		Δ F	3.395		Δ F	9.896*		Δ F	10.295*	
SEE	14.32		SEE	15.40		SEE	13.21		SEE	12.70	

*p-value <.050, **p-value < 0.001; N=88, Crete set as 0.

321

Summary table for hierarchical regression of multiple models and sample as categorical predictor.

	Model 21 + sample			Model 22 + sample			Model 23 + sample			Model 24 + sample	
Variable	B	β	Variable	B	β	Variable	B	β	Variable	B	β
Constant	96.863**		Constant	96.707**		Constant	125.570**		Constant	129.903**	
On.Ar	-900.375**	-0.492	On.Ar	-1061.64**	-0.580	On.Pm	-92.782**	-0.539	On.Pm	-108.778**	-0.63
Ct.Ar	-0.680	-0.303	Ct.Ar/Tt.Ar	-22.190	-0.151	Ct.Ar	-0.606**	-0.270	Ct.Ar/Tt.Ar	-16.662	-0.01
Sample	9.868	0.277	Sample	8.7*	0.244	Sex	9.649**	0.271	Sex	8.605	0.24
R2	0.506		R2	0.462		R2	0.536		R2	0.498	
F	30.726		F	25.906		F	34.511		F	29.776	
Δ R2	.074		Δ R2	.058		Δ R2	.071		Δ R2	.057	
Δ F	13.048*		Δ F	9,364*		Δ F	13.305**		Δ F	9.871**	
SEE	12.60		SEE	13.10		SEE	12.18		SEE	12.67	

*p-value <.050, **p-value < 0.001; N=88. Crete set as 0

Appendix B.10 Simple and Multiple Linear Models by SEX

Males

Residuals vs fitted plot, Q-Q plot,
Scale-location plot, Residuals vs Leverage´s values

MODEL 27: 15.15 + 2.904(OPD)

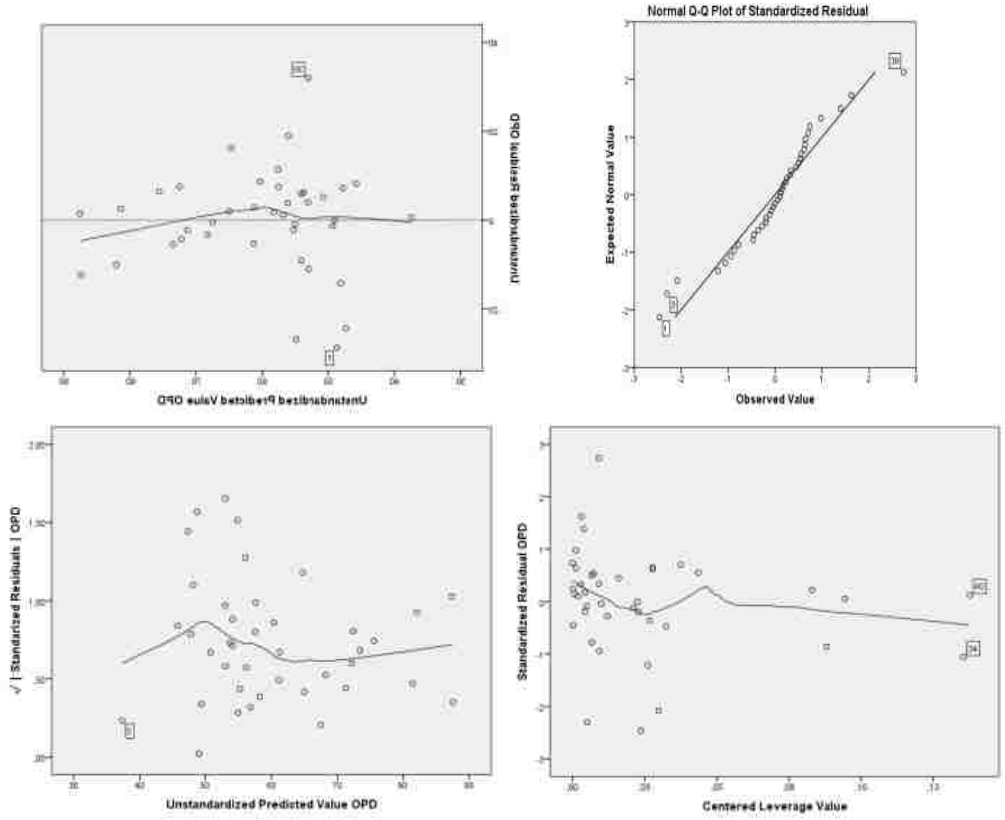

MODEL 28: -402.715 + 507.025(On.Cr)

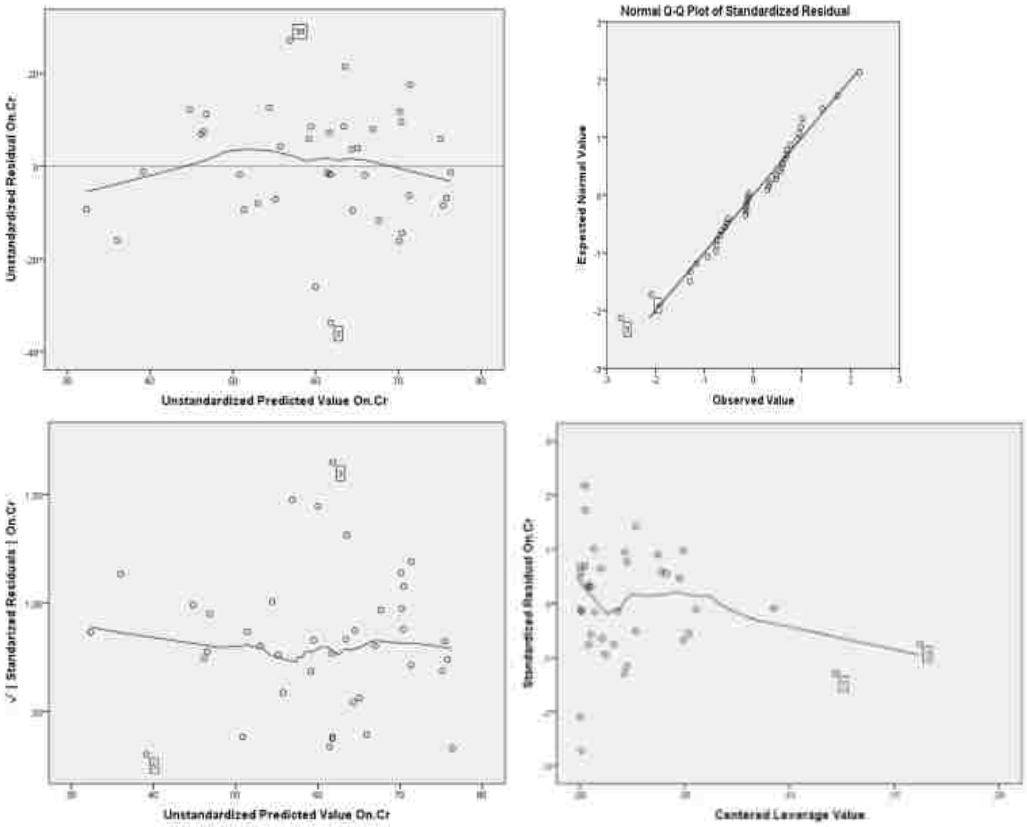

MODEL 29: -247.98 + 2.04(OPD) + 302.931(On.Cr)

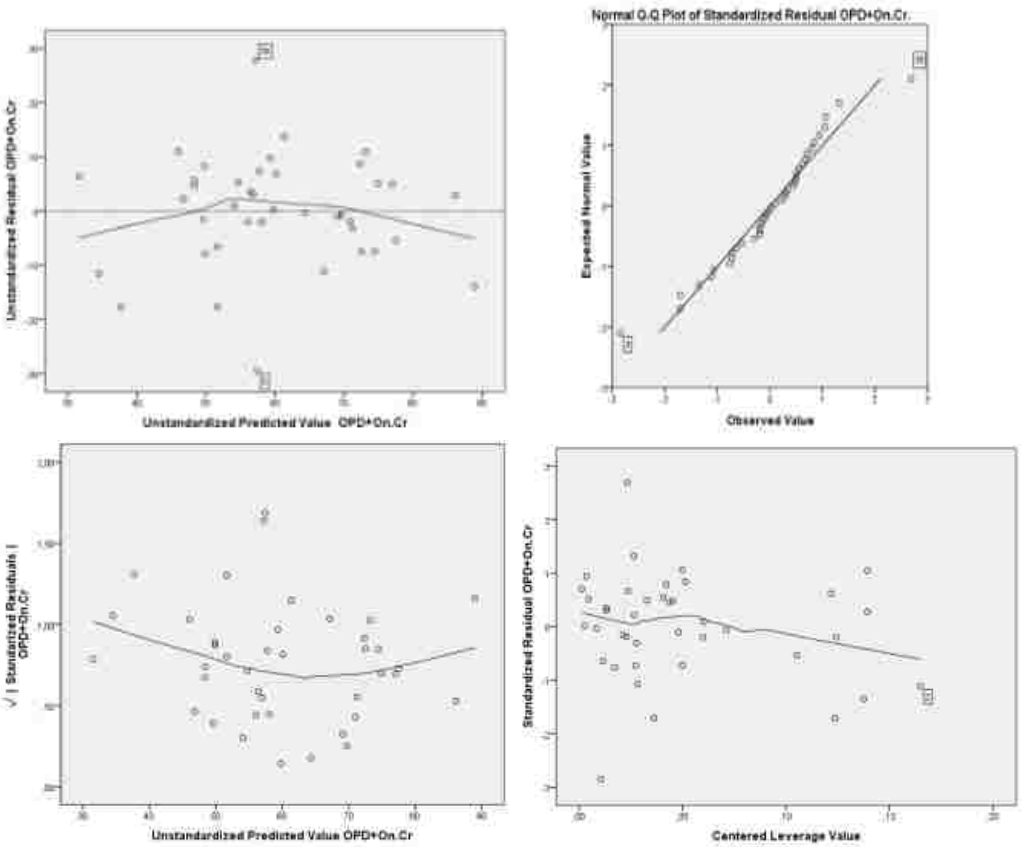

Females

MODEL 30: 23.511 + 5.753(OPD(F)

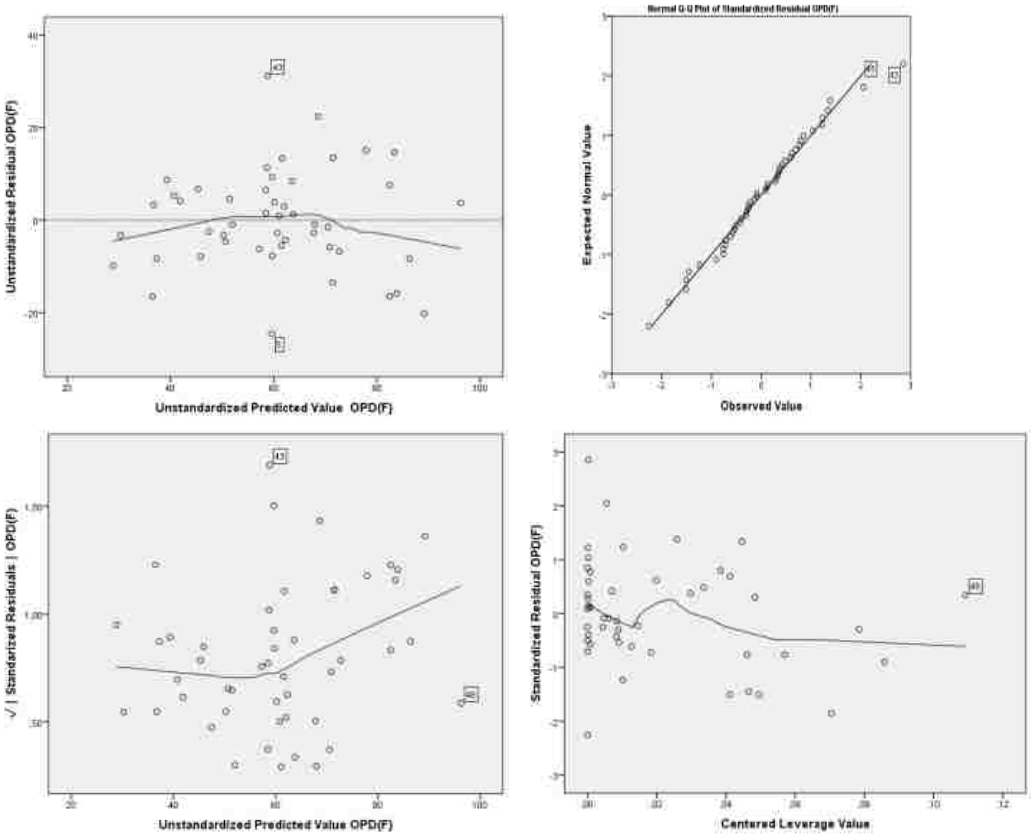

MODEL 31: 95.428 – 1.984(Ct.Ar)

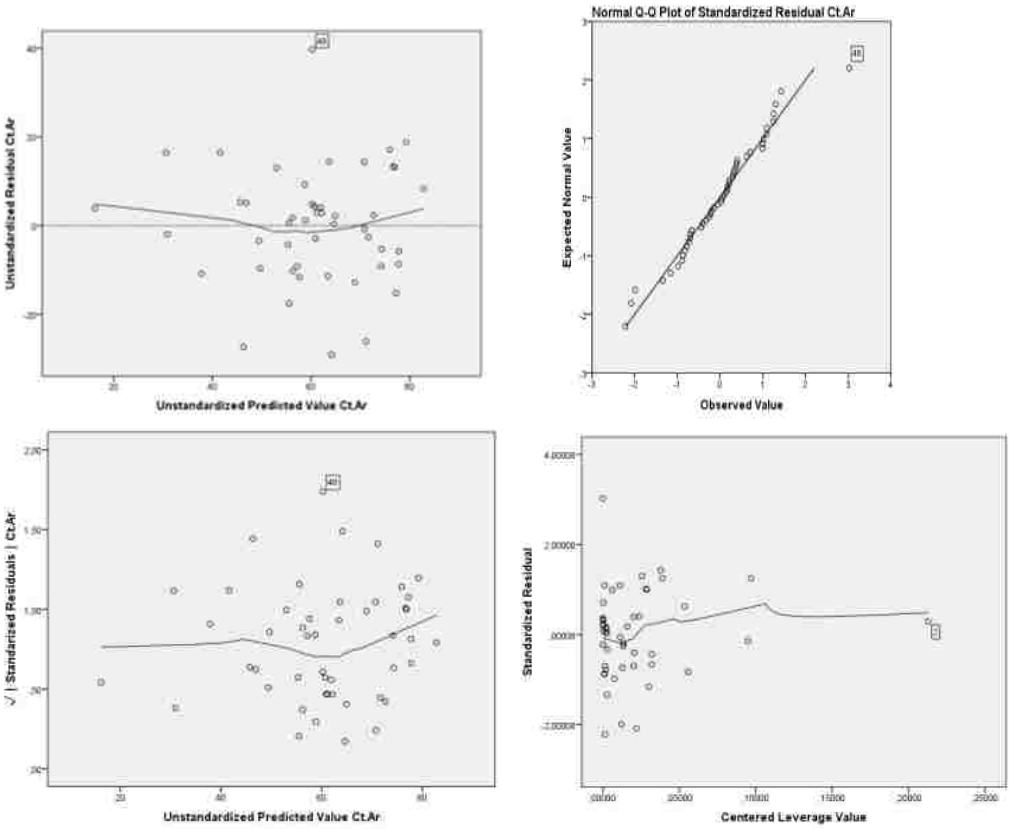

MODEL 32:128.742 – 74.338(On.Pm) – 1.220(Ct.Ar)

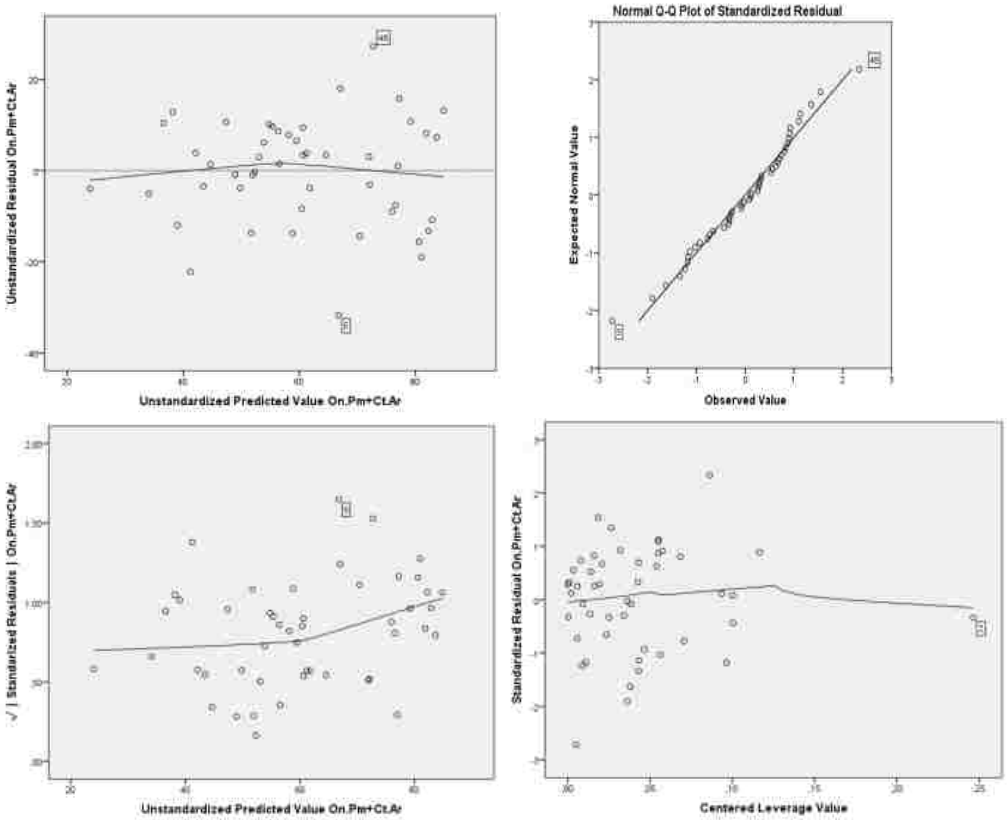

MODEL 33: -276.939 – 399.886(On.Cr) – 1.453(Ct.Ar)

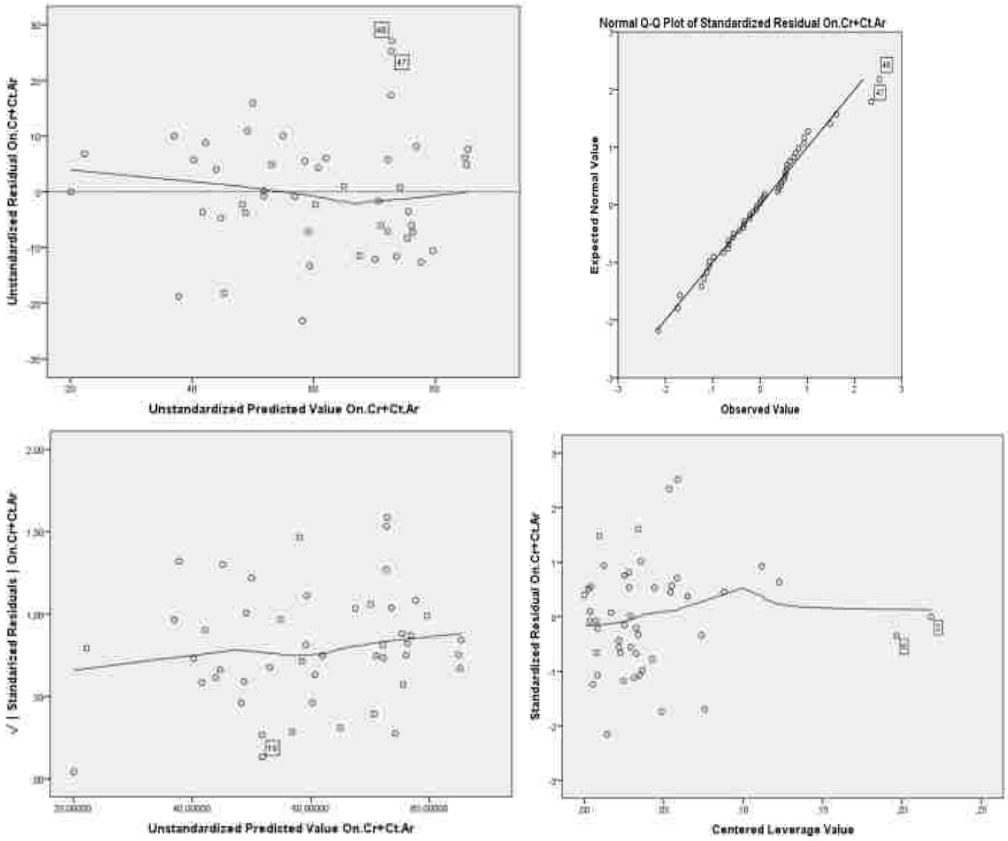

MODEL 34: 52.44 + 4.21(OPD(F)) – 1.080(Ct.Ar)

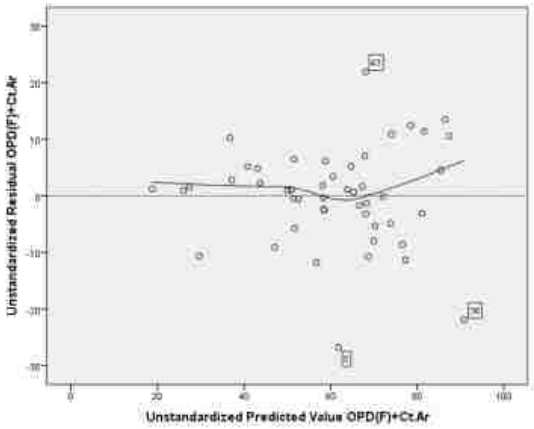

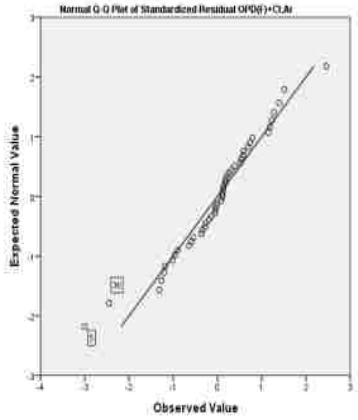

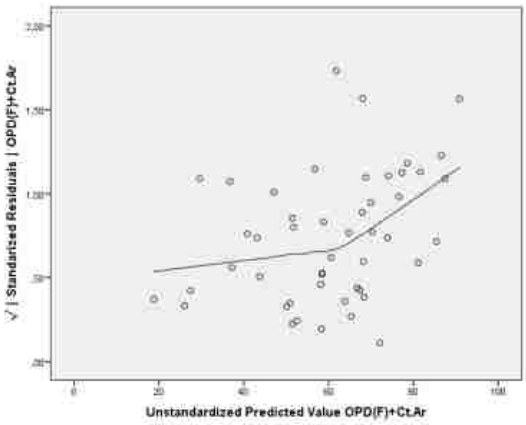

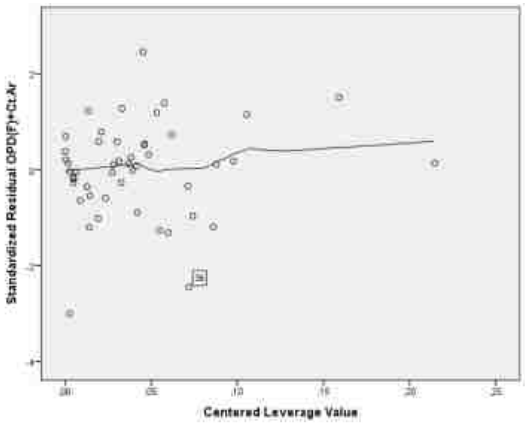

Appendix B.11 Simple and Multiple Linear Models for CYPRIOTS

Residuals vs fitted plot, Q-Q plot, Scale-location plot, Residuals vs Leverage´s values

MODEL 35: 32.66+ 4.417(OPD(F))

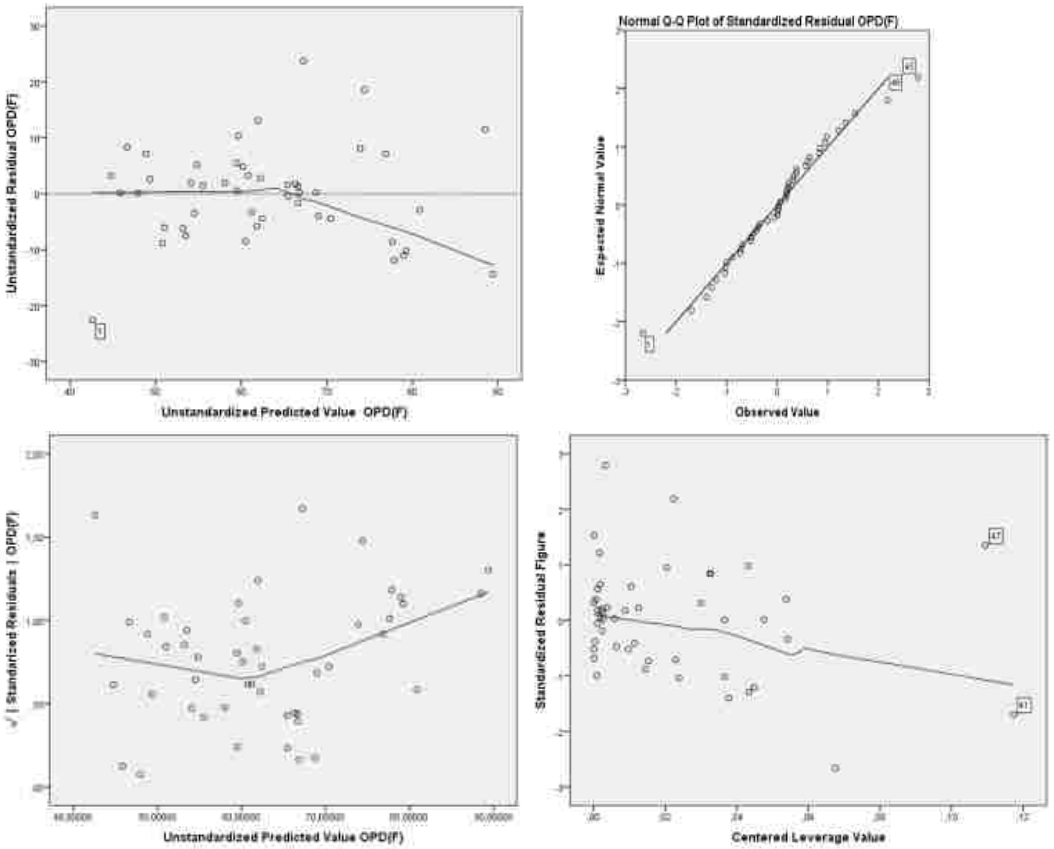

MODEL 36: 21.36+ 2.549(OPD)

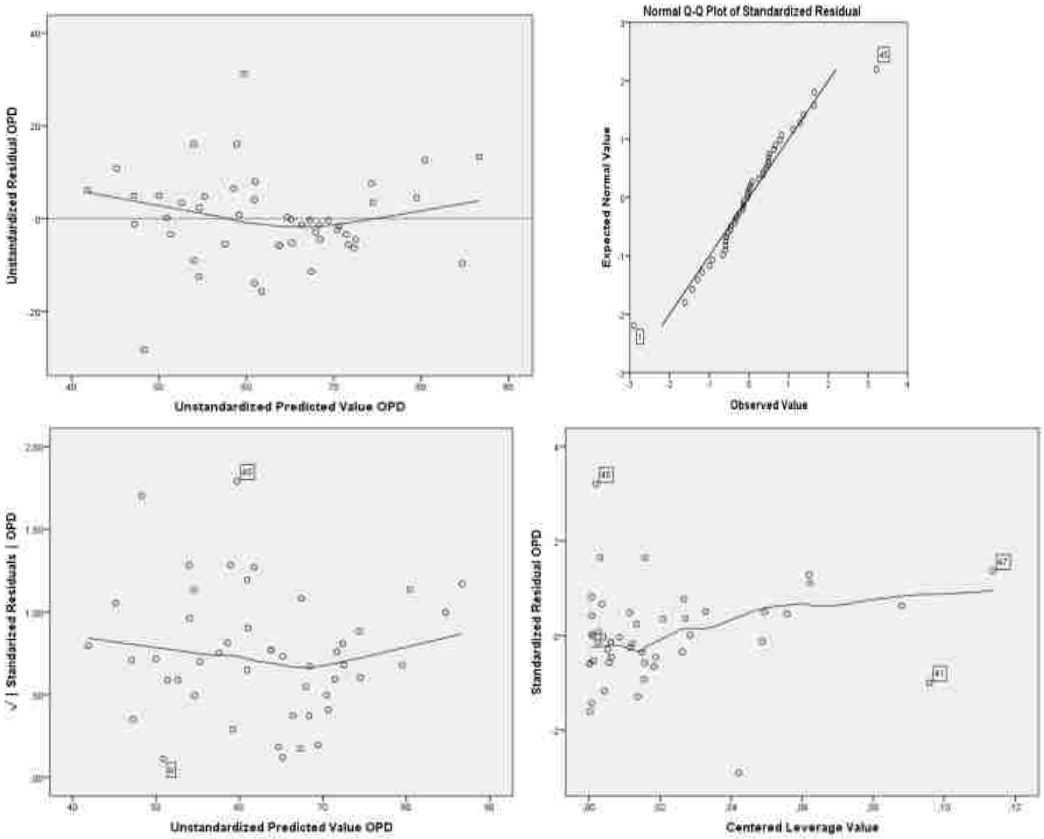

MODEL 37: 89.238 – 80.95(Ct.Ar/Tt.Ar)

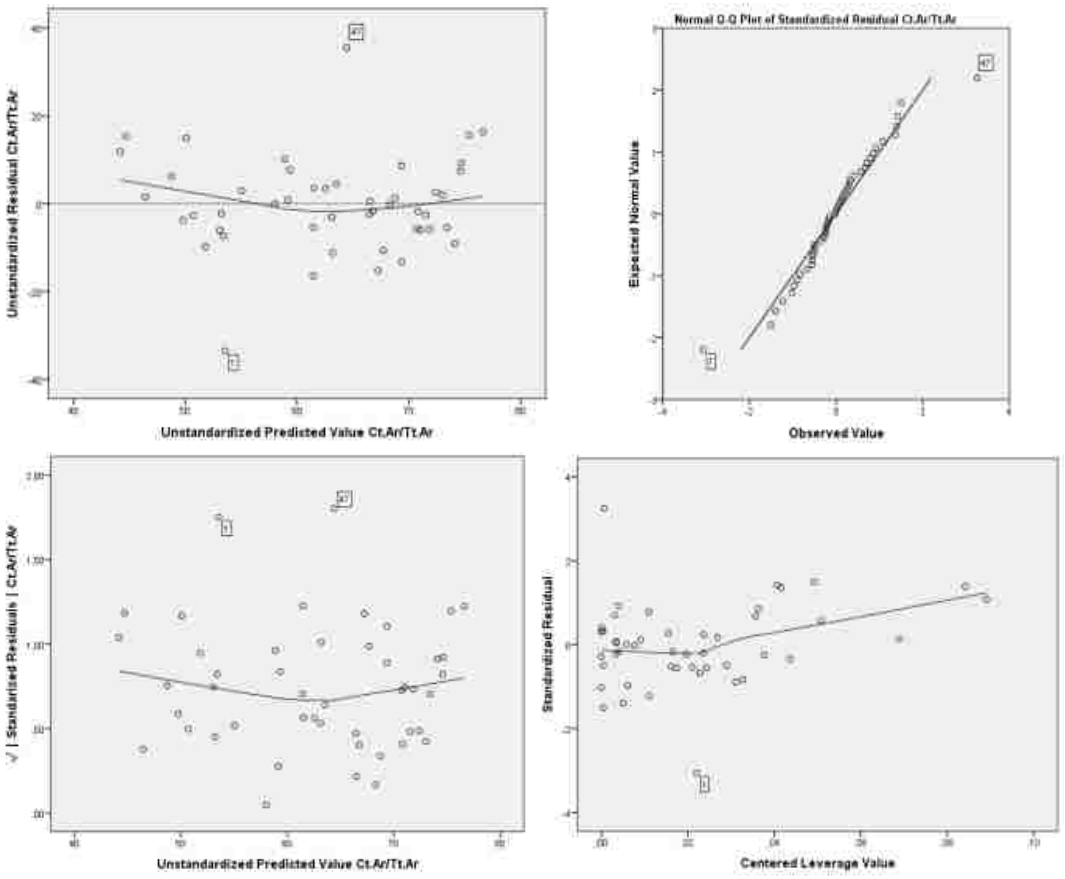

MODEL 38: 136.234 – 113.681(On.Pm)

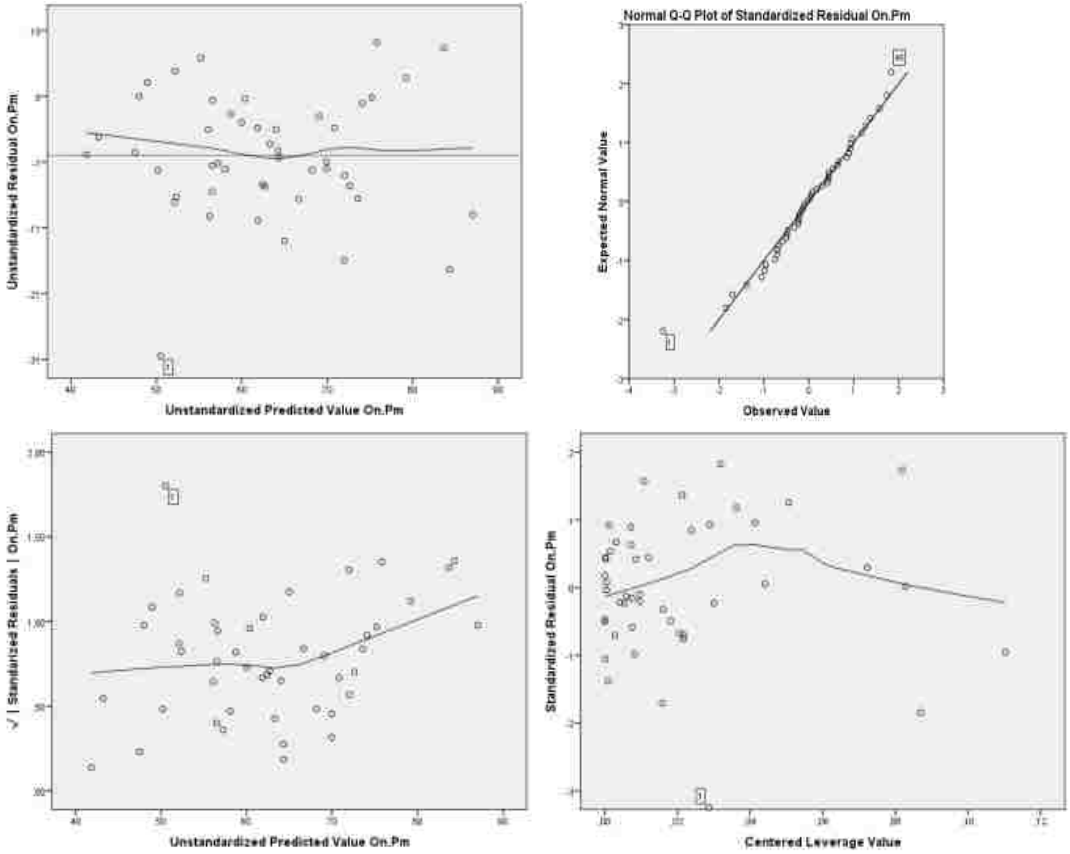

MODEL 39: 78.819 + 2.97(OPD(F) – 56.171(On.Pm)

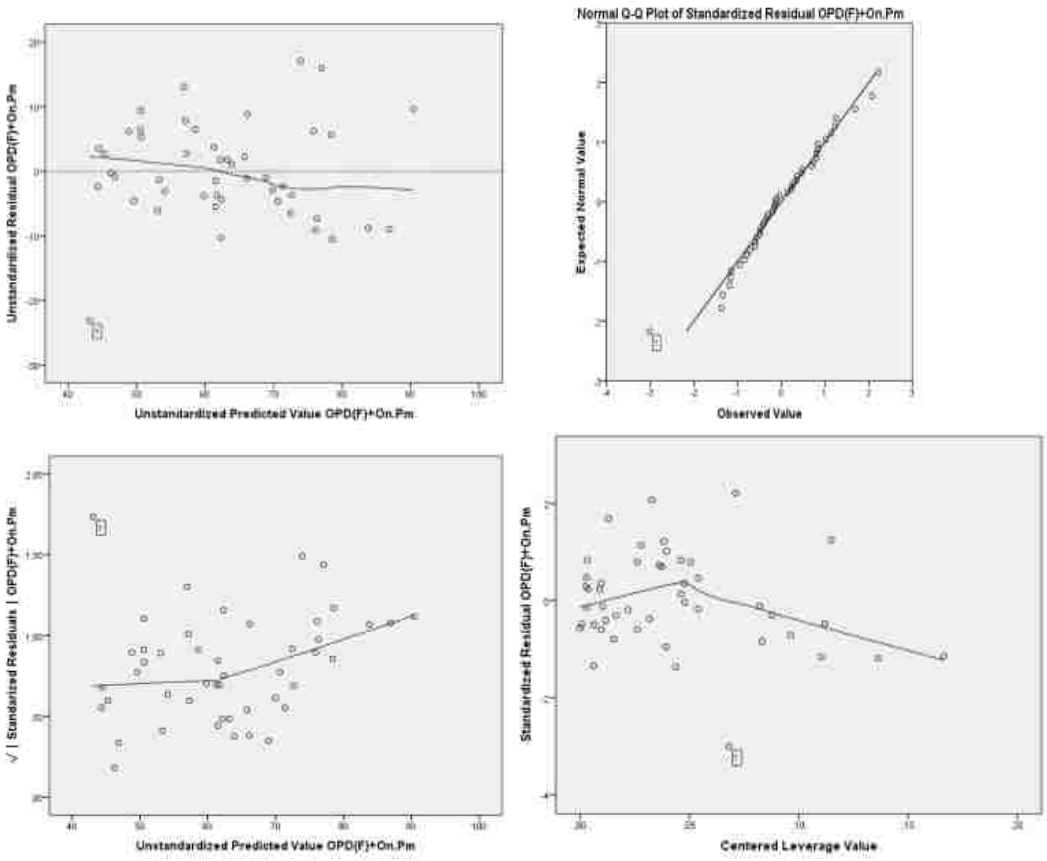

MODEL 40: 85.982 + 1.507(OPD) – 73.831(On.Pm)

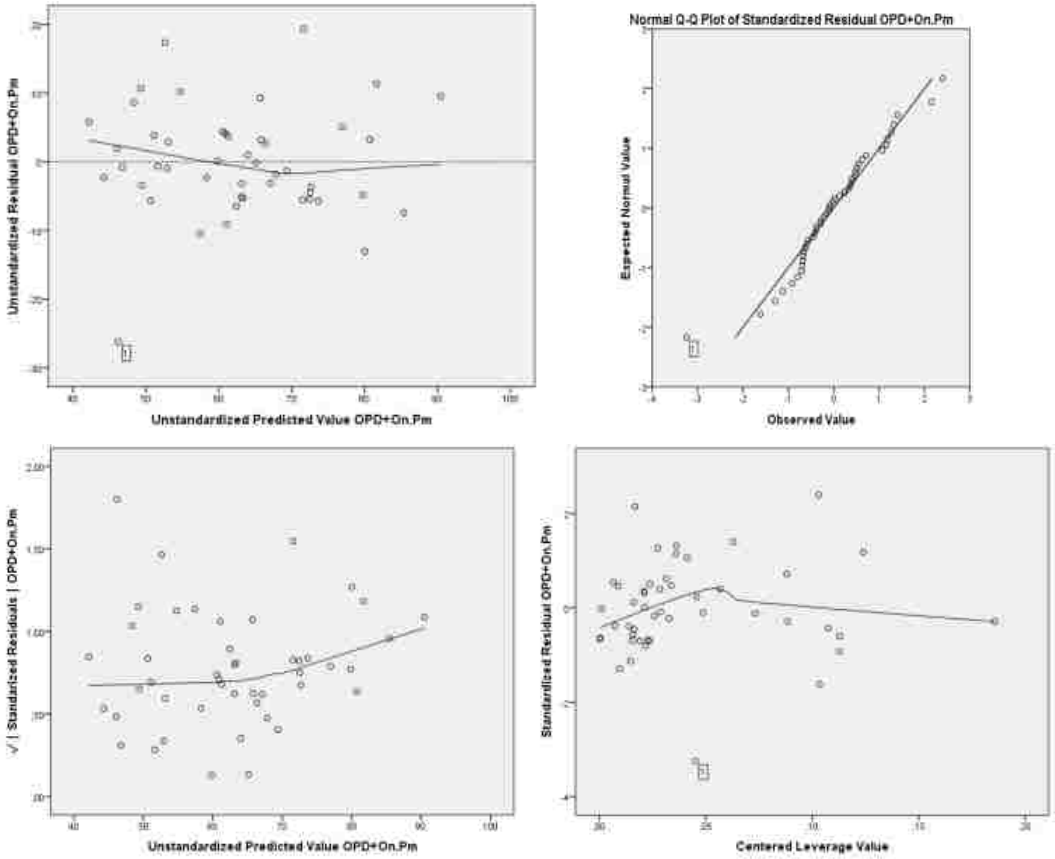

MODEL 41: 131.744 – 86.248(On.Pm) – 40.518(Ct.Ar/Tt.Ar)